A role for a leaky gut and the intestinal microbiota in the pathophysiology of Myalgic Encephalomyelitis/Chronic Fatigue Syndrome (ME/CFS)

Daniel T. Vipond BSc (Hons), MRSB

Quadram Institute Bioscience & Norwich Medical School

A thesis submitted for the degree of Doctor of Philosophy to the University of East Anglia

September 2018

Abstract

The field of ME/CFS research is challenged by many often confusing and conflicting reports of immune, neuroendocrine, autonomic, neurological dysfunction. During the prodromal phase of this condition patients often report flu-like symptoms, persistent chronic fatigue and gastro-intestinal symptoms including abdominal pain and discomfort.
Its study is complicated by the lack of specific biomarkers and criteria to accurately define the illness, relying on the exclusion of other fatiguing illnesses. Recent publications suggest an altered intestinal microbiota and increased intestinal permeability are associated with ME/CFS. Further evidence is accumulating for dysfunctional energy, lipid and amino acid metabolism that may indicate oxidative stress and/or immune-mediated damage to mitochondria, disrupting the efficiency of aerobic respiration, explaining the effect of post-external malaise (PEM), a unique characteristic for the diagnosis of ME.

In this study, Next Generation Sequencing (NGS) and Nuclear Magnetic Resonance (NMR) spectroscopy probed the composition of the intestinal microbiota and faecal and serum microbiomes in 17 severe, house-bound patients and house-hold healthy controls (HHC). Severe, house-bound patients account for 0.5% of all ME/CFS research, yet it is estimated they represent 25% of the patient population. We found *Faecalibacterium prausnitzii* was significantly reduced in severe patients ($p = 0.018$) but did not replicate individual differences in faecal and serum metabolites that others have previously reported. We further enhanced a flow cytometry technique for detecting IgA coated bacteria in faecal suspensions and analysed the proportional differences between patients and HHCs. This demonstrated a trend for increased IgA-coated bacteria in most patients; however, this trend was reversed when repeated with a second sample produced a year on.

Since the initial concept for this study, several advances have been made in sequencing methods and quality control standards for metagenomic and metabolomic studies. Based on these, we conclude further investigations are warranted using whole genome sequencing and targeted metabolomics to address the emerging hypotheses in ME/CFS research, with an emphasis on the study of severe, house-bound ME patients.

Table of contents

Chapter Six

List of figures

Abbreviations

αSn	alpha-synuclein
16S	16S ribosomal RNA
4EPS	4-ethylphenylsulfate
ABC-TP	Adenosine-triphosphate binding cassette transporter permease
ACTH	Adrenocorticotropic hormone
ADL	Activities of Daily Living
ANA	Antinuclear antibodies
ANS	Autonomic Nervous System
APCs	Antigen presenting cells
AQP4	Aquaporin-4
ASD	Autism Spectrum Disorder
ASO	Antisense Oligonucleotide
BBB	Blood Brain Activation
BDNF	Brain-derived Neurotrophic Factor
bp	Base pairs
CBT	Cognitive Behavioural Therapy
CCC	Canadian Consensus Criteria
CD	Cluster of Differentiation
CDC	Centers for Disease Control and Prevention
CDI	Clostridium Difficile Infection
CF	Chronic Fatigue
CFS	Chronic Fatigue Syndrome
CFU	Colony forming unit
CLOCK	Circadian Locomotor Output Cycles Kaput
CNS	Central Nervous System
COX	Cyclooxygenase
CRF	Corticotropin-releasing Factor
CRP	C-Reactive Protein
EAE	Experimental Autoimmune Encephalomyelitis
EBV	Epstein-Barr Virus
ENS	Enteric Nervous System
ESR	Erythrocyte Sedimentation Rate
FFAR2	Free fatty acid receptor 2
FM	Fibromyalgia
FMT	Faecal Microbiota Transplantation
GABA	Gamma-aminobutyric acid
GALT	Gastro-intestinal associated lymphoid tissue
GB	Guillain Barre

GC/LC-MS	Gas Chromatography/Liquid Chromatography-Mass Spectrometry
GF	Germ Free
GI	Gastrointestinal
GR	Glucocorticoid receptor
HADS	Hospital Anxiety Depression Scale
HHC	House-Hold Control
HPA	Hypothalamus Pituitary Adrenal axis
HT	High-Throughput
IBD	Inflammatory Bowel Disease
IBS	Irritable Bowel Syndrome
ICC	International Consensus Criteria
ICD	International Case Definition
IFNγ	Interferon-gamma
IgA	Immunoglobulin A
IgG	Immunoglobulin G
IgM	Immunoglobulin M
IL	Interleukin
ILCs	Innate Lymphoid Cells
IM	Infectious Mononucleosis
IOM	Institute of Medicine
IP	Intestinal Permeability
KO	Knock-Out
LEfSE	Linear Discriminant analysis Effect SIze
LPB	Lipopolysaccharide-binding protein
LPS	Lipopolysaccharide
M	Mild/moderate ME
Mϕ	Macrophage
MBP	Myelin basic protein
MDD	Major Depressive Disorder
ME	Myalgic Encephalomyelitis
MHFD	Maternal High Fat Diet
MHFD	Maternal High Fat Diet
MIA	Maternal Immune Activation
MOG	Myelin oligodendrocyte glycoprotein
MS	Multiple Sclerosis
MyoD88	Myeloid differentiation primary response 88
NGS	Next Generation Sequencing
NHL	Non-Hodgkin's Lymphoma
NICE	National Institute for Health and Care Excellence
NMDA	N-methyl-D-aspartate (NMDA)
NMO	Neuromyelitis Optica
NPY	Neuropeptide Y
OTU	Operational Taxonomic Unit
oxLDL	Oxidized Low-Density Lipoprotein
PAMP	Pathogen Associated Molecular Pattern
PCoA	Principle Coordinate Analysis
PCR	Polymerase chain reaction
PD	Parkinson's Disease

PEM	Post-Exertional Malaise
PGE2	Prostaglandin E2
PGN	Peptidoglycan
POTS	Postural Orthostatic Tachycardia Syndrome
PP	Peyer's Patches
PPR	Pattern Recognition Receptor
PVFS	Post-Viral Fatigue Syndrome
PVN	Paraventricular Nucleus
RA	Relative Abundance
ReA	Reactive Arthritis
RhA	Rheumatoid Arthritis
ROS	Reactive Oxygen Species
RR	Relapsing-Remitting
S	Severe ME
sCD14	Soluble Cluster Differentiation 14
SCFA	Short Chain Fatty Acids
SD	Standard Deviation
SEID	Systemic Exertional Intolerance Disorder
SF-36	Short-form 36 item questionnaire
SFB	Segmented Filamentous Bacteria
SLE	Systemic Lupus Erythematosus
SPF	Specific-pathogen free
TDA	Topological Data Analysis
TFT	Thyroid Function Test
TGR5	Takeda G-protein receptor 5
Th1/Th2	T-helper 1/T-helper 2
TJ	Tight Junction
TLR	Toll-like Receptor
TNFα	Tumour Necrosis Factor Alpha
UPGMA	Unweighted Pair Group Method with Arithmetic Mean
V4-V5	Hypervariable regions of 16S ribosomal RNA
WGS	Whole Genome Sequencing

Acknowledgements

I would to thank Richard & Pia Simpson and all at Invest in ME Research UK for funding my studentship to allow me to complete this work. As the first Ph.D. student to undertake ME/CFS research in Norwich, this was an ambitious and daunting project right from the beginning. There have been many times over the years where I (and others) did not think I would succeed. It gives me great pleasure and satisfaction that persistence and refusal to give up has finally made this achievement possible. For the most, I must thank my supervisors, Prof. Simon Carding, Prof. Tom Wileman, Dr. Amolak Bansal; and especially Dr. Melissa Lawson for your reassurance and intervention at a critical moment which saved me from giving into tough criticism – I will always be grateful to you for this.

To Dr. Linda Harvey and Dr. Mark Wilkinson; thank you both for helping me along the difficult journey towards getting research ethics approval and access to the Norwich Biorepository. To the staff and ME/CFS patients at Epsom & St. Helier NHS hospital; thank you for your interest and support of this work. In particular, Mrs. Jackie Cunningham for promoting the research within the immunology department, and to Dr. Rhea Bansal for assisting in blood sample collection during some of the home visits.

Special thanks must go to Dr. Alister Noble; you provided with the first glimmer of hope that I may be able to achieve some sort of result during this project. I appreciate your kindness and help you gave me to generate the data in the final chapter of this thesis. Dr. Lesley Hoyles, your expertise and time you have invested in helping me analyse this first attempt to characterise the metagenome of severe, house-bound ME/CFS patients is greatly appreciated.

In Chapter 4, I was drawn to explore the metabolome in our severe, house-bound patients. To that end, I am grateful to Dr. Ian Colquhoun and Mr Mark Philo for their expertise in ^{1}H-NMR and LC/MS respectively. Without your involvement in this project I wouldn't have the data to produce a publication based on this thesis project – thank you.

Over the years I have had several medical students interested in ME/CFS research who have followed me around and kept me company in the laboratory and during long

journeys to London to visit patients and the clinic. Therefore, my future healthcare should be no cause for concern. It has made the experience a whole lot more enjoyable; Dr. Verity (Veritas) Griffiths, Dr. Vinitha Soundararajan, Dr. Navena Navaneetharaja and Dr. Bharat Harbham - I congratulate you all as you embark on your medical careers. Verity; credit to you for coining the word “Viponderings” to describe the times I would prattle on incoherently about random thoughts I had about science, ME/CFS and Lana Del Rey.

Finally, my thanks and best wishes to my colleagues and now friends, Katharine Seton, Fiona Newberry and Shen-Yuan (Ernie) Hsieh. It is you who will be next in line to succeed in getting your Ph.D. My advice to you all is, don’t let others get you done – you’ve got this.

To my nan, the first female mortuary technician in the U.K., you inspired my interest and desire to pursue biomedical research - this is for all the times you would drive an hour there and back to pick me up from school.

Lastly, to the behind-the-scenes sponsors of this project, mum and dad, I hope you agree that this has been worth it. I owe you both so much.

For mum & dad

Chapter One

1 Introduction

1.0 Background to ME

Myalgic Encephalomyelitis (ME) has been classified by the World Health Organisation (WHO) since 1969 as a disease of nervous system (ICD-10; G93.3) and until recently included Chronic Fatigue Syndrome (CFS) under the same classification code. This enigmatic and ill-defined condition primarily affects young to middle aged adults, more often women, and is usually of sudden onset in apparently healthy and otherwise active individuals. Typically, ME/CFS is preceded by a 'flu-like' illness or viral infection associated with immunological abnormalities culminating in highly disabling physical and mental fatigue. The name ME implies a recognised (neuro-)pathology consisting of muscle pain (myalgia) and inflammation in the brain (encephalomyelitis), that so far the has not be established consistently within all patients (Blomberg et al., 2018). The use of ME is preferred by many patients who argue CFS reduces the seriousness and presents the illness in the context of a psychosomatic disorder (Dickson et al., 2007; Looper & Kirmayer, 2004). However, clinical examination and routine blood tests provide no obvious explanation for this pathological fatigue and variety of other symptoms including: cognitive dysfunction, muscle pain, exhaustion after minimal physical or mental exertion, orthostatic intolerance (Bansal, 2016; Haney et al., 2015). This list is not extensive, and symptoms vary in frequency and severity from patient to patient. Many illnesses can be represented by some or all of these symptoms and therefore must be ruled out before ME/CFS can be diagnosed.

Evidence is gathering to support a hypothesis of an infectious trigger causing long-lasting fatigue and immunological and gastrointestinal symptoms that could give rise to wider multi-systemic dysfunction involving signalling between intestinal microbes and the central, autonomic and enteric nervous systems, in addition to signalling between the (neuro-)immune and neuroendocrine systems and the brain. Other syndromes closely associated with ME include fibromyalgia (FM) and irritable bowel syndrome (IBS) which may represent a discrete subsets of ME patients.

- *Prevalence*

It is unclear how many people suffer with ME/CFS worldwide. A recent indication from the Institute of Medicine (IOM) suggests between 836,000 and 2.5 million Americans have ME/CFS (Reynolds et al., 2004). In the UK between 0.23-1.29% of the population are affected (Science Media Factsheet, 2018). The only prescribed treatment to these patients

consists of psychological-led interventions such as Cognitive Behaviour Therapy (CBT) for management of anxiety and depressive-like symptoms that manifest as a result of being chronically ill.

- *Early reports*

An illness that appears synonymous with characteristics of ME/CFS first described in 1869 became known as neurasthenia (Van Deusen, 1869). Symptoms included fatigue, headaches, dizziness, weakness, and emotional disturbances (Beard, 1869). It was originally associated as a result of physical isolation of farmer's wives who were socially inactive, but was also attributed to stress and a busy lifestyle (Beard, 1869; Van Deusen, 1869). To that end it was viewed as a psychogenic, rather than organic illness which altered the behaviour of the individual. From 1938 up until 1955 several apparent outbreaks of an illness with similar symptoms to poliomyelitis were described. These followed patterns of discrete clusters firstly, in Los Angeles in 1938 where the disease was called "atypical poliomyelitis" with symptoms of muscle weakness and severe pain aggravated by exercise (Gilliam, 1938). In Switzerland, in 1939, 73 soldiers developed low grade fever, with autonomic disturbances, fatigability and loss of concentration that was labelled epidemic neuromyasthenia. What appeared to a case of poliomyelitis in 1948 developed into another outbreak, involving 488 cases in rural areas around Akureyri, Iceland leaving patients severely paralysed particularly within the 15-19 age group, and occurred in 49% of pupils resident at a high school within Akureyri. Seventy percent of these patients had characteristic low grade fever, muscle tenderness, whilst 30% had muscle weakness with pyrexia (Parish, 1978). Other areas of outbreaks of a "polio-like" illness include Denmark, South Africa and Australia (Patarca-Montero, 2004).

1.1 Controversy of ME

ME/CFS controversy is driven by the lack of a defined pathophysiology with routine clinical and physical examination, including blood biochemistry revealing no obvious medical abnormalities as a specific cause. Over the decades separate definitions have been generated for ME and CFS with patients who do not meet either criteria diagnosed with idiopathic chronic fatigue which is classified as mental and behavioural disorders (ICD F48.0). An apparent outbreak of this disease was reported in 1955 describing patients suffering from malaise, tender lymph node, sore throat, pain and appeared to be infectious with signs of encephalomyelitis from limb spasms (Staff, 1957). Despite the appearance of

an epidemic of viral encephalomyelitis, the cause was never established and a lack of physical symptoms in these patients convinced many doctors that they were not physically ill, labelling it as 'benign myalgic encephalomyelitis' since no one died as a result the illness (IOM, 2015). This along with other reported outbreaks were explained by psychiatrists as a "psychosocial phenomena caused by one of two mechanisms; either mass hysteria on the part of the patients or altered medical perception of the community" and the fact most patients were female fitted with the hypothesis of epidemic hysteria considered characteristic among females (McEvedy & Beard, 1970; IOM, 2015).

Over 200 cases of this chronic illness were documented by Dr Melvin Ramsay, a physician at the Royal Free hospital, who later published the first criteria for ME to refute its proposed psychological aetiology based on apparent involvement of the central nervous system (Staff, 1957). Interestingly some sporadic cases were reported at the time have following a viral infection and had been diagnosed as post viral fatigue syndrome (PVFS) (Lewis Price, 1961; Speight, 2013). Similar epidemics had previously occurred in 1934 and 1947 in Los Angeles and Nevada, respectively (Speight, 2013). These outbreaks have been documented in the literature as poliomyelitis and were indistinguishable from Ramsay's patients, with a similar neuromuscular condition.

- *Psychiatry and ME*

Psychiatry has dominated the media and public interpretation of ME/CFS and has had unfortunate consequences for the treatment of patients. Patients can easily be accused of malingering or being ill in the mind. Many doctors and nurses formulate their own opinion based on various psychiatric explanations labelling the condition as a disease of the mind and is largely down to the fact very little or no training is given on how to manage these patients. Therefore, patients are easily stereotyped as neurotic or attention seeking. Other suggested causes include the stress of modern day living and 'middle class' disease (Speight, 2013). In the past it is fair to say the media has marginalised campaigns for biomedical research and excluded their voices in favour of the psychosomatic argument (Blease & Geraghty, 2018). This has created a significant amount of frustration for patients who are desperate for answers to this debilitating and life-threatening illness. This is not unusual throughout medical history which tends to favour a psychological explanation when there is no convincing somatic origin. Asthma was once considered one of the 'holy seven' psychosomatic illness during the 1930-50s with talking therapy as an alleged cure

(Opolski & Wilson, 2005). Indeed, psychiatric conditions such as depression do have a negative effect on symptoms in somatic illnesses, like asthma, with a reduction in quality of life, that are not aetiologically relevant to its pathogenesis (Opolski & Wilson, 2005).

1.2 The challenge for ME/CFS Research

The foundations of ME/CFS research rely on the description of self-reported symptoms and clinical expertise when assessing the patient before making a diagnosis of ME/CFS. The application of reliable and highly specific criteria would be a significant breakthrough for research and in primary care. Indeed, the psychological concept for this condition is still a problem in front line care with 20% of staff believing CFS is all in the patient's head. International agreement on how we study the ME/CFS population is not forthcoming and is still frequently discussed until the medical and research communities agree on how this heterogenous group of patients be further stratified according to specific symptoms and severity other than subjective categories of: mild, moderate, severe and very severe. How these categories are defined is still a matter of clinical opinion and varies significantly from country to country. Further confusion is generated by the various names that have been introduced to describe unexplained and persistent fatigue. ME and CFS remain the most frequently used, however others including post-viral fatigue or post-infectious fatigue syndrome are named so after the apparent infectious event triggering long-term symptoms. There is symptom overlap with these illnesses makes it unclear if these are separate conditions or all the same (Twisk, 2014).

1.3 Diagnosing ME/CFS

The diagnosis of ME/CFS relies entirely on the exclusion of medical or psychiatric conditions associated with fatigue or any other symptoms presenting in the patient (Bansal, 2016). As a minimum criteria, fatigue must persist beyond four months according to current NICE guidelines. Fatigue is a universal symptom making it difficult to distinguish patients who each present their own set of unique symptoms. An added complication for accurate diagnosis is that many of the symptoms are not disease specific and encompass marked variability in severity and a daily and even hourly basis (Bansal et al., 2011). It is perhaps more helpful to view ME/CFS as an umbrella term for a number of conditions defined by chronic persistent fatigue that cannot currently unexplained, that may have discrete pathogenic aetiologies.

- *Assessing fatigue*

Fatigue effects an individual's ability to function physically and mentally. However, the concept that fatigue can manifest as illness without a pathological explanation called idiopathic fatigue, suggests a psychogenic cause since very little is known about the physiological mechanisms for the sensation of fatigue. Indeed, this makes fatigue difficult to assess with no objective physiological marker. Ultimately, it relies upon highly subjective measures and assessments including patient interviews and completing questionnaires regarding their perception of fatigue and how it impacts their daily functioning. Self-reported scales of fatigue such as the Chalder Fatigue Scale (Chalder et al., 1993) and measures of the impact fatigue has on a patients' function such as the Short-Form 36 item questionnaire (SF-36) have been used extensively in ME/CFS research (Jason et al., 2009).

The "envelope theory" proposed in 1999 suggests patients pace themselves according to the perceived amount of total energy they have available (Jason et al., 2012). To this end, crashes or worsening of symptoms can be avoided my limiting energy expenditure within this 'envelope'. Patients kept an activity record to provide a self-assessment report on feelings of fatigue, pain, type and intensity of activity and enjoyment every 30 min to build a comprehensive picture how CFS impacted their daily functioning. Using this method, CFS patients were found to experience fatigue more of the time and to spend 2.5 times more resting than those with major depressive disorder and 4 times longer than the healthy control group after low intensity activity (Hawk et al., 2007; Jason et al., 2012).

However, a review of 39 measures of fatigue has highlighted that no single method encompasses the full nature of fatigue in ME/CFS (Whitehead, 2009). Researchers are challenged as to how to use this subjective information to identify potential underlying physiological aetiologies. However, there are some aspects of the type and severity of fatigue experienced in the ME/CFS population that would not be perceived as normal part of experiencing fatigue that appear to separate these patients from other fatigue-related illnesses (Bansal, 2016). This is the most significant and characteristic symptom of ME, described as a delayed reaction to minimal physical or mental exertion, referred to as post-exertional malaise (PEM).

- *alternative sickness behaviour*

The similarities between ME/CFS and sickness behaviour have been extensively reviewed (Morris et al., 2013). The behaviour responses to infection have been modelled in mice challenged with Lipopolysaccharide (LPS) derived from Gram-negative bacteria, which have shown systemic inflammation can lead to neuroinflammation and sickness behaviour (Biesmans et al., 2013). Behavioural disturbances seen in LPS-treated animals cause depressive-like symptoms and withdrawal from social interaction and the environment. Many ME/CFS patients present with symptoms of "infection" that may drive proinflammatory cytokines IL-1β, IL-6, and TNFα able to trigger vagal nerve stimulation (the nerve from the gut to the brain) or activate brain microglial cell to produce proinflammatory cytokines locally (Hoogland et al., 2015). In humans, an extreme example of sickness behaviour may manifest as delirium, a common and severe neuropsychiatric syndrome, delirium causes confusion, agitation and attentional deficits (MacLullich et al., 2009; Pandharipande et al., 2013). Delirium is associated with aging, a period defined by a declining in the microbiota and therefore insults on the intestinal microbiota may alter brain function causing neuroinflammation and alter a person's behaviour or response to physical, mental stress or infection (Di Sabatino et al., 2018; Vaiserman et al., 2017).

The overriding issue with ME/CFS research is that patient selection still remains highly ambiguous with interchangeable use of ME and CFS and case definitions. In a systematic review evaluating the application of case definitions, the authors highlighted the existence of over 20 sets of case definitions with significant overlap (Brurberg et al., 2014). As a result healthcare providers do not feel confident in about ME/CFS (Bowen et al., 2005; Brimmer et al., 2010). The lack of specificity and accuracy in the diagnosis of ME/CFS is evident in the fact that CFS-like fatigue has been reported in 30.5% of 9050 randomly selected adults in the Netherlands using the Center for Disease Control (CDC) criteria by questionnaire, commonly referred to as Fukuda criteria (Fukuda et al., 1994; Van'T Leven et al., 2010). Moreover, this application of broader case definitions has led to a lack of reproducibility in ME/CFS research further fuelling the perception that this illness is psychogenic. A recent critical review has argued that there is 'no convincing pathogenesis model for CFS' (Mm & Ssung, 2017).

- *Case definitions*

In the absence of a definitive diagnostic clinical test, guidance is set out in a series of case definitions used to described symptoms of ME/CFS to the detriment of having a homogenous patient population with varying degrees of overlapping symptoms, figure 1.1.1. This has many limitations such as selection criteria biases and methodologies to assess patients and will be influenced by researchers' own preconceptions of disease aetiology (Morris & Maes, 2013b). Application of case definitions in an apparently multisystem disorder such as ME/CFS can require multiple medical specialities to assess each symptom meets any threshold requirements, e.g. frequency and duration. This can generate difficultly comparing studies using different definitions and criteria to score fatigue and severity. Moreover, many symptoms included in the following case definitions risk including groups of patients that do not suffer from the same disease, with more general criteria including a group of patients in some cases with very little symptom overlap (IOM, 2015).

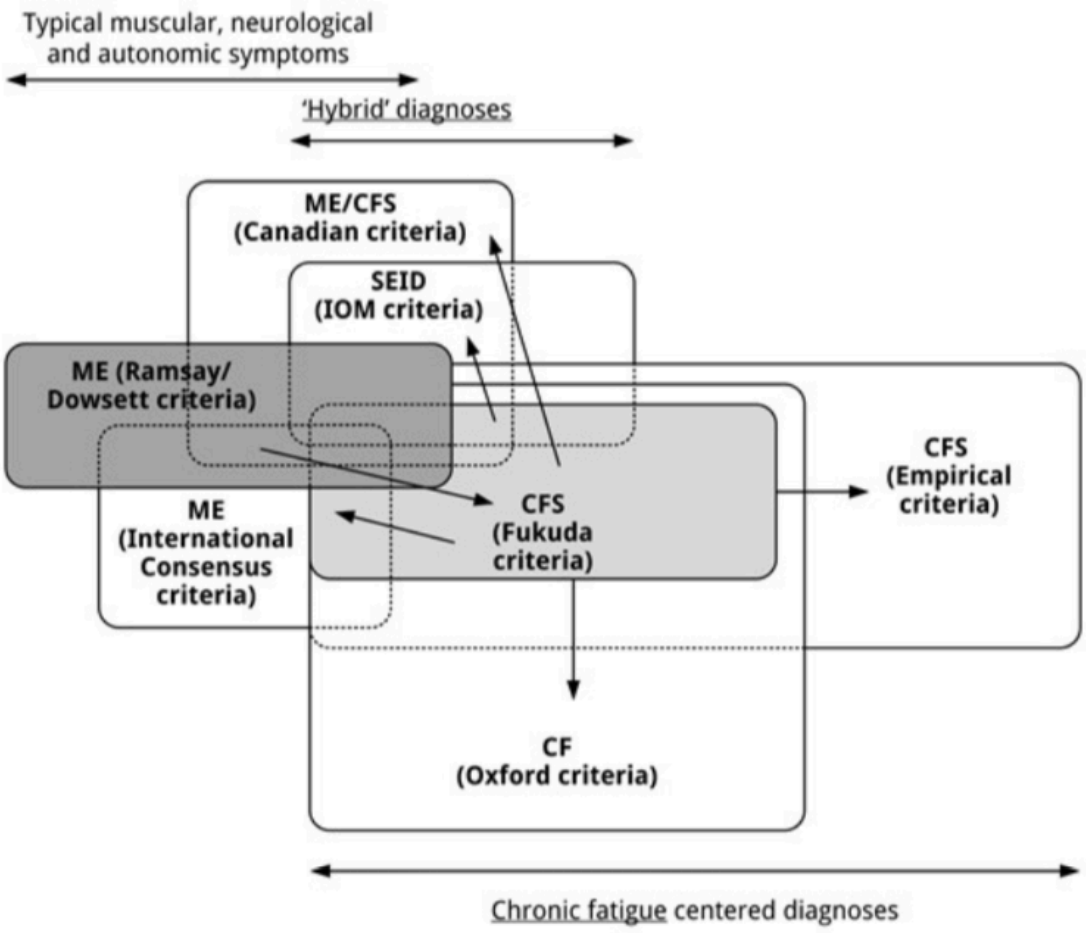

⇐**Figure 1.1.1 Overlapping case definitions can result in patients being diagnosed with ME/CFS with very little symptoms shared between cases.** Fukuda criteria sets out symptoms required for diagnosing CFS and it the most widely used case definition. The larger the area within circle of each case definition reflects the more encompassing rather than specific it is for defining patients with broad number of symptoms, in addition to mandatory chronic persistent fatigue. Figure from (Twisk, 2017).

- *Ramsay (1986)*

The acceptance of ME as a neurological condition by the WHO was attributed to the work of Dr Melvin Ramsay, a clinician at the Royal Free at the time of the 1955 outbreak, who proposed ME was a polio-like, neuromuscular disease and refuted any argument for it being psychogenic based on opinion of psychiatrists reviewing patients notes. The original criteria proposed by Ramsay generally considered most accurate and specific to the nature of ME symptoms including muscle weakness/tenderness, and pain after only minor exertion lasting for days, concentration and memory impairment, sleep disturbance, cold extremities, hypersensitivity and orthostatic tachycardia. Ramsay also documented the fluctuating nature of many of the symptoms and the dramatic effect of exercise upon muscle function which are not observed in IM or 'glandular fever' cases (Ramsay, 1986). Here, ME was described as distinctive from poliomyelitis as it did not cause paralysis or resulted in death and was termed 'benign Myalgic encephalomyelitis'.

- *Holmes (1988)*

In 1988 the Centres for Disease Control (CDC) introduced the name CFS and provided the first definition. Holmes et al. (1988) produced this criteria to standardise the population and distinguish CFS from potentially viral infection aetiologies that had be associated with outbreaks of EBV infection (Holmes et al., 1988)(Holmes et al., 1987). CFS was described as persistent or relapsing fatigue for at least 6 months severe enough to impair the persons daily activities below 50% of previous capacity before becoming ill. It also stated that 8 or more other symptoms from a list of 11, including 'neuropsychologic complaints' had to be present. This led to the inclusion of patients with psychiatric problems such as depression base on generalised overlapping symptoms (Friedberg & Jason, 1998).

- *Oxford (Chronic Fatigue)*

This criteria was established in the 1990s that has been criticised since it only requires severe and disabling fatigue and no longer used for its lack of specificity for diagnosis of CFS, or any neuro-muscular symptoms of ME described by Ramsay in 1987.

- *Fukuda (1994) (Chronic Fatigue Syndrome)*

In 1994 the CDC introduced a new definition commonly referred as the Fukuda criteria after its primary author. Similar to the Holmes criteria, the criteria Fukuda criteria does not provide guidance on interpreting these symptoms and has been criticised for being too broad and encompassing of all cases (Reeves et al., 2003). This sets out the requirement for moderate or severe fatigue lasting at least 6 months in addition to four or more of eight symptoms: post-exertional malaise, unrefreshing sleep, impairment in memory or concentration, headaches, muscle pain, joint pain, sore throat, or tender lymph nodes (Fukuda et al., 1994). None of these symptoms are characteristics of ME are mandatory in the Fukuda definition of CFS; but also, are rather unspecific and potential inclusive of other medical and psychiatric disorders.

It is still the most widely used case definition that has largely been adopted in clinical practice (Brurberg et al., 2014). However, this criteria is frequently judged too vague and polythetic, essentially highlighting a group of patients with chronic fatigue as the predominant factor in their illness. Not all CFS patients will have post-exertional malaise and memory/concentration impairment as these are not strictly required to satisfy Fukuda criteria. The review of the original ME criteria established by Ramsay (1987) suggest a distinct disease that is more than persistent chronic fatigue, with particular emphasis on neuro-immunological exhaustion (Dowsett et al., 1990). In the patients from the Royal Free outbreak, muscular pain, autonomic symptoms and malaise following any form of physical or mental exertion where triggered after a flu-like illness are the hallmarks of ME which Fukuda does not require but help differentiate true cases of ME from ones with general chronic fatigue.

Patients with major depression may also be misdiagnosed with CFS (Jason et al., 1999). It is also possible for patients which very little symptom overlap to be diagnosed with CFS, with the only primary feature of unexplained fatigue being shared with Ramsay's criteria for ME. Further heterogeneity is introduced when some CFS patient fit the criteria for ME and vice

versa. ME and CFS are used interchangeable or combined as ME/CFS, given many patients satisfy various diagnostic criteria for both. However, there is little understanding about the pathophysiology of ME and how it is separate from CFS, although the delayed exhaustion to minimal physical or mental exertion is considered unique to ME.

- *Canadian Consensus Criteria (2003) for ME/CFS*

The 1955 definition of ME involves post-exertional malaise and impairment of memory and concentration as distinguishing features that are not absolutely required by Fukuda (Dowsett et al., 1990). Thus, the shortcomings of the Fukuda criteria lacking overall specificity for ME, led to the introduction of the Canadian Consensus criteria which had more emphasis on ME-like symptoms requiring two or more neurological/cognitive symptoms and at least one symptom of autonomic, neuroendocrine and immunological dysfunction, as well as post-exertional malaise (PEM) which often causes a delayed exacerbation of all symptoms. The inclusion of more core symptoms identifies patients overlapping with the Ramsay criteria, but also because of the increased number of possible symptoms, like the Holmes criteria, introduces higher rates of psychiatric co-morbidity (Katon & Russo, 1992; Williams, 2014).

The early 2003 criteria required several other symptoms (see figure 1.1.3) in addition to two core symptoms referred in the previous paragraph (Jason et al., 2010). Up to 75% of CFS cases identified with Fukuda also satisfy the Canadian (2003) criteria for ME/CFS (Jason et al., 2013a; Nacul et al., 2011; Jason et al., 2012a.) To address this problem, the updated Canadian Consensus Criteria (2010) introduced structured questionnaires (DePaul Symptoms Questionnaire; SF-36) to gather standardised information in addition to operational definitions for assessing symptoms that must be present within 6 categories (see figure 1.1.3) and must be of moderate severity for at 50% of the time as well as scoring sufficiently low on the SF-36 for substantial reduction in functioning Jason et al., 2014; Jason et al., 2010; IOM, 2015). This is viewed as a stricter definition than Fukuda with a focus on more severe patients since it does require PEM and memory/concentration impairment and indication of minimum frequencies and severity of symptoms. Fewer patients met this revised definition compared with using the 2003 version and with Fukuda. To this end, the revised Canadian Consensus Criteria perhaps represents severe group of CFS patients with significantly more frequent psychiatric co-morbidity. By contrast, the

original 2003 Canadian Consensus highlighted patients with less psychiatric co-morbidity than Fukuda (Services et al., 2015).

- *ME International Consensus Criteria (ICC)*

The International Consensus Criteria (ICC) for the diagnosis of ME essentially evolved from the Canadian Census Criteria for ME/CFS. Introduced by Carruthers et al. in 2011 it recommended a distinction of ME based on recent research of "widespread inflammation and multisystem neuropathology" (Carruthers et al., 2011). Delayed exhaustion following minimal physical or mental exertion (PEM), termed post-exertional neuroimmune exhaustion by the authors, is an absolute requirement. In addition, neurocognitive impairments, pain, sleep disturbance, neurosensory, perceptual or motor disturbances must be present. Importantly, at least one symptom has to be present from 3 of 5 immune, gastro-intestinal and genitourinary categories – including flu-like symptoms, recurrent viral/bacterial infections, GI discomfort and sensitivities to food, medicines, odours, chemical sensitivities had to be present. Finally, at least one symptom associated with energy production/transportation impairments including cardiovascular/respiratory symptoms, intolerance to extremes of temperature also needs to be present (Twisk, 2017; IOM, 2015).

- *Systemic Exertional Intolerance Disorder (SEIDS)*

An extensive review was conducted by the Institute of Medicine, USA in 2015 of the published studies of ME/CFS and the implementation of case definitions and subsequent diagnosis made from these (IOM, 2015). As a result, the report introduced SEIDS to replace ME/CFS. To qualify for diagnosis of SEIDS, fatigue, PEM and non-refreshing sleep, cognitive deficits and orthostatic intolerance are absolute requirements. Although the application of this criteria is straightforward and simpler (see diagnostic algorithm, figure 1.1.2) than other case definitions, it can still miss symptoms attributed to neuro-immune, neuromuscular and neuroendocrine dysfunction that are the hallmarks of Ramsay's original ME criteria meaning this definition could essentially still include cases with little symptom overlap.

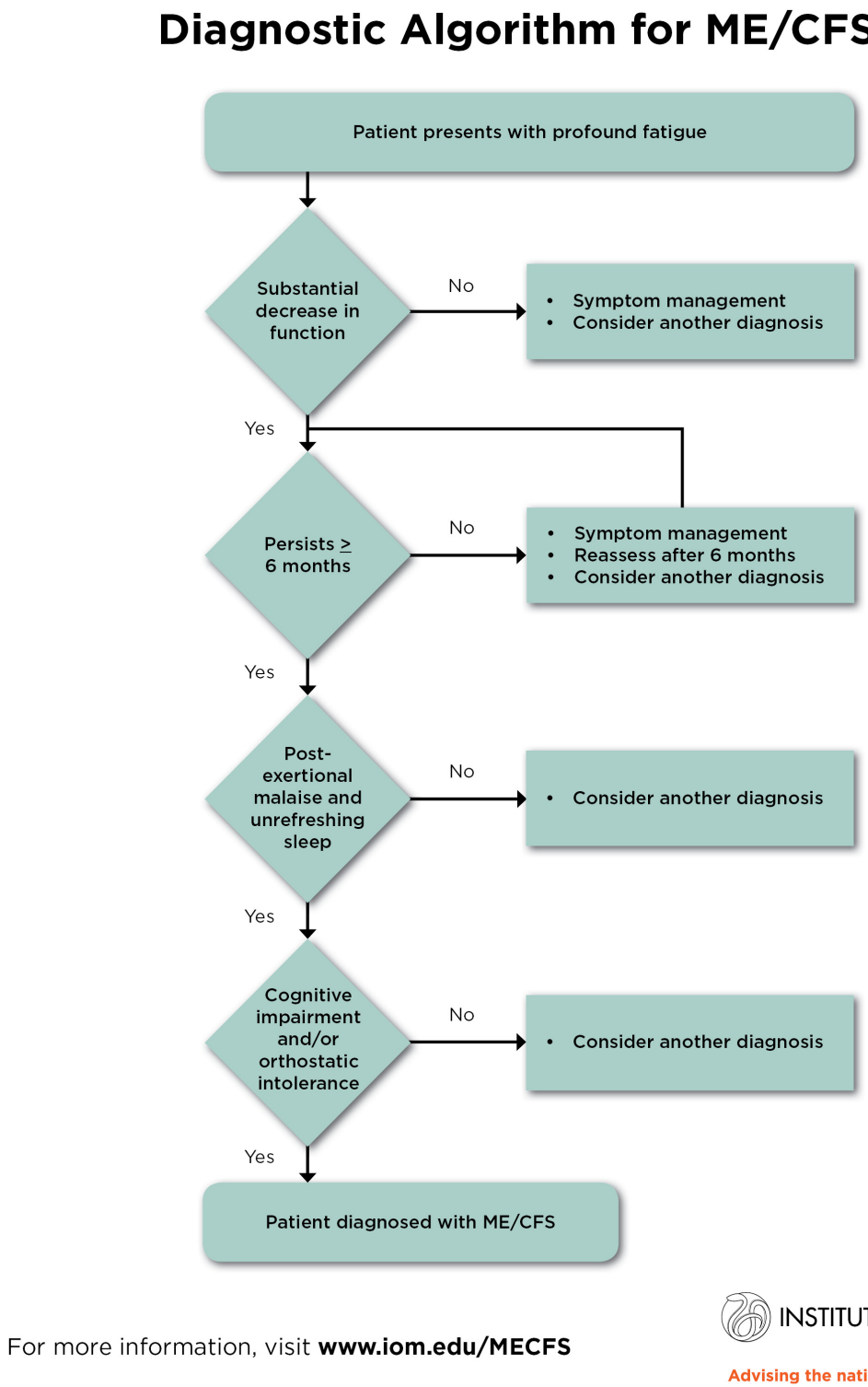

Figure 1.1.2 Pathway to the diagnosis of Systemic Exertional Intolerance Disorder (SEID) produced by the Institute of Medicine, USA in 2015.

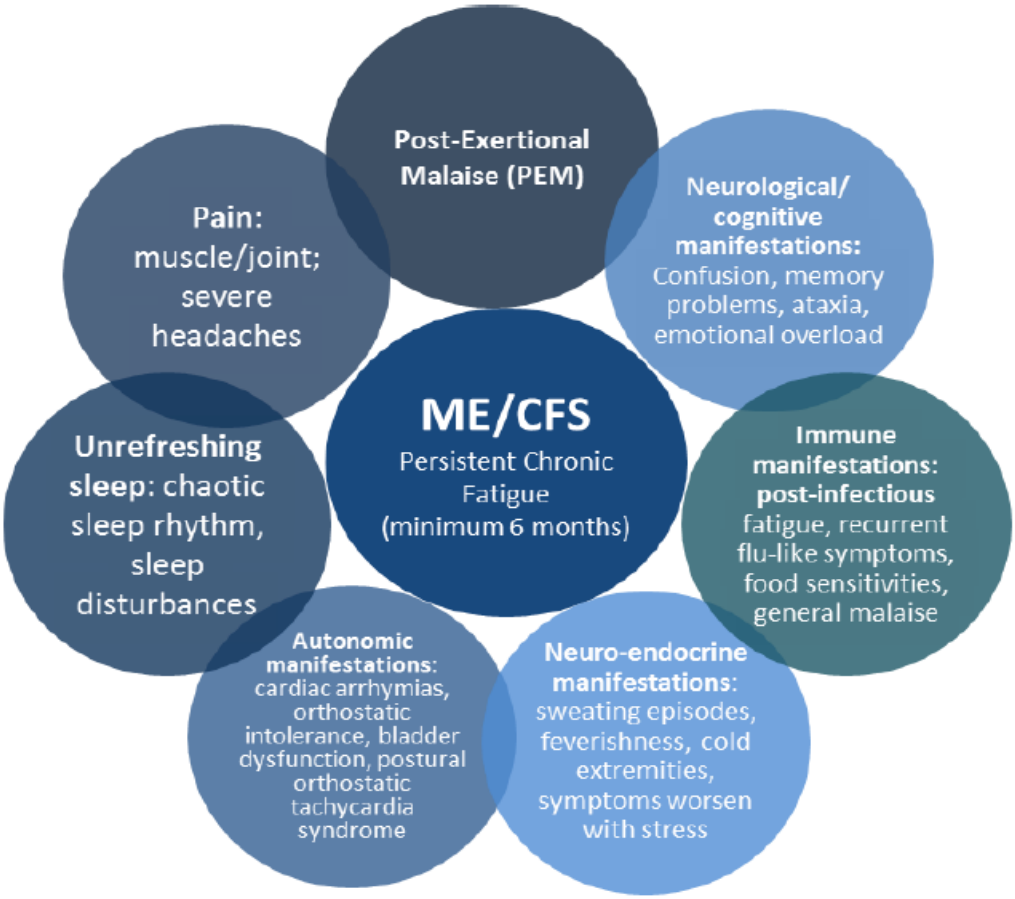

Figure 1.1.3 Common symptoms of ME/CFS shared across various case definitions Figure adapted from (Online, 2018) assessed 29th September 2018, with additional information included from (Jason et al., 2010).

- *Symptoms*

The case definitions for ME/CFS (CCC), and ME (ICC), and the IOM replacement of ME/CFS with SEID are not entirely satisfactory criteria since they still include patients with other medical and psychological illness that are not defined by neuro-muscular features, delayed muscle fatigability with an apparent prodromal phase that precedes a very serious chronic illness. The list of symptoms and references below are taken from the 2015 IOM report, and provide an overview of all the different symptoms that stand out across multiple studies implementing CFS, ME/CFS and ME criteria, these include: persistent fatigue and unrefreshing sleep, orthostatic intolerance, widespread pain (myalgia), cognitive dysfunction, and immune dysregulation, along with secondary anxiety and depression, contribute to the burden imposed by fatigue in this illness:

- Neurocognitive symptoms defined as slowness of thought; mental fog; and problems with concentrating, memory, or understanding (Arroll and Senior, 2009; Hickie et al., 2009; Jason and Taylor, 2002; Ray et al., 1992).

- Musculoskeletal factors: muscle or joint aches and pains and weakness (Brimacombe et al., 2002; Hickie et al., 2009; Nisenbaum et al., 2004; Tseng and Natelson, 2004);

- Infectious symptoms: a "viral flu-like" factor that includes such complaints as fever, sore throat, and tender lymph nodes (Brimacombe et al., 2002; Nisenbaum et al., 1998, 2004; Tseng and Natelson, 2004);

- Psychological emotional distress or mood or anxiety disturbance factor (Arroll and Senior, 2009; Fostel et al., 2006; Hickie et al., 2009; Ray et al., 1992);

Other common symptoms of the autonomic nervous system include GI disturbances, such as constipation, diarrhoea, nausea, increased bowel sounds, mild bloating and abdominal tenderness are reported by majority (92%) of patients. It is typical for symptoms of IBS to precede onset of ME/CFS that become closely associated with worsening of fatigue, mood, malaise, and severity of muscular and joint pain.

- *Post-exertional malaise (PEM)*

The CCC and ICC emphasise post-exertional malaise (PEM) to help clinicians rule out cases of idiopathic fatigue. It however can still be viewed as a symptom of ME/CFS rather than exclusively belonging to ME, based on its requirement in the Canadian criteria. PEM generally causes a global worsening of all ME/CFS symptoms for which the trigger can be patient specific and can take different periods for recovery. PEM can be described as a "crash", "relapse" or "collapse" of varying degrees of duration, severity, impairment, and symptoms that are exacerbated by minimal physical or mental activity (IOM, 2015). Objectively testing the extent of a patients' PEM by inducing a stressor or forcing the patient exercise is considered unethical given the disabling effects and pain that can last up to days. Therefore, self-reported experiences of PEM and associated triggers are frequently recorded in questionnaires of the patient's previous experience. How these questions are asked and their wording can influence how the patient responds (Leonard et al., 2015).

PEM is considered a unique symptom of ME/CFS that distinguishes it from cases of idiopathic chronic fatigue, anxiety, depression and other psychiatric and/or fatiguing disorders fatigue-related illness, yet it is still largely an ill-defined and vague. It has been suggested, PEM be further described by the period of delay in its onset, and how long the period of the exacerbation of all ME/CFS symptoms last. For instance, PEM may be more immediate in some patients, as little as 3 hrs, or delayed up to 12-24 hrs after completion of a specific activity, and can endure longer than 24 hrs in severe cases (Bansal, 2016). Interestingly there is a subtle difference between PEM which entails a full-body sensation of malaise and post-exertional muscle weakness observed in Ramsay's ME patients. Indeed it has now been proposed the PEM be categorised according to its nature either as a general factor of exacerbating illness, or extreme muscle pain and weakness, both following from minimal physical or mental exertion (McManimen et al., 2016).

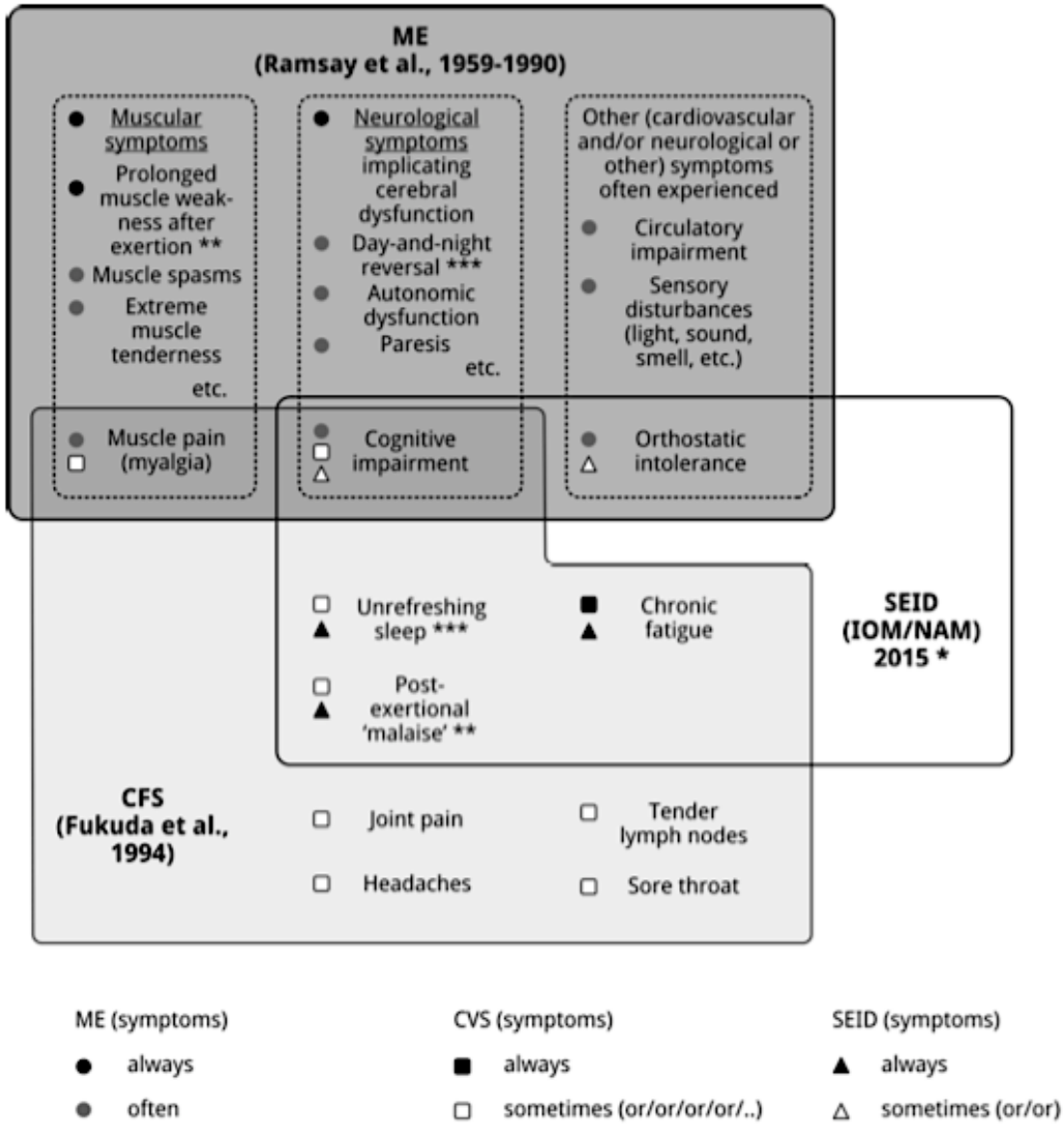

Figure. 1.1.4 The IOM definition of SEID sits between the Fukuda cases definition for CFS and Ramsay's proposed criteria for ME in 1988. SEID does not have require muscle pain (myalgia) with optional orthostatic intolerance. Figure from (F. Twisk, 2018)

- *Summary*

There is currently no clear agreed distinction between CFS and ME. The Fukuda criteria upon which the majority of clinical research has implemented to date, has perhaps hindered consistent findings because the patients it diagnoses includes various disease entities which share persistent fatigue; including Chronic Fatigue, Chronic Fatigue Syndrome and ME – see figure 1.1.1. The 2010 Canadian definition attempts to separate CFS by defining more symptoms of a neurological nature but is still has considerable overlap with the earlier CFS definition and therefore attracts a heterogeneous ME/CFS patient population with varying degrees of symptom overlap. The IOM criteria for SEID has been suggested to replace 'ME/CFS' and uses simpler criteria than CCC and ICC definitions which should be relatively straightforward to translate into the clinic.

The CDC introduction of the term CFS on the back of the Holmes criteria has led to the confusion of CFS and ME being the same disease (Twisk, 2018). All it has served is to identify a group of patients who share persistent fatigue and does not give insight to the seriousness and severity of the original cases highlighted by Dr Ramsay (Dowsett et al., 1990; FNM, 2017). The more recent Canadian and International ME criteria hybridise CFS/ME with emphasis on PEM and reduce the frequency of depressive disorders with this criteria more successfully selecting against those individuals in whom depression may be a significant factor in their chronic fatigue symptoms (Jason et al., 2012).

The most recent SEID definition attempts to bridge together Fukuda and Ramsay criteria but completely lack requirement for muscle-specific symptoms and will therefore likely continue to represent a heterogenous patient population that remain very distinct the condition of ME described by Ramsay and colleagues (Dowsett et al., 1990). Many symptoms used by Ramsay relating to neuro-muscular pathology, including: muscle weakness particularly after exertion, spasms, extreme tenderness, as well as neurological symptoms such as light and sound sensitivities are unique to ME, yet not defined specified or used as absolute requirement by other case definitions.

In 1990, the year of the death of Ramsay and therefore his last publication before his death, the criteria for ME is re-iterated: "a syndrome commonly initiated by respiratory and/or gastrointestinal infection, but an insidious or more dramatic onset following neurological, cardiac or endocrine disability occurs…features are general or local muscle

fatigue following minimal exertion with prolonged recover"(Dowsett et al., 1990). A table for this paper (reproduced as table 1.1.1) lists the symptoms and signs in 420 patients monitored during the Royal Free outbreak. Ramsay discusses the epidemiological evidence for ME being caused by "non-immune individuals of widespread subclinical non-polio enteroviruses (NPEV)" based on the neurological manifestations for which many NPEVs had been associated with. Out of the 420 cases, 205 (33%) of these had coxsakie B virus neutralisation tests that revealed an ongoing infection (Dowsett et al., 1990) . Of course, it cannot be said for certain these cases were a result of an enterovirus, but enteroviruses are well-known causes of acute respiratory and/or gastrointestinal infections and non-specific flu-like illness. Interestingly more recently enteroviruses have been suggested a common trigger, along with EBV, for causing ME/CFS in a subgroup of patients (Zhang et al., 2010). Indeed, many patients show ongoing signs of bacterial/viral infection that could explain their long-term sickness behaviour. These observations have led an infectious-neuro-immune hypothesis model which will now be introduced in the next section.

Table II Symptoms and signs in 420 patients with ME

Commonly found (>50%)	*No.*	*%*	*Less commonly found (<50%)*	*No.*	*%*
Muscle fatigue	420	100	Gastrointestinal symptoms****	205	49
Emotional lability†	411	98	Disturbance of micturition§	160	38
Myalgia††	336	80	Recurrent lymphadenopathy§§	152	36
Cognitive disturbance†††	323	77	Arthralgia	118	28
Headache	310	74	Orthostatic tachycardia	88	21
Giddiness, disequelibrium	302	72	Recurrent abacterial conjunctivitis	68	16
Autonomic dysfunction††††	289	69	Orchitis/prostatism in young males	15/113	13
Auditory disturbances*	289	69	Seronegative polyarthritis	42	10
Reversal of sleep rhythm	268	64	Vasculitic skin lesions	42	10
Visual disturbances**	260	62	Myo/pericarditis	34	8
Parasthaesia, hypo & hyperasthaesia	256	61	Positive Romberg sign	25	6
Intercostal myalgia/weakness	247	59	Thyroiditis in female patients	15/307	5
Fasciculation, spasm, myoclonus	239	57	Mesenteric adenitis§§§	5	1
Clumsiness***	235	56	Paresis and muscle wasting	3	1

†Includes frustration, elation, depression; ††characteristically affects limbs, shoulder girdle, spinal muscles; †††memory, concentration, anomia, dyslexia; ††††especially circulation and thermoregulation; *hyperacusis, deafness, tinnitus; **mainly loss of accomodation, photophobia, nystagmus; ***usually due to impaired spatial discrimination; ****nausea/disturbance of intestinal motility; §frequency incontinence, retention; §§enlargement, recurrent after prodrome; §§§surgical intervention for abdominal pain.

Table 1.1.1. Symptom repertoire of patients diagnosed with ME used Ramsay criteria in 1988. This list is presented as a summary of symptoms found in 420 patients at the Royal Free Outbreak in 1955, highlights muscle fatigue is the defining characteristic of ME with 49% of patients experiencing gastro-intestinal disturbances. Table reproduced from (Dowsett et al., 1990).

1.4 A proposed infection-neuro-immune disease mechanism in ME/CFS

ME/CFS is a complex multifaceted disease involving disruptions to the neurological, neuroendocrine and immune systems. An infectious aetiology can be appreciated from the early documented cases of a fatiguing neuro-muscular condition, that became known as ME. The polio-like nature and symptom onset suggest a systemic infection, possibly originating from the gut which influences immune-inflammatory events responsible for causing sickness behaviour and other symptoms prevalent among neuro-psychiatric conditions where the behaviour may be a result of persistent immune activation and chronic stress and anxiety surrounding not getting better. Persistent infections are known to increase intestinal permeability. This may then explain the self-perpetuating nature of ME, since increased exposure of intestinal immune cells to commensal bacterial antigens such as LPS across the intestinal bacteria can activate the immune system and proinflammatory cytokines that have been documented to cause sickness behaviours but also trigger autoimmunity. Moreover, increased permeability is already known to occur during periods of stress and is significantly influenced during early colonization of microbes along the GI tract. In an attempt to bring order to the sequences of events, this model proposes a step by step process leading to intestinal barrier leakiness as a result of persistent immune activation and disruption to centres of the brain regulating the physiological response to systemic infections.

The following sections of this chapter, present various aspects of this model and explore it in the context of the current observations in ME/CFS, but also wider studies mainly performed in animals attempting to unravel crossover interactions with the immune system, neuroendocrine system and signalling with the brain via the hypothalamus-pituitary-adrenal (HPA) axis. This pathway has been most studied in animal models of infection where in becomes activated leading to distinct physiological changes. Moreover, evidence is emerging of the gut microbiome providing physiological input to the regulation of the immune system and HPA axis during stress test situations.

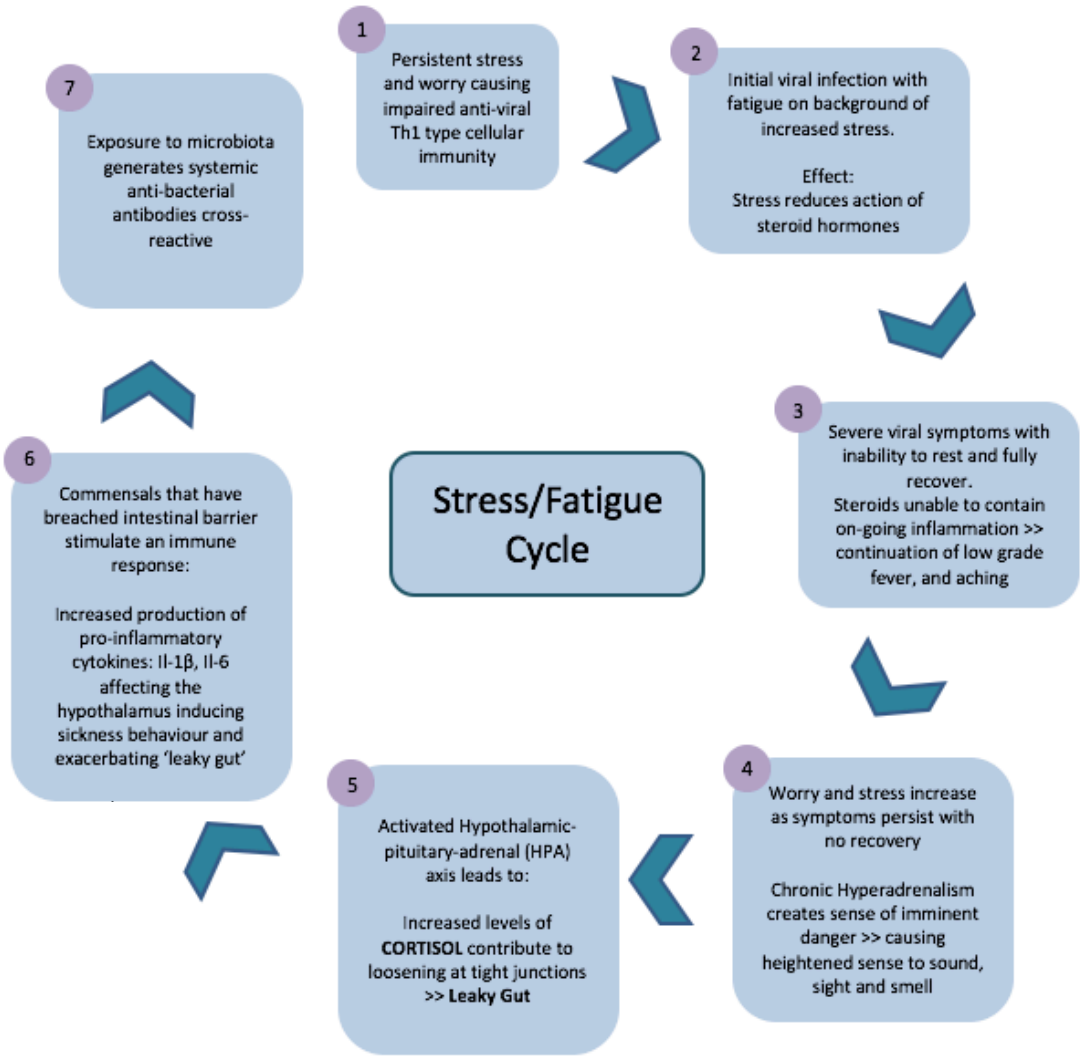

Figure 1.1.5 Current psycho-biology model for the pathophysiology of ME/CFS. Several symptoms of ME/CFS, chiefly among which post-exertional malaise (PEM), are suggestive of a dysfunctional Hypothalamus-Pituitary-Adrenal axis during times of stress. Stressors can originate from psychological processing of emotions and negative thoughts. Chronic stress can also weaken immunity and cause susceptibility towards infection. Long term exposure stress hormones can also impair intestinal barrier function, causing a "leaky gut" and exposure to intestinal microbes (Lambert, 2009). The immune system reacts with commensal bacteria previously hidden from immune cells, as a result this causes inflammation and further tissue damage and low-grade inflammation resulting from increased exposure to endotoxin (bacterial LPS). Serum antibodies IgM and IgA antibodies have been detected in ME/CFS are raised against intestinal microbes and may potentially cross-react with the CNS engender neuroinflammation and altered behaviour (Maes, Kubera, Leunis, & Berk, 2012; Morris, Berk, Galecki, & Maes, 2014). Finally, health anxiety and the damaging social impact resulting from this illness can causing further stress and GI-disturbances which appear to perpetuate this cycle.

1.5 The Hypothalamus-Pituitary-Adrenal (HPA) axis

The HPA axis is a major gut-brain pathway that protects the body from the dangers of stress. Components of this axis include the immune, neuroendocrine and central, autonomic, and enteric nervous systems, with various positive and negative feedback mechanisms designed to coordinate physiological and behavioural adaptations collectively called the stress response. This response is governed by several pathways (figure 1.1.6) and by the balance of immune (cytokines), endocrine (cortisol) and neural inputs from the intestines (vagus pathway and enteric nervous system) (Rea, Dinan, & Cryan, 2016). Activity of the HPA axis is determined by the release of corticosterone-releasing factor (CRF) from neuro-endocrine neurons from the paraventricular nucleus (PVN) of the hypothalamus during stress (Watts, 2005). Neuro-anatomical tracing studies reveal the suprachiasmatic nucleus (SCN) found in the anterior hypothalamus contains vasopressin-releasing neurons in close proximity to neurons in the PVN which can strongly inhibit corticosterone release during daytime (Kalsbeek et al., 1992). In response to actual or perceived (psychological) stress, CRF stimulates release of adrenocorticotrophic hormone (ACTH) from the anterior pituitary triggering successive release of glucocorticoids (cortisol in humans, corticosterone in animals), catecholamine (adrenaline and noradrenaline), mineralocorticoids (aldosterone) from the adrenal cortex into the systemic circulation causing mobilisation of gluconeogenesis (energy production), increased awareness (hypersensitivity), increased heart rate and blood pressure, and altered behaviour commonly referred to as the “fight or flight” response (Dallman et al., 1993; Rea et al., 2016; Taub, 2008).

Control of the PVN integrates signalling from catecholaminergic, glutamatergic and serotonergic neurotransmitters and is inhibited by the GABA-ergic neurons (Bellavance & Rivest, 2014). Glucocorticoid receptors (GR) expressed in the hippocampus and prefrontal cortex provide autoregulatory feedback to prevent HPA hyperactivity (Herman et al., 2012). The SCN has master control over the release of corticosteroids from the HPA axis, defined by the CLOCK system relying light and dark signals on photosensitive retina ganglion cells to coordinate circadian rhythm of peripheral CLOCKS throughout the body via humoral and neural connections (fig 1.1.6) (Tsigos et al., 2016). The release of CRF follows a circadian and ultradian rhythms measured by glucocorticoids in plasma revealing a day/night cycle and clustering of 6 to 9 surges in plasma cortisol in the very early hours of the morning and before getting up to facilitate awakening and arousal to start the day (Kalsbeek et al., 2012).

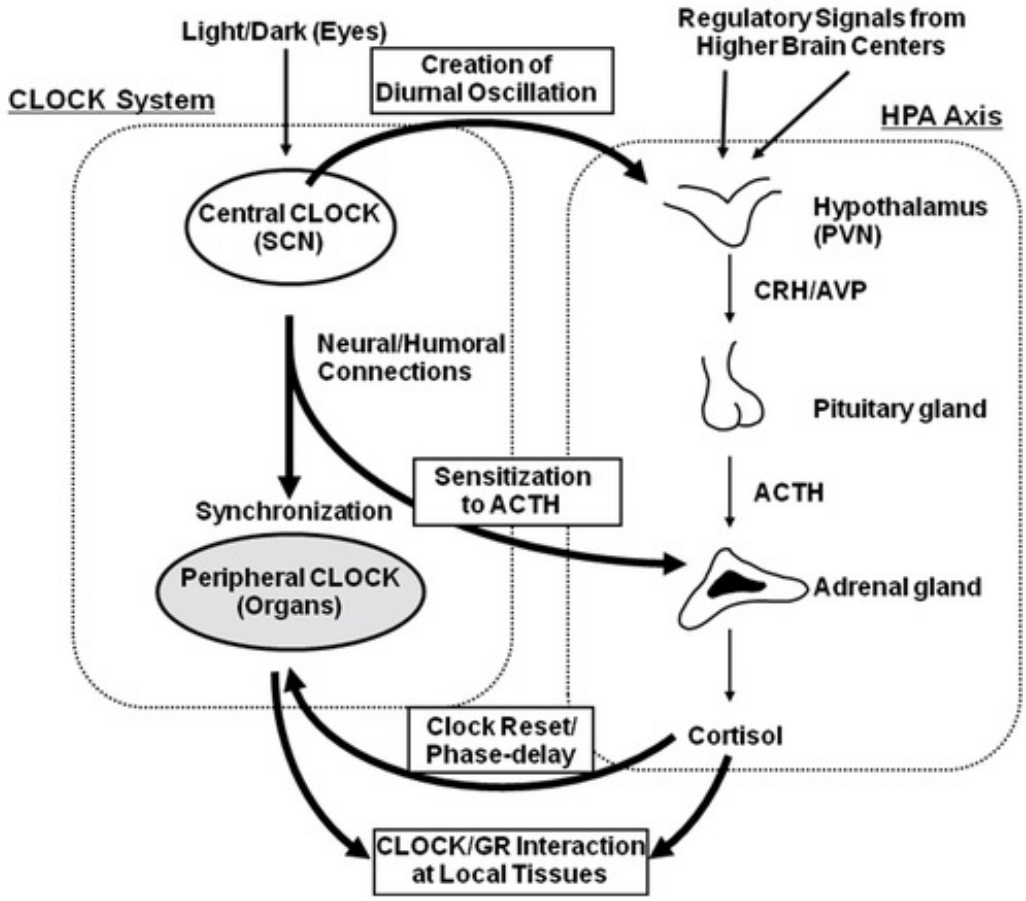

Figure 1.1.6 Daylight activates the central CLOCK in the suprachiasmatic nucleus (SCN) which coordinates the daily circadian rhythm for releasing glucocorticoids via neural inputs to CRH/AVP-containing neuron in the PVN of the HPA axis. Secreted glucocorticoids also synchronise peripheral CLOCKs by causing expression of CLOCK-related genes in local tissues. CRH: corticotropin-releasing hormone; AVP: arginine vasopressin; PVN: paraventricular nucleus. Figure from (Tsigos et al., 2016).

- *HPA disruption in ME/CFS*

Sleep disturbances are common in ME/CFS patients and is acknowledged this can have an impact on the daily rhythm of cortisol secretion (Jackson & Bruck, 2012). Circadian rhythm may also be perturbed in some patients who cannot withstand light and therefore disrupt daylight signals to the SCN via the retino-hypothalamic tract giving inadequate environmental cues when transitioning between day and night (Balbo et al., 2010). Low cortisol in CFS compared with healthy controls were reported to be related to the "low arousal state" in CFS patients (Demitrack et al., 1991). Generally, reduction in cortisol levels are more apparent in women and are associated with worse symptoms (Papadopoulos & Cleare, 2012; IOM, 2015). One report has found patients with more severe symptoms had

lower awakening cortisol and a flatter diurnal curve suggesting dysfunction within HPA signalling (IOM, 2015) However, not all studies have generated consistent data to support blunted HPA activation in all cases of ME/CFS. Interestingly, hyperactivity of CRF-releasing neurons have been associated to early life exposure to stress and is a risk factor in primates for developing major psychiatric disorders in adulthood (Coplan et al., 1996). Early life stress can also be conferred by viral infections such as Epstein-Barr Virus commonly associated with risk for developing ME, as well as enteroviruses which may precipitate a pre-programmed altered HPA response. As a result of a blunted HPA axis, immune-mediated inflammation may persist even with minor physical or psychologic stressors.

- *Intestinal microbiota programmes the HPA response*

There is evidence to support that stressful insults (antibiotic exposure, bacterial/viral infections) which impact the early intestinal microbiota composition can increase the risk neurodevelopmental behaviour disorders (Borre et al., 2014; O'Mahony et al., 2017). Excessive corticosteroid exposure during postnatal development influences the developing brain and neuronal complexity within areas such as the amygdala, hippocampus, and pre-frontal cortex in addition to GR expression (Borre et al., 2014). The hippocampus has inhibitory effects on HPA activation, however, stress causes reduced synaptic plasticity and decreased expression of NR_1 and NR_{3B} subunits of the N-methyl-D-aspartate (NMDA) receptor contributing towards HPA hyperactivity (Farzi et al., 2018).

Later in life stress can increase intestinal permeability and activate proinflammatory cytokines and prostaglandins with stimulate the HPA axis (De Punder & Pruimboom, 2015). Hyperactivation of HPA axis decreases GR expression and negative feedback to immune cells resistance to anti-inflammatory properties of cortisol which further weaken the intestinal barrier (Farzi et al., 2018; Kelly et al., 2015). Systemic inflammation and increased circulating cortisol is associated in stress-related neuropsychiatric disorders, particularly Major Depressive Disorder (MDD) (Doolin et al., 2017; Jacobson, 2014). Stress and negative emotions are also a major factor in the development of Irritable Bowel Syndrome (IBS) where peripheral neuro-immune interactions can contribute to abdominal hyperalgesia (Elsenbruch, 2011). As with ME/CFS case definition criteria is applied to the diagnosis of IBS, with 50-90% of patients having an associated psychiatric co-morbidity (Singh et al., 2012). IBS has been found to increase the risk of depressive, anxiety, sleep, and bipolar disorders. Furthermore, gastroenteritis, prior to anxiety and depression are risk factors for the subsequent development of post-infectious IBS (Lee et al., 2015).

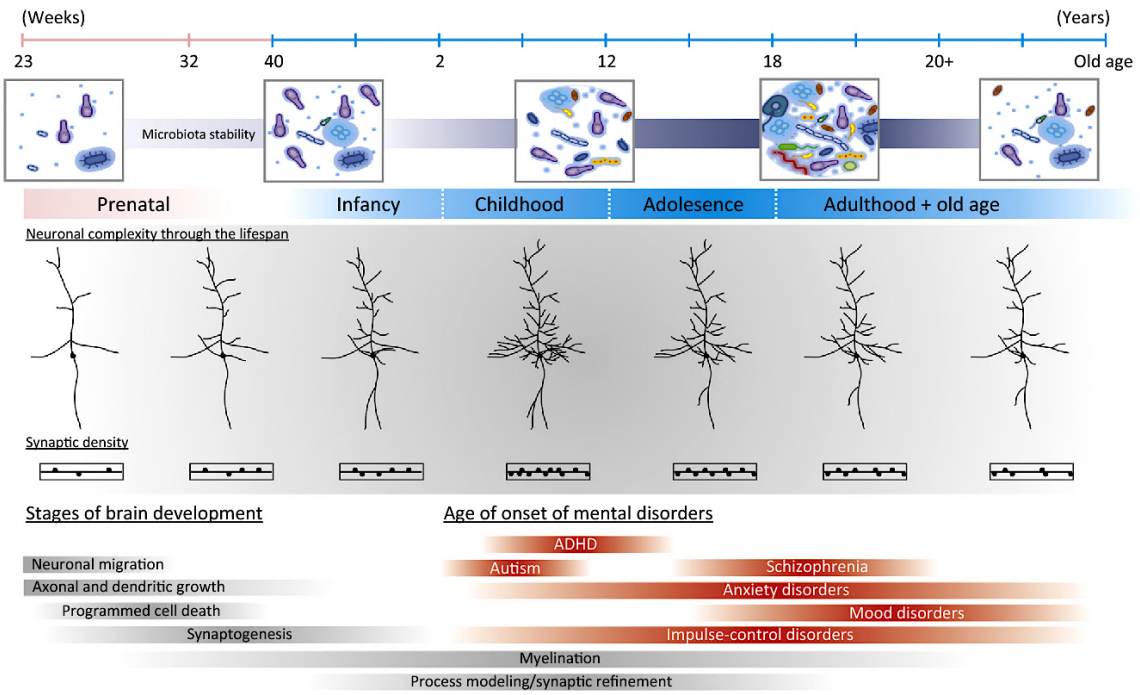

Figure 1.1.7 Critical windows between the development of neurons, diversity of the intestinal microbiota and the age of onset of neuropsychological disorders. The stability of the intestinal microbiota can affect development of the neural complexity of the CNS in early life. Early life physical and mental stressors (antibiotic treatment, psychological abuse) can impact the composition of the intestinal microbiota and increase the risk of developing psychiatric illnesses in adult life. Animal studies have shown bidirectional communication between intestinal microbes and the central nervous system that is essential for neurodevelopment and programming of stress-responsivity responses governed by the HPA axis. Figure from (Borre et al., 2014).

The intestinal microbiota colonisation occurs during a critical window of neurogenesis during which time neuronal structures within the CNS are undergoing axonal and dendritic growth and forming synaptic connections (fig 1.1.7). The networks of neuronal connections are complex and highly plastic during this development. Early insults on the intestinal microbiota during this process can cause life-long changes in behaviour and physiological response to stressors later in life. The majority of this work is pre-clinical and predominantly conducted on animal models with targeted manipulation to the intestinal microbiota to observe how these animals respond behaviourally and physiologically to a variety of physical and immune stressors.

Gnotobiotic mice continue to be the most accessible tool for neurobiologists to explore the capacity of the intestinal microbiota to influence the HPA axis and behaviour via immune and neuro-endocrine systems as well as central, autonomic and enteric nervous systems,

(figure 1.1.8) (Cryan & Dinan, 2015; Farzi et al., 2018). High levels of ACTH and corticosterone concentrations are found in germ-free (GF) mice in response to restraint stress and are consistent with HPA hyperresponsiveness (Sudo et al., 2004). GF mice have less brain-derived neurotrophic factor (BDNF) important in neuronal growth, differentiation and survival (Sudo et al., 2004). Some of the differences in GF mice are dependent on sex; for example serotonin concentration is higher in the hippocampus of GF mice with decreased 5-HT_{1A} receptor expression only in female mice (Clarke et al., 2013). GF status appears to disrupt the programming of the HPA axis response via permeant reduction of GR and mineralocorticoid receptor (MR) gene expression in the hippocampus and increasing hippocampal volume (Luczynski et al., 2016).

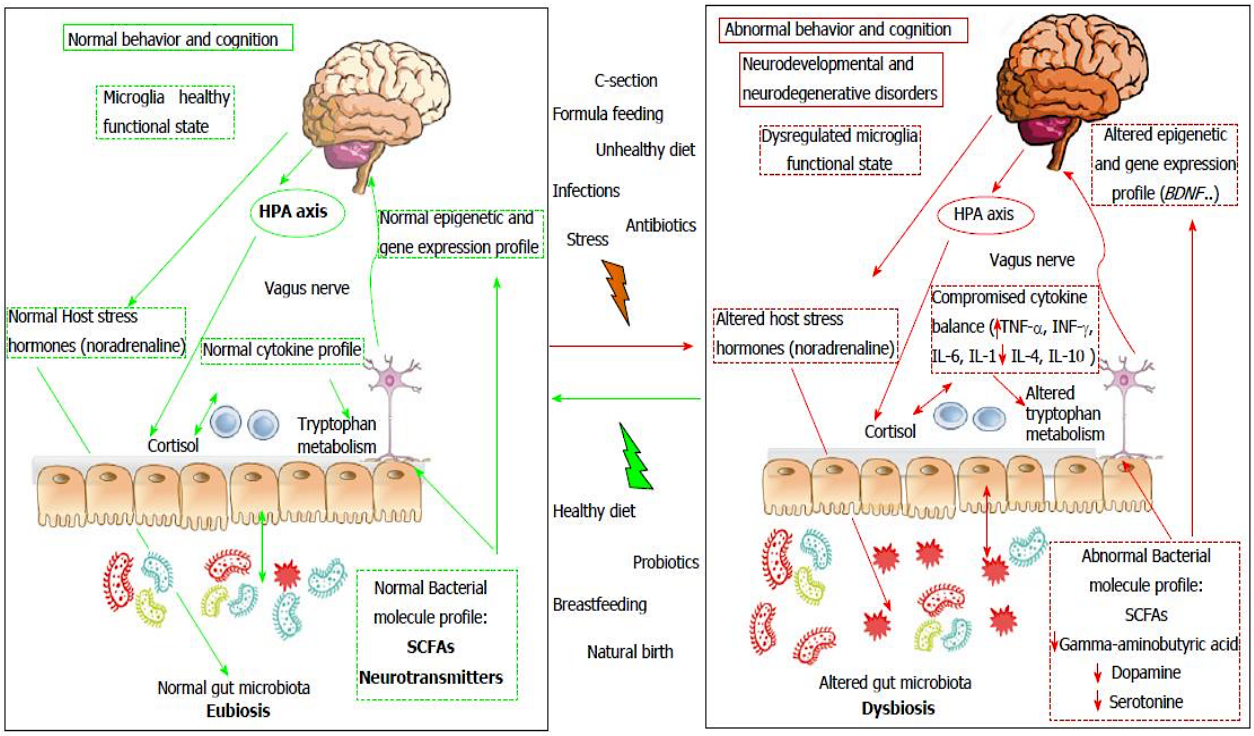

Fig. 1.1.8 Neural and humoral signalling pathways between the intestine and the brain. These pathways together represent the microbiota-immune-gut-brain axis. The architecture and formation of the CNS and brain occur during early life, when intestinal microbes provide external environmental cues at specific windows of time. Additional factors later in life, such as diet, stress, infections, antibiotic exposure, can also influence the microbiota and its function via the production of microbial specific metabolites, that mimic neurotransmitters, can impact on signalling via the gut-brain axis. The immune system also interacted with the microbiota and can become activated in response to dysbiosis, causing changes in intestinal permeability and production of pro-inflammatory cytokine that can trigger sickness behaviour and activated microglial cells in the brain that increase the risk of neurodegenerative disorders affecting cognition and memory. Figure from (Cenit et, 2017).

Probiotic administration of a single strain, *Bifidobacterium infantis*, restored normal HPA response to stress in GF mice, whilst reduced anxiety behaviour and increased locomotor activity could only be reverted in young mice, not adult mice, with adoptive transfer of SPF microbiota (Sudo et al., 2004). Early life disruptions to the colonisation of the intestinal microbiota occurs simultaneously during neurodevelopment of the brain and CNS and it emerges there are temporal critical windows for colonisation to ameliorate HPA dysfunction later in life (figure 1.1.9).

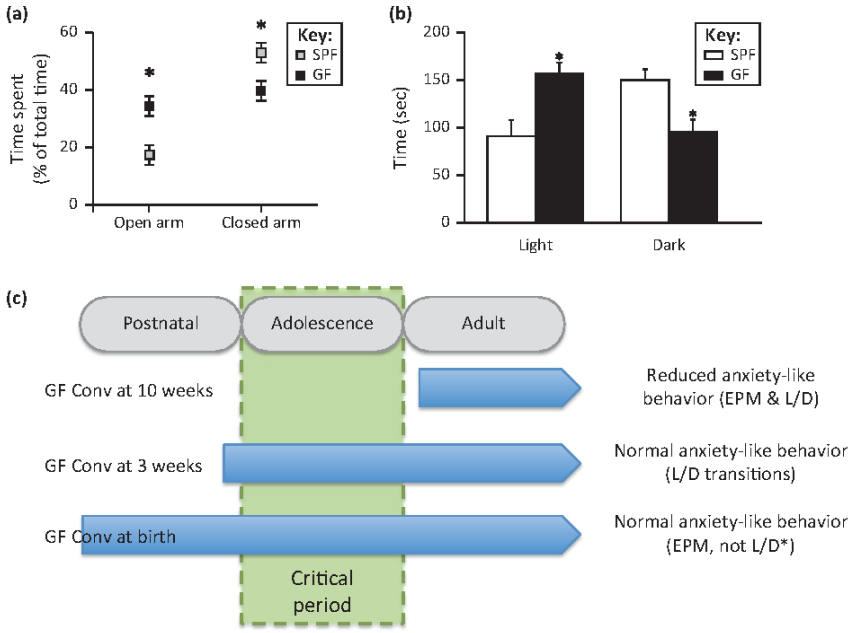

Figure 1.1.9 Germ free mice raised without exposure to microbes display reduced anxiety-like behaviour which cannot be reversed by recolonization following adolescence. GF mice spend more time in the light and more time spent in the open arm of the elevated plus maze, suggesting they are less anxious. Adolescence is a critical period when the intestinal microbiota influences anxiety-like behaviour, that can have life-long effects. From (Foster et al., 2013).

Altered hippocampal gene expression and increased serotonin production may explain why GF mice display reduced anxiety-like behaviour and increased locomotor activity compared with specific-pathogen free (SPF) mice with a normal microbiota (Neufeld et al., 2011). Antimicrobial treatment in SPF mice alters the composition of the microbiota and increased exploratory behaviour and BDNF expression; and transfer of stress-prone BALB/c mice microbiota into GF NIH Swiss mice transferred anxiety-related behaviour, while transfer of SW microbiota to GF Balb/C mice had an anxiolytic effect, suggesting a direct causal link between the intestinal microbiota and behaviour (Bercik et al., 2011).

Post-natal development can be influenced by antibiotic exposure during the microbial "colonisation window" causing visceral hypersensitivity in adult male rats, without perturbing anxiety, cognition and immune-related stress responses (O'Mahony et al., 2014). Conversely, antibiotic depletion later in life of the microbiota in rats causes depressive behaviour, cognitive deficits, and reduces visceral pain sensitivity (Hoban et al., 2016). Reduction in the number of bacterial species (richness) is associated with depression with evidence for beneficial treatment using lactobacillus and bifidobacterial species to modulate depressive symptoms (Bravo et al., 2011). A stable and diverse microbiota is attributed to colonisation resistance to effectively limit colonisation and overgrowth of pathogens as well as supporting a balance of anti- and pro-inflammatory responses (Lawley & Walker, 2013). Transferring the intestinal microbiota from depressed patients to rats induced anxiety-like behaviour and anhedonia characteristic of depression which suggests a causal role for intestinal microbes in the pathogenesis of depression (Kelly et al., 2016).

It seems paradoxical that GF exhibit both exaggerated HPA activity in response to stress and yet have reduced-anxiety and increase locomotor activity highlighting the complexity of microbiota-gut-brain signalling. Both the amygdala and hippocampus are enlarged in these animals, along with differential gene expression pattern involved in neuronal plasticity, neurotransmission and morphology, and evidence of defects in a subpopulation of immune cells, resident in the brain, called microglial cells (Farzi et al., 2018; Stilling et al., 2015). There is evidence that Blood-Brain-Barrier (BBB) permeability in increased in GF mice with a similar effect in antibiotic-induced disruption to the intestinal microbiota causing tight-junction defects in specific brain regions, predominantly the hippocampus and amygdala (Braniste et al., 2014). Antibiotic treatment has the capacity to effect brain neurochemistry evidenced in the depletion of the SFP mice microbiota during the human equivalent of adolescence causing reduced anxiety, memory impairment, altered tryptophan metabolism, and reduced BDNF, oxytocin, and vasopressin expression in the hypothalamus (Desbonnet et al., 2015).

- *Maternal Immune Activation*

Maternal Immune Activation (MIA) offspring display an altered composition of intestinal microbiota compared to control offspring (Hsiao et al., 2013). These offspring result from pregnant dams injected with viral mimic poly(I:C) to simulate maternal infection link to an increased risk of autism probably caused by elevated level of inflammatory molecules in the maternal blood (Hsiao et al., 2013). Altered intestinal permeability was measured in

MIA offspring was attributed excess leakage of gut-derived metabolites into systemic circulation and consequently is demonstrated to alter the serum metabolome. Administration of *B fragilis* to MIA offspring every other day for 6 days at weaning was able to ameliorate GI barrier defects associated with an improvement in intestinal permeability. The impact *B fragilis* has on gut barrier integrity and is shown to be through a mechanism involving changes in expression of claudins 8 and 15 in the colon, but not in the small intestine, consistent with the fact that the majority of the microbiota including *B fragilis* resides in the colon and therefore may be an effective treatment for restoring gut permeability defect, at least in MIA offspring. Serum metabolites significantly altered by MIA treatment (around 8% of all 322 serum metabolites detected in adult sera by GC/LC-MS based metabolomics profiling) were restored by *B fragilis* treatment revealed the most dramatically affected metabolite, 4-ethylphenylsulfate (4EPS) (Hsiao et al., 2013). 4EPS exhibited a 46-fold increase in serum levels of MIA offspring. This is interesting because conventional germ-free mice do not have detectable levels of 4EPS indicating it originates from intestinal microbes. This work remains preclinical so its relevance to humans with autism and similar neurodevelopmental disorders is uncertain.

- *Maternal separation and stress*

Depressive-like behaviours are noted during maternal separation of new born mice causing HPA activation, immune activation and visceral hypersensitivity akin to IBS-like symptoms in humans (O'Mahony et al., 2011). The integrity of the intestinal microbiota is susceptible during maternal separation in infant monkeys; in addition to stress-related behavioural changes caused by elevated cortisol, these infants had significant decreases in faecal *Lactobailli*, and were more susceptible to bacterial infection and associated emotional behaviour, and stress to disruption to the immune system (Bailey & Coe, 1999). Maternal prenatal stress measured by consistent elevated salivary cortisol during pregnancy induced a higher relative abundance of Proteobacteria and lower *Lactobacilli* and *Bifidobacterium* that are hallmarks of inflammatory diseases and GI symptoms and did cause infant GI symptoms related to changes (Zijlmans et al., 2015).

- *Intestinal microbiota and neural communications*

The autonomic nervous system (ANS) integrates the communication between the CNS and the gut viscera, with resident microbiota signalling interacting with enteric nervous system influencing the brain and the perception of abdominal pain. Primary functions of the enteric nervous system (ENS) include control of movement and transmucosal fluid in maintaining mucosal barrier function and absorption of nutrients – as well as modulation of the immune system through the neuroendocrine system. Several classes of neurotransmitters can be synthesised by specific bacterial species including γ-aminobutyric acid (GABA), serotonin, catecholamines and acetylcholine (Cenit et al., 2017). Strains of *Lactobacillus spp.* and *Bifidobacterium spp.* are known to contribute to the synthesis of GABA; *Escherichia spp*. *Bacillus spp*., and *Saccharomyces spp*. produce noradrenaline; *Candida spp., Streptococcus spp., Escherichia spp*. and *Enterococcus spp*. produce serotonin; *Bacillus spp*. produce dopamine, while *Lactobacillus* have been shown to make acetylcholine (Barrett et al., 2012; Cenit et al., 2017; Dinan et al., 2013). Neuronal communication between intestinal microbes and the brain is evidenced by benefits of probiotic treatment of social and emotional behaviour. Administering *Lactobacillus rhamnosus* to mice had a reduction on stress-induced level of corticosterone and on GABA receptor regional expression in the brain. GABA-nergic neuron projecting from the hypothalamus to PVN inhibiting CRF neurons, serving as a gate keeper for PVN activation and receive projections of glutamatergic neurons from the hippocampus and prefrontal cortex – indeed lesions in these brain areas exacerbate responses to psychogenic stress (Figueiredo et al., 2003; Herman et al., 2016). Alteration to GABA receptor expression is known to be implicated in anxiety and depressive states and is also the main CNS inhibitory neurotransmitter. Alterations in the GABAergic system have pathological implications for stress-related psychiatric conditions, as such; these receptors are also main targets for anti-anxiety agents such as benzodiazepines (Bravo *et al.,* 2011).

- *Immune system and HPA axis*

Systemic infection via pro-inflammatory cytokines can activate the HPA-axis and trigger release of corticosterone in animals (Dunn, 2000; Turnbull & Rivier, 1999). However, the HPA axis is normally tightly regulated during infection providing negative feedback to the immune system via immune cells glucocorticoid receptors to downregulate CRF and limit pro-inflammatory cytokine production enabling host adaption to the ongoing stress and to effect certain behavioural changes (Silverman et al., 2005). Stress effects on the immune

system include reduced NK cell activity, changes in peripheral lymphocyte subsets and proliferation, diminished antibody production and reactivation of latent viral infection (Taub, 2008). Early life exposure to LPS in mice causes life-long HPA hyperresponsiveness measured by elevated ACTH and corticosterone reduced GR-mediated negative feedback (Shanks et al., 1995).

The composition of the intestinal microbiota influences the host's susceptibility and response to infection; mouse enteropathogenic Citrobacter *rodentium* infection is mild in NIH Swiss mice (resistant) compared to lethal in C3H/HeJ mice, however antibiotic depletion of the microbiota in resistant mice and transfer the microbiota from C3H/HeJ to the resistant mice made them more susceptible to infection; although not lethal, this highlights additional factors including genetic background, but also demonstrated the microbiota can influence host resistance seen by transfer of NIH Swiss microbiota into HeJ mice which delayed pathogen colonisation and mortality (Willing et al., 2011). *C. rodentium* can drive anxiety like behaviour in CF-1 male mice, challenged at nine weeks old their immune cytokine levels were unchanged, but displayed elevated c-Fos (marker of neuronal activity) within vagal afferent neurons suggesting vagal stimulation confers this type of behaviour rather than immune mediated inflammatory cytokines (Bullitt, 1990; Lyte et al., 2006).

E. coli a gut pathogen which elicits activation of the HPA axis and the secretion of pro-inflammatory cytokines causing changes in the hypothalamus regulation of body temperature, e.g. fever. The adrenal cortex is sensitive to ongoing pro-inflammatory molecules, such as Prostaglandin E2 (PGE2) and correlated with rising corticosterone (Zimomra et al., 2011). The rise in circulating corticosterone is a product of COX-induced prostanoid synthesis which correlates with PGE2 production (Dinan & Cryan, 2012). Psychopathologies with evidence of HPA hyperactivation may therefore be associated immune responses to ongoing infections. Activation of the HPA may be triggered by increased intestinal permeability caused by stress, coupled with short term exposure to stress causing disruption to the microbiota (Bailey et al., 2011; Galley et al., 2014) (De Punder & Pruimboom, 2015).

Neonatal immune challenge with LPS during neurodevelopment increases activity of tyrosine hydroxylase needed to catecholamine synthesis (Shanks et al., 1995). Stress-induced increases in neuroendocrine hormones noradrenaline and dopamine can support growth of intestinal Gram negative bacteria and are a source LPS (Lyte & Ernst, 1992).

Infection elicits HPA activation with challenges using E.coli and LPS in rats causing IL-1 and neuroinflammation leading to memory impairment after a second inflammatory challenge in adulthood (Bilbo, 2005). Interestingly, maternal high fat diet (MHFD) increases circulating pro-inflammatory cytokines and negatively affects the neurodevelopment and microbiota of the foetus (Sullivan et al., 2014). Moreover, HFD is associated with an altered intestinal microbiota and increased vulnerability of anxiety-like behaviour.

- *Stress and neuroinflammation*

Neuroinflammation is synonymous with microglial cell activation; these are innate immune cells resident through the CNS and brain and undergo extreme morphological changes during ageing consistent with them being in an activated, pro-inflammatory state (figure 1.1.10). Innate immune cells display pattern recognition receptors (PPRs) which recognise common microbial and virus structures known as pathogen associated molecular patterns (PAMPS) for example, bacterial cell wall components such as peptidoglycan (PGN) and lipopolysaccharide (LPS) recognised as non-self by Toll-like Receptors (TLR) leading to activation and downstream intracellular signalling associated with myeloid differentiation primary response gene MyoD88 and NF-kB activation of pro-inflammatory cytokines (Mogensen, 2009). In the absence of bacterial or viral infection, the primary function of microglial cells during resting state (M0) is to carry out immune surveillance within the brain and CNS (Kettenmann et al., 2011). The sensing of these bacterial products may regulate the neurodevelopment of the CNS in health as well as triggering neuroinflammation in pathological states. A recent study suggests PPR interactions with the intestinal microbiota are needed for brain development; PGN-recognition proteins and NOD-like receptors are highly expressed during the postnatal window of colonisation, occurring simultaneously with the developing brain (fig. 1.1.7), are sensitive to changes in the intestinal microbiota (Arentsen et al., 2017). Fragments of PGN have been reported to cross the BBB in postnatal development of healthy mice (Arentsen et al., 2017). Using PGN-recognition protein 2 knockout mice lead to the development of changes in social behaviour similar to GF or antibiotic treated mice (Arentsen et al., 2017). Thus translocation of PGN across the BBB and activation of PRRs during neurodevelopment appears to a mechanism for mediating early programming of neuronal circuits associated with emotions, cognitive and motor activity (Arentsen et al., 2017).

GCs are also expressed on microglial cells and thus their immune status, morphology, and number are influenced by peripheral immune events and stress-induced HPA activity

(Sierra et al., 2008). Cytokine and other inflammatory markers such as PGE2 caused due to peripheral events, such as infection, can traverse the chorus plexus and BBB as well as promote prostaglandin release from endothelial cells within the vascular of the PVN and activate microglial cells and the stress response (Rivest, 2001). Moreover, vagal nerve stimulation can transmit information of peripheral inflammation in the gut to the brain to influence the HPA stress response and feedback to the peripheral immune system (Rea et al., 2016).

- *Microglia activation and polarisation*

Under steady state conditions (M0) microglial labelled with CX3CR1-GFP in mice, time-lapse two-photon microscopy shows they have multiple processes which continue to survey their environment (Nimmerjahn et al., 2005). Recognition of bacterial or viral PAMPS by PPRs will stimulate an innate immune response. Bacterial LPS (endotoxin) binds to TLR4 which activates microglia (M1 polarisation) to adopt an amoeboid morphology, show increased motility and production of pro-inflammatory cytokines and reactive species (oxygen or nitrous derived) designed to engulf pathogens and mobilise CD4+ IFNγ-producing Th1 cells and trafficking of immune cells to the brain (Nakagawa & Chiba, 2014). Microglial cells are a prime target for glucocorticoids to control this pro-inflammatory phenotype (Sierra et al., 2008). Figure 1.1.10 shows M1 activated microglial cells produce pro-inflammatory cytokines and chemokines such as IL-1β, IL-6, TNFα, CCL2, ROS, NO that are associated with sickness behaviour (Parnet et al., 2002). Depending on the cytokine milieu, Th2-derived cytokines, IL-4 and IL-13 can promote activation and polarisation of M2 microglia which express anti-inflammatory cytokine IL-10 (Nakagawa & Chiba, 2014). The lowered threshold for microglial activation, known as “microglial priming” is associated with ageing and neuroinflammation, consequently animal studies of neurodegenerative diseases find microglial cells are primed or activated (M1) and are more sensitive to peripheral immune activation (Perry & Holmes, 2014; Perry & Teeling, 2013). Thevaranjan and colleagues recently reported ageing in mice is also associated with decline of the intestinal microbiota (dysbiosis) and increased permeability of the intestinal barrier as well as the BBB triggers chronic systemic inflammation whilst GF mice are protected from these effects (Thevaranjan et al., 2017).

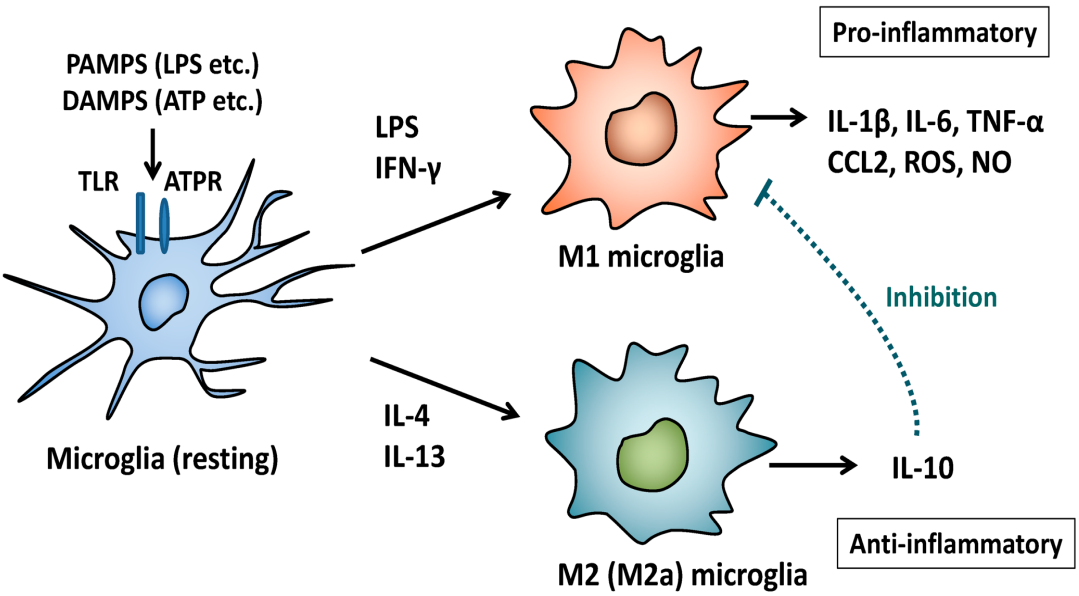

Figure 1.1.10 Polarisation and differentiation of microglial cells resident in the brain and CNS. Microglial cells are frequently referred to as the tissue-resident macrophages of the CNS and have an immunoregulatory function. M1/M2 polarisation occurs when resting microglia are stimulated by pattern and/or danger associated molecular patterns, e.g. LPS, via TLR receptors. M1 microglia are associated with pro-inflammatory cytokine responses and release of PICs into the CNS. Conversely, M2 activation is stimulated by Th2-assocated cytokine IL-4 and IL-13 which causes microglia to secrete anti-inflammatory IL-10. Reproduced from (Nakagawa & Chiba, 2014).

As a consequence of damage to the intestinal microbiota, caused by stress or infections, increased intestinal permeability may facilitate increases in plasma endotoxin which activate innate immune responses. Initial (primary) exposure to LPS did not increase IL-1β in the brain, however, long-term repeated dosages of LPS (secondary infection) in mice resulted in increased brain IL-1β, TNFα and IL-12 and an activated (M1) microglial phenotype and exaggerated response to infection with S. *typhimurium* (Püntener et al., 2012). The characteristics of microglia during stress are similar to ageing, and are likely explained fact both lead to microglial priming, neuroinflammation and heightened reactivity to peripheral immune stimuli caused by low grade inflammation (Jurgens & Johnson, 2012). To this end, prolonged stress could be facilitating the acceleration microglial age-associated M1 polarisation and driving neuroinflammation. The effect of stress is paradoxical since under normal circumstances stress hormones releasing GCs are considered anti-inflammatory causing inactivation of immune cells via GRs. However, stress prior to immune activation in rats enhanced NF-kB activation and proinflammatory cytokine production in the frontal cortex and hippocampus, but was blocked by pre-treatment of an GC receptor antagonist (Munhoz, 2006).

As discussed, early intestinal microbiota colonisation is necessary for postnatal development of the CNS and microbial-gut-brain signalling pathways in coordinating stress and immune responses. Defects in microglial cells are emerging as an important mediator of neuropsychiatric and neuroinflammatory disorders and may also be vulnerable to disruption in the intestinal microbiota. The importance of acquisition of the microbiota in early life for microglial homeostasis is apparent in GF mice which display immature neurons and BDNF. During early life, microglia support neuronal survival, modelling and pruning synaptic pruning as well as producing various neurotrophic factors to promote neuronal circuit development and synaptic formation (Erny et al., 2015). However, a number of downregulated genes required for microglial activation were discovered in GF mice microglial, including type 1 interferon receptors, Janus kinase 3 (Jak3) and signal transducer and activator of transcription 1 (Stat1) are evident compromised immune function and immaturity of microglia cells (Erny et al., 2015). Disruption of synaptic pruning by microglial cells during development is evident in mice lacking Cx3CR1 chemokine receptors, these mice had significant reduced number of microglial cells, and lacked functional neuronal connectivity, and display autism-related behaviour (Zhan et al., 2014).

In addition to the variety of neurotransmitters produced by the intestinal microbiota, Short Chain Fatty Acid (SCFA) production can effect changes in brain neurophysiology being readily absorbed across the BBB and contribute to microglial homeostasis (Rea et al., 2016). GF free mice re-introduced to a normal microbiota reversed deficits in microglial cell numbers, morphology and maturity, however SCFA alone were sufficient in reproducing this outcome (Erny et al., 2015). Moreover, mice deficient for SCFA receptor, FFAR2, also produce the same microglial phenotypic defects seen in GF mice with increased BBB permeability, yet under normal conditions FFAR2 is not expressed in any cell type in the brain and CNS (Braniste et al., 2014; Erny et al., 2015). Psychological stress causes prolonged HPA activation, and alteration in the microglial phenotype may involve trafficking of peripheral monocytes from the spleen (Wohleb et al., 2015). Thus, the intestinal microbiota may regulate microglial activation and neuroinflammation through trafficking of immune cells dependent on the production of SCFA (Rea et al., 2016). Interestingly faecal SCFAs have been reported significantly higher in children with autism spectrum disorder compared with control, suggesting increased fermentation process within the microbiota (Wang et al., 2012).

Studies in GF mice show their microglial cells are less efficient at mounting pro-inflammatory responses to pathogens. It is also revealed the intestinal microbiota can influence BBB permeability since butyrate-producing bacteria can increase expression of tight junction (TJ) protein occludin in the hippocampus and frontal cortex; in addition, transfer of SPF microbiota to GF decreased their BBB permeability (Braniste et al., 2014). Antibiotic-induced intestinal dysbiosis reduces bacterial metabolites in plasma, enhances HPA activity, with similar altered expression to TJ proteins seen in GF mice (Fröhlich et al., 2016). To this end, hyperactivation of HPA and BBB permeability defects may facilitate circulating pro-inflammatory cytokine directly interacting with microglial cells during systemic infections.

Indeed, neuropsychiatric disorder bi-polar and schizophrenia show involvement of the immune system as both TNFα and CRP are elevated in both conditions. Increasingly psychiatric disorders including these, and anxiety and depression are being characterised by neuroinflammation. Ageing is also associated to this immune profile and is termed "inflammageing" with profound effects on mood and emotion (Frasca & Blomberg, 2016) Recently a study collecting cerebral spinal fluid (CSF) in relation to psychiatric symptoms and cognitive dysfunction found CSF-resident microglia patients with schizophrenia and bi-polar disorder have activation markers including CD14, a co-receptor for TLR4 (Johansson et al., 2017). Detection of soluble CD14 in CSP was associated with psychotic symptoms in twins with psychotic disorders compared with their un-unaffected twin (Johansson et al., 2017). It is unclear what may be driving these differences, however, it is tempting to speculate increased exposure to bacterial components may drive neuroinflammation as a consequence of increased intestinal permeability (Kelly et al., 2015).

- *Stress impacts the intestinal barrier function*

Stress-induced increases in intestinal permeability are well documented in animal models for behaviour and in colitis where it is discussed as causing exposure of the body to huge quantities of antigenic material derived from the microbiota which interacts with innate immune cells to drive low grade chronic inflammation (De Punder & Pruimboom, 2015; Fasano, 2012; Kelly et al., 2015; Visser et al., 2009). Stress-response and systemic inflammation in mice is dependent of PPR recognition of bacteria via TLR4 and do not respond to Gram negative bacteria when this receptor is knocked out (Gosselin & Rivest, 2008). Negative emotions and stress-related hormones and neurotransmitters exert influence on the intestinal microbiota and alter physiological of the immune and neuro-

endocrine pathways in complex humoral pathway and neuronal circuits (Rea et al., 2016). Maternal separation in rats, causes increased expression of choline acetyltransferase (ChAT) and hyperactivation of cholinergic neurons belonging to the ENS and is linked to stress-induced CFR activation of CRF-receptor 2 (CRFR2), a G-protein coupled receptor (GPCR) expressed on enteric neurons to induce barrier dysfunction (Gareau et al., 2007). The mechanism was further uncovered by the work of Overman et al., who revealed CRF mediated its permeability effects in this cholinergic neural pathway via activation and release of TNFα and proteases from mast cells, including histamines that impact tight junction proteins (Overman et al., 2012). The expression of PRRs (e.g. TLRs) present on enteric neurons suggests that microbes may interact directly with afferent nerve terminals belonging to the ENS and provide further feedback to the ENS and HPA axis via vagal stimulation (Dinan & Cryan, 2012; Rhee et al., 2009).

Stress is known to induce endotoxin and low-grade inflammation by increasing intestinal permeability and may also cause neuroinflammation by altering permeability of the blood brain barrier through disruption to vascular endothelial tight junctions (De Punder & Pruimboom, 2015; Verma et al., 2006). The genus *Lactobacillus* is significantly reduced in mice exposed to social stress and in early life stress (Galley et al., 2014; O'Mahony et al., 2011). In rats, probiotic treatment may offer solution to prevent increased permeability following oral administration of *Lactobacillus farminis* for 2 weeks resulted in decreased circulating LPS and attenuated HPA responses to acute psychological stress (Ait-Belgnaoui et al., 2012).

Further to the work published on germ-free models and maternal separation of animals, GI barrier defects and alterations in the microbiota have been explored in a disease mouse model for autism, as well as in children (Hsiao et al., 2013; Luna et al., 2017). Increased intestinal permeability appears to be an influencing factor in pathogenesis of autism; increased permeability was found in 36.7% of adults patients with ASD, and in 21.2% of their relatives, compared to just 4.8% in healthy children (De Magistris et al., 2010). Similar changes in intestinal permeability have been reported to precede onset of type 1 diabetes in a study of 81 preclinical/new-onset/long-term patients versus 40 healthy controls using the lactulose/mannitol urinary excretion test (Bosi et al., 2006).

An alternative stress signalling pathway may be via enterochromaffin cells which may act as signal transducers between the luminal microbiota and underlying enteric neuronal network by secreting various signalling peptides and hormones including serotonin, CRF, cholecystokinin and somatostatin (Rhee et al., 2009). Low-grade chronic inflammation is associated with an altered intestinal microbiota in depression, with low abundance of butyrate-producing *Faecalibacterium* and high levels of *Enterobacteriaceae* (Jiang et al., 2015). Targeting these changes in the microbiota may influence intestinal immunity and consequently the level of inflammation that is detriment to causing increased permeability (De Punder & Pruimboom, 2015). Potential future therapies for stress-related and behavioural defects may redress the microbiota's input using probiotics in neuropsychiatric disorders appears promising (Dinan et al., 2013).

- *Summary*

The microbiota is essential to the development and training of neuroendocrine and neuroimmune pathways in neurodevelopment and the HPA axis. Early life stress (antibiotics, infections) can impact the intestinal microbiota and disrupt temporal environmental cues to this process which have life-long consequences for stress handling and response to infection and can lead to priming of microglia in the brain. Many of the symptoms of ME/CFS, such as cognitive impairment, memory deficits, sleep disturbance, malaise, fatigue, are synonymous with ageing, a period where a decline in the diversity of the intestinal microbiota is paralleled with weakened immunity, and GI functions of digestion and motility is often compromised. Low-grade inflammation associated with ageing is apparent from increased levels of TNFα, IL-6 and CRP, and are known to affect cognitive functions and mood (Frasca & Blomberg, 2016). Just as the intestinal microbiota is necessary for post-natal neurogenesis and maturation of macrophage-related microglial cells, perturbations of the intestinal microbiota in later years influences the state of neuroinflammation and risk for neurodegenerative conditions with similar symptoms of cognitive defects and sickness behaviours influenced by peripheral inflammatory events caused by progressive priming and activation of microglial cells via vagal, HPA signalling and inflammatory immune mediators, altering their morphology and function in the brain to the effect of behavioural changes and social deficits similar to anxiety and depression. Finally, intestinal dysbiosis and increased intestinal permeability are plausible mechanisms for exposing the body to non-self antigenic material, predominantly, LPS and PGN from the microbiota which activate innate immune responses and activate microglial cells in the

brain and promote the pathogenesis of neuroinflammatory disorders. Animal models are leading the way in deciphering the relative impact GI function has in neuropsychiatric disorders; GF mice for example show exaggerated stress response and depletion of BDNF that can be rescued with *B. infantis* (Bercik et al., 2011; Sudo et al., 2004); reveal SCFAs are required for maturity and function of microglial cells (Erny et al., 2015).

1.6 Immune Abnormalities in ME/CFS

Immunological studies attempting to characterise immune dysfunction in ME/CFS, are further complicated when stress and disruption to sleep is a known impact on the immune system and is prevalent among the patient population. The main immunological factors that vary between ME/CFS and healthy individuals are serum/plasma levels of chemical of cytokines, which facilitate crosstalk between the innate and the adaptive immune system. The available literature provides a conflicting view on the status of the immune system in ME/CFS (Theorell et al., 2017). Despite this, imbalances in the regulation of the immune system of ME/CFS patients have been documented in multiple studies, ranging from individual case studies to moderately sized patient cohorts (Broderick et al., 2010; Fletcher et al., 2009)Lorusso et al., 2009). The cytokine profiles reported are more indicative of an ongoing immune response to an underlying infection rather than being specific to ME/CFS. However, more recently a specific cytokine immune profile has emerged during early onset of ME/CFS which may help early diagnosis. In these immunological surveys there is potential evidence in some patients of a persistent stimulus triggering the immune system, which results in activation of immune-inflammatory pathways and is highly likely to account for many of the symptoms of ME/CFS including sickness behaviour (Morris & Maes, 2013). However, individual patient cytokine profiles may also depend on patient subgroup and staging of the disease, acute flares versus partial remission, and render it difficult to study the precise nature of the immune dysfunction seen in ME/CFS. Without effective grouping with ME/CFS patient there is a limit the value of determining cytokine levels in patients' serum due to intraindividual differences and varying methodologies to detect them.

- *Inflammation*

Early reports suggested ME/CFS presented with activation of a chronic low-grade inflammatory responses by the presence of pro-inflammatory cytokines such as TNFα, IL-1β, IL-6 which positively correlates with symptoms of fatigue and the feeling of experiencing an infection, or flu-like illness (Maes et al., 2012) (Morris & Maes, 2013). It is known these cytokines can impact tight-junction protein causing leakiness in the gut and in the blood brain barrier and correlate strongly with sickness behaviour of fatigue and malaise commonly experienced during viral infections. (Morris et al., 2013).

- *Cytokine network analysis*

In an analysis of the cytokine networks of CFS, Broderick and colleagues studied the co-expression of interleukins: 1α, 1β, 2, 4, 5, 6, 8, 10, 12, 13, 15, 17, 23, IFNγ, lymphotoxin-α and TNFα and found distinct modules signalling a shift in the paradigm of Th1, Th2, and Th17 responses of CFS patients versus healthy controls (Broderick et al., 2010). Th1 responses promote inflammatory cytokines secreted by innate immune cells and the activation of cytotoxic T cells as well as natural killer cells (Segerstrom & Miller, 2004), Conversely, Th2 responses produce anti-inflammatory cytokines, which promote humoral immunity by differentiation of B cells into antibody-secreting B cells and antibody class switching to IgE (allergy response). Associated cytokines belong to Th1 and Th2 and typically inhibitory of one another and high anti-inflammatory response reduce the risk of inflammation but can allow existing intracellular infections to persist if there are not adequately cleared.

The association network pattern demonstrated significant attenuation of cytokines IL-1β, IL-4, IFNγ and TNFα promoting Th1 and Th17 responses with higher expression of Th2-inducing cytokines to be responsible for driving the inflammatory milieu in CFS (Broderick et al., 2010). IL-4 concentration was observed three-fold in CFS while IL-2, IFNγ and TNFα remained unchanged. Anti-inflammatory cytokine IL-10 also increased substantially in CFS in contrast to IL-13, 17 as well as IL-5 and 6 which were diminished in the CFS network (Broderick et al., 2010) .

Interestingly this supports the bias towards a Th2 response as IL-4 demonstrates an antagonistic effect on Th1-inducing cytokines such as IFNγ and IL-2 (Brenu et al., 2011; Hornig et al., 2015). Ordinarily, IL-2 is associated with Th1 response but can also act as a growth factor for NK-cells which is are consistency found to be diminished in CFS patients (Brenu et al., 2011; Broderick et al., 2010) . Moreover, the direct antagonistic role of IL-2 on IL-17 production maintained in healthy controls was removed in CFS and in concert with IL-1β emerges as another network within CFS permissive of an IL-23/Th17/IL-17 inflammatory response (Broderick et al., 2010). A question that is remaining is what causes this disruption within cytokine networks? It may partially be answered by a decreased sensitivity to IL-12 released by macrophages and dendritic cells during viral infection. Normally IL-12 production stimulates Th1 differentiation driven by IL-2 and their subsequent release of IFNγ and TNFα would consequently enhance NK activation and

proliferation during viral clearance. By contrast, in CFS recurrent viral infection may be as a result of reduced NK cell cytotoxicity and elimination of virus-infected cell as shown by the lower expression of activation marker CD69 associated with a reduction in IL-2 and IFNγ in an IL-4 dominant milieu (Mihaylova et al., 2007). An earlier study in 2004 by Skowera *et al.* demonstrated increases in IL-4 producing CD4 and CD8 T cells; which together with the loss of Th1 antiviral responses may be a factor in decreased NK activity, a bias towards Th2 responses, consistent with a latent viral infection (Skowera *et al.,* 2004).

- *Cytokine profiles in early versus long-term ME/CFS diagnosis*

Pro- and anti-inflammatory cytokines have been evaluated in early cases (< 3years) of ME/CFS and compared with long-term patients (> 3 years) demonstrating a significance of disease progression in cytokine analysis (Hornig et al., 2015). An immune response was noted by IFNγ associated with CD4+ and CD8+ T-cell, and NK cell activity in the early phase, with decreased CD40L expression. CD40L is necessary for B cell class switching; and its deficiency causes susceptibility to infection triggering progressive neurologic and cognitive decline (Bishu et al., 2009). In long-term cases many cytokines were reduced below levels found in healthy control (Hornig et al., 2015). Elevated TGFβ has emerged as the most consistent finding based on a meta-analysis (Blundell et al., 2015). Montoya and colleagues have studied the association of 51 cytokines with disease severity and found that 13 pro-inflammatory cytokines may contribute to long term immunological changes. None of these were statistically higher in ME/CFS, but measurement for severe patients were found to be in the higher range for controls, whereas mild/moderate cases were in the lower range (Montoya et al., 2017). This may explain why past studies using heterogenous CFS criteria have yielded confusing and conflicting analyses of the immune system.

Finally, increases in TGFβ in ME/CFS may have a negative effect on persistent infections, during an of the immune system to downregulate persistent inflammation. Despite its anti-inflammatory properties via the induction of T(regs), TGFβ has been found in the gut mucosa of IBD patients with active disease (Shen et al., 2015) and thus ongoing pro-inflammatory milieu observed in ME/CFS may alters its role (Morikawa et al.2016). Interestingly mice with T-cell targeted inactivation of TGFβ signally develop systemic autoimmunity with spontaneous colitis highlights the importance of the TGFβ signalling pathway in immunity (Gorelik & Flavell, 2000). Also the higher prevalence of Non-Hodgkin's Lymphoma in older ME patients may result from immunosuppression by TGFβ and

upregulation of CD70 expression which is found to inhibit T cell memory effector function referred to as T cell exhaustion (Yang et al., 2014). These defective CD8+ T cells do not produce cytokines such as IL-2 and lose their ability to proliferate during chronic viral infection (Wherry, 2011). Severity of CD8+ T cell exhaustion also depends on the viral load (Wherry, 2011). Decreased CD8+ responses to the lytic phase of EBV reaction in virus-infected B cells have been found during all stages of Multiple Sclerosis (MS) and in CFS patients highlighting impaired viral immunity (Loebel et al., 2014; Pender et al., 2017).

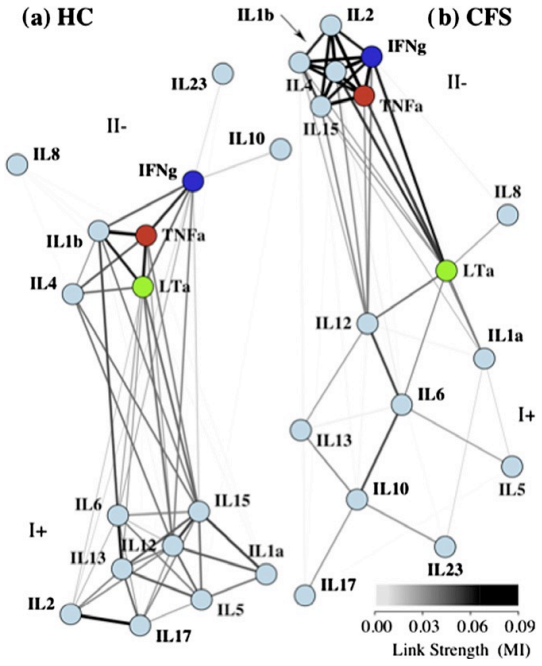

Fig. 1.1.11 Formal analysis of plasma cytokine networks in 40 female Chronic Fatigue Syndrome patients and 59 female Healthy Controls. HC and CFS display significantly different network topologies than expected by chance; CFS cluster II- being more "hub-like" design integrating a distinct subnetwork in CFS consisting of cytokines: Il-1b, 2, 4, IFNγ, and TNFα. Note cytokine nodes in CFS cluster I+ are more sparsely connected compared to HC. Figure obtained from (Broderick *et al*., 2010).

Macrophages stimulated by IFNγ during an ongoing pro-inflammatory response produce neopterin, a marker of cell-mediated immunity and indicator to ongoing oxidative stress (Murr et al., 2002). Interestingly some evidence has been found for increased IFNγ production and elevated neopterin in ME/CFS, as well as IL-12 associated with Th1 immune response and positively correlated with fatigue and flu-like symptoms (Morris & Maes, 2013a). One study that has separated ME from CFS using PEM lasting longer than 24 hr as

the hallmark symptom of ME showed that ME patients had higher levels of IL-1, TNFα and compared to the CFS (Maes et al.,2012).

- *Natural Killer (NK) cell deficiency*

In addition to cytokine profiles, immunophenotyping of peripheral blood mononuclear cells (PBMCs) has shown various of immunological abnormalities in ME/CFS patients with significant increases in IL-10, IFNγ, TNFα, and reduction in cytotoxic activity of NK and $CD8^{+}$T cells (Brenu et al., 2011). Reduced cytotoxicity in NK cells has been found in ME/CFS and has been attributed to an ongoing virus infection, although this has not been consistently found across all studies (Rivas et al. 2018). This may be down to technical factors some as using fresh whole blood versus frozen PBMCs as well as the time taken to analyse the sample in which small molecule such as cytokines may diminish in concentration (Rivas et al., 2018). CD69 expression is lower in ME/CFS and normally functions to stimulate T cell and NK cytotoxicity (Mihaylova et al., 2007) . Indeed, perforin expression has been found lower in patient compared with healthy controls, and is intrinsic to NK cytotoxic effects since it enables membrane disruption to cells targeted by NK cell to allow granzymes to enter and cause apoptosis (Baran et al., 2009; Mihaylova et al., 2007). Finally, a recent article has failed to reproduce previous findings regarding altered NK function which brings it to question any potential use of NK activity and other immunological abnormalities as a diagnostic marker in ME/CFS (Theorell et al., 2017).

- *Virus Infection*

Infectious mononucleosis, IM (*Glandular Fever*) bears resemblance to CFS but is usually self-limited to recovery within 12 weeks after onset. Typically, around 25% of teenagers and young adults infected with the Epstein Barr Virus (EBV) will go on to develop infectious mononucleosis and a further subset of these cases will also develop CFS after recovery from initial infection, suggesting that CFS may be a prolonged mononucleosis syndrome. EBV infection is common across the population, but the infection usually passes silently in most people without any obvious clinical symptoms. The virus initially targets mucosal epithelium before gaining entry to memory B cells, after which life-long latency usually ensues and is controlled by NK and $CD8^{+}$ T cell responses. However, the virus may be reactivated and emerge in immune suppressed individuals. The frequency of EBV detection in those with no history of infectious mononucleosis shows that most individuals acquire

adaptive immunity, with the frequency of detection in CFS being no different to the rest of the general population. The idea that EBV is responsible for causing CFS remains controversial. Moreover, viral load and serological responses detected in CFS are inconsistent and are not helped by the use of different viral antigens in different serological assays (Bansal *et al.,* 2011). CFS patients have demonstrated a mixture of enhanced and diminished specific antibody titres towards EBV suggesting possible latent reactivation caused by immune dysfunction in these patients. Diminished NK cytotoxicity and reduced NK-derived perforin production remain concurrently reported and specific to CFS (Brenu *et al.,* 2013), suggesting chronic immune activation by viral infection may be responsible for clonal exhaustion and subsequent depletion of memory T cells (Maher *et al.,* 2005). Regulatory T cells are seen to be increased in ME/CFS and may hinder antigen presentation by dendritic cells through interaction with CD80 and CD86 markers on the surface of DCs. Furthermore, this may contribute to the altered pattern of cytokine secretion by Th cells, favouring a type 2 immune response (Brenu et al., 2014) (Corthay, 2009; Serra *et al.,* 2003).

Despite scepticism surrounding EBV infection as a cause of ME/CFS, some evidence suggests underlying immune abnormalities and stress can promote reactivation of the virus and would likely contribute to the relapsing nature of ME/CFS. Circumstantially, the onset of symptoms with viral infections, apparent outbreaks of the illness, persistence of infections in ME/CFS individuals and beneficial treatment of EBV and human herpesvirus 6 infection is consistent with an immune response to infection. Abnormalities within the HPA axis occur in CFS and can be affected by physical and psychological stressors e.g. anxiety and depression. This could play a role in ME/CFS pathogenesis as glucocorticoids secreted as part of the signalling axis are known to drive Th2 polarity and furthermore could support the latent reactivation of EBV leading to chronic recurrent viral infection (Webster *et al*., 2002). Relentless exposure to virus infection is likely to drive $CD8^+$ T cells to exhaustion and may be further exacerbated by high levels of IL-10 (Angelosanto & Wherry, 2010). An example is HIV infection where IL-10, IFNγ, and TNFα correlate with chronic infection and viral load (Couper *et al.,* 2008).

A recent publication exposed deficient EBV-specific B- and T-cell responses in CFS patients [Loebel *et al,* 2014]. Serum IgG derived from long-lived plasma cells can persist years after primary infection. Therefore, the authors looked at the memory B cell function, *in vitro,* toward specific EBV antigens and found low to undetectable antibody responses against

EBNA-1 and VCA antigens in 76% of CFS patients despite normal titres of IgG antibodies to VCA found in serum. This could represent an inability to generate significant numbers of EBV-specific memory B-cells during primary infection or loss of memory B cells in ME/CFS. EBV-specific T cell responses were analysed after stimulation with fragments consisting of overlapping 15-mer peptide derived from EBNA-1 protein normally expressed during early latency phase. Frequency of EBV-specific CD4 and CD8 triple producing $TNF\alpha^+$, $IFN\gamma^+$, $IL\text{-}2^+$ memory T cells were significantly lower in 58% of cases (n=23) than the non-fatigued control group (n=17).

Vast numbers of studies have assayed for sero-prevalence of viral DNA using RT-PCR and conducted sero-analysis of antibodies to different viral antigens leading to mixed results (Bansal *et al*., 2011). However, no evidence linking a single pathogen, viral or bacterial, to causing ME/CFS pathology has been found. Instead, CFS may be caused by an aberrant response to infection (Hickie *et al.,* 2006) therefore, multiple viral infections may perpetuate a chronic persistent immune activation by exploiting the Th2 bias and disruption to NK cytotoxic function.

- *Summary*

There is no consistent cytokine profile in ME/CFS. Nevertheless, there is a tendency for IL-1, IL-2, IL4, IL-10, IL-17A, IFNγ and TNFα to be elevated in ME/CFS patients particularly with respect to illness (Hornig et al., 2015) . Given the high prevalence of GI symptoms in ME/CFS it is interesting to note proinflammatory cytokines, IL-1, TNFα are also found at high levels in patients with inflammatory bowel disease (Strober & Fuss, 2011). Reduced natural killer (NK) cell activity is a common observation in ME/CFS, with multiple studies reporting elevations in $FoxP3^+$ Tregs which may further limit NK cell activity (Brenu *et al.,* 2013b). The cause for this elevation Tregs and heightened IL-10 production is unknown but could represent a counter mechanism to attenuate pro-inflammatory responses during chronic persistent infection in ME/CFS.

1.7 Autoimmunity in ME/CFS

No consistent autoantibodies have been identified in all ME/CFS patients, with those that have been identified overlapping with other autoimmune disorders. Mild to moderate improvement in 67% CFS patients (10/15) was seen treated with Rituximab®, an anti-CD20 B cell depletion therapy (Fluge *et al.,* 2011). This drug works but causing targeted depletions of the CD20 B cell population with a delayed response of 2-7 months before both self-reported and physician-assessed fatigue scores were significantly improved. The trial authors speculate delay in clinical response is due to the gradual elimination of serum autoantibodies (Fluge *et al.,* 2011). Prior to this finding, increases in the naïve/transitional B cell population had been reported in a study by Bradley and colleagues, as well as marked depletion in the plasmablasts.

Blood taken from 56 ME/CFS patients and 37 healthy controls, show ME/CFS may be characterised by increased levels of plasma peroxides and serum oxidised LDL (oxLDL) antibodies which demonstrate ongoing oxidative stress caused by chronic immune activation (Maes et al.,, 2011). Evidence is emerging that many ME/CFS patients have increased levels of oxidative stress following exercise (Jammes et al., 2005). Interestingly there have been reports of autoimmune responses in some ME/CFS patients against self-epitopes as a result of damage caused by intermediate reactive oxygen species (ROS) from immune processes. These include components of lipid membrane, palmitic, myristic and oleic acid, and anchorage molecules, S-farnesyl-L-cysteine which undergo conformational changes, presenting to the immune system as neoepitopes (Maes et al., 2006; Morris & Maes, 2014). ROS are essential for killing of bacterial pathogens, however overproduction or inadequate removal of these intermediates by redox pathways may cause significant tissue damage and disruption to the intestinal epithelial barrier (Aviello & Knaus, 2017). These observations in ME/CFS posit the theory that chronic immune activation and ROS cause self-epitopes to be damaged and become a target for the immune system (Morris et al., 2014; Morris & Maes, 2013a). Microbial infection may drive chronic inflammation and cause autoimmune cross-reactivity by a process of molecular mimicry explained by sharing of amino acid sequence homology between bacterial antigens and host self-antigens leading to autoantibodies targeting both (Morris & Maes, 2013a). Increased bacterial translocation is increasingly evident as a result of increased intestinal permeability now demonstrated several human diseases including Crohn's disease and in liver cirrhosis (Pastor-Rojo *et al.,* 2007; Pijls *et al.,* 2013).

Autoimmune reactions lead to inflammation, increased permeability of blood vessels and migration of lymphocytes to sites of injury that contribute towards patient fatigue and malaise (Maes et al., 2013). The nature of the stimuli and antigen(s) responsible for generating any auto-antibodies in ME/CFS remains to be determined. Several autoantibodies have been documented in ME/CFS patients however, the profiles vary between patients. The most interesting are anti-5-HTA receptor antibodies since the majority of serotonin is produced in the gut (Maes et al., 2013). Additional evidence supports a subset of ME/CFS (29.5%) patients have antibodies against one or more M acetylcholine and β adrenergic receptors (Loebel et al., 2016). Remarkedly those patients with elevated antibody levels pre-treatment of Rituximab were the majority of clinical responders; their total IgG, IgA and IgM levels post-treatment were lower, but not significantly different compared to non-responding patients (Loebel et al., 2016). The presence of these antibodies is not disease specific but have been found in autoimmune diseases that share common features with ME/CFS including fatigue and autonomic dysfunction. An example is postural orthostatic tachycardia syndrome (POTS) is estimated to affect 10-20% of CFS patients, where β1 and β2 adrenergic receptor antibodies have also been reported, as well as in orthostatic hypotension cases (Thieben et al., 2007; X. Yu et al., 2012).

- *Infection elicited autoimmunity*

It is known that microbial-derived stimuli can influence the nature and function of immune cells in the intestinal mucosa, and when dysregulated can lead to systemic inflammation (Strober, 2013; Maloy & Powrie 2011; Tanoue et al., 2010). For example, Guillain-Barre (GB) syndrome has been associated with certain bacterial infections including Campylobacter *jejuni*, Haemophilus *influenza* and Mycoplasma *pneumonia* (Heikema et al., 2010). LPS exhibit structural homology to human gangliosides, found chiefly on neuronal ganglia that are major constituents of neuronal cell membranes, and are possible target for cross-reactive antibodies found in the serum of GB patients in response to bacterial infection (Nishimura, 1996). Reactive arthritis (ReA) has been strongly associated with the HLA-B27 allotype and is triggered by diverse bacteria (Alvarez-Navarro 2013). HLA-B27-restricted epitopes of bacterial and self-antigens cross-react to activate cytotoxic lymphocytes and therefore play a role in ReA. The role of HLA-B27 in inflammatory rheumatic diseases also highlights the importance of HLA allotypes being factors in autoimmune disease.

Both viral and bacterial infections have long been associated with pathogenesis in autoimmunity, notably mycoplasma infection in Rheumatoid Arthritis (RA). Mycoplasma-derived antigens are capable of generating cytotoxic cross-reactive effector lymphocytes, which upon isolation from the synovial tissue of RA patients bear the same receptor-targeted specificity to Mycoplasma arthritidis antigen (MAM) (Oldstone, 1998; Cole et al., 2000; Sherbet, 2009). The occurrence of viral infection preceding onset of autoimmunity has been recognised in ME/CFS patients (Morris et al., 2013), and in type 1 diabetes (van der Werf et al., (2007). However, it is difficult to dissect and validate the mechanisms, e.g. molecular mimicry, by which viruses generate autoimmunity.

Reduced cytotoxic T-cell responses to EBV can also increase activating autoreactive B cells as a result of exposure to gut-derived microbial antigens that induce chronic inflammation and T cell exhaustion (Loebel et al., 2014). Blomberg and colleagues have reviewed various aspects of the ME/CFS and suggest a mechanism of microbial infection driving autoimmune processes which impacts on the severity of ME/CFS symptoms (Blomberg et al., 2018). Emerging data supports disruption to intestinal microbiome in ME/CFS and changes in intestinal permeability that are likely to have negative consequences for mucosal tolerance to commensal bacteria as well as wider implications for the immune system that have not yet been explored in ME/CFS.

1.8 The Human Intestinal Microbiota

Intestinal microbes represent the greatest concentration of microbes than any other area on or in the human body whose genetic repertoire (the microbiome) is estimated between 2-20 million genes which vastly exceeds the genetic information of the ~20,000 genes representing the human genome (Kurokawa et al., 2007). Most are bacteria, consisting of more than 1000 different species whose inhabitancy affording functional benefits have become fully integrated with biological pathways controlling our metabolism, immune system, neuro-endocrine system, and development of the brain and central nervous system (Heijtz et al., 2011; Kawamoto et al., 2014; Qin et al., 2010; Round & Mazmanian, 2009; Sudo et al., 2004). Initial colonisation of the intestinal tract occurs immediately after birth and is dominated by *Bifidobacterium* species belonging to the phyla *Bacteroides* and runs in parallel with the developing mucosal immune system (Rodríguez et al., 2015). Data from the Human Microbiome Project classifies intestinal bacteria into 5 distinct phyla, listed here from highest to lowest proportional abundance: *Firmicutes*, *Bacteriodetes*,

Actinobacteria, *Proteobacteria* and *Verrucomicrobia*, the only representative of this last phyla in humans being an intestinal species called *Akkermansia muciniphila* (Li et al., 2014). Members belonging to *Firmicutes* (F)and *Bacteroides* (B) contribute approximately 92% of the microbiota (Eckburg et al., 2005). The ratio of F:B in infants begins at 0.4 (3 weeks to 10 months) , evolving to 10.9 in adulthood (25-45 years old) and declining towards 0.6 in the elderly (70-90 years old) (Mariat et al., 2009). The average person's faecal samples contains approximately 160 different species and regardless of the variation in diversity and composition of the intestinal microbiota between different people, there is similarity in their metabolic statuses, which may be more important in defining aspects of health (Huttenhower et al., 2012; Moya & Ferrer, 2016; Rodríguez et al., 2015). For example, a core microbiota of 57 species has been reported to exist in more than 90% of individuals which suggests these species have critical metabolic functions (Qin et al., 2010). However, defining the composition of a 'healthy' microbiota is complex due to variations in host genetics, diet, lifestyle, age, fitness, stress, geographical location, antibiotic exposure and history of infections, between individual persons (Huttenhower et al., 2012). This variability in the composition of the microbiota from person to person and in disease versus healthy will influences it the metabolic and immunological functions and has driven interest in defining the role of individual species involved in these processes (Rowland et al., 2018). Specific members of microbiota stimulate an equilibrium between pro- and anti-inflammatory immune responses to control diversity and growth of bacterial populations. Altering the composition of the microbiota, through diet, stress, mediations, antibiotics exposes it to possible pathogenic bacteria which promote inflammation and outgrowth over members of the community (Baümler & Sperandio, 2016).

Compositional differences within the profile of gut bacteria have been observed in several human diseases, including ME/CFS, when compared to healthy subjects (Bajaj et al., 2014; Carding et al., 2015; Clemente et al., 2018; Giloteaux et al., 2016; Joossens et al., 2011; Norman et al., 2015; Quigley, 2018). Most strikingly, these observations are not limited to GI disorders such as IBD and IBS (Carding et al., 2015). There is increasing evidence to suggest intestinal bacteria contribute towards systemic chronic inflammatory-based disorders such as obesity, metabolic disorders have now been linked to changes in gut permeability, immunity and the composition of this microbiota referred to as gut dysbiosis (Carding et al., 2015; Fasano, 2012).

The function of the intestinal microbiota is largely mediated through diet. The composition of the diet can substantially alter growth of specific members microbiota as well as its metabolic activity which influences availability of bacterial-derived metabolites to the host. For example, SCFAs are the products of fermentation of dietary fibres which can reduce the pH affecting the growth of pH-sensitive species (*Escherichia coli* and *Salmonella spp*.) within the intestine (Cherrington et al., 1991). SCFA production is reduced by the consumption of high levels of animal saturated fats from meat, and low complexity (refined) carbohydrates (David et al., 2014). Moreover, refined sugars increases the risk of opportunistic pathogen colonisation, e.g. *Clostridium difficile* and *Clostridium perfringens* (Brown et al., 2012). High sugar consumption has been shown to elevate *Enterobacteriaceae* associated with brain and intestinal inflammation and deficits in cognitive capabilities in hepatic encephalomyelitis which is seen as a complication of liver cirrhosis associated with endotoxin exposure and increasing intestinal barrier dysfunction (Bajaj et al., 2012). SCFAs are relevant to inflammatory disorders since the can support immune tolerance by promoting anti-inflammatory responses towards commensals of the intestinal microbiota and have been shown to reduce inflammation in the dextran sulfate sodium (DSS)-induced colitis mouse model (Atarashi et al., 2011). As we age the composition of the microbiota changes towards an increased abundance of *Bacteroidetes* and *Clostridium cluster IV*, however, the capacity to produce SCFAs appears to be reduced and is understood to contribute to the increasing pro-inflammatory tone as we age (Biagi et al., 2010; Claesson et al., 2011; Frasca & Blomberg, 2016). SCFAs also act as signalling molecules via activation of GPCRs, GPR41 and GPR43 also called FFAR2 which have been associated with in reducing pro-inflammatory cytokines; and affecting pathway involved in epithelial integrity, fatty acid oxidation via the activation HDAC (Kimura et al., 2014; Vanhoutvin et al., 2009; Waldecker et al., 2008).

- *Intestinal microbiota and mucosal immunity*

The gut-associated lymphoid tissue (GALT) is home to the majority of immune cells in the body, containing over 70% of the immune system (Vighi et al., 2008). A key function of the immune system is to discriminate between the threat of pathogens and commensal (non-pathogenic) members of the microbiota. To that end, there are several mechanisms the immune system employs which help shape the intestinal microbiota and limit pathogen colonisation.

GF mice has proven valuable in understanding how the intestinal microbiota influences the developing immune system and sets the inflammatory tone through mediating the balance of pro and inflammatory mechanisms. GF mice are more susceptible to pathogen infections compared to conventional mice and have fewer intestinal antigen-presenting cells (APCs) and defects in gut-associated lymphoid tissues (GALT) compared with SPF mice (Kim et al., 2017). Lymphocytes structures for presentation of antigen, for example Peyer's Patches (PP) and mesenteric lymph nodes (MLN) are sites for , are missing in GF mice but can be restored with intestinal bacteria, or PGN derived from Gram-negative bacteria (Bouskra et al., 2008; Falk et al., 1998).

The microbiota regulates the differentiation of T helper (Th) cells and therefore the balance of T(reg) and Th1/Th2/Th17 subsets which respond accordingly to the presentation of bacterial protein antigens via MHC complexes on dendritic cells (DCs) and macrophages (Mϕ) patrolling the lamina propria (Kim et al., 2017). Figure 1.1.12 summaries the functions of each T cell subset and its associated cytokine profile and transcription factors. TLRs are also present on the apical surface of intestinal epithelial cells exposed to bacterial antigens and are themselves significant producers of cytokines contributing to the cytokine milieu (Akira & Hemmi, 2003). The cytokine environment is important as it will influence the activation of a particular T cell subset upon antigen presentation. For example, under normal circumstances, antigen presenting cells (APCs) reside within PPs and produce significant amounts of anti-inflammatory IL-10 to promote T(reg) differentiation and immune tolerance (Iwasaki & Kelsall, 1999). Moreover, Mϕ cells do not produce pro-inflammatory cytokines upon activation of TLRs by common bacterial antigens such as LPS (Smythies et al., 2010).

In addition to the defects in secondary lymphoid structures, GF mice have significantly fewer CD4+ T cells in the lamina propria which an imbalance towards a Th2 immune response (H. J. Wu & Wu, 2012). In addition to SCFA production, specific members of the microbiota are known to induce T(reg) cells which include those belonging *Clostridia clusters IV* and *XIVa* (Atarashi et al., 2011), polysaccharide A of *Bacteroides fragilis* (Telesford et al., 2015), and *Faecalibacterium praunitzii* (Qiu et al., 2013). However, there are also certain groups of bacteria such as segmented filamentous bacteria (SFB) are capable of elicit higher numbers of Th1 and Th17 cells critical in the induction of autoimmune pathogenesis and the acceleration of experimental autoimmune

encephalomyelitis (EAE) (Forbes et al. , 2016; Lee et al., 2011). Further close protection of the epithelial barrier is afforded by a specialised class of immune cells, called innate lymphoid cells (ILCs) whose role includes the release of IL-22 during infection and in addition to its association with Th17-mediated inflammation, is it protective and counter-active in IBD of mice (Zenewicz et al., 2008).

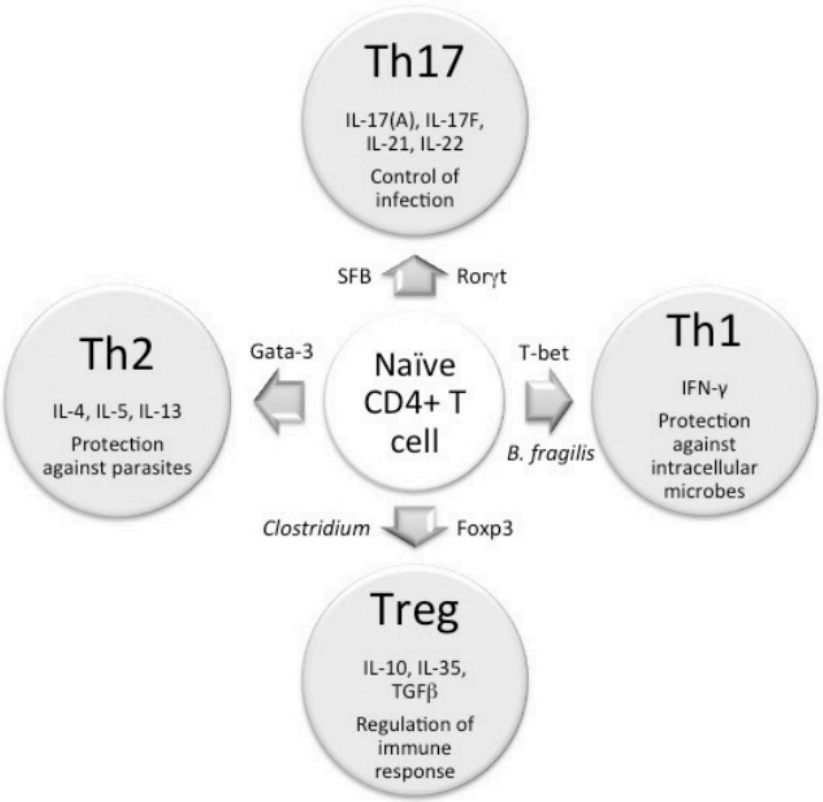

1.1.12 Commensal bacteria induce T cell differentiation. Each T cell subset is defined by its own transcription factor associated cytokine production. Th1 responses are critical in responding to intracellular infections, whereas Th2 is associated in allergy responses. Th17-mediated inflammation controls infection but also has been attributed to the pathophysiology of several chronic auto-inflammatory disorder, including IBD. T(reg) cells induce tolerance and inhibit T cel differentiation into the other subtypes. Several beneficial intestinal bacteria are known to stimulate T(reg) responses which control inflammation. Figure reproduced from (Wu & Wu, 2012).

In addition to stimulating T(regs), secretory IgA (sIgA) enables the immune system to coordinate a response without causing inflammation and protect the epithelial barrier from invasion. Further evidence that single strains of bacteria can alter the balance of pro- and anti-inflammatory responses was demonstrated in probiotic treatment with *Lactobacillus*

kefiri CIDCA 8348 in Swiss mice for 21 days increased the production of faecal IgA and moreover stimulated IL-10 (Carasi et al., 2015). The production sIgA can occur through T cell-dependent and T cell-independent pathways. DCs and Mϕ present antigen to naïve B cells at Germinal Centres (GCs) for interaction with Th cells in order to effect differentiation and class switching to become IgA secreting plasmablasts before homing to the intestinal lamina propria as resident IgA producing plasma cells, figure 1.1.13 (MacPherson et al., 2008; Macpherson & Uhr, 2004). IgA production is another feature compromised in GF mice as a result of poor maturation of naïve B cells and underpins the requirement for exposure to intestinal microbes to coordinate commensal-specific IgA production and may also contribute to intestinal barrier defects (Kim et al., 2017). IgA responses are induced following the introduction of commensal bacteria to a reversible colonisation of GF mice however, following repeated dosage of commensal bacteria, IgA responses were in recognition of the exposure of microbes at that time and therefore IgA induction lacks immunological memory or prime boost effect as is the case with systemic vaccination (Hapfelmeier et al., 2010).

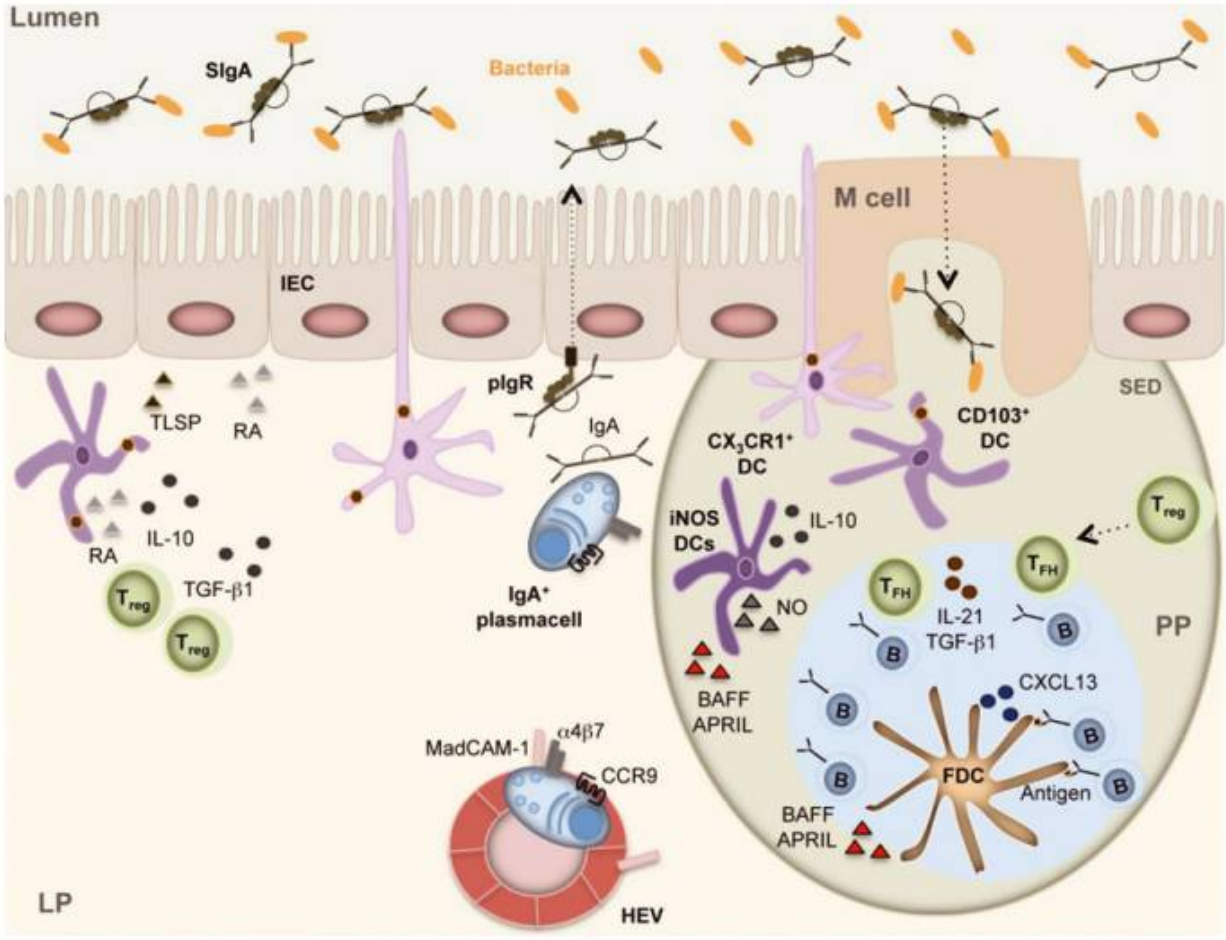

⇐ **Figure 1.1.13 Induction of Immunoglobulin A at Peyer's Patches (PP).** Specialised epithelial cells, called M cells, capture luminal antigens at PPs for uptake by CD103+ dendritic cells which migrate within the PP to establish contact with CD4+ T(regs) cells which remain tolerant to the commensal microbiota and support IgA-production. This response requires DC-derived retinoic acid, TGFβ, IL-10 for T(regs) to differentiate into T-follicular (Tfh) helper cells which interact with antigen-specific naïve B cells to become activated. Once activated B cells then migrate towards the follicle (blue area) where they interact with follicular dendritic cells which retain antigen, enabling rapid expansion of B cells and induction of SHM, IgA CSR and affinity maturation in response to CD40L, IL-21 and TGF-β secreted by Tfh cells. IL-10, retinoic acid further enhances this process and IgA production within the germinal centre by inducing gut-homing markers on B cell, such as α4β7 and CCR9. B cells eventually differentiate into plasmablasts and long-lived plasma cells within the lamina propria that secrete IgA which following pIgR-mediated transcytosis across the epithelial barrier comes into contact with luminal microbes. Figure and description adapted from (Gutzeit, Magri, & Cerutti, 2014).

- *Microbial-neuro-immune interaction*

Afferent vagal neurons are in close contact with the mucosal and display receptors for common signalling molecules such as cytokines that are released from activated immune cells such as macrophages. The explanation therefore for sickness behaviour during infection is best explained as cytokine-mediated activation of the vagus nerve in response to inflammatory changes. In these instances, peripheral cytokines influence the CNS are coupled with mucosal production of other inflammatory mediators many effective upon receptors expressed on enteric neurons such as TNFα receptors, overall facilitating sensitization and perception of abdominal pain via afferent neurons which innervate the gut wall (Mayer, 2011). The basic mechanisms of sensing the microbiota, primary neurons of the ENS, immune cells and enteroendocrine cells are at the forefront of signalling in the gut-brain axis linking functionality of the HPA axis, the neuroendocrine system and the immune system together in gastrointestinal function.

Neuronal signalling is a vital component for modulating immune responses at the intestinal epithelial barrier - particularly controlling mucosal inflammation. Enteric neurons express TNFα receptors (TNFR1 and R2), but neuropeptide Y (NPY) KO mice produce less endogenous TNFα compared with wild-type mice; which has been shown to activate expression of NYP in the ENS leading to changes in intestinal permeability (Chandrasekharan et al., 2008). NPY has a role for pro-inflammatory effects in the GI tract

and is shown to induce changes in permeability via tight-junction protein, claudin-2 (Chandrasekharan et al., 2008). Enteric neurons also express PPR immune signalling receptors, including Toll-like receptors 2, 3, 4 and 7. Mice lacking expression of TLR2 and TLR4 exhibit defects within the architecture of their ENS, abnormal mucosal secretion and reduced motility, where similar to mice with a depleted microbiota; however Tlr2(-/-) mice developed more severe form of colitis than wild-type mice following SSD treatment (Brun et al., 2013) As a consequence of an underdeveloped ENS, TLR2 KO mice exhibited severe colitis supporting the notion that intestinal microbes are necessary for enteric development and maturation of the mucosal immune system later in life (Sharkey & Savidge, 2014).

1.9 Stress and neuroendocrine manifestations in ME

Psychological stress is a critical factor in the pathological development and maintenance of ME/CFS symptoms. As well as reports of flu-like illness preceding ME, significant life events hyper-activate the stress response through cortisol production as well as from the pressure to perform well at work or school and to succeed. Individuals of this kind are highly ambitious and competitive and have a desire to feel in control with a direction in their lives. However, many ME/CFS patients appear to reach a state of burnout and are unable to fully recover and become increasingly distressed and anxious as well as physically exhausted in pursuit of great expectations. Emotions and negative thoughts lead to further stress, underpinning a psycho-biological mechanism (figure 1.1.5, page 40), this is likely to become self-perpetuating as the stress of not being able to recover and return to normal life will have negative effects on the immune system and consequently the gut microbiota and gut barrier. Thus, the characteristics of inability to rest and unwind, may represent dysfunction within the negative feedback pathways integrated with HPA axis, immune system and the central nervous system.

Further symptom-based evidence for altered stress-responsivity manifests within post-exertional malaise, the main symptom of ME/CFS which highlights the effect physical and psychological stressors endure on patients. Patient's undertaking any form of physical or mental challenge can expect severe worsening of their symptoms after an initial delay of 12 hours or more in severe ME/CFS. Interestingly, the delay in the effect of PEM is an unusual phenomenon as it is not symptom that has been associated with any other disease, other than ME. Speculatively, PEM may represent a variation of stress response regulated by the

HPA axis. Dysfunctional HPA-axis is also substantiated further by symptoms of cold hands and feet since the hypothalamus regulates the body temperature. Usually body temperature is elevated in response to peripheral infection, but is not in ME/CFS, potentially a weakness in developing infections or allowing reactivation of latent infections such as EBV (Bansal, 2016). Finally, HPA dysfunction is also implicated in the pathophysiology of anxiety and depression and ongoing low-grade chronic inflammation in these conditions.

1.10 Intestinal microbiota impacts neuropathology

Neurological and neuropsychiatric illnesses are strongly linked to intestinal dysbiosis and physical and emotional stressors (Cryan & Dinan, 2015). In addition to immunomodulation, intestinal microbiota can influence the ENS and communicate with the CNS to alter animal behaviour and social stress. This has been demonstrated by faecal microbiota transplantation (FMT) from depressed patients into GF rats inducing alterations in tryptophan metabolism and characteristics of depression, such as increasing anxiety and anhedonia (Kelly et al., 2016). For instance, lactic acid producing bacteria (LAB) are known produces of GABA. Moreover, *Lactobacillus rhamnosus* (JB-1) induces GABA receptor expression throughout the brain, but is dependent of neuronal transmission between the intestine and brain via the vagus nerve, just as the effect of Bifidobacterium longum since its anxiolytic action was blocked in vagotomised mice (Bercik et al., 2011; Bravo et al., 2011). Stress is implicated in hyperactivity and hyperresponsivity of the amygdala (the brain centre for emotions and emotional behaviour) and upregulation of CRF expression and is concomitant with a lack of inhibitory control by GABA neurotransmitter signalling. Such dysfunctional GABAergic signalling is associated with anxiety, depression and schizophrenia and abnormal HPA dysfunction (Wang et al., 2016). Glucocorticoid production by the HPA regulates GABA receptor expression and induces atrophy in GABAergic neurons in early life development, thus chronic activation of the HPA contributes to stress and mood disorders by blocking inhibitory GABA feedback in the amygdala (Wang et al., 2016).

There are other factors that may compound dysbiosis such as leakiness of the gut epithelial barrier which is known to be impacted by chronic stress. The enteric nervous system responds to CRF to change gastrointestinal functions during stress events which include during response to pathogen infection. This can heighten visceral pain perception, and to

stimulate inflammatory responses within the gut and CNS. In addition to vagal nerve stimulation, sensory neurons within the ENS can sense specific molecular patterns of molecules expressed on commensal bacteria via TLRs, providing feedback to the brain and immune system. Given the high frequency of GI disease in neurological and neuropsychological disorders these microbiota-derived physiological inputs are emerging critical to the formation of pro-inflammatory conditions as a requisite to developing (and progressing) autoimmune disorders affecting the brain and CNS.

MS is a chronic autoimmune inflammatory disease driven by autoreactive T cells causing demyelination of the CNS. It manifests with similar neurological impairment and gradual degeneration presented in ME/CFS with symptoms including muscle weakness, paresthesia, fatigue, cognitive impairment, numbness and relapsing (flares) and remitting nature affecting the CNS. In addition to genetic susceptibly, the state of the composition intestinal microbiota is emerging as a contributor towards risk of developing autoimmune disease. Clinical studies on patients with relapsing-remitting (RR) onset Multiple Sclerosis (MS) exhibit differences in the composition of intestinal microbes at the taxonomic level compared with healthy controls (Chen et al., 2016; Jangi et al., 2016; Miyake et al., 2015). In a cohort of Japanese patients, these taxa comprise of significant changes to 21 species, of which a depletion of 19 was in RR MS samples; 14 belonging to *Clostridia clusters XIVa* and *IV*.

In terms of the richness, the number of species the MS patients (α-diversity) did not differ from healthy controls, unlike in IBD which is characterised by significantly lower species richness (Gong et al., 2016). Therefore, intestinal dysbiosis in MS appears distinct from other inflammatory disorders which have lower α-diversity. In a separate study, species richness also did not separate RR MS from healthy controls, rather active disease patients compared to RR MS showed decreased species richness and warrants further longitudinal studies to determine if and how compositional changes within the intestinal microbiota relate to progression of MS or enhance its severity, or frequency of relapses (Chen et al., 2016).

Interestingly there is very little overlap between the *Clostridia species* found reduced in RR MS and those that have been documented in IBD (Atarashi et al., 2013). *Clostridia* are known producers of Short Chain Fatty Acids (SCFAs), particularly butyrate which is a used as an energy source and stimulates anti-inflammatory responses and induction of colonic

T(regs) in the support of immune tolerance towards commensal bacteria (Zhang et al., 2016). In experimental colitis models, SCFAs effect epigenetic changes via inhibition of histone deacetylase 1 (HDAC-1). In particular, *Faecalibacterium prausnitzii*, one of the most abundant bacteria in the intestinal microbiota found less abundant in RR MS, has been identified to regulate Th17/T(reg) differentiation by inhibition of HDAC-1 which blocks IL-6/signal transducer and activation of transcription 3 (STAT3)/IL-17 pathway, causing Foxp3 induction of T(regs) and differentiation (Zhou et al., 2018). T(regs) can produce TGFβ an anti-inflammatory cytokine in order to suppress pro-inflammatory Th1/Th17 cell responses.

Peripheral events leading up to, or during the onset, and progression/exacerbation of neurological diseases are being studied. In a recent pilot study comparing the intestinal permeability of RR MS patients with 18 age and sex-matched healthy controls, the ratio of lactulose/mannitol measured in urine was significantly higher in 16/22 patients ($p=0.0284$) (Buscarinu et al., 2017). Increased intestinal permeability is a proposed mechanism for developing autoimmune disease that develops over time and in response to intestinal dysbiosis (Fasano, 2012). The interactions between intestinal microbes and the immune system in MS remain unclear and challenging to study in humans. Experimental Autoimmune Encephalomyelitis (EAE) is generated in rodents through peripheral immunisation with CNS antigens including; myelin basic protein (MBP) and myelin oligodendrocyte glycoprotein (MOG). As a result, pro-inflammatory infiltration of autoreactive T cells into the brain and CNS of mice, causing chronic inflammatory demyelination that resembles clinical aspects of MS in humans (Stromnes & Goverman, 2006).

In addition to exposure to MOG peptide, T-cell mediated neuroinflammation in EAE requires IFNγ producing Th1 cells and IL-17 and expression of $\alpha4\beta1$ integrin for extravasation across the BBB. There is some evidence to suggest systemic infections increased the chances of relapse in MS patients (Correale et al., 2006). Systemic challenge with lipopolysaccharide (LPS) is used to model systemic inflammation. The induction of proinflammatory cytokines including IL-1β, IL-6 and TNFα can influence sickness behaviour and delirium commonly associated with CNS disorders. Pro-inflammatory stimuli and ongoing CNS neuroinflammation induce cyclooxygenase-2 (COX-2) which causes astrocytes supporting the BBB to secrete prostaglandin E2 (Font-Nieves et al., 2012). The induction of fever during infection is described by the IL-6-COX2-PGE2 axis which culminates in the

activation of EP3 receptors expressed in thermoregulatory neurons within the hypothalamus to induce fever and malaise (Eskilsson et al., 2017; Evans et al.,, 2015).

B cell mediated autoimmunity may also influence RR MS since the intestinal microbiota has been shown necessary to drive autoantibody-producing B cells and for stimulating myelin-specific CD4+ T cells in the process of spontaneous RR EAE (Pöllinger et al., 2009). RR mice are transgenic SJL/J mice predisposed to spontaneously developing EAE due to increased TCR expression specific for MOG peptide 92-106 (Pöllinger et al., 2009). In contrast to induced EAE, RR mice develop the characteristic remission and relapsing nature of RR MS in humans which leads to neuroinflammation causing demyelination throughout the CNS. B cell autoantibodies enhance demyelination and severity since mice deficient in MOG antigen or with depleted B cells do not develop spontaneous RR EAE (Pöllinger et al., 2009).

Latent EBV reaction have been documented to cause serious neurological complication in paediatric patients, with long term consequences including cognitive impairment and epileptic seizure and symptoms of Alice in Wonderland Syndrome affecting sense of vision, sensation, touch, hearing and perception of one's own body (Fine, 2013). The lytic phase of EBV infection is reactivated when memory B cells undergo differentiation into plasma cells. Normally EBV-specific CD8+ T cells target EBV-infected B cells. However, defective control of EBV reactivation may facilitate generating autoreactive B cells in MS who display defective T cell control of EBV infection with a reported decrease of CD8+ T cells against lytic phase EBV (Pender et al., 2017).

B-cell targeted therapies have been trialled in CNS autoimmune disorders MS and neuromyelitis optica (NMO) despite being considered T-cell mediated (Fillatreau, 2018). Anti-CD20 therapy called Rituximab® has been successful in reducing inflammatory brain lesions and clinical relapses in RR MS during a 48-week trial in 104 patients (Hauser et al., 2008). B cell are potent cytokine produces and also antigen presenting cells, thus engagement with T cells through CD40 and produce IL-6 that enhances Th17 differentiation (Barr et al., 2012). Depletion of B cells may reduce ongoing proinflammation cytokine production as well as removing auto-reactive B cells that may contributing towards pathogenesis. For example, NMO, also called Devic's disease, is a variant of MS that represents demyelination restricted to the optic nerve and spinal cord. However, IgG1 autoantibodies produced by B cells target AQP4, an aquaporin, expressed in astrocytes to attack myelin. These autoantibodies belong to the class IgG1 and require direction of T-follicular helper cells for class switching and maturation of plasma cells of this antibody

isotype. Rituximab® clinical trials in NMO deplete B cells decreased rate and severity of relapses (Etemadifar et al., 2017).

Analysis of the intestinal microbiota in NMO patients identified enrichment at the species level of Clostridium perfringens, compared with healthy controls (Cree et al., 2016). AQP4-reactive T cells are elevated in NMO patient and specificity mapped to amino-acid residues 63-76. This immunodominant region revealed 90% sequence homology (207-216) to an adenosine-triphosphate binding cassette transporter permease (ABC-TP) expressed by C. perfringens (Zamvil et al., 2018). To put this finding into perspective, myelin-specific T cell responses in MS, reveal less sequence homology between immunodominant T-cell targeted epitopes in myelin and microbiota-derived antigens (Zamvil et al., 2018).

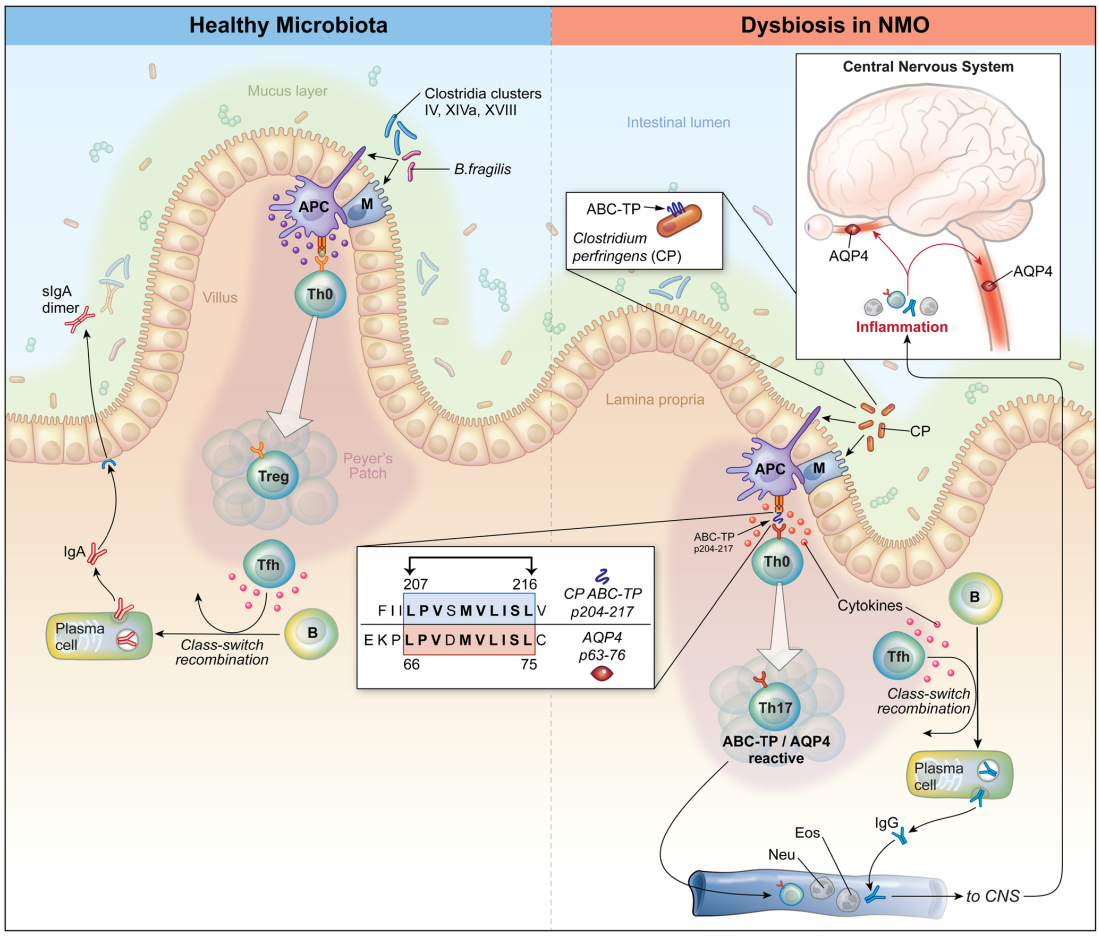

Figure 1.1.14 Pathogenesis of NMO arises from *Clostridium perfringens* molecular mimicry driving autoantibodies against AQP4 channels in the central nervous system. Bacteria become internalised by M cells at the PPs and delivered to dendritic cells which in a healthy microbiota promote anti-inflammatory cytokines and naïve T cells to different into regulatory T cells and T follicular cells which support the induction of IgA secretion. Specific IgA responses to members of the intestinal microbiota can protect against disease and inflammation (Kawamoto et al., 2014; Kubinak & Round,

2016). Overgrowth of *C. perfringens* is thought to contribute to the development of NMO, which becomes internalised by M cells for presentation to immune cells. ABC-TP(p204-217) shares sequence homology with Aquaporin 4, AQP4 (p63-76) and leads to the activation and expansion T cells which recognise both antigens (Oldstone, 1998). Dysbiosis may alter the balance between pro and anti-inflammatory T cell responses in the immune system, causing Th17-polarisation and expansion of auto-reactive ABC-TP/AQP4-specific Th17 cells which promote B cells to differentiate into antibody secreting plasma cells. These pathogenic antibodies further mediate destruction of AQP4 within the CNS causing inflammation of the optic nerves and spinal cord. Figure from (Zamvil et al., 2018).

Clostridia strains from *clusters IV*, *XIVa* and *XVIII* are considered as producers of SCFA and promote TGFβ (Atarashi et al., 2013). *C. perfringens* is not included within these clusters and may well contribute to long-chain fatty acids, similar to Segmented Filamentous Bacteria (SFB) which promote Th17 differentiation (Ivanov et al., 2009). Indeed, CD4+ T cells isolated from NMO patients are characterised by IL-17 production as well as IFNγ and IL-6, inducing Th17 differentiation (Ochoa-Repáraz & Kasper, 2018; Varrin-Doyer et al., 2012).

The intestinal microbiota strongly influences the balance between proinflammatory and anti-inflammatory immune reactions, leading to either protection or induction/progression of disease. Mice SFB induce fewer Th17 cell in the small intestine (Ivanov et al., 2009). Commensal members of the microbiota influence the balance of T(regs)/Th17 in the intestine and so it can be seen the dysbiosis would potential altered this balance. GF mice are in fact protected against EAE producing lower IFNγ and IL-17 as well as having more FoxP3+ T(regs). Re-colonisation with *B. fragilis* producing capsular polysaccharide Ag maintains protection against EAE , as well as some Clostridia species through enhanced stimulation of IL-10 producing FoxP3+ T(regs) (Atarashi et al., 2013; Ochoa-Reparaz et al., 2010). *B. fragilis* has also been shown to be effective at correcting IP in MIA offspring, and alters microbial composition to the benefit of ameliorating ASD-like behaviour and GI complications in these mice (Hsiao et al., 2013).

Intestinal permeability determined by histological sectioning of duodenum, jejunum and ileum of EAE mice show they develop increased intestinal barrier permeability preceding the onset of neurological symptoms (Nouri et al., 2014). Indeed there have been observations of increased intestinal permeability preceding clinical onset and relapses in Crohn's Disease and type 1 diabetes (Bosi et al., 2006; Fasano, 2011; Irvine & Marshall,

2000). Th1 associated proinflammatory cytokines, TNFα and IFNγ in combination with IL-17 may trigger overexpression of zonulin and disorganisation of TJs to increase intestinal paracellular transit (Nouri et al., 2014). Metabolic disorders have been well studied with an association between low-grade chronic inflammation sustained by systemic endotoxin measured in obese and diabetic mice with evidence of dysbiosis characterised by increased *Proteobacteria* abundance which are Gram negative bacteria with presence of endotoxin on their outer membrane (Rizzatti et al., 2017). Endotoxin-induced inflammation is driven microbiota dysbiosis in these animals recognised by the fact that antibiotic treatment reduced circulating endotoxin, improved insulin sensitivity, and lowered systemic inflammation and oxidative stress caused by the immune system (Cani et al., 2008; Rizzatti et al., 2017).

Epithelial tight junctions in the intestine are similar to the endothelial tight junctions of microvascular in the brain and are equally susceptible to endotoxin. Circulating endotoxin can disrupt the blood-brain-barrier (BBB) and activate microglia in the brain via PRRs leading to the recruitment of leukocytes during neuroinflammation. Preventing the extravasation of autoreactive T-cells by blocking $\alpha4\beta1$ integrin disrupts trafficking across the BBB and has yielded some clinical benefit in the treatment of RR MS.

- *aging microbiota and neurodegeneration*

There is a striking parallel between the onset of neurodegenerative disorders such as Parkinson's Disease and Alzheimer's and age-related changed within the intestinal microbiota. Age-related decline of the intestinal microbiota is associated with increasing proinflammatory cytokines and deteriorating IP in mice (Thevaranjan et al., 2017). The ageing intestinal microbiome appear to alter in composition with a reduction in alpha diversity, and increased presence of proteobacteria (Rizzatti et al., 2017). Significant decreases have been reported in *Bifidobacteria, Bacteroides,* and *Clostridium cluster IV* (Zwielehner et al., 2009).

Enrichment of *Proteobacteria* are a common observation in inflammatory conditions (Rizzatti et al., 2017). Age-associated intestinal dysbiosis may arise as a consequence of an ageing immune system (immunosenescence) and potentially enhanced susceptibility towards infections, inflammation and autoimmunity. Risk of neurological inflammatory driven pathologically increase as we age, susceptibility to diseases and increased morbidity and mortality due to low-grade inflammation caused by endotoxemia (Singh &

Newman 2011; Freund et al. 2010). The intestinal microbiota is potentially a large source of endotoxin. Concomitantly, ageing causes priming of microglial cells in the brain making them more sensitive to a secondary inflammatory stimulus (Perry & Holmes, 2014). It is not understood why this occurs during a process what is termed inflammageing; however microglial susceptible to activation by circulating pro-inflammatory cytokines caused by a systemic trigger (i.e. infection) may facilitate a leaky blood-brain barrier (BBB) and trafficking of pathogenic T cells that promote various neurogenerative conditions (Bachstetter et al., 2015; Dilger & Johnson, 2008)(Blaylock & Maroon, 2011).

- *Parkinson's Disease (PD)*

Sleep disorder, cognitive impairment and mood disturbance are common non-motor symptom in PD (Yu et al., 2018). However, the origins of Parkinson's Disease (PD) may begin in the intestine. It has been suggest that GI symptoms, particularly constipation can precede motor symptoms up to 20 years prior to diagnosing PD and may predict onset of PD (Yu et al., 2018). The production of SCFAs by the intestinal microbiota are known to modulate microglia and enhance PD in genetically susceptible mice (Sampson et al., 2016). Overexpression of α-synuclein (αSn) in these mice causes aggregation within neurons and culminates in progressive deficits in motor function as well as intestinal motility dysfunction (Sampson et al., 2016).

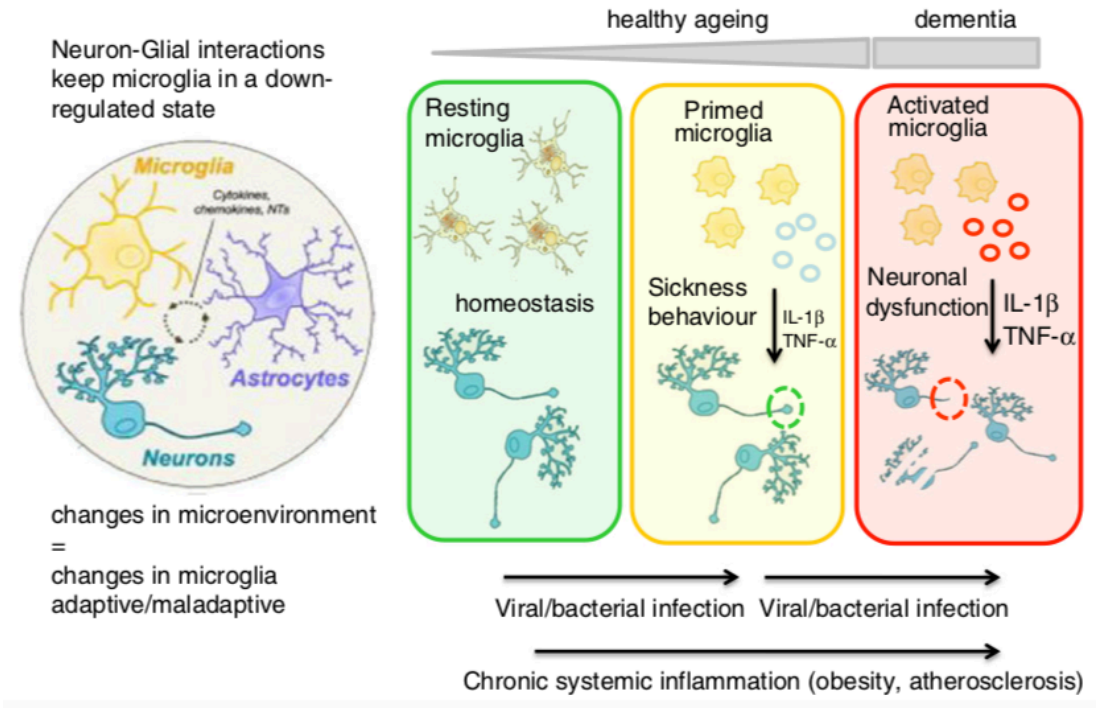

Figure 1.1.15 Microglial activation is induced by systemic inflammation and contributes towards behaviour adaptions to infection. Ageing and low-grade systemic inflammation causes progressive priming of microglial cells in the brain that alters their morphology and neural function. Later in life, viral/bacterial infections may cause irreversible activation of microglial cells that increases the risk of illnesses affecting memory, and cognition such as dementia, characterised by neuronal dysfunction, and activated of pro-inflammatory cytokines in the brain. From (Perry & Holmes, 2014).

Microbial production of SCFAs during viral infection have been described as activating microglial cells, the resident tissue macrophage in the brain and CNS (Erny et al., 2015). Indeed, transfer of faecal material from human PD patient donor into αSn-overexpressing mice revealed an altered profile of SCFAs, which was capable of activating microglia alone within PD disease-susceptible GF mice (Sampson et al., 2016). Activation of microglia passes the threshold known as priming of microglial, and induces neuroinflammation observed through morphological changes, including on specific administration of SCFAs in this experiment.

- *Increased intestinal permeability in Major Depression*

Major depression is a psychiatric disorder with a defined abnormal immune component and suspected changes in intestinal permeability. Patients display high serum IgM and IgA antibodies reactive with LPS (endotoxin) of multiple Gram-negative enterobacteria. The levels of these antibodies are associated with a global worsening of symptoms, including fatigue, autonomic and gastro-intestinal symptoms (Maes *et al.,* 2008). These results also suggest 'leaky gut' plays a role by increasing the exposure of bacterial LPS causing an inflammatory immune response marked by proinflammatory cytokines IFN-γ and IL-6. Chronic low-grade inflammation or immune activation that underlies the aetiology of IBS is also a driving risk factor in mood disorders (O'Malley et al., 2011).

- *Increased intestinal permeability in ME/CFS*

Increased serum IgM and IgA responses have also been documented in CFS patients against the LPS of enterobacteria using an ELISA method (Maes et al., 2007). Given the year of publication of this article it is important to note that the Canadian ME/CFS and/or international ME criteria could not have been applied. As discussed earlier, Fukuda CFS criteria has significant overlap with psychiatric comorbidities.

More recent studies that have assayed for surrogate markers of intestinal permeability, Including LPS, LBP, sCD14, I-FABP as well as surveying a number of pro-inflammatory

cytokines conclude that bacterial translocation in ME/CFS may be stimulating the immune system (Giloteaux et al., 2016). Together with recent data showing a reduction in the diversity of the ME/CFS microbiome appear to add further support to this concept, however, there is no additional information related to differences in local gut immune reactions towards intestinal microbes, or how these permeability markers reflect severity of ME/CFS.

1.11 Leaky gut hypothesis in ME/CFS

'Leaky gut' is an informal term used to described increase intestinal permeability that may result in bacterial translocation and exposure to the host immune system. It has been suggested that 'leaky gut syndrome' is a mechanism for immune dysfunction and auto-inflammation and autoimmunity (Fasano, 2012). Indeed, there have been several reports of changes in intestinal permeability that are frequently in tandem with evidence for dysbiosis in a selection of neurological and autoimmune diseases (Bosi et al., 2006; Fasano, 2012; Manfredo Vieira et al., 2018; Pijls et al., 2013; Rojo et al., 2007; Sapone et al., 2006). Of course, details for how the microbiota cause the immune system to produce autoantibodies is unclear and in to response to which particular microbes in the gut. It is tempting to speculate an unknown infection in ME/CFS initiates neurological complications in some patients, similar to Guillain-Barré (GB) syndrome where LPS derived from *Campylobacter jejuni* elicit cross-reactive antibodies through molecular mimicry of host gangliosides (Yu *et al*., 2006). From this, the pathological consequences to the CNS and effects on behaviour appear to be precipitated by immune dysregulation driven by bacterial infection. However, serial pieces of evidence are missing to support this hypothesis.

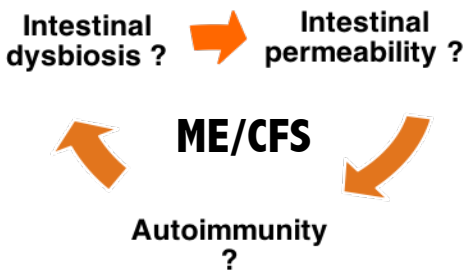

Figure 1.1.16 An explanation for ME/CFS incorporating intestinal dysbiosis, intestinal permeability and autoimmunity. Our hypothesis is that the pathogenesis of ME/CFS is driven by intestinal dysbiosis that results in increased Th1/Th17 immune responses towards intestinal microbes and

increased intestinal permeability. Increased anti-microbial reactivity to luminal microbes may engender cross reactivity through molecular mimicry with the CNS and brain that so far has not been established in ME/CFS. Identifying intestinal dysbiosis and alterations in intestinal permeability are plausible mechanisms for induction of autoimmunity and have been associated with several autoimmune diseases (Fasano, 2012).

- *Concluding remarks*

The cause(s) of ME/CFS is not known but is suspected to involve cytokine infiltration of the brain, neuro-inflammation, low NK cell function and frequently follows viral infections suggesting a link with the immune system. Environmental and/or microbiological triggers originating from the gastrointestinal tract are thought to be a cause of the disease or perpetuate symptoms and pathological illness.

Autoimmune reactions lead to inflammation, increased permeability of blood vessels and migration of lymphocytes to sites of injury. Microglia within the brain can be primed during chronic inflammatory diseases but can then induce inflammation in the brain when they are triggered by a second inflammatory challenge such as a systemic microbial infection (Blaylock & Maroon, 2011). This raises the possibility that the damaging neuro-inflammation seen during ME may be triggered by systemic infections. Indeed, several autoantibodies have been documented in some but not all ME/CFS patients. An interesting example are anti-5-HTA receptor antibodies since the majority of serotonin is produced in the gut (Maes *et al.,* 2013b).

Many ME patients have gastrointestinal disturbance, are more likely to develop irritable bowel syndrome, and may have a “leaky” gut barrier (Lakhan & Kirchgessner, 2010) Together these observations suggest that changes in intestinal barrier integrity, which may be driven by or are a consequence of intestinal dysbiosis, as a result, for example, of a gut infection could contribute to ME by increasing exposure of host mucosal and systemic immune cells to microbe-derived antigens and drive systemic inflammation and/or influences the microbiota-gut-brain axis.

1.1.12 Overall study aim, hypothesis & objectives

- *Central Hypothesis*

Severe ME/CFS patients have a compositionally and functionally altered intestinal microbiota compared to their house-hold relative, which promotes ongoing intestinal epithelial permeability and systemic, chronic (auto)-inflammation.

- *Thesis Aim*

The first aim was to recruit an apparently healthy, house-hold control participant to match with their respective house-bound, severe ME relative; the second, to characterise the composition and metabolic of activity of the intestinal microbiome and to test for evidence of intestinal epithelial permeability in these patients.

Recent metagenomic and metabolomic studies have focussed exclusively on mild to moderately affected ME/CFS patients with respect to conventional age and gender matched healthy controls. If these findings translate into severe, house-bound ME/CFS patients in unknown.

- *Specific Objectives:*

Chapter 3: To compare metagenomic sequencing methods to characterise the composition of the intestinal microbiota in severe, house-bound patients, in order to determine:

i) if there is evidence for intestinal dysbiosis;

ii) the identify of key bacterial species belonging to a novel “microbial signature” which may help define severe, ME patients from those mild to moderately affected;

iii) the effect of the contribution of external environmental factors known to influence population-level microbiome variation by using house-hold controls

Chapter 4: To define the faecal and serum metabolome of severely affected ME/CFS patients, in order to determine if:

i) altered microbial composition (dysbiosis) influences the faecal and blood serum metabolism;

ii) there is any evidence for alterations in aerobic energy metabolism or of a hypometabolic state, which have recently been reported in studies on mild to moderately affected ME/CFS patients;

iii) severe, ME patients have a distinct bile acid metabolic profile using targeted HPLC-mass spectrometry.

Chapter 5: To evaluate methods for detecting anti-microbial antibodies using solid phase and liquid phase assays by establishing:

i) if lab-cultured bacterial isolates, representative of the human intestinal microbiome, can be immobilised onto nitrocellulose-coated glass slides;

ii) a whole cell bacterial microarray to rapidly screen serum using microarray scanner detection;

iii) the relative abundance of IgA-coated faecal microbes in severe ME/CFS patients versus matched house-hold controls using faecal flow cytometry;

iv) the intestinal permeability status of severe ME patients versus house-hold controls based on serum detection of lipopolysaccharide (LPS) and LPS-Binding Protein (LBP);

v) if IgA reactivity towards faecal microbes correlates with these existing measures of intestinal permeability.

Chapter Two

2 Overall study design

2.1 General study rationale

This thesis project is a pilot study focussed on severe ME/CFS patients who were identified as being house and/or bed-bound. Housebound and bedbound ME/CFS patients account for approximately 25% of the patient population, yet fewer than 0.5% of studies carried out to date include these patients (Pendergrast et al., 2016). Studies of the intestinal microbiota of ME/CFS patients suggest a reduction in microbiota diversity and the number of species of bacteria (Fremont et al., 2013; Giloteaux et al., 2016; Nagy-Szakal et al., 2017). Other culture-based studies using the Fukuda criteria to identify patients, described an increased number of D-lactate producing *Enterococcus* and *Streptococcus* spp. in ME/CFS patients providing a plausible explanation for neurological impairment (see symptoms fig 1.1.3) in ME/CFS similar to patients with D-lactic acidosis (Sheedy et al., 2009).

Relatively few studies compare the microbiota of patients with healthy same house-hold individuals as controls despite the benefit of controlling for important environmental factors. Various factors affect the microbiota, chiefly among are diet and lifestyle (Zhernakova et al., 2016). It is a reasonable assumption that members of the same house-hold will share food and be exposed to similar habitat associated factors and microbes. To this end, house-hold members act as a useful environmental control. Finally, the majority of house-hold controls used in this study were relatives of the patient and share a similar genetic background which contributes to microbiota diversity shaping of the host immune response to commensal intestinal microbes.

At the time of writing, this work represents the first insight of the intestinal microbiota of house-bound ME/CFS patients and disease-free members of the same house-hold. The data from this analysis is presented in the following chapter, chapter 4. Host and microbiota metabolism analysed through metabolomics-based approaches has identified alterations energy and lipid metabolism, amino acids and products of microbial metabolism including lactate and SCFAs (butyrate) derived from fermentation of dietary carbohydrates. However, none of these studies have included severe patients or healthy house-hold controls (Armstrong et al., 2015; Germain et al., 2017; Naviaux et al., 2016). In chapter 5 detection of faecal IgA-coated bacteria is determined using flow cytometry as a surrogate for intestinal permeability that has previously been applied to assessing intestinal barrier dysfunction in colitis (Palm et al., 2014).

In total seventeen home visits were carried out across the South of London and neighbouring counties (see heatmap, figure 2.2.1) to collect faecal samples from 17 severe patients and 10 house-hold controls (two being full-time carers). Of these, additional faecal samples were provided by seven patients and five house-hold controls.

During 2015 faecal samples were obtained from twenty-five mild/moderate severity ME/CFS patients recruited from the Chronic Fatigue Service (CFS) at the Epsom & St Helier NHS Foundation Trust University Hospital, Carshalton, UK.

2.2 Study Participants

All patients were registered at the St. Helier CFS service under direct supervision of Dr Amolak Bansal, Consultant Immunologist and Director of the CFS service. This has over more than 10 years registered more than 7000 patients enabling it to establish a substantial clinical history and clinical definition of ME/CFS leading to the development of a 13-point scoring system (figure 1.2.1) based on the most frequent symptoms of ME/CFS (Bansal, 2016) and an absolute requirement for PEM symptom, which scores a maximum of 3 points.

Since 2008 over 2000 patients have been diagnosed using this system and it has remained a robust and rigorous in that during the past decade with no other explanations for fatigue being forthcoming in any patients diagnosed with ME/CFS (Bansal, 2016). Common symptoms in the vast majority (>90%) of patients within this service includes aching muscles and muscles weakness, stress aggravated fatigue, impaired concentration and non-restorative sleep (Bansal, 2016). Additional symptoms include an increased respiratory rate with 70% of moderate to severe and very severe patients presenting with persistent cold hands and feet (Bansal, 2016).

Factor	Score
Delayed prolonged post-exertion malaise after increases in physical, mental and emotional activity	3
Non-restorative sleep with frequent difficult initiating and/or maintaining sleep	2
Impaired concentration that is reduced further by external stimuli	1
Reduced short term memory with word finding difficulty	1
New onset headaches (>2/mth and different in character from previous headaches)	1
Sore throat with cervical tenderness/recurrent flu-like episodes	1
Arthralgia affecting several joints with stiffness > 1 hr but no swelling	1
Myalgia affecting multiple groups and exacerbated by mild exertion	1
Postural instability feeling unstable on standing or sitting	1
Hypersensitivity to sounds and lights (smells and to a lesser degree taste also)	1

Table 2.2.1 Adapting Fukuda, CCC and ICC case definitions into a 13-point scoring system used by Epsom and St Helier CFS service List of symptoms and respective scores to characterise CFS/ME.

- *Inclusion criteria*

Patients diagnosed with ME/CFS must fulfil the Canadian, International Consensus and Fukada criteria to be part of the St. Helier CFS service. The selection of patients from this service for inclusion in this study were identified by Dr Bansal as described above (Bansal, 2016) with symptoms persisting for a minimum 50% of any period (Jason et al., 2014). Patients must also score a minimum of 8 using this system. The results of previous clinical investigations including blood tests were used to exclude other common causes of persistent tiredness, including psychiatric illness. These tests include full blood counts, levels of C-Reactive Protein (CRP), Erythrocyte Sedimentation Rate (ESR), tests for renal, hepatic (LFT) and thyroid (TFT) function, presence of anti-nuclear antibodies (ANA) to exclude systemic lupus erythematosus (SLE), and serum immunoglobulin levels and gluten sensitivity tested. The patient's clinical and psychiatric history were also examined to identify potential causes for fatigue. The Hospital Anxiety Depression Scale (HADS) was used to assess any underlying depression and anxiety. The Chalder Fatigue Scale and additional fatigue scale are used routinely to assess the degree of fatigue.

- *Exclusion criteria*

Antibiotic usage 4 weeks prior to enrolment was the only major exclusion criteria with patients given the opportunity to be recruited to the study after completing their antibiotic treatment and after recommendation by Dr Bansal. The other specific exclusion criteria was a HADS score of greater than 7. Anxiety and depression are known to affect the immune system causing stress and disturbances in sleep. Nonetheless, given the chronic state of this illness a degree of depression and anxiety, and stress, is likely to feature in all patients but is distinct from major depressive symptoms including guilt and low motivation. Probiotic consumption was not an exclusionary criterion as this would have restricted patient recruitment.

- *Disease severity*

Patients were grouped based on the severity of their ME/CFS defined by the St. Helier CFS service. Mild/moderate patients were distinguished from severe (house/bed-bound) patients by their ability to attend to repeat hospital visits. This is reflected by descriptions of daily living (ADL) activities used by the service (table 2.2.2). Patients beyond the level of moderate severity cannot or rarely leave the house and are defined as severe in this study.

Mild	Moderate	Severe	Very Severe
Still working, mobile, reduction in family and leisure activities	Not working, sleeping in daytime. Reduced mobility, but can leave the house	House-bound, (rarely leaves house) with severe worsening of symptoms under physical and mental exertion	Bed-bound, light and noise sensitivities. Requires someone else to wash and feed them

Table 2.2.2 Definitions of Activities of Daily Living (ADL) determining the level of severity of symptoms in ME/CFS patients

- *Eligibility of House-Hold Controls (HHC)*

With the exception of 2 out of 10 HHCs, who were full-time carers of the patient, all these individuals were family relatives of each respective severe ME/CFS patient living in the same house-hold. These participants were recruited on the basis of their 'apparent' healthy status and could not be clinically assessed, or medical records obtained prior to their inclusion in the study. However, HHCs were advised not to participate with any known medical or psychiatric history, particularly associated with gastrointestinal symptoms.

Figure 2.2.1 Heatmap of location of patient home visits 2016-2017 using Google Maps. A total of 17 home visits were completed to severe, house-bound ME/CFS patients registered at the CFS service in Epsom and St Helier, Surrey.

2.3 Research Ethics Approval

The original study proposal was reviewed by the University of East Anglia Faculty of Medicine and Health Sciences (FMH) Research Ethics Committee in 2014 and subsequently approved (reference FMH20142015-28). This approval allowed for the inclusion of faecal and blood samples collected from patients within the Epsom and St Helier CFS Service using the Norwich Biorepository, approved from the Cambridge East Committee of the National Research Ethics Service (NRES). Copies of approval letters from the committee and the research and development department are provided in supplementary figures 2.1 and 2.2.

The original research proposal included recruitment to assess the intestinal permeability of 140 ME/CFS patients including 35 mild/moderate, 35 patients defined as severe, 35 controls, and 35 ME/CFS with specific GI symptoms. It became apparent that this target was ambitious and could not be completed in the time allowed and it was later revised to focus exclusively on home visits severe patients.

- *Informed consent*

Patient information sheets containing information about the study were provided to patients upon request at the St. Helier CFS service or discussed in routine consultation with Dr Bansal (see appendix). Severe patients were informed of the study by telephone consultation with Dr Bansal who forwarded the information and advised patients interested in participating to contacted myself using email or the study dedicated telephone number. Patients expressing an interest in participating were mailed study documents in advance of any home visit and advised to contact myself via email or telephone to discuss the study further.

- *Inclusion of House-Hold Controls (HHCs)*

The inclusion of a same household control was not an absolute study inclusion criteria in order to enable severe, house-bound patients to participate in this research. Prospective HHCs were approached by the patients themselves before contacting myself to discuss the research and provided with a stool samples kit.

- *Ethical considerations*

The study's ethical approval did not allow any data collection such as the use of questionnaires for assessing level of functional GI disorders or clinical history to be obtained. As a researcher, it was not possible to conduct a physical examination of the patient to ascertain parameters such as an individual response to painful stimuli or sensitivity to light and sound. There were also several occasions where it was not physically possible to obtain a blood sample for patients. ME/CFS patients can exhibit collapsed or inaccessible veins. In other instances, blood samples could not be acquired without causing distress to the patient and therefore it was deemed unethical to obtain these samples. For example, in severe patients with extreme light sensitivity or with heightened sensitivity to touch and pain stimuli.

2.4 Sample collection & Storage

Samples were collected and stored within 1-6 h at -80^{0}C at St Helier prior to transfer to the Norwich Biorepository at a later date. All samples were processed and analysed together.

- *Mild/moderate ME/CFS patients*

Twenty-five mild/moderate ME/CFS patients were recruited in 2015 from St Helier CFS service.

- *Home visits*

A minimum of 2 visits were carried out between 2016-2017 to each of the 17 severe patients, first to consent patient and provide them with the stool sampling kit and instructions for collection (see appendix).

- *Stool sample*

All study participants were instructed to collect their intact faecal sample in a FECOTAINER® (AT Medical B.V., Enschede, Netherlands), figure 2.2.2 no later than 24 hours prior to a scheduled home visit. Samples were stored at 4^0C prior to collection from the patient home and transported on ice to St. Helier hospital. Participants donating stool in 2017 collections were also provided with an AnaeroGen™ Compact anaerobic sachet (Cat No. AN0010, Oxoid Ltd., United Kingdom) to activate as soon as they produced their sample to eliminate environmental oxygen conditions and promoting the survival of obligate anaerobic microbes. On return to the hospital, samples were manually homogenised with a sterile autoclaved metal spatula, aliquoted and either processed immediately or stored at -80^0C for future use.

Figure 2.2.2 FECOTAINER® collection device used to collect stool sample. (Reproduced image accessed via www.fecotainer.eu on 12th September 2018).

- *Blood sample*

Where possible patients and house-hold controls (HHC) were also bled using S Monovette® Z-Gel for serum collection (Cat No. 02.1388.001, Sarstedt AG & Co., Nümbrecht, Germany). For home visits, it was not always possible to attempt to collect blood from severe patients and HHCs due to unavailability of a phlebotomist to accompany myself.

Chapter Three

3 Characterising the composition of the gut microbiome associated with severity of ME/CFS

3.1.1 Introduction

There is an urgent need to identify validated biomarkers for the diagnosis of ME/CFS. Altered intestinal microbiota composition (dysbiosis) has emerged as a feature of neuro- and immuno-inflammatory diseases, suggesting a causal relationship (Round & Mazmanian, 2009). Gastrointestinal inflammation is associated with abdominal pain and altered bowel movements (Neufeld, 2013). Stress, anxiety and depression are well known psychological disorders, which frequently make GI symptoms worse, particularly in IBS. Intestinal dysbiosis may be a driver of altered gut-brain signalling and pain perception. Thus, IBS is described as a functional disorder, and like ME/CFS appears absent of physical, structural or biochemical abnormalities and is instead identified by characteristic symptoms (Häuser et al., 2012). IBS-like symptoms are common among ME/CFS patients with as many as 92% of all ME/CFS having IBS at some time during the development of ME/CFS (Lakhan & Kirchgessner, 2010). The mechanism for IBS-related abnormal pain and discomfort is thought to be driven by inflammatory derived immune signals, such as cytokines and release of prostaglandins in response to an infection and through direct bacterial activation of the nervous system.

Chui and colleagues have shown that infection by *S. aureus* activates nociceptors causing mechanical and thermal hyperalgesia in mice, the severity of which correlated with bacterial load (Chiu et al., 2013). Furthermore, LPS stimulation of afferent sensory neurons require TRPA1 ion channel mediated calcium influx and release of neuropeptides which enhance local inflammation and hyperalgesia (Meseguer et al., 2014). Although sensory neurons express the receptor for LPS, TLR4, the sensory responses to LPS in tlr4-deficient mice did not differ (Meseguer et al., 2014). Visceral pain perception has become a target for pharmacological intervention using drugs to block or alter gut-brain signalling and neuroimmune pathways to alleviate symptoms (Farzaei et al., 2016). Increased intestinal permeability in a subset of IBS patients with diarrhoea symptoms enhances severity and hypersensitivity to visceral stimuli (Zhou et al., 2009). Increased bacterial translocation would therefore facilitate direct contact with afferent sensory neurons, which further stimulate visceral hypersensitivity through engagement of bacterial antigens. Given the role of intestinal bacteria in activating nociceptors, management of visceral hypersensitivity in IBS and other disorders with GI symptoms may benefit from targeting the intestinal microbiota as well as the (“leaky”) intestinal epithelial barrier.

The intestinal microbiota is significant in the development of post-infectious IBS in mice where probiotic preparation of *Bifidobacterium* and *Lactobacillus* strains ameliorate IP and inflammatory cytokine production, reducing intestinal inflammation and alleviating hypersensitivity (Wang et al., 2014). An overlapping profile of plasma cytokines has been reported in IBS and ME/CFS driven by IL-6, IL-8 IL-1ß and TNF (Scully et al., 2010). Systemic circulation of these cytokines to the brain induces sickness behaviour causing symptoms of extreme malaise and severe fatigue (Dantzer et al., 2008).

- *Dysbiosis linked to low-grade chronic inflammation*

Intestinal inflammation and bacterial translocation can lead to systemic infection and low-grade chronic inflammation in ME/CFS (Lakhan & Kirchgessner, 2010). Changes in the intestinal microbiota in metabolic disorders are associated with higher plasma concentrations of LPS and development of endotoxemia (Cani et al., 2008). It is well documented that the relative abundance of *Firmicutes* exceeds *Bacteroidetes* in metabolic disorders. However, the increased prevalence of Proteobacteria is a potential microbial signature for inflammatory-dependent intestinal and extra-intestinal diseases (Rizzatti et al., 2017). In addition, the aging microbiota is represented by an increase in Proteobacteria and decrease in *Bifidobacteria* and may alter the balance between anti- and pro-inflammatory responses of Treg/Th17 immune cells in the intestine (Biagi et al., 2010).

Proteobacteria are Gram-negative and a potential source of LPS which could induce endotoxemia in the development of metabolic disorders. Beyond metabolic disorders, a more recent study has shown that Parkinson's Disease patients have increased abundance of *Proteobacteria*, but it is unclear how dysbiosis enhances progression and impairment of motor control and decline in neurocognitive functioning. A possibility is that increased intestinal permeability may expose Proteobacteria to the internal environment. Indeed, faecal markers for intestinal inflammation and intestinal permeability, (including zonulin overexpression) are significantly elevated in a cohort of PD patients compared to age-matched healthy controls (Schwiertz et al., 2018). Moreover, intestinal biopsies taken from 9 PD patients showed a positive correlation between intestinal αsynuclein aggregation and serum endotoxin in early PD in response to increase exposure to intestinal bacteria (Forsyth et al., 2011). Whilst these pathological features do not distinguish PD patients from other (neuro)-inflammatory disorders associated with GI barrier dysfunction, it does lead to speculation of a common cause for generating low-grade inflammation and

increased physiologic input from the microbiota in the activation innate immune receptors such as TLR4 and nociceptors in afferent sensory neurons behind a compromised intestinal barrier.

- *Microbiota-derived intestinal metabolites*

It is not known if or how intestinal dysbiosis influences the pathogenesis of ME/CFS. Many of the symptoms of ME/CFS, severe fatigue, malaise, unrefreshing sleep, cognitive impairment, memory deficits, autonomic disturbances including blood pressure changes, orthostatic intolerance, overlap with neurodegenerative and neuropsychiatric disorders, as discussed above. Significantly, an altered microbiota will impact on the profile of microbial products, particularly those with the capacity to act as neurotransmitters and modulators of inflammation. For example, secondary bile acid metabolism (see next chapter) is regulated by certain intestinal bacteria with specialised enzymes (bile salt hydrolases, BSH) modifying structural and chemical changes to primary bile acids produced by the liver. These secondary bile acids are lipophilic and can be absorbed across the intestinal barrier, interacting with cells beyond the intestinal epithelial barrier via TGR5 which has emerged as a key receptor in the mediation of bile acid neural-humoral signalling with an impact on energy homeostasis and inflammation (Bunnett, 2014).

Altered microbiota in PD patients has been associated with alterations in the proportions of SCFAs (Unger et al., 2016). SCFA are significant metabolites produced by the microbiota, the most abundant of which are acetate, propionate and butyrate that are an important source of energy for intestinal epithelial cells. Understanding how the intestinal microbiota changes in disease states will help understand the impact dysbiosis may have on disease pathogenesis. For instance, *Bacteroides thetaiotaomicron* is a major producer of acetate and propionate. *Clostridium tyrobutyricum* produces high levels of butyrate that inhibits HDAC activity and upregulation of TJs proteins such as zonulin, which if dissociated from the TJ complex leads to increased serum levels which is a useful marker for altered intestinal permeability (Bordin et al., 2004; Sapone et al., 2006). However, PD patients have an overall reduction in faecal SCFAs (Unger et al., 2016). In PD patients, members of the phyla Bacteroidetes which includes the family *Prevotellaceae* were reduced with increased abundance of Enterobacteriaceae which includes Proteobacteria (Unger et al., 2016). Significantly ASO mice, engineered to overexpress a-synuclein are genetically susceptible to PD, but do not develop the PD-like phenotype if maintained under germfree conditions or

are treated with antibiotics to eliminate gut microbes. Conventionalisation of these germfree or antibiotic-treated mice restored the PD phenotype, with the transplantation of faecal microbiota from PD patients greatly exacerbating the PD phenotype compared to animals conventionalised with faecal microbiotas of healthy individuals (Sampson et al., 2016). Moreover, SCFAs derived stool samples from PD patients were sufficient alone to enhance motor dysfunction and activate microglial in GF ASO mice (Sampson et al., 2016).

Defects in Blood Brain Barrier (BBB) permeability in the offspring from germfree mice have been observed after intravenous administration of Evans blue dye which accumulates in the brain parenchyma (Al-Asmakh & Hedin, 2015). However, the prior introduction of SCFAs producers, *C. tryrobutyricum* (butyrate) and *B. thetataiotaomicron* (acetate/propionate), enhanced BBB integrity via unknown effects on TJ complexes (Braniste et al., 2014). SCFAs activate the GPR41 and GPR43 G-protein coupled receptors, with physiological effects including of reducing GI transit, energy balance, and anti-inflammatory signals (Al-Asmakh & Hedin, 2015). Gpr43 deficient mice develop colitis, arthritis and asthma (Maslowski et al., 2009). Moreover, butyrate has a neuroprotective effect limiting neuronal damage and prevents α-synuclein accumulation by enhancing autophagy (Liu et al., 2017).

Although the role of SCFAs in the pathophysiology of inflammatory diseases is unclear, associated intestinal dysbiosis appears to have a role in driving pathology in various neurodegenerative diseases (Mulak, 2018). α-synuclein aggregates form in the enteric nervous system many years prior to the onset of PD which raises the question, do neurodegenerative disease begin in the intestine? Mouse models demonstrate that the intestinal microbes contribute to driving neuropathology, further highlighting the need to understand how microbial compositional changes impact microbial metabolite production, for example SCFAs, that may contribute to pathogenesis.

Unlike PD, RR, MS, NMO introduced earlier in chapter 1, there is no animal model for ME/CFS. The observations that the intestinal microbiota can have a wide range of physiology input in metabolic disorders, to neuro-immune and neurodegenerating disorders with similar symptoms including severe fatigue, cognitive deficits, visceral sensitivity and GI disturbances, warrants investigation into ME/CFS to establish potential aetiological causes.

- *Treating intestinal dysbiosis*

Faecal Microbiota Transplant (FMT) is the practice of transferring a healthy donor stool sample into a patient in an attempt to treat intestinal dysbiosis by restoring a diverse intestinal microbiota (Borody & Khoruts, 2012). In clinical practice it has proven to be very effective in the treatment of recalcitrant *Clostridium difficile* infection (CDI), which arises as a result of antibiotic treatment leading to the loss of many members of the microbiota, leading to germination of *C. difficile* spores and bacterial overgrowth.

Bacteriotherapy involving trans-colonoscopic infusion of 13 anaerobic enterobacteria has been trialled in 60 ME/CFS patients. Amongst the ME/CFS patients, 52 had IBS comorbidity. Just over half of these patients responded to an initial infusion, of which 88% no longer experienced GI symptoms. Ten patients that did not respond with significant improvements in refreshing sleep, lethargy, fatigue, did see some improvement in their GI symptoms. Although the initial success rate was encouraging, this trial did not adequately follow up the long term benefit this treatment in these patients. Twelve patients that were followed up of which 7 remained cured of CFS which the other 5 describing relapsing CFS symptoms between 18 months to 3 year following bacteriotherapy (Borody et al., 2012).

3.1.2. Profiling the intestinal microbiota

The relatively few studies that have profiled the composition of intestinal bacteria in ME/CFS are summarised in Table 2.2. It must be appreciated that these studies rely on a small number of patients defined by the use of the Fukuda (1994) criteria for CFS. Moreover, these studies have varied in their experimental approach and according to the technical capabilities at the time. Prior to recent advances in DNA sequencing technology, traditional culture-based techniques were used to study the human intestinal microbiota. In fact, the concept that the composition of the microbiota changes in health is not new and was first reported in 1973 using culture techniques (Tannock & Savage, 1974). However, in the past decade improvements and cost reductions in sequencing technology have made it possible to profile the bacterial composition across different microbiotas on and inside the human body. This is evidenced by the rapidly increasing number of publications shown as year on year increases in figure 3.1.1, as the technology has improved and reduced in cost.

The introduction of high-throughput (HTP) next-generation sequencing (NGS) technology has allowed researchers to exploit the highly conserved bacterial 16S gene for their reliable identification without the necessity of isolating and culturing them, on a massively parallel scale. Sequenced-based molecular identification of bacteria entails a choice 9 hypervariable regions of 16S rRNA gene using universal primers flanking these regions to amplify the DNA prior to high-throughput next generation sequencing. This generates sequences that are typically 250 base-pairs long, referred to as reads. Each read can then be processed and collectively analysed using bioinformatics software to such as Qiime, to assign each of the reads to their operational taxonomic units (OTUs) (D'Amore et al., 2016). The software utilises reference databases to identify each OTU.

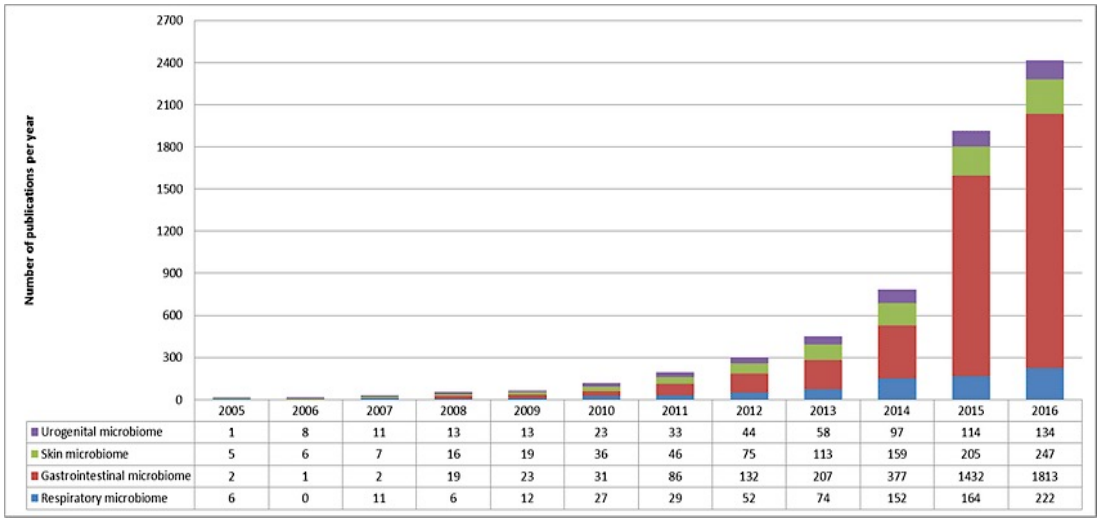

	2005	2006	2007	2008	2009	2010	2011	2012	2013	2014	2015	2016
Urogenital microbiome	1	8	11	13	13	23	33	44	58	97	114	134
Skin microbiome	5	6	7	16	19	36	46	75	113	159	205	247
Gastrointestinal microbiome	2	1	2	19	23	31	86	132	207	377	1432	1813
Respiratory microbiome	6	0	11	6	12	27	29	52	74	152	164	222

Figure 3.1.1 The rise in the number of microbiome-based studies between 2005 – 2016 Scientific Figure on ResearchGate. Available from: https://www.researchgate.net/Bibliometric-parameters-of-microbiome-studies-Representations-were-limited-to-the-four_fig1_320728834 [accessed 10 May, 2018]

- *Limitations of 16S gene-based sequencing studies*

16S rDNA gene amplicon sequencing has become the most widely used method of NGS to profile of the human gut microbiota. However, its domain is restricted to bacteria and archaea and it is limited to profiling bacteria at the genus level and therefore it is not possible to discriminate bacteria at a species or strain level (Jovel et al., 2016; Ranjan et al., 2016). Furthermore, the choice of 16S hypervariable region and primers introduce a bias for particular bacteria taxonomic groups (Ghyselinck et al., 2013).

- *Faecal DNA extraction*

Faecal samples are the most complex and diverse microbiome samples that can be isolated from on or inside the human body and therefore obtaining a good quality and high yield of DNA from all faecal bacteria can be challenging when studying such a diverse and complex community of microbes which have varying cell membrane and cell wall strengths encapsulating their DNA context. To that end, commercially available DNA extraction kits have been shown to vary in efficiency and quality of DNA extraction. A recent study compared 6 of these kits, including the MP Biomedicals FastDNA® Spin kit for soil used in this study (Turlej-Rogacka et al., 2017). For 16S-based studies all kits produced adequate DNA for PCR amplification, sufficient to provide a product which could be sequenced. However, the kits did vary significantly in obtained DNA concentration and purity using ($A_{260/280}$) ratio (Turlej-Rogacka et al., 2017). For shotgun metagenomic studies high-molecular weight genomic DNA will maximise the quality of output for downstream applications (Bag et al., 2016). However, total recovery of genomic DNA is a significant challenge for commercially available kits using minimal amounts (~250 mg) of faecal material and naturally these methods can have different biases towards the efficiency of DNA extraction from different bacterial species (Brooks et al., 2015). Accurately quantifying the concentration DNA in your sample can depend on the method of choice with more that 10-fold higher DNA concentrations using NanoDrop versus Qubit (Turlej-Rogacka et al., 2017).

- *Evidence of intestinal dysbiosis in ME/CFS using culture-based techniques*

Before the advent of NGS technology, investigators relied on traditional microbiology and bacterial cultures to grow and identified individual isolated bacteria. During an early investigation by Sheedy and colleagues, they likened the neurological impairments of ME/CFS to another condition where lactic acid producing bacteria are responsible for severe cognitive dysfunction. D-lactic acidosis is a metabolic disorder, which usually manifests in patients as a complication of having short bowel syndrome (SBS). SBS describes the inadequate absorption of nutrients by the small intestine, diarrhoea and dehydration enabling colonic bacteria to ferment carbohydrates causing excess D-lactic acid to accumulate in the blood. The effects of D-lactic acid on the CNS are apparent from other studies where it causes neurological impairments such as confusion, slurred speech, muscle weakness and inability to think. Faecal bacteria were grown in selective cultures from 108 CFS patients and 177 controls to generate viable counts (Sheedy et al., 2009). The

number of D-lactic acid producing Enterococcus and Streptococcus species were significantly higher in patients than controls (p=0.01) (Sheedy et al., 2009). The possible cause or mechanism for the accumulation of these bacteria is unclear, though their presence will lower the intestinal pH and may explain intestinal permeability increases associated with systemic endotoxemia (Henriksson et al., 1988; Maes & Maes, 2009).

Another report in the same year, outlines the effect of a 4-week programme of administering twice daily (x2 20ml) probiotics containing 10^8 CFU/ml of *Lactobacillus* F19, *L. acidophilus* NCFB 1748 and *B. lactis* Bb12 in 15 CFS patients with high fatigue and disability scores (Sullivan et al., 2009). During the four-week follow up, 6 patients reported significant improvement in cognitive function, but not in fatigues or physical activity scores compared to pre-treatment, with no significant changes found in their intestinal microbiota PCR-based methods for identification *Lactobacilli* and CFU counts (Sullivan et al., 2009). The authors remarked on the high variability in patient responses demonstrating the heterogeneity of the study group, moreover, the benefits were on a case by case basis, with those benefitting reporting sustainable improvement to cognitive function up to 70 days later (Sullivan et al., 2009).

The depression and anxiety characteristics in 39 CFS were studied in a separate cohort following an 8 week intervention consuming a daily dose of 2.4 x 10^{10} CFU of L. *casei* strain Shirota (LcS) spread across 3 smaller doses of 8 x 10^9 CFU after each meal (Rao et al., 2009). Overall, a significant rise in *Lactobacillus* and *Bifidobacteria* spp. was seen in patients receiving the probiotic treatment (n=19), as well as a reduction in levels of anxiety, versus those patients (n=16) who have received the placebo control (Rao et al., 2009).

- *16S rDNA-targeted amplicon sequencing in ME/CFS*

Fremont and colleagues published the first ME/CFS study using HT 454 pyrosequencing performed on 16S V5-V6 region generating reads of at least 240 bp long (Fremont et al., 2013). On average, 6000-7000 reads were obtained for each patient/control of which 98% could be assigned to specific phyla, and 129 different bacterial genera identified (Fremont et al., 2013). This ME/CFS cohort included patients from Norway and Belgium with respective healthy controls from the same countries. The majority of patients were female and diagnosed by Fukuda criteria. Dysbiosis was more significant in the Norwegian patients with a reduction in firmicutes: *Roseburia, Syntrophococcus, Holdmania, Dialister* and a x20

increase in *Lactonifactor*, and a 3.8 increases in *Bacteroidetes* genus, *Alistipes* (Fremont et al., 2013). Interestingly reduction of *Roseburia*, a Gram-positive butyrate producer, is reported to be a defining characteristic of dysbiosis in ulcerative colitis patients, and thus consistent with intestinal inflammation (Machiels et al., 2014). Moreover, *Alistipes* (and *Enterobacteriaceace*) were over-represented in patients with depression (Jiang et al., 2015). In contrast, Belgian patients were less distinct from their respective healthy controls, except for x45 increase in *Lactonifactor* in patients thus remarkedly similar to the 20 -fold increase of this genera in Norwegian patients (Fremont et al., 2013).

Since this 2013 study, Roche® 454 sequencing has been replaced by the Illumina® MiSeq platform. The fundamental difference is an ability of 454 sequencing to achieve longer reads (up to 700 bp with 99.9% accuracy and 0.7Gb/run) compared on average with Illumina® NGS, between 150-300 bp (L. Liu et al., 2012). However, the Illumina® MiSeq v2 platform offers 2 x 250 bp (paired-end, PE) reads yielding a total coverage of 44-50 million reads equivalent to 7.5-8.5 Gb of data per run (Goodwin et al., 2016). Thus, Illumina® provides much more sequencing depth and number of reads than earlier Roche® 454, as well as a more rapid turnaround time of as little as 4 h making it more cost-effective. It can now produce up to 15 Gb output making it the most widely used NGS platform to date (Ravi et al., 2018).

High-throughput is further achieved by multiplexing and pooling samples in an individual sequencing run; allowing a large number of samples, up to 384, to be analysed simultaneously (Illumina, 2014). During DNA library preparation of each samples, specialised DNA adaptors and bar codes (or sequencing indexes) are hybridised to each DNA fragment. Each read sequenced is identified to a particular library representing a unique sample. For example, the Nextera XT library preparation kit manufactured by Illumina® provides 40 unique indexes; two are used in unique combination per DNA fragment enabling up to 384 samples to be analysed in a single sequencing run (Illumina, 2014).

A recent application of NGS Illumina® MiSeq sequencing performed in ME/CFS compared the 16S rDNA V4 sequences from faecal samples of 48 patients compared with 39 healthy controls (Giloteaux et al., 2016). Most of these patients (n=34) reported GI symptoms including constipation, diarrhoea, and abdominal pain/sensitivity (Giloteaux et al., 2016). In

total, 8,534,117 reads were obtained with an average of 98,093 reads per sample (Giloteaux et al., 2016). The primary finding was a reduction of bacterial diversity in ME/CFS patients, (P=0.004, W=1268; figure 2.2). To define the diversity of a sample, sufficient number of sequences must be obtained from each sample to identify all present bacterial taxa. The rarefaction curve in figure 2.2 shows as the number of reads increase the number of identifiable taxa increases up to a plateau. Beyond this point despite increasing the vast number of additional reads, very few or no additional taxa will be identified (Hanson & Giloteaux, 2017). However, too few reads (below 5000, green area) will cause underestimation of bacterial diversity. This puts into perspective the relatively low number of reads achieved by Fremont and colleagues in the earlier study, where 6000-7000 reads per sample did not distinguish α-diversity within ME/CFS samples compared to controls using the same indices of diversity within a sample (Shannon H evenness, Chaos1 and PD richness).

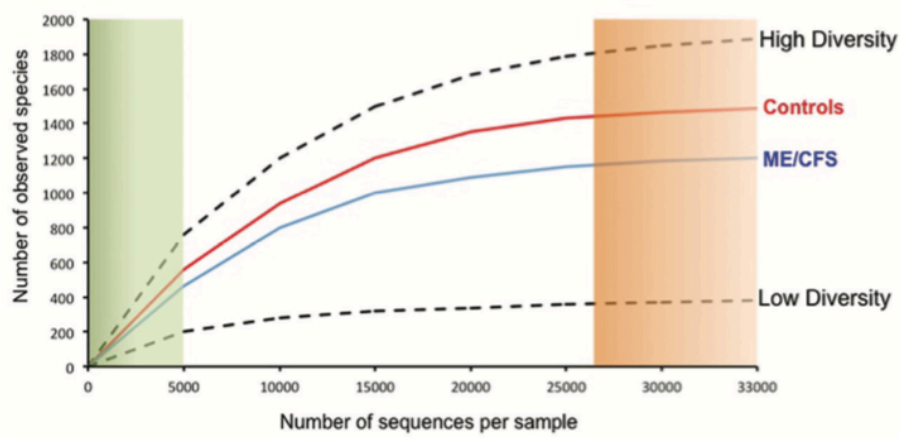

Figure 3.1.2 Sequence-based rarefaction curve of Phylogenetic diversity across ME/CFS and Control samples using 16S targeted rRNA sequencing. Based on the same number of sequences per sample, the diversity of assigned bacterial taxa (observed species) is higher in controls compared with ME/CFS patients. Figure reproduced from (Hanson & Giloteaux, 2017)).

Gilateaux et al. reported a reduction in *Bifidobacterium* and *Faecalibacterium* species in ME/CFS patients (figure 2.3) (Hanson & Giloteaux, 2017). Individually the genera in fig. 2.3 represent only 1% of the gut microbiome. At the phylum level, firmicutes were reduced in patients at 35% relative abundance (RA) versus 46% in controls with a relative increase in the abundance of proteobacteria, belonging to the family *Enterobacteriaceae*; 6% in ME/CFS versus 3% in controls (Giloteaux et al., 2016).

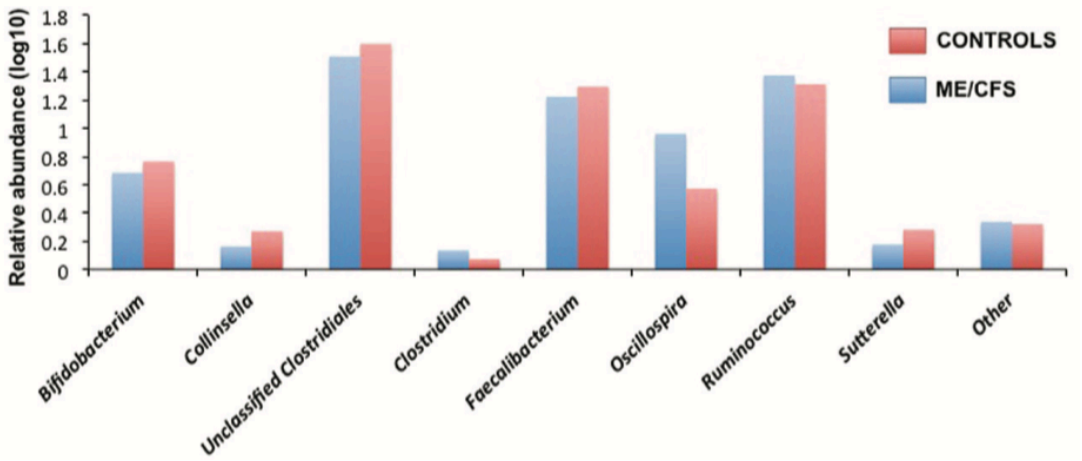

Figure 3.1.3 Comparison of relative abundances of bacterial genera between ME/CFS patients and Healthy Controls. Shows relative abundance on a log10 scale. Figure reproduced from (Hanson & Giloteaux, 2017).

The majority of 40 OTUs found to be different in ME/CFS were within Firmicutes; including *Ruminococcaceae* family members *Oscillospira* spp, *F. prausnitzii*, *Ruminococcus*; and *Lachnospiraceae* such as *Coprococcus* spp. (Giloteaux et al., 2016).Although butyrate production was not measured in this cohort, a reduction in butyrate producers and lactic acid promoting bacteria (beneficial to barrier function) is similar to individuals with IBD and IBS and will influence the production of PICs and consequently the risk of immune activation and increases in intestinal permeability demonstrated by higher levels of LPS, sCD14 and LBP in the plasma of ME/CFS patients (Giloteaux et al., 2016).

- *Whole-Genome 'Shot-gun' (WGS) sequencing*

Whole genome sequencing, WGS (also called Shotgun metagenomics) is unrestricted to specific target amplicons, like 16S, and is able to resolve the microbiota beyond the genus level, including sequencing information derived from other members of the microbiota such as fungi and viruses. WGS can determine low abundance species as well as functional capacity of the sample microbiome based on the mapping of individual genes (Ranjan et al., 2016). From this, the potential metabolic pathways that enable the microbiota to function, and more critically identify pathways that are disrupted in disease can be deduced. This in combination with other 'omics technologies, particularly metabolomics (in the next chapter) may provide a more informative description of intestinal dysbiosis in ME/CFS

patients according to the metabolic function of their intestinal microbiota rather than just changes in composition.

The first WGS-based study was performed in ME/CFS sub-grouped according to the presence of IBS symptoms. Out of the 50 ME/CFS patients recruited, 21 had been diagnosed with IBS with no cases of IBS in 50 healthy controls. Shotgun metagenomic sequence data collected from this cohort is fundamentally different to earlier ME/CFS microbiome studies in that it will not be subject to amplification biases of 16S based sequences; furthermore species-level assignments are possible using MetaPhlan taxonomic assignment, in addition to identification of biological pathways. Increases in unclassified *Alistipes* and *Faecalibacterium* emerged as microbial markers of ME/CFS with IBS, whist robust statistical testing agreed decreased RA of *B. vulatus* defined ME/CFS without IBS (Nagy-Szakal et al., 2017). Differences with bacterial species in ME/CFS were driven by IBS co-morbidity including a reduction in RA of *Faecalibacterium* species, *R. obeum*, *E. hallii*, and *C. comes* (Nagy-Szakal et al., 2017). Table 2.1 lists the bacterial species taken from the Nagy-Szakal et al. (2017) study that are the strongest predictors for subgroups of ME/CFS with/without IBS.

"ME/CFS"	"ME/CFS + IBS"	"ME/CFS – IBS"
C. *catus*	Faecalibacterium cf.	Bacteroides *caccae*
P. *capillosus*	Bacteroides vulgatus (decreased	P. *capillosus*
D. *formicigenerans*	RA distinguishes from ME/CFS –	P. *distasonis*
F. *prausnitzii*	IBS, on all statistical tests)	Bacteroides *fragilis*
C. *asparigiforme*		Prevotella *buccalis*
Sutterella *wadsworthensis*	Additional 9 added:	Bacteroides *xylanisolvens*
A. *putredinis*	F. cf.	D. *formicigenerans*
Anaerotruncus *colihominis*	F. *prausnitzii*	
	B. *vulgatus*	
	A. *putredinis*	
	C. *catus*	
	A. *caccae*	
	D. *formicigenerans*	
	A. *colihominis*	
	C. *asparagiforme*	

Table 3.1.1 Lists of bacterial species extracted from text of Nagy-Szakal paper, relevant to their predictive model to distinguish ME/CFS subgroups from controls

Interestingly, there were significant correlations between certain bacterial species and symptom severity scores using the SF-36 and Multidimensional Fatigue Inventory (MFI). Decreased RA of *Faecalibacterium* spp, *R. obeum*, *E. hallii*, *C. comes* and *Coprococcus* spp were associated with IBS-like hypersensitivity, bloating and abdominal discomfort (Nagy-Szakal et al., 2017).

- *Summary*

Both Giloteaux et al. (2016) and Nagy-Szakal et al. (2017) have used different methods to produce lists of bacteria at various taxonomic levels (partly on whether the data is 16S or shotgun) which are putatively overrepresented in either patients or controls. Both studies assess the size of the effect that each taxon has on the difference between groups, using the same method of Linear Discriminant analysis Effect Size, (LEfSE). Significant differences were found in 40 OTUs (out of ~1,330 OTUs per sample), but only appear to name corresponding species for some of them despite this being 16S data. Moreover, even if all taxa were distributed randomly between patients and controls, you are likely to get a small number, which appear, by chance, markedly more abundant in one group compared to the other. To that end, if this study were to be repeated it would be surprising if all of these genera listed were found to be significantly more/less abundant in ME/CFS again because of major environmental factors, such as diet known to contribute to population-level variation of the microbiota on a daily basis. Figure 2.4 is taken from Fig. S2 in this paper, to highlight the difficultly in equating these taxa to differences for separation of ME/CFS from Controls in these plots.

The 2017 study additionally presents functional pathways overrepresented in ME/CFS with or without IBS compared with controls. In their statistical analyses, “ME/CFS” is referred distinctly from “ME/CFS + IBS”, and “ME/CFS – IBS”, and “controls” (no ME/CFS, no IBS), suggesting the “ME/CFS” is a supergroup being compared with subsets of itself. Critically this paper lacks an IBS-only disease control group. Parts of the methods to this work suffer ambiguity, particularly with respect to the tools used to create the topological data analysis (TDA) and machine learning approach to identify difference across groups; the lack of detail here does not makes this easily reproducible. The machine learning approach was successful in the Giloteaux et al. (2016) study as a way to see what combination of microbial taxa and various plasma markers could successfully predict whether a subject is a patient or control, using most of the data as a training set and then making predictions on the remaining samples. Finally, there is consistency between TDA, the rank-based test, the LEfSe, and features identified by machine learning for species belonging to *Faecalibacterium, Roseburia, Dorea, Coprococcus, Clostridium, Ruminococcus*, and *Coprobacillus* as significantly different in “ME/CFS” compared with “controls” (Nagy-Szakal et al., 2017).

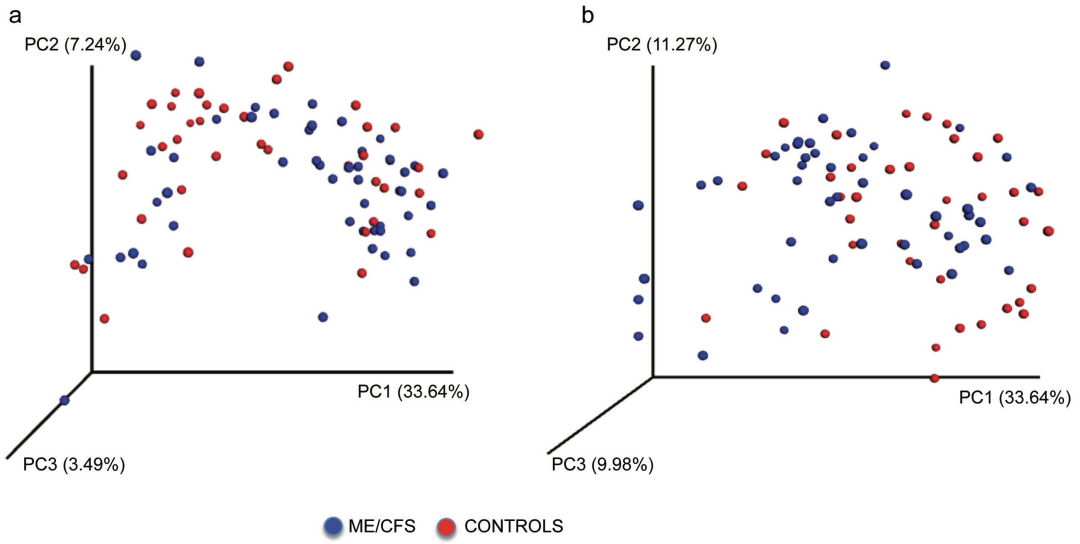

Figure 3.1.4 Principal Coordinate Analysis (PCoA) plot of healthy controls versus ME/CFS based on 32223 sequences per sample using targeted 16S rRNA gene sequencing. 16S rRNA derived microbial community analysis reveals no difference in beta-diversity between patients and controls. Clustering distances calculated with weighted UniFrac (a) and unweighted UniFrac (B). Figure reproduced from (Giloteaux et al., 2016), supplementary figure S2.

- *Confounders of microbiome diversity*

The differences found between Norwegian and Belgium ME/CFS patients highlight the importance influences the environment, diet and genetic background have on the composition of the intestinal microbiota (Fremont et al., 2013). Most studies offer gender and age matching of healthy controls to their patients, with no consideration of the above factors. Cohousing mice is a routine and regular practice in studying the effects of the intestinal microbiota and to control for dietary influences. Interestingly a recent paper studying the enteric virome in IBD in humans demonstrates the importance of having house-hold controls to increase the power of detecting disease-associated changes. Then natural variability in intestinal bacteria and viruses in non-household controls and patients makes it more difficult to see such disease-specific alterations (Norman et al., 2015). It is also expected house-hold controls will more likely share a similar diet and will normally share a similar genetic background mother-daughter or father-son. In these circumstances age of course cannot be matched; however, researchers have to decide which factors to give the priority towards controlling and will depend upon individual study design and the hypothesis. So far, no study investigating the microbiome in ME/CFS has attempted to recruit house-hold controls.

Indeed, comparison of multiple studies in microbiome research is complicated by the fact that different researchers opt for different study designs, extraction methods, sequencing platforms and favour different bioinformatic tools to interpret the data (D'Amore et al., 2016). Nagy-Szakal et al. (2017) acknowledge that their work cannot be directly compared to the earlier 16S rDNA analyses but support intestinal dysbiosis in ME/CFS based on increases/decreases of the RA of specific bacterial species (table 2.1). However, they have made a first attempt to correlate specific symptoms and severity with patterns of dysbiosis in ME/CFS although their study design did not make severity a focus. Impact of severity included scores associated with emotional wellbeing, motivation, fatigue and pain, however the relatively small cohort make it difficult to predict ME/CFS severity using their microbiome data in this study.

Study	Sequencing method	Recruitment criteria	Sample size	Platform	Av. number of reads	16S rRNA variable region	Significant Observations/Conclusions
Sheedy et al. (2009)	Culture-based assays	Holmes (1988) /Fukuda (1994)/ Canadian (2003)	108 ME/CFS 177 controls	N/A	N/A	N/A	↑D-lactate *Enterococcus* and *Streptococcus spp.*
Fremont et al. (2013)	16S targeted amplicon	Fukuda (1994)	43 ME/CFS 36 controls	454 FLX (Roche®)	6000-7000 per sample, min 240 b.p.	V5-V6	Belgian patients: x45 < *Lactonifactor genus* Norwegian patients: x20 < *Lactonifacor genus* 3.8 fold < in *Bacteroidetes genus Alistipes* Decreased *Firmicute* sub-populations
Hanson et al (2016)	16S targeted amplicon	Fukuda (1994)	48 ME/CFS (34 report GI disturbances) 39 controls	Illumina® MiSeq 2x250 bp	98,093 ± 29,231 reads per sample	V4	Reduced *Bifidobacteria* and *Faecalibacteria spp.* Positive plasma markers for increased intestinal permeability: LPS, LBP, sCD14 PD metric: ME/CFS less diverse than Healthy Controls
Lipkin et al. (2017)	Shotgun Metagenomic	Fukuda (1994)/ Canadian (2003)	50 ME/CFS 50 controls	Illumina® HiSeq 4000 2x100 bp	~35 million reads per sample 10 samples/pool 350 million reads per pool	N/A	Family level: ↓ *Lachnospiraceae* & ↓*Porphyro-monadaceae* in ME/CFS Genus level: ↓*Dorea*, ↓ *Faecalibacterium*, ↓*Coprococcus*, ↓*Roseburia*, & ↓*Odoribacter* ↑*Clostridium* and ↑*Coprobacillus* in ME/CFS

Table 3.1.2 Summary of microbiome studies performed in ME/CFS with relevant findings and overview of methods to determine these differences Up arrows denote increased relative abundance; down arrows denote reduction in relative abundance of bacterial taxa.

3.1.3 Aim and Objective

There is limited evidence to suggest ME/CFS is associated with an altered intestinal microbiota and increased permeability. It is not known how well these findings replicate in other patient cohorts or according to disease severity. Existing published ME/CFS research has made no attempt to stratify patients based on specific symptoms and severity. Often such studies are indirectly comparable due to lack of protocol standardisation and agreement on the best inclusion and exclusion criteria to recruit patients.

The aim for this first results chapter was two-fold. The first, to focus recruitment on patients who are house-bound with severe symptom severity, postulating that the severity of gut dysbiosis may be directly linked to extreme fatigue and neurological symptoms in these patients. The second, to compare house-bound patients with a house-hold control in order to:

- control for environmental factors known to cause population-level variations in microbiome data;
- use 16S targeted gene marker sequencing and whole genome “shotgun” metagenomic sequencing to assess for evidence of or any pattern of intestinal dysbiosis that may;
- support conclusion from existing metagenomics studies in ME/CFS, and;
- identify key bacterial species belonging to a novel “microbial signature” which may help define severe ME patients from those mild to moderately affected.

3.3.4 Hypothesis

Severe, house-bound ME/CFS patients have a distinct microbial signature for dysbiosis that is reflected by their profile of gut bacteria; the composition and reduction of diversity of which, separates them from house-matched healthy controls and when compared to existing metagenomics data from the general ME/CFS population.

3.2 Materials & Methods

3.2.1 Patients

For the work presented in this chapter, a total of 52 individuals (42 ME/CFS and 10 controls) were recruited and consented between 2015-2017 to provide faecal samples to this study. Of these ME/CFS patients, 17 were severe, house-bound and 25 mild/moderate. An additional faecal sample one year on was available in 2017 from 8 previous participants (4 severe ME matched to 4 house-hold controls), bringing the total to 60 faecal samples processed for microbial DNA extraction and sequencing across 16S and whole genome metagenomic platforms.

Prior to any home visits, mild/moderate ME patients were the first participants to be recruited and sequenced in 2015 using 16S rDNA V4 sequencing generating "Dataset A". Home visits to severe patients were conducted in 2016 ("Dataset B") and 2017 ("Dataset C") with modifications made to stool sample collection method that have been used for mild/moderate patients (described below). All samples were initially stored at -80^{o}C at St Helier Hospital, Carshalton, London. At the end of the study recruitment phase, all samples were packaged in dry ice containment and collected by an authorised courier for them to be deposited within the Norwich Biorepository. Samples were the accessible from the Biorepository to be used in experiments.

- *Stool sampling kits*

The original stool kit used for recruitment of mild/moderate patients included the following items: a Protocult^{TM} collection device (Product #500 Ability Building Centre, Rochester, MN, USA), OMNIGene® GUT stool device (OMR-200, DNA Genotek, ON, Canada), x4 30 ml Universal tubes with spatulas, and zipped bags for packaging. Using this method patients took samples from their own stool and equally divided as much of the sample as possible across the four tubes. As per instructions on the package insert of the OMNIGene® (figure 3.1.1), patients were asked to transfer equivalent of a pea-sized amount of faeces into the yellow tube top and scrape horizontally. After replacing the purple cap, the device is shaken back and forth as hard as possible by hand, for a minimum of 30 seconds to allow mixing with the stabilising liquid.

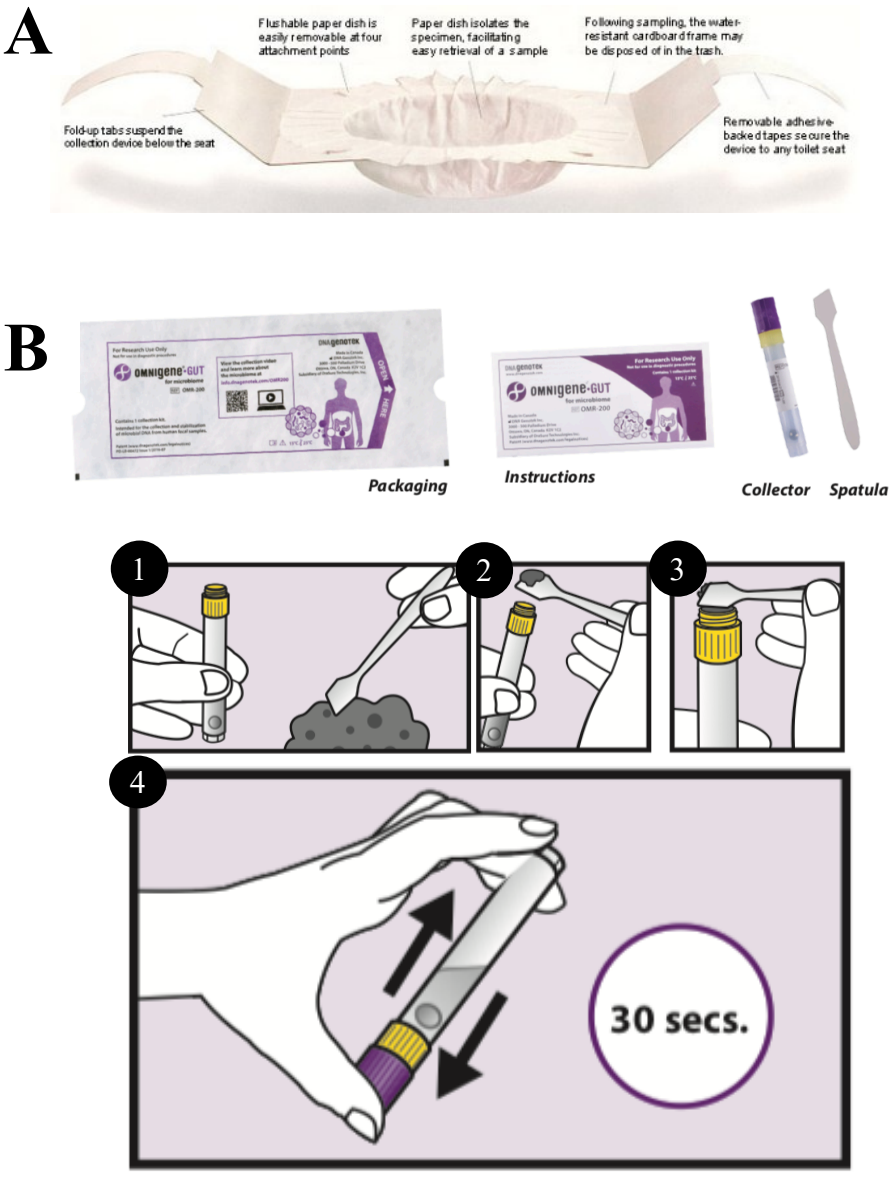

Figure 3.2.1 Instructions for OMNIGene® GUT collection device used to collect mild/moderate ME/CFS samples in 2015. Patients collected their stool using the paper Protocult™ collection device (A), and then taking a 'pea-sized' spot sample from their stool transferred this to an OMIGene™ GUT® tube (B) and followed the visual instructions (1-4) as shown in this figure. The rest of the faecal sample was then divided equally across four 30 ml Universal tubes. Images obtained from: https://www.dnagenotek.com/us/products/collection-microbiome/omnigene-gut/OMR-200.html [assessed 10 March 2019].

- *Improvements to stool sample collection in 2017*

In 2017 changes were made to improve faecal sample collection to facilitate entire stool sample collection for the purposes of homogenisation. This step was particularly necessary for preparation of faecal water samples, as spot sampling from different areas of the same stool sample has been shown to produce varying results (Gratton et al., 2016a). Severe and house-matched participants were instructed to collect their entire faecal sample into a device called a FECOTAINER® (AT Medical B.V., Enschede, The Netherlands), figure 2.2.2 no sooner than 24 hours before a scheduled home visit, and to keep it in the fridge at 4^0C in double containted in plastic bags provided. This kit also contained an AnaeroGen™ Compact anaerobic sachet (Cat No. AN0010, Oxoid Ltd., United Kingdom) to activate as soon as participants produced their sample to minimise oxygen conditions limiting any aerobic growth and activity. On return to the hospital, samples were manually homogenised with a sterile autoclaved metal spatula and processed according to their downstream application and stored at -80°C until required.

3.2.2 Faecal DNA extraction

The method for DNA extraction from human faeces was obtained from the Hall Lab at Quadram Institute Bioscience, with minor adaptions to the manufacturer's kit protocol. Prior to experimenting, faecal DNA extracts were prepared from frozen faecal aliquots that had been pre-weighed (~250mg) into a sterile Lysing Matrix E tubes from the FastDNA SPIN kit for Soil (Cat. No. 116560200, MP Biomedicals, UK). Samples were stored at -80°C as soon as possible on the same day of collection. Earlier samples obtained using the OMNIGene GUT device began the exact same process to be described here, instead taking 250 µl of faecal homogenate.

On the day of the experiment, faecal aliquots were thawed, after which 978 µl sodium phosphate buffer and 120 µl MT buffer was added and homogenised using the FastPrep® Instrument for a duration of 45 seconds and repeated for a total of 3 cycles. Each cycle was separated by placing each sample in ice for 60 seconds to reduce heat. Following the mechanical destruction of bacteria cells within the faeces, cell debris and other faecal particulate were removed by centrifuging at 14,000 x g, for 15 min. The supernatant was transferred into a sterile 2.0 ml Eppendorf tube, to which 250 µl of PPS was added to precipitate protein from the solution. The supernatant was transferred in 15 ml tubes

containing 1 ml of Binding Matrix and inverted by hand for 2 minutes to allow DNA binding. Tubes where then placed in a rack and allowed to settle for 3 minutes after which 500 µl of the supernatant was discarded with care not to disturb the settled Binding Matrix. The remaining resuspended Binding Matrix solution containing bound DNA was passed through a SPIN filter tube at 14,000 x g, for 1 minute. DNA captured on the column was washed using DNase-free salt/ethanol wash (SEWS-M). Subsequently, a second dry spin was performed and each SPIN filter air dried for 10 minutes at room temperature to remove excess alcohol. Finally, DNA was eluted in 50 µl of DNase/Pyrogen free DNA water (DES) pre-incubated at 50 degrees to enhance DNA recovery and stored at 4^{o}C short term, or at -20^{o}C for a longer period. DNA was quantified using Qubit® and Agilent Tapestation.

3.2.3 Acquisition of 16S rRNA gene sequence data

V4 16S rRNA gene sequencing was performed in two batches for mild/moderate patients in 2015 and severe and house-hold controls in 2017. Following microbial DNA was extraction as described above, these samples were sent to sequencing companies for further downstream processing as described below:

- *Mild/moderate ME/CFS (n=25)*

DNA extracted from 25 faecal samples from *mild/moderate* ME/CFS patients was submitted to Animal Health and Veterinary Laboratories Agency (AHVL) for PCR amplification of the V4-V5 region of the 16S rRNA gene (primers: U515F, 5'-GTGYCAGCMGCCGCGGTA-3'; U927R, 5'-CCCGYCAATTCMTTTRAGT-3') and (Illumina MiSeq) sequencing. 16S rRNA gene sequence data were processed using QIIME 1.9 (Caporaso et al., 2010). Demultiplexed read files were supplied by the sequencing provider. For each read file, paired-end reads were joined using fastq-join (Aronesty, 2011); minimum acceptable Phred quality score was Q20; primers were removed from reads using cutadapt leaving reads of ~370 nt in length (Martin, 2011). The read files were concatenated and OTUs picked using usearch (99 % mapping, similarity, gg_13_8), which also performs chimera checking (Edgar, 2010). Sequences were aligned using PyNAST (Caporaso et al., 2009). Taxonomy was assigned using gg_13_8 (99 %), with annotations for the representative sequence set checked and corrected where necessary (e.g. in Greengenes, members of the family *Rikenellaceae* are poorly annotated and newly described prokaryotes are not annotated). Singletons and reads representing < 0.001 % of total reads were filtered from the OTU table. For descriptions of data in terms of abundance,

rarefaction was performed on the OTU table (*n* = 8,750) so that the number of reads compared per sample was identical.

- *Severe ME/CFS (n=21) and House-hold controls (n=12)*

Faecal DNA extracted from severe house-bound patient and their respective house-hold controls were submitted to Novogene® for 16S sequencing. DNA concentration and purity were checked on 1% agarose gels. According to the concentration, DNA was diluted to 1ng/μL using sterile water. The V4 region of the 16S rRNA gene were amplified using specific primers, U515: F, 5'-GTGYCAGCMGCCGCGGTA-3'; and U806, R, 5'-CTACCRGGGTATCTAATCC-3' (Caporaso et al., 2011). All PCR reactions were carried out with Phusion® High-Fidelity PCR Master Mix (New England Biolabs). PCR products stained with Sybr Green nucleic acid stain were separated on a 2% agarose gel and bands selected between 400-450bp of length. These PCR products were mixed in equidensity ratios. Then, the mixture of PCR products was purified with Qiagen Gel Extraction Kit (Qiagen, Germany). Libraries were generated using the NEBNext® UltraTM DNA Library Prep Kit for Illumina and sequencing performed on the Illumina® MiSeq platform. Paired-end reads was assigned to samples based on their unique barcode and truncated by cutting off the barcode and primer sequence. Demultiplexed read files were supplied by the sequencing provider.

Acquisition of Shallow Shotgun Metagenomic sequence data

- *Dataset B*

DNA extracted from 11 severe ME/CFS patients and 8 house-matched controls were quantified using Qubit® Broad Range Assay and submitted to Dr Gemma Kay at the Bob Champion Biomedical Research Building, University of East Anglia, UK, for library preparation. An additional sample of containing 20 μl DES H_2O was processed alongside the faecal samples to act a negative control and to highlight potential kit contamination. Illumina library construction was prepped using the Nextera XT DNA kit (Illumina Inc. USA) containing barcoding sequences and i5 and i7 primer adaptors. Raw sequencing reads were pre-processed using Trimgalore (v 0.4.4) for end trimming and filtered to exclude low-quality and low-complexity reads. Adaptor sequences were removed using cutadapt contained with the Trimgalore wrapper. Human sequences were subtracted from the dataset using BBMap 38.06 to align them against the Human reference (hg38), keeping

only unaligned reads for further processing. Bacterial composition (relative abundance) was obtained from raw sequencing data using MetaPhlAn (v1.7.8).

Dataset	Year	Study type	Sample Size	ME/CFS status	Platform	Av. number of reads	Analytical methods & bioinformatics tools
A	2015	16S rRNA targeted amplicon U515F, U927R	n = 25 ME/CFS No controls	Mild/ moderate	Illumina® MiSeq x2 300 bp V4 region	70,769 (rarefied to 8,750)	16S rRNA gene sequence data were processed using QIIME 1.9, species annotation by Greengenes assigned 99% similarity OTU clustering Few *Actinobacteria* (*Bifidobacteria* and *Coriobacteria*
B	2016	"Shallow" shotgun metagenomics	n = 19 11 female ME/CFS 8 house-matched control (7 female, 1 male)	Severe, bed bound	Illumina® MiSeq x2 300bp	960,260 (ranges 253,000 - 2,168,000)	MetaPhlAn 2.0. Capacity to determine species level and functional capacity Microbial community analysis performed using MEGAN 6.0
C	2017	16S rRNA targeted amplicon U515F; U806R	n = 33 21* females ME/CFS 12* house-matched controls	Severe, bed bound	Illumina® HiSeq 2500 x2 250 bp V4 region	150,882 (rarefied to 47,985)	QIIME 1.7 97% similarity OTU clustering, species annotation by SILVA database Microbial community analysis performed using MEGAN 6.0

Table 3.3.1 Summary and descriptions of metagenomic datasets (A-C) collected in 2015, 2016 and 2017.

Sample Summary:
Dataset A (2015)

	Status	Sex	Age	DV**	Reads	Observed OTUs
28	Mild/Moderate	M	54	22	68,165	310
30	Mild/Moderate	F	28	15	58,752	289
31	Mild/Moderate	M	41	24	48,775	142
32	Mild/Moderate	F	65	17	66,839	278
33	Mild/Moderate	M	48	18	65,459	222
35	Mild/Moderate	M	37	21	64,504	284
37	Mild/Moderate	F	60	1	140,262	238
38	Mild/Moderate	F	43	2	91,835	352
39	Mild/Moderate	F	39	3	82,192	338
40	Mild/Moderate	F	44	4	118,137	283
41	Mild/Moderate	F	54	5	77,531	238
42	Mild/Moderate	F	45	6	87,229	318
43	Mild/Moderate	M	47	7	77,101	366
44	Mild/Moderate	F	25	8	106,107	113
45	Mild/Moderate	F	48	10	58,552	332
46	Mild/Moderate	F	72	11	71,712	345
47	Mild/Moderate	F	30	12	61,424	225
48	Mild/Moderate	F	55	13	54,967	336
49	Mild/Moderate	F	33	14	46,834	306
50	Mild/Moderate	M	58	16	68,534	300
51	Mild/Moderate	F	53	19	9,064	229
52	Mild/Moderate	F	27	20	75,622	235
53	Mild/Moderate	F	32	23	76,883	327
54	Mild/Moderate	F	21	26	57,916	216
55	Mild/Moderate	F	59	27	34,851	171

Table 3.3.2 Sample summary of dataset A containing 25 mild/moderate patients (44.72 ± 13.40 years old). Note: these samples were processed using OMNIGENE gut collection tube prior to DNA extraction and 16S gene sequencing.

Sample Summary:
Datasets B & C

	Status	Sex	Age	'Shallow" Shotgun 2016	16S (V4 region) 2016	2017
1	Severe	F	63	ME_8	F26	
2	Severe	F	56	ME_5		F15
3	Control	F	55	CTR_4	F31	F6
4	Control	F	69	CTR_17	F30	F4
5	Severe	F	44			F3
6	Control	F	70			F20
7	Control	F	55	CTR_18		F19
8	Severe	F	38	ME_13		F2
9	Severe	F	21	ME_3	F33	F10
10	Severe	F	37			F9
11	Control	F	64			F11
12	Severe	F	18	ME_12	F27	F7
13	Severe	F	61			F1
14	Severe	F	40			F17
15	Severe	F	54			F18
16	Severe	F	58	ME_1	F21	F13
17	Control	M	60	CTR_2	F22	F14
18	Severe	F	27	ME_6	F23	F12
19	Control	F	60	CTR_16	F28	F8
20	Severe	F	63			F5
21	Severe	F	32	ME_7	F24	
22	Severe	F	31	ME_11	F25	
23	Control	F	54	CTR_15		
24	Control	F	29	CTR_14		
25	Severe	F	56	ME_10	F32	
26	Severe	F	30	ME_19	F29	
56	Control	F	34	CTR_9	F34	

Table 3.3.3 Sample summary of datasets B & C consisting of 17 Severe, house-bound patients (42.88 ± 15.16 years old) and 10 house-hold control (55 ± 13.62 years old). Samples obtained during 2016 and 2017. This table also highlights the cross over between datasets B and C in terms of DNA sequencing technology used to survey the ME microbiome.

3.3 Results

3.3.1 16S phylogenetic abundance in mild/moderate ME patients (n=25)

- *Dataset A*

Phylogenetic abundance data was generated from 21 females and 6 male mild/moderate patients. It was not possible to obtain samples from suitable control subjects. Raw sequences were trimmed using cutadapt to remove primers. In total, 1, 769, 247 reads were generated across 25 samples. The mean number of paired end (PE) reads at 250bp long obtained was 70,770 ±25,581 S.D. per sample. Reads which clustered together with 99% sequence homology generated a total of 686 Operational Taxonomic Units (OTUs) across all samples. Sequenced-based rarefaction curves were produced at 8750 (figure 3.3.1) and 34000 reads per sample, which demonstrated diversity of all 25 samples was covered by sampling at 8750 reads. A minimum number of 2 samples were required for each particular OTU to be observed in order for that OTU to be retained. After filtering OTUs of less than 0.01% relative abundance, on average, 272 ± 52 SD OTUs were obtained per sample.

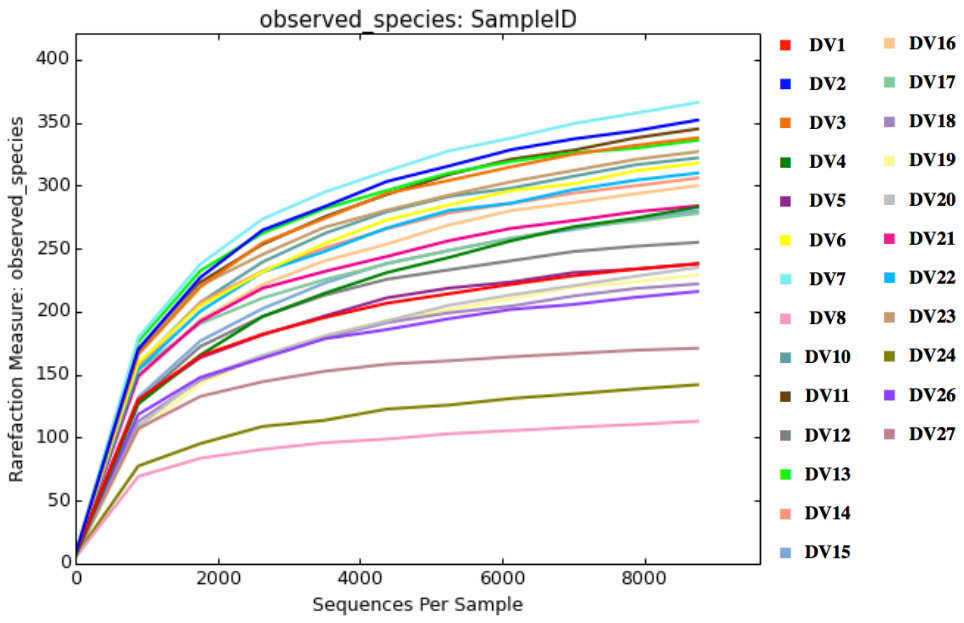

Figure 3.3.1 Rarefaction curve for the intestinal microbiota of 25 mild/moderate ME patients recruited from walk-in appointment at the CFS service. Each sample has been rarefied to 8750 reads. As the gradient of each curve increases less species are discovered within each sample. The higher the curve the greater number of species have been found within that sample.

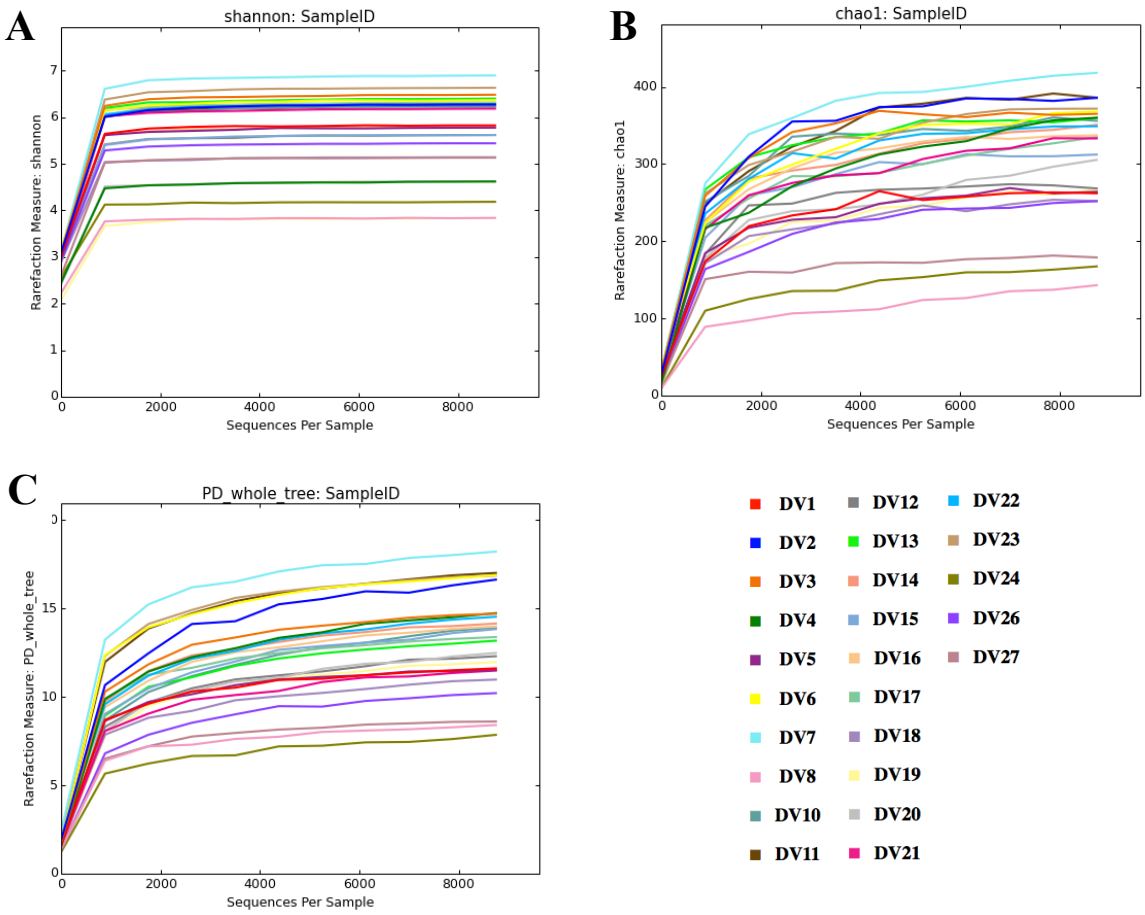

Figure 3.3.2 Alpha diversity plots showing community evenness (Shannon H) A, and richness (Chao1, and PD), B and C, of 25 mild/moderate ME/CFS faecal samples derived from dataset A. As the gradient of each curve decreases and reaches a plateau the diversity (number of species identified) within that sample does not increase.

All samples were rarefied to 8750 reads, which was below the sample with the least number of reads, sample DV19 (table 3.3.3). The number of observed "species" represented by number of reads clustering with 99% sequence similarity to form unique OTUs was used to calculate the alpha diversity within the mild/moderate ME/CFS group. Figure 3.3.2 shows the respective curves for community evenness using the Shannon H index, and indices for community richness; Choa1 and Phylogenetic Diversity (PD). These plots show as the number of reads increases the curve approaches a plateau beyond which the diversity of each sample does not increase with increasing number of sequence reads. Based on rarefying to 8750 read per sample, Shannon indices produced a value of H = 5.68 $\pm$ 0.70 SD, whilst indices for community richness produced 309.92 $\pm$ 59.12 SD, and 12.18 $\pm$ 2.20 SD for Choa1 and PD respectively.

Of the 686 OTUs found across all samples, 62 were assigned to bacterial genera using the Greengenes database. OTUs which could not be assigned were classified as unknown. The relative abundance of all OTUs and assigned OTUs were outputted into Microsoft™ Excel® to provide tables at each different taxonomic level from kingdom to the genus level. Four samples DV2,6,7,23 had detectable *Archaea* ranging from 0.01% - 0.38% of all classifications.

- *Phylum level observations*

Compositional taxonomic analysis based on bacterial phyla (figure 3.3.3) identified *Firmicutes* and *Bacteroides* as the most abundant members of the microbiota at 49.02% and 47.80% respectively. *Tenericutes* were found in relative high abundance in two samples DV7 and DV23, 5.94% and 14.56% respectively.

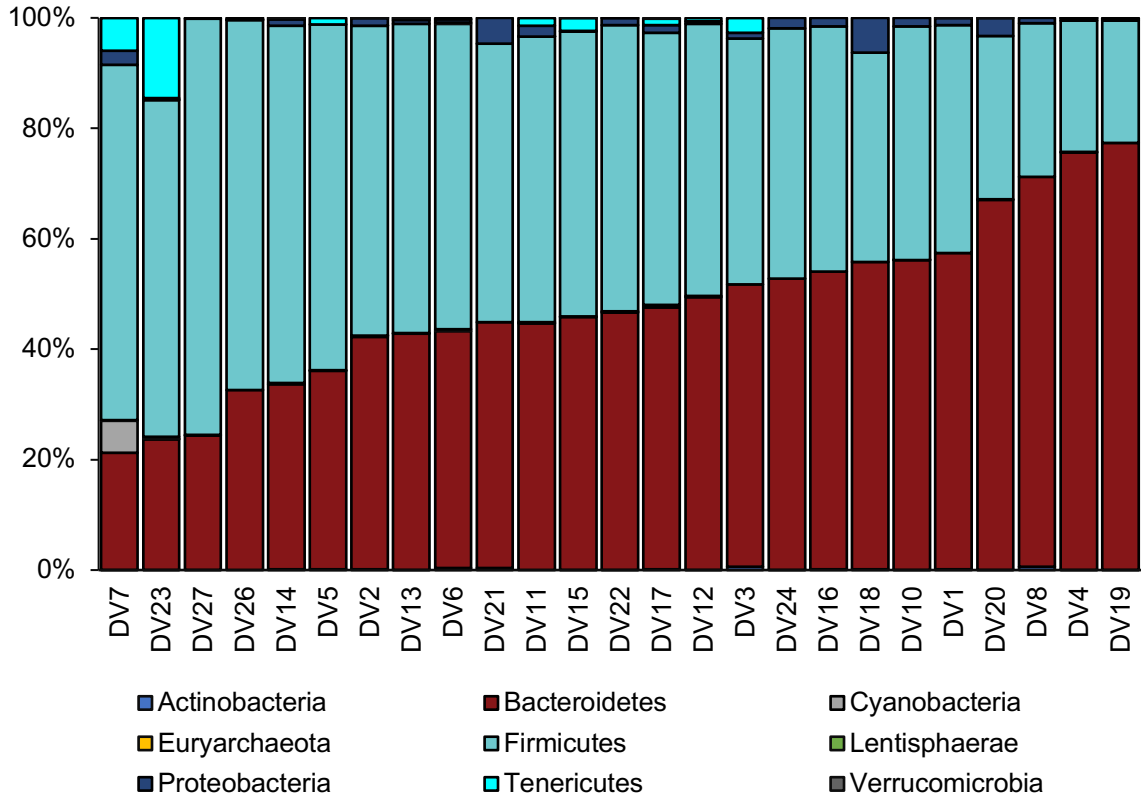

Figure 3.3.3 Relative abundance (%) of bacterial phyla provides a community composition profile of 25 mild/moderate ME/CFS patients. *Bacteroidetes* (red) and *Firmicutes* (turquoise) are the most dominant bacterial phyla within all samples

- *Genus level observations*

Genus abundance is the highest taxonomic level that can be achieved in 16S-based microbiome studies. On average 41.12 ± 3.62 SD genera (figure 3.3.4) were identified per sample, ranging from the lowest, 32 genera in sample DV27, to the highest, 47 genera in sample DV2. Four samples were distinguished by high abundance of *Prevotella*, particularly DV4 at 60.27% of all genera present. Few Actinobacteria which include members of *Bifidobacterium* (0.04%), *Coriobacteria* (0.19%) and *Eggerthella* (0.02%) were identified across all samples. On average, 12.27% ± 8.61 SD of genera (purple bars, fig 3.3.4) were classified as unknown.

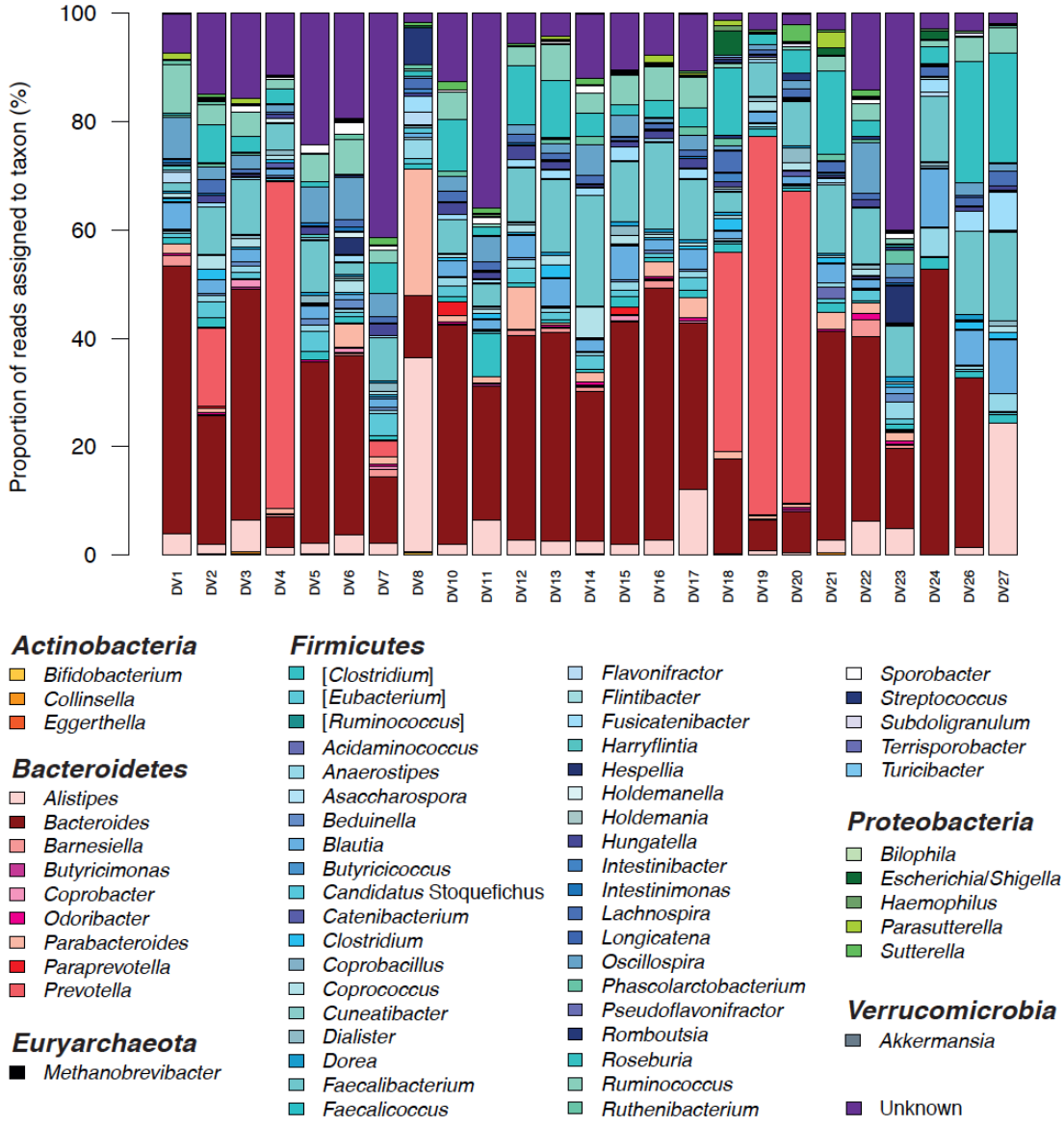

Figure 3.3.4 Genus-level abundance data produced sampling at 8750 reads per sample from faecal samples obtained from 25 mild/moderate ME/CFS patients collected in 2015.

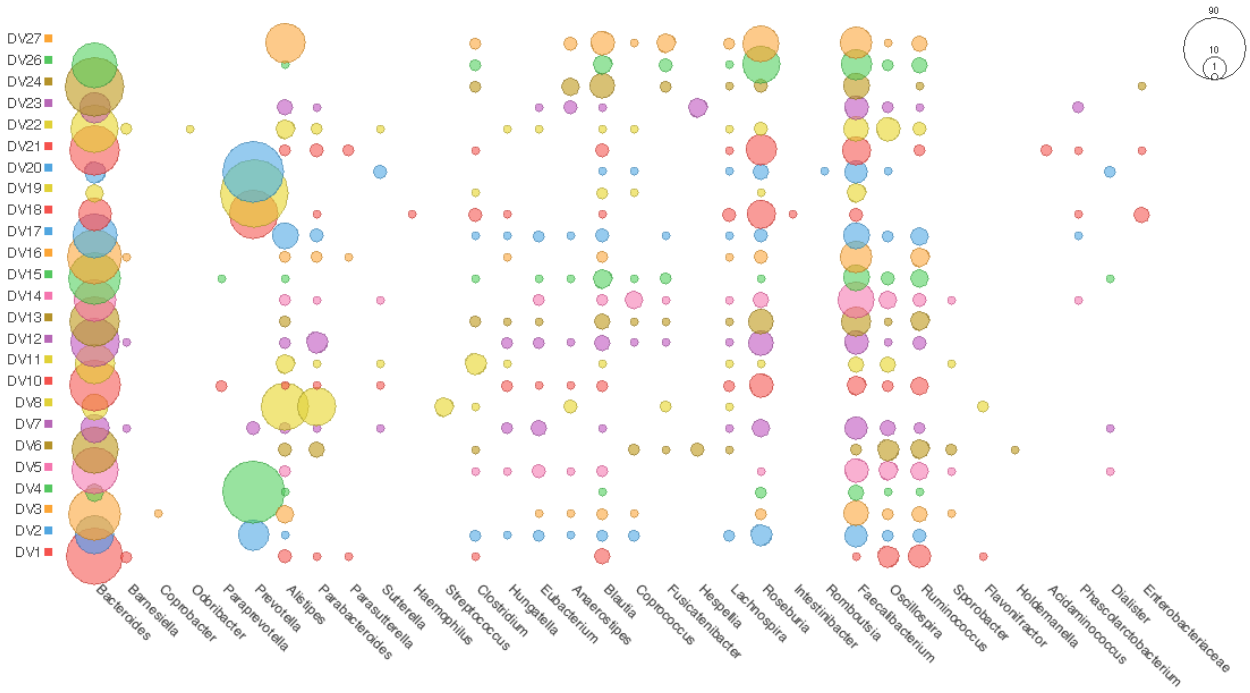

Figure 3.3.5 Summary of 34 top genera observed in 25 mild/moderate ME/CFS patients based on 16S V4 region sequencing identification. Circle size relative to percentage abundance.

The raw abundance tables were imported into MEGAN 6.0 for composition community analysis to visualise and compare each sample with the rest of the group. The top 34 most abundant genera are presented in figure 3.3.5. *Bacteroides* was the most abundant genus present in 24 samples at 28.06% ±12.60 SD. This genus was not detected in sample DV27; however, this sample had the third lowest number of reads. *Faecalibacterium* was prevalent in almost all samples at 9.27% ± 3.86 SD. No healthy sample control group processed at the same time of this sequencing to compare this data to. However, this data highlights some qualitative difference between patients that may influence the ME/CFS microbiota. For example, *Roseburia* is more abundant (6.01% ± 4.82 SD) in some patients than others ranging from 0.38% to 22.42% RA of the total ME/CFS microbiome. A similar pattern was seen for *Oscillospira* and *Ruminoccoccus* observed at 3.06% ± 2.04 SD and 3.54% ± 1.96 SD RA respectively.

Taxonomic profiles for all 25 samples was analysed using MEGAN which performed analysis of overall compositional differences samples within the group using multiple comparison tests for beta-diversity and applied to Principal Coordinate Analysis (PCoA) using Bray-Curtis dissimilarity. Near-neighbour network representation was generated to reveal any sample grouping (fig 2.3.6).

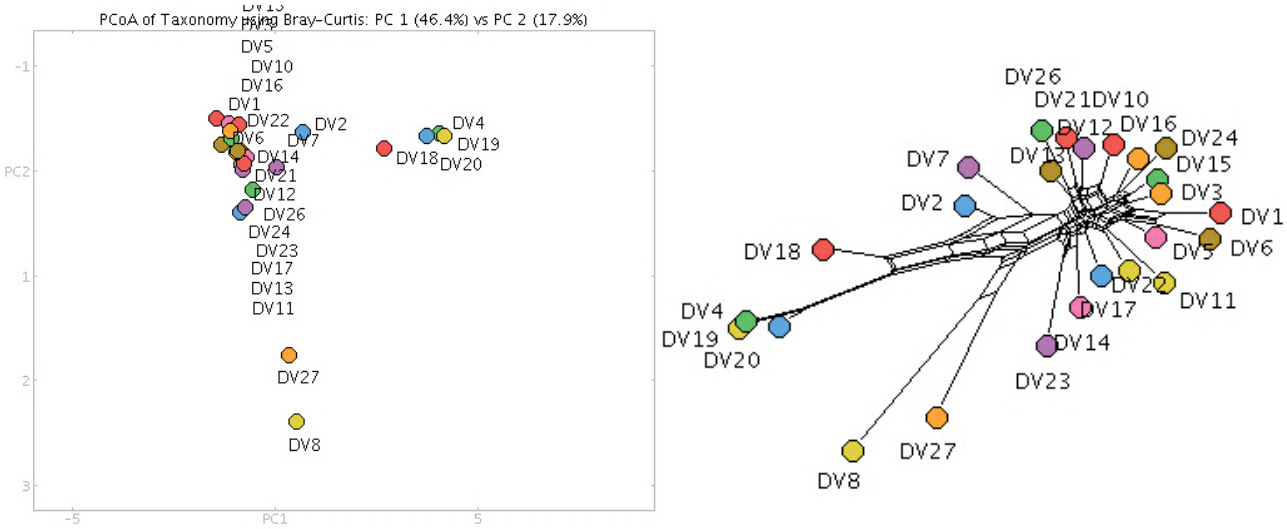

Figure 3.3.6 Principal Co-ordinate Analysis using Bray-Curtis dissimilarity and Nearest-Neighbour network analysis comparing all 62 genera across 25 mild/moderate ME/CFS patients. Figures created using MEGAN 6.0. Left, PCoA separates samples into clusters, the closer samples cluster together the more compositionally similar they are. Right, Nearest-neighbour network groups.

Bray-Curtis is influenced by the most abundant taxa within a sample. For example, DV4, DV18, DV19 and DV20 form a discrete cluster due to the higher RA of *Prevotella* in these samples 45% ± 19.72 SD. Other outliers include DV7 represented by 41.39% of unknown genera, and DV8 with the highest (35.93%) RA across all samples for *Alistipes*.

3.3.2 Shallow shotgun metagenomics

- *Dataset B*

Shotgun metagenomic sequencing of 11 severe, house-bound ME/CFS patients and 8 same house-hold healthy controls (HHC) relatives generated FASTQ files accumulating to 19.24 GB of sequence data from 300 bp, paired end reads from a single lane on the Illumina™ MiSeq® platform. The range of sequence reads obtained was between 230,000 and 2,168,000 for these samples. After QC clean up, there were no reads associated with sample CNEG-20 which was a blank control to exclude any DNA extraction kit contamination and 'kitome' effect. A high number of human-associated reads were found in all samples ranging from 7-44% of all reads and removed before analysing sequences using MetaPhlAn. A total of 152 species of bacteria were observed across all samples of which 143 were from within the severe ME/CFS groups compared to 88 found in the HHC group. On average the number of species per sample was 38.64 ± 6.28 and 34.62 ± 8.97 in ME/CFS and HHCs respectively.

- *Phylum level observations*

Firmicutes were the most abundant bacterial phyla within most samples for patients and HHCs, in figure 3.3.7 (turquoise bars) at 58.17% ± 21.6 in ME and 56.11% ± 12.92 SD in HHC. *Bacteroides* were less dominant at 17.90% ± 15.26 SD in ME versus 26.66% 13.54 SD in HHC. *Actinobacteria* (blue bars) were more abundant in ME compared with HHC, at RA of 14.59% ± 8.41 SD versus 11.72% ± 6.72 respectively. *Euryarchaeota* (yellow bars) were found in 3 ME/CFS samples, the highest RA in 1_ME at 15.89%, and in a single HHC sample, 4_HHC at 2.05% RA. These samples were not from the same house-hold. Sample 4_HHC was also notable for having the highest number of human reads at 43.77% of all 253, 484 reads generated. After filtering human reads only 169,707 were useable for metagenomic characterisation. Table 2.3.2 present summary of number of reads associated with each sample.

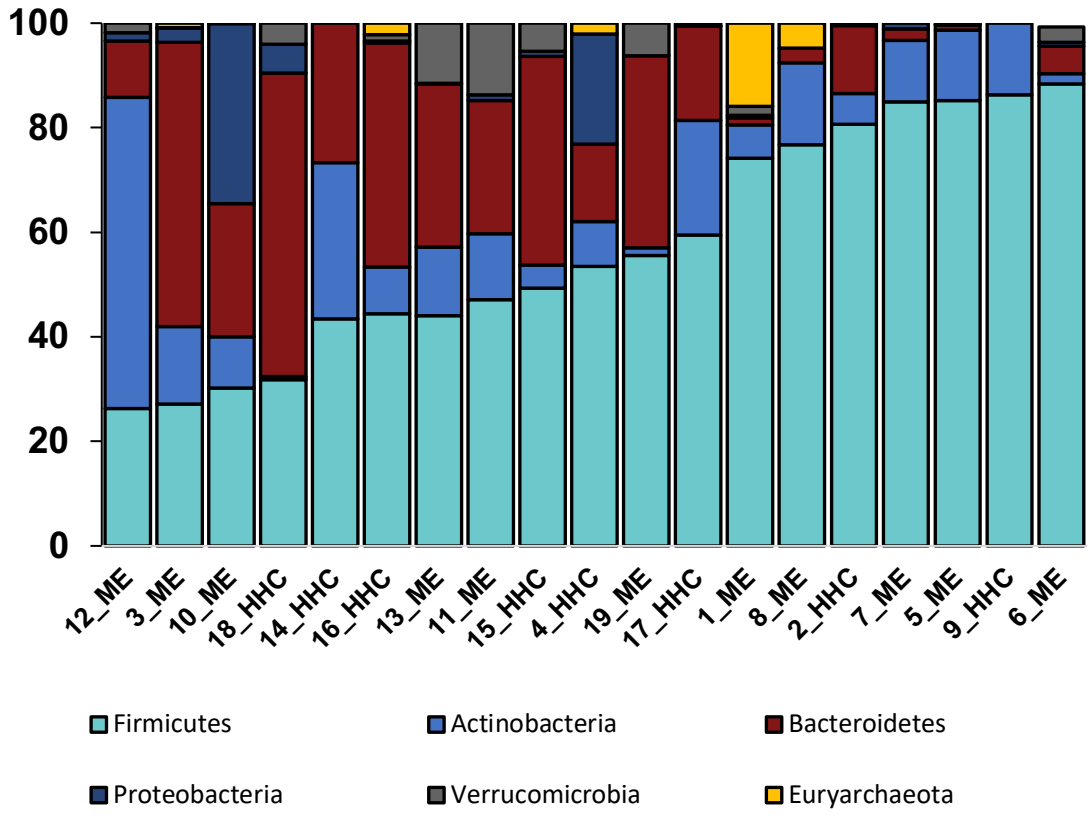

Figure 3.3.7 Relative abundance of bacterial phyla observed across all 19 samples (severe ME=11, HHC=8) using Illumina™ MiSeq® sequencing platform. There are no proportional differences in these bacterial phyla between both groups.

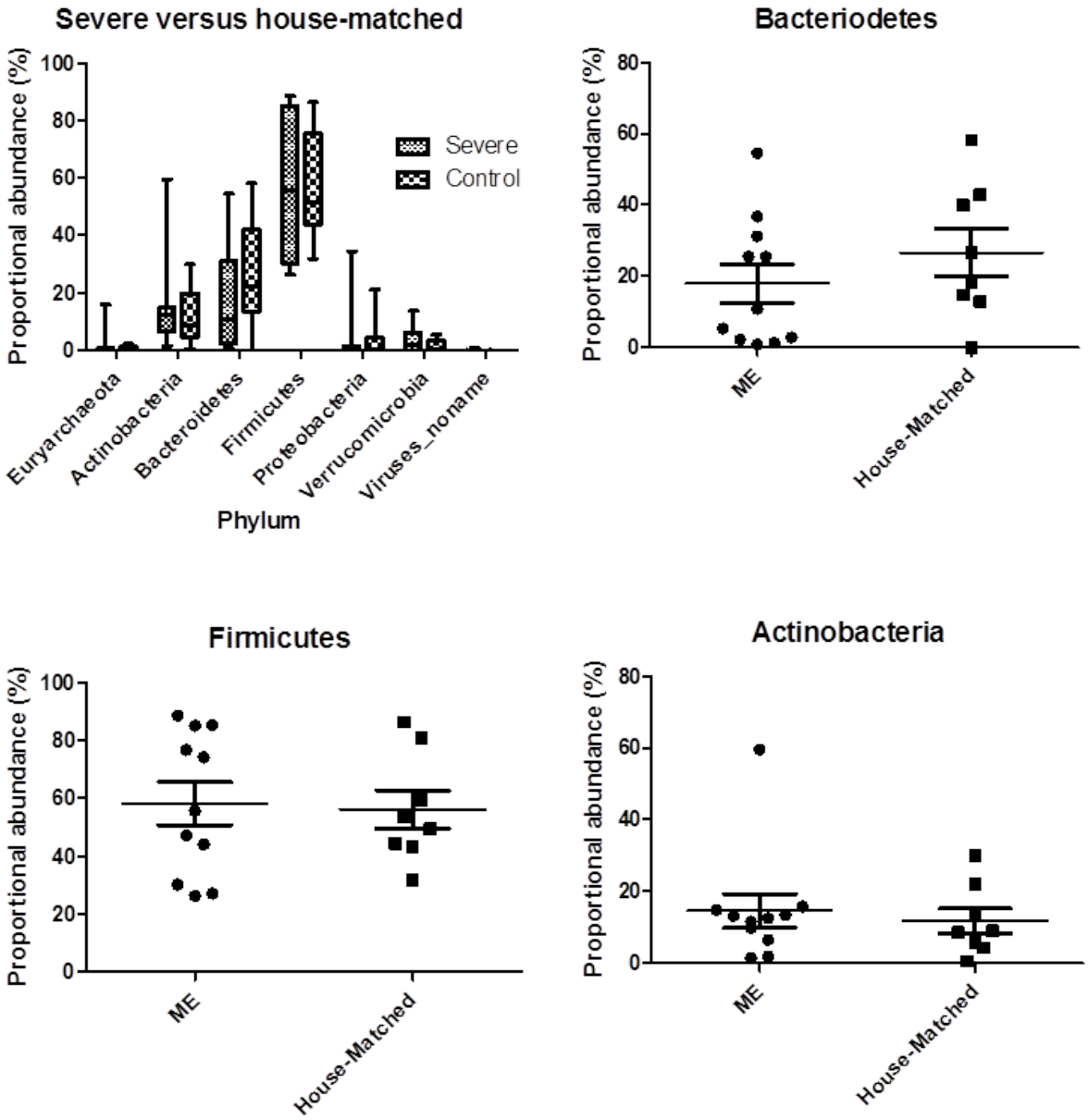

Figure 3.3.8 Statistical plots for bacterial phyla: Bacteroides, Firmicutes and Actinobacteria in ME and HHC. Top left, box plot of all phyla observed, central line represents median percentage of group severe vs. house-hold control; error bars indicate max and min values for each observation. Top right and bottom, each dot represents a single sample; central line is mean percentage, error bars are the standard error (SE). No significant differences.

The RA of *Bacteroides*, *Firmicutes* and *Actinobacteria* were plotted in graphs (figure 3.3.8) and statistically analysed with the non-parametric Mann-Whitney test for differences between ME and HHC. There were no statistically differences for observed relative abundances across the bacterial phyla between ME and HCC at 5% significance level.

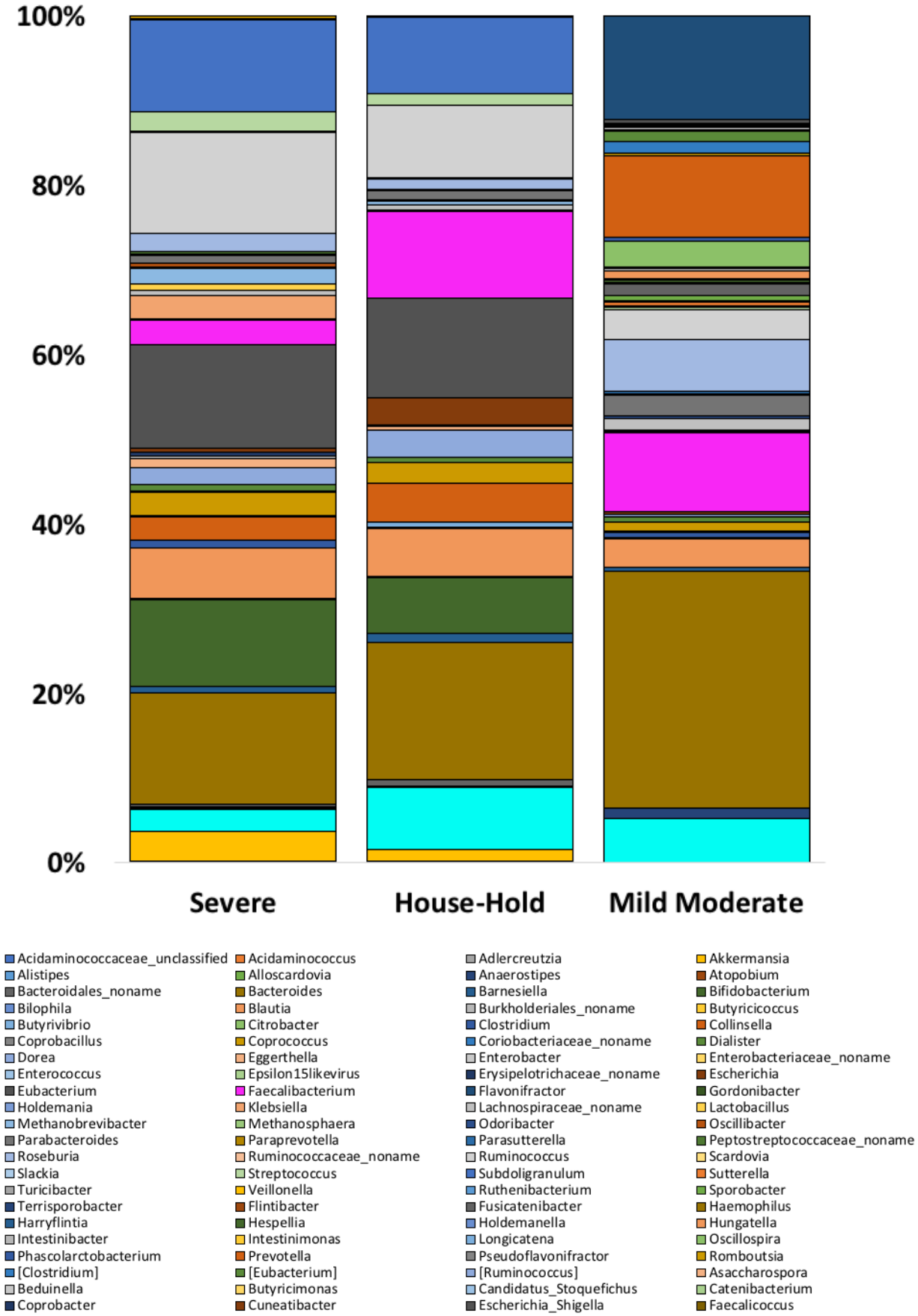

Figure 3.3.9 : Comparison of relatives abundance (%) of bacterial genera in severe (n=11), mild/moderate (n=25) ME/CFS compared with HHCs (n=8).

- *Genus level observations*

Genus-level abundance detail of the severe ME microbiome is of qualitative comparative interest to the earlier mild/moderate ME/CFS dataset (figure 2.3.9). A total of 57 bacterial genera were identified across severe ME and HHC samples. These observations were correlated with bacterial genera observed in mild/moderate ME/CFS, of which 29 genera of these were not identified in either severe ME or HHCs. Table 2.3.4 lists the 57 bacterial genera found and their RA in Severe ME and HHCs. This approach highlighted possible genus-level trends across sample groups. For example, *Bacteroides* (fig. 3.3.9, brown) abundance is follows for the trend M>H>S, at 28.06%, 16.14% and 13.1% respectively.

Bacterial Genus	Severe	House-Hold	Mild Moderate
Acidaminococcaceae_unclassified	0.0063	0.0000	ND
Acidaminococcus	0.1592	0.0000	0.09
Adlercreutzia	0.0927	0.1505	ND
Akkermansia	3.4569	1.4131	0.01
Alistipes	2.5854	7.4204	5.17
Alloscardovia	0.1686	0.0000	ND
Anaerostipes	0.2074	0.1067	1.23
Atopobium	0.0192	0.0000	ND
Bacteroidales_noname	0.2808	0.7948	ND
Bacteroides	13.110	16.140	28.06
Barnesiella	0.7925	1.1171	0.49
Bifidobacterium	10.186	6.5995	0.04
Bilophila	0.2289	0.0921	0.01
Blautia	5.9221	5.7447	3.30
Burkholderiales_noname	0.0000	0.0888	ND
Butyricicoccus	0.0014	0.0000	0.10
Butyrivibrio	0.0000	0.6657	ND
Citrobacter	0.0183	0.0000	ND
Clostridium	0.9115	0.0079	0.69
Collinsella	2.7422	4.5425	0.06
Coprobacillus	0.0822	0.0000	0.02
Coprococcus	2.8474	2.4623	1.13
Coriobacteriaceae_noname	0.1021	0.0000	ND
Dialister	0.8483	0.5147	0.56
Dorea	1.9255	3.2903	0.37
Eggerthella	0.9899	0.4304	0.02
Enterobacter	0.3085	0.0000	ND
Enterobacteriaceae_noname	0.0177	0.0000	ND
Enterococcus	0.0285	0.0000	ND
Epsilon15likevirus	0.0700	0.0000	ND
Erysipelotrichaceae_noname	0.4662	0.1554	ND
Escherichia	0.4830	3.1811	0.33
Eubacterium	12.152	11.868	ND
Faecalibacterium	2.9294	10.233	9.27
Flavonifractor	0.0028	0.0000	0.27
Gordonibacter	0.1350	0.0148	ND
Holdemania	0.0374	0.0000	0.07
Klebsiella	2.6349	0.0706	ND
Lachnospiraceae_noname	0.6953	0.6304	1.39
Lactobacillus	0.6840	0.0000	ND
Methanobrevibacter	1.9334	0.5275	0.03
Methanosphaera	0.0421	0.0000	ND
Odoribacter	0.0112	0.0076	0.28
Oscillibacter	0.4695	0.0797	ND
Parabacteroides	0.9784	1.0373	2.43
Paraprevotella	0.1379	0.1425	0.18
Parasutterella	0.0000	0.0079	0.37
Peptostreptococcaceae_noname	0.2556	0.0000	ND
Roseburia	2.1468	1.3018	6.01
Ruminococcaceae_noname	0.0569	0.1169	0.01
Ruminococcus	11.931	8.5893	3.54
Scardovia	0.0344	0.0000	ND
Slackia	0.1176	0.0000	ND
Streptococcus	2.3592	1.2583	0.39
Subdoligranulum	10.799	9.0340	0.09
Sutterella	0.1550	0.1134	0.48
Turicibacter	0.0208	0.0000	0.06
Veillonella	0.2164	0.0451	ND

Table 3.3.4 Genus-level abundance data from dataset B. Values expressed in this table are an average percentage (%) of the relative abundance (RA) of genera across groups: severe, house-hold, mild/moderate A total of 58 genera were observed across all samples from severe patients and house-hold controls. Of these, only 34 out of 62 matched to genera from 16S analysis of mild/moderate patients (dataset A). *ND, not detected*

The *Faecalibacterium* genus, shown in pink in this figure, was found lowest in severe ME (2.93%) compared with mild/moderate and HHCs at RA of 10.24% and 9.27% respectively. Finally, *Alistipes spp.* (fig. 3.3.9 pale blue) were diminished in Severe ME at 2.59% versus 7.42% in HHC and 5.17% in the mild/moderate 16S-derived microbiota.

Using the 25 most abundant genera found in severe ME and HHCs, a heatmap was generated in MetaPhlAn. In this figure (3.3.10), samples to the right of ME-3 tend to feature more controls (6) versus samples to the left are more dominated by ME samples with the exception of 2 HHCs. Based on the low number of samples collected in this cohort is difficult to identify any findings that distinguish the severe ME microbiome separate from HHC. The *Bacteroides* genus tends to be more abundant in HHCs, whilst *Collinsella spp.* is absent in some ME samples and at low-high abundance in HHCs. In addition, *Coprococcus spp.* is identifiably more abundant (dark blues) in at least 4 of severe ME patients and one ME patient higher (red). Notably, *Oscillibacter spp*. was found present in 8 of the severe ME patients whilst only one HHC had this genus.

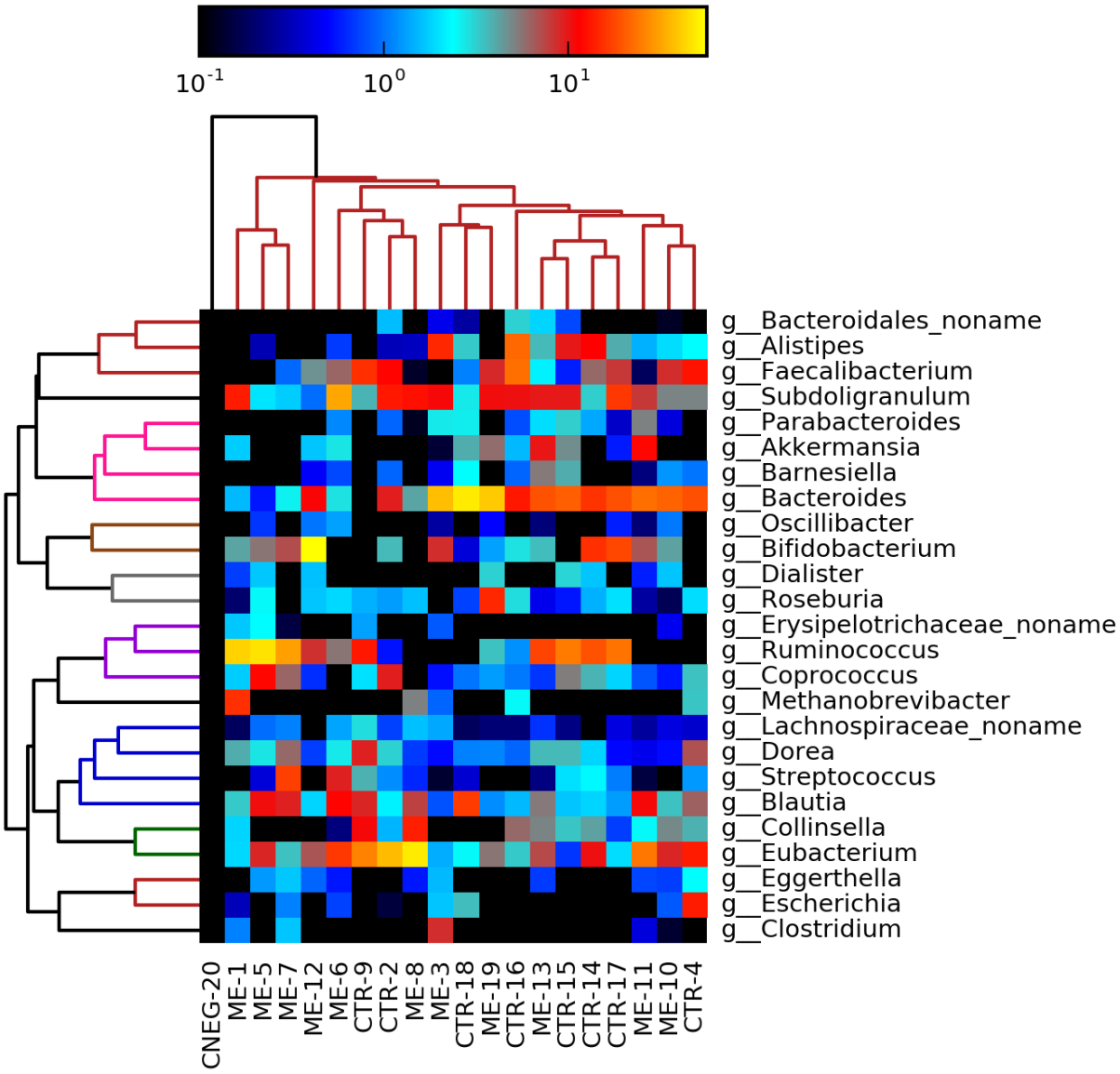

Figure 3.3.10 Heatmap of 25 most abundant bacterial genera seen in severe ME (n=11) and matched house-hold controls, HHC (n=8). Genera list (g_name) on the right of map. Red colours indicate this genus is present at a higher RA in samples, whereas blue genera are less abundant and black indicates absence of this genera. CNEG-20 is water, used as a kit control (kitome) for sequencing.

- *Species level observations*

A total of 152 species were classified across all samples using MetaPhlAn 1 in 2016. The same raw sequencing data was re- analysed with the more update version of MetaPhlAn 2.0 in 2018. However, this did not significantly alter the outcome of this data. Table 3.3.5 summaries the total number reads associated with each sample and the total number of species observed in it. DNA concentration was measured and recorded prior to dispatch to the sequencing provider who also performed in-house QCs checks for DNA fragment length. The lowest quantity of DNA sent for sequencing was 700 ng of total DNA in 20μl water, in sample CTR-15. The highest number of observed species was 52 in ME-10, and the lowest number 20 in CTR-9.

Sample	DNA (ng/μl)	Reads	Species
ME-1	172	1,188,807	44
CTR-2	196	765,785	40
ME-3	372	818,307	43
CTR-4	73	169,707	24
ME-5	294	1,324,046	41
ME-6	548	1,468,535	38
ME-7	76.4	1,258,690	46
ME-8	468	480,512	23
CTR-9	137	345,280	20
ME-10	300	1,038,416	52
ME-11	47	990,786	37
ME-12	270	1,222,374	40
ME-13	65.2	1,267,583	39
CTR-14	199	344,530	24
CTR-15	35	1,185,795	40
CTR-16	324	1,090,871	40
CTR-17	264	1,511,959	47
CTR-18	144	873,110	42
ME-19	78	899,956	22

Table 3.3.5 Sample sequencing statistics for extracted DNA concentration from 250 mg of raw faecal stool and number of paired end reads obtained following QC and trimming. This data was generated from 20μl of undiluted DNA sent to an external sequencing provider. Number of reads obtained after removal of human sequences. Number of species assigned to reads using MetaPhlAn 2.0.

A

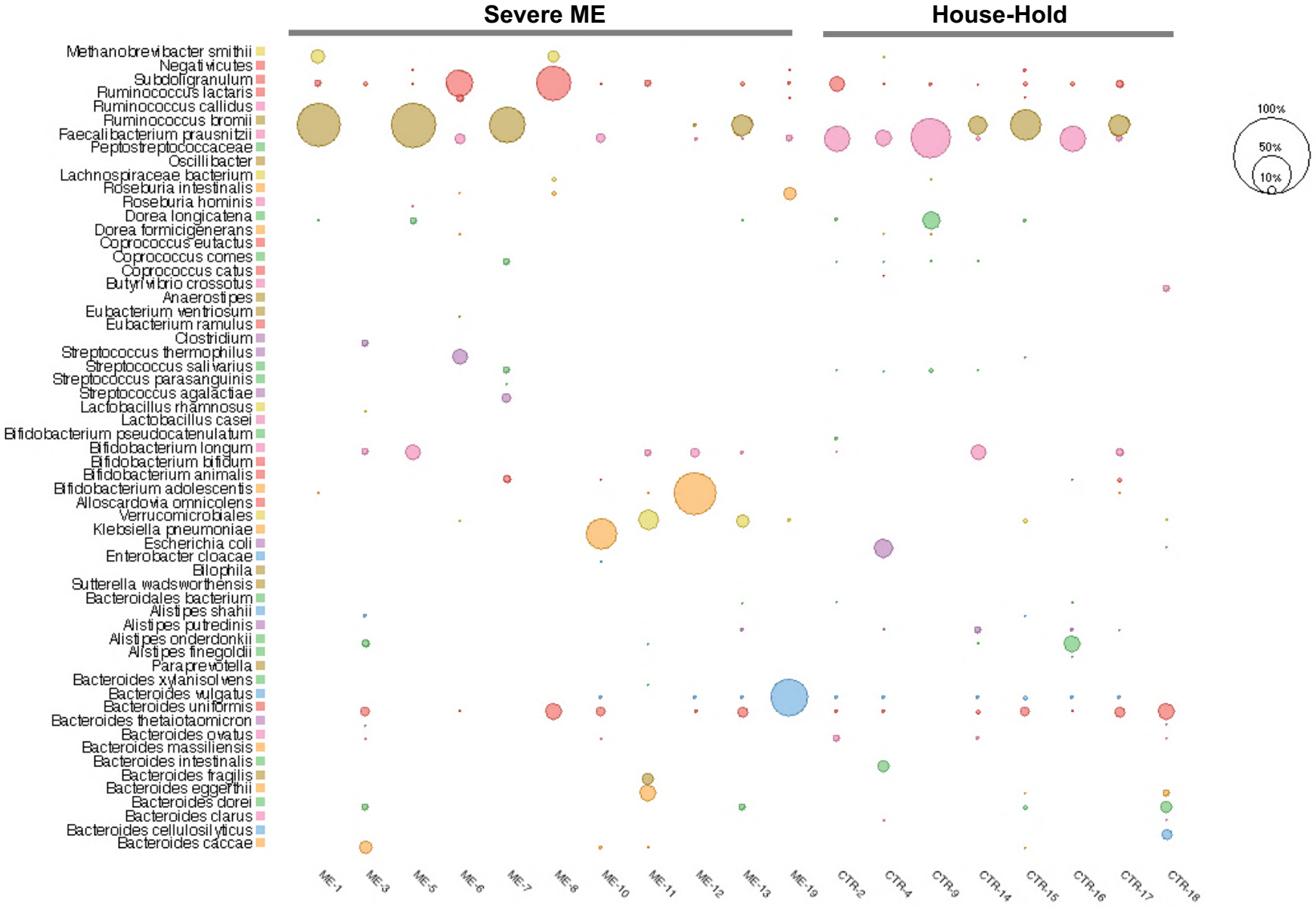
Severe ME
House-Hold
Methanobrevibacter smithii
Negativicutes
Subdoligranulum
Ruminococcus lactaris
Ruminococcus callidus
Ruminococcus bromii
Faecalibacterium prausnitzii
Peptostreptococcaceae
Oscillibacter
Lachnospiraceae bacterium
Roseburia intestinalis
Roseburia hominis
Dorea longicatena
Dorea formicigenerans
Coprococcus eutactus
Coprococcus comes
Coprococcus catus
Butyrivibrio crossotus
Anaerostipes
Eubacterium ventriosum
Eubacterium ramulus
Clostridium
Streptococcus thermophilus
Streptococcus salivarius
Streptococcus parasanguinis
Streptococcus agalactiae
Lactobacillus rhamnosus
Lactobacillus casei
Bifidobacterium pseudocatenulatum
Bifidobacterium longum
Bifidobacterium bifidum
Bifidobacterium animalis
Bifidobacterium adolescentis
Alloscardovia omnicolens
Verrucomicrobiales
Klebsiella pneumoniae
Escherichia coli
Enterobacter cloacae
Bilophila
Sutterella wadsworthensis
Bacteroidales bacterium
Alistipes shahii
Alistipes putredinis
Alistipes onderdonkii
Alistipes finegoldii
Paraprevotella
Bacteroides xylanisolvens
Bacteroides vulgatus
Bacteroides uniformis
Bacteroides thetaiotaomicron
Bacteroides ovatus
Bacteroides massiliensis
Bacteroides intestinalis
Bacteroides fragilis
Bacteroides eggerthii
Bacteroides dorei
Bacteroides clarus
Bacteroides cellulosilyticus
Bacteroides caccae
ME-1
ME-3
ME-5
ME-6
ME-7
ME-8
ME-10
ME-11
ME-12
ME-13
ME-19
CTR-2
CTR-4
CTR-9
CTR-14
CTR-15
CTR-16
CTR-17
CTR-18
100%
50%
10%

B

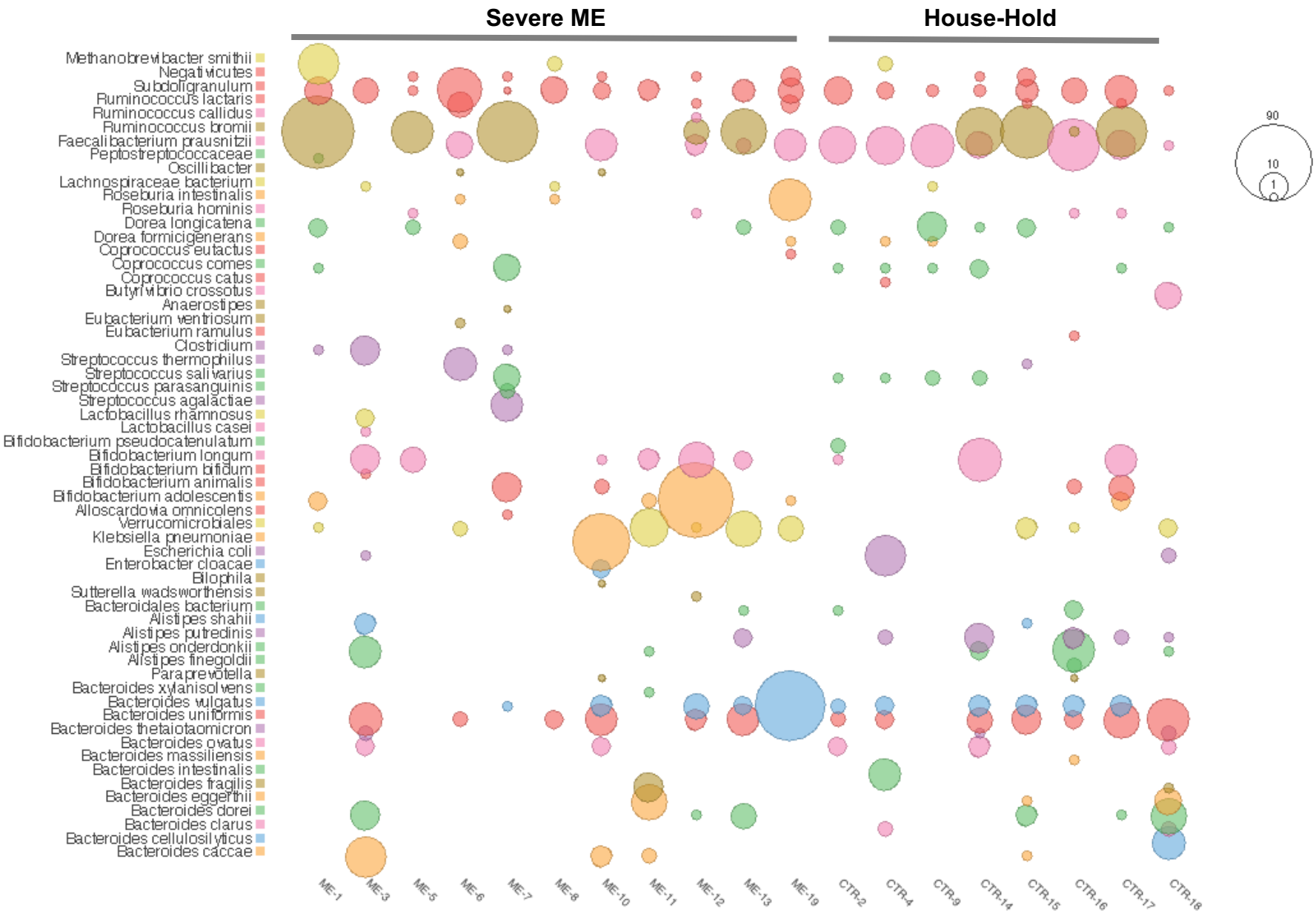
Severe ME
House-Hold
Methanobrevibacter smithii
Negativicutes
Subdoligranulum
Ruminococcus lactaris
Ruminococcus callidus
Ruminococcus bromii
Faecalibacterium prausnitzii
Peptostreptococcaceae
Oscillibacter
Lachnospiraceae bacterium
Roseburia intestinalis
Roseburia hominis
Dorea longicatena
Dorea formicigenerans
Coprococcus eutactus
Coprococcus comes
Coprococcus catus
Butyrivibrio crossotus
Anaerostipes
Eubacterium ventriosum
Eubacterium ramulus
Clostridium
Streptococcus thermophilus
Streptococcus salivarius
Streptococcus parasanguinis
Streptococcus agalactiae
Lactobacillus rhamnosus
Lactobacillus casei
Bifidobacterium pseudocatenulatum
Bifidobacterium longum
Bifidobacterium bifidum
Bifidobacterium animalis
Bifidobacterium adolescentis
Alloscardovia omnicolens
Verrucomicrobiales
Klebsiella pneumoniae
Escherichia coli
Enterobacter cloacae
Bilophila
Sutterella wadsworthensis
Bacteroidales bacterium
Alistipes shahii
Alistipes putredinis
Alistipes onderdonkii
Alistipes finegoldii
Paraprevotella
Bacteroides xylanisolvens
Bacteroides vulgatus
Bacteroides uniformis
Bacteroides thetaiotaomicron
Bacteroides ovatus
Bacteroides massiliensis
Bacteroides intestinalis
Bacteroides fragilis
Bacteroides eggerthii
Bacteroides dorei
Bacteroides clarus
Bacteroides cellulosilyticus
Bacteroides caccae
90
10
1
ME-1
ME-3
ME-5
ME-6
ME-7
ME-8
ME-10
ME-11
ME-12
ME-13
ME-19
CTR-2
CTR-4
CTR-9
CTR-14
CTR-15
CTR-16
CTR-17
CTR-18

⇐ **Figure. 3.3.11 Bubble chart summary of 59 bacterial species and 9 genera in 11 severe ME patients versus 8 House-Hold Controls.** Colours representative of individual genera or species. (A) Size of circle is proportional to the relative abundance (RA) of that genus or species with the individual total microbiota. (B) Size of circle represent RA values on a square-root scale to reveal differences between less abundant and minor members of the intestinal microbiota.

Figure 3.3.11 A and B were produced using MEGAN 6.0 to summarise composition differences between species in ME and HHC; which reveals several HHCs had a higher RA of *Faecalibacterium prausnitzii* (pink circles) 10.23% ± 6.04 SD versus 2.93% ± SD 3.15 in HHCs. *Ruminococcus bromii* (brown circles) was higher in 3 of the ME patients; 41.24%, 23.04% and 33.15% respectively in figure 3.3.11B. This part of the figure also shows *Bacteroides vulgatus* (pale blue circles) was missing is 6 patients compared to just two in the HHCs. However, ME-19 had a RA of 36.79% for this species compared to an average of 2.70% ± 1.62 in across all HHCs. Almost half of the relative abundance of species within ME-12 was attributed to *Bifidobacterium adolescentis* (orange circles, fig. 3.3.11B) at 45.39% which was absent in most ME patients and only appear in a single HHC at RA of 3.71% (CTL-17).

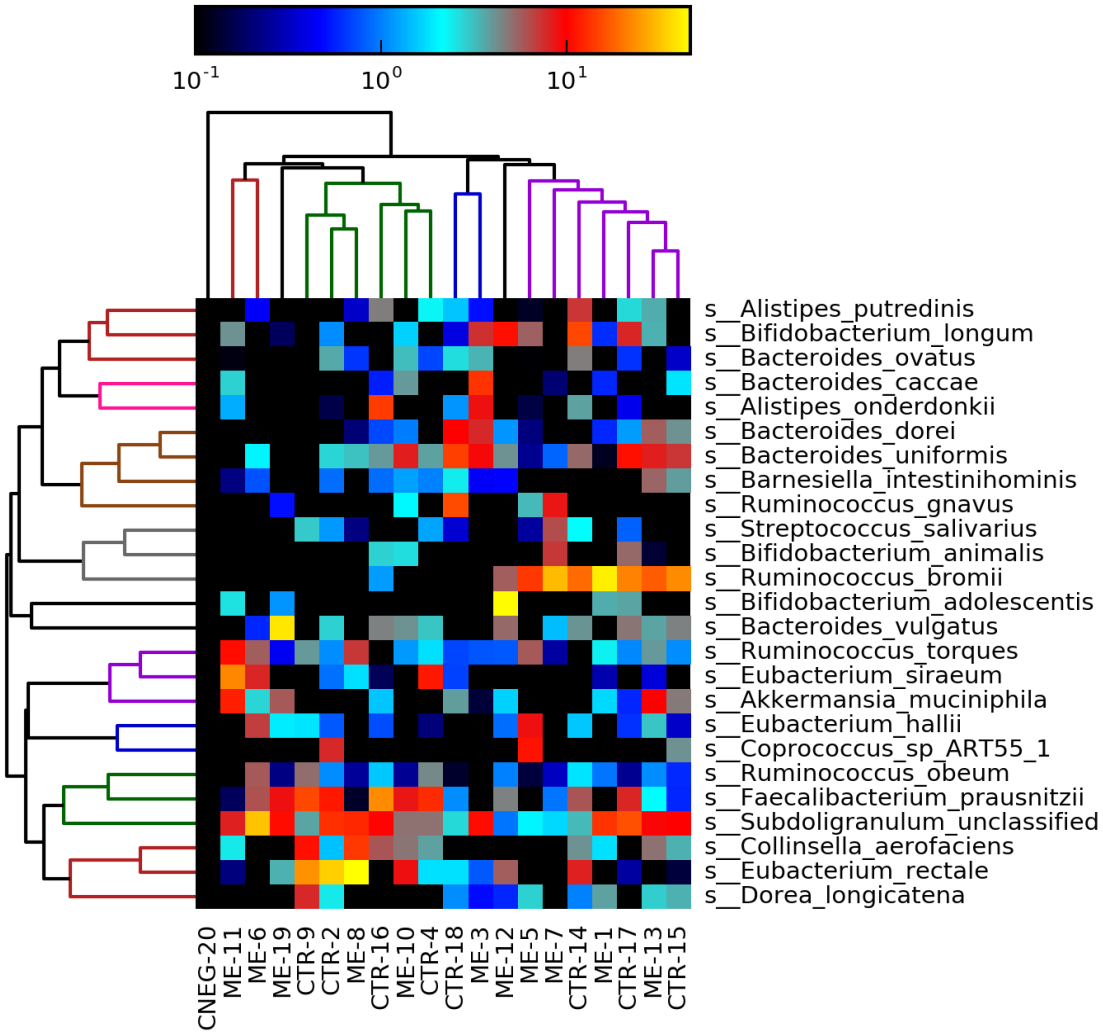

⇐ Figure 3.3.12 Twenty-five most abundant bacterial species across all samples identified using MetaPhlAn 2.0 in 2018.

Sequnce read originally analysed in 2017 were re-analysed using a more recent version of MetaPhlAN. Additional species were identified in most samples; however, this did not exceed 12 per sample. It is important to note that these were not new species and instead represented assigning of previously identified species to more samples across both groups. A heatmap was generated in Figure 3.3.12 from MetaPhlAn 2.0 to compare the RA of the top 25 species which varied the most between patients and HHCs.

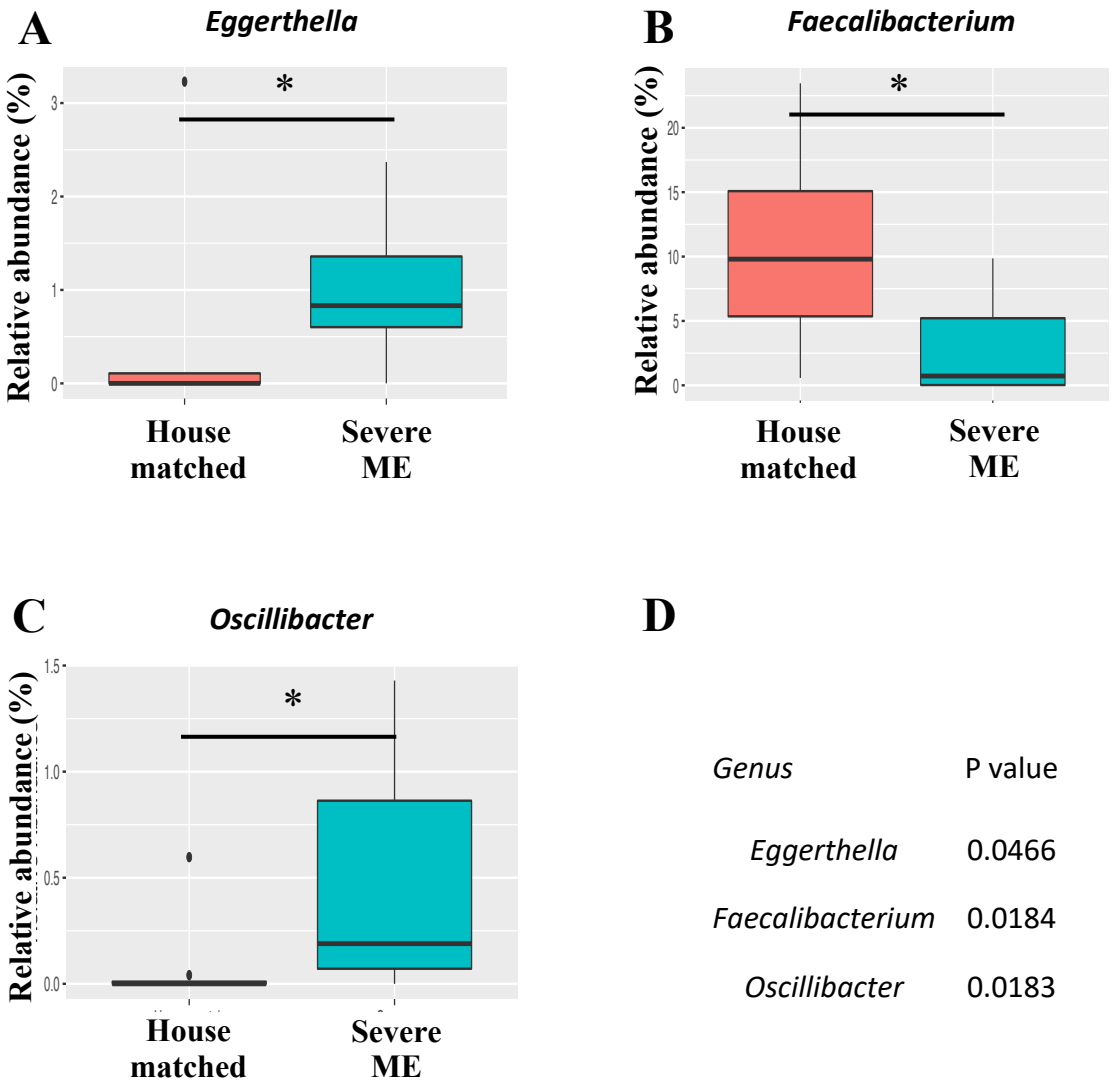

Fig. 3.3.13 Status by bacteria genus reveals differences between severe ME and house-matched controls for Eggerthella, Faecalibacterium & Oscillibacter. Statistical analysis and graphical output completed using RStudio®.

- *Statistical comparison of bacterial genera in severe ME versus HHC*

Taxonomic abundance tables were analysed using R Studio for significance testing between ME and HHC at the genus level. Figure 3.3.13 presents the statistical plots generated for this analysis using an unpaired Mann Whitney U test with Benjamin Hochberg p value adjustment. This identified three bacterial genera with a p value <0.05. Members of *Oscillibacteria spp.* and *Eggerthella spp.* were statistically more abundant (p values 0.0183 and 0.0466, respectively) in the severe ME microbiota compared with the HHC group. Conversely, the genus *Faecalibacterium* were significantly lower (p=0.0184) within the severe ME microbiota compared to HHCs. No species belonging to the genus of *Oscillibacteria* or *Eggerthella* were identified whilst *F. prausnitzii* was the only species found within *Faecalibacterium spp.*

- *Bray-Curtis Dissimilarity Analysis*

The beta-diversity between the microbiotas of severe ME and HHCs was calculated using MEGAN 6.0. PCoA of taxonomy using Bray-Curtis distances are based on measures of the most abundant bacterial taxa within that sample. Figure 3.3.14 the direction of clustering of samples and has been labelled with the dominant species within these samples driving this spatial separation. Significantly, *Facalibacterium prausnitzii* emerges as the main principle component in most CTR samples. Other discrete clusters are for ME samples driven my *Ruminoccus bromii* and *Bacteroides uniformis* however, these are explained by typically one of two outlier ME samples compared to the rest of the group, see fig. 3.3.11b.

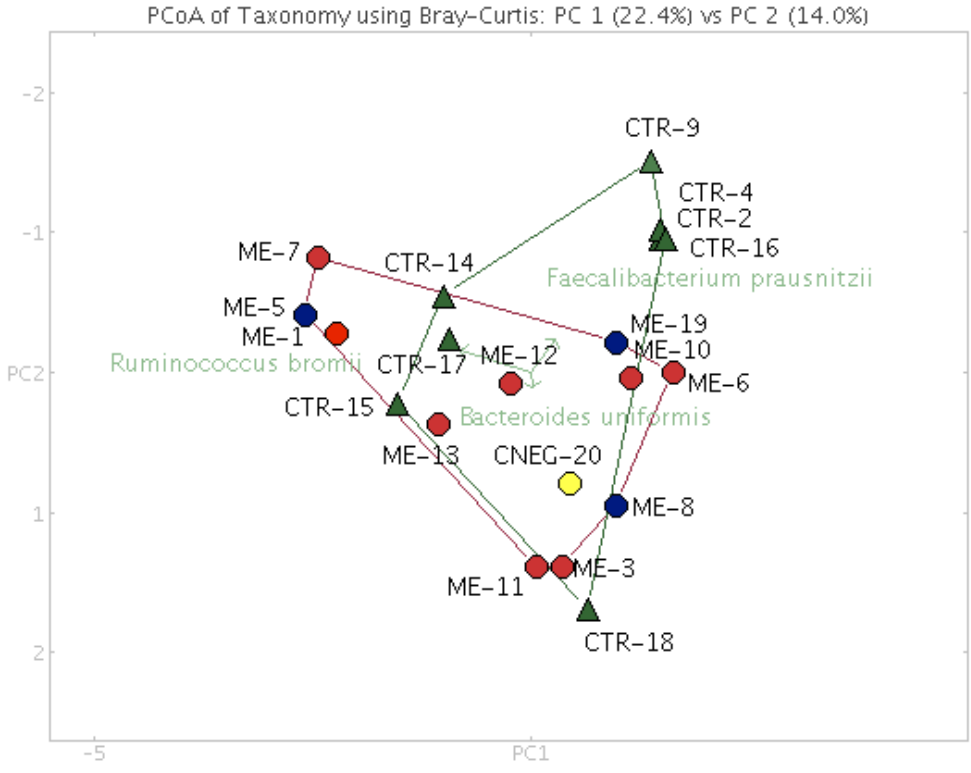

⇐ **Figure. 3.3.14 PCoA analysis using Bray-Curtis dissimilarity to compare compositional differences in beta-diversity between severe ME and HHCs groups.** Analysis draws conclusion of most abundant bacterial species (annotated in figure) associated with separations of samples, e.g. *Faecalibacterium prausnitzii* is more abundant in CTR-2, CTR-4, CTR-9 & CTR-16.

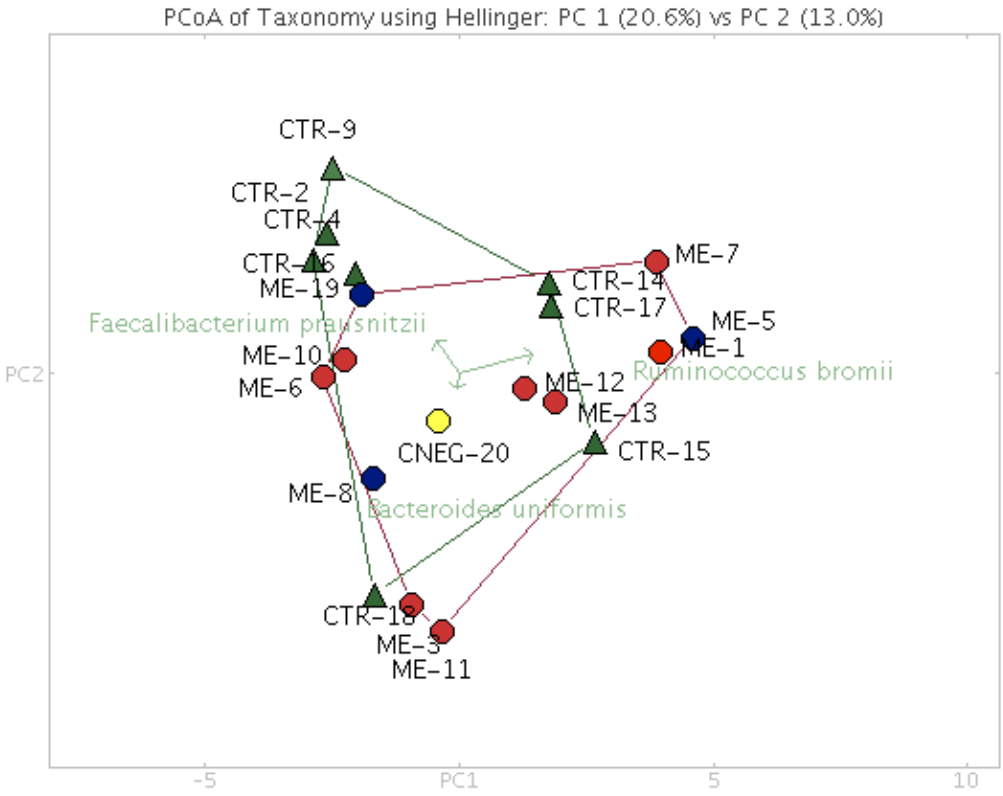

Figure 3.3.15 PCoA analysis using Hellinger distances to measure the difference in compositional taxa between severe ME and HHCs. Plot annotated with bacterial species relevant to driving separation of samples.

PCoA analysis was also performed using Hellinger distances to separate samples based on proportions of taxa observed between each dataset and is considered more representative of proportional differences between taxa between groups of samples. Sample which cluster together are more compositional similar. Another standard tool for microbial community analysis is Unweighted Pair Group Method with Arithmetic Mean (UPGMA) based on UniFrac distances which is a hierarchical clustering method for sample classification used in ecology studies. Samples with the closest distance cluster together as a node. Unweighted UPGMA (figure 3.3.16A) considers the clustering of samples on composition alone, whilst the weighted version (figure 3.3.16B) consider both abundance and composition.

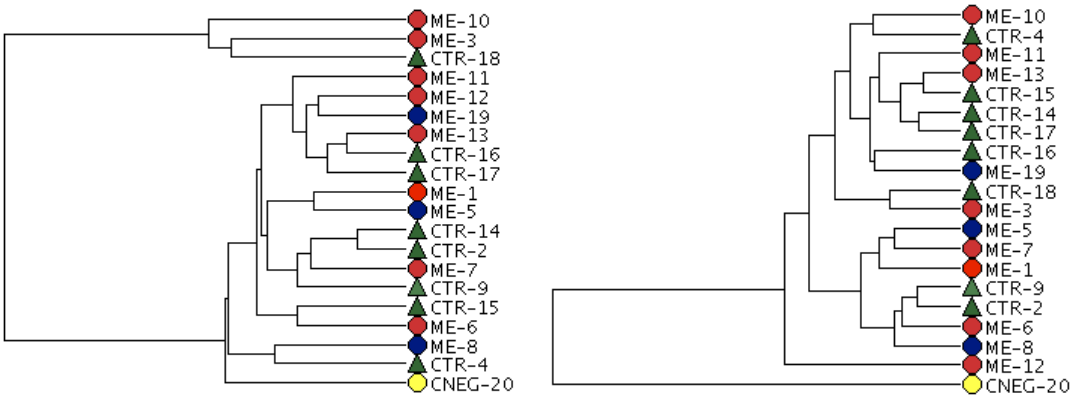

Figure 3.3.16 UPGMA clustering unweighted (A) versus (B) weighted UniFrac distances performed in MEGAN using severe ME and HHC samples. Matched severe ME (red circles), unmatched severe ME (blue circles); matched house-hold controls (green triangles); negative control (yellow circle).

- *Comparison of severe ME and HHC core microbiomes*

Core microbiomes were calculated as a feature of MEGAN 6.0 using a sample threshold of 50% and class threshold of 1%. This analysis provided an interesting output and revealed a distinct difference in the number of species determining the core microbiome in patients compared with HHCs. Patients have 6 members of a core microbiota (fig 3.3.17A), represented by *Bacteroides uniformis*, *Verrucomicrobiales, Bifidobacterium longum*, *Eubacterium spp*., *Dorea spp.*, *Ruminococcus spp.* and *Subdoligranulum spp*. Figure 3.3.17B shows there are 8 members within the core microbiome of HHCs distinct from ME and include *Bacteroides vulgatus*, *Alistipes putredinis, Streptococcus salivarius, Coprococcus comes, Dorea longicatena, Ruminococcus bromii, Faecalbacterium prausnitzii*, and *Ruminococcus bromii.*

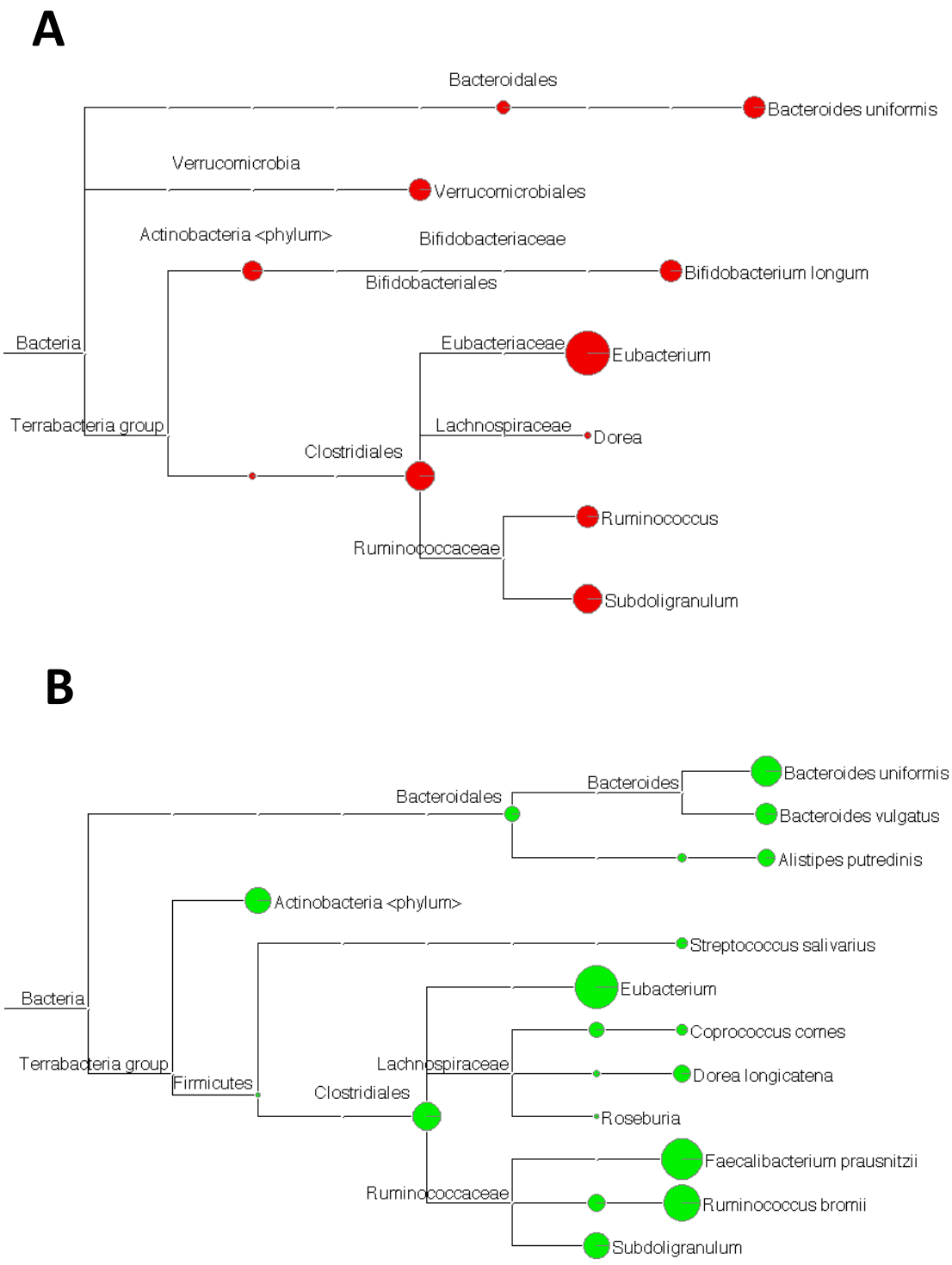

Figure 3.3.17 Phylogenetic trees featuring the members of bacterial taxa identified as part of a core microbiome within 11 severe ME sample and 8 HHCs. Size of circle is proportional to the relative abundance of taxa within these samples. A: represents common features shared between 11 severe, house-bound ME patients. B: represents 8 house-hold controls related to severe, house-bound patients.

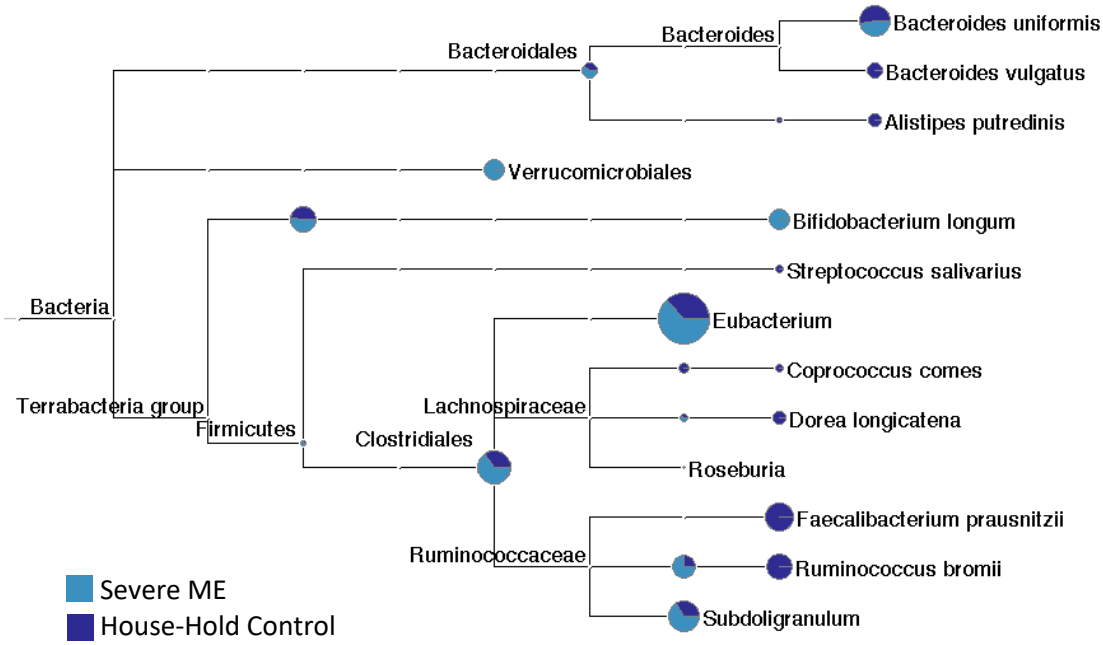

Figure 3.3.18 Phylogenetic tree representative the comparison between the shared core microbiome of 11 severe patients and 8 house-hold controls. Colours and size of circles are proportional of the RA contributing to the microbiome. Patients are in light blue versus HHCs in purple.

Figure 3.3.18 provides shared features of a core microbiome in patients and HHCs compares the compositions of these members between groups. For example, ME (light blue) is less abundant in *Bacteroides vulgatus, Alistipes putredinis, Coprococcus comes, Faecalibacterium prausnitzii*, and *Ruminococcus bromii* but highly more represented by *Eubacterium spp.*

16S phylogenetic abundance in severe ME and HHCs

- *Dataset C*

This final data provided insight into the 16S V4 region microbiome of 17 female severe, house bound patients and 8 HHCs recruited in 2016/2017 using the enhanced methods for faecal sample collection which required the entire intact stool and was protect using Anaerogen™ Compact® sachet to limit oxygen exposure. Left over sample from the previous year (2016) in conjunction with additional samples produced in 2017 available from 4 patients and their respective HHCs bringing the total number of samples to 21 ME versus 12 HHC.

Table 2.3.6 shows faecal DNA extraction yield was notably lower in samples that had been stored in the -80^{0}C freezer. The minimum concentration yielded was 12 ng/µl in a total volume of 65 µl of ddH_2O. The average number of reads per sample was 150,882 ± 35,890. A total 2520 OTUs were observed across all samples. Of these 2282 (figure 3.3.19) were clustered together with ≥97% DNA sequence similarity and annotated to 866.15±75.80 SD bacterial genera across both groups. OTU abundance was normalised corresponded to sample F4 with the least number of reads at 47,985. On average the number of genera observed per sample in each group was 877±56.40 SD in ME versus 847±108 SD in HHCs.

Sample	Status	DNA (ng/μl)	Year	Reads	Ave Len(nt)	Q20	Q30	GC%	Assigned OTUs
F1	ME	803	2017	243,161	253	99.34	98.68	53.14	910
F2	ME	466	2017	163,179	253	99.37	98.71	53.9	926
F3	ME	731	2017	223,279	253	99.36	98.71	53.39	877
F4	HHC	448	2017	47,985	253	99.34	98.68	55.47	467
F5	ME	648	2017	222,044	253	99.4	98.77	54.03	932
F6	HHC	610	2017	182,173	253	99.37	98.73	52.68	825
F7	ME	515	2017	150,931	253	99.36	98.72	54.25	865
F8	HHC	544	2017	195,424	253	99.39	98.74	52.95	903
F9	ME	403	2017	117,136	253	99.36	98.7	53.04	934
F10	ME	526	2017	109,282	253	99.37	98.71	52.67	842
F11	HHC	2154	2017	172,826	253	99.4	98.78	53.13	1265
F12	ME	244	2017	166,377	253	99.35	98.7	52.21	805
F13	ME	171	2017	213,772	253	99.33	98.65	53.12	896
F14	HHC	978	2017	135,073	253	99.34	98.66	53.49	935
F15	ME	326	2017	188,528	253	99.34	98.68	53.41	915
F17	ME	233	2017	219,965	253	99.37	98.71	55.02	881
F18	ME	822	2017	163,722	253	99.37	98.72	52.89	799
F19	HHC	576	2017	116,316	253	99.36	98.71	53.56	884
F20	HHC	476	2017	171,177	253	99.35	98.68	53.21	894
F21	ME	336	2016	107,094	253	99.36	98.68	53.18	876
F22	HHC	385	2016	101,151	253	99.36	98.69	52.99	849
F23	ME	147	2016	150,529	253	99.38	98.75	53.47	1215
F24	ME	90.2	2016	148,620	253	99.34	98.67	52.56	812
F25	ME	66.5	2016	196,539	253	99.35	98.68	53.86	830
F26	ME	44.9	2016	141,569	253	99.36	98.7	54.11	823
F27	ME	466	2016	190,187	253	99.33	98.66	53.85	785
F28	HHC	454	2016	92,279	253	99.38	98.73	53.18	782
F29	ME	12	2016	159,789	253	99.4	98.77	53.21	859
F30	HHC	351	2016	144,861	253	99.38	98.73	52.91	732
F31	HHC	672	2016	101,084	253	99.37	98.71	53.35	812
F32	ME	237	2016	159,332	253	99.37	98.71	53.25	794
F33	ME	183	2016	91,557	253	99.35	98.68	53	843
F34	HHC	29.2	2016	84,446	253	99.36	98.7	52.89	816

Table 3.3.6 Summary of sample status and number of paired-end reads, including quality score (Q20 and Q30), DNA concentration, GC% content obtained per sample from 33 samples supplied to sequencing provider.

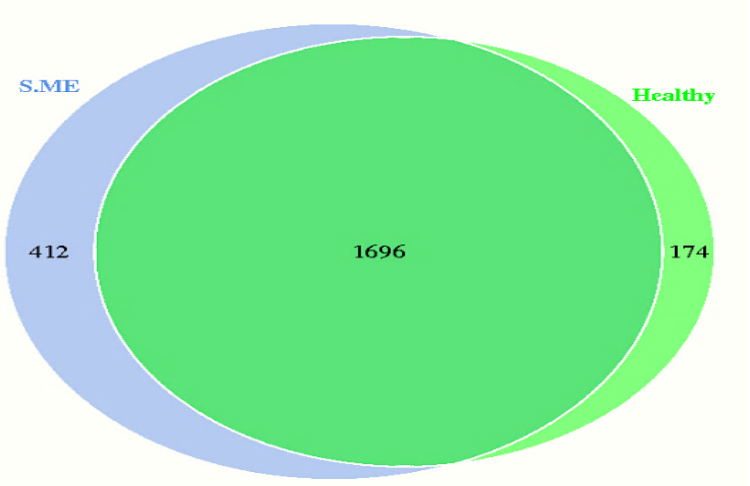

Figure. 3.3.19 Venn diagram of observed OTUs in severe ME (n=21) and HHCs (n=12) samples. Values in overlapping parts represent common OTUs. The numbers refer to specific OTUs unique to that sample group.

Rarefaction curves were plotted for each sample (figure 3.3.20A) using reads rarefied to 47,985 reads. As the number of sequenced reads increases the number of observed species gradually reaches a plateau.

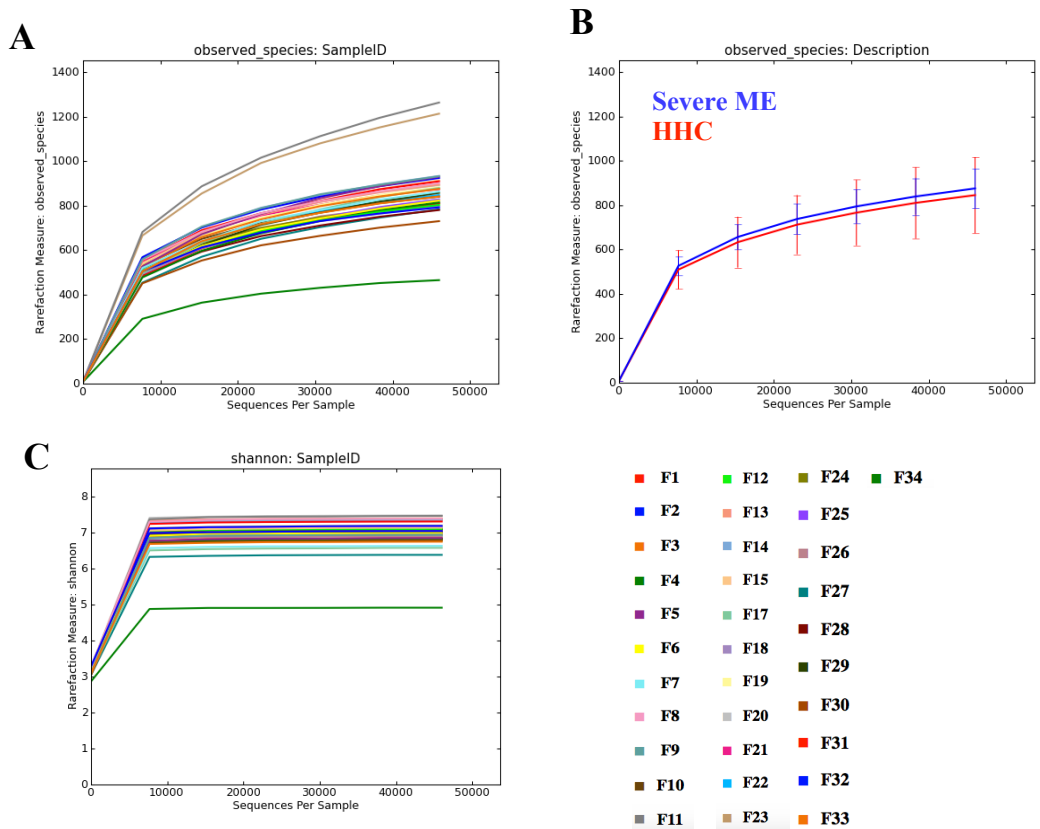

Figure 3.3.20 Rarefaction curves per sample (A) and averaged species abundance (B) and alpha diversity (C) measured using the Shannon Index, H.

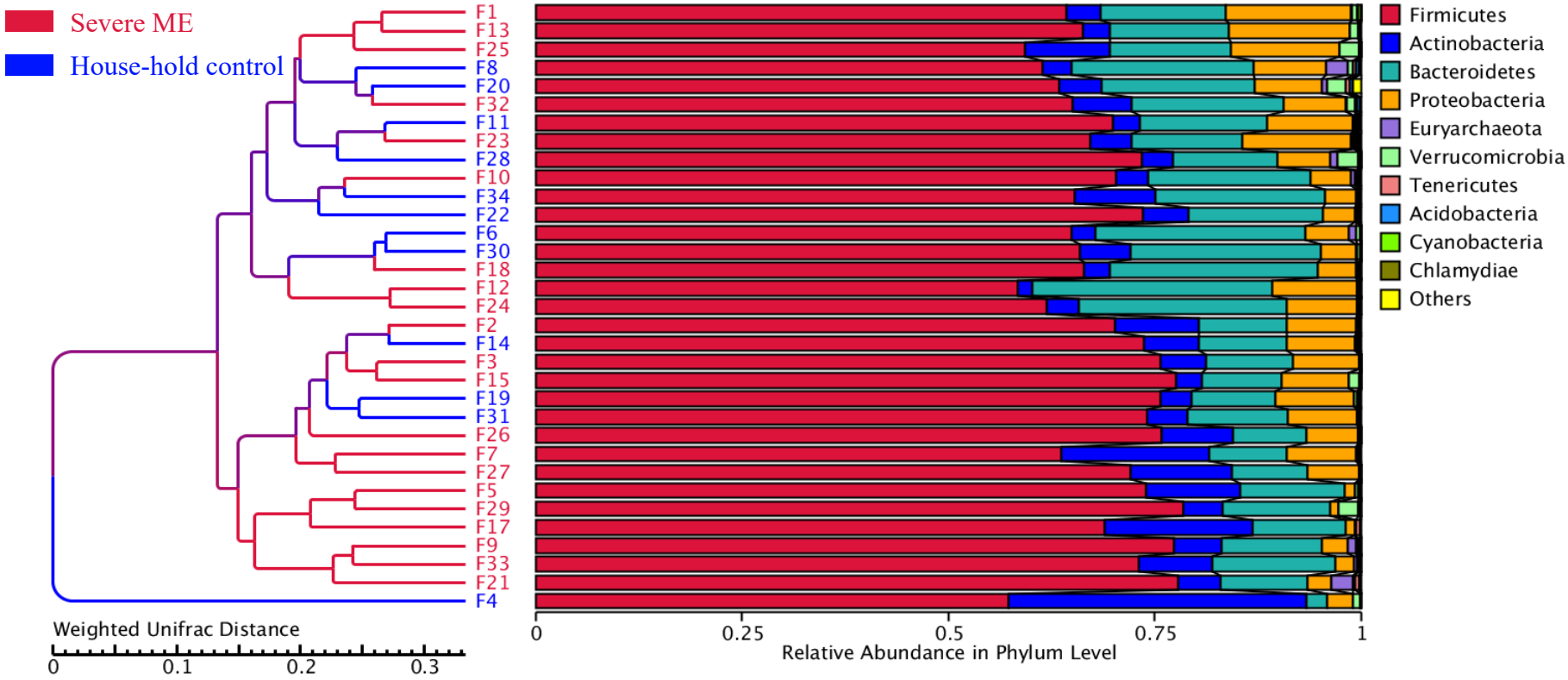

Figure 3.3.21 WPGMA cluster analysis using weighted UniFrac distances to reveal hierarchical clustering of samples based on composition and relative abundance of bacterial phyla in 21 severe ME patients and 12 House-Hold Controls. Weighted pair group method with arithmetic mean (WPGMA) is a hierarchical clustering tool used in ecological studies to classify samples. The clustering tree (left) is constructed on the basis of sequence similarity among different samples. The Weighted Unifrac Distance is calculated as an average between clusters of samples with similar sequences forming a node, followed by branching and clustering of samples with more distant sequences.

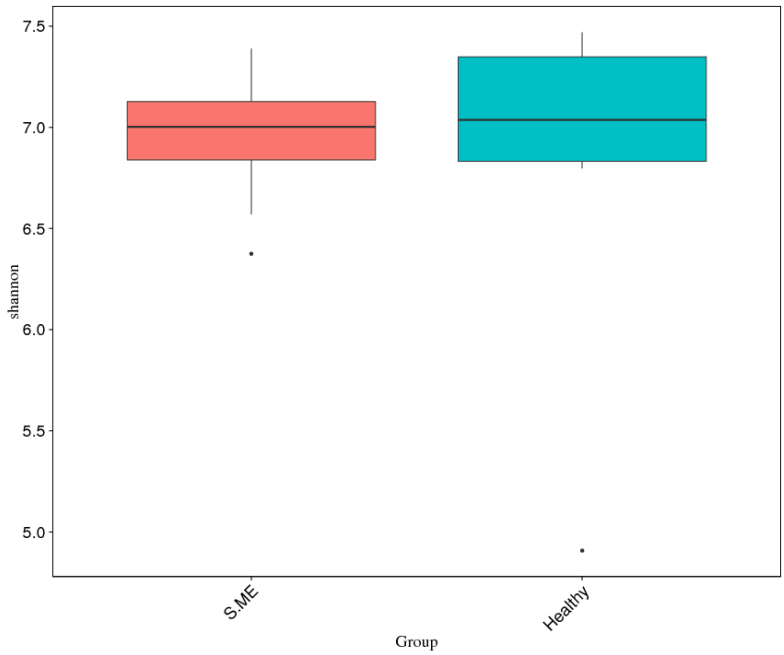

Figure 3.3.22 Box plot of Alpha Diversity indices between 21 severe ME patients and 12 House-Hold Controls using the Shannon (H) index. Plot highlights no intra-individual sample differences for species diversity within patient and control groups. Diversity of severe ME appears no different from house-hold control samples.

Alpha diversity is used to assess the diversity of microbial composition. This was performed on this dataset using the cut-off of 45,995 reads per sample assigned to OTUs at 97% similarity in DNA sequencing. Classification of these OTUs provides microbial composition. The Shannon H index measures microbial composition in each individual sample (figure 3.3.20C). The difference in H indices obtained from samples within both groups, severe ME and HHCs are presented in figure. 3.3.22.T-test and Wilcox tests were performed on this data and showed no significant difference between these groups in terms of microbial composition.

- *Phylum level observations*

Weighted UniFrac distances were applied to PGMA to visualise clustering of samples at the phylum level. Figure 3.3.21 is the output from this analysis and shows a proportion of severe ME patients cluster at this level. However, averaging the RA of phyla between groups shows there were no significant observations in terms of RA at the phylum level. *Firmicutes, Bacteroides, Proteobacteria* and *Actinobacteria* were observed the most abundant bacterial phyla in that order within both groups (figure 3.3.23).

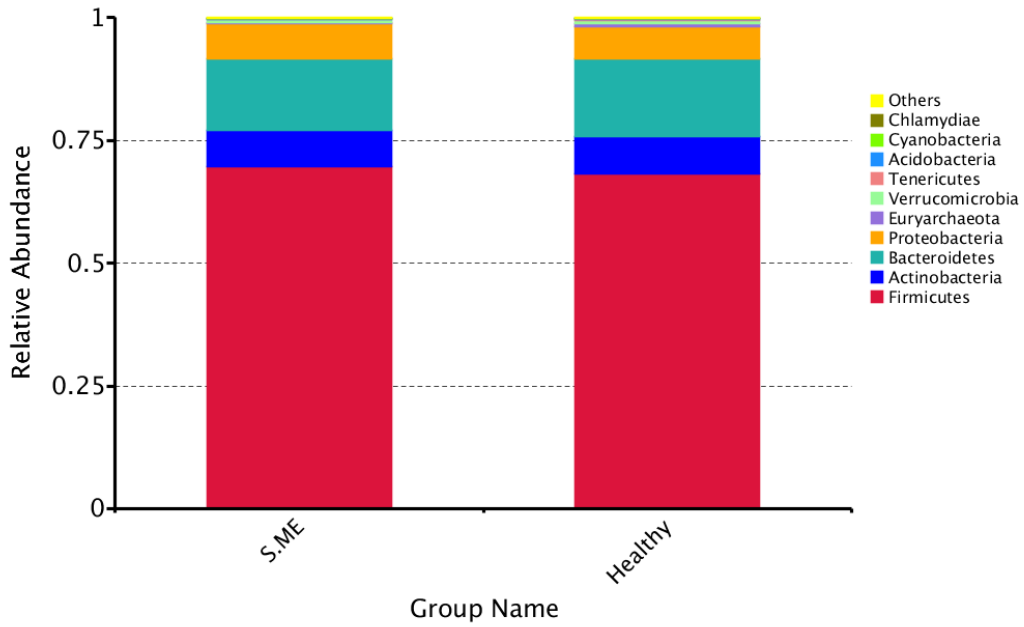

Figure 3.3.23 Relative abundance ratio of bacterial phyla observed in severe ME versus HHC. "Healthy" refers to House-Hold Controls (HHCs). There is no significant or observable difference in the proportions of bacterial phyla comparing severe ME with a respective house-hold control.

- *Genus level observations*

The abundance of the most dominant 35 genera among all samples was investigated in terms of distribution between severe patients and HHCs. The majority of the most dominant genera were found within *Firmicutes*. This was based on the analysis of clustering of samples as well as taxa. Interestingly the most abundant dominant genera were found in individual severe ME samples, including *Holdemanella, Streptococcus, Anaerostipes, Prevotella, Dialister, Bifidobacterium, Subdoligranulum, Collinsella, Lachnospiraceae, Dorea, Escherichia-Shigella* and *Mucilaginibacter.*

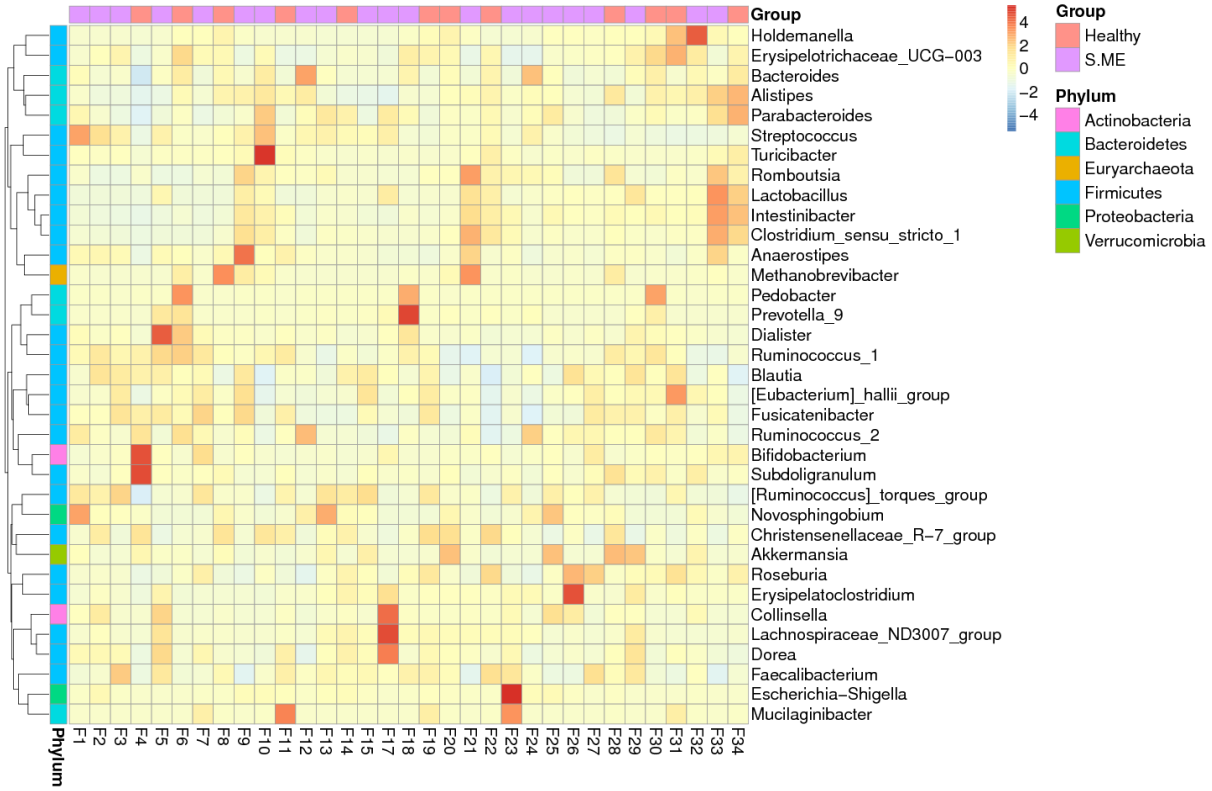

Figure 3.3.24 Heatmap of relative abundance of the most dominant genera in 21 severe ME versus 12 HHCs. The abundance distribution of the dominant 35 genera among all samples was displayed in this species abundance heatmap. Based on the clustering results of samples and taxa, samples may be clustered or not according to their similarity or differences, observed in this heatmap. Names on right side of heatmap represent bacterial genus. The absolute value of Z represents the distance between the raw score and the mean of the standard deviation across all samples in that group. Z is negative (blue) when the raw score is below the mean and vice versa when the score is above the group mean (red) for that sample.

- *Statistical analyses*

Principle component analysis (PCA) uses complete multivariate data based on OTUs from each sample to compare the structure of the data from the two groups. PC1 (17.19%) and PC2 (PC 7.42%) in figure 3.3.25 show the maximum variation in this data. The similar the microbial composition between samples, the closer the distance corresponding to their position of the plot. Most samples cluster together suggesting a similar microbial composition is shared in both groups. However, four patients and one HHC are compositional distinct from this cluster and appear as outliers.

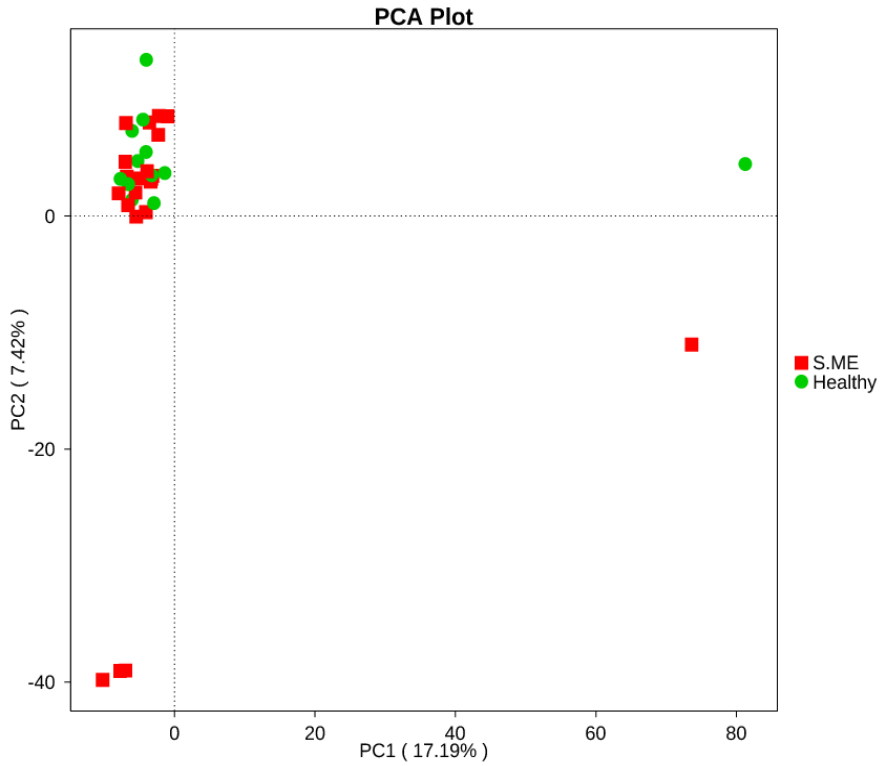

Figure 3.3.25 Principal Component analysis based on differences of composition of assigned OTUs to bacterial taxa in 21 severe ME patients and 12 HHCs. Each dot represents a sample plotted against principal components, PC1 (17.19%) versus PC2 (7.42%). Samples which share a similar community composition of bacteria, the closer they are represented on the plot. Based on similar group clustering of ME and HHC samples, plot reveals no difference between the beta-diversity of patient and control group.

A series of comparisons between patients and HHCs using ecological indices explored in PCoA plots using Bray-Curtis dissimilarity, Chi-Square and Goodall similarity index to determine pair-wise similarity between observations of composite multivariate OTU datasets in the two groups. As discussed earlier, Bray-Curtis measures focus on the most abundant bacterial taxa, which were found to be *Bacterdoides vulgatus, Turicibacter spp.* and *Clostridium celatum.* Patients in the plot (figure 3.3.26) are represented by dark blue red are matched, whilst un-matched ME patients are the dark blue circles. All HHCs (green triangles) are matched to their respective severe ME patients.

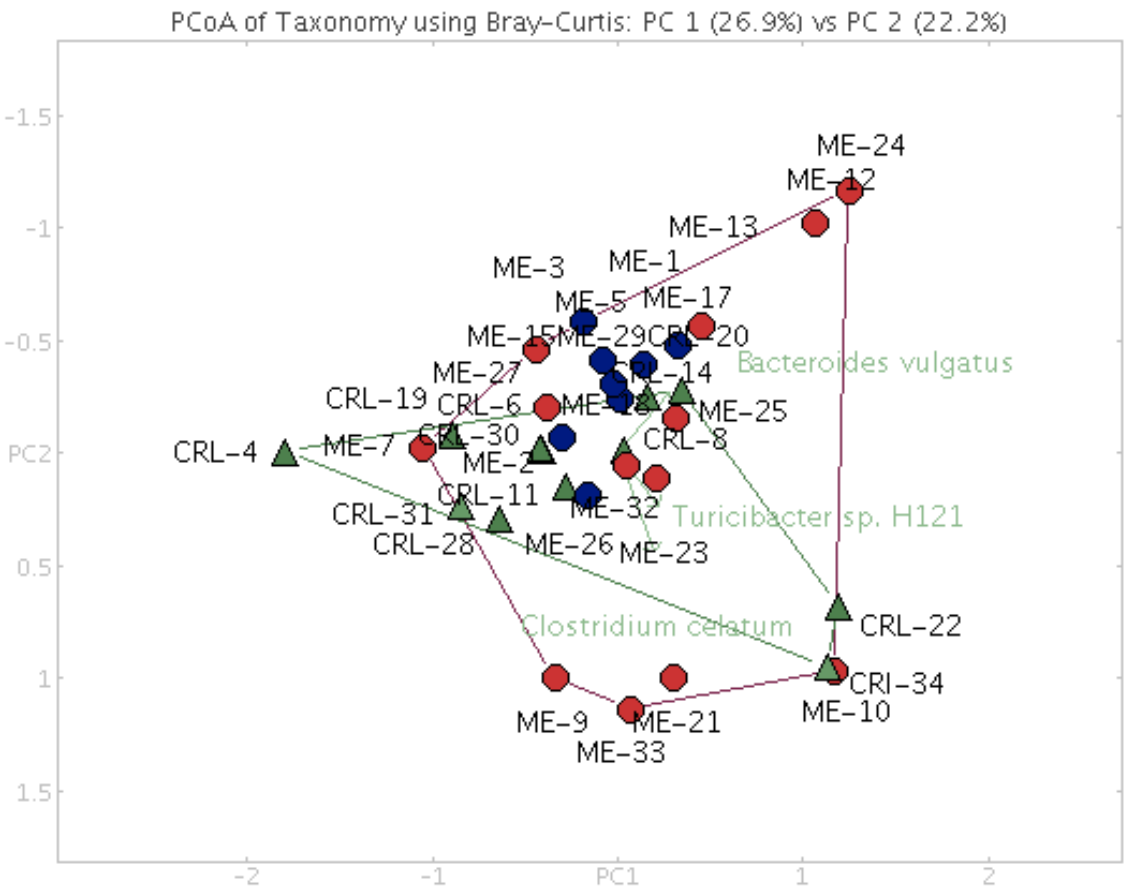

Figure 3.3.26 PCoA using Bray-Curtis distances to separate 21 severe ME patients from 12 HHCs
High species composition similarity between samples are plotted closer together. There appears to be a reduced similarity comparing between severe ME patient samples, compared to both unmatched and house-hold controls which appear much more similar to one another. *Red circles*, matched severe ME; *dark blue circles*, unmatched severe ME; *green triangles*, house-hold controls. Plot annotated with bacterial species relevant to driving separation of samples.

MEGAN 6.0 was also used to compute PCoA plots using Chi-Square distances and the Goodall's similarity index. The former (figure 3.3.27) has the added advantage over Bray-Curtis for considering the differences in proportions of the taxa instead of summarising the most abundant. Using this method, the same bacterial taxa emerge samples in the respective region of the plot. In both methods, un-matched ME patients cluster more closely as do HHCs with exception to CRL-4, -22 and -34.

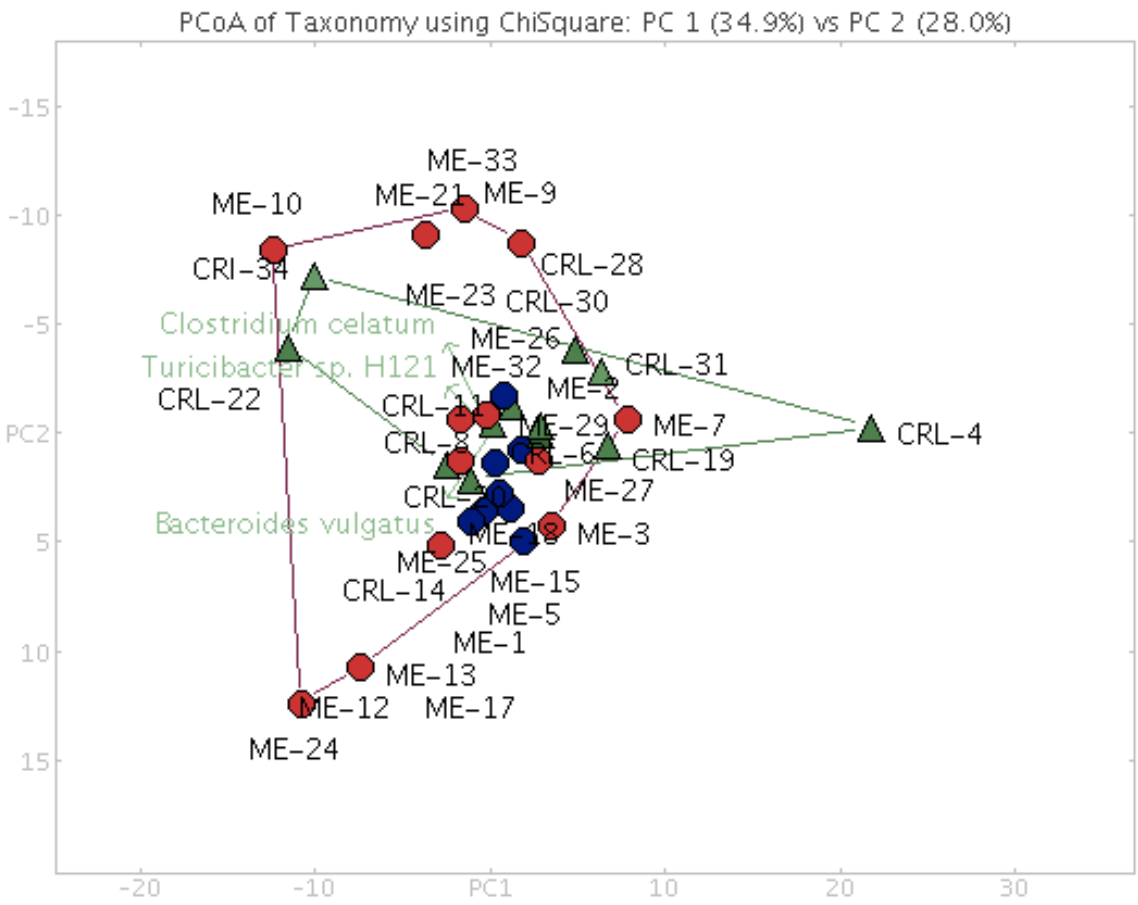

Figure 3.3.27 PCoA plot using Chi-Square distance separation between 21 severe ME patients and 12 HHCs. Conventional unmatched controls (blue) cluster together revealing similar proportions of bacterial taxa. Contrastingly, severe ME samples (red) display more dissimilarity within their own group and with their respective House-Hold control (HHC), green triangles. Fewer than expected HHCs share similar proportions of the same bacterial taxa identified in their ME patient counterpart.

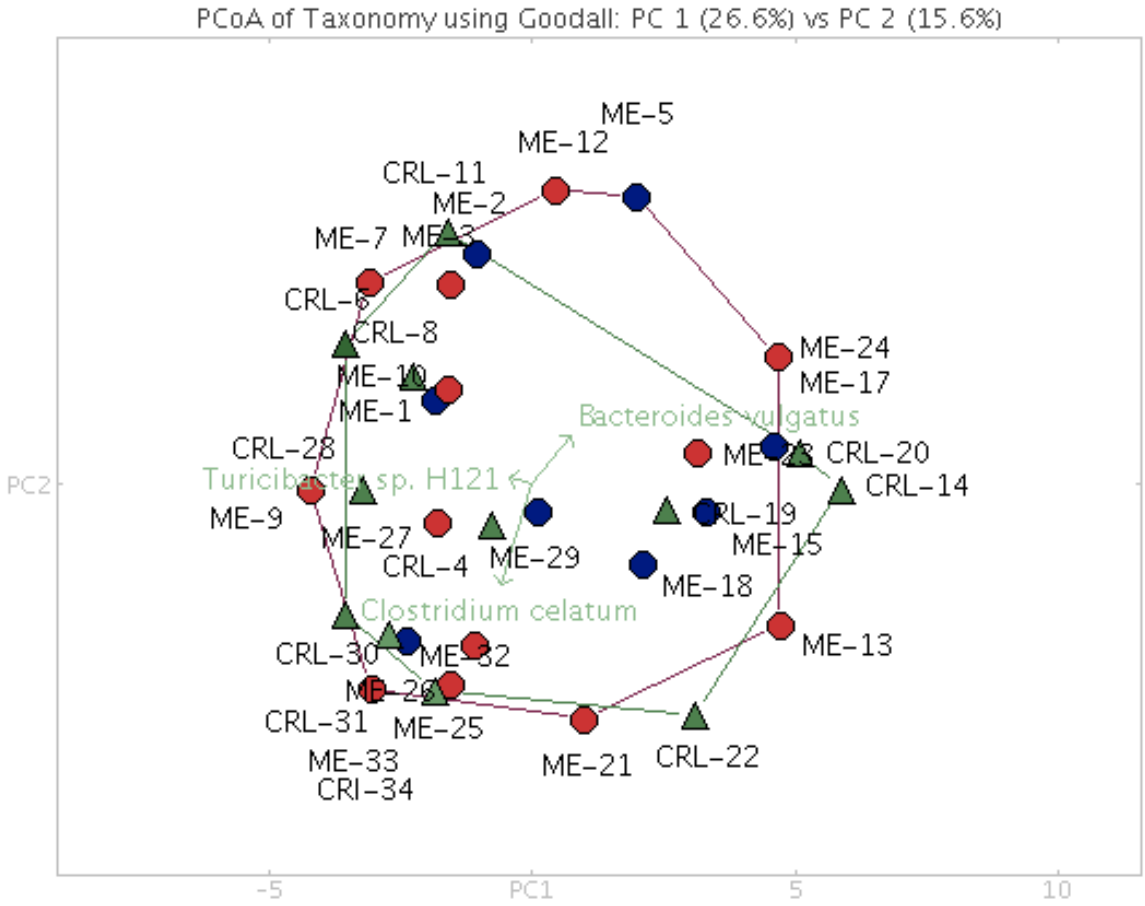

Figure 3.3.28 PCoA plot using Goodall's similarity index to compare 21 severe ME patients and 12 HHCs. This measure assigns greater similarity between severe ME (red) and HHCs (green) identifying the sharing of rarer bacterial genera regardless of the high abundance of other genera. These less represented genera found in severe ME and HHCS are much less likely to be found in samples from the conventional (unmatched) control group.

Goodall's similarity index (figure 3.3.28) is an non-parametric measure designed to examine pairwise similarity between observations of composite multivariate data and is used to give more weight to differences between rarer bacterial taxa rather than comparing the most abundant genera within a group (Mitra et al., 2010). This had the dramatic effect of reducing the clustering of samples compared to the other PCoA plots. Finally, UPGMA was used to visualise the distances between the clustering of samples according to the unweighted and weighted UniFrac method and is frequently used to compare microbiological community structures. In contrast to Bray-Curtis, the relative relatedness of community members by observation of phylogenetic distances between observe species within a sample is used to compare samples. This analysis was performed using MEGAN 6.0 and presented in figures 3.3.29A (unweighted) and 3.3.29B (weighted). Unweighted only accounts for clustering of OTUs compared to weighted which considers the RA in addition.

A, Unweighted

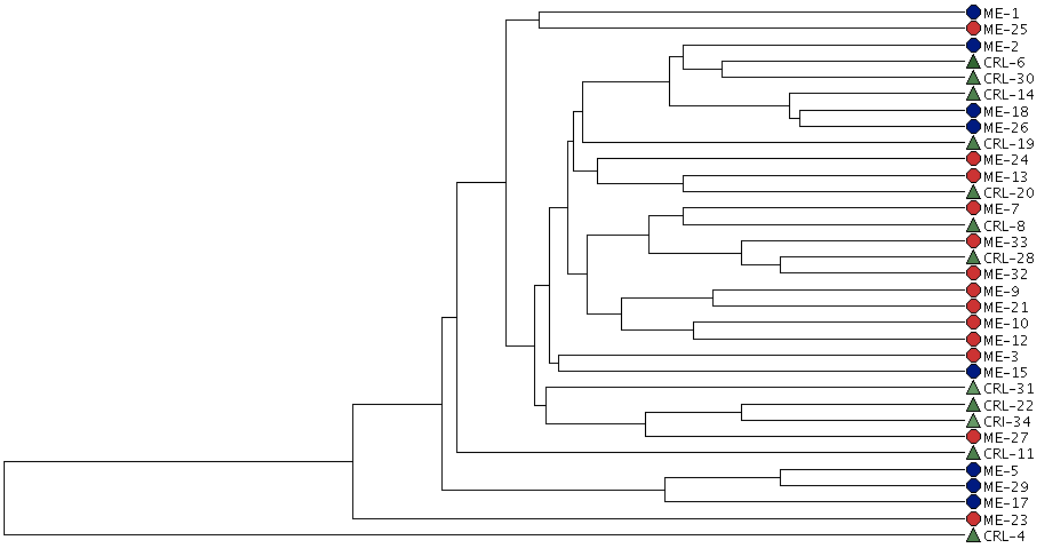

B, Weighted

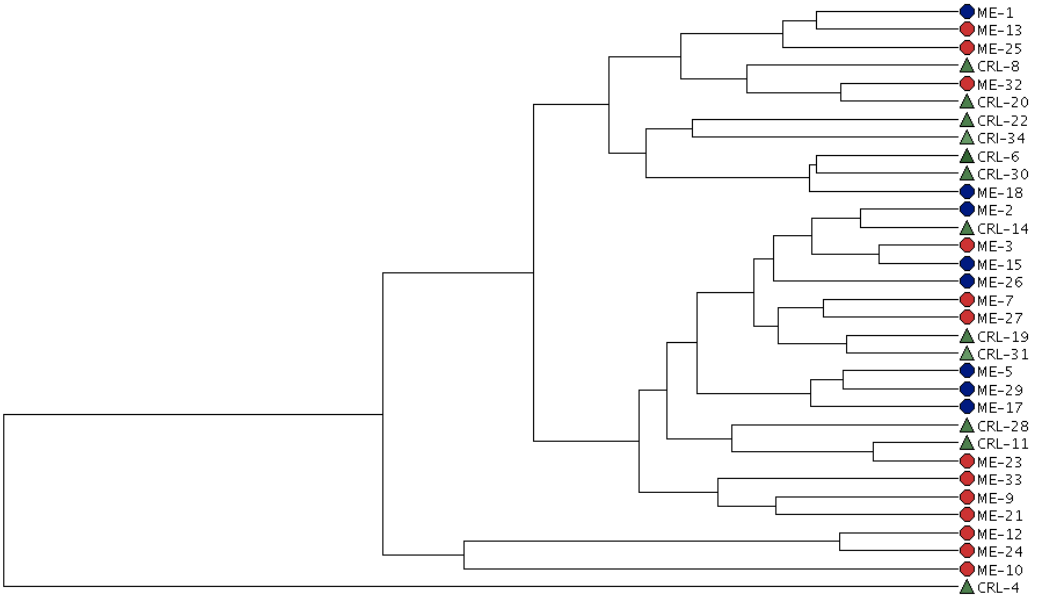

Figure 3.3.29 UPGMA clustering based on unweighed (A) and weighted UniFrac (B) distances between 21 severe ME patients and 12 HHCs. Analysis represents the comparing of microbial ecological communities across all samples using phylogenetic distances to generate a tree. Unweighted corresponds to differences in low-abundance taxa, whereas weighted calculates branch length according to the observed abundance of shared and unshared bacterial taxa across both groups and is less sensitive to lower abundance taxa. *Red circles*, matched severe ME; d*ark blue circles*, unmatched severe ME; *green triangles,* house-hold controls.

- *Species variation between severe ME and HHC*

T-test was performed to determine species with significant variation between groups (p value < 0.05) at various taxonomic ranks including phylum, class, order, family, genus, and species.

Figure 3.3.30 shows the significant species variation in abundance between both groups. The class of *Bacilli spp.* appear more (p = 0.004) in severe ME. Conversely, the phylum *Sphingobacteria* was higher (p = 0.045) in the HHC group. Significant intra-group variation were detected using MetaStat produced in RStudio which used multiple hypothesis-test for sparsely sampled features and Benjamin Hochberg false discovery rate (FDR). *Fusobacteria spp.* emerged from this analysis as significant (q < 0.05) in severe ME patients.

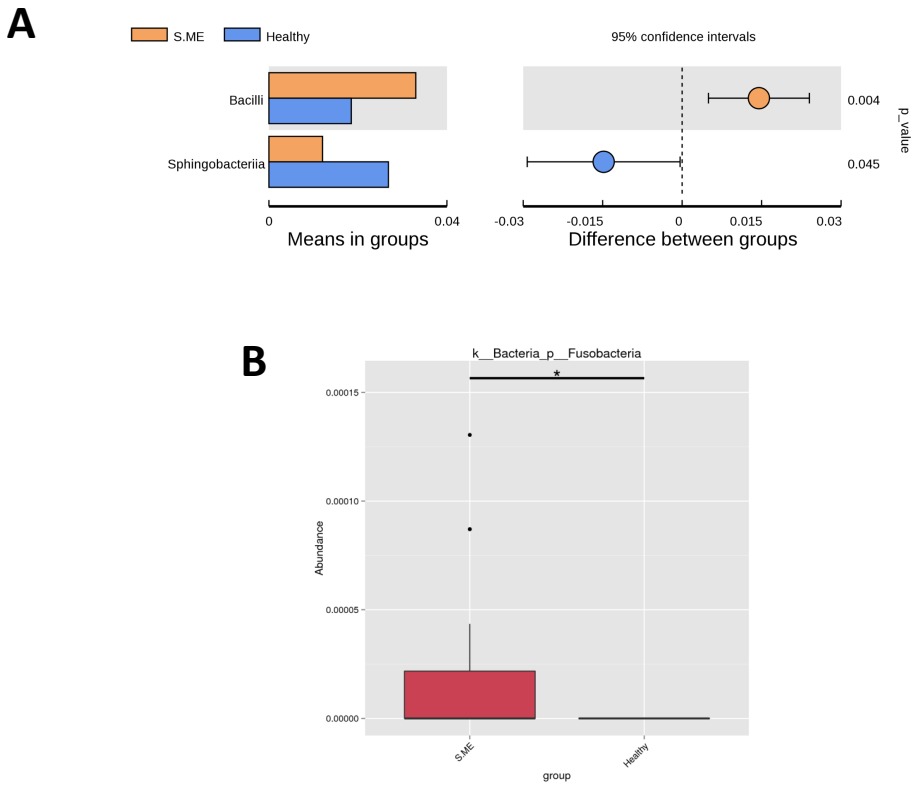

Figure 3.3.30 The bacterial phylum, Fusobacteria are significantly more varied in ME and absent in HHCs (A) Intergroup variation: left panel, each bar represents the mean value of the abundance in each group of the species showing significant between group variation. The right panel shows the confidence interval between these group variations. The centre each circle represents the difference of the mean value. (B) Intra-group variation detected *Fusobacteria* were significantly (q <0.05) more varied within patient compared to HHCs were they were absent.

As a final summary of this data, MEGAN was used to generate a phylogenetic tree (figure 3.3.31) of the top 10 most RA genera across also samples and to highlight the relative contribution these have within the two groups. This revealed *Collinsella spp., Blautia spp*. and *Lachnospiraceae spp*. were more common in some patients (fig. 3.3.32). Conversely, *Bifidobacterium spp., Subdoligranulum spp.* were more common in HHCs. Interestingly, *Faecalibacterium spp.* was similarly abundant in both groups.

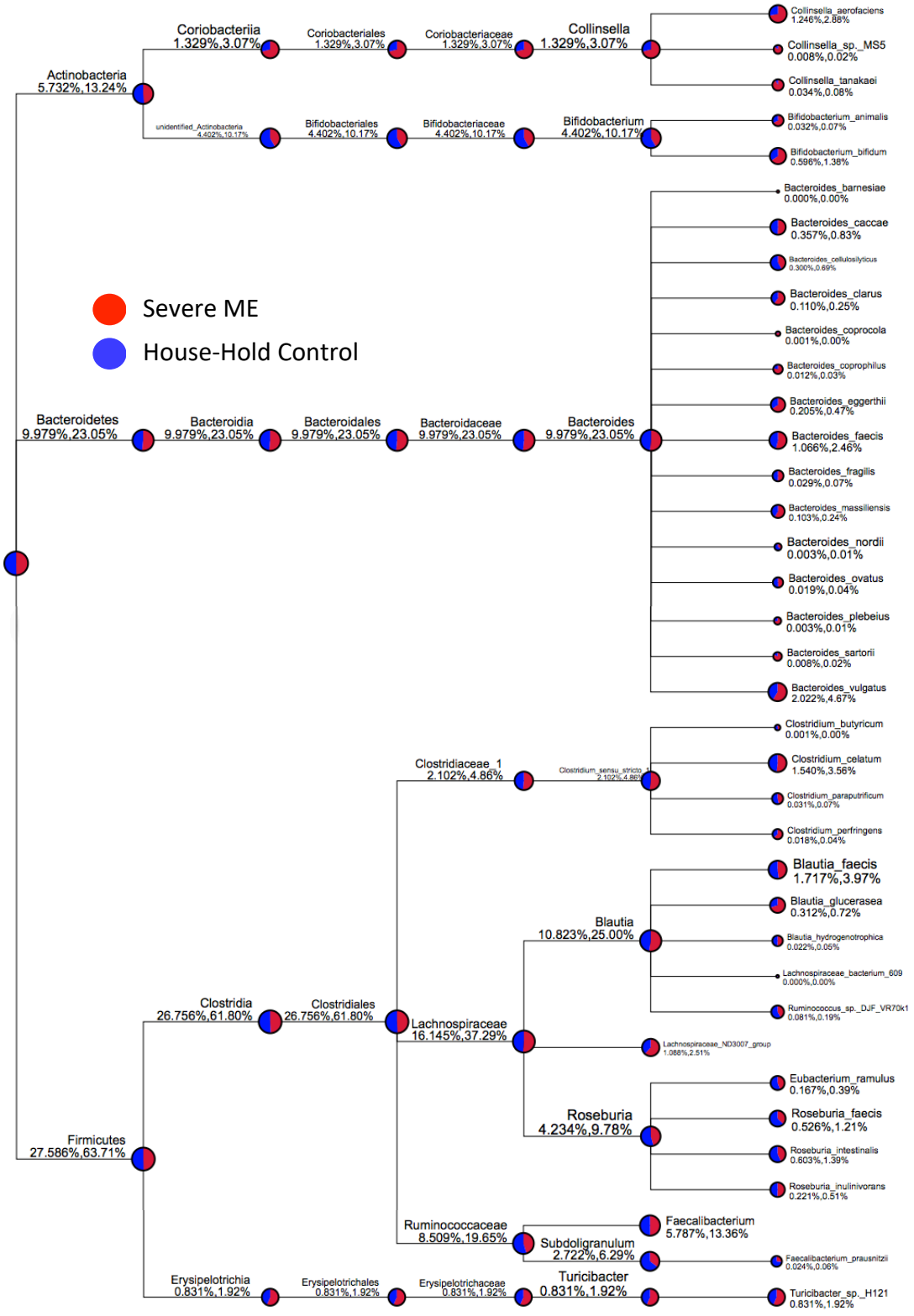

Figure 3.3.31 Top 10 bacteria genera found common in 21 severe ME patients and 12 HHCS. The size of circle represents the size of its relative abundance in samples. Each colour represents a sample group and the proportion of dominance that taxa has within the sample group. The first number below the taxonomic name represents the percentage in the whole taxon, while the second number represents the percentage in the selected taxon. Tree highlights no observable differences between these top 10 genera in patients and HHCs; *Collinsella; Bifidobacterium; Bacteroides; Clostridium; Blautia; Lachnospiraceae; Roseburia; Faecalibacterium Subdoligranulum; Turicibacter.*

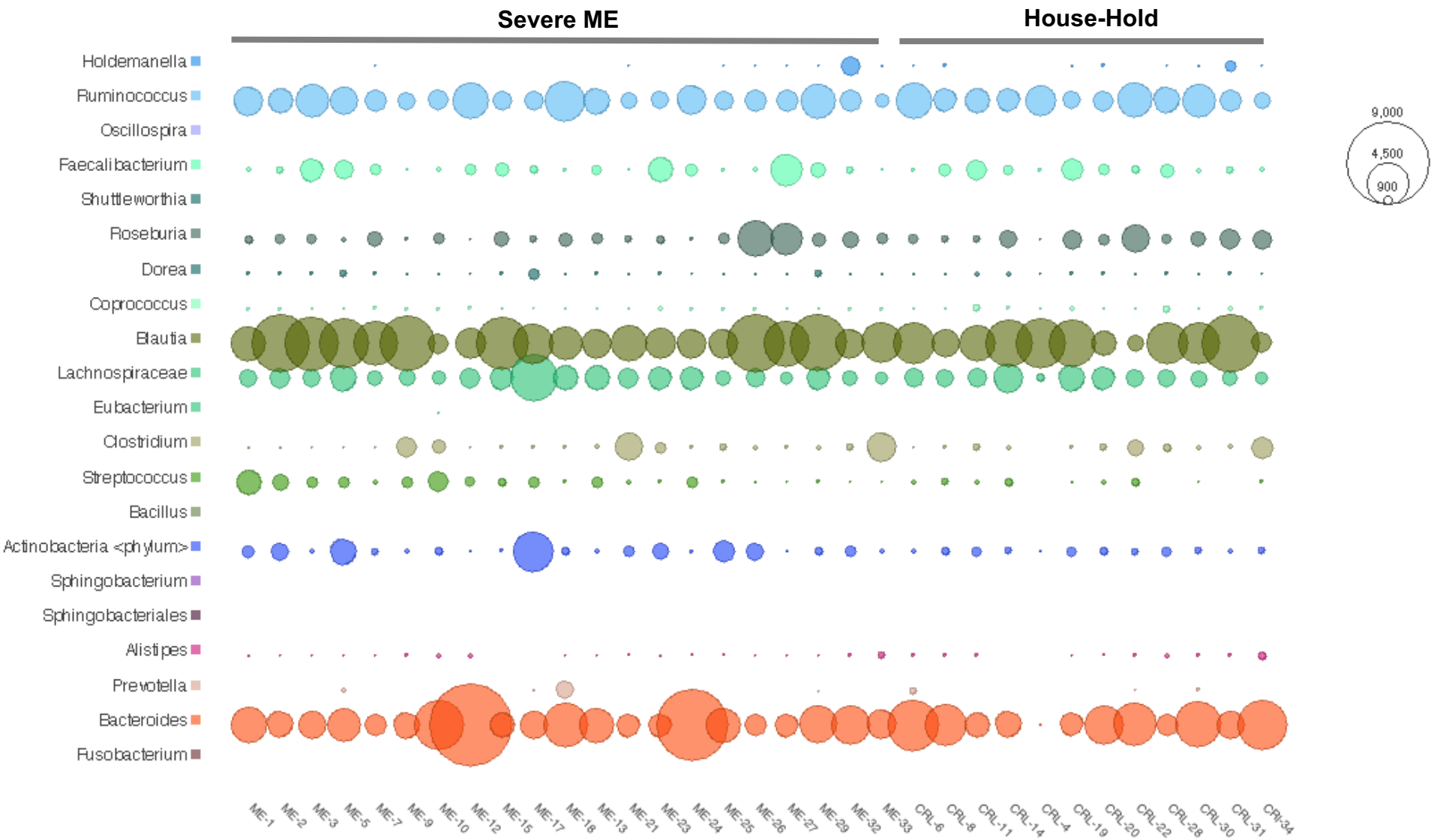
Severe ME
House-Hold
Holdemanella
Ruminococcus
Oscillospira
Faecalibacterium
Shuttleworthia
Roseburia
Dorea
Coprococcus
Blautia
Lachnospiraceae
Eubacterium
Clostridium
Streptococcus
Bacillus
Actinobacteria <phylum>
Sphingobacterium
Sphingobacteriales
Alistipes
Prevotella
Bacteroides
Fusobacterium
9,000
4,500
900
ME-1
ME-2
ME-3
ME-5
ME-7
ME-9
ME-10
ME-12
ME-15
ME-17
ME-18
ME-13
ME-21
ME-23
ME-24
ME-25
ME-26
ME-27
ME-29
ME-32
ME-33
CRL-6
CRL-8
CRL-11
CRL-14
CRL-4
CRL-19
CRL-20
CRL-22
CRL-28
CRL-30
CRL-31
CRL-34

⇐ **Figure 3.3.32 Bubble plot summary of 21 selected genera across 21 severe ME patients and 12 HHCs.** Analysis provides individual sample summary of bacterial abundance. There are no obvious differences in abundance of these shared genera between patients and HHCs. Plot generated using MEGAN 6.0. Colour corresponds to bacterial genera listed to the left. Size of bubble given proportional the square root scale of the relative abundance in each sample.

3.4 Discussion

The initial design and concept for this microbiome study was conceived in late 2013. At this time there was very little published guidance on designing the perfect microbiome study. The overwhelming majority of intestinal microbiome research uses faecal samples collected by the participant and DNA extracted using a range of commercially available kits. Since 2013 several reports have highlighted that sample collection represents a crucial step in ensuring uncompromised sample integrity and that stability is maintained for downstream application of Next-Generation Sequencing (NGS) (Panek et al., 2018). Prompt downstream processing of faecal samples should be completed within 2-3 hours with immediate stabilisation for longer term storage (Panek et al., 2018). Relatively short term exposure to room temperature for up to 2 h prior to DNA extraction does not affect the stability of the microbiota composition according to comparison with samples that had been frozen immediately (Guo et al., 2016).

Freezing the faecal sample at -80^{0}C as soon as possible after collection is regarded as the most appropriate method for preserving microbial composition (Choo et al., 2015). This was not possible considering the majority of samples were obtained from house-bound patients who had collected their sample within 24 hrs of a scheduled home visit. Last minute house visits could not be conducted to minimise this time because of the 150-mile distance between the research laboratory and patients living in the South London area. Instead patients were asked to store their sample in the fridge until collection. Refrigeration of up to 72 hours has been shown not to adversely affect the microbiota diversity of composition and is reassuring that this covers the time required to collect the faecal samples from the patients home (Choo et al., 2015). However, all samples were left without refrigeration between collection from the patient's home and delivery to the hospital laboratory, before storing at -80^{0}C. The time delay was dependent on a number of factors including traffic delays and distances between patient's homes and the hospital and could be between 1-6 hrs until the sample was frozen may contribute to changes microbial composition. This study also praised OMNIgene GUT® as an alternative method to

refrigeration. These devices contain a patented stabilisation mixture and where initially used in 2015 for the collection of faecal samples from 25 mild/moderate patients in dataset A. Early attempts to extract faecal DNA from -80^{0}C frozen OMNIgene GUT devices failed to produce a readable concentration of DNA using the MOBIO Powersoil® DNA extraction kit and Nanodrop. Instead, the FastDNA® Spin kit for soil was found to extract the minimum 5ng/μl for PCR 16S V4 amplification performed by the sequence provider.

Storage of the OMNIGene GUT at -80^{0}C is only recommended up to 1 month (DNAGenotek, 2017). Samples from mild/moderate patients (dataset A) were kept at the hospital at -80^{0}C for much longer (~9 months) before they were received at the institute for DNA extraction. Notably, these samples have very low abundance of *Actinobacteria* which includes members of *Bifidobacterium spp.* and *Coriobacteria spp.* This observation was found not to be the case in dataset C (fig. 3.3.7) in severe ME patients who had 14.59±8.41% RA of *Actinobacteria* and may be regarded as a technical artefact. The turnaround time dataset C was much quicker, as these samples had their DNA extract within 3 months of being stored at -80^{0}C. Interestingly Table 3.3.6 shows some of samples from 2016 collections yielded a lower DNA concentration compared to 2017 samples. Studies of long-term storage of faecal material at -80^{0}C has been investigated for samples stored for 2 years and 14 year showing they can be used for 16S but with a reduction in observed OTUs and increased abundance for *Lactobacillus spp.* and *Staphylococcus spp.,* none of which were detected in our mild/moderate ME patients (Kia et al., 2016; Shaw et al., 2016; Vandeputte et al., 2017). Long term freezing causes substantial DNA shearing compared to fresh faecal extractions and may have greater implications for shotgun metagenomic studies which require high quality input DNA (Kia et al., 2016).

Following sample collection and storage, several processing steps can introduce data bias caused by the DNA extraction protocol and during 16S rDNA library preparation (Rintala et al., 2017). For example, detection of Gram-positive bacteria, particularly *Bifidobacterium spp*. requires adequate bead-beating during sample DNA extraction and optimisation using modified primers targeting V1-V3 regions (Walker et al., 2015). 16S microbiota profiles are based on the reported relative read abundances of OTUs derived from 16S amplicons; thus PCR amplified DNA can only be representative of the quantitative abundance of all bacteria in faeces if this step is efficient for all strains of bacteria (Wintzingerode et al., 1997). Universal primers U515F and U927R/U806R in datasets A and C respectively, were chosen

to span the 16S V4-V5 region for highest taxonomic resolution of bacterial and archaeal ribosomal gene (Wang & Qian, 2009). This leads to the assumption that the PCR primers have equal access for hybridisation to a specific 16S-targed V region in all bacteria, however DNA extraction also determines this property depending on how sufficiently the extraction kit causes bacterial cell disruption in order to access the genetic material (Wintzingerode et al., 1997).

Since 16S-based microbiome studies are restricted to short nucleotide (nt) read lengths (100-300bp) on the Illumina platform (compared to 250-400bp using 454 methods), the outcome of the relative abundance of amplicons can also favour different bacteria depending which variable region of the 16S gene is targeted and the specificity of primer sets used. For example, primers spanning hypervariable regions V1-V2 do not adequately reproduce proportional abundance of reads that reflect the contribution of all species in the female genital tract compared to the V3-V4 region which identifies a greater number of taxa (Graspeuntner et al., 2018). There is also consensus that targeting V4-V5 regions in intestinal microbiome studies produces a greater number of recognised OTUs and observed microbial diversity compared to V3-V4 using the Shannon H index (Rintala et al., 2017). Elsewhere, sequencing regions V4-V6 have been suggested to represent the majority of diversity of bacterial phyla for taxonomic classification (Yang et al., 2016).

Amplicon sequencing is suggested to be more sensitive to lower abundant species since utilities a PCR application step in preparation of a library of amplicons to be sequenced (Edgar, 2017). However, primer bias and mismatches can occur during PCR amplification and can bias the relative abundances of amplicon produced in the library (Robinson et al., 2016). Although datasets A and C are 16S-derived sequencing of the same V4 region they were collected by different methods and do not contain overlapping samples to determine the batch effect and therefore cannot be directly compared. Moreover, the library preparation of these datasets use different PCR protocols provided by the sequencing provider at the time. It has been suggested PCR primer length, amplicon length, reaction temperatures and number of cycles, and different polymerases can influence the efficiency for amplification and shown to provide contrasting estimates for community structure (Wu et al., 2010).

The design of the perfect 16S study cannot be achieved because different microbiotas have vastly different microbial structures which makes deciding the most suitable V-region, set of optimal primers and recommended read length a substantial challenge to accurately reflect the correct community profile. Mock microbial community analysis using 16S amplicon read abundances have been independently compared with shotgun metagenomic sequences showing significant deviation away from the 16S estimated bacterial composition compared to the known community structure (Edgar, 2017). To obtain accurate measurement of the full taxonomic diversity within a complex community sample such as human faeces, near complete characterisation of the 16S gene is needed to assign specific bacterial species (Yarza et al., 2014). Therefore species-level abundances using 16S have no meaningful use because they are based on such short read lengths of 250-300bp compared to the available length of the 16S rRNA is around 1400-1900bp (Karst et al., 2018) Closely related bacteria are more difficult to resolve using V4 alone. To that end the species-level assignment given in figure 3.3.31 are not reliable based on this sequence information. Another problem encountered can be 16S copy number variation which will bias the PCR amplification step and influence the predicted microbial composition (Edgar, 2017). Moreover, the choice of storage method, DNA extraction protocol, primer design and sequencing platform will influence the outcome of the result. For consistency, the 16S-derived microbiota in datasets A and C were processed using the same extraction kit and targeted at the V4 of 16S PCR amplification. In future, to avoid any batch effects samples must be analysed together using the same experimental PCR protocols, conditions and at the same time.

Dataset C produced on average 80,122 more reads per sample than those in dataset A, which allowed over 4 times the number of classifiable OTUs to be taxonomically assigned. This fact demonstrates how the collection method, primer sequences, PCR protocols and sequencing length can affect data output and has been explored more in depth using mock microbial populations highlight a need for a standardised approach (Fouhy et al., 2016). Alpha diversity (figure 3.3.22) and beta diversity measurements were not found to be significantly different between Severe ME patients and HHCs. *Actinobacteria* were present in all samples (figure 3.3.21), as they were also in the “shallow” shotgun, dataset B (figure 3.3.7), adding further convincing evidence that the lack of these species in dataset A, mild/moderate patients is not a genuine finding. In contrast to findings from Giloteaux et al. (2016), the number of observed species in patients was higher than in HHC (figure

3.3.20A and 3.3.20B). A key difference between this study and theirs are the inclusion of controls living within the same house-hold of the patient. It was expected that similar features in microbiota populations would be shared between the microbiotas of patient and their respective HHC. It was expected PCoA analysis would show closer distances between patient and their matched control based on overall community composition. The reverse is found in figures 3.3.26 and 3.3.27 which show house-hold controls are more compositionally related to un-matched ME patients. Goodall's similarity test was chosen as it specifically considers the fact these samples are paired. It can be seen from figure 3.3.28 that the patient and HHC group are positioned in an overlapping ring formation with some unmatched patients within the centre of the plot. To that end, given the description of this analysis by (Mitra et al., 2010), Goodall dissimilarity more accurately reflects the relationship between severe ME and HHCs. The lack of forming discrete clusters within this PCoA plot also demonstrates how compositionally diverse both patients and HHCs from other members within their respective group. UPGMA UniFrac considers the presence or absence of OTUs distances and did show clustering of some severe ME patient that matched HHCs (fig. 3.3.29) (Jovel et al., 2016). However, UniFrac is a method of determining the phylogenetic relationship tree structures compared between samples, and so given the shallow sequencing and number of observed OTUs this method is perhaps not the most suited to this data, whereas non-phylogenetic measures of ß-diversity, including Bray-Curtis (fig 3.3.26) which does account for zero abundances within the raw data, but is still heavily influenced by more dominant OTUs which overshadow smaller changes in less abundant, rarer OTUs (see supplementary S2.1 and S2.2) (Bray & Curtis, 1957; Jovel et al., 2016). Among the top 10 genera highlighted from MEGAN in figure 2.3.31 that shared between ME and HHC, includes *Lachnospiraceae, Roseburia,* and *Faecalibacterium,* that have previously been associated with the ME/CFS (Giloteaux et al., 2016; Nagy-Szakal et al., 2017). *Lachnospiraceae* the family to which the genus *Lactonifactor* belongs, found to increased x20 in Norwegian CFS patients and x40 in Belgian CFS patient compared to healthy controls, did not differ between patients and HHCs in dataset B (table 3.3.4) and dataset C (fig. 3.3.11B) (Fremont et al., 2013).

Finally, dataset C did not reproduce findings from dataset B, for significant changes in the relative abundances for *Faecalibacterium prausnitzii*, *Oscillibacter* and *Eggerthella*. *Fusobacteria* were associated with 1-3 OTUs (figure. 2.3.30) per sample, in patients only. These were samples ME_5, ME_17, ME_27 and ME_29. Fusobacterium are increased in

colorectal cancer (CRC) and have diagnostic relevance as an additional microbial marker for faecal immunochemical testing patient faeces increasing sensitivity of testing to 92.3% from 73.1% to supplement diagnosis of advanced CRC (Wong et al., 2017).

- *Shotgun metagenomics attempt*

In order to overcome the potential biases of 16S gene marker approaches and achieve better taxonomic resolution, shotgun metagenomics (dataset B) was attempted from 2016 visits to 11 house-bound patients. Unfortunately, the term "shallow" shotgun metagenomics was adopted to describe the low sequencing depth of reads with this dataset. Lipkin et al. 2017, acquired on average 7GB of sequence data per sample equivalent to around 35 million reads, compared to our lowest sample which had 253, 484 raw sequencing reads (Nagy-Szakal et al., 2017). This may partly be due to MiSeq platform used to sequence these samples which is limited to 15GB of data with a maximum output of 44-50 million 300bp PE sequencing reads with the MiSeq Reagent Kit v3 (Illumina, 2015). It is difficult to advise exactly how many reads are required to generate an accurate representation of the total microbiome which also includes members of archaea, fungi and viruses. Cost is a significant factor per sequencing run, individual coverage of these samples is balanced by the total number of samples processed simultaneously in each run by multiplexing up to 96 or 384 samples at a time using dual indexes (barcodes) during library preparation (Quince et al., 2017). Based on the number of reads obtained, this dataset exceeds both average number of reads for 16S in the other datasets. Significantly as it is SMS, it is not restricted to the 16S gene and therefore contains random sequencing across the total microbiome which MetaPlAn has compared against reference genomes available from (www.bitbucket.org/biobakey/metaphlan2). This has had some benefit in being able to apply a species-level identification to dataset B.

As highlighted already, application of SMS to metagenomic studies of diverse microbiotas requires high-quality molecular weight DNA. This aspect was not considered during preparation of dataset B; at the time DNA was quantified using Qubit, which uses a fluorescent dye to hybridise with the sample DNA and is considered superior at providing more accurate concentration than the NanoDrop. Added to this, lack of sequencing depth has since been explained by the fact that libraries were prepped using Illumina® Nextera XT, which is recommended for use in low-biomass starting material of 1ng/μl. As with 16S studies, the choice of method for preparation of library preparation for shotgun

metagenomic sequence data has been evaluated in faecal samples which show Nextera XT performs poorly in these samples with 28% low quality reads compared the more expense Illumina TruSeq PCR-free kits (Jones et al., 2015). The low DNA input for Nextera XT is possible because of a whole genome amplification (WGA) step, but given the diversity of the intestinal microbiome, there will be the familiar amplification biases that will also cause the RAs of different bacteria to change (Probst et al., 2015). It has been proposed that PCR-free approaches to metagenomic library prep are implemented, however, these are more expensive but will likely be more representation of the true community structure of the faecal microbiota (Quince et al., 2017).

Another explanation for the loss of sequencing depth may be a result of the beat betting used by the FastDNA® spin kit which would create shortened DNA fragments that are suitable enough for 16S, but not for shotgun library preparation with the Nextera XT kit which uses a technique called "tagmentation" (Quince et al., 2017). This causes enzymatic fragmentation of sample DNA and transfers transposons (tags) onto the both ends of dsDNA to allow partial overhang of Illumina® sequencing adaptors. The concentration of the kit's reagents and the concentration of sample DNA can limit transposome complex transposase activity (figure 3.4.1) and tagging of DNA fragments. Thus, the distribution of tagged DNA within the library will influence the proportion of the library that gets sequenced. For example, samples that are >1ng can therefore lead to under-tagmentation (Caruccio et al., 2009; Holmes et al., 1988; Illumina, 2014; Syed et al., 2009). Prior to sending samples to the sequencing provider for dataset C, they were analysed on the Bioanalyzer™ Tapestation® which produces gel images to assess DNA fragment sizes. Although this dataset produced 16S data, DNA quality can also affect tagmentation. The Nextera XT transposome requires minimum of 300bp to efficiently cut the DNA into fragments for transposon tagging and therefore if the sample DNA is degraded this will cause few tagmented fragments to be sequenced and will cause an under-representation of species diversity (Illumina, 2014).

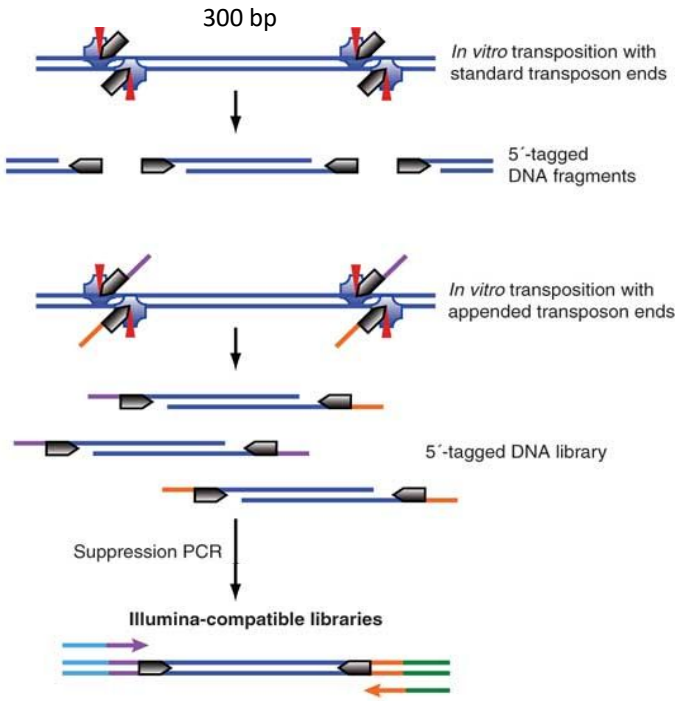

Figure. 3.4.1 Nextera XT fragmentation causes breaks within dsDNA and transposon tagging across the sample DNA. Diagram adapted from**,** (Caruccio et al., 2009)

Despite the technical issues with this data, there were some interesting findings comparing severe patients with HHCs. The first is the lower RA of *Faecalibacterium prausnitzii* in patients shown in figure 3.3.11. This is in agreement with another report of this species being significantly reduced in ME/CFS patients with IBS (Nagy-Szakal et al., 2017). It is suggested to account for 5% of the total bacteria resident in the intestinal microbiota and a reduction in this species in linked to dysbiosis in intestinal inflammatory diseases such as Crohn's Disease (Miquel et al., 2013). Significantly higher RA of *Eggerthella spp*. 0.98% ME versus 0.43% HHC (table2.3.4) was seen comparing across the genus level using non-parametric Mann-Whitney U test in figure 3.3.13. The abundance tables for this dataset are included in the supplementary section (S3.1 and S3.2). *Eggerthella spp.* are Gram-positive anaerobes belonging to the phylum *Actinobacteria* normally found in the human intestinal microbiota but have been associated with abdominal sepsis (Gardiner et al., 2014).This finding in severe ME patients was also something reported by Lipkin et al (2017) in ME/CFS without IBS (Nagy-Szakal et al., 2017).

- *Summary*

Seventy-seven samples were analysed using next generation sequencing to determine differences in the composition of the intestinal microbiota between ME/CFS patients and house-hold controls. The composition of the intestinal microbiome of ME/CFS patients has been suggested to be less diverse than that of healthy controls (Fremont et al., 2013; Giloteaux et al., 2016; Nagy-Szakal et al., 2017). We compared and contrasted sequencing of the V4 hypervariable region of the 16S gene, a single genetic marker against recovery of non-targeted, random 150bp DNA sequences representing the entire (meta)genome content extracted from faeces. The data generated from these two methods did not show variation in the diversity of species identified in ME/CFS and HHCs. However, using shallow shotgun sequences, patients had a 5-fold reduction in *Faecalibaterium prausnitzii* compared to HHCs. Other significant differences were at the genus level included increased abundance of *Oscillibacter* and *Eggerthella* in severe ME compared to HHC. Comparison of the members of the core microbiota (defined by bacterial taxa appearing in 50% of all samples) revealed qualitative and quantitative differences between severe ME and HHCs based on 16S sequencing. Severe ME patients have few members of the core microbiota than HHC. No evidence for increased abundance of *Proteobacteria* (a source of bacterial LPS) was found in any of the datasets. The genus contains several known human pathogens and is suggested as a microbial signature for low-grade inflammation sustained by exposure to LPS (Rizzatti et al., 2017).

A recent review highlights the need for best practices for designing and analysing microbiome studies which address some of the issues surrounding reproducibility of microbiome data (Knight et al., 2018). Several sources of confounding factors are generated through every step of a microbiome study. Every microbiome study faces challenges for establishing an experimental design to generate the best source of data and relies on the of methods of sample collection, protocols to standardise faecal DNA extraction and library preparation and PCR biases, choice of sequencing platform, pre-processing of reads, and bioinformatics pipelines to analyse sequence data to generate a microbial profile. Therefore, the output of multiple metagenomics studies is very difficult to compare without establishing good practices to address these differences.

In conclusion, the total data in this chapter represents a pre-screening of the composition the intestinal microbiota of severe ME patients compared to HHCs. We have shown the

taxonomic capabilities of 16S sequencing does not allow sufficient taxonomic resolution to reveal differences between patients and house-hold controls. Our shallow shotgun data utilised non-targeted, random “shotgun” sequencing of the intestinal microbiome but failed to provide adequate coverage based on the low number of sequence reads generated. Despite this, the number of reads generated far exceed the output of both 16S datasets and were processed using MetaPlAn to compare sequences against known bacterial reference genomes. Here, we did reveal a significant reduction in the relative abundance of *Faecalibacterium* and increased *Eggerthella* and *Oscillibacteria* in severe ME compared to HHCs. This study represents the first of its kind to explore the microbiota composition in severe patients matched with their respective healthy house-hold control. We consider this an important strength to this study, but future work should sample from patients diagnosed with IBS to exclude to possible dysbiosis by this cause. Our analysis did not sufficiently replicate those of other ME/CFS metagenomic studies carried out in mild to moderately affected ME/CFS patients. Given the known impact diet has of the microbiota, future studies should give consideration to recording food intake. Future work should also resolve both technical and logistical concerns raised throughout this discussion.

Chapter Four

4 Profiling the faecal and serum metabolome in house-bound, severe ME patients

4.1.1 Introduction

The human metabolome is complex, particularly within the gut since factors including diet, lifestyle, age, medications, and environmental contact with microbes influence experimental data and outcome. Metabolomics, a major contributor among the 'omics'-based technologies, is being exploited to better understand the role of the functional capacity of gut microbes in the context of health and disease. The majority of research on the intestinal microbiota has focused on genome-based studies that have led to associations of changes in the composition of intestinal bacteria in a broad spectrum of (auto)-immune/inflammatory disorders from: obesity, type II diabetes, cancer, and (neuro)-immune/endocrine pathologies such as multiple sclerosis, autism and depression and anxiety-based disorders. Gradually metagenomics has started to become integrated with metabolomics to functionally annotate the microbiota and characterise its metabolic activity and relative contributions in health and disease. The advent of NGS metagenomics over the last decade has evolved in its high-throughput capacity to identify thousands of targets within the complex samples such as human faeces for a comprehensive sequenced-based identification of a diverse range of bacterial species. Previously it was suggested bacteria outnumber cells in the human body by a ratio of 10:1, however this estimate has been downgraded to be in the same order of the number of cells in the body (Sender et al., 2016). The Human Microbiome Project and MetaHIT have shown the taxonomic diversity of the human microbiota through the number of bacterial species varies enormously from person to person (Ehrlich, 2011; Human Microbiome Project, 2012). However, a number of different communities of bacteria as well as individual bacterial species within the microbiota are able to perform exactly the same metabolic biochemical functions in a healthy microbiome. This functional redundancy allows the microbiota to adapt to environmental changes, or perturbations by changing gene expression to continue to deliver the same functional benefits to the host (Heintz-Buschart & Wilmes, 2018). Nearly 10 million genes have been catalogued from the human gut microbiome with little known about their biochemical function and contribution towards host metabolism (Li et al., 2014). The functional benefits of the microbiota are being recognised in faecal microbiota transplants from healthy donors and has been suggested to be successful in treating some ME/CFS patients (Borody & Khoruts, 2012). Understanding the composition of intestinal bacteria alone is not enough to understand the complex relationship between the intestinal microbiota and host. Depending on the method of prediction between 40-70% of

the protein-coding metagenome has unknown function and is a limitation to metagenomic approaches to unravel disease mechanisms (Heintz-Buschart & Wilmes, 2018). The shift towards shotgun metagenomic provides an overview of the genetic information encoded by the microbiota however, additional 'omics technologies need to become integrated with this strategy to address the expression of this metagenomic material and characterise its metabolic features which interact with the host and relate to its functions in health and in disease.

The principle technologies of metabolomic profiling uses a combination of platforms including Nuclear Magnetic Resonance (NMR), Gas Chromatography /Mass Spectrometry (GS/MS) and Liquid Chromatography/Mass Spectrometry (LC/MS) in non-targeted and targeted experiments to cover a range of metabolites with accuracy and sensitivity. The aim of this is to combine metabolite profiles with a functionally annotated intestinal microbiome to help identify diagnostic biomarkers as well as unravel diseases mechanisms associated intestinal dysbiosis with limited bias and data-driven approach to biomarker discovery. The biggest challenge remains in the extent of metabolite coverage in a single experiment. In fact multiple methodologies are needed because of the physical biochemical diversity of metabolites ranging from hydrophilic to hydrophobic compounds (Dias & Koal, 2016). The experimental design and choice of workflow to quantify metabolites, as well as differences in the range of signal detection, when comparing NMR data derived from a 600 MHz versus 750 MHz magnetic field strength machine, will alter the signal to noise ratio in NMR spectra and sensitivity towards metabolite detection. Indeed, this can make inter-study comparison difficult not least because of the heterogenous patient cohorts used in ME/CFS research but also differences in size of reference compound libraries to compare against experimental spectra can vary between studies. This is made further difficult in non-targeted experiments when it is not clear which metabolites are of particular interest to that cohort. A combination of targeted and non-targeted approaches using multiple metabolic platforms is for example preferred to identify and quantify as many metabolites as possible. As a result, studies often examine different sets of metabolites and number of metabolites that can be identified can make it challenging to compare studies linking metabolites variation to a particular disease state.

4.1.2 The metabolome in ME/CFS

Suppression of general energy metabolism and mitochondrial dysfunction are thought to be involved in the aetiology and long-term maintenance of the two most significant and highly debilitating symptoms in ME/CFS patients: chronic persistent fatigue and post-exertional malaise (Fluge et al., 2016). Whilst onset of ME/CFS is often described by a flu-like illness, many potential pathogens that have been linked with the disease are not consistently found in all patients, suggesting that they may be acting as a potential trigger to a series of pathological events yet to be defined rather than being a direct cause in itself (Buckwold et al., 1996). The gut acts as a major player within the immune system, since its epithelial cell surface barrier remains exposed to the microbiota. Microbial dysbiosis resulting in altering the diversity profile of gut bacteria has been reported in ME/CFS, but it is unknown how microbial metabolites may conspire to alter local intestinal (and systemic) homeostasis or contribute to the severity of fatigue.

Given that a key microbiota function is in digestion and extracting energy from food and current research highlighting metabolic disruption in energy and lipid metabolism in ME; additional insights may be obtained from studying the severest, most fatigued patients, would provide a test for reproducibility and further substantiate confidence in these findings. Severe patients represent the most fatigue and disabled individuals within the ME spectrum and may represent a subset of patients whom fundamental changes have occurred within their energy metabolism as a product of immune activation (Hornig et al., 2015), on-going inflammation, neuroendocrine dysregulation, autonomic dysfunction and/or cardiovascular anomalies. This highlights the complexity of multi-system dysfunction that have been found to occur in ME/CFS. It is a reasonable assumption to suspect that blood metabolism may be exerting homeostatic shifts across these systems. Moreover, blood metabolism is influenced by gut metabolism and diet, and in general, increasing evidence suggests gut health plays a significant part in many extra-intestinal diseases, including neuro-psychological and neuro-inflammatory disorders (Carding et al., 2015; De Punder & Pruimboom, 2015; Kelly et al., 2016; Moos et al., 2016; Sampson et al., 2016). For example, a study between the relationship of the intestinal microbiota and plasma metabolites show strong correlations, (e.g. microbiota-derived plasma levels of Trimethylamine N-oxide (TMAO)) with microbial community structures and an individual's body mass which influenced the risk of developing glucose tolerance (Org et al., 2017).

4.1.3 Faecal metabolome in ME/CFS

The relationship between host and changes in gut bacterial populations within the ME/CFS are currently at the correlation level with very little previous reports to comment on the faecal metabolome in these patients. One study by Armstrong *et al.* (2017) examined the faecal metabolites from 34 female patients using 750MHz ^{1}H-NMR (see table 4.1.1) to correlate the data with changes in bacterial populations and systemic metabolism by taking blood serum and urine samples (Armstrong et al., 2017). Their findings were consistent within ME/CFS for a decrease in faecal lactate and increase in faecal butyrate, isovalerate and valerate. Small Chain Fatty Acids (SCFAs) such as these, particularly butyrate are utilised by intestinal epithelial cells as an energy source as a by-product of the fermentation of indigestible food in the colon (Inoue et al., 2014). They act by binding to G protein-coupled receptors (GPR41 and GPR43) to signal conversion of adenosine monophosphate-activated protein kinase (AMPK) to the phosphorylated (pAMPK) (Kimura et al., 2014). This facilitates increased fatty acid oxidation and expression of glucose transporter (GLUT4). Moreover, increased gut permeability thought to be present in ME/CFS, and may be exacerbated by higher levels of SCFAs and will enter the blood circulation in increased concentration and have further influence on systemic energy metabolism, but particularly in liver and muscle cells (Armstrong et al., 2017; Giloteaux et al., 2016) . Armstrong's observations support this idea, since propionate from the gut can enter gluconeogenesis via succinyl-CoA in the liver to generate aspartate and glucose which were positively correlated within serum and urine metabolomic profiles, respectively (Armstrong et al., 2017).

To summarise, the faecal metabolite differences found SCFAs in ME/CFS suggest increased bacterial fermentation that appears facilitated by changes within the microbiome profile. Armstrong used traditional culture methods to simultaneously analysis bacterial species, as such, *Clostridium spp.* were increased and are interestingly shown to ferment lactate and amino acids in the production of butyrate (Smith & MacFarlane, 1998). Indeed, acetate, propionate and butyrate were all increased in the ME/CFS faecal metabolome, with butyrate being the most significant. Lactate was unexpectedly found to have decreased despite an earlier finding which found an increase in lactic acid producing bacteria in ME/CFS (Armstrong et al., 2017; Sheedy et al., 2009).

4.1.4 Systemic metabolome in ME/CFS

Blood serum and plasma have previously been studied in ME/CFS using NMR and LC-MS and produced intriguingly consistent results that is even more surprising given the extreme heterogeneity which is normally a drawback in studies of these sizes, (see Table 4.3.1) (Armstrong et al., 2015; Germain et al., 2017; Naviaux et al., 2016). Such consistency may be indicative of the blood metabolome being fundamentally different in ME/CFS. Armstrong first reported anomalous energy and oxidative stress pathways in ME/CFS derived from serum NMR experiments 2015 (Armstrong et al., 2015). Using this 2015 data of 29 metabolites identified and quantified in sera, these were later combined with faecal metabolite concentrations in 2017 to conclude SCFAs maybe entering the circulation, especially propionate to cause mitochondrial dysfunction and oxidative stress and may further be exacerbated by increased gut permeability ME (Armstrong et al., 2015, 2017; Giloteaux et al., 2016). Further correlations were made between the faecal and blood metabolomes summarised in table 4.1.1.

In conclusion, current evidence points towards suppression of energy metabolism, fatty acid metabolism and oxidative stress as common pathways altered in ME/CFS and to which there is some consistency within the literature. But it is not clear how these pathways relate to the context of severity of ME or from observations of the faecal microbiome or why these observations are so consistent given the heterogeneity of the ME population included in these studies so far. Naviaux et al. published a landmark paper in 2016 detailing abnormalities within 20 metabolic pathways from plasma, including reduced lipid metabolism, amino acid metabolism, and purine metabolites, and mitochondrial metabolism (Naviaux et al., 2016). Another study using the Fukuda CFS criteria suggested that the ratios of plasma metabolites pyruvate/isocitrate and ornithine/citrulline, related to the TCA and urea cycles, respectively, may have diagnostic relevance (Yamano et al., 2016). Germain et al., who later published from a much smaller pilot cohort using distinct mass spectrometry techniques (see Table 4.1.2), supported the vast range of conclusions drawn from Naviaux's earlier work targeting 612 metabolites in total. Among the 361 detected, 74 metabolites were significantly different with a similar trend to Naviaux's finding for a hypometabolic state with 80% of these altered metabolites being lower in ME/CFS versus controls.

4.1.5 Investigating bile acid metabolism in ME

As a follow up to NMR, targeted High-Performance Liquid Chromatography-mass spectrometry (HPLC-MS) was used in faecal water and serum to accurately quantitate 26 bile acids – based on previous observation of decreased taurine in ME/CFS plasma (Niblett et al., 2007). Taurine conjugates with bile acids to form bile salts necessary for lipid absorption which were also found to be negatively affected in patients belonging to the Germain study (Germain et al., 2017). To date, no other studies have targeted the role of bile acids within ME/CFS metabolism; especially in severe, house-bound patients. Moreover, the gut microbiota provides a functional role in the regulation of bile acid metabolism which is vitally important in host lipid and energy metabolism.

Bile acids (BA) are steroidal compounds synthesised in the liver from cholesterol and regulated via negative feedback through their binding to nuclear farnesoid X receptors (FXRs) in the liver and gut, see figure 4.1.1. There are two pathways that have been identified for BA synthesis: the "classical" and "alternate" pathways also shown in figure 4.1.1. The classical pathway is responsible for most BA synthesis and is controlled by the enzyme cholesterol 7α-hydroxylase (CYP7A1) which is inhibited by FXR activation through expression and binding of FGF15/19 to FGF4/ßKlotho receptor. As much as 95% of the total BAs secreted are reabsorbed from the gut and delivered to the liver via the hepatic portal vein. Chenodeoxycholic acid (CDCA) and cholic acid (CA) are the two most abundant primary bile acids produced by humans in the liver which serve to facilitate lipid emulsification and digestion. Upon secretion into the duodenum, the bile acid pool may be further altered by the gut microbiota to produce secondary bile acids (Wahlström et al., 2016). Indeed, the gut microbiota can therefore alter the distribution of bile acids as a consequence of dysbiosis within its community structure. In fact, several disease states including inflammatory bowel disease (IBD), liver disease, *C. difficile* infection, metabolic syndrome, and various cancers are now associated with changes to bile acid metabolism (Staley et al., 2017). Thus, alterations within bile acid metabolism may be indicated by changes of the ratio of primary to secondary bile acids, could be indicative of a disease-associated microbiome.

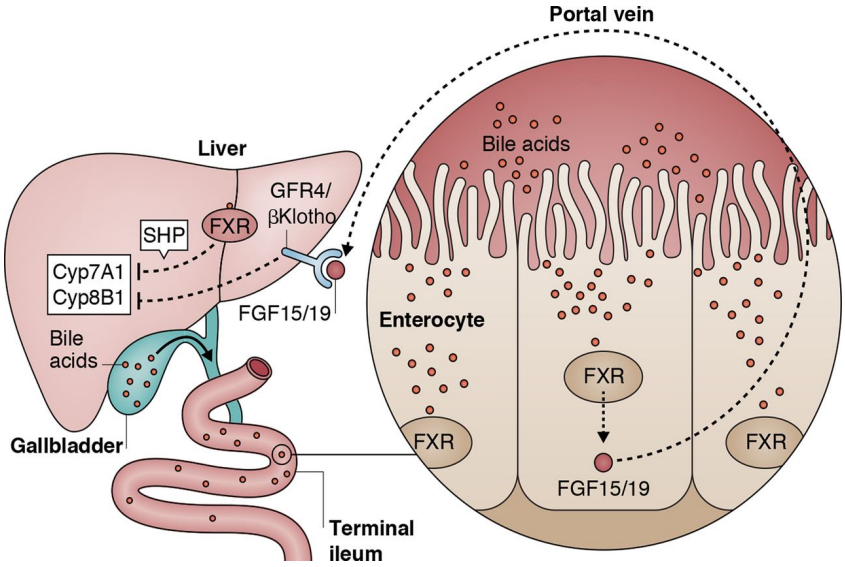

Figure. 4.1.1 Bile acid synthesis is dependent on expression of CYP7A1 in the liver and is regulated by a negative feedback loop mediated by the induction of FXR. Primary acids are produced in the liver. CYP7A1 codes for the enzyme 7α-hydroylase which converts cholesterol to 7α-hydroxycholesterol. FXR activation inhibits CYP7A1 and is activated by hydrophobic (non-polar) primary and secondary bile acids (CDCA, CA, DCA, LCA). Intestinal activation of FXR induces the release of FGF15/19 into enterohepatic circulation back to the liver where it binds to GFR4/βKlotho receptors on hepatocytes to inhibit CYP8B1, another hydrolase involved in BA synthesis. FXR – farnesoid X receptor; FGF -fibroblast growth factor. (Shapiro et al., 2018)

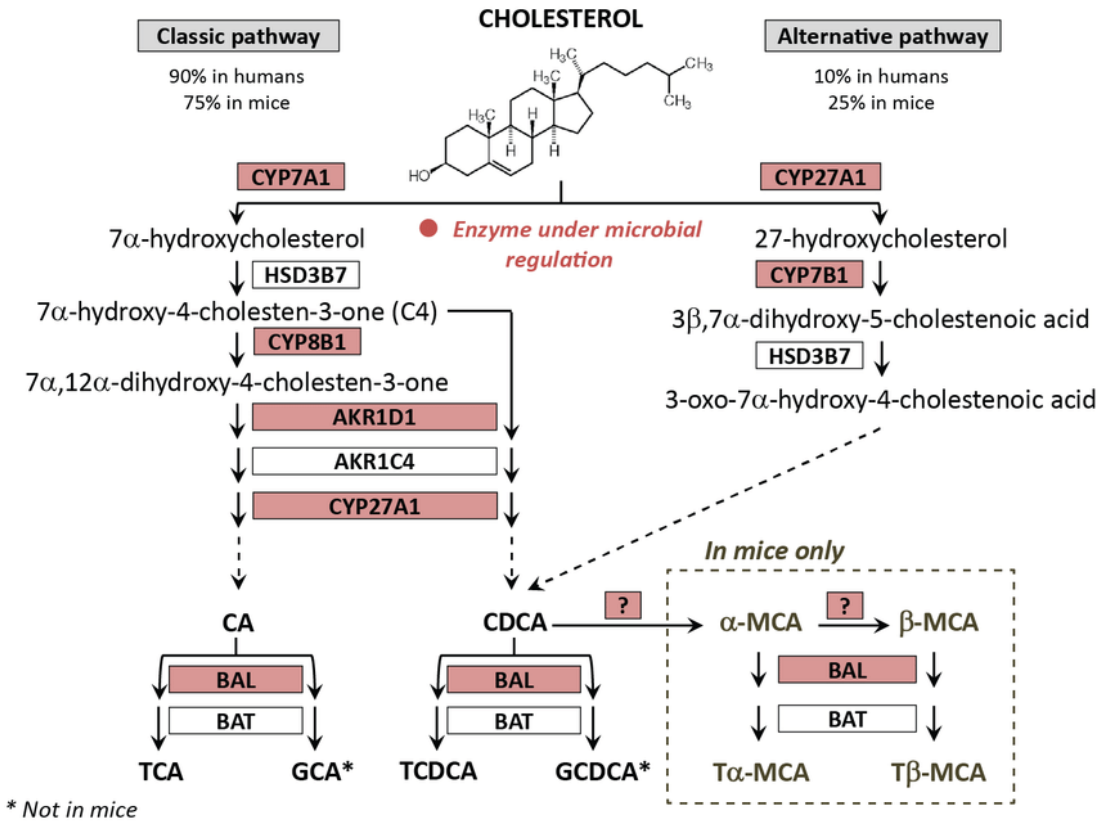

Figure 4.1.2 Summary of "Classical" and 'Alternative" pathways for bile acid synthesis in humans and mice. Classical pathway occurs in hepatocytes and accounts for 90% of total bile acid production in humans. Cholic acid (CA) and chenodeoxycholic acid (CDCA) are the predominant primary BAs in humans; whereas CDCA is converted in muricholic acids (MCAs) in mice. Whilst in the liver, BAs are conjugated to either glycine or taurine regulated by bile acid-amino acid transferases (BAT) and bile acid CoA ligase (BAL) prior to bile secretion into the duodenum. Genes coloured in red have been identified as being under the regulation of the intestinal microbiota. The major difference in mice is the conversion of CDCA into αMCA and β-MCA in the mouse liver. Figure has been reproduced from an open access publication – access to this is available from: https://www.researchgate.net/Schematic-overview-of-pathways-involved-in-the-hepatic-synthesis-of-primary-bile-acids-in_fig2_317376112 [accessed 11 Jul, 2018].

BA composition differs significantly in mice, due to the conversion of CDCA through hydroxylation at the 6β-position to form alpha-muricholic acid (αMCA), whereas βMCA is formed from ursodeoxycholic acid (UDCA) (Takahashi et al., 2016). Whilst UDCA is a secondary bile acid in humans, in mice produce is as a primary bile acid (Wahlström et al., 2016). It has been shown in the absence of a microbiota in germ-free mice, the bile acids pool is largely made up of primary conjugated bile acids, including MCAs such as T- αMCA and T-βMCA which are typically more hydrophilic in comparison to human BAs where the

total bile acid pool is more hydrophobic (Wahlström et al., 2016). However, the biochemical pathway for this conversion from CDCA to MCA is unclear; but a recent report suggests Cyp2c70 is a gene required for MCA synthesis in mice which leads to this

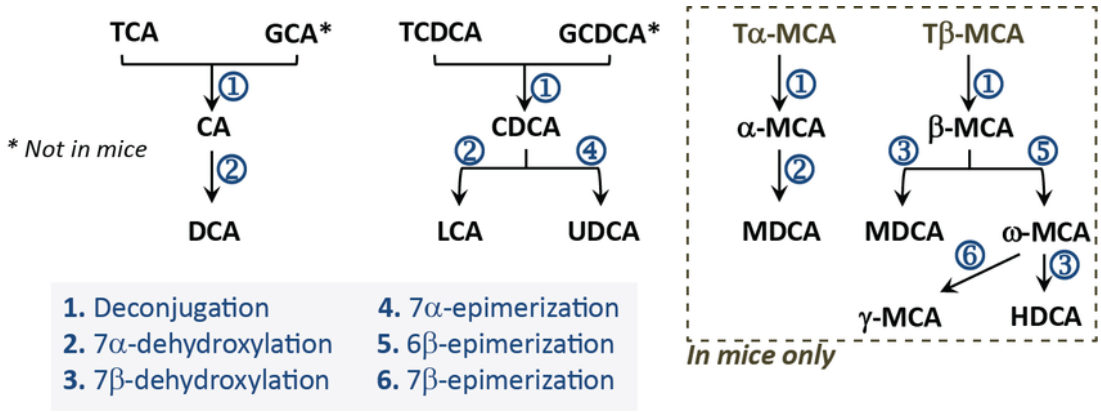

Fig. 4.1.3 Secondary bile acid metabolism. Microbial metabolism facilitates transformation of primary bile acids via deconjugation and 7α/β-dehydroxylation. Further heterogeneity can be introduced into the BA pool through step-by-step epimerization, oxidation and reduction by 7α/β-hydroxysteroid dehydrogenases to produce stereochemical distinct oxo-bile salts. Upon recirculation to the liver, DCA and LCA are conjugated to glycine or taurine just as primary bile acids are synthesised before being reintroduced into the bile acid pool. In mice, CDCA is converted to muricholic acids (MCAs) and contributes to a distinct secondary bile acid profile compared with humans. Figure has been reproduced from an open access publication – access to this is available from: https://www.researchgate.net/Schematic-overview-of-pathways-involved-in-the-hepatic-synthesis-of-primary-bile-acids-in_fig2_317376112 [accessed 11 July, 2018].

species variation (Takahashi et al., 2016). Human primary bile acids are mostly conjugated to glycine in the liver but can also include taurine (more frequently in mice), via an enzymatic step involving bile acid-amino acid transferase (BAT) before they are released in the duodenum (Claus et al., 2008). The human gut microbiota influences the bile acid pool from a functional perspective by providing enzymes for deconjugation, dehydrogenation and dehydroxylation of primary bile acids. In the liver primary BAs are found to have hydroxyl groups attached at the 3, 7, 12-carbon positions under regulation of at least 14 enzymes, of which some of these are shown to be under the regulation of unknown factors derived by the gut microbiota. (Sacquet et al., 1983; Sayin et al., 2013). Further biochemical modifications can involve oxidation of these hydroxyl groups and reversible

epimerization by microbial enzymes which alter their stereochemical orientation during transformation providing a heterogenous secondary bile acids pool within the gut (Staley et al., 2017). The biochemical steps involved in secondary bile acid metabolism is summarised in figure 4.1.3. The small quantity of BAs that do not get reabsorbed, undergo deconjugation of taurine and glycine by hydrolases ubiquitous throughout the microbiota, and various oxidation steps which serve to alter the chemical properties, particularly the toxicity and hydrophobicity of each bile acid. For example, deoxycholic acid (DCA) is a secondary BA transformed in the large intestine following deconjugation to free cholic acid (CA) and subsequent 7α-dehydroxlyation by intestinal clostridia. Deconjugation enhances detergent properties which lead to the greater disruption of bacterial cell membrane potential (Ridlon et al., 2014). Furthermore, accumulation of DCA has been reported to be associated with a "Western diet" (Dermadi et al., 2017).

Increased concentrations of bile acids appear to favour gram-positive bacteria belonging to the firmicutes which also include *Clostridium cluster XVIa* bacteria capable of 7α-dehydroxylation to generate secondary bile acids, DCA from CA, and LCA from CDCA. Conversely, gram-negative bacteria are less resistant to bile acids and prefer lower BA concentrations (Ridlon et al., 2014). Such observations are based on patients presenting with hepatic encephalopathy. These patients exhibit certain neuro-psychiatric abnormalities as a result of liver failure during its severe stages. During these stages, bacterial dysbiosis was observed and linked to low bile acid concentrations and reduction of gram-positive bacteria *Blautia* and *Rumminococcaceae* (Bajaj et al., 2014).

BAs are also recognised as important signallers, which act as steroid hormones associated in the regulation of triglyceride and glucose homeostasis. To that effect, BA metabolism has come under increasingly scrutiny to better understand how microbial dysbiosis may contribute in various disease states including type 2 diabetes, cardiovascular disease, non-alcoholic fatty liver disease and cancers. However, a substantial amount of research on BA metabolism to date has been performed in germ-free, specific knock-out and conventional mice; and given the differences between mice and humans, these experimental outcomes limit any translation benefit in human disease and future development of therapies targeting bile acid metabolism. For this reason, it was decided to explore the BA profile for the first time in severe, house-bound ME patients.

4.1.6 Experimental design overview

Various platforms (NMR versus MS) and methods lead to great differences in the power of discovery in the field of metabolomics (Dias & Koal, 2016). Greater accuracy for quantification of metabolites is needed, but it is also desirable being able to detect a greater number of metabolites in a single run. For instance, at the time of writing, the Serum Metabolome database contains 4651 small molecules identified in human serum (Psychogios et al., 2011). The expanse of metabolites which can be targeted falls dramatically short of expectation in comparison to genomics-based technologies which can identify millions of target genes in a single experiment, although 40-70% of their biochemical function is not known (Heintz-Buschart & Wilmes, 2018). This makes current observations and consistencies within the ME/CFS metabolome even more interesting given its heterogenous nature. Here, the result of a small pilot study is presented examining the faecal and serum metabolome profiles from 11 severe, house-hold ME/CFS patients using 600 MHz ^{1}NMR spectroscopy.

Where possible, each patient was matched with a house-hold control, and both samples collected and processed for analysis simultaneously. Only samples collected during 2017 were included in this work due to changes made to sample collection protocols requiring faecal homogenisation and faecal water extraction on the day of sample collection. It is important to note that sample preparation and processing were performed in accordance to the methods described by Armstrong et al., 2017. It is highly important to make every endeavour to control for method variation to give more power in comparing studies and towards unravelling multiple aetiologies conspiring to cause ME/CFS symptoms.

Study	Selection Criteria	Cohort Size	Biofluid	Type	Metabolites targeted	Observations/Conclusions
Naviaux et al. (2016)	IOM (2015), Canadian (2003), & Fukuda (1994)	45 ME/CFS (n = 22 men and 23 women) CFS males were 53 (±2.8) y old vs. females 52 (±2.5) y old 39 control subjects (n = 18 men and 21 women) age- and sex-matched.	Blood Plasma	HILIC-ESI-MS/MS*	612 (from 63 biochemical pathways)	Abnormalities in 20 metabolic pathways – 80% ↓ consistent with hypometabolic syndrome: ↓ plasma sphingo- and glyco- sphingolipids in patients who had CFS Diagnostic accuracy in males using 8 metabolites versus 13 in female. Posit ME is hypermetabolic response to stress from environment similar to dauer.
Germain et al. (2017)	Fukuda (1994)	17 female ME/CFS (age 53.9±8.6y) 15 female controls (age 51.9±6.2y)	Blood Plasma	Q-Exactive ME (QE-MS) method	361 (74 altered in ME)	20% of metabolites disrupted in ME/CFS 31 metabolites↓ in ME incl. lipid metabolism and several amino acids, ↓glucose, ↓ATP, ↓ADP ↓primary bile acids & taurine, ↑palmitate
Armstrong et al. (2017)	Canadian (2003)	34 females with ME/CFS (34.9±1.8 SE) y old 25 female controls (33.0±1.6) y old	Faeces, Blood serum & urine	^{1}H NMR – (800MHz) Bruker Avance II US	Total of 83 identified metabolites in: faeces (24), urine (30) & serum (29)	14 metabolites altered,↓faecal lactate,↑faecal butyrate ↑microbial fermentation of fibre and amino acids to produce SCFA
Vipond et al. (unpublished)	Canadian (2003), International Consensus (2011) & Fukuda (1994)	11 <u>severe</u> female ME/CFS 8 <u>house-matched</u> controls (7 female, 1 male) 14 mild/moderate CFS	Faeces & blood serum	^{1}H NMR (600MHz) Targeted HPLC-MS	45 in faeces 53 in serum 26 Bile Acids	Faecal gamma-butyrobetaine notably↑in 3 patients Faecal taurine detected only in 2 patients ↑Glycocholate in severe patients (p=0.03) No significant findings from serum.

Table 4.1.1 Summary of publications relating to the study of the metabolome in ME/CFS *Hydrophilic Interaction Liquid Chromatography-ElectroSpray Ionization-Tandem Mass Spectrometry

4.1.7 Aim & Objective

The aim of this chapter was to define the faecal and serum metabolome of severely affected ME/CFS patients compared to house-hold controls, in order to understand how metabolic features may be related to neurological and behavioural aspects associated with greater severity compared to mild and moderately affected patients.

Three recent independent studies on the general ME/CFS population have contributed consistent data revealing various biochemical pathways and metabolites in patients that are associated with a reduction in lipid and energy metabolism (Armstrong et al., 2017; Germain et al., 2017; Naviaux et al., 2016). Whilst these metabolomics-based studies of mild to moderately affected ME/CFS patients have identified such alterations, it is not known if these findings translate to severely affected ME/CFS patients. In order to determine this, the following objectives were established:

- to address the functional capacity of the severe ME/CFS microbiome using NMR spectroscopy to measure low molecular weight metabolites;
- by preparing faecal water and serum samples in accordance to methods set out by a previous NMR study by Armstrong and colleagues in 2017;
- to determine if an altered microbial composition (dysbiosis) influences faecal and serum metabolism in severe ME compared with house-hold controls;
- to determine if severe ME patients display a distinct bile acid metabolic profile using targeted HPLC-mass spectrometry which may described altered energy metabolism in these patients.

4.1.8 Hypothesis

The functional capacity of the intestinal metabolome in severe ME/CFS patients is altered through a decline in the compositional diversity of intestinal bacteria to the detriment of host metabolism, causing the faecal and serum metabolomes of severe, house-bound ME/CFS patients to reflect a hypometabolic state in accordance with altered energy and bile acid metabolism.

4.2. Materials & Methods

4.2.1 Sample preparation and storage

Briefly, the entire stool sample was collected in a FECOTAINER® collection device (AT Medical B.V., Enschede, Netherlands), figure 2.2.2 no sooner than 24 hrs before visiting the patient's home for collection. During this time before our arrival to collect, patients were advised to keep their sample inside the fridge in double containment using the packaging provided. An AnaeGen™ Compact anaerobic sachet (Cat. No AN0010, Oxoid. Ltd.) was also provided for insertion and activation inside the FECONTAINER® as soon as the sample was produced by the patient.

On return to the hospital the entire stool sample was homogenised manually using a sterile autoclaved metal spatula. Faecal water was extracted from homogenate of each sample with a 2:1 ratio of molecular grade water. It is recommended ~15g of faecal material is used with 30 ml of water but is dependent of amount of original sample provided. This mixture was vortexed for 5 min and centrifuged at 18,000 x g, for 10 min, or 3,500 x g, for 30 min. The supernatant is then divided in to multiple aliquots and stored at -80 degrees prior to analysis.

4.2.2 Preparation for ^{1}H NMR spectroscopic Analysis

- *Preparation using serum samples*

Samples were prepared for NMR using a method modified from a previous study (Armstrong et al., 2017). Serum samples were thawed from -80^{0}C, from which 250µL of serum was added to 250µL ice cold deuterated chloroform and 250µL ice cold deuterated methanol and mix by vortexing. Samples were then left on ice for 15 mins before centrifuging (16100 x g) at 4^{0}C for 10 mins to produce hydrophilic phase of water/deut. methanol and lipophilic phase of deuterated chloroform. 300µL of the top hydrophilic layer was transferred to 300µL of NMR buffer (0.26g NaH_2PO_4,1.44g K_2HPO_4,17mg TSP, 56.1mg NaN_3 in 100 ml D_2O), and mixed mix before transferring 550µL to NMR tube. In addition, 0.9% saline solution (0.9g NaCl in 100ml D2O) was made to combine with serum, using 200µL serum mixed with 400µL saline solution, before transferring 550µL in to NMR tubes.

- *Preparation using faecal water extracts*

Samples were prepared for NMR using a method modified from a previous study (Armstrong et al., 2017). One millilitre aliquot from each sample were thawed from -80^{0}C. 250µL faecal water was transferred in 250µL ice cold deuterated chloroform and 250µL ice cold deuterated methanol. Samples were mixed by vortexing and left on ice for 15 mins before centrifuging at 16100 x g at 4^{0}C for 10 mins to produce hydrophilic phase of water/deuterated methanol and lipophilic phase of deuterated chloroform. 300µL of the top hydrophilic layer was transferred in to 300µL of NMR buffer (phosphate buffer, pH 7.4 in D_2O, containing 1mM d_4-TSP), and mixed thoroughly before all samples were transferred into NMR tubes. Additional faecal extracts were prepared without chloroform/methanol extraction from 300µL of faecal water in 300µL NMR as described above.

- *Acquisition of NMR data*

High resolution ^{1}H NMR spectra of faecal water extracts were recorded on a 600 MHz Bruker Avance III HD spectrometer fitted with a 5 mm TCI cryoprobe and a 60 slot autosampler (Bruker, Rheinstetten, Germany). Sample temperature was controlled at 300^{0}K and the D_2O signal was used as lock. Each spectrum consisted of 1024 scans of TD = 65,536 data points with a spectral width of 20.49 ppm (acquisition time 2.67 s). The *noesygppr1d* presaturation sequence was used to suppress the residual water signal with low power selective irradiation at the water frequency during the recycle delay (D1 = 3 s) and mixing time (D8 = 0.01 s). A 90^0 pulse length of approximately 8.1 µs was used, with the exact pulse length determined for each sample by the Bruker automation routine (*au_prof1d*). Spectra were transformed with 0.3 Hz line broadening and zero filling and were automatically (*proc_prof1d*) phased and referenced (to TSP) using the TOPSPIN 3.2 software. The *noesygppr1d* sequence avoids the need for a first order (PHC1) phase correction or for baseline correction. The resulting Bruker 1r files were converted to Chenomx (.cnx) format using the 'Batch Import' tool in the Processor module of Chenomx NMR Suite v8.12. The only additional processing during conversion was a shim correction to remove any line-shape irregularity and the concentration of the reference compound, TSP, was set to 0.5 mM.NMR spectra of serum extracts were recorded and processed in exactly the same way except that the number of scans was 512 and the 90^0 pulse length was approximately 8.6 µs. NMR spectra of the serum/ saline solution samples were also obtained using the diffusion edited pulse sequence to emphasise signals from lipoproteins and other large molecules.

Metabolites were identified from the Chenomx library (337 compounds) with in-house additions (ca. 40 compounds), the HMDB database (http://www.hmdb.ca), literature and by use of the 2D-NMR methods, COSY, TOCSY, HSQC and HMBC on selected samples. The 2D methods were useful in obtaining precise chemical shifts which could differ slightly from literature values since the samples contained some methanol in addition to water. Concentrations of up to 45 compounds per sample were obtained using the Chenomx Profiler module and the concentrations of all samples were exported to an excel file. Diffusion edited spectra were analysed using variable width buckets (added graphically to spectra using Bruker AMIX software).

- *Data analysis*

Statistical analysis for individual compounds was carried out in GraphPad Prism v5.01 (GraphPad Software, San Diego, CA) using the Mann-Whitney test for comparison of two groups or the Kruskal-Wallis test for three groups, followed in the latter case by Dunn's Multiple Comparison test for pairwise comparison. Data plots were also produced for the compounds showing the median and interquartile range for each group.

Multivariate statistical analysis (Principal Component Analysis, PCA) was carried out using the PLS Toolbox v8.01 (Eigenvector Research Inc., Wenatchee, WA) running within Matlab R2015a (The Mathworks Inc., Natick, MA). For the PCA any missing values (zero concentrations) in the data table were replaced with a very small value, the rows were normalised (sum of concentrations made the same for each sample) and the columns (compound concentrations) were scaled to unit variance.

4.2.3 Targeted bile acid quantification by mass spectrometry

Faecal water extracts and serum were analysed using HPLC – mass spectrometry operated in multiple reaction monitoring (MRM) mode. Each sample (5 µl) was analysed using an Agilent 1260 binary HPLC coupled to an AB Sciex 4000 QTrap triple quadrupole mass spectrometer. HPLC was achieved using a binary gradient of solvent A (Water + 5mM Ammonium Ac + 0.012% Formic acid) and solvent B (Methanol + 5mM Ammonium Ac + 0.012% Formic acid) at a constant flow rate of 600 µl/min. Separation was made using a Supelco Ascentis Express C18 150 x 4.6, 2.7µm column maintained at 40°C. Injection was made at 50% B and held for 2 min, ramped to 95% B at 20 min and held until 24 minutes. The column equilibrated to initial conditions for 5 minutes.

The mass spectrometer was operated in electrospray negative mode with capillary voltage of -4500V at 550°C. Instrument specific gas flow rates were 25ml/min curtain gas, GS1: 40 ml/min and GS2: 50 ml/min. Dwell time for each MRM was 20 ms. Quantification was applied using Analyst 1.6.2 software to integrate detected peak areas relative to the deuterated internal standards.

4.3. Results

4.3.1 Patient cohorts and datasets obtained

This chapter presents various datasets using faecal water and blood serum samples collected from 2016- 2017. Table 4.3.1 summarises the types of samples collected and from which group of participants. This has given rise 4 distinct datasets (4A-4D), which have displayed and described in table 4.3.2. Each dataset here is presented in its order collection and the result of each described in the following text in that order. All samples within each dataset have been included in the same experiment.

4.3.2 Identification of faecal metabolites using NMR

Proton Nuclear magnetic resonance (^{1}H-NMR) spectroscopy was used to identify metabolites within faecal water from 11 female severe house-bound ME patients (42.1 $\pm$ 4.8 SE years) versus 6 house-matched controls (63 $\pm$ 2.4 SE years). The resultant cohort was matched on the basis of each healthy control living with a patient. With the exception of one matched healthy control, paired samples were gender matched and typically represent mother as control, and daughter as patient. Due to this relationship it was not possible to control for age differences. A total of 45 compounds were examined and quantified as absolute concentrations down to the low micromole per litre range. Figure 4.3.1 shows the multiple spectra obtained using AMIX (Bruker) to colour individual spectra by group (e.g. patient/control). The peaks were used to determine concentrations of individual metabolites by fitting the spectra of known single compounds from the reference library to the experimental spectra. Ice cold methanol/chloroform was mixed with serum to create biphasic separation of upper hydrophilic layer containing low molecular weight metabolites. It is this fraction in which the data has generated from.

Prior to statistical testing no assumption was made on distribution of individual metabolite concentration; to this end *p-values* were determined with the non-parametric Mann-Whitney test in GraphPad prism. In some samples the compound concentrations were below the limit of detection were set at 0.0001 mM to avoid having zeroes for the statistical analyses. The outcome of these p-values is summarised with the table included as part of figure 4.3.2.

	Status	Sex	Age	Faecal water	Serum NMR *2016*	Serum NMR *2017*	Bile Acid analysis *faeces*	Bile Acid analysis *serum*
1	Severe	F	63		X			X
2	Severe	F	56	X	X	X	X	X
3	Control	F	55		X	X		X
4	Control	F	69	X			X	X
5	Severe	F	44	X		X		X
6	Control	F	70	X		X	X	X
7	Control	F	55	X		X	X	X
8	Severe	F	38	X	X		X	X
9	Severe	F	21	X	X	X	X	X
10	Severe	F	37	X				
11	Control	F	64	X			X	
12	Severe	F	18	X		X	X	X
13	Severe	F	61	X			X	
14	Severe	F	40	X			X	
16	Severe	F	58	X	X		X	X
17	Control	M	60	X	X		X	X
18	Severe	F	27	X	X		X	X
19	Control	F	60	X	X		X	
20	Severe	F	63	X		X	X	X
22	Severe	F	31		X			X
23	Control	F	54		X			X
24	Control	F	29		X			X
25	Severe	F	56		X			X
26	Severe	F	30		X			X
27	Mild ME	F	30		X			X
28	Mild ME	M	54		X			
29	Mild ME	F	26		X			X
30	Mild ME	F	28		X			X
31	Mild ME	M	41		X			X
32	Mild ME	F	65		X			X
33	Mild ME	M	48		X			X
34	Mild ME	M	43		X			X
35	Control	M	37		X			X
36	Mild ME	F	43		X			X
37	Mild ME	F	60		X			X
49	Mild ME	F						X
50	Mild ME	M	58					X
57	Mild ME	F	60					X
58	Mild ME	M	54					X
59	Mild ME	F	27					X

Table 4.3.1 Summary of participant samples acquired for metabolic profiling.

15 Severe (age 42.9± 4.04 SE years), 15 Mild/Moderate (age 44.7±3.49 SE years), and 9 Control (age 57.3±4.04 SE years). Status for each participant is given. 'X' identifies year sample was collected and the analysis performed.

Dataset	Biofluid	Platform	Sample size	ME/CFS status	Sample prep.	Metabolite coverage	Summary of findings
4A	Faecal water	^{1}H-NMR (600MHz)	**n=17** 11 ME/CFS, 6 House-matched controls	Severe	Ice-cold deuterated Methanol/chloroform Extraction of hydrophilic phase As described by Armstrong et al. 2015	45	Increased glycocholate (p=0.03) Hypoxanthine (p=0.05) Methylsuccinate (p=0.06)
4B	Faecal water	HPLC-MS	**n=14** 8 ME/CFS 6 House-matched controls	Severe	200µl faecal water	26 Bile acids	No significant findings Kruskal-Wallis Traces of muricholic acids High concentration of HDAC in some patients
4C	Blood Serum	^{1}H-NMR (600MHz)	**n=34** 25 ME/CFS, 9 House-matched controls	Severe (n=14), Mild/moderate (n=11)	Ice-cold deuterated Methanol/chloroform Extraction of hydrophilic phase Diff. edited NMR: Saline-diluted serum	53	No significant findings Kruskal-Wallis with Dunn's test
4D	Blood Serum	HPLC-MS	**n=46** 26 ME/CFS, 7 House-matched 6 IBD	Severe (n=14) & Mild/moderate (n=14)	200µl undiluted serum	26 Bile acids	Significant variances across samples within dataset Traces of muricholic acids HDCA higher in some severe ME patients

Table 4.3.2 Overview of datasets presented in this chapter and metabolite coverage generated using NMR and HPLC-MS metabolomic profiling of participants recruited between 2015-2017. Datasets are organised in chronological order for each experiment: "A" represents the first dataset; and "D" being the final dataset to be completed.

- *dataset 4A*

Scatter dot plots were generated in GraphPad Prism for each metabolite for comparison between the severe ME group and matched healthy controls. These have been summarised and presented as supplementary figures (S4.1 and S4.2) included within the appendix. The horizontal lines indicate the max, median and min.

In an attempt to separate severe ME (S) from House-Hold Controls (H), principal component analysis (PCA) was performed to identify any metabolites as a source of variation between the two groups (figure 4.3.5). The first principal component (PC1(41.69%)) represents the largest possible variance. This is determined to a large extent by interindividual differences, particularly samples with unusually higher values, although an attempt was made by normalising the sum of concentrations in each sample to the same value. PC3(8.92%) versus PC4(6.80%) in the right plot of figure 4.3.5 shows severe (S) in red separates from house-matched (H) in green. The numbers refer to the individual samples driving these differences. In order to understand the source of this variation, figure 4.3.6 provides an annotated PCA plot with specific faecal metabolites. This is useful in identifying specific metabolites within individual samples causing the variance. Here compounds: formate, ethanol, lactate, succinate, methylamine, glutarate, methylsuccinate, taurine and 3-phenylpropionate are found higher in patients 6, 14 and 15 and not in the severe (S) groups in general. To that end, there is very little statistical power based on the observations made in this experiment. For many compounds there are one or two samples with very high values – often these come from the same sample, for example sample 9 (and 12) is high in amino acids and sample 15 is very high in succinate and lactate, (figures 4.3.7 & 4.3.8).

The conclusion is that a weak separation is found between patients and control. Of the 45 compounds examined only one showed $p<0.05$. This compound was the nearest calibrated standard that was available in our reference library, which was “glycocholate”, although it should be considered of as a general bile acid signal. The inclusion of this compound along with another seen in very high concentration in 3 of the severe patients was γ-butyrobetaine. This present in very low concentration in patients and controls and is a gut metabolite of L-carnitine and intermediate in the conversion of carnitine to trimethylamine and TMAO (Koeth et al., 2014). L-carnitine is associated with a lot of meat in the diet, however it is more likely that these patients have been taking L-carnitine supplements. PCA

separation with the addition of these compounds is included in figure 4.3.7. In this plot, PC1(39.99%) demonstrates that severe (S) samples 6, 9, 12, 14, 15 in red, are the source of this variation of which, the compounds have been annotated to the plot in figure 4.3.8. Metabolites shown in the positive region f PC3 are more likely to be in higher concentration in severe (S) patients, versus the negative region which reveals compounds more likely to be higher in house-matched (H) control. A more detailed analysis of the bile acids by mass spectrometry in a targeted analysis appears later in this chapter as a follow up to the apparent bile acid signal detected significantly higher in patients. The next nearest significant difference was hypoxanthine (p=0.05) and methylsuccinate (p=0.06), see box plot in figure 4.3.3.

A box plot summary presents the entire dataset was and highlights the lack of evidence for differences in individual metabolites (figure 4.3.3). Some of the trends identified are at variance with earlier publications suggesting short chain fatty acids are in higher concentration within the ME/CFS populations. The data obtained for this in figure 4.3.4 shows no evidence of this in severe ME patients. No differences were found for pyruvate or ornithine or any of the detected amino acids in this experiment. Alas, these other studies had more participants, but nevertheless the clinical severity of patients used in our study made this finding even more disappointing. From Armstrong et al. (2017), table in Fig 1e and Sec 3.4 in this paper find significant differences between patients and controls for isovalerate, lactate and valerate – in each case with a higher level in patients. Although not significant they also report a higher level of total SCFA in patients. Although none of these are found to be significant in this small cohort of severe patients there does appear to be a trend for all of them to be higher in controls (isovalerate, valerate, acetate, butyrate, propionate), but not in patients. The PCA loadings with figure 4.3.8 agree with this since all these metabolites appear in the negative region of PC3 and are likely to be higher in house-matched (H) samples, according to this experiment.

Faecal Water ^{1}H-NMR

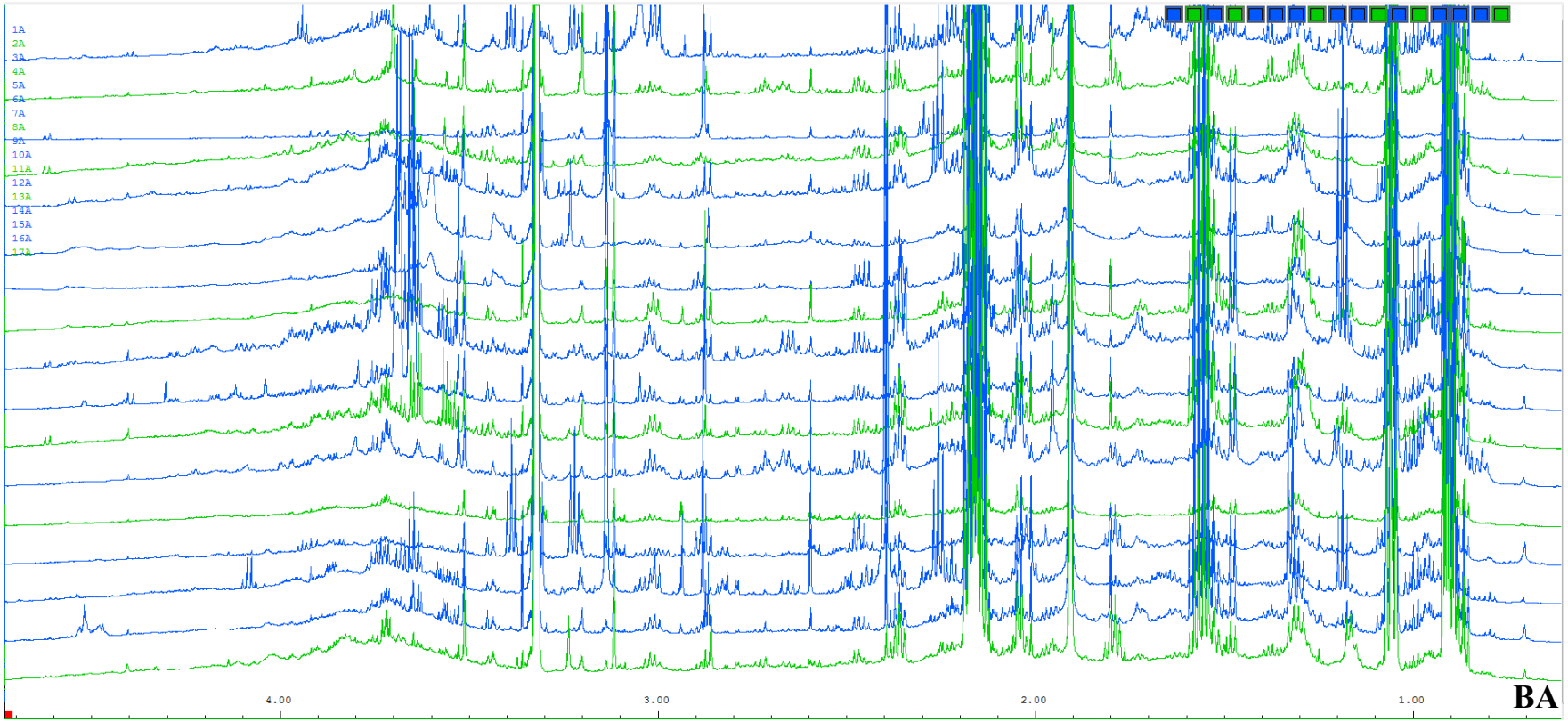

Figure 4.3.1 Partial 600 MHz ^{1}H-NMR spectra from faecal water extractions used for biphasic separation in methanol/chloroform to extract the hydrophilic layer for small metabolites quantification. 1-17 are shown. Severe (S) are in blue. House-Matched (H) are green. γ-gain increased to reveal smaller peaks. All metabolites assigned to the reference spectra using Chemomx software. "BA" = bile acid peak, quantified as "glycocholate".

Metabolite	*p-value*
1,3-Dihydroxyacetone	0.3361
2-methylbutyric	0.2913
3-Phenylpropionate	0.2901
5-Aminopentanoate	0.9599
Acetate	0.8016
Alanine	0.5804
Aspartate	0.8802
Butyrate	0.725
Caprate	0.6537
Caproic acid	0.3112
Ethanol	0.0779
Formate	0.9599
Fumarate	0.8404
Glutamate	0.9599
Glutarate	0.6503
Glycerol	0.8397
Glycine	0.451
Hypoxanthine	0.0561
Isobutyrate	0.2478
Isoleucine	0.3654
Isovalerate	0.3397
Lactate	0.7992
Leucine	0.1193
Lysine	0.3397
Methionine	0.6468
Methylamine	0.5136
Methylsuccinate	0.0628
Nicotinate	0.222
Phenylacetate	0.2913
Phenylalanine	0.0786
Proline	0.3549
Propionate	0.9599
Serine	0.5947
Succinate	0.1193
Taurine	0.3237
Threonine	0.9195
Trimethylamine	0.5804
Tyrosine	0.2478
Uracil	0.58
Valerate	0.2478
Valine	0.3397
Glucose	0.2657
p-Cresol	0.2823
Gammabutyrobetaine	0.2478
"Glycocholate"	0.0347

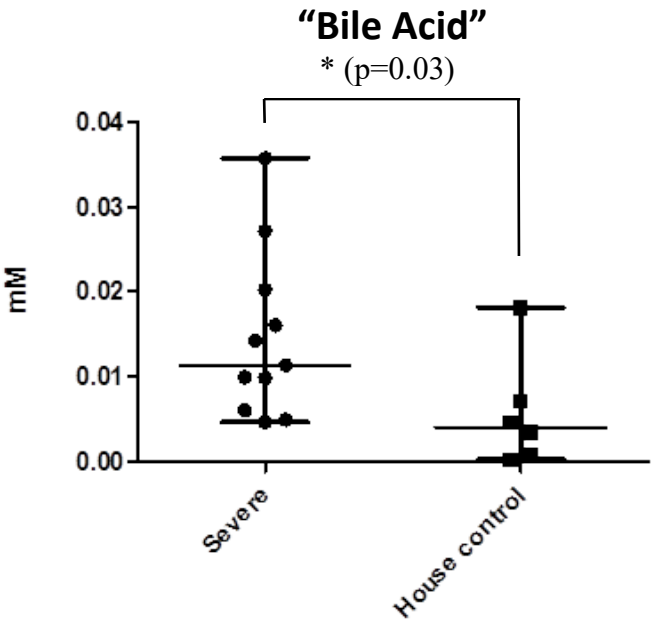

Figure 4.3.2 The 45 metabolites detected across faecal water samples using 600 MHz ^{1}H-NMR spectroscopy. Table (left) provides the name of each metabolite compound and *p-value* generated from the Mann Whitney test. Out of the 17 faecal water samples from (11) severe, house-bound ME/CFS patients and (6) house-matched control, the only significant difference was reported from a potential bile acid signal. The scatter plot for this compound display the absolute concentrations in mM from individual samples. Severe mean = 0.015mM vs control = 0.0058mM

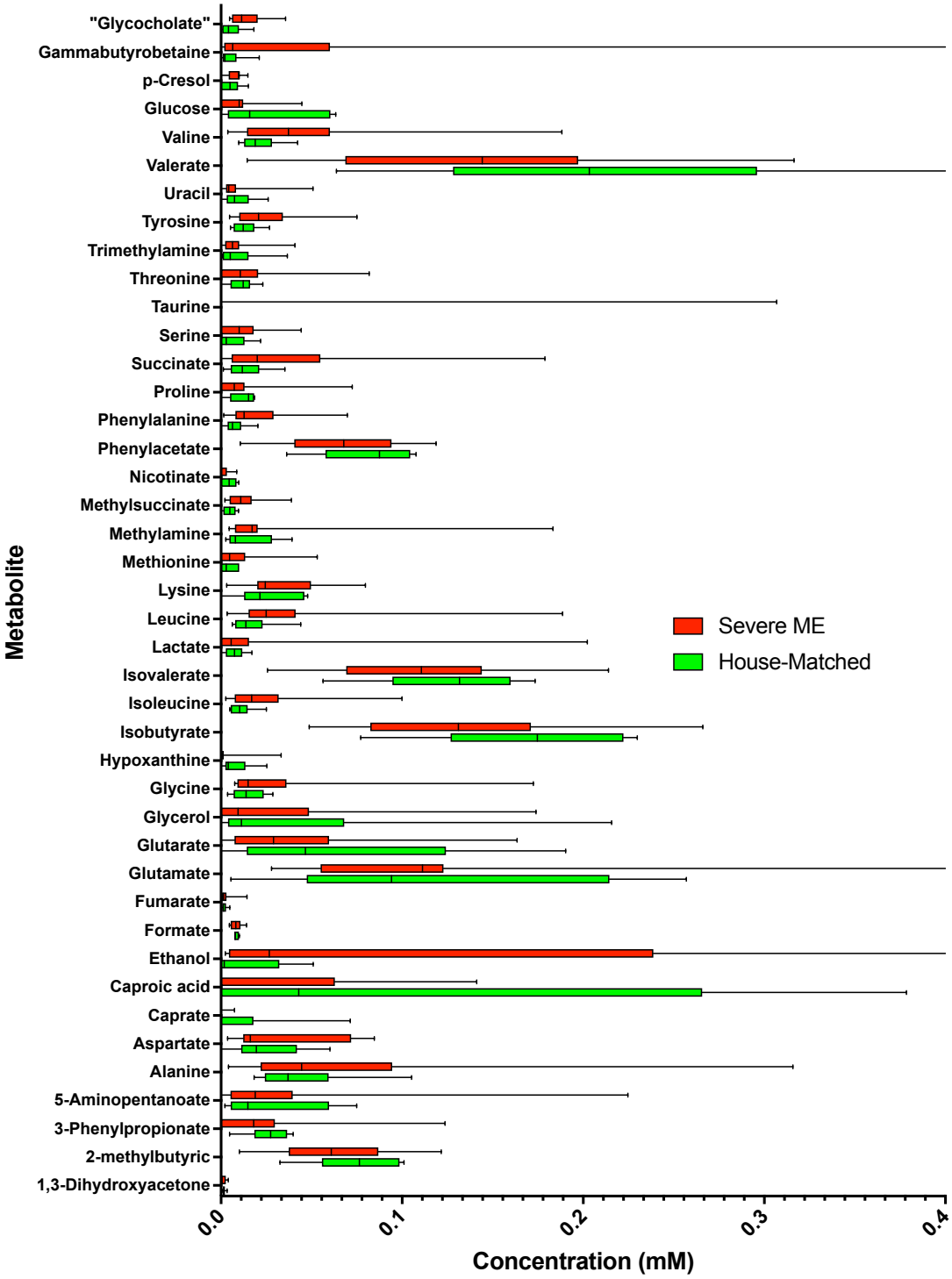

Figure 4.3.3 Box plot representation of 42 out of 45 faecal water low molecular weight metabolites in severe (s) red, versus House-matched (H) green samples. The magnitude of the concentration of the other 3 metabolites could not be presented in this plot. Each household control (H) is matched to an individual severe (S) ME patient. Both samples were collected and analysed simultaneously on a 600MHz ^{1}H-NMR Bruker machine. Central line of each box represents the median. Width denotes the interquartile range, with error bars positioned to show Min and Max

concentration detected across that group. “Glycocholate” has been labelled with inverted commas as the closest assigned bile acid fitting the experimental spectra.

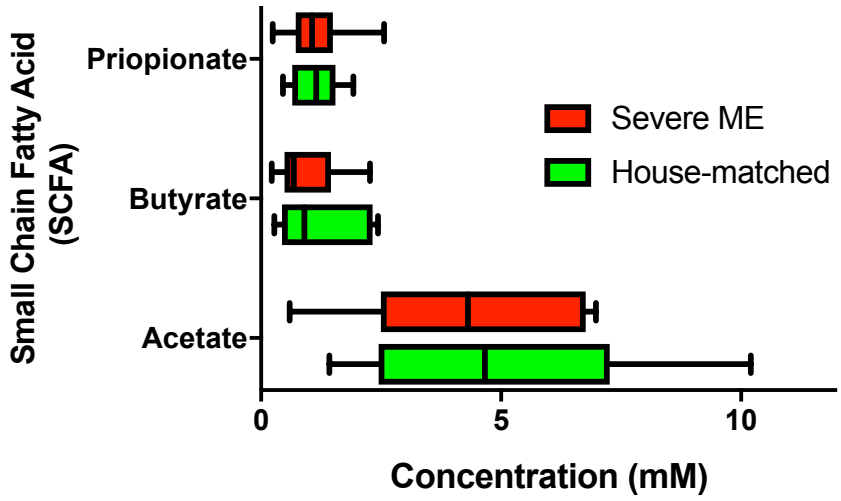

Figure 4.3.4 Summary of Short Chain Fatty Acid (SCFA) compounds whose range of concentrations detected across all samples were too extreme to include with other low molecular weight metabolites quantified using NMR spectra. Box plot with whiskers. Concentrations were analysed using the Mann-Whitney test at 5% significance level. Severe (n=11) versus House-Matched (n=6). Acetate: severe mean = 4.21±0.64 SE mM versus House-Matched mean = 5.00±1.25 SE mM. Butyrate: severe mean = 0.97±0.19 SE mM versus House-Matched mean = 1.21±0.38 SE mM. Propionate: severe mean 1.15±0.19 SE mM versus House-Mathced mean = 1.14±0.21 SE mM. P values were 0.80, 0.73 and 0.96 respectively.

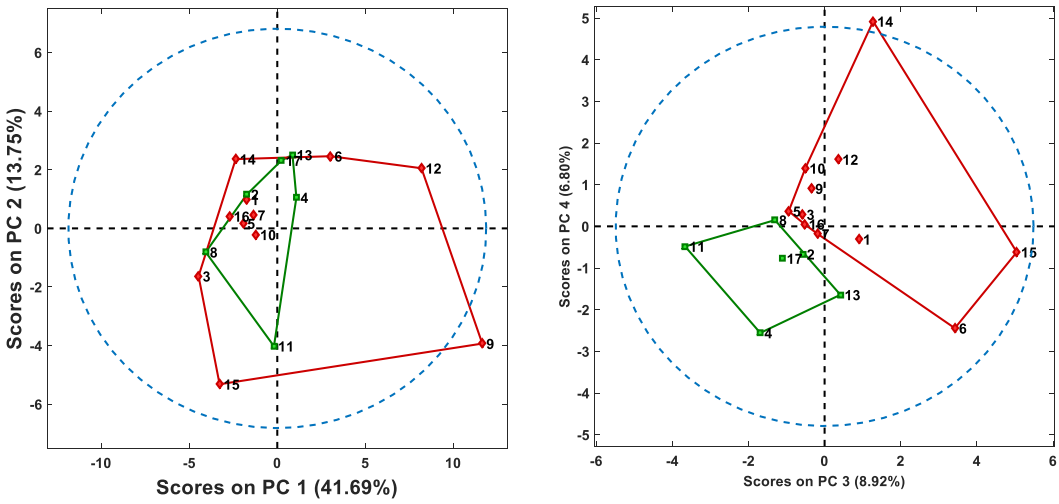

Figure 4.3.5 PCA plots showing interindividual variation of faecal water NMR metabolomic profiles based on 45 absolute concentrations for low molecular weight metabolites. PC1 vs PC2 & PC3 vs PC4 scores. Severe (S), red, House-Matched (H), green. Separation between severe and control group is seen on PC3. Data Row normalised and autoscaled.

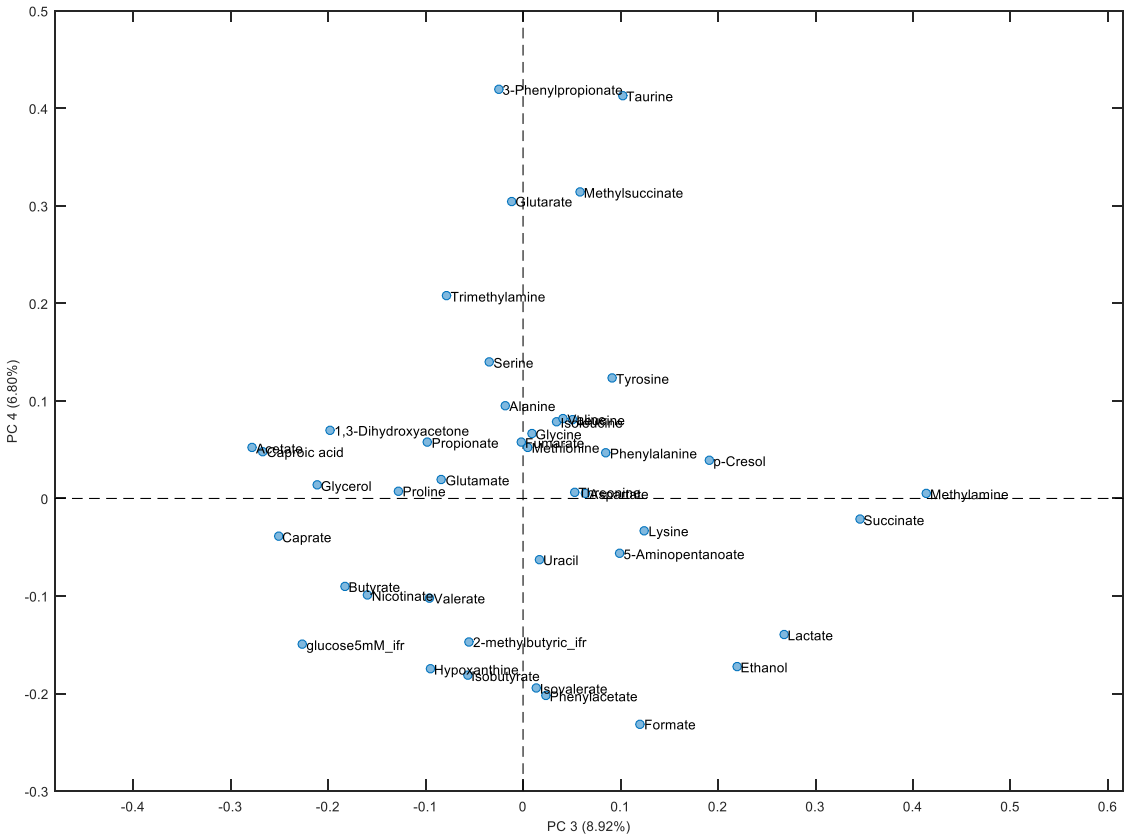

Figure 4.3.6 Metabolite labelled PCA plot identifying metabolite compounds influencing spatial separation. Row normalised and autoscaled. PC3 vs PC4 Loadings.

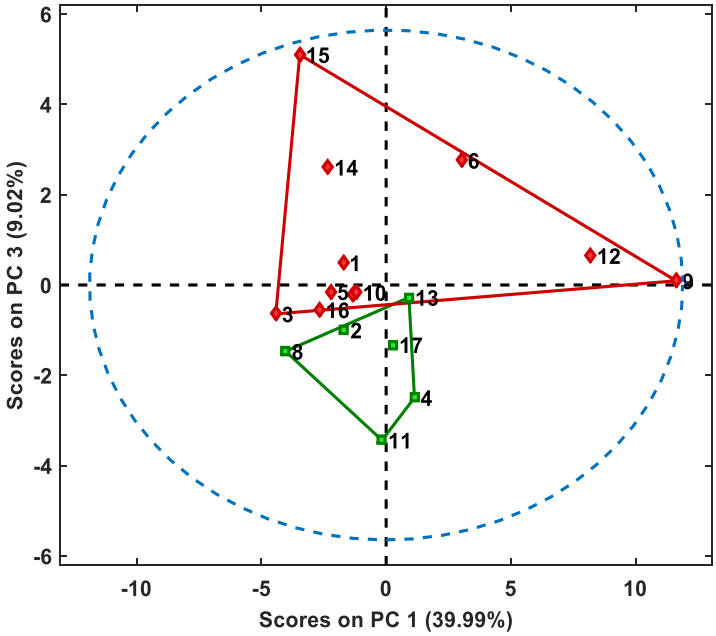

Figure 4.3.7 PCA plot showing a weak separation between severe (S) and House-Match (H) groups including glycocholate and gammabutyrobetaine. Row normalised and autoscaled. PC1 vs PC3. Severe (S), red, House-Matched (H), green.

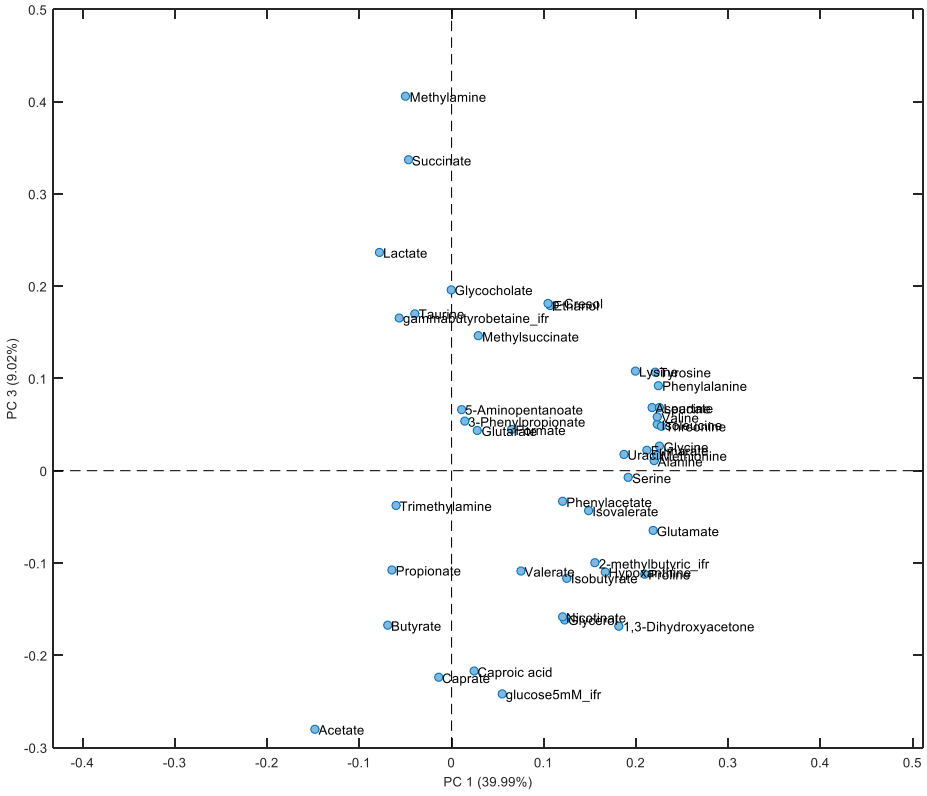

Figure 4.3.8 Metabolite labelled PCA plot showing individual metabolites influencing group separation between severe (S) and House-Match (H). Analysis includes glycocholate and γbutyrobetaine. Row normalised and autoscaled. PC1 vs PC3 Loadings. Metabolites in the positive part of PC3 are expected to be higher in patients and those in negative part to be higher in controls.

4.3.2. Serum metabolome

- *dataset 4C*

Direct quantification of a total of 53 metabolites was conducted in a slightly larger patient cohort representing 14 severe (S), as well as 11 mild/moderate (M) ME patients and 9 house-matched (H) controls. Table 4.3.1 highlights that paired samples 3 and 9 where included twice in this dataset due to the availability of further serum collected approximately one year later.

A similar and more comprehensive set of metabolites were measured using the same method of extraction in methanol/chloroform, producing a biphasic with a top hydrophilic layer, as in Armstrong et al., (2015). They found significant difference for acetate, glucose, glutamate, hypoxanthine, lactate and phenylalanine. Scatter plots presented in figure 4.3.9 highlight the fact that none of these findings were replicated within severe (S) patients. Indeed, following a log transformation of all absolute metabolite concentrations across groups and summary of the distribution of all data points within a box plot demonstrates a lack of evidence for differences, figures 4.3.12 and 4.3.13. Many of the bars show extreme overlapping variation in all groups: (S), (M) & (H). The three groups were analysed statistically according to the response variable of absolute metabolite concentration in millimolar (mM). As with the earlier data on the severe ME faecal metabolome, no assumption was made about the distribution of concentration values. In order to not assume statistical significance by chance, a non-parametric analysis of variance was carried out using the Kruskal-Wallis (KW) test. A post-hoc Dunn's multiple comparison test was applied since the response variable in this case in ordinal (severe(S)/mild-moderate (M)/house-matched (H)) rather than nominal, i.e. treatment. This allows for determination of which pairs of groups (S v M, S v H, M v H) is significantly different from the other.

Out of all the tests only one was found to be significant – 2-hydroxyisovalerate, which had a p value of 0.02 with S v M as the pair that was significantly different (M>S). This has been identified in urine and is associated with lactic acidosis, where lactic acid accumulates in the body and can result in the lowering of blood pH. It is also among several hydroxycarboxylic acids which form ketone bodies from the ketogenesis of amino acids valine, leucine and isoleucine (Liebich & Först, 1984). Unfortunately, none of the other

observations for these amino acid concentrations were helpful in supporting any form of hypothesis surrounding this finding, except that is likely that these patients were in a fasting period during the sample was taken. Although no diet information or pattern of eating was recorded during the study.

With respect to glutamate, one of the healthy samples appeared as an obvious outlier at 0.15mM. In figure 4.3.10 this sample has been removed to resolve any visible separation across the groups. On repeat of a KW test, there was a significant difference across the groups for glutamate ($p=0.03$), however Dunn's multiple comparison did not confirm which paired groups were significantly different. An attempt to view the data with other clear single outliers within scatter plots for hypothanthine (within the Mild group) and phenylalanine (within House-Matched group) were excluded and re-plotted (not shown). These outliers did not make any difference to reveal at specific trend. Tau-methylhistidne included in this figure, is another increased metabolite that may be slighter higher within some severe (S) patients, however, given the distributions of concentrations derived from house-hold controls (H) and the small ranges in concentration difference it is hard to conclude anything from this. Suffice to say, Tau-methylhistinde is an amino acid largely present in actin and myosin, and can be used as a surrogate for indirect determination of muscle myofibrillar protein degradation (Lowry et al., 1985; Röuthig et al., 1984). Indeed, in the context of severe, house-bound patients, this is not a surprising finding.

Two other metabolites from serum did appear interesting based on the possible subset distribution of concentration in severe (S). Figure 4.3.11 presents the scatter plots for an unknown metabolite at 2.69ppm, and for acetoacetate. In both these plots, there appears to be an emergence of two discrete, severe (S) patient populations. Higher levels of acetoacetate are indicative of ketosis during a fasting state. Indeed, many of the severest patients, who remain bed-bound the entire time, eat very little and at inconsistent times of the day. Dehydration is also common among them and is reflected by the Bristol scores, most which score 1, being the most dehydrated stool presenting difficult to pass for the patient.

Finally, as a statistical summary for all metabolite concentrations measured in serum, table 4.3.3 provide mean concentrations (mM) and the standard error for each of 53 metabolites

measured in serum along with their respective p value for KW test performed with Dunn's multiple comparison test. Despite a more comprehensive overview of the coverage of 53 serum metabolites none of the previous findings based of just 24 serum metabolites could be replicated (Armstrong et al., 2017). Armstrong et al. acknowledged no investigation was performed on their serum samples using the apolar layer extracted during methanol/chloroform extract. In the next result section, for the first time in ME/CFS research, an attempt has been made to study the lipid profile of ME/CFS serum.

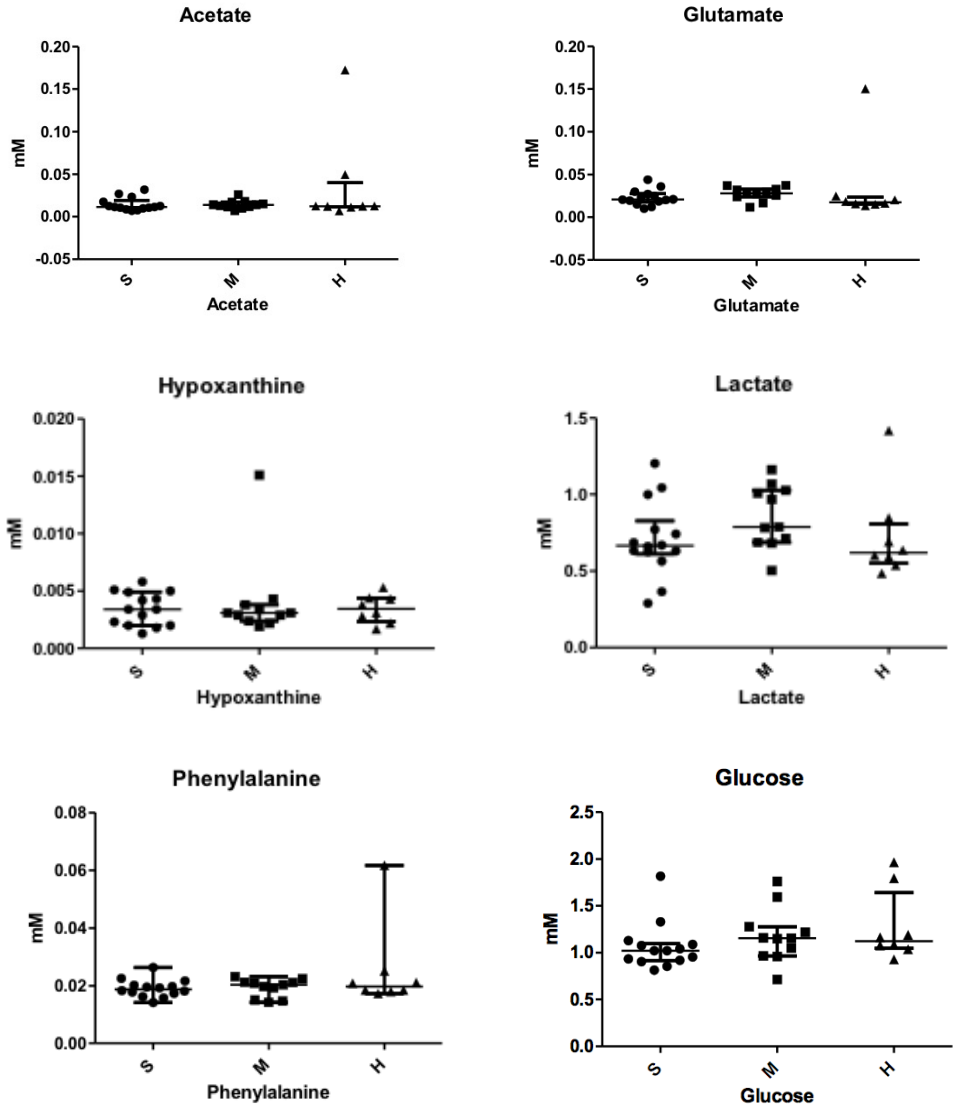

Figure 4.3.9 Selected scatter plots of 8 metabolites previously reported to be altered within the ME/CFS patient population but were not observed to be significant altered in this study. Plots were generated using GraphPad Prism. Each dot represents a single participant. Horizontal line represents the median concentration (mM) value. Error bars represent the Max and Min values observed from each experimental group.

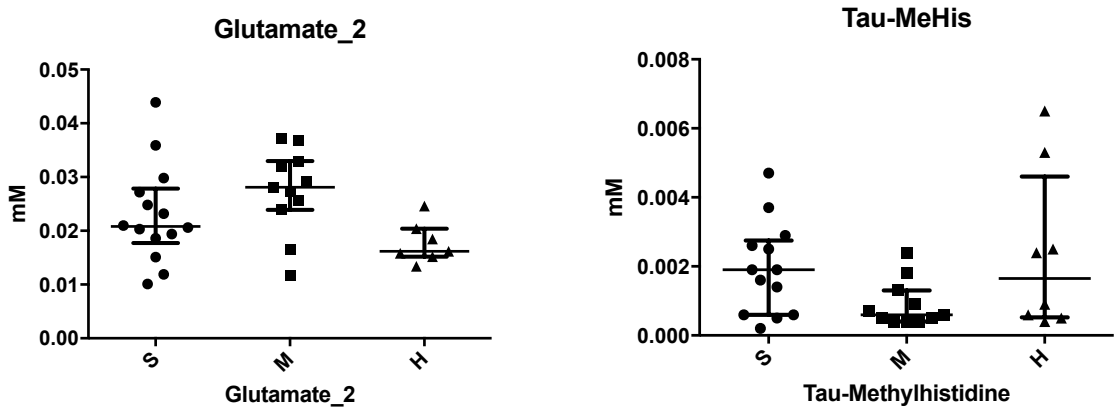

Figure 4.3.10 Amended scatter plots excluding extreme values included in the initial plot (Fig. 4.3.11) for Glutamate and Tau-MeHis. Glutamate (p=0.03, M>H). Tau-MeHis (p=0.07)

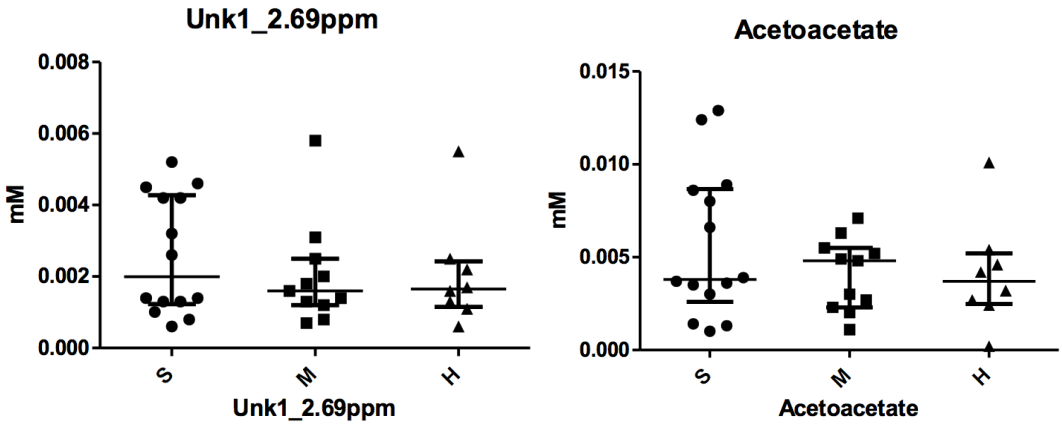

Figure 4.3.11 Scatter dot plots for unknown small metabolite and acetoacetate. Significance tested using Kruskal-Wallis test with Dunn's post-hoc test, no significances observed. Distribution of concentrations (mM) plotted appear to indicate a trend in metabolite concentration across groups, S>M>H for both metabolites. (p=0.81 and p=0.66 respectively).

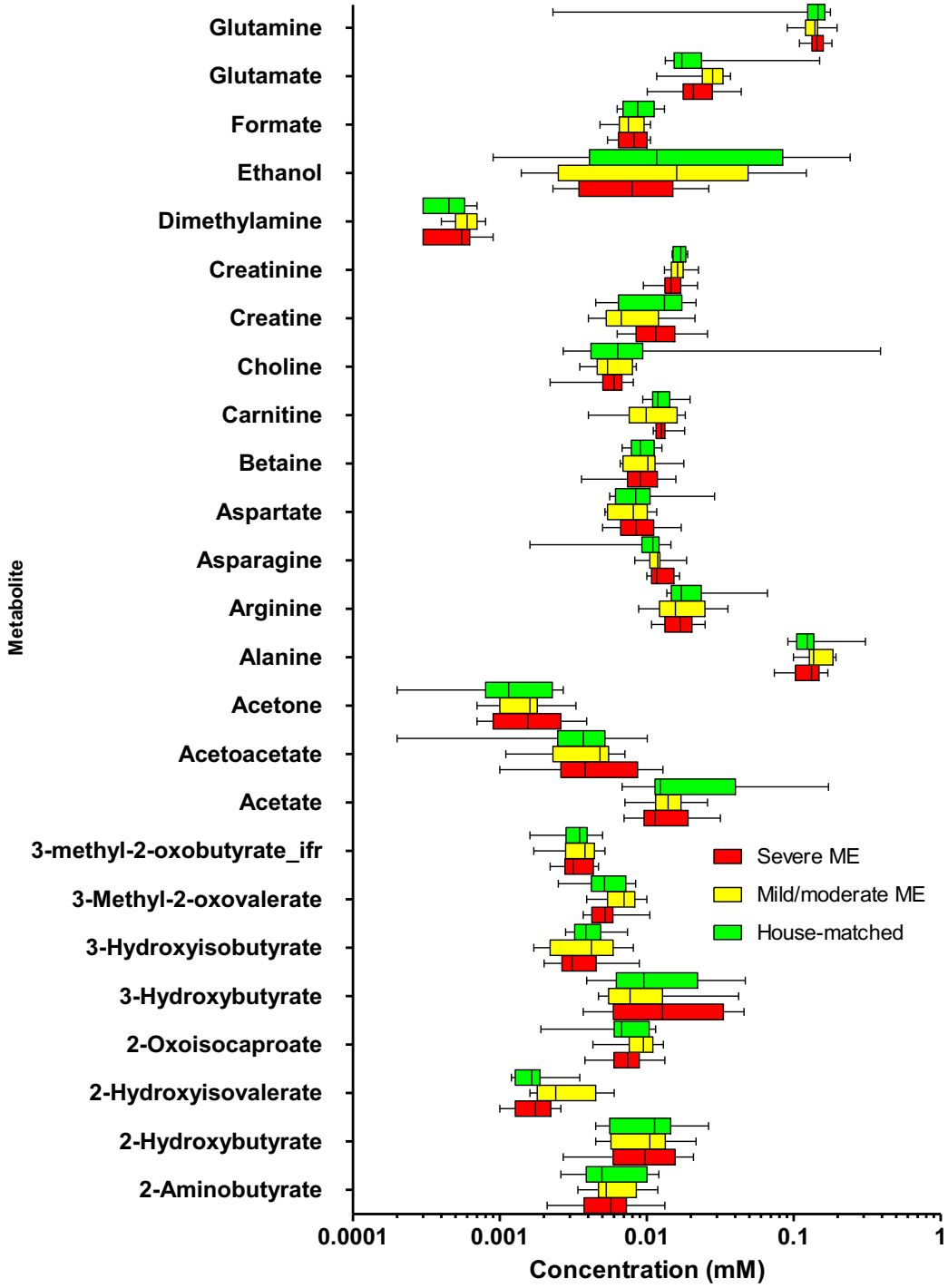

Figure 4.3.12 Box plot summary including 25 of 53 serum metabolites detected using 600MHz ^{1}H-NMR. Frozen storage (-80^{o}C) serum collected from severe (S), mild/moderate (M) and House-Matched (H) were analysed simultaneously. Analysis was performed blinded using experimental spectra compared with reference spectra of known small compounds. Absolute concentrations were obtained in milli-molar (mM) before undergoing log transformation and plotting data using GraphPad Prism. Three groups S, M, & H were analysed for statistical significance using the Kruskal-Wallis test with Dunn's post correction. *(2-hydroxyisovalerate, p=0.02).

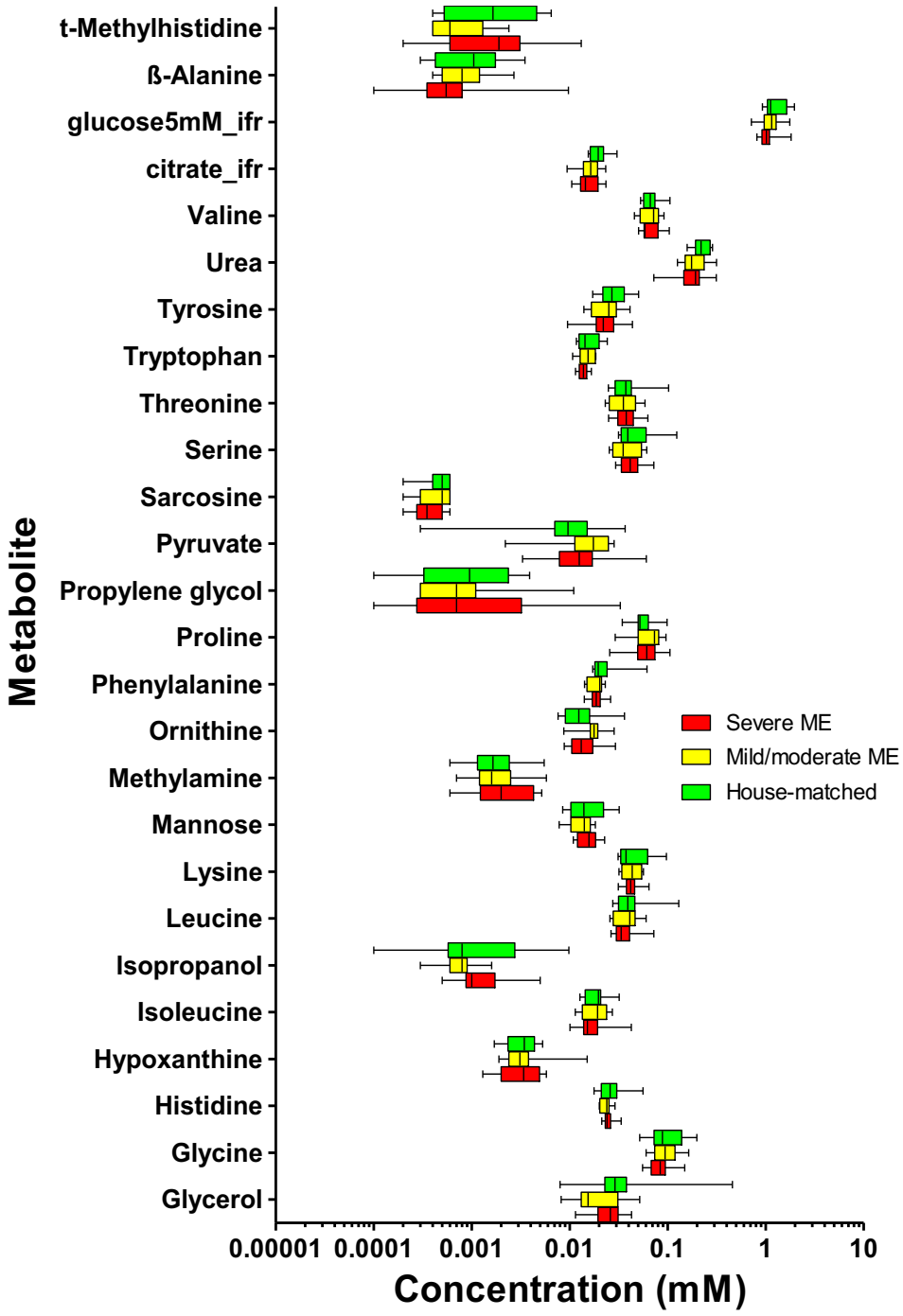

Figure 4.3.13 Remaining 26 out of 53 metabolites found in serum. All samples were analysed simultaneously using 600 MHz ^{1}H-NMR. Central line of boxes represents median value for each compound; error bars show samples were the max and min concentration was detected. Width of box shows the interquartile range. Absolute concentrations were determined from measurement of peak intensity. Compounds were identifiable based on comparison of the experimental spectra with known reference spectra in the library. No significant differences were observed across groups: (S), (M) & (H).

Metabolite	P value	Severe		Mild/moderate		House Matched	
		Mean	St. Err	Mean	St. Err.	Mean	St. Err.
2-Aminobutyrate	0.95	0.0062	0.00082	0.0062	0.00077	0.0063	0.001247
2-Hydroxybutyrate	0.94	0.0106	0.00149	0.0104	0.00155	0.0117	0.002476
2-Hydroxyisovalerate	0.02*	0.0017	0.00013	0.0030	0.00046	0.0018	0.000260
2-Oxoisocaproate	0.25	0.0076	0.00066	0.0092	0.00076	0.0075	0.001112
3-Hydroxybutyrate	0.75	0.0179	0.00385	0.0125	0.00353	0.0151	0.005106
3-Hydroxyisobutyrate	0.57	0.0039	0.00052	0.0043	0.00061	0.0043	0.000524
3-Methyl-2-oxovalerate	0.13	0.0056	0.00052	0.0070	0.00054	0.0055	0.000684
3-methyl-2-oxobutyrate	0.65	0.0034	0.00021	0.0037	0.00031	0.0034	0.000352
Acetate	0.62	0.0144	0.00203	0.0143	0.00149	0.0362	0.020025
Acetoacetate	0.66	0.0056	0.00106	0.0041	0.00058	0.0041	0.001024
Acetone	0.58	0.0019	0.00025	0.0016	0.00022	0.0014	0.000305
Alanine	0.29	0.1264	0.00800	0.1493	0.00994	0.1420	0.024365
Arginine	0.67	0.0171	0.00115	0.0178	0.00244	0.0236	0.006239
Asparagine	0.36	0.0128	0.00065	0.0123	0.00099	0.0102	0.001357
Aspartate	0.76	0.0092	0.00086	0.0081	0.00067	0.0105	0.002707
Betaine	0.78	0.0096	0.00090	0.0103	0.00095	0.0094	0.000712
Carnitine	0.75	0.0128	0.00047	0.0116	0.00151	0.0130	0.001132
Choline	0.99	0.0057	0.00042	0.0060	0.00052	0.0542	0.048057
Creatine	0.09	0.0124	0.00140	0.0087	0.00151	0.0128	0.002179
Creatinine	0.82	0.0153	0.00092	0.0168	0.00088	0.0168	0.000576
Dimethylamine	0.2	0.0005	4.93681E-05	0.0006	3.9207E-05	0.0005	5.34522E-05
Ethanol	0.53	0.0103	0.00224	0.0364	0.01350	0.0505	0.029978
Formate	0.49	0.0083	0.00048	0.0079	0.00053	0.0092	0.000870
Glutamate	0.03*	0.0230	0.00242	0.0274	0.00238	0.0343	0.016630
Glutamine	0.39	0.1460	0.00552	0.1354	0.00807	0.1312	0.019423
Glycerol	0.35	0.0262	0.00242	0.0218	0.00398	0.0807	0.054000
Glycine	0.47	0.0855	0.00669	0.0980	0.00886	0.1034	0.017186
Histidine	0.57	0.0250	0.00084	0.0238	0.00082	0.0284	0.004210
Hypoxanthine	0.94	0.0035	0.00038	0.0041	0.00111	0.0035	0.000429
Isoleucine	0.48	0.0184	0.00238	0.0194	0.00166	0.0193	0.002131
Isopropanol	0.08	0.0014	0.00030	0.0008	0.00010	0.0022	0.001138
Lactate	0.11	0.7062	0.06555	0.8540	0.06157	0.7263	0.105928
Leucine	0.58	0.0385	0.00372	0.0400	0.00324	0.0493	0.011746
Lysine	0.88	0.0440	0.00237	0.0434	0.00272	0.0481	0.008200
Mannose	0.29	0.0157	0.00095	0.0131	0.00099	0.0162	0.002826
Methylamine	0.45	0.0026	0.00044	0.0020	0.00043	0.0021	0.000534
Ornithine	0.06	0.0145	0.00148	0.0179	0.00145	0.0148	0.003233
Phenylalanine	0.76	0.0190	0.00081	0.0192	0.00095	0.0251	0.005307
Proline	0.34	0.0635	0.00616	0.0678	0.00618	0.0575	0.006659
Propylene glycol	0.97	0.0039	0.00232	0.0016	0.00094	0.0014	0.000472
Pyruvate	0.19	0.0157	0.00369	0.0177	0.00249	0.0124	0.003852
Sarcosine	0.23	0.0004	3.69564E-05	0.0004	4.52724E-05	0.0005	4.9099E-05
Serine	0.39	0.0435	0.00304	0.0391	0.00392	0.0519	0.010921
Threonine	0.84	0.0387	0.00267	0.0366	0.00354	0.0434	0.008674
Tryptophan	0.31	0.0139	0.00042	0.0154	0.00086	0.0160	0.001569
Tyrosine	0.42	0.0237	0.00222	0.0244	0.00253	0.0295	0.003739
Urea	0.19	0.1878	0.01646	0.1940	0.01734	0.2247	0.015689
Valine	0.85	0.0672	0.00392	0.0695	0.00463	0.0695	0.005800
Citrate	0.12	0.0158	0.00102	0.0166	0.00136	0.0203	0.001703
Glucose	0.1	1.0639	0.06742	1.1821	0.08797	1.2798	0.134884
β-Alanine	0.44	0.0012	0.00065	0.0010	0.00022	0.0013	0.000386
τ-Methylhistidine	0.07	0.0027	0.00086	0.0009	0.00020	0.0024	0.000827

Table 4.3.3 Summary statistical for absolute concentration (mM) of low molecular weight (hydrophilic) metabolites in serum. Mean values and standard error were calculated using Microsoft Excel. Data was plotted using Prism (see scatter plots in supplementary materials). Kruskal-Wallis test was applied for determining level of significance at 5% followed by Dunn's multiple comparison test to compare across groups: (S) vs (M) vs (H).

4.3.4 Diffusion edited NMR using saline diluted serum

- *dataset 4C*

A separate dataset was collected using saline-diluted serum to explore spectral contributions from lipoproteins and other macromolecules as opposed to small molecular metabolites. Diffusion edited NMR spectra were analysed by summing the intensities within each variable width bucket. As far as possible each bucket was assigned by comparing spectral features with reference spectra in the literature. At the time of writing, no previous data using ^{1}H-NMR has looked at the contribution of lipoproteins in this disease. Blood serum contains various proteins and lipoproteins which contribute strongly to ^{1}H-NMR spectra with smaller metabolites such as amino acids superimposed as sharp peaks. The larger molecules generate much broader resonances figure 4.3.14 compared with the earlier NMR generated spectrum (figure 4.3.1). This is characteristic of larger macromolecules such as lipoproteins due to their faster relaxation properties of protons associated with aromatic and aliphatic chemical groups. By alternating the NMR pulse sequence during the acquisition of the samples this generates a diffusion edited NMR spectrum (figure 4.3.15). This approach utilises an echo phenomenon to recover certain signals after a delay in diffusion - as such, macromolecules behave as 'sluggish' movers.

The data provides a spectral overview of CH groups of lipids within lipoprotein particles, table 4.3.4. This was then analysed by summing the intensities within each variable width bucket, shown as black bars along the chemical shift axis in figure 4.3.15. Each bucket is labelled with a chemical shift at the centre of each bucket (ppm). The integrated intensities from each sample are presented in dot plots comparing Severe (S), Mild/moderate (M) and House-Matched (HM) – see supplementary figure (S 4.3) in appendix. These intensities were normalised by setting the sum of intensities in each spectrum to 1 to allow for concentration difference. Table 4.3.4 presents the identities of the chemical shifts relating to each variable width bucket. These have been assigned using the resonances observed from high resolution 750 MHz ^{1}H-NMR using normal human blood plasma (Foxall et al., 1995).

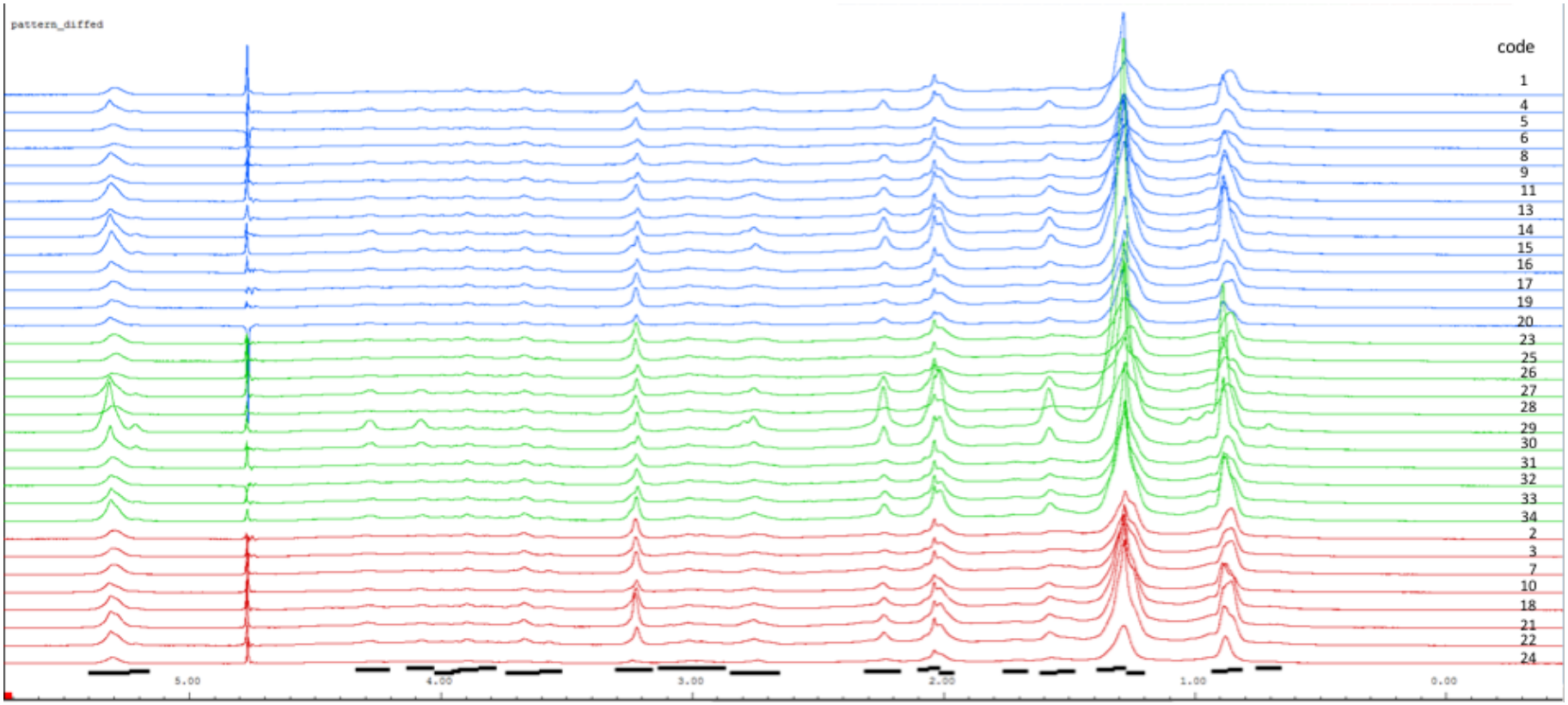

Figure 4.3.14 600 MHz ^{1}H diffusion edited NMR spectra of all serum samples (n=34) with patient codes and colouring: severe (S) – blue; mild (M) – green; healthy (H) – red.

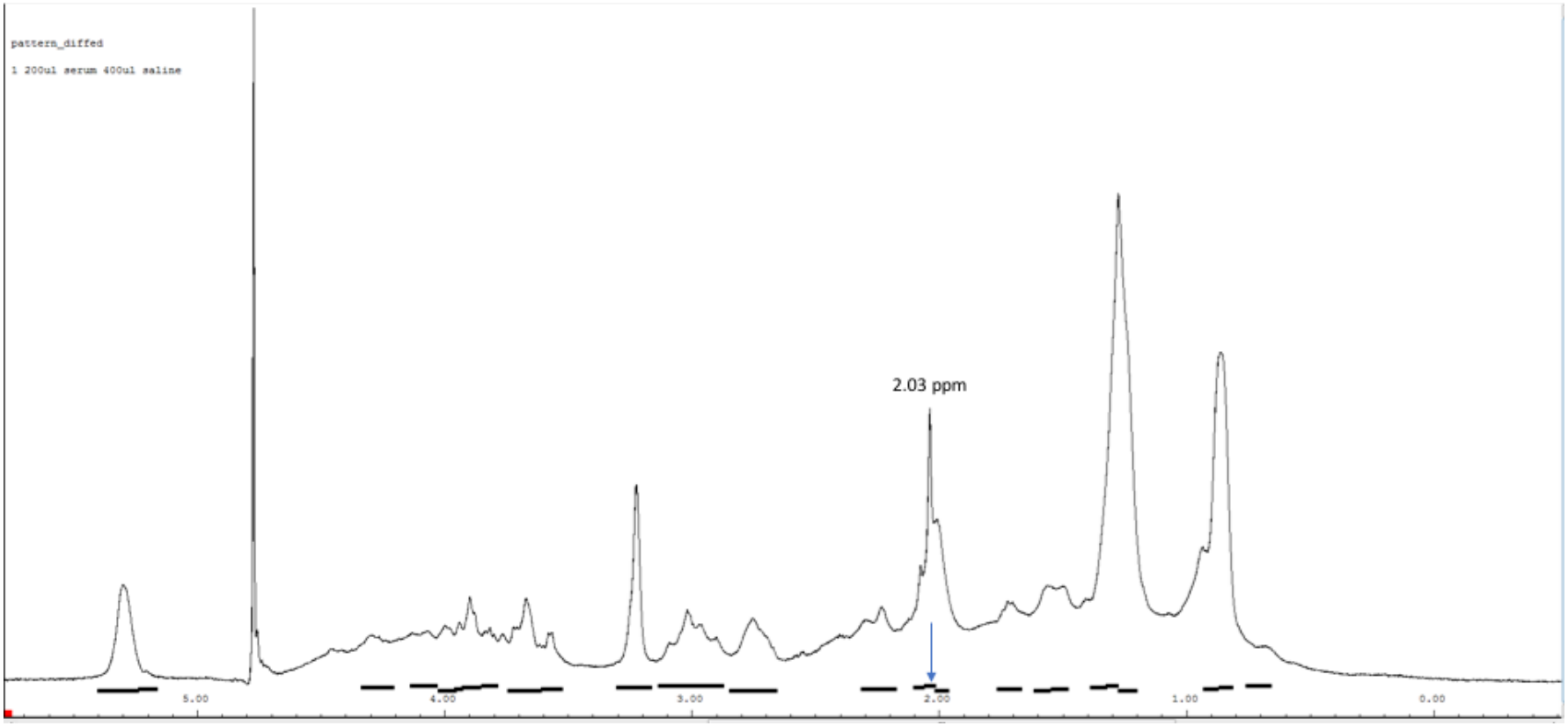

Figure 4.3.15 600 MHz 1H 'diffusion edited' NMR spectrum of saline diluted serum (sharp lines from low mol. wt. metabolites are suppressed). The data are analysed by summing the intensities within each variable width bucket (black bars below the spectrum). Each bucket is labelled with the chemical shift at the centre, e.g. the arrowed bucket is labelled '2.03' in the supplementary statistical plots.

Metabolite	Chemical Structure	Chemical shift (ppm)	Assigned	Observed
Unsaturated lipid	=CHCH2CH2	5.31690001	5.31	1D, COSY, HMQC
Glyceryl of lipids	CHOCOR	5.1967001	5.2	COSY
Glyceryl of lipids	CH2COR	4.26854992	4.25	HMQC
myo-inositol	CH2	4.08055019	4.06	JRES
Unknown		3.98484993	3.98	JRES
Unknown		3.93875003	3.93	JRES
Glycerol	C2H	3.88940001	3.87	JRES, COSY
Unknown		3.81389999	3.83	JRES, COSY, HMQC
Choline (lipid)	NCH2	3.67209995	3.66	JRES, COSY, HMQC
Glycerol		3.56110001	3.56	1D, COSY, HMQC
Choline	N(CH3)	3.22959995	3.21	JRES, HMQC
Albumin lysyl	e-CH2	3.000000	3.01	1D, JRES, COSY, HMQC
Lipid	C=CCH2C=C	2.74849999	2.72	1D, COSY,
Lipid	CH2CO	2.23970008	2.23	COSY
Unknown		2.07934999	2.08	1D, JRES, COSY
Glycoprotein (acetyls)	NHCOCH3	2.03464997	2.04	1D, COSY, HMQC
Lipid	CH2C=C	1.98540002	2	COSY
Lipid	CH2CH2C=C	1.71249998	1.69	COSY, HMQC
Lipid	CH2CH2CH2CO	1.3513	1.32	JRES, COSY, HMQC
Lipid (mainly VLDL)	CH2CH2CH2CO	1.29580003	1.29	1D, CPMG, JRES, COSY
Lipid	CH3CH2CH2	1.23405004	1.22	HMQC
Cholesterol C21	C21	0.89815	0.91	HMQC
Lipid (mainly VLDL)	CH3(CH2)n	0.8364	0.84	1D, JRES, COSY, HMQC
Cholesterol C18	C18	0.70524999	0.7	HMQC
Lipid (mainly VLDL)	CH2CH2CO	1.57999998	1.57	JRES, COSY, HMQC
Unknown		1.509		

Table 4.3.4 Experiment spectra peak assignment based on observed chemical shift and reference to known lipid molecules detected in normal human plasma. Using 750MHz ^{1}H-NMR.

The only significant difference discovered was across two groups (p=0.009, S>H) for a signal at 2.03ppm. This signal was identified as N-Acetyl groups from α_1-acid glycoprotein (figure 4.3.16). The next closest significant signals were detected at 2.24ppm, 1.23ppm and 1.58ppm. The signal at 1.58ppm (figure 4.3.17) appears to follow a trend (S>M>H) and appears to correspond to citrulline based on the observed resonances recorded in Nicholson & Foxall, (1995). However, in this particular experiment small molecules such as citrulline are known to be excluded. The earlier set of samples processed using methanol/chloroform extraction would have detected low molecular weight metabolites such as this, but unfortunately did not detect citrulline either.

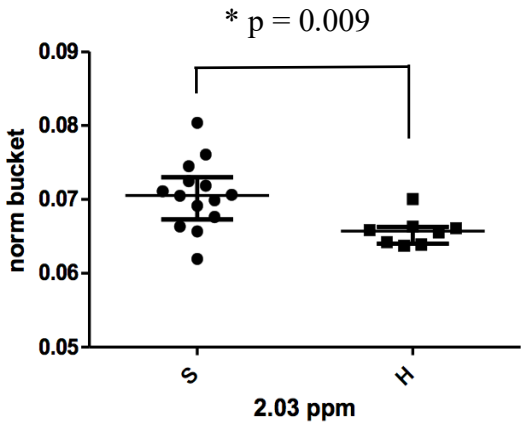

Figure 4.3.16 N-acetyl group from glycoproteins The points in the statistical plot shows the integrated intensities of the bucket labelled with a chemical shift of 2.03ppm. These intensities have been normalised i.e. the sum of intensities in each spectrum has been set to 1 to allow for concentration differences. (p=0.009).

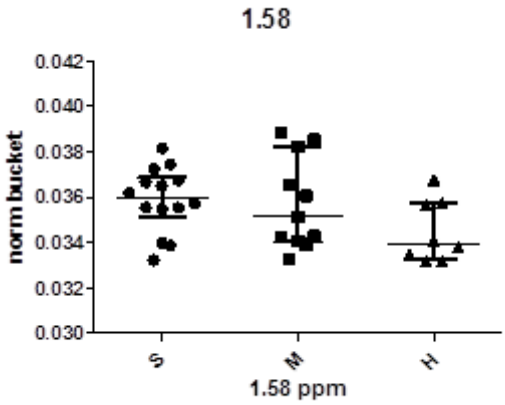

Figure 4.3.17 Integrated signal intensities within bucket width at 1.58ppm. No significant p value. There appears to be a trend (S>M>H).

Citrulline was detected in2D NMR experiments used for signal identification but it was too low in concentration and lacked clear-cut signals that could be used for quantification by NMR. Armstrong et al., claim to have quantified it using the same method as they had access to a 900 MHz NMR, the 600 MHz machine. Citrulline has previously been suggested as a surrogate marker for increased intestinal permeability as well as intestinal insufficiency relating to short bowel syndrome in patients (Curis et al., 2007; Fragkos & Forbes, 2018). In a 2018 review, the authors conclude citrulline is 'quite reasonably' a marker of intestinal function and absorption (Fragkos & Forbes, 2018).

4.3.5 Targeted bile acid mass spectrometry

- *dataset 4B*

As an extension to the 45 metabolites identified using ^{1}H-NMR in severe ME faecal water; additional aliquots for available samples were used for a targeted analysis of 26 bile acids (Table 4.3.5) using Liquid-Chromatography – Mass Spectrometry (LCMS) in multiple reaction mode (MRM). A total of 14 samples were analysed including 8 severe ME (S) patients versus 6 House-Matched (H) controls. The range of concentrations observed across the 26 bile acids varied dramatically and for the purposes of summarising this data across the two groups (S v H), log transformation of absolution bile acid concentrations enabled visualisation on a box plot (figure each bile acid, 4.3.18). Individual metabolites were compared between severe (S) and house-matched (H) using the Mann-Whitney test, except where multiple samples gave zero concentrations, using GraphPad Prism. Beta-muricholic acid (β-MCA), a primary bile acid that is one of the main forms of major bile acids found in germ-free mice, was significantly higher in severe patients, p value = 0.0416) (Eyssen et al., 1976). The literature is clear that the presence of this bile acid is not expect in humans but been reported to be detected in low concentrations in urine (Goto et al., 1992). Tauro-conjugated forms of alpha- and beta- muricholic acids were also detected in (S) and (H) faecal metabolomes. Table 4.3.5 provides statistical summary of mean bile acid concentrations (ng/ml) and standard errors and respective p value.

The bile acid, temporarily designated as ‘glycocholate’ based on earlier collected NMR spectra which showed a weak separation between severe (S) and house-matched (H), did not produce any significant result, with a recorded p value of 0.4162. For some bile acids, one or two severe ME (S) samples were observed to have unusually higher concentration values outside the rest of the group (see Figure 4.3.19).

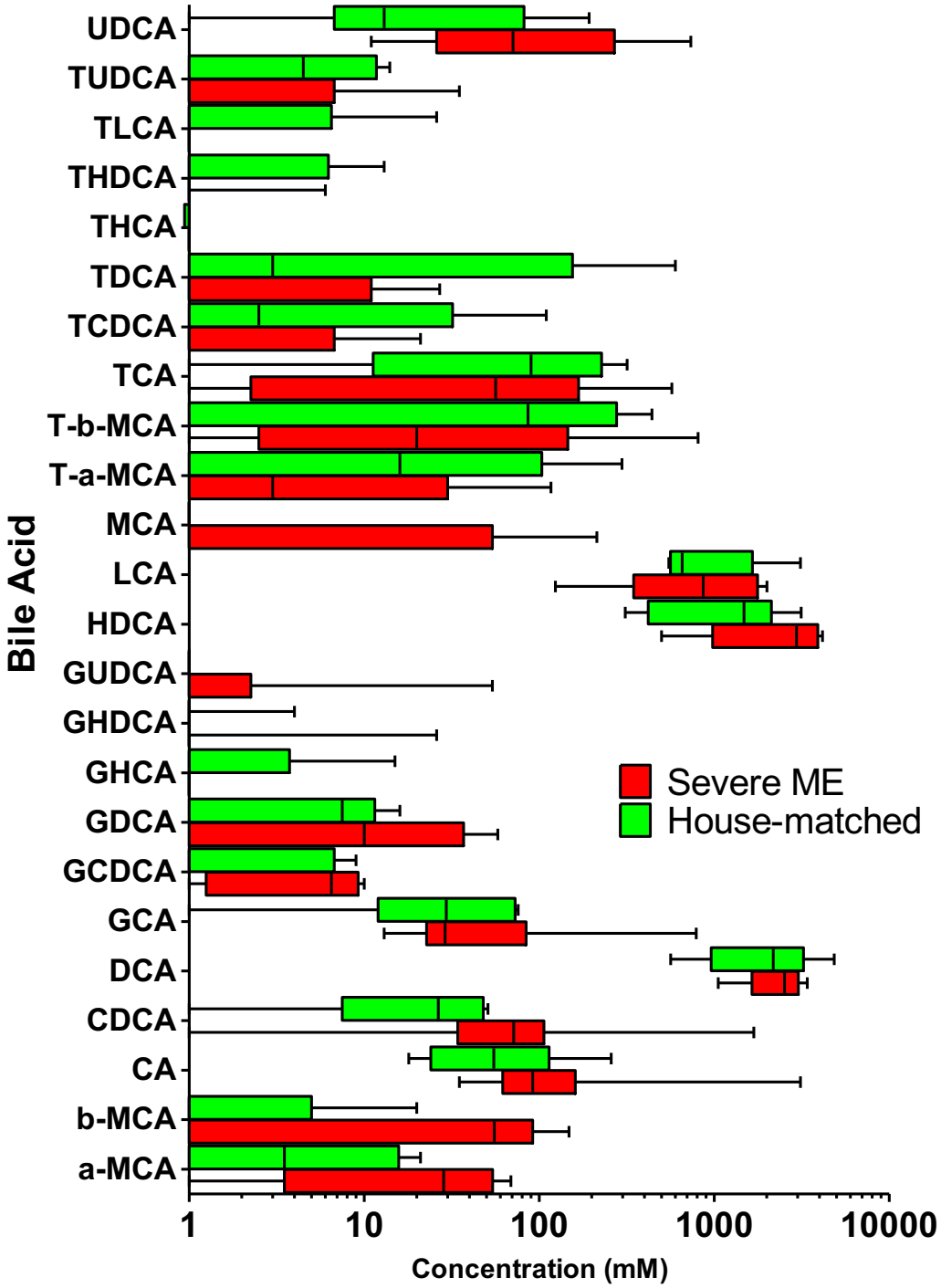

Figure 4.3.18 26 Bile Acid targeted Mass Spectrometry analysis of faecal water from 8 severe (S) and 6 House-matched controls (H) Box plot used to compare range of log of concentrations (mM) detected within (S) and (H) groups. Line inside each box represent the median. Error bars indicate the extreme Max and Min values.

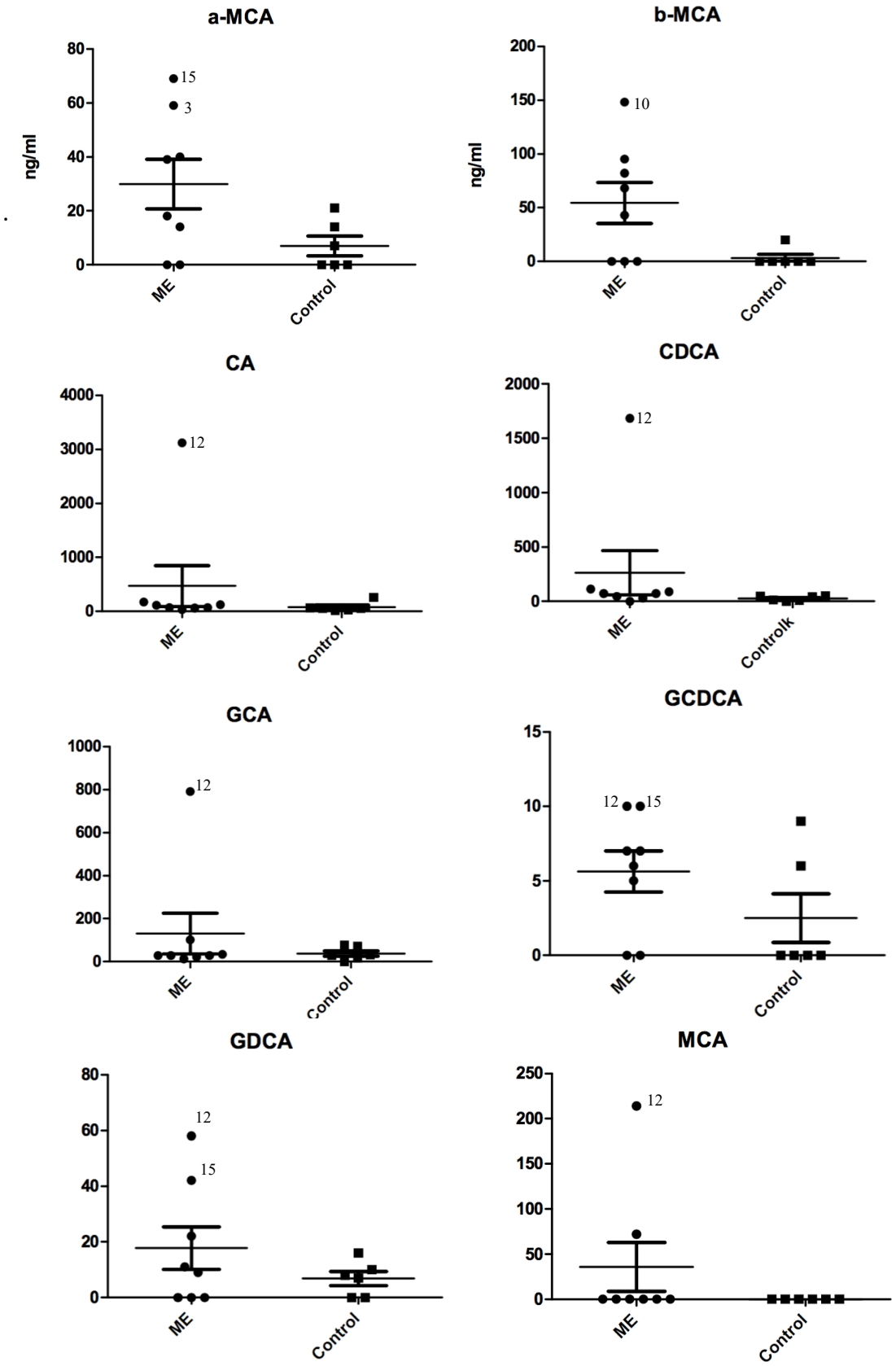

Figure 4.3.19 Summary scatter plot for 8 out of the total 26 Bile Acids (BA) targeted faecal water in 8 severe ME patients versus 6 House-Matched controls. Horizontal lines indicate the max, median, and min. Patient numbers 12 and 15 were consistency revealed as outliers across at least 3 BAs. Data was analysed by Mann-Whitney test at the 5% significance level. Plots are labelled with the abbreviated name of each BA listed in Table 4.3.5.

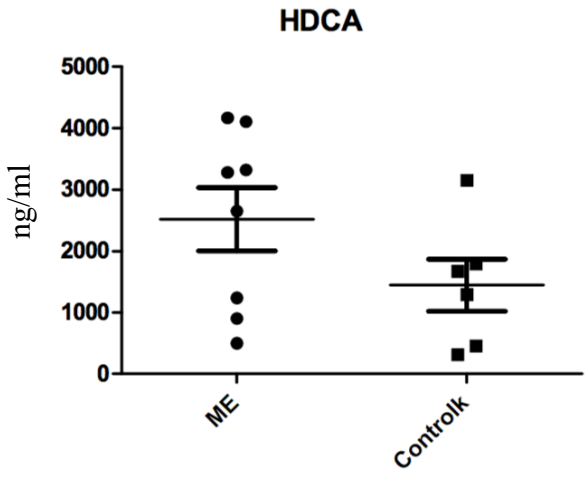

Figure 4.3.20 Faecal metabolome concentration of HDCA (ng/ml) in severe (S) ME versus House-Matched controls. No significant different report by Mann-Whitney test (p=0.15).

Hyodeoxycholic acid (HDCA) showed a cluster of patients with almost double the concentration detected within the House-matched (H) group. The scatter plot in figure 4.3.20 has been annotated with a red box to highlight these patients. It has been documented that HDCA is formed from muricholic acid and hyocholic acid by an unknow Gram-positive rod shaped bacterium originating from the gut of rodents (Eyssen et al., 1999). It is therefore considered to be a secondary bile acid formed in humans as a metabolic by-product of intestinal bacteria. It is not normally present in the urine of healthy humans (Almé et al., 1977); but most interesting has also been cited as being absorbed well across the gut barrier based on its excretion in urine (Sacquet et al., 1983) in patients with cholestatic disease and others with purported intestinal malabsorption (Almé et al., 1977; Summerfield et al., 1976) . Interestingly, HDCA has been shown to be effective in treating rodents for metabolic disorders and a diet enriched in HDCA was protective of atherosclerotic plaque formation in LDL receptor knockout mice by reducing intestinal absorption of cholesterol (Shih et al., 2013).

Bile Acid	Abreviation	Type	Faeces Un-paired t test				
				Severe (S)		House-Matched (H)	
			P value	Mean	St. Err.	Mean	St. Err.
alpha-muricholic acid	α-MCA	Primary (mouse)	0.0631	21.90	9.20	7.0	3.60
beta-muricholic acid	β-MCA	Primary (mouse)	0.0416*	43.75	20.37	5.6	3.30
Cholic acid	CA	Primary (mouse)	0.3948	661.90	20.00	59.4	36.50
Chenodeoxycholic acid	CDCA	Primary (mouse)	0.3397	355.40	16.60	19.7	9.10
Deoxycholic acid	DCA	Secondary	0.8786	639.80	373.20	1076	615.10
Glycocholic acid	GCA	Glyco-conjugated	0.4162	165.10	3.10	24.6	12.50
Glycochenodeoxycholic acid	GCDCA	Glyco-conjugated	…	3.00	1.40	3.30	1.60
Glycodeoxycholic acid	GDCA	Glyco-conjugated	0.2583	17.20	3.60	4.60	2.50
Glycocholic acid	GHCA	Glyco-conjugated	…	0.00	0.00	4.20	2.50
Glycohyodeoxycholic acid	GHDCA	Glyco-conjugated	…	5.70	0.00	1.10	0.70
glycolithocholic acid	GLCA	Glyco-conjugated	…	0.00	0.00	0.00	0.00
Glycoursodeoxycholic acid	GUDCA	Glyco-conjugated	…	11.70	0.50	0.00	0.00
Hyodeoxycholic acid	HDCA	Secondary	0.1511	1128.50	598.90	757.7	422.3
Lithocholic acid	LCA	Secondary	0.7645	621.50	287.70	681.9	409.7
Muricholic acid	MCA	Primary (mouse)	…	53.60	12.00	0.00	0.00
Tauro-a-muricholic acid	Tα-MCA	Tauro-conjugated	0.3989	27.10	18.90	78.6	47.70
Tauro-b-mucricholic acid	Tβ-MCA	Tauro-conjugated	0.983	169.70	130.90	128.1	69.20
Taurocholic Acid	TCA	Tauro-conjugated	0.9303	127.50	91.60	97.3	50.30
Taurochenodeoxycholic acid	TCDCA	Tauro-conjugated	…	5.60	3.50	29.9	18.00
Taurodeoxycholic acid	TDCA	Tauro-conjugated	…	7.20	2.20	165.9	99.6
taurodehydrocholic acid	TDHCA	Tauro-conjugated	…	0.00	0.00	0.00	0.00
trihydroxycoprostanic acid	THCA	Secondary	…	0.00	0.00	0.83	0.50
Taurohyodeoxycholic acid	THDCA	Tauro-conjugated	…	0.00	0.00	3.80	2.10
Taurolithocholic acid	TLCA	Tauro-conjugated	…	0.00	0.00	7.20	4.30
Tauroursodeoxycholic acid	TUDCA	Tauro-conjugated	…	8.25	5.70	5.70	2.60
Ursodeoxycholic acid	UDCA	Secondary	0.2567	179.10	116.00	49.20	30.1

Table 4.3.5 Statistical summary table for 26 bile acids (BA) quantified in faecal water samples from severe (S) ME patients versus house-matched (H) controls. Mean concentrations are provided in ng/ml with standard error in measurements. Both groups were compared for statistical significance at the 5% level using the Mann-Whitney test, p values are displayed in table

Bile Acid	Abbreviation	Type	P value	Severe (S)		Mild (M)		Healthy		IBD	
			KW	Mean	St. Err	Mean	St. Err	Mean	St. Err	Mean	St.Err
alpha-muricholic acid	α–MCA	Primary (mouse)	0.55	30.12	2.77	25.21	1.91	27.5	1.98	33.00	6.01
beta-muricholic acid	β–MCA	Primary (mouse)	0.16	11.12	9.21	0.00	0.00	11.25	4.81	9.67	9.67
Cholic acid	CA	Primary (mouse)	**0.01***	78.29	14.79	102.21	29.43	155.91	58.29	240.33	54.77
Chenodeoxycholic acid	CDCA	Primary (mouse)	**0.003****	57.21	12.11	109.5	37.65	137.00	49.06	233.00	65.45
Deoxycholic acid	DCA	Secondary	0.33	267.07	106.47	189.5	55.78	230.25	54.37	130.67	24.05
Glycocholic acid	GCA	Glyco-conjugated	0.47	143.64	23.58	185.57	49.04	188.75	33.51	172.83	27.00
Glycochenodeoxycholic acid	GCDCA	Glyco-conjugated	0.59	354.86	67.04	553.86	107.18	453.33	85.75	439.17	105.08
Glycodeoxycholic acid	GDCA	Glyco-conjugated	0.19	270.00	60.85	225.64	44.62	267.33	68.02	87.83	21.28
Glycocholic acid	GHCA	Glyco-conjugated	**0.02***	0.64	0.64	6.92	2.49	1.00	1.00	0.00	0.00
Glycohyodeoxycholic acid	GHDCA	Glyco-conjugated	0.27	14.29	0.54	11.36	1.34	13.42	1.48	9.67	3.15
glycolithocholic acid	GLCA	Glyco-conjugated	0.16	16.07	2.04	16.42	1.94	21.67	4.72	10.83	1.28
Glycoursodeoxycholic acid	GUDCA	Glyco-conjugated	0.15	15.21	1.33	13.71	0.79	16.00	1.00	16.67	0.92
Hyodeoxycholic acid	HDCA	Secondary	n/a	0.00	0.00	0.00	0.00	0.00	0.00	0.00	0.00
Lithocholic acid	LCA	Secondary	0.10	59.57	47.91	1.71	1.71	32.42	24.22	0.00	0.00
Muricholic acid	MCA	Primary (mouse)	0.84	75.5	16.87	136.29	38.63	105.41	28.43	88.67	32.71
Tauro-□-muricholic acid	T□-MCA	Tauro-conjugated	0.21	17.86	8.69	2.07	1.42	5.50	3.00	20.83	9.51
Tauro-□-mucricholic acid	T□-MCA	Tauro-conjugated	0.06	319.93	126.3	124.93	18.66	220.08	48.64	122.83	28.32
Taurocholic Acid	TCA	Tauro-conjugated	0.11	123.21	24.16	77.14	10.36	149.5	32.2	147.83	56.52
Taurochenodeoxycholic acid	TCDCA	Tauro-conjugated	0.93	90.71	24.22	81.5	18.8	98.25	25.88	79.17	24.36
Taurodeoxycholic acid	TDCA	Tauro-conjugated	0.13	85.43	17.71	50.57	8.32	73.67	21.79	30.50	6.17
taurodehydrocholic acid	TDHCA	Tauro-conjugated	0.30	0.00	0.00	2.07	2.07	0.00	0.00	6.50	6.50
trihydroxycoprostanic acid	THCA	Secondary	n/a	0.00	0.00	0.00	0.00	0.00	0.00	0.00	0.00
Taurohyodeoxycholic acid	THDCA	Tauro-conjugated	0.13	15.07	0.66	12.57	12.3	13.58	0.50	15.17	1.08
Taurolithocholic acid	TLCA	Tauro-conjugated	0.17	16.00	0.94	13.79	1.41	17.00	1.79	12.33	1.02
Tauroursodeoxycholic acid	TUDCA	Tauro-conjugated	0.60	21.21	2.89	15.00	2.13	16.83	1.98	15.67	3.61
Ursodeoxycholic acid	UDCA	Secondary	0.36	17.57	4.35	39.93	11.77	30.67	6.95	36.50	10.89

Table 4.3.6 Statistical summary of serum bile acid concentrations (nM) in Severe (S), Mild/moderate (M), Healthy, and IBD. Included 26 targeted bile acids quantified using mass spectrometry. Significant p values are in **bold.** Colour shading for ease of separation of values corresponding to 12 severe ME (red), 14 mild/moderate ME (yellow), 7 healthy (green) and 6 IBD (blue) samples. Mean concentrations and standard error per metabolite, per group. P values calculated using Kruskal Wallis test at 5% significance: *denotes $p < 0.05$, ** denotes $p < 0.01$.

4.3.6 Bile Acid analysis of ME serum

- *dataset 4D*

Targeted HPLC mass-spectrometry of the same 26 bile acids was accurately quantified in a total of 46 serum samples collected between 2015-2017. This represents the largest and final dataset (designated 4D, Table 4.3.2) acquired during the study. Twenty-six ME/CFS patients where included in the experiment were categorised as follows: 12 severe (S), 14 mild/moderate (M). In addition, 7 House-Matched (H) and 6 IBD serum samples were also included. Sera collected the previous year (2016) was available at the time, for 2 of the severe patients (n=12+2, severe) and their respective House-Matched control (n=7+2). A further 3 conventionally healthy samples were provided as a gift along with the 6 IBS serum samples kindly given by Dr Alistair Noble (Imperial College London, UK), bringing the total sample size to 46.

The synthesis of primary bile acids takes place within the liver where major bile salts are produced when conjugated with taurine and glycine, forming tauro-chenodeoycholate (TCDCA) and glycochenodeoxycholate (GCDCA) respectively (Germain et al., 2017). Both of these have been reported significantly reduced in ME/CFS patients. In contrast, within severe (S) and Mild/moderate (M) patients there was no statistically relevant difference for either. However, upon review of the scatter plot for GCDCA (fig. 4.3.21), it does appear as if severe patients have a lesser concentration compared with the other groups which would be in agreement with these previous reports. Although it is worth noting that this trend was not identified in the faecal water metabolome of the same participants (figure 4.3.19).

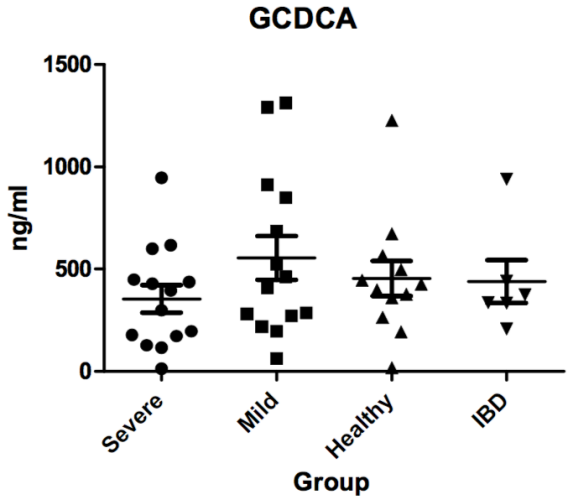

Figure 4.3.21 Concentration (ng/ml) of glycochenodeoxycholic acid (GCDCA) across 4 groups. KW test revealed no significant differences at 5% significance.

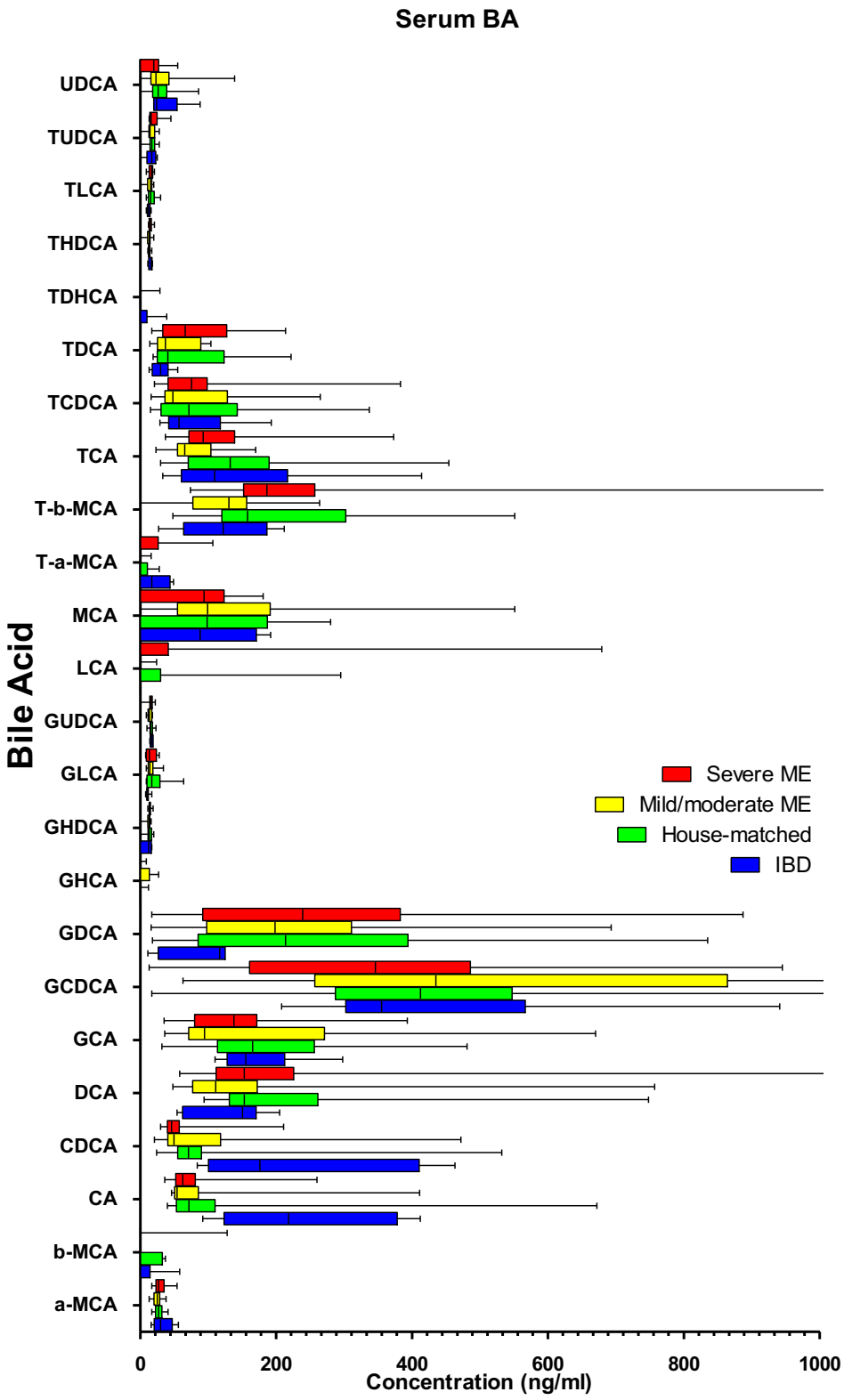

Figure 4.3.22 Mass Spectrometry targeting on 26 bile acids in serum. Four groups compared: 14 severe (S), 14 Mild/moderate (M), 14 House-Matched (H) and 6 IBD serum. Statistical analysis was performed in GraphPad Prism using one-way ANOVA with Dunnett's Multiple comparison to House-Matched (H). No significance was observed.

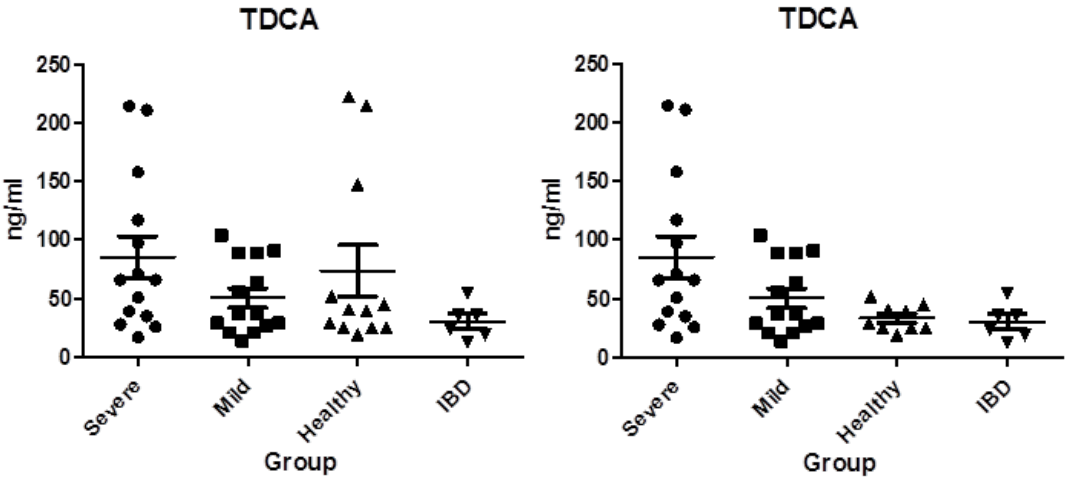

Figure. 4.3.23 Scatter plots summarising concentrations found of tauro-deoxycholic acid (TDCA) found across the 4 groups labelled. Kruskal-Wallis with Dunn's multiple comparison test reveal the following values (left plot) p= 0.132, (right plot) p=0.047.

Another interesting trend emerged from a primary bile acid produced in the liver called taurodeoxycholic acid TDCA. The initial Kruskal-Wallis (KW) test performed for this bile acid did not show significant differences in accumulation between different groups. Review of the scatter plot highlighted 3 healthy outliers. These samples were subsequently removed from the plot (figure 4.3.23), given the limited criteria for the condition of healthy was based on participants 'apparently healthy'. After which, the KW test re-applied to show higher, significant difference between groups, at a p value of 0.047. Alas, Dunn's multiple comparison was unsuccessful is demonstrating which pair of groups were significantly different, but the trend appears to be S>M>H. Tauro-congutated bile acids are more typically found in mice, compared to human bile acids which more frequently conjugate with glycine.

In an attempt to summarise this work, as with previous datasets 4A-C, a box plot was constructed comprising serum bile acid concentrations (ng/ml) across severe (S), mild/moderate (M), house-matched (H) and IBD groups. Statistical summary of the data is provided by Table 4.3.6 with mean BA concentrations and standard errors, including p values determined by individual KW tests. As with the faecal metabolome, several muricholic derived bile acids were detectable and quantified in serum, with possibly the highest concentrations detected in a few of the severe (S), see table 4.3.6. However, in a recent metabolomic study profiling bile acids in human plasma from patients with Alzheimer's disease (AD) various muricholic acid forms were below the limit of detection (Pan et al., 2017).

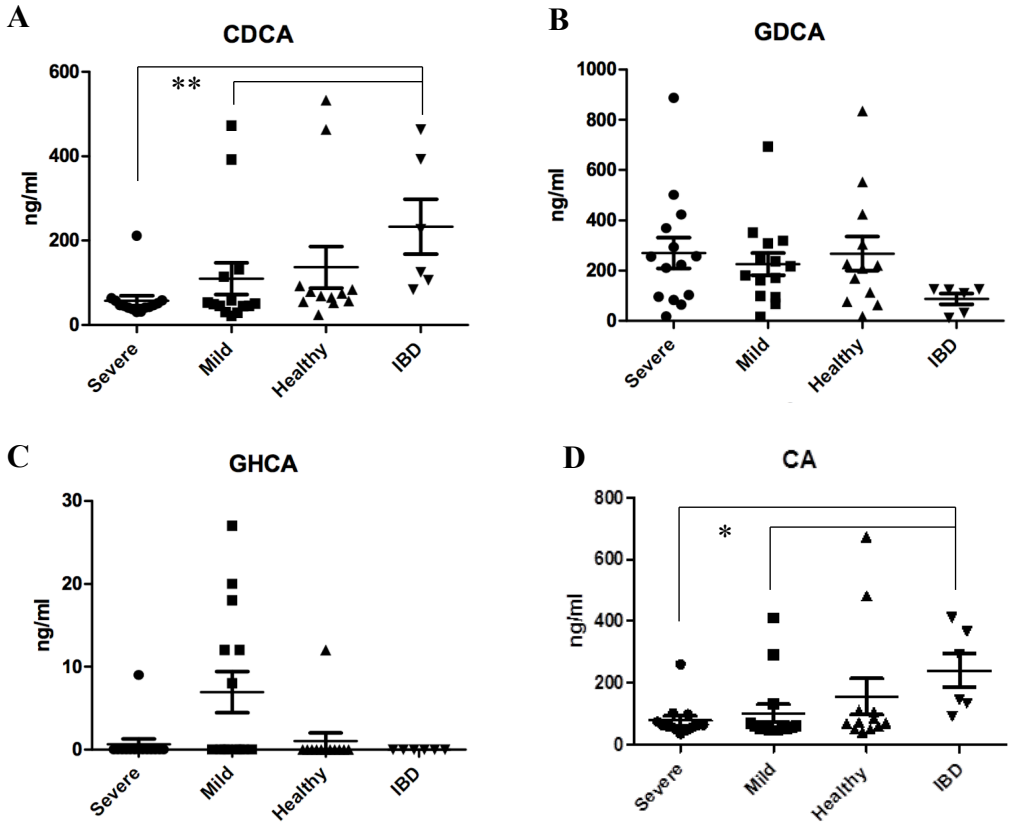

Figure 4.3.24 Selected scatter plots for absolute bile acid concentration across 4 bile acids in serum. Consistently the same patients are the represented as outliers within their respective group (S), (M), (H) for these particular bile acids. No clinical information was provided for IBD serum samples used in this analysis. KW test revealed GHCA group differences generative p value of 0.02, but failed Dunn's multiple comparison. CDCA **p=0.003 CA *p= 0.01

Chenodeoxycholic acid (CDCA) and cholic acid (CA) are considered primary bile acids that undergo synthesis in both the livers of humans and mice before conversion by intestinal microbes to lithocholic acid (LCA) and deoxycholic (DCA) respectively (Hu et al., 2014). CDCA is usually abundant in human bile, but is not compared with mice where is it converted to muricholic acids (Zhang & Klaassen, 2010). Higher serum concentration of CDCA and other bile acids such as GCA, GCDCA, TCDCA are noted with respect to liver injury and disease (Luo et al., 2018). No evidence, as such, is presented within these data to suggest severe (S) ME or mild/moderate (M) patients display signs of liver injury or disease. On the contrary, the CDCA scatter plot presented in figure 4.3.24 was highly significantly different ($p=0.003$) based on KW test and Dunn's multiple comparison, for the following trends, S<IBD, M<IBD. CDCA is normally abundant in human bile compared with mice where is converted to muricholic acid. Indeed, the earlier observation of higher faecal HDCA is also intriguing as it can be formed from MCAs.

4.4 Discussion

Metabolomics was used to profile metabolites derived from serum and the faecal microbiota of ME/CFS patients compared to HHCs. The composition of the intestinal microbiota was explored in the previous chapter in ME/CFS using metagenomics increasingly interprets the functional gene diversity, rather than its taxonomic profile, needed to carry out important functions including vitamin, short chain fatty acid production, amino acid synthesis, secondary bile acid metabolism and fermentation of non-dietary carbohydrates (Vernocchi et al., 2016). Metabolomics is able to compliment functional metagenomic interpretations, by providing a metabolic profile as an intermediate between microbiota-host interactions. Until now recent metabolome studies to date, have suggested some consistencies for alterations with the ME/CFS faecal and blood metabolome. These findings have been substantiated by independent research groups and by the application of different metabolomics methods using ^{1}H-NMR and Mass Spectrometry (MS). Based on this, it was expected that the severe ME patient cohort examined here would exhibit similar metabolic disturbances relating to their energy and lipid metabolism. Furthermore, given their severity of clinical status it was hypothesised that the scale of such metabolic difference may be accentuated in severe ME compared with the general mild/moderate ME patient population. The data presented in this chapter based on serum did not support this hypothesis. Indeed, the lack of any particular finding in either faecal and serum metabolome was surprising and appear to reject our hypothesis.

Faecal water collected from 11 severe ME patients and 6 house-matched controls were the first samples to be examined. These samples were collected in 2017 following changes made to sample collection where the patient was asked to provide samples from their own stool specimen which, did not allow for control of location of the sample from the entire stool. In an attempt to address the issues around the lack of standardisation frequently the case in microbiome-based studies, it was decided to collect the entire stool sample from each participant. Gratton *et al.* (2016) show that faecal homogenisation is an important step in overcoming sample variability according to where you sample even within same stool specimen (Gratton et al., 2016b). Transport time was also an additional factor when attempting to conduct patient home visits. There was considerable journey time for some sample collections depending on where they lived with respect to the site of sampling processing.

There may be a consensus regarding reduced butyrate production in the faecal metabolome in ME/CFS patients, although this was not seen in this study. No assumptions were made about the distribution of metabolite concentrations prior to statistical testing. To that end, a conservative approach was made in the decision to use non-parametric testing to compare differences across different groups. In contrast to parametric testing, this approach is more stringent, with less assumption but also does not account for the fact that each house-matched control is paired with a severe ME patient. However, this does not negate that upon review of the data in figures 4.3.3. there is great overlap in individual metabolite concentrations between the groups. Earlier work by Armstrong et al., (2017) using 900MHz ^{1}H-NMR, provided the most relevant incite in to the ME systemic metabolome since it also used ME/CFS serum, but only had the capacity to detect 29 metabolites. With the emphasis on the severity of ME with our patient cohort, the lack of any result is puzzling given that in the analysis of serum 53 metabolites there were detected and quantified in severe ME, again, no significant conclusions can be justified.

The lack of reproducibility continues to be a challenge for ME research, however this is layered with further challenges when considering potential methodological differences may be contributing dramatically to the outcome of the result. As discussed, sample collection and processing must also be controlled. Review of table 4.1.1 highlights serum versus plasma as the most obvious factor in accounting for variability with respect to small metabolites that appear to be more stable in plasma than in serum based on the lack of any consistent findings that have previously reported. Both serum and plasma analyses have been performed in ME patients using mass spectrometry but only those done using plasma highlight significant overlap in observed differences in metabolic pathways. Unfortunately, it was not possible to include plasma in this work since serum collection was originally prioritised for the purposes of identifying the presence of (auto)-antibodies towards gut microbes in future work. Serum is the preferred standard for antibody-based discovery. Moreover, serum collected from house-bound patients experienced variable delays (1-4 hrs) in transport to the laboratory for processing and storage at -80^{o}C. It is unknown if this causes further enhanced loss of some metabolites or if plasma would be more resilient. For future sample collection is would be highly preferably to include mobile refrigeration during transportation to maintain constant temperature of all samples.

Other methodological difference include NMR platform technology and equipment used. Armstrong *et al.* produced their data on a 900 MHz ^{1}H-NMR machine – which is 1.5 times stronger than the 600 MHz machine used in this chapter. Briefly, when a sample is placed in a strong magnetic field the nuclear spins allocate themselves to two energy levels: low ('spin up') and high ('spin down'). The energy level difference is small compared with thermal energy so the difference in number of nuclei in the lower and upper energy levels is very low e.g. 1 in a million. It is only this difference that we can detect. The difference in energy levels is greater and more detectable using 900 MHz machine versus 600 MHz. Moreover, signals are 1.5x more spread out at 900MHz, across 0-10 ppm, the full range of signals for hydrogen. For these reasons, a signal of interest that is overlapped with an interfering signal at 600 MHz may be better resolved at 900 MHz.

Contrary to Armstrong et al. (2017), no evidence has been found for increased fermentation within this severe patient cohort. Particularly no difference was found for faecal butyrate or any other SCFAs. Often the faecal specimen provided by the patient was significantly less than that from house-matched control and appear very hard and dehydrated. Taking into account the disabling nature which confines these patients to the house and bed, often patients eat very little and do not drink enough. This most likely decreases gut transit and is a process that is known to increase the pH in the gut environment (Thursby & Juge, 2017). Studies have documented the effect of higher pH to show increased SCFA production and a decrease in lactate concentration, another metabolite in which no significant difference was observed (Belenguer et al., 2007).

One interesting metabolite detected was γbutyrobetaine. This could be measured at a low level in most samples (patients and controls) but was notably higher in 3 of the patients. It is a gut microbial metabolite of L-carnitine (Koeth et al., 2014) and an intermediate in the conversion of carnitine to trimethylamine and TMAO. L-carnitine is found in meat, fish and eggs, however could also suggest these patients are taking a supplement with carnitine. Another possible explanation could be these patients lack bacteria that effect the conversion to TMA or TMAO. Increased *Lactonifactor spp.* belonging to the family *Lachnospiraceae spp.* and *Ruminococcus spp.* can produce TMAO, whilst *Bacteroides spp.* has been found to be less abundant in its presence (Wang et al., 2015). Another metabolite that was only found in two patients was taurine. Taurine may be relevant since it is known to conjugate to primary bile acids in the liver whose function is important in lipid metabolism and consequently energy homeostasis. Like, L-carnitine, taurine is also

found in many health and energy supplements which we were unable to obtain any information regarding their consumption by ME or control subjects included in this study.

The liver is the site for bile acid synthesis from cholesterol. Tauro-chenodeoxycholate (TCDCA) and glyco-chenodeoxycholate (GCDCA) have already been reported to be reduced in ME/CFS, which may suggest potential liver damage, although more the status of more conventional markers for this are unknown in ME/CFS (Germain et al., 2017). Bile acids are an important aspect to lipid metabolism since they facilitate the digestion and absorption of lipids within the small intestine. Interestingly, high fat diets may lead to partial intestinal permeability dysfunction; thus, bile acid metabolism was explored in these severe ME patients in the context of a role for a leaky gut in ME/CFS as providing a potential mechanistic role in these circumstances. Moreover, an unidentifiable suspected 'bile acid', to which the closest reference match was glycocholate, appeared significantly higher in severe patients (fig. 4.3.2) based on NMR resonances observed from their faecal water. Out of the 45 metabolites, this unknown bile acid was the only significantly different metabolite (KW, $p=0.03$).

Global metabolite profiling uses an untargeted approach in the field of biomarker discovery, however different platforms can be limited to the size and chemical properties of metabolites they detect. Increasing the number of metabolites identified requires authenticated standards included in the analysis to compare mass spectra and retention time with sample metabolites (Roessner, 2001). The choice of sample extraction solvent can allow for separation of polar and apolar metabolites. With our NMR work, chloroform/methanol was used for biphasic solvent extraction, thus our focus was on small soluble metabolites in serum and faeces. The sensitivity and resolution of NMR is considered inferior the MS-based methods, therefore better coverage of the metabolome uses both of these in combination. Together ^{1}H-NMR and MS are the most powerful metabolomic techniques that define the number of metabolites in clinical samples (Collino et al., 2013). Other published ME/CFS studies have been able to detect a wide variety of metabolites with a range of physical chemical properties. Germain and colleagues used plasma to quantify 361 metabolites using Q-Exactive MS (QE-MS) and found ADP, ATP, pyrimidines and many amino acids were significantly decreased in ME (Germain et al., 2017). Indeed, it would be interesting to undertake similar sophisticated workflows and MS, as previously described, to examine these pathways in severe ME patients. However the majority of the "signature"

metabolites identified from the analysis of much larger numbers of metabolites (Armstrong et al., 2017; Germain et al., 2017; Naviaux et al., 2016) whose abundance was altered in mild and moderately affected ME/CFS patients; whilst of those metabolites overlapping with our study were found unaltered in severe ME/CFS patients.

The previous chapter discovered that severe ME patients tended to have less *F.prausnitzii* compared to HHCs.(fig. 3.3.11B). A reduction in this species has been well-established with IBD and considered an important contributor to intestinal health (representing 5% of the total microbiota) providing energy to colonocytes through butyrate production and simulating anti-inflammatory signalling pathways (Arumugam et al., 2011; Cao et al., 2014; Miquel et al., 2013; Qiu et al., 2013). Our expectation was to find a reduction in faecal butyrate. However, Armstrong and colleagues suggested ME/CFS patients to display increased microbial fermentation correlated with *Clostridium spp.* and *Bacteriodes spp*. producing higher levels of SCFAs, valerate, isovalerate and butyrate (Armstrong et al., 2017). None of these were found any different between our severe patients and HHCs, (figure 4.3.3) or from our sequencing data. Microbial volatile organic acids may be better targeted using GS/MS compared to NMR as the current agreement between metabolic studies in ME/CFS have been focused on using MS techniques (Germain et al., 2017; Naviaux et al., 2016).

Targeted bile acid mass spectrometry did not reveal any significant changes in bile acid composition between patients and controls and was not helped by the relatively low sample group sizes. This was in exception to serum CDCA found significantly lower in severe ME patient serum and is known to be reduced in fasting states (J. Zhang et al., 2017). Surprisingly, the alpha and beta forms, as well as tauro-conjugated muricholic acids were detectable across all samples in faecal water and serum even though it has been suggested that the human gut microbiota is unable to metabolize CDCA into βMCA (Martin et al., 2007, 2008; Sacquet et al., 1984, 1985). Conversely, mice can hydroxylate chenodeoxycholic acid (CDCA) in the liver at the 6β-position to form α-muricholic acid (MCA) and ursodeoxycholic acid (UDCA) to form βMCA. Cyp2c70 is the principal enzyme involved in MCA production and is responsible for the differences in bile acid metabolite profile between humans and mice with further heterogeneity introduced in secondary bile acid metabolism by intestinal microbiota where taurine/glycine conjugated primary bile acids undergo deconjugation by intestinal bacteria using bile salt hydrolases (BSHs). Tauro-

alpha/beta-muricholic acids (T- α/βMCAs) were also detected in patients and controls, despite also normally being considered as species-specific primary bile acids in mice that are lacking in humans. Notably, tauro-beta-muricholic acid has been studied as a farnesoid X receptor (FXR) antagonist in mice models for metabolic disorders including obesity and insulin resistance, where reduction of bacteria with BSH activity protected against obesity and improved insulin sensitivity (Prawitt et al., 2011). Further work is needed to explore the BA profile in ME/CFS due to it roles in participating in different signalling pathways involved in lipid, glucose, and energy metabolism.

Targeted analysis conducted in this way does have a drawback in that other less abundant, minority isoforms may go unnoticed in humans, such as muricholic acids. For instance, (García-cañaveras et al.,, 2012) were able to detect for the first time T-αMCA in healthy human serum using UPLC MRM MS, where in mice MCAs form >80% of the total primary acid pool (García-cañaveras et al., 2012). Analysis of faecal bile acid composition also revealed high levels of a mouse secondary bile acid, hyodeoxycholic acid (HDCA) shown in figure 4.3.20, in some severe ME patients. Although this result is not statistically significant, it appears convincingly higher in concentration for five severe patients (red box), at over twice the median concentration compared to the control group. In fact the conventional mouse gut microbiome is able to convert T-βMCA through bile salt hydrolase (BSH) and bile acid 7α-dehydroxlase forming β-MCA and hyodeoxycholic acid (HDCA; 3α,6α-Dihydroxy-5β-cholan-24-oic acid) respectively (Ridlon et al., 2014) . The higher levels of HDCA in severe patients is unusual and obscure when reviewing the current published literature which purport hydroxyl groups in human primary bile acids to mainly occupy the 3, 7, 12-position, whilst only mice can also add hydroxyl groups at the 6-postion forming HDCA and α/β/γ-MCAs (Sacquet et al., 1983). Indeed, the only difference between deoxycholic acid (DCA) and HDCA is the position of the hydroxyl group, which is at the 12-postion in DCA. To that end, HDCA is considered to be a major murine secondary bile acid, absent in humans, that is microbially generated from the primary bile acids αMCA and βMCA (Studer et al., 2016).

The microbiome is a source of various bile salt hydroxylases (BSHs) that can perform deconjugation of glycine and taurine to liberate free primary bile acids and 7α-dehydroxylating bacteria facilitating bile acid conversion. Member of *Lactobacillus spp.* and *Bacteroides spp.* are known to produce BSH, none of which we found correlations in our

earlier discussed sequencing of the ME/CFS metagenome (De Smet et al., 1995; Stellwag & Hylemon, 1976). An unidentified Gram-positive rod-shaped bacteria capable of dehydroxylation of the 7β-hydroxy group and epimerization of the 6β-hydroxy group into a 6α-hydroxy group converting βMCA into HDCA was isolated from rat intestines (Eyssen et al., 1999). Therefore, this makes the higher levels on detection in some severe samples, in tandem with low levels of MCAs a possible interesting finding. HDCA does not appear to be used as a substrate for further conversion by intestinal bacteria and has been reported to be well absorbed in the human intestine, although serum levels were unremarkable in severe ME serum (Sacquet et al., 1983).

Thus, mice and humans have different bile acid pools that may affect signalling through bile acid receptors and host physiology very differently across species further highlighting the microbiome's role interaction in host species metabolism. This warrants caution when translating the bulk of research literature performed in mice to explain human disease states. For instance, germ-free mice have revealed that a lack of a gut microbiota not only changes the bile acid pool within the entero-hepatic circulation and serum but also reduces availability of SCFAs, such as butyrate used as an energy substrate by colonocytes (Bäckhed et al., 2007; Wichmann et al., 2013). Consequently, these animals display hyperglycaemia and insulin resistance causing disruption to glucose metabolism. SCFAs are considered necessary for gut health, since lack of butyrate-producing bacteria has been associated with type 2 diabetes. Furthermore, in a recent report using mice with a disrupted microbiota caused by antibiotic treatment there was improved glucose homeostasis and insulin sensitivity compared to their GF counterparts. (Zarrinpar et al., 2018). Conflicting reports such as these and the known metabolic difference between mice and man highlight the complexities of microbial metabolic interactions with host metabolism and physiology. More observation led studies must be applied in human disease states, such as this work in severe ME to decipher how apparent changes in the gut microbiota may be altering host metabolism and physiology particularly with respect to host lipid and energy metabolism.

Our data is most relevant for comparison with Armstrong and colleagues, based on ^{1}H-NMR measurements in faecal water and serum, whereas the other studies use plasma and MS in in combination with different workflows. Serum versus plasma is another consideration that has to be made when comparing studies and the respective metabolomic profile will be different (Yu et al., 2011). The coagulation and separation of serum within the gel

collection tube can alter the metabolite profile and, as with metagenomic research, highlights the important for sample collection and processing standardisation (Liu et al., 2018). Moreover, blood transport time and storage were significant cofounding factors given that these samples were obtained from home visits and had various delays in processing for long term storage (Jobard et al., 2016). The drawback is that we have been unable to detect and quantify a large number of metabolites that have been reported to alter various aspects of ME/CFS metabolism. Targeted acquisition of metabolites in these pathways can be sought with more sophisticated workflows using MS, as previously described (Germain et al., 2017). As an example, we targeted bile acids in our analyses, and acknowledge their biological importance to energy metabolism and glucose homeostasis (Shapiro et al., 2018; Wahlström et al., 2016). Blood serum levels of BAs are difficult to interpret given the known impact diet and the time of taking the sample. However, TDCA was significantly higher ($p = 0.047$) in severe ME (fig. 4.3.22) and may directly inhibit colon motility and slow intestinal transit time and gastric emptying as shown in mice (Abdu & Albaik, 2016). Interestingly, bile acids can inhibit LPS-induced TNFα secretion, while conjugated bile acids can act as signalling molecules for TGR5 pathways to modulate inflammation (Chang et al., 2018). Moreover, TCDA may also decreases systemic inflammatory cytokines by increasing immune-regulatory cells (Chang et al., 2018).

In conclusion, despite the adoption of similar sample processing and acquisition of NMR metabolic profile, we were unable to replicate the observations reported by Armstrong and colleagues. Despite the relative reduction in *F. prausnitzii* in severe ME patients reported in the previous chapter, faecal butyrate concentration was not decreased compared to house-hold controls. Of note, the levels of muricholic acid and their derivatives cholic acid and chenodeoxycholic acid (CDCA), which are the most important human primary bile acids, were significantly lower in the serum of severe ME/CFS patients. Analysis of faecal bile acid composition also revealed high levels of a mouse-associated secondary bile acid, hyodeoxycholic acid (HDCA) in severe ME. HDCA is considered to be a major murine secondary bile acid, absent in humans, that so far, has only reported to be microbially generated within the rat intestinal microbiome from primary bile acids αMCA and βMCA (Eyssen et al., 1999; Studer et al., 2016). Further work exploring the significance of specific alterations of bile acid profile in ME/CFS may yield new mechanistic insights into how the alterations in primary bile acids impacts on signalling pathways involved in lipid, glucose, and energy metabolism that are a general feature of ME/CFS.

Chapter Five

5 Detection of IgA-coated faecal bacteria in severe ME/CFS patients

5.1 Introduction

Increased intestinal permeability, or "leaky gut" is not currently recognised as a standalone medical disorder that can be diagnosed and treated. In health, the intestinal epithelial barrier acts as a physical barrier protected by a immunologically active mucus layer with bacteriostatic and bactericidal properties, such as anti-microbial peptides, called defensins, to stop invasion and translocation of harmful microbes and toxins that may elicit inflammatory damage from infection injury (Khounlotham et al., 2012). Increased gut permeability represents a major loss of this barrier function causing increased exposure of intestinal microbes to the intestinal immune system with the risk of translocating bacteria entering the systemic circulation and other sites in the body triggering widespread systemic immune system activation (Fasano, 2012). Finally, the intestinal microbiota represents an entity that can be manipulated with diet and pre-/probiotic interventions, and in extreme cases with faecal transplantation of the microbiota in an attempt to treat a "leaky gut" and ameliorate inflammatory-driven intestinal barrier tissue damage.

Bacterial and viral infections are commonly reported prior to, and during the onset of autoimmune disease where intestinal permeability may increase the exposure of immune cells to intestinal microbes and environmental triggers (e.g. food, medications) which does not normally occur in good health (Fasano, 2012). This can then be contributing to a mechanism where reactivity against foreign bacterial and viral antigens leads to cross-reactive antibodies towards self-epitopes which share a common protein sequence similarity during a process referred to *a molecular mimicry* (Oldstone, 1998). The concept of molecular mimicry was first described in 1983 where monoclonal antibodies to measles virus P protein (MV-P) were found to react with intermediate filament protein, vimentin (Fujinami et al., 1983). Neurological symptoms are triggered during *Campylobacter jejuni* infection in some individuals. This food-borne pathogen is a major cause of gastroenteritis that can trigger Guillain-Barre syndrome (GBS). During the infection antibodies are made reactive to lipooligosaccharide (LOS) structures on the outer surface membrane of *C. jejuni*. Structural analysis of LOS includes sialyated moieties homologous to human gangliosides leading to antibody cross-reactivity directed against peripheral nerves as well as *Campylobacter* (Heikema et al., 2010). Infection appears to initiate these pathological events, but after pathogen clearance autoimmunity persists suggesting there are additional perpetuating factors which drive this phenomenon, which may be explained by long lived auto-antibodies and/or persistent regeneration of new autoantibodies.

Less than 10% of persons with a genetic risk for developing type 1 diabetes develop disease. Antigen presenting cells, such as macrophages and dendritic cells, are in close proximity to the intestinal barrier and their responsiveness is dependent on individual genotypes of HLA class I and II molecules for presentation of antigen to T cells. To that end, a genetic predisposition is not sufficient for disease development. Increased intestinal permeability may have a key role in a pre-autoimmune mechanism which initiates or progresses autoimmunity in T1D patients causing auto-destruction of insulin producing pancreatic β cells (Visser et al., 2009).

Evidence for existence of leaky gut in patients with type 1 diabetes (T1D) and their relatives, is based on expression of the tight junction protein, zonulin which is frequently upregulated in autoimmune disease and causes disassembly of tight junctions between gut epithelial cells (Fasano, 2011; Sapone et al., 2006). This is further correlated with increased intestinal permeability measurements of sugar absorption greater in 42% out of 339 diabetic patients in comparison to age-matched controls (Sapone et al., 2006). A separate independent study also found increased intestinal permeability preceding clinical onset of T1D by comparing the intestinal permeability to sugars in 18 preclinical subjects with 28 new onset and 35 long-term with 40 healthy controls (Bosi et al., 2006). These findings underpin the concept that a leaky gut may shift the balance towards contribution of various environmental factors including changes in the gut microbiota, in conjunction with genetic factors and immune responsiveness which conspire to cause the pathogenesis of T1D. However, the detail of the precise order these events following increased intestinal permeability is not known and therefore in the various conditions associated with increased permeability it is not known how important altered intestinal permeability relates as a cause or consequence across these disease pathologies.

T1D patients have also shown high titres of antibodies against glutamate decarboxylase (GAD), an enzyme found in pancreatic β cells, which has sequence similarity to coxsackie B viral protein p2-C suggesting a viral trigger for this disease. Interestingly, PBMCs isolated from patients with autoantibodies to islet cells proliferated in response to GAD and this viral peptide. However, it is unclear what are the most significant environmental triggers are or the sequences of such events in the development of T1D although there is some evidence that diabetogenic T cells are initially primed in the intestine in response to dietary

gluten and is therefore associated in pathogenesis (Antvorskov et al., 2014; Visser et al., 2009).

- *Measuring intestinal permeability in patients*

The current method to assess intestinal permeability in patients is not routinely used in NHS clinical practice because it is invasive and requires medical supervision with delayed sample collection of urine to measure the rate of excretion of low to high molecular weight sugars, lactulose/mannitol/sucralose (Andre *et al.,* 1988). High molecular weight molecules such as lactulose rely on much slower transcellular uptake across the epithelial barrier as opposed to paracellular transit of smaller sugar probes such as mannitol into the circulation. Determining the ratio between the concentrations of these two molecules in the patient's urine after 5-6 hrs requires sophisticated analytical equipment such as HPLC/MS not found in conventional NHS hospital laboratories. Moreover, results obtained generally reflect changes in small intestinal permeability as lactulose is degradable by bacteria in the colon (Bischoff et al, 2014).

In their review Bischoff et al., 2014 described at almost 100 publications linking intestinal permeability to disease. In the 4 years since their review on this topic the majority of the methods used to assess intestinal permeability have not advanced in attempt to address their limitations. Another common choice of method is to examine patient serum/plasma for levels of bacterial endotoxin (LPS) using the lysate from horseshoe crabs, which is highly sensitivity to bacterial endotoxins forming a gel clot. This is known as the Limulus-Amoebocyte Lysate (LAL) assay. Such assays can be technically challenging to perform since the enzymes in the clotting cascade in this crab can be inhibited by various protein factors in human blood in addition to EDTA and heparin anticoagulants found in blood collection tubes can all effect endotoxin recovery. Manufactures of LAL kits do not recommend its use in clinical samples without undertaking special precautions to minimise these effects. In addition to circulation levels of LPS, other surrogate markers such as soluble CD14 and LPS-Binding Protein (LPB) which bind help to and sequester LPS have been documented for many diseases (Buscarinu et al., 2017; De Kort et al., 2011; Irvine & Marshall, 2000; Maes et al., 2007; Rojo et al., 2007). LPS measurement may be the preferred surrogate marker for intestinal permeability for its obvious advantages over the L/M test which requires significant patient intervention. Despite the technical complications assaying for LPS in plasma, data published comparing the disease activity of IBD patients correlated increased

LPS with clinical worsening of the patients' condition (Rojo et al., 2007). Plasma LPS level could also separate patients in inactive and active Crohn's disease which had significantly higher circulating LPS compared with inactive and active Ulcerative Colitis (UC) patients.

In the pursuit of diagnostic biomarkers, systemic antibodies reactive towards intestinal microbes, as well as autoantibodies resulting from intestinal inflammation, have been explored in the context of leaky gut in IBD where increased intestinal permeability has been associated in the onset of pathology as well as the relapse or progression of disabling symptoms (Macpherson et al., 1996; Mitsuyama et al., 2016; Palm et al., 2014; Sapone et al., 2006; Tibble et al., 2000). A predisposition to increased intestinal permeability may explain why certain individuals are prone to developing IBD since mice genetically engineered to lack junctional adhesion molecule A (JAM-A) and adaptive immune cells develop colitis (Khounlotham et al., 2012). Whereas JAM-A deficiency alone did not cause colitis because of compensatory mechanism leading to an enhanced adaptive immune cell response and increased IgA secretion (Khounlotham et al., 2012). The combined loss of barrier and adaptive immune cells exaggerated acute mucosal injury in these mice (Khounlotham et al., 2012). Many IBD patients report stressful life events prior to episodes of illness. Stress has been implicated with negative consequences for the immune system and increasing intestinal permeability and may be an etiological factor in promoting a leaky intestinal barrier (Ait-Belgnaoui et al., 2012; Glaser & Kiecolt-Glaser, 2005; Vanuytsel et al., 2014).

It has been proposed that autoantibodies reactive with the intestinal microbiota and intestinal epithelial tissue be useful markers in IBD patients and provide insight to its immune-mediated pathogenesis. Indeed, a diagnostic test to differentiate IBD from non-IBD, and Crohn's from Ulcerative colitis, has been commercialised by Prometheus® Laboratories (Nestlé Health Science) called IBD sgi Diagnostic®. Now its 4th generation of this screening panel including 9 serological markers (Prometheus Laboratories, San Diego, CA). The test uses the ELISA platform to quantify anti-microbial antibodies such as anti–*Saccharomyces cerevisiae* antibody (ASCA), antibody to *Escherichia coli* outer membrane porin C (OmpC), antibody to *Pseudomonas fluorescens*–associated sequence (anti-I2), and antibody to flagellin Cbir1 (anti-CBir1) (Targan et al., 2005). A report by Benor et al. in 2010 highlighted an earlier version of this test, IBD7, based on 7 serological markers without any genetic or inflammatory markers now included in the up-to-date version, was not successful at predicting IBD in children referred for suspected IBD and initial clinical

evaluation and diagnostic by conventional endoscopy and histopathology (Benor et al., 2010); Here, detection anti-flagellin antibodies only had a specificity of 53%. Elevated IgG antibody titres have been reported in 120 Crohn's patients compared with 120 non-IBD, age-matched controls, against a cocktail antigen preparation derived from *B. vulgatus* and another using 20 mucosal-associated gut bacteria, and is consistent with loss of barrier function causing increased exposure to microbial antigens and an altered immune response (Adams et al., 2008). It still remains that clinical diagnosis of IBD requires invasive endoscopy and histopathology to inform differential diagnosis of clinical forms such as Crohn's Disease and Ulcerative Colitis.

- *Antimicrobial antibodies to assess intestinal permeability*

Despite substantial evidence for increased intestinal permeability in neurological/neuropsychiatric pathologies such as MS, Parkinson's disease, stress, anxiety, depression, autism spectrum disorders, as well as in ME/CFS, there is limited data available on systemic antibody responses towards intestinal commensal bacteria in health and disease (Hollander, 1999; Vanuytsel et al., 2014). How intestinal permeability contributes towards a disease mechanism is poorly understood in these conditions although there is some evidence to suggest increase intestinal permeability precede years before onset of diabetes and Parkinson's Disease and first degree relatives of these patients also have higher intestinal permeability (Bosi et al., 2006; Forsyth et al., 2011). Anti-microbial antibodies may be more informative and evident of decreased compartmentalisation between the local intestinal immune system and systemic immunity, which may increase the presence of anti-microbial antibodies to intestinal bacteria in samples of peripheral blood. Indeed, systemic IgA, IgG and IgM antibodies reactive against *E.coli, E. faecalis, E. coli Nissle, B. fragilis, K. pneumoniae, and B. thetaiotaomicron* have been measured in 29 IBD patients (a combination of mild/active and active CD and UC) and 19 controls using live bacterial fluorescence activated cell sorting (FACS) (Haas et al., 2011). It is perhaps not surprising that severe chronic enteropathy is associated with IBD patients to have higher antibody titres in IBD patients probably due to increased exposure in the gut arising from damage caused to the intestinal barrier. The same study highlights chronic HIV-1 infection association with enteropathy and B cell disturbances, with data suggesting bacterial translocation arises from circulating LPS, sCD14 and butyrate potential driving chronic immune activation. However, comparison of systemic antibodies to gut commensals in these patients to healthy controls were no different and did not support their hypothesis

for gut bacteria driving this chronic immune activation. The authors acknowledge lack of data on local immune responses in the gut of these patients since faecal samples were not available to study IgA-responses to gut commensals where distinct reactivity to certain members of the intestinal microbiota provides an IgA +/- index of specific antibodies that have been identified in IBD (Palm et al., 2014). As a result, the earlier reports of increased bacterial translocation and LPS exposure in HIV-1 appear misleading since Haas et al. did not replicate increased LPS or endoCAb levels. To that end, increased intestinal permeability does not appear relevant cause for immune activation in chronic HIV-1 infection.

The gut bacteria in the lumen do not normally cause a systemic immune response as the gut is considered a separate closed compartment (MacPherson & Uhr, 2004). On the basis a leaky gut reduces the compartmentalisation between the gut immune system and systemic immunity, blood serum is becoming an attractive sample for quantifying antibodies against gut commensals. Previously where elevated LPS, sCD14, LPS-bind protein (LBP) in serum has indicated leaky gut, by identifying high titres of commensal antibodies in peripheral blood as well as confirming a series of specific Here there is a requirement for a rapid, high-throughput method for simultaneous detection of multiple commensal antibodies in a single serum sample.

Current methods such as live bacterial FACs and traditional ELISA can only quantify antibody titres towards a select number of commensal isolates whilst it is estimated that there are 1000 species of gut bacteria present in a healthy gut (Qin et al., 2010). In an attempt to address this problem, in this chapter a new technique for a leaky gut microarray chip is presented as well as a flow cytometry to measure anti-microbial antibodies to faecal bacteria. This technique uses existing DNA microarray printers to deliver whole cell bacteria onto a glass slide coated with substrate designed to immobilise cells. Following incubation with a minimal amount of patient serum, such slides can be screened with a secondary anti-human IgG antibody for reactivity against several candidates of the microbiota, figure 5.1.1 using a standard microarray scanner.

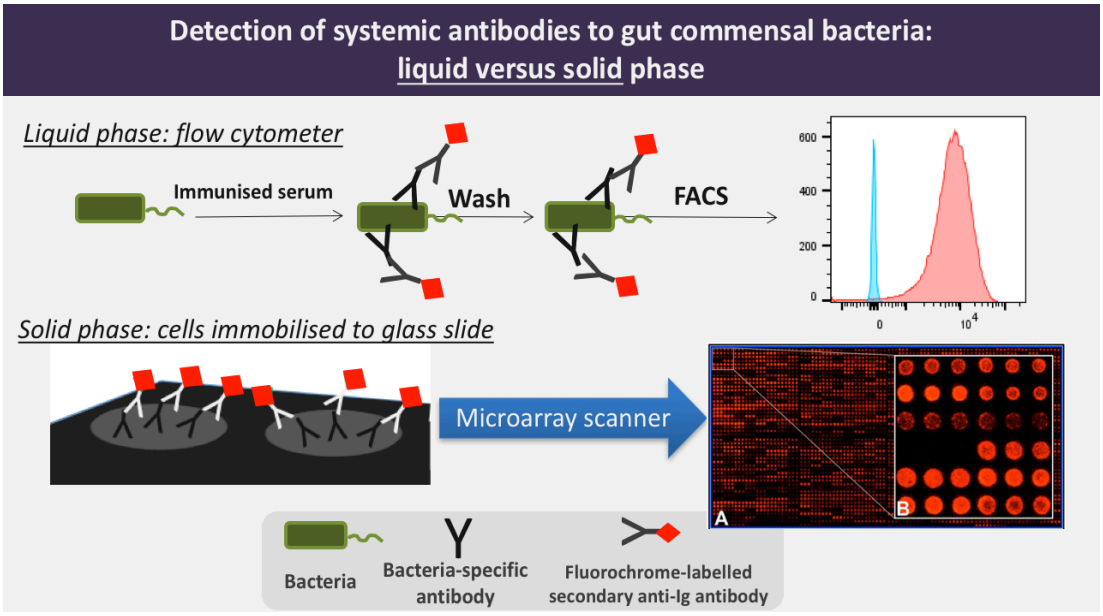

Figure 5.1.1 Comparison of methods used in this chapter for detecting antibodies against intestinal microbes in faeces (top) and serum (bottom). Top: isolated faecal bacteria suspended in liquid can be incubated with IgA-specific and binding detected using a flow cytometer. Bottom: in adaptation to a method reported by Thirumalapura et al., 2006 simultaneous screening of serum against multiple intestinal bacteria immobilised onto nitrocellulose can be assessed using a conventional DNA microarray scanner and microarray printing equipment.

Bacteria have previously been immobilised onto nitrocellulose-coated glass slides used for the detection of antibodies in sera of dogs infected with *Francisella tularensis* (Thirumalapura et al., 2006). The method used both Gram positive and Gram-negative bacteria and reported successful immobilisation onto commercially available nitrocellulose-coated glass slides. An immunoassay of this kind has not been reported for use in human serum antibody detection. As a platform, microarrays offer high-throughput capability that would favour screening multiple serum samples for reactivity against potentially hundreds of bacterial isolates from the human gut microbiota. In a single experiment this format would aid simultaneous antibody and help identify specific titres of antibody relevant to disease pathology and the status of the immune system. This assay would not only be useful for ME/CFS research but may also facilitate other areas of research with difficultly in establishing a causative role for increased gut permeability.

- *Evidence of increased intestinal permeability in ME/CFS*

Evidence of raised concentrations of serum IgA and IgM against LPS in CFS patients for a limited number of enterobacteria isolates has been obtained in several studies, concluding that serum IgA levels to selected isolated bacterial species also correlated with severity of illness using the Fibro-fatigue scale (Maes et al., 2007). These isolates include *Hafnia alvei, Pseudomonas aeruginosa, Morganella morganii, Proteus mirabilis, Pseudomonas putida, Citrobacter koseri,* and *Klebsiella pneumonia* (Maes et al., 2007). It has been proposed that severity of symptoms of fatigue, IBS symptoms, and failing memory/concentration in some ME/CFS patients originated from having a leaky gut which drives inflammation and cell mediate immune activation and altered cytokine production (Maes & Maes, 2009). In a case report on a 13 year old girl who showed high titres for IgM against LPS of enterobacteria, normalisation of leaky gut led to complete remission of her symptoms using a combination of antioxidants, zinc and glutamine, with immunoglobulin therapy (Maes et al. 2007). Maes also report higher serum antibody titres for the same enterobacteria in patients with major depression disorder (MDD). In 2013, Maes reported autoimmunity in some ME/CFS patients and increased IgA responses towards commensal enterobacteria, all of which were associated with increased fatigue, neurocognitive and autonomic symptoms, sadness and a flu-like malaise (Maes et al., 2013). Leaky gut may well support autoimmunity but with limited data of the types of antibodies made to only a few commensal bacteria it is difficult to decipher the source of this phenomenon.

In summary, the current methods for defining intestinal permeability are not without limitation, open to misinterpretation, and are not widely used in clinical practice. Without improved methods to assess intestinal permeability and the role of the microbiota in disease, current therapeutics such as prebiotic and probiotics, and especially faecal microbiota transplantation may be ineffective. Detection of systemic IgG and gut mucosal IgA antibodies towards commensal bacteria as a surrogate for intestinal permeability in patients has yet to be explored in ME/CFS.

- *The role of mucosal IgA antibody in protecting the intestinal barrier*

The intestine generates several grams of IgA per day, secreted from large numbers of plasma cells from beneath the surface of the layer of epithelial cells which form the intestinal barrier and is the main mediator of intestinal mucosal immunity (Pabst, 2012). IgA antibody responses can be produced by T cell dependent and independent pathways (Macpherson et al., 2012). The majority of commensal bacteria have been found to mostly stimulate IgA production in a T cell independent manner resulting in low affinity or non-specific "natural" IgA antibodies which contribute to the shaping of the gut microbiota (Bunker et al., 2015; Rescigno, 2014). In contrast, T-cell dependent mechanisms for IgA production lend towards reactivity against non-self, bacterial derived specific antigenic proteins presented by dendritic cells and macrophages in Peyer's patches and mesenteric lymph node (mLNs) during infection (Bunker et al., 2015). Mucosal IgA also appears to have as significant role in immune compartmentalisation between the local and the systemic immune system since mice deficient in IgA produce higher serum antibodies towards gut commensals (Macpherson & Uhr, 2004; Sait et al., 2007).

More recently, in mice, the majority of the reactivity of sIgA appears to be naturally polyreactive against the commensal microbiota instead of being specific to individual bacteria taxa (Bunker et al., 2017). Whilst its primary function is to promote immune exclusion of intestinal pathogens by neutralising them for phagocytosis, the commensal member *B. fragilis* adapts it outer-membrane surface structures to promote IgA-binding, to gain access and colonise mucosal niches providing intimate contact with gut barrier epithelial cellular innate immune receptor such as TLRs (Donaldson et al., 2018). Another study found a proportion of the IgA repertoire contains reactivity towards specific commensal antigens that appears to be dependent on T cell pathways (Benckert et al., 2011). T cell independent pathways obliterated by MyD88/TRIFF double KO mice are deficient in 'naturally' polyreactive IgA antibodies and instead show systemic antibodies reactivity towards the intestinal microbiota (Slack et al., 2009). Supportive of systemic antibody production are Th1 and Th2 cytokines IFNγ and IL-4 known to trigger CSR to IgG1 and IgG2a and IgE in allergy, respectively (Mitsdoerffer et al., 2010) Finally, in the event of increased intestinal permeability, we hypothesis exposure to the intestinal microbiota will initiate pro-inflammatory T cell mediated responses that are known support B cell proliferation and affinity maturation within the gut-associated lymphoid tissue (GALT) enhanced antibody production (Mitsdoerffer et al., 2010). In humans, CD27+ and CD27-

IgA+ circulating memory B cells are known to exist which operate under T-cell dependant and independent pathways, respectively (Berkowska et al., 2015). T cell dependent CD27+ IgA+ circulation memory B cells may become activated in a pro-inflammatory milieu and secrete more sIgA. Conversely, CD27- IgA- circulating memory B cells are T cell independent and their IgA reactivity profile has shown to be polyreactive towards commensal members of the intestinal microbiota (Berkowska et al., 2015). Under normal homeostatic conditions, T(reg) and DCs derived cytokines IL-10 and TGFB would favour T cell independent B cell proliferation and CD27- IgA+ memory B cell production of "natural" polyreactive antibodies against the commensal microbiota, thus support the immunological barrier against bacterial translocation (Berkowska et al., 2015).

Based on studies carried out in animal models in a healthy gut microbiota, Foxp3+ T regulatory cells promote immune tolerance toward the commensal microbiota by supressing inflammation and regulating the diversity of IgA repertoire through selection in Peyer's patches enriched with antibody secreting B cells (Kawamoto et al., 2014). Foxp3+ T cells differentiate into T-follicular helper (Tfh) cells in germinal centres where they interact with naïve B cells to stimulate differentiation into gut homing IgA-secreting plasma cells whose quantity of IgA antibody production and specificity influences the composition of the gut microbiota (Kawamoto et al., 2014; Rescigno, 2014). Absence or dysregulation of IgA production severely impacts the composition of the gut microbiota (Kawamoto et al., 2012; Suzuki et al., 2004; Wei et al., 2011). M cells have a major role in the uptake of luminal antigens presented by APCs in Peyer's Patches and in their absence GCs in mice fail to maturate causing a decline in the total production of sIgA (Rios et al., 2016). Tolerogenic DCs suppress Th7/Th19 inflammatory responses through releasing retinoic acid, IL-10 and TGF-B with promote Foxp3+ T regulatory cells and can further differentiate into Tfh cells with express CD40L and IL-21 to induce B cell mediated IgA production in the germinal centres (GCs) (fig 5.1.2) (Gutzeit et al., 2014). A disrupted microbiota can also lead to altered antigen presentation and loss of tolerance potentially overwhelming the regulatory T cell maintenance of GCs and instead activate pro-inflammatory Th1/Th17-cell dependent IgA production. Further, increased intestinal permeability would facilitate increased uptake of bacterial luminal antigens by DCs which migrate to LNs where they interact with naïve T cells to trigger clonal expansion and differentiation into Th1/Th2/Th17 T cell subsets with their associated cytokine profiles influencing B cell interactions.

Elevated levels of secretory IgA are an apparent compensatory mechanism for compromised intestinal permeability and has been reported in mice deficient in junctional adhesion molecule A (Khounlotham et al., 2012). Interestingly in IBD the identification of taxa-specific levels of IgA-coating faecal bacterial has revealed distinct patterns of the colitogenic microbiota in IBD (Palm et al., 2014). Therefore, measurement of IgA-coated bacteria may be a future diagnostic marker for the outcome of the interactions between the immune system and gut bacteria. The status of IgA+/IgA- coated bacteria in addition to specific systemic antibody responses to gut microbes are not known in ME/CFS.

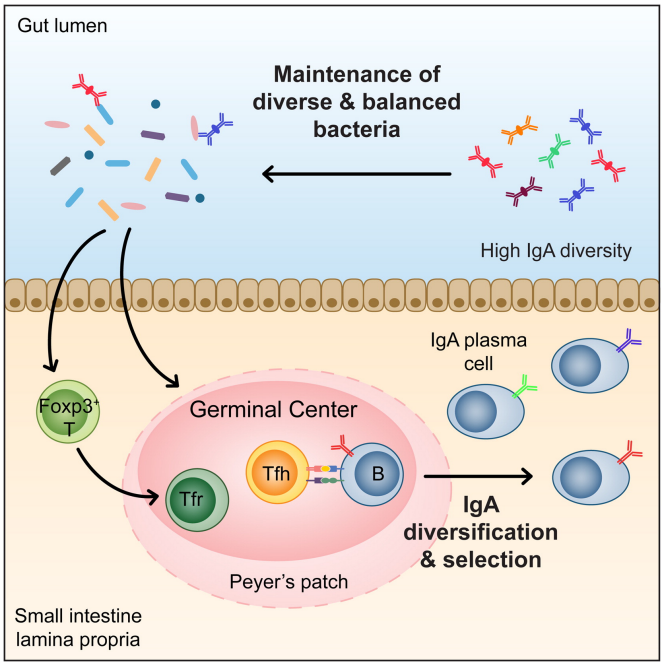

Figure 5.1.2. A healthy intestinal microbiota promotes Foxp3+ regulatory T cells to interact with B cells to undergo class switch recombination (CSR) and somatic hypermutation (SHM) in germinal centres to generate polyreactive or "natural" IgA antibodies to maintain microbial diversity. B cells residing in germinal centres interact with T-follicular cells which migrate to germinal centres (GCs) by expressing CXCR5 chemokine receptor (King et al., 2008) to stimulate B cell maturation into long-lived IgA-secreting plasma cells. Graphical abstract taken from Kawamoto et al., 2012

- *Experimental approach*

Observations of IgA-coated faecal bacteria can be easily assessed with minimal invasiveness to the patient since no blood extraction is needed. Intestinally secreted IgA antibody can be visualised using an anti-human IgA secondary antibody conjugated to APC and measured by flow cytometry as a proportion of total faecal bacteria (Palm et al., 2014).

With the necessary antibody isotype control for excluding nonspecific binding, flow cytometry has a major advantage over traditional ELISA methods and western blotting techniques, which usually test single bacterial antigen (LPS) extracted from bacterial lysate as opposed to whole cell bacteria which maintain the integrity and full complement of bacterial cell antigens to which the host immune system would be exposed to in vivo.

Patient antibodies which target bacterial surface antigens in pure culture and in human faeces have been explored using flow cytometry (Moor et al., 2016; van der Waaij et al., 1994). This has an added advantage over more traditional techniques such as an ELISA since the bacteria are in liquid suspension and do not require immobilisation to a micro-titre plate or glass slide. It is also much easier to adjust bacterial densities in liquid phase and to detect discrete bacteria populations within a faecal bacteria suspension to which antibodies have bound to. Moreover, faecal flow cytometry examines the entire faecal bacteria cell population unique to that individual which can lead to the identification of specific bacterial subpopulations. Until now, faecal IgA production has not been explored in the ME/CFS population and may be useful additional marker for increased intestinal permeability. The benefit being this is a potential non-invasive method that can determine this status without the need a blood sample.

5.1.2 Aims & Objectives

The first aim of this chapter was to determine the suitability of a whole-cell bacterial microarray ("chip") to assess ME/CFS patient serum antibody reactivity against representatives of the intestinal microbiota using immunofluorescence and high-throughput microarray scanning.

In order to achieve this aim, the following objectives were set out:

- to determine the stability of lab-cultured intestinal bacteria once immobilised onto nitrocellulose-coated glass microscopy slides;
- establish an assay protocol using a microarray scanner to detect polyclonal anti-microbial antibodies generated in rabbit from a stool sample provided from a healthy donor (positive control);
- following validation of the microarray, screen blood serum from severe ME/CFS patients and house-hold controls;
- to detect serum antibody reactivity against this microarray to determine intestinal permeability status in ME/CFS versus house-hold controls.

The second aim of this chapter was to assess intestinal IgA reactivity against faecal microbes, isolated in a faecal liquid suspension from patients and house-hold controls using a modified method of flow cytometry:

- to exclude faecal contaminants by using a nuclei acid stain to resolve microbes;
- in order to determine if severe ME patients have a higher relative abundance of IgA-coated faecal bacteria compared with their house-hold controls;
- to assess faecal IgA reactivity against intestinal bacteria with serological markers such as LPS and LBP, to see how IgA-bound faecal bacteria may serve as a surrogate marker for interpreting intestinal permeability in patients.

5.1.3 Hypothesis

Patients with severe ME/CFS have increased intestinal permeability, which causes a loss of compartmentalisation between the intestinal and systemic immune systems (fig. 5.1.4). This exposes the intestinal microbiota to the immune system leading to increased T-cell dependant mucosal IgA production and reactivity towards faecal bacteria. Secretory IgA is therefore a potential biomarker for intestinal dysbiosis and increased barrier permeability (fig 5.1.3).

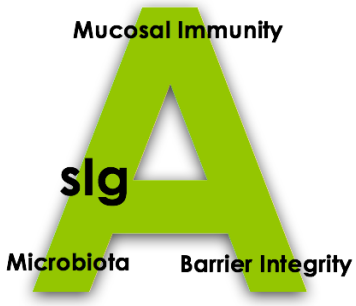

Figure 5.1.3 Secretory IgA regulates gut microbiota composition and protects the intestinal barrier. IgA is the predominant antibody isotype found in the intestine and recognises a broad range of members of microbes. Levels of IgA coating intestinal bacteria may be a marker for increased intestinal permeability in an attempt to neutralise commensal bacteria as well as enteric pathogens that may be relevant to ME/CFS pathophysiology. Increased IgA-bound bacteria may also indicate dysbiosis resulting from the interactions between intestinal microbes and the immune system in these patients.

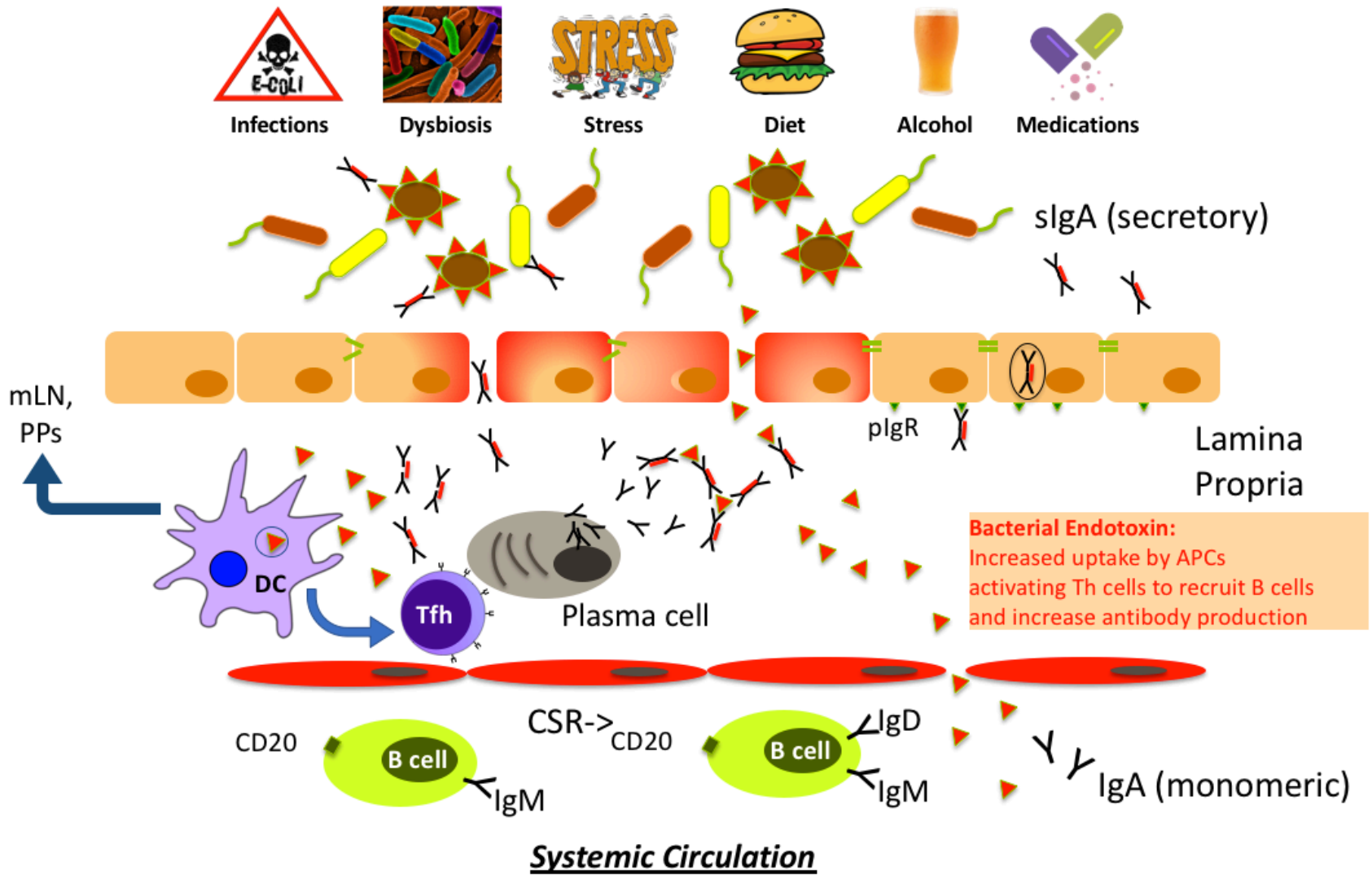
Infections
Dysbiosis
Stress
Diet
Alcohol
Medications
sIgA (secretory)
mLN,
PPs
pIgR
Lamina
Propria
Bacterial Endotoxin:
Increased uptake by APCs
activating Th cells to recruit B cells
and increase antibody production
DC
Tfh
Plasma cell
CD20
B cell
IgM
CSR->CD20
B cell
IgD
IgM
IgA (monomeric)
Systemic Circulation

⇐ **Figure 5.1.4 Increased intestinal permeability facilitates translocation of bacterial endotoxin (LPS) and exposure of mucosal-associated bacteria**. Antigen presenting cells (APCs) interact with members of the microbiota to present bacterial antigens to T-helper cells which stimulates polyclonal B cells activation and expansion to produce antibodies towards these members of the intestinal microbiota. Flow cytometry can be used to identify IgA-bound bacteria within mixed faecal bacterial suspensions obtained from patients and their house-matched control. Higher levels of IgA-coated bacteria may a valid indicator of intestinal permeability in accordance with other serological marker for evidence of bacterial translocation. Diagram created in Microsoft® PowerPoint® by Daniel Vipond

5.2 Materials & Methods

5.2.1 Solid versus liquid phase assay for bacterial antibody detection

The methods used in this chapter attempt to probe human serum and faeces to elucidate immunoreactivity against whole cell faecal bacterial surface antigens presented on a solid slide and in liquid suspension.

5.2.2 Bacteria Microarray

The protocol for a whole cell bacterial microarray was based on the method of Thirmulalapura and colleagues using Gram positive and Gram negative bacteria immobilised onto nitrocellulose-coated glass slides to detect antibodies in canine infected serum (Thirumalapura et al., 2006).

- *Strain preparation*

Bacterial cells were resuscitated from a -80^{0}C glycerol stock and grown for 16 h under appropriate growth conditions. Cells were harvested by centrifuging at 6000 x g for 10 min. Cells were washed in PBS and adjusted to an optical density (OD) of 1.0 ± 10% at 600 nm and plated onto solid agar media for CFU counting. For visualisation purposes, bacteria were fluorescently stained using 1µl/ml Baclight® Red or Sybr Green nuclei acid (x10,000) stain, diluted 1:10,000 for 30 min. Bacteria were inactivated by fixing in 1% paraformaldehyde (PFA) for 15 min to preserve whole cells structure before use in experiment. Based on colony counting experiments, one millilitre of cell suspension represents approximately 10^8 cells.

- *Microarray construction and use*

The ProPlate® microarray slide module (Grace Bio-Labs, Sigma cat. GBL204839) was inserted onto the surface of a SuperNitro Microarray substrate glass slide containing a 150 µm layer of nitrocellulose (Arrayit® item no. SNM) to create 64 discrete wells for pipetting sample. 50 µl of fixed bacterial cells in PBS suspension was pipetted into each well and any remaining wells filled with PBS. The slide coupled with its silicone gasket was held in place with snap clips before being placed into a makeshift polystyrene block enclosed within a centrifuge swing bucket and monitored whilst operating at 700 rpm (99xg) for 15 min to pull down cells onto the slide surface. The slide was left overnight at 4^{0}C to facilitate binding of bacteria to the nitrocellulose coating on the slide.

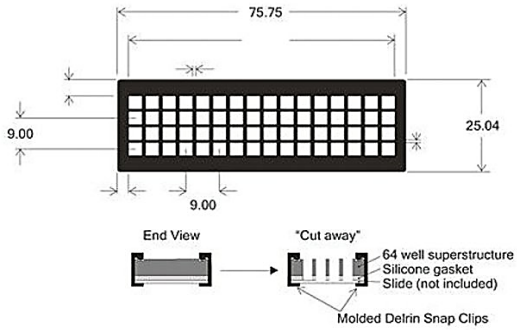

Figure 5.2.1 Grace-Biolab ProPlate® 64-well microarray slide module to create wells on a nitrocellulose glass microscope slide. Dimensions are given in millimetres (mm).

- *Primary antibody/rabbit serum slide incubation*

The printed bacterial microarray was blocked with 2-10% BSA (Sigma cat. no. 05470) in PBS (pH 7.4) for 1 h on a gently shake at 4^{o}C inside sterile a Petri dish. If using serum, the sample was heated to 56^{0}C in a heat block for 30 min to inactive complement proteins and kept on ice afterwards. All primary antibody/rabbit serum dilutions were performed in sterile-filtered PBS, 2%BSA, typically at dilutions of 1:50, 1:100, 1:200. Primary antibody or rabbit serum was pipetted into each well and left overnight at 4^{0}C. The next day, the slide was washed twice with sterile-filtered PBS in Petri Dish for 5 min, while gently shaking.

In later experiments, the slide was spin dried using a makeshift polystyrene insert for swing bucket modules designed for that specific centrifuge. These slides were then incubated with the rabbit OmpA monoclonal antibody or rabbit serum samples for 30 min at room temperature. After incubation, the slides were washed twice for 10 min each with PBS-T.

Bound antibody was detected using 50 µl/well secondary goat anti-rabbit-IgG antibody conjugated to Dylight® 550 (5µg/ml) at 1:200 in PBS, 2% BSA for 30 min. The ProPlate® gasket was retained on the glass slide throughout the entire experiment and through a single PBS wash bath step and dried at 50^{0}C. The slides were then immediately scanned for fluorescence on the GenePix® 4000B Microarray Scanner using 635 nm and 532 nm lasers, and the images acquired using the scanner's native GenePix® Pro 6.0 software.

- *Anti-faecal microbe anti-sera*

Rabbit polyclonal antibodies were generated by CovalAb UK (Cambridge, United Kingdom) against faecal bacteria isolated from a single healthy human stool sample. Two female rabbits were immunised accordingly to the regime over 67 days in table 5.2.1 and included four injections per animal.

Day 0	**Pre-immune bleed** (4 - 5 mL) and storage at -20°C Intradermal injection (1 mL / rabbit) 0.5 mL of 10^6 fixed bacteria + 0.5 mL incomplete Freund's adjuvant
Day 14	Intradermal injection (1 mL / rabbit) 0.5 mL 10^6 fixed bacteria + 0.5 mL incomplete Freund's adjuvant
Day 28	Intradermal injection (1 mL / rabbit) 0.5 mL 10^6 fixed bacteria + 0.5 mL incomplete Freund's adjuvant
Day 39	**Test bleed** (4 - 5 mL) and storage at +4°C Dispatch of sera D0 & D39 - 15/09/2015
Day 42	Subcutaneous injection (1 mL / rabbit) 0.5 mL of 10^6 fixed bacteria + 0.5 mL incomplete Freund's adjuvant
Day 53	**Test bleed** (10 - 15 mL) and storage at +4°C Dispatch of sera D53 - 29/09/2015
Day 67	**Terminal bleed** (50 - 70 mL) and storage at +4°C

Table 5.2.1 67-day immunisation protocol used in rabbit to generate polyclonal antibodies against human faecal bacteria isolated from a single healthy donor.

Faecal bacteria were extracted from 1g of fresh human stool by homogenisation with PBS and centrifuging at 300 x g for 5 min to remove large particulates. One millilitre of the bacterial supernatant was taken and washed twice in PBS (3,500 x g, 10 min) to produce a biomass of 400 µg for immunisations.

- *Validating of rabbit sera anti-microbial activity*

Faecal bacteria from the same donor were extracted in PBS and diluted across the slide in a series of 1:10 dilutions and blocked with 2% BSA for 1hr before being incubated with serum at a dilution of 1:100 for a further 1hr. Slide washes were performed for removal of blocking and after each primary and secondary antibody incubation using a 0.5l PBS bath The slide was developed with a secondary goat anti-rabbit IgG-conjugated to Dylight®650 for 1 hr. Dylight® 650 provides far-red fluorescence with excitation/emission at 652/672 nm respectively.

- *Microarray assay validation*

Polyclonal antibody generated in rabbit for outer-membrane protein A (OmpA) (1.74mg/ml) was kindly provided by Dr Régis Stentz (Quadram Institute Bioscience, Norwich). OmpA is widely expressed among Gram-negative bacteria. In addition, a strain of *Bacteroides thetaiotaomicron* engineered to lack OmpA protein, GH290, was also made accessible as a negative control species for immobilisation on the microarray in experiments to enable determination of optimal assay conditions as well as the limit of antibody detection. In a further attempt to provide proof-of-concept an *E.coli* RaFC "deep rough" mutant was also immobilised and used as an additional control, onto a slide and probed used an anti-*E coli* FITC antibody (1:500) for 1hr at RT. The slide was imaged immediately using the 532 nm (green) laser on the microarray scanner and signal gain adjusted in relation to wells left as blanks.

5.2.3 Patient and control serum

Bacterial endotoxin (LPS) and LPS-Binding Protein (LBP) were quantified in patient and house-hold control (HHC) serum samples collected into 9 ml polypropylene blood collection tube using the S-Monovette® Z system containing a clotting activator (Sarstedt, Germany, order: 02.1063.001). Collection tubes were centrifuged 2000 x g for 15 min to extract the serum. Serum samples were kept stored at -80^{0}C until required.

- *Serum Endotoxin*

Endotoxin testing was performed on severe ME (S), House-Hold Control (HHC) and earlier Mild/moderate ME/CFS (M) samples using the same batch of reagents provided the Kinetic-QCL Limulus-Amoebocyte Lysate (LAL) kit manufactured by (Lonza Ltd., Switzerland, Cat. No. 50-650U). Serum was diluted 1:10 in LAL water certified as pyrogen-free and inactivated by heating to 56^{0}C for 30 min. After cooling, serum was then kept on ice and stored overnight at 4^{0}C. Endotoxin standards were made using E. coli 055:B5 by reconstituting the supplied vials in a volume of LAL water provided on the certificate of analysis. All serum samples, endotoxin standards and a negative control (LAL water) were dispensed in a volume of 100 μl into wells on endotoxin-free microplate and preincubated in the microplate reader at 37^{0}C for 10 min. Reconstituted LAL reagent was prepared by adding 2.6 ml of LAL water to lyophilised mixture of lysate prepared from circulation amoebocytes from the horseshoe crab and kept at 4^{0}C and used on the same day. 100 μl of

LAL reagent into each well on the microplate as quickly as possible before activating the microplate reader. This assay has been designed to measure ΔOD over time, (Reaction Time, RT) to increase the initial absorbance measurement by 200 mOD. To this end, each well was simultaneously measured for absorbance OD at 405 nm every 50 seconds for 2 hr on the BioRad® Benchmark Plus plate reader using Microplate Manager software. Individual OD readings for each well was then exported to a Word® Excel® file and kinetic plots generated for each sample and controls. A standard curve of known endotoxin concentration ranging from 0.005 EU/ml to 50.0 EU/ml was established. Using a four-parameter linear regression model, a mathematical formula representing the kinetic plots from each serum sample was generated to calculate the precise Reaction Time (RT) for a ΔOD of 200mOD. The concentration of endotoxin is inversely proportional to the RT.

- *Serum LPS-Binding Protein (LBP)*

The same aliquots of serum analysed for endotoxin that had been kept at 4^0C overnight were used to measure LPS-binding protein (LBP) by a Human LBP ELISA kit according to kit instructions (RayBio® Inc., item code: ELH-LBP). Briefly, serum samples were diluted in LAL water to a final 1:100 concentration. Duplicate testing was performed on 100 μl of diluted serum per sample well and concentrations of LBP ranging from 0.819 ng/ml to 200 ng/ml and a zero standard after transferral to the LPB microplate immobilised with anti-human LBP. Following a 2.5 hr incubation at room temperature, a secondary biotinylated anti-human LBP antibody was added for 1 hr at room temperature with gently shaking. The plate was then washed four times before incubating with HRP-streptavidin for 45 min at room temperature. After plate washing, 100 μl of the supplied 3,3,5,5'-tetramethylbenzidine (TMB) was added as a substrate for 30 min in the dark. 50 μl of 0.2M sulfuric acid was added per well to stop the reaction, and readings for each well measured at 450 nm using the BioRad® Benchmark Plus and native Microplate manager software.

5.2.4 Faecal bacteria flow cytometry

- *Sample preparation*

Stool samples were homogenised manually using a metal spatula for 5 min. Six aliquots containing 100 mg of raw faecal pellet was prepared from each stool sample and designated use in flow cytometry experiments. These were stored at -80^{0}C before the experiment. On the day of the experiment, a single 100 mg aliquot of raw faeces was taken for each study participant and initially thawed whilst resting on wet ice and then gradually up to room temperature to mitigate any protease activity causing degradation of IgA antibody. It is estimated that 1g of healthy stool contains anywhere between 10^9-10^{10} bacteria cells. Based on this, all 100 mg faecal homogenates were diluted to 1:100 which is equivalent to 10^6 cells in a final volume of 4 ml and stained with Sybr Green (1:10,000) and anti-human IgA-APC (1:100). To do this, 1ml of sterile-filtered Dulbecco's phosphate-buffered saline (Sigma, cat. D8537) was used to homogenise each 100 mg of faeces using a plastic pestle and mot for 5 min. This faecal homogenate was then centrifuged at 300 x g for 5 min to produce a faecal bacterial suspension. This suspension was then further diluted 1:10 in PBS before staining. Sybr green nuclei acid stain was provided as a gel stain at a x10,000 concentration in DMSO (Sigma, cat. S9430) and diluted in each sample to a final concentration of 1/10,000 and added to 20 μl sample of the faecal bacterial suspension in PBS to a FACS tube containing 80 μl PBS containing SYBR green to make a further 1:10 dilution. To this, 1 μl of anti-human IgA-APC antibody (Miltenyi Biotec, order no. 130-116-879) was incubated at room temperature for 30 min before fixing in 350 μl of 1% PFA and temporarily placed onto ice whilst awaiting to be analysed.

- *Flow cytometry data acquisition*

Flow cytometric analysis was performed on faecal bacteria suspensions stained with Sybr green (1:10,000) and anti-human IgA-APC (1:100) using the BD FACSCanto™ II and BD FACS Diva software for data acquisition. Forward and side scatter voltages were adjusted to capture events within the space of the plot. Non-fluorescently labelled cells were used to set PMT voltages for APC (IgA-detection) and FITC (Sybr Green) and position these events on the bottom left area of the plot. Events captured in the bottom right of the plot were positive for Sybr green, and events observed top left were IgA-APC position. Anti-human IgG-APC (1:100) was used in each sample as an isotype control for non-specific binding.

5.3 Results

5.3.1. Sample acquisition

Home visits were conducted during May 2016 and at the end of February 2017. A total of 17 severe ME patients were recruited and included in this chapter (Table 5.3.1) Nine household controls were recruited and linked to their respective ME participant. It must be noted that out of these nine house-matched controls, two were unrelated full-time carers of these severe ME patients. This was the best achievable environmental control in these instances, since these carers worked long hours in close contact with the patient and in the preparation of meals.

Figure 5.3.1 shows a map of the locations of the 11 home visits carried out in 2016. Due to the availability of a suitably trained medical profession, it was not possible to obtain blood samples from all these home visits. Blood taking from these patients proved difficult for most severe patients and was deemed unethical to pursue further attempts to take blood. The difficulties in obtaining blood was another turning stone to switch strategies from systemic microbial antibody detection, to using less invasive faecal samples to access IgA reactivity in faecal bacteria.

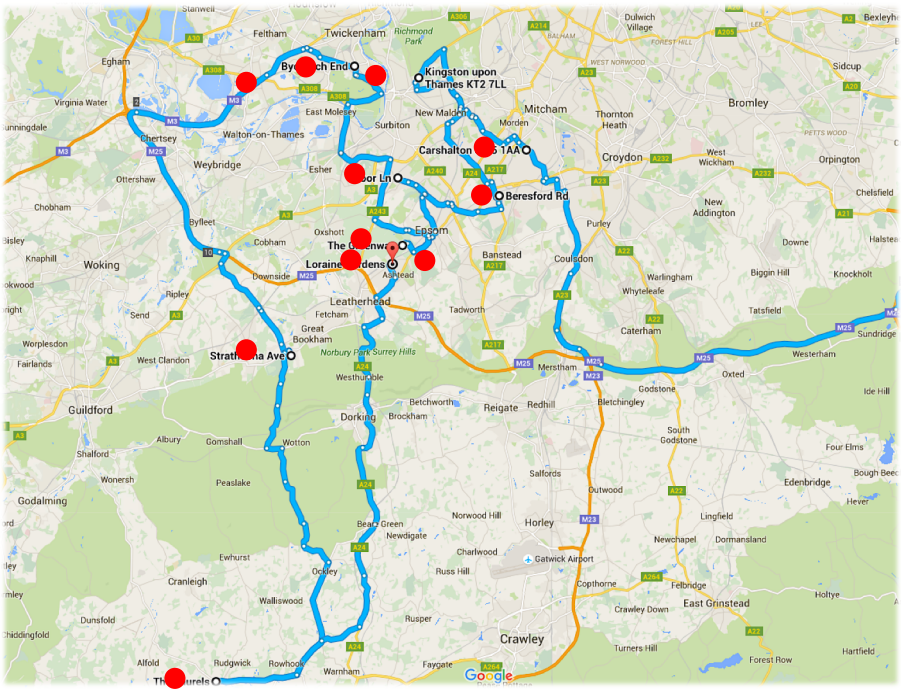

Figure. 5.3.1 Maps of locations for 11 home visits attended across South London, UK, during 2016

Sample Collection Summary

Sample	Status	Age	Sex	Collection year 2016	2017	Paired samples
1	Severe ME	63	F	X	X	
2	Severe ME	56	F	X	X	
3	House Control	55	F	X	X	1
4	House Control	69	F	X	X	2
5	Severe ME	44	F		X	3
6	House Control	70	F		X	3
7	House Control	55	F	X	X	4
8	Severe ME	38	F	X	X	2
9	Severe ME	21	F	X	X	1
10	Severe ME	37	F		X	5
11	House Control	64	F		X	5
12	Severe ME	18	F	X	X	4
13	Severe ME	61	F		X	
14	Severe ME	40	F		X	
15	Severe ME	54	F		X	
16	Severe ME	58	F	X	X	6
17	House Control	60	M	X	X	6
18	Severe ME	27	F	X	X	7
19	House Control	60	F	X	X	7
20	Severe ME	63	F		X	
21	Severe ME	32	F	X		10
22	Severe ME	31	F	X		8
23	House Control	54	F	X		8
24	Carer	29	F	X		9
25	Severe ME	56	F	X		9
26	Severe ME	30	F	X		
56	Carer	34	F	X		10

Table 5.1.1 Patient Demographics: Severe ME (n=17) plus House-Hold controls (n=9)

"X" denotes sample collected. Severe ME (age 42.9±13.2 years) and House-matched controls (age 57.3±8.8 years). Yellow highlights patients followed up for a second sample

In 2017, additional faecal samples were made available from 7 of the original severe ME patients recruited in 2016, with another 6 new severe ME patients included in final home visits to conclude the entire study. Again, owing to the difficulties of organising a suitable trained clinical professional to take blood as well as these patients being exceptionally challenging to acquire a suitable vein for bleeding, not all severe ME patients and their controls contributed blood serum to this study.

5.3.2 Bacterial Microarray

Attempts to design and develop a useful bacterial microarray for patient systemic serum antibody detection was carried prior to research ethics approval and therefore these experiments were conducted in advance of any patient or control sample collections. The rationale for its design was to allow for ease of detection of serum antibodies in human serum against multiple faecal bacterial isolates and for the simultaneous detection of these antibodies using high-throughput microarray printing and array scanning.

Early attempts used single cultured intestinal isolates immobilised onto a nitrocellulose-coated slide. *Bacteroides thetaiotaomicron VPI 5482* was chosen for its ability to withstand oxygen exposure on the lab bench and due to the availability from within the research group culture collection and that of an outer-membrane protein A deficient strain, GH290 ($OmpA^-$). This was also one of the species used for anti-microbial detection by Haas et al., 2011 in HIV-1 infection and IBD patients (Haas et al., 2011).

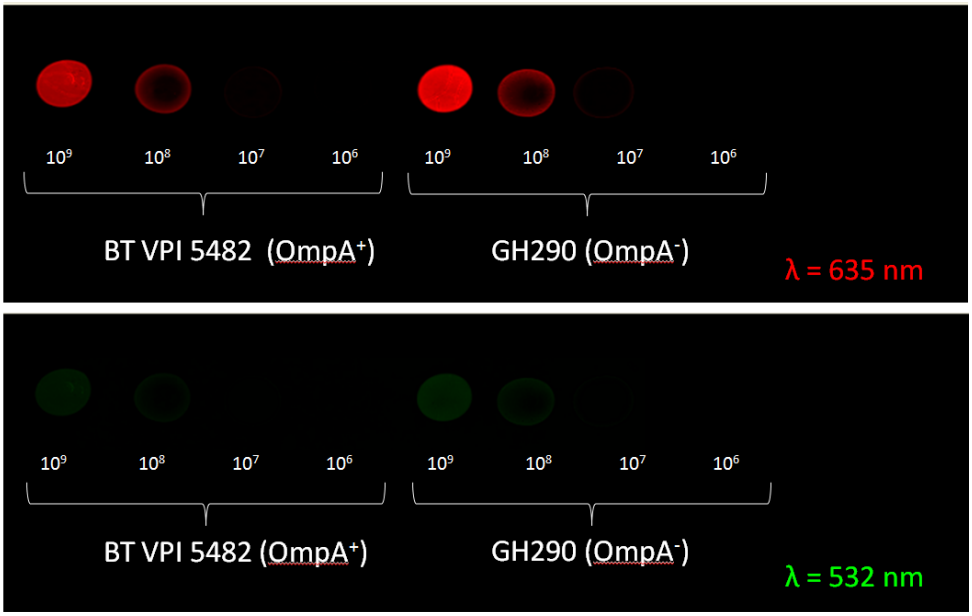

Figure 5.3.1. Bacteroides thetaiotaomicron $OmpA^+$ and $OmpA^-$ can be immobolised onto a nitrocellulose-coated glass microscope slide. Baclight Red® stain was incubated with cells before transfer of 10 µl to slide. Slide was dual laser imaged on the GenePix Microarray scanner. Fluorescence cells appear detectable, read at wavelength of 635 nm versus 532 nm .

In preparation to access the effect of CFU numbers on the detectability of Baclight® Red signal during the microarray scan; PBS suspended *VPI5482* (10^9 cells/ml) and *GH290* (10^9

cells/ml) cells were stained with Baclight® Red (100 µM, working dye solution) in a final 1:1000 dilution. The desired cell number (ranging from 10^9, 10^8, 10^7 or 10^6 cells per array spot) was achieved by serial dilution in PBS. Figure 5.3.1 shows an example of these cells deposited onto the microarray using a 10 µl printing volume. The Baclight® red fluorescence intensity was recorded using the red laser (λ = 635 nm). The slide was also scanned for fluorescence on the green channel of the microarray scanner (λ = 532 nm) and shows background fluorescence may interfere with downstream signal detection of antibodies on this channel. It was difficult to quantitate the intensity of Baclight® fluorescence at this stage, however OmpA$^-$ cells did appear more fluorescent from this image.

In slide-independent studies using flow cytometry (figure 5.3.2), Baclight® Red was demonstrated to only have fluorescent properties when it was associated with both Gram positive and negative bacterial cells, confirmed also by the manufacturer's protocol and gave reassurances that Baclight® detection was a reliable visual indicator of the presence and location of cells on the microarray slide. Figure 5.3.2 shows *E. gallinarum* (Gram positive) and *A. muciniphila* and *B. thethaiotoamicron* (both Gram negative) cells can be sort for fluorescence using Baclight signal intensity.

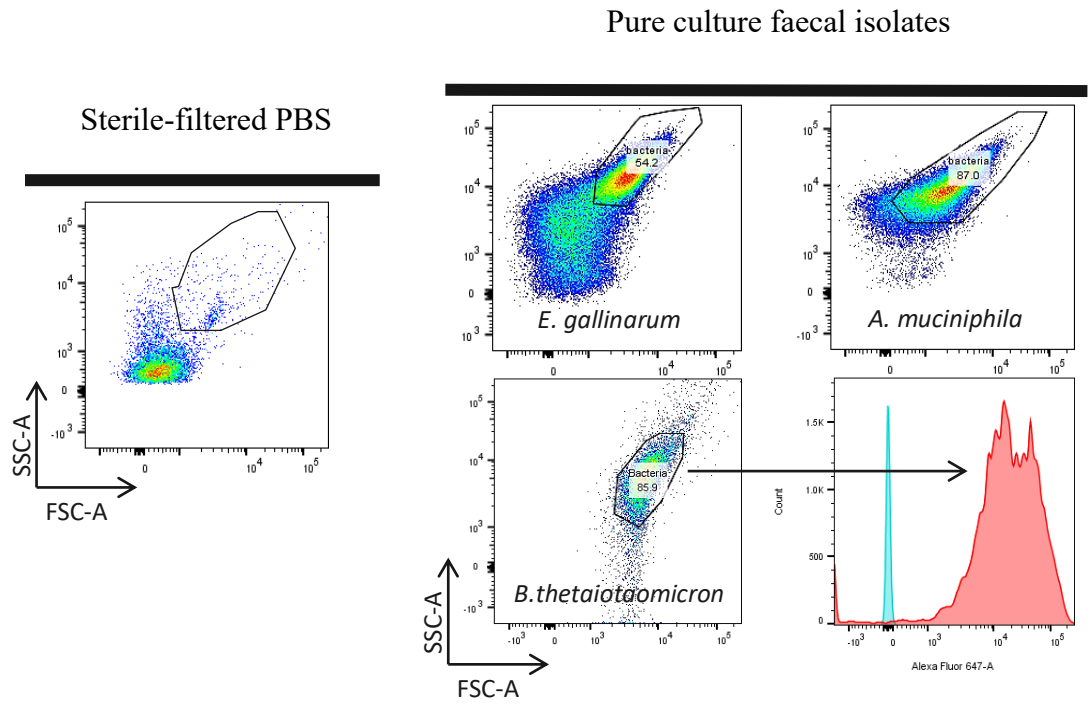

Figure 5.3.2 Visualising bacteria stained using Baclight® red by flow cytometry. Threshold set to a minimum of <100 ets/s based on sterile-filtered PBS (left plot). Bacterial cells were positioned within the plot using forward (FSc) and side scatter (SSc) light properties which are proportional the size of

individual cells (FSc) and intracellular complexity (SSc). Histogram measured the Baclight® intensity, cells accumulate to the right of this plot are positively stained. Pseudo-colour represents concentration of cells where a region of interest (gate) has been added to exclude culture debris and non-specific events. Number inside gate is a percentage of all events processed. These were then gated and measured for Baclight signal in the histogram (red).

- *Microarray assay validation*

Immobilisation of OmpA$^{+/-}$ strains of *Bacteroides thetaiotaomicron* on nitrocellulose-coated glass slides was used to optimise the antibody detection protocol using a polyclonal anti-OmpA antibody and a secondary goat anti-rabbit-IgG conjugated to Dylight®550 (Thermo-Scientific) for green fluorescence that could be detected on the microarray scanner's second laser at 532 nm. To facilitate multiple antibody conditions on single glass slide, a multiarray chamber (fig. 5.2.1), was integrated with the glass slide to produce 64 individually spaced wells similar to a microtiter plate. Binding of the OmpA antibody would be expected using the wild-type VPI5482 strain, with GH290 (OmpA^{-}) representing a negative control.

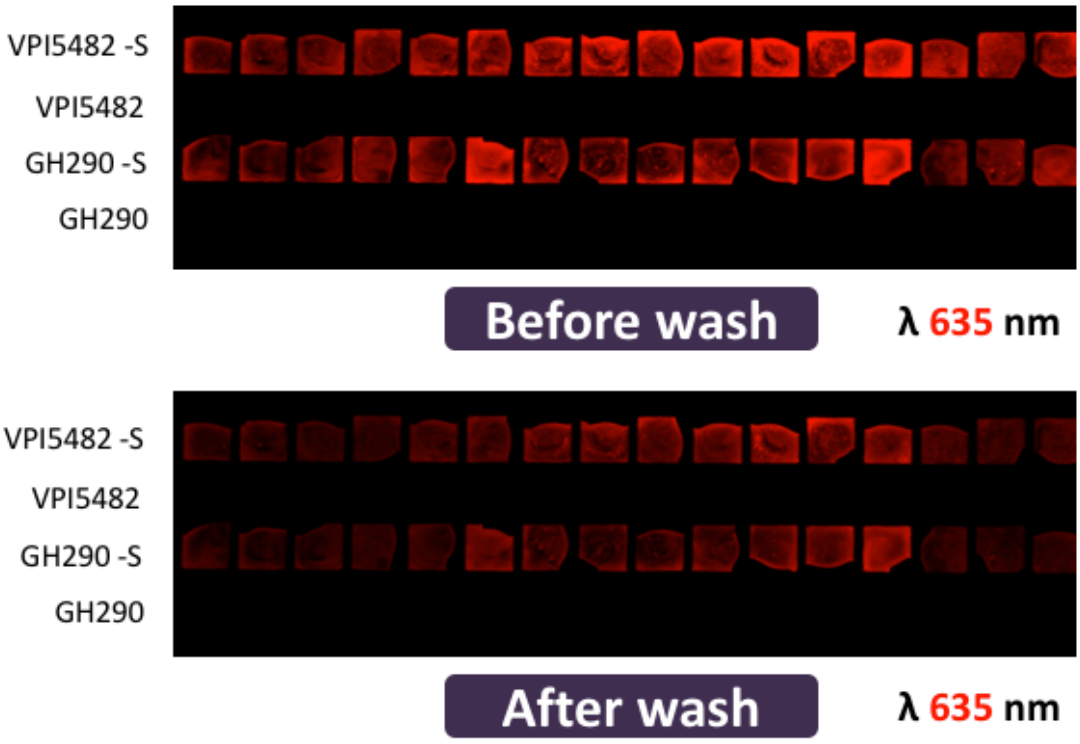

Figure 5.3.3 Slide washing causes loss of bacterial cells. 10 µl of bacterial suspension (10^9 CFU/ml) of stained and unstained VPI5482 and GH290 cells per well (10^8 cells) was air dried onto slide and subjected to three separate washing steps by submersing slide in a 5L bath of PBS-T (0.05% Tween 20) and left to dry in between each wash. After the final wash the slide was left to dry at 37^0C before scanning.

An experiment was required to test if immobilised bacteria can withstand a minimum of three PBS-T wash steps to allow for application and removal of (1) a suitable blocking reagent, (2) serum/antibody, and (3) removal of unbound primary/secondary antibody.

Bacteroides thetaiotaomicron strains remain partially immobilised onto the slide after three washing steps (figure 5.3.3). Efficiency and stability of cells immobilisation appears to vary across different regions of the slide since loss of fluorescence occurs more to wells at the ends of the slide. There appeared to be no differences between $OmpA^{+}$ or $OmpA^{-}$ cells.

Using the ProPlate 64-well gasket configuration, VPI5482 and GH290 cells were immobilized onto separate slides with the application of primary OmpA antibody concentrations (1:100, 1:200, 1:500) titrated against secondary goat anti-rabbit IgG-Dylight®550 (1:100, 1:100, 1:500). Figure 5.3.5 shows two slides with annotations for antibody incubated against $OmpA^{+/-}$ *Bacteroides*. Cells incubated with antibody were not stained with Baclight® Red to avoid any signal bleed over onto the 532 nm laser used to detect secondary antibody binding. Both slides contained 10^8 cells per well which were deposited onto the slide in 10 µl volume/well in an attempt to coat the entire well surface. Six wells did contain 10^9 cells stained with Baclight® Red as a control and for the purposes of monitoring following slide washing.

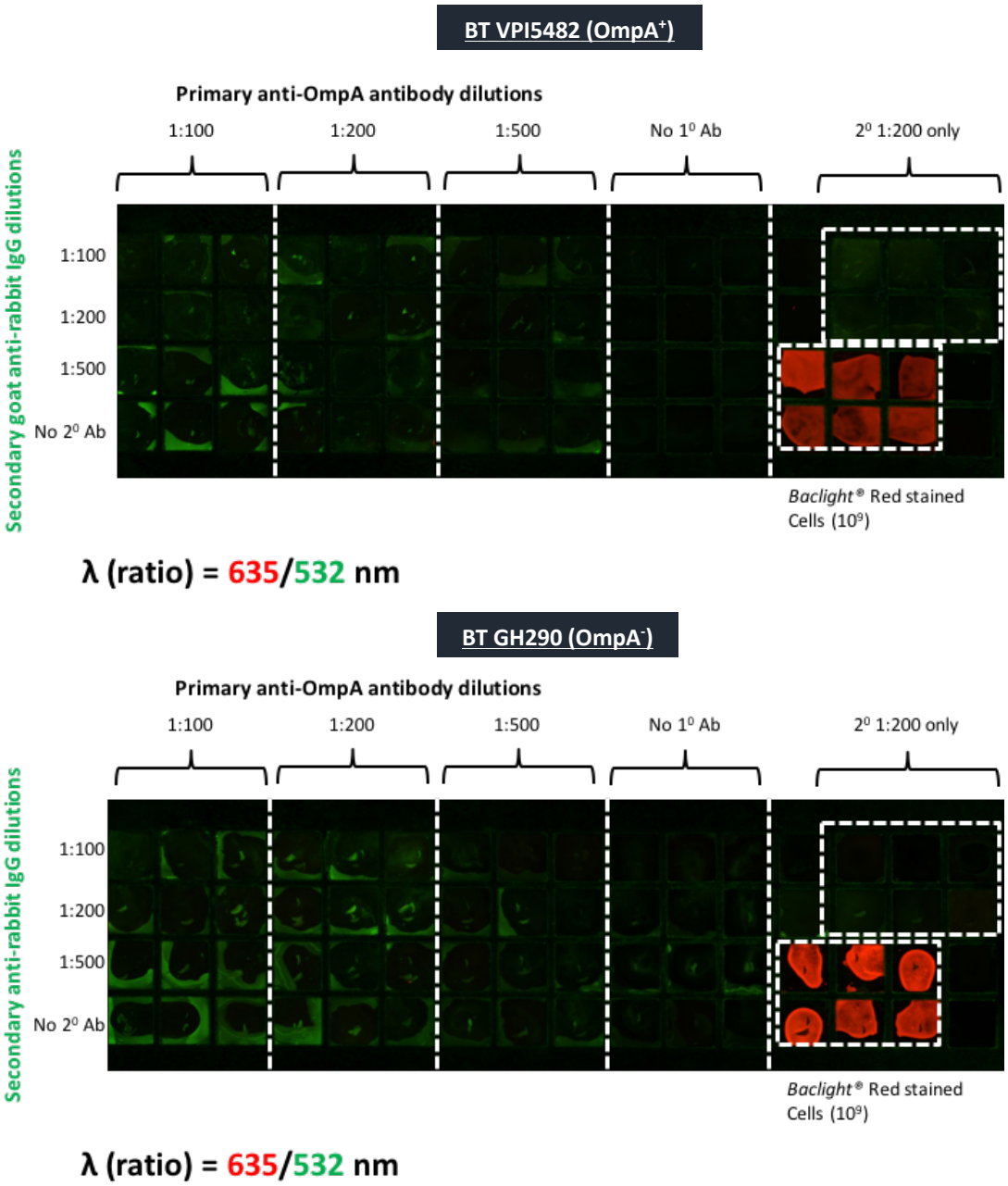

Figure 5.3.4 Polyclonal rabbit OmpA antibody was used to test for specificity and reactivity against immobilised VPI5482 bacteria.

Several attempts were made using OmpA antibody to provide proof-of-concept for this method of antibody detection. A makeshift polystyrene insert for a centrifuge swing bucket was created to introduce centrifugal force to maximise contact between cells and the slide surface. Blocking with BSA was attempted at 2% and increased to 10% to minimise slide background signal in fig. 5.3.4. However, scanning of both slides at 532 nm did not reveal specific binding of antibody to the wild-type (OmpA$^+$) *Bacteroides*.

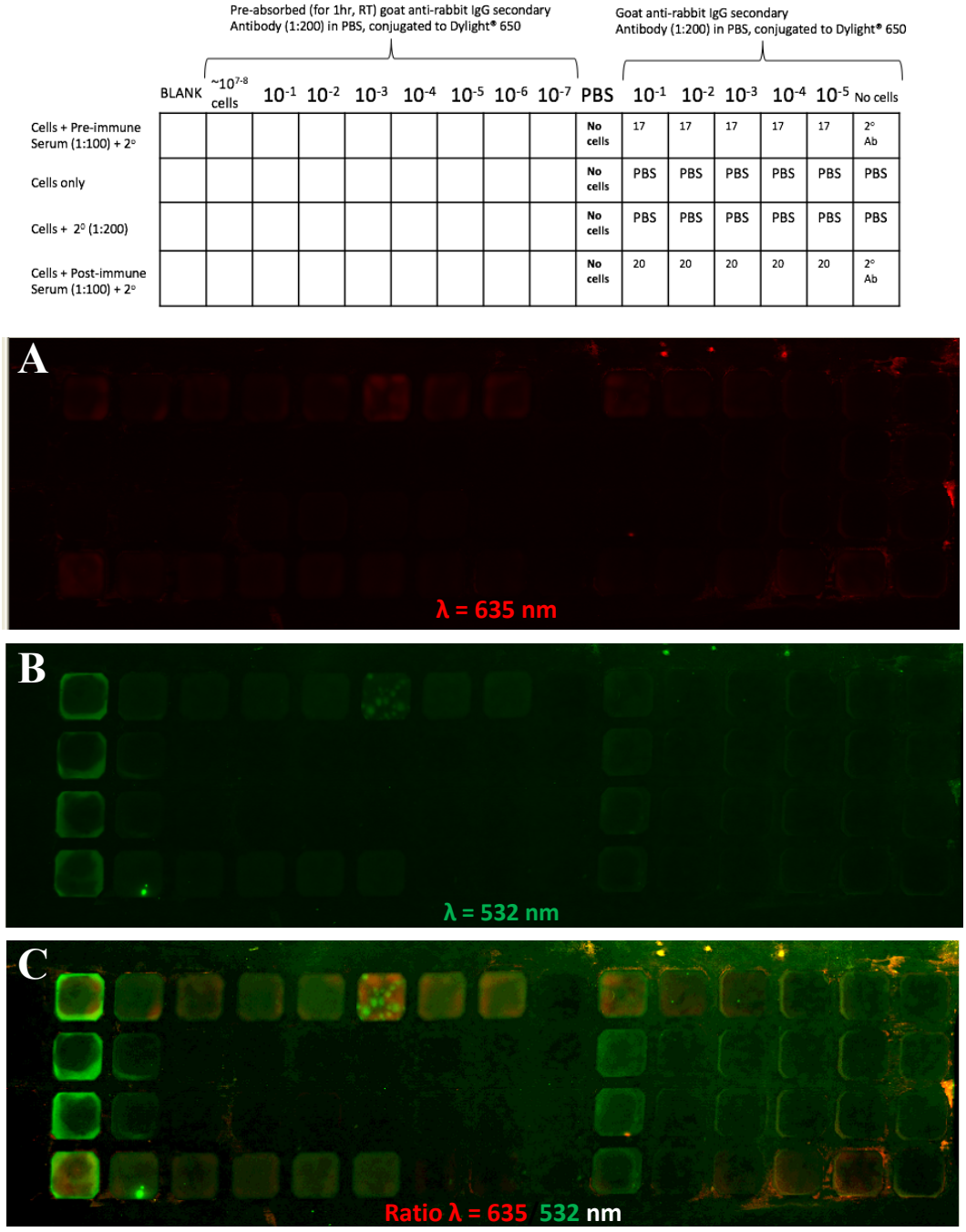

Figure 5.3.5 Reactivity of polyclonal anti-microbial rabbit serum tested against faecal bacteria extracted from human faeces. Donor faecal bacteria used to immunise rabbit was used on this slide, starting at 10^8 cells diluted across the slide using PBS. Top: slide map shows the position of cell dilutions and antibody staining concentration. (A) single (red)laser, λ = 635 nm, scan of slide to detect secondary antibody binding produced no reactivity. (B) single (green) laser, λ = 532 nm measures background fluorescent activity. (C) dual laser (λ = 635/532 nm) with increased gain show no specific antibody reactivity to faecal bacteria.

Rabbit sera raised against faecal bacteria isolated from a single human donor was tested using this microarray format in figure 5.3.5. However, no fluorescence was detected on the array scanner at 635 nm.

An attempt using pooled serum from rabbits “17” and “20”. In this experiment, blocking was increased by using 10% BSA and the serum was left overnight at 4^0C. The slide was then processed and developed as previously performed and scanned for fluorescence (figure 5.3.6). Detection using the green channel shows the slide surface to be highly auto-fluorescent. Combined post-immune sera was compared directly with the pre-immune bleed for anti-microbial activity to donor faecal bacteria titrated against cell number, but this produced little or no detectable antibody binding (fig. 5.3.6, right).

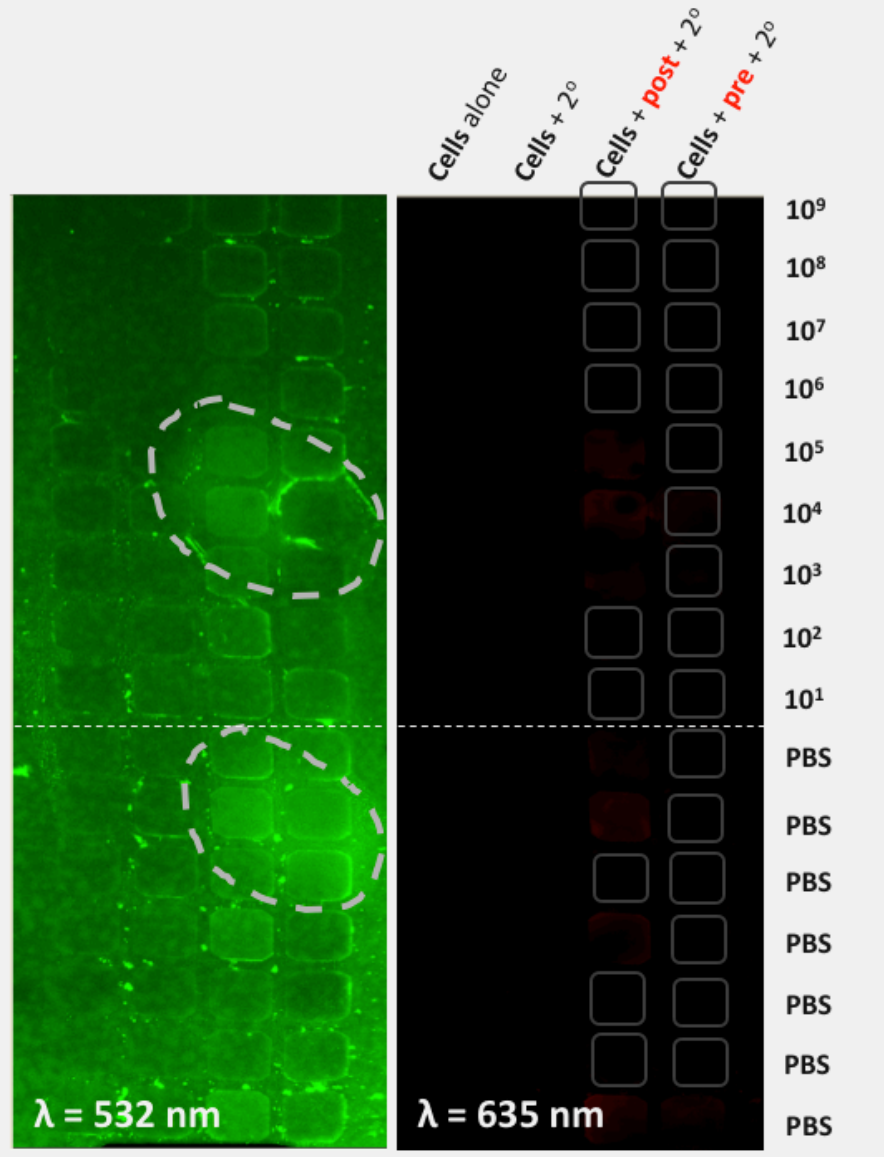

⇐ **Figure 5.3.6 Post-immunised rabbit sera shows no anti-microbial reactivity using donor faecal bacterial immobilised onto a nitrocellulose-coated glass microscope slide.** Anti-microbial reactivity towards faecal bacteria was compared using pre- and post-immune rabbit sera. Faceal bacteria were diluted from 10^9 – 10^1 cells using PBS only as a negative control. Slide was imaged on separate laser channels, λ = 635 nm, green (left) and λ = 635 nm, red (right). Regions of interest (boxes) indicate wells created to deliver cells onto slide.

- *Automated microarray printing*

A microarray printer was used to deliver cells onto the nitrocellulose-coated slide in the same fashion described by Thirumalapura and colleagues. To that end, a microarray printing buffer was recreated using PBS containing 20% Ficoll 400 and 4% glycerol to suspend VPI5482 bacterial cells at a density of 10^9 cell/ml. Figure. 5.3.7 shows example of cells printed with each array spot representing ~25,000 cells. PBS/Ficol/Gycerol was compared with PBS alone, which provided a better quality of array spot. The bottom image in fig. 5.3.7 shows a scan of the entire slide surface and the differences in the quality of spotting. During imaging of the slide, signal gain was adjusted in relation to areas of the slide out of range of the microarray printer and was kept constant during re-imaging of the same slide following slide washing.

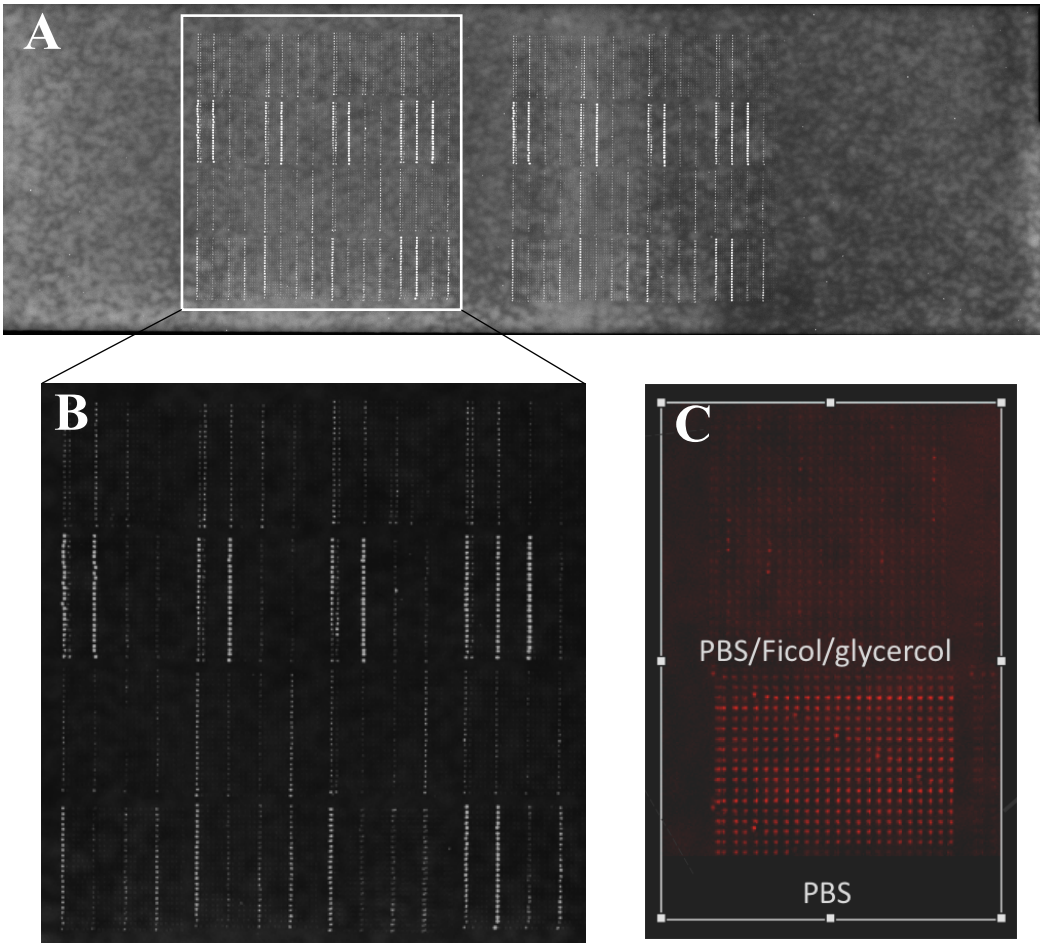

⇐ **Figure 5.3.7 Automated microarray printing of Baclight® Red stained *Bacteroides thetaiotaomicron VPI5482 (OmpA⁺)*.** Cells were robotically printed onto a nitrocellulose-coated glass slide and imaged using a microarray scanner. (A) Entire slide surface imaged using single (red) laser, λ = 635 nm. (B) represents enlarged view of area in white box in A. (C) Compared Baclight® signal intensity (λ = 635 nm) from bacterial cells suspended in either PBS and PBS/Ficol/Glycerol printing buffer

Baclight® signal was quantified using pre-defined analysis modes within the native GenePix® software on the array scanner. Based on the microarray printing pattern, regions of interest could be placed around each array spot and its fluorescent signal recorded and exported into an Excel file.

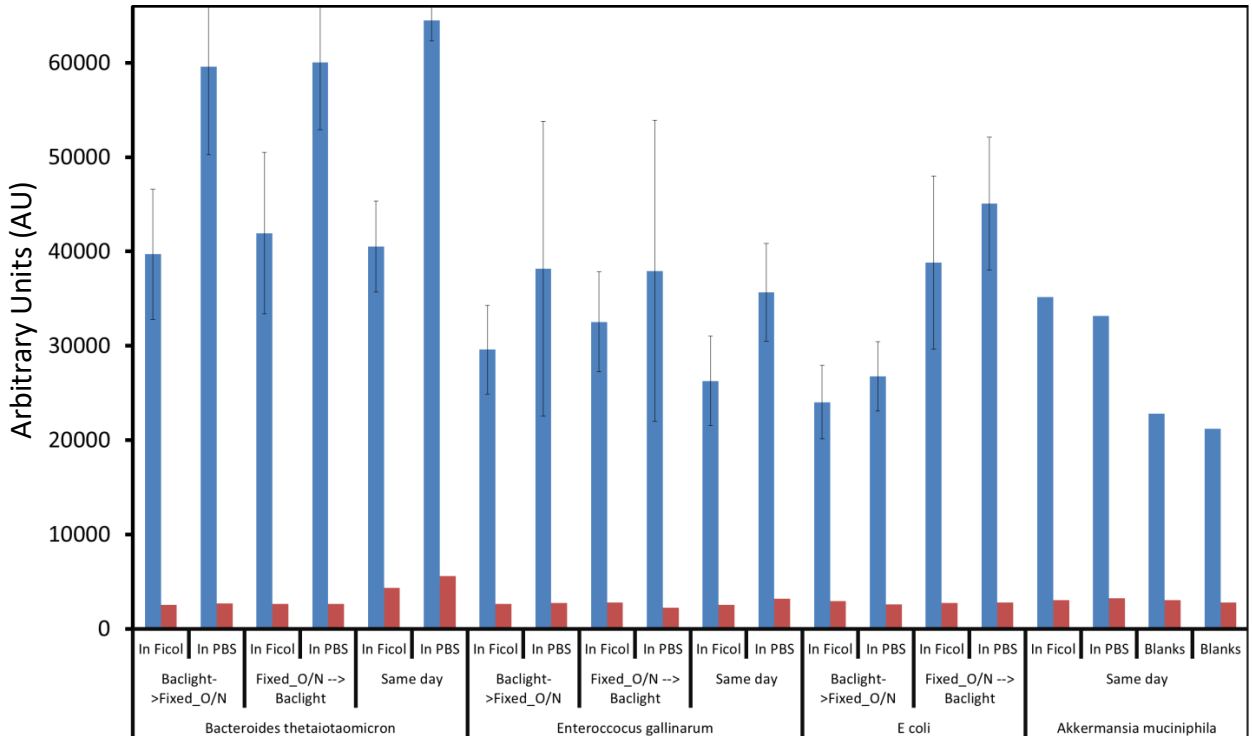

Figure 5.3.8 Washing causes the majority of cells to be lost from the microarray slide surface. Two printing buffers, PBS and PBS/20%Ficol/4% glycerol were used to robotically print bacterial cells from *Bacteroides thetaiotaomicron* (Gram negative)*, Enterococcus gallinarum (*Gram positive)*, E.coli* (Gram negative)*,* and *Akkermansia muciniphilia* (Gram negative) on to a nitrocellulose glass slide. Cells were stained with Baclight® Red according to different conditions; either before or after fixing cells overnight or staining unfixed cells and printing on the same day. Blue bars indicate Baclight® Red fluorescence pre-wash, compared to the red bars at post-wash. Mean fluorescence values were recorded in arbitrary units (AU) following scanning of entire slide surface. Error bars give the range of standard deviation.

Figure 5.3.8 (blue bars) compares the intensity of Baclight® signal in PBS versus PBS/20% Ficoll/4% Glycerol. Given the final version of this assay would require tens or even hundreds of different representatives of the human gut microbiota, such an assay would require advanced preparation and staining of these bacteria before they could be immobilised onto the array. Baclight® intensity was a third higher in cells printed in PBS alone for *B. thetataiomicron*. However, it did not make any notable difference if cells have been stained the previous day and kept at 4^0C compared to staining these cells the same day to be printed. The order of fixing cells before or after Baclight® staining did not make a difference for *B. thetaiotaomicron* or *E.gallinarum*; with the exception for E.coli that was more advantageous to stain these cells on the same day of printing. Interestingly the difference in fluorescence between the printing buffers for *Akkermansia muciniphila* was the least in contrast to the other strains that performed better in PBS, highlighting optimal printing and staining conditions are dependent on the bacterial strain. Reimaging the slide following washing revealed complete loss of Baclight® signal from all strains suggesting these cells have been lost from the slide surface.

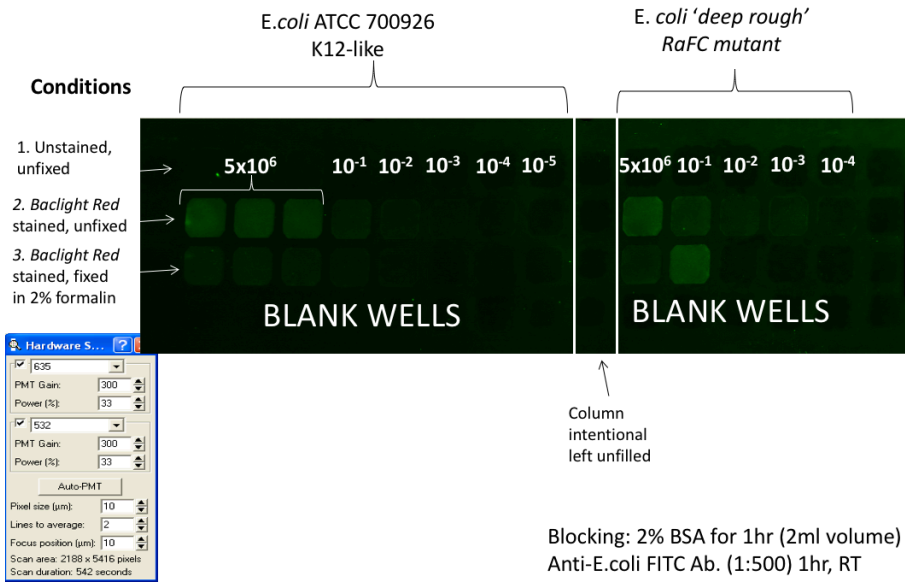

Figure. 5.3.9 Anti-E.coli-FITC antibody reactivity towards for wild-type *E.coli* ATCC 700926 and ΔRaFc 'deep rough' mutant E.*coli* immobilised onto nitrocellulose-coated slide. $5x10^6$ cells transferred onto slide and diluted in series 10^{-1}-10^{-5}. Each row of the slide indicates condition of cells prepared (1) unstained and unfixed, or Baclight® Red stained in unfixed (2) and 2% formalin (3).

A final attempt was made to generate a working slide assay using a 'deep rough' mutant raFC mutant E.*coli*. A FITC-conjugated goat polyclonal anti-*E.coli* antibody was tested against ATCC 700926 cells, including a K-12 like E.coli strain and a 'deep rough' mutant *E.coli.* This antibody reacts with most *E.coli* given the 95% homology across all strains. It was anticipated this experiment would work based on reducing the number of washing steps since no secondary antibody was required, however figure 5.3.9 is a scan of result of this experiment at 532 nm and show no specific antibody reactivity towards wild-type *E.coli*. Non-specific binding appeared to have occurred but was due to bleed over of Baclight® Red signal, as previously observed in figure 5.3.1. Fixing did appear to reduce this effect. Based on independent experiments using rabbit serum, OmpA and *E.coli* antibodies it was determined that this assay, in our hands, was not suitable to continue for future detection of serum antibodies in patient samples. At this time in the study it became apparent an alternative method was needed to evaluate anti-bacterial antibodies in patient samples.

5.3.3 Faecal detection of IgA-coated faecal microbes

Sybr green was used to label faecal bacteria isolated from homogenised stool samples of patients and house-hold controls. Figure 5.3.10 is an early experiment with faecal bacteria isolated from a single healthy donor stool. The flow plots reveal a subpopulation of cells that are Sybr green positive. Bacterial cells can also be identified using light scatter characteristics alone providing an adequate threshold of detection has been established so that no more than a rate of 100 events per second are detected using sterile-filtered PBS alone. PBS containing unstained/stained bacterial cells were diluted to an approximate range of 5000 events per second to minimise risk of clogging the cytometer.

The protocol for visualising faecal bacteria using Sybr green in a flow cytometer was based on a protocol used by Dr Alistair Noble (Imperial College London) to stain intra-epithelial microbes isolated from biopsy samples of patients with inflammatory bowel disease (IBD). Here, Sybr green staining has been used as a refinement to earlier published work using faecal flow cytometry where no attempts have been made to separate faecal bacteria from other particulates within stool (Palm et al., 2014).

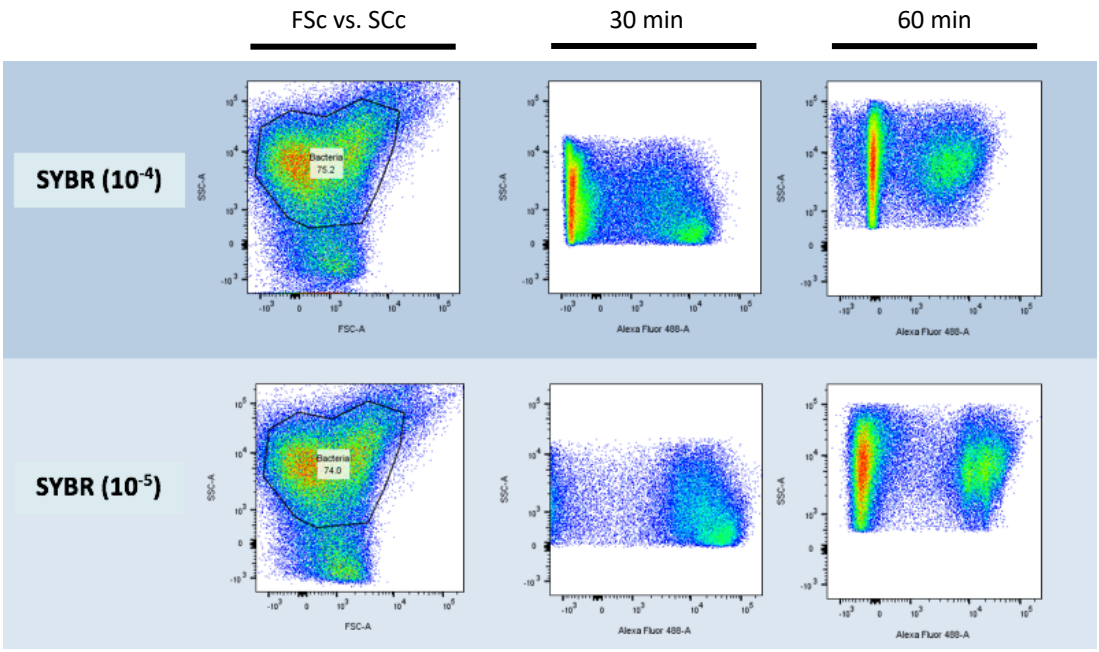

Figure 5.3.10 Optimisation of concentration required to visualise faecal bacterial cells with Sybr Green nucleic acid staining using flow cytometry. Faecal bacteria were extract from a single donor provided as 100 mg aliquot for homogenisation and diluted 1:100 in PBS. FSc and SSc properties were used to identify faecal microbes from faecal debris. Identifying faecal bacteria was enhanced with with Sybr green staining diluted to 1/10,000 versus 1/100,000 for 30 min or 60 min and inspected on the flow cytometer.

Further optimisation of Sybr green was performed with anti-human IgA and compared against faecal bacteria in an ME and HHC sample, by 1:100 and 1:1000 dilution of faecal bacteria in sterile-filtered PBS. We found 1:100 dilution most suitable for staining (see supplementary figures 5.1 and 5.2).

A total of 19 samples were analysed from 2016 collections. The method for faecal IgA detection presented here was tested in an early experiment using a single matched severe ME patient and house-hold control. The percentage of IgA^{+} bacteria in the severe ME (57, F) patient was 21.3% compared to 6.37% in the HHC (60, M) (figure 5.3.11). The percentage of non-specific binding was 0.16% and 0.27% from patient and HHC respectively. The Sybr green staining was recorded at 52.7% in the patient versus 81.9% in the HHC. Although the percentage of Sybr Green is higher in the control, this should not make any difference to the percentage recorded for IgA detection.

The effectiveness of the Sybr green positive staining appeared to vary in both patients and HHCs. As an example, Sybr green staining pattern did not appear consistent in identifying bacteria within the faecal homogenate shown in the house-hold control (HHC), although the percentages suggested more were identified in the ME (21, F) patient compared to the HHC (55, F) at 54.8 % in ME and 66.4% in HHC (figure 5.3.12). In this pair, the percentage of isotype non-specific bind was recorded at 0.17% for the patient and 3.60% for the HHC. The percentage of IgA^+ bacteria was the second highest in its group at 36.6%, over double the percentage compared to 16.5% measured in the HHC. This pair represented the greatest difference in percentage between patient and HHC. This patient is also the second youngest at 21 years old and remains entirely bed-bound.

As a third example of this dataset, another female ME (38, F) and HHC (69, F) pair showed more consistent $Sybr^+$ green positive staining for faecal bacteria at 51.8% versus 70.1% in ME and HHC respectively (figure. 5.3.13). This patient presents the third highest percentage at 31.8% IgA^+ bacteria compared with 17.0% IgA^+ in the HHC control. Sybr Green positive staining was 51.8% versus 70.1% for ME and HHC respectively. Non-specific bind with isotype antibody was 4.85% in ME versus 0.72% in HHC.

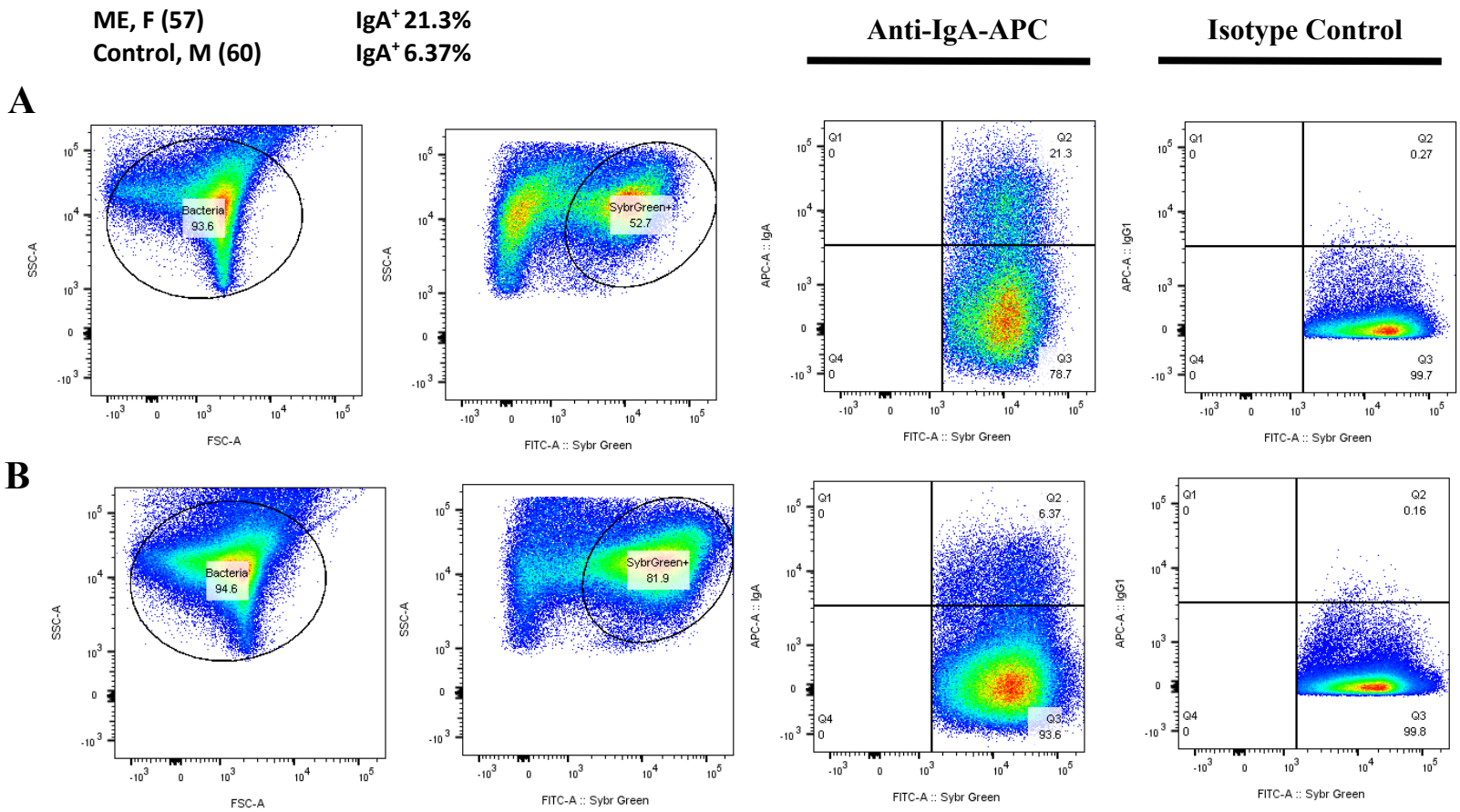

Figure 5.3.11 Flow cytometry data using faecal bacteria isolated from severe ME patient (top row) and their house-hold control (bottom row). Bacteria are gated using Sybr green fluorescence and measured for anti-IgA-APC binding to these cells recorded in the top right quadrant of IgA plots. Isotype control provides indicator for non-specific binding events. Pseudo-colour shows areas of increasing cell numbers. Numbers within each gate, represent the percentage out of total events recorded.

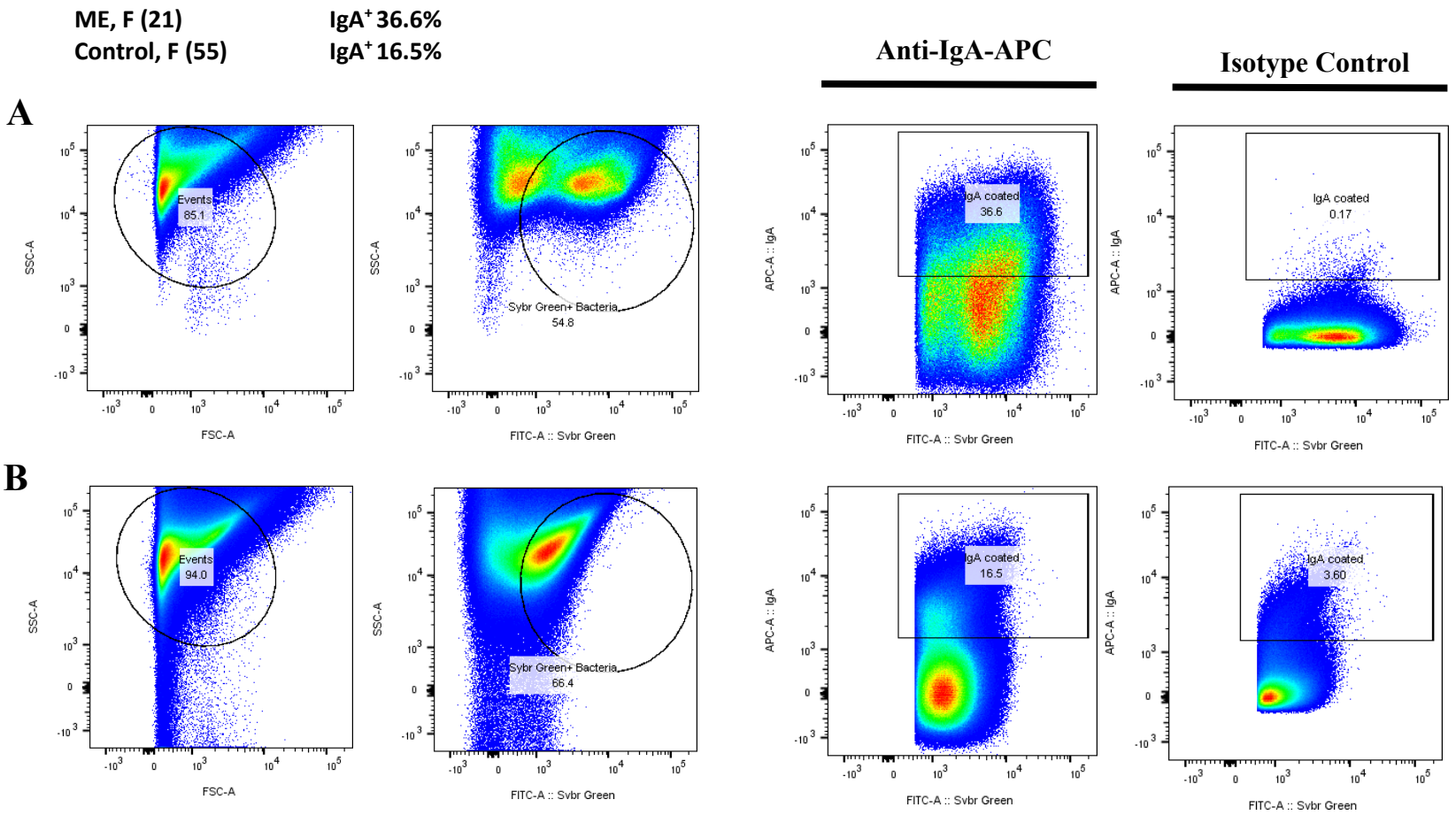

Figure 5.3.12 Flow cytometry data using faecal bacteria isolated from severe ME patient (top row) and their house-hold control (bottom row). Bacteria are gated using Sybr green fluorescence and measured for anti-IgA-APC binding to these cells recorded in the top right quadrant of IgA plots. Isotype control provides indicator for non-specific binding events. Pseudo-colour shows areas of increasing cell numbers. Numbers within each gate, represent the percentage out of total events recorded.

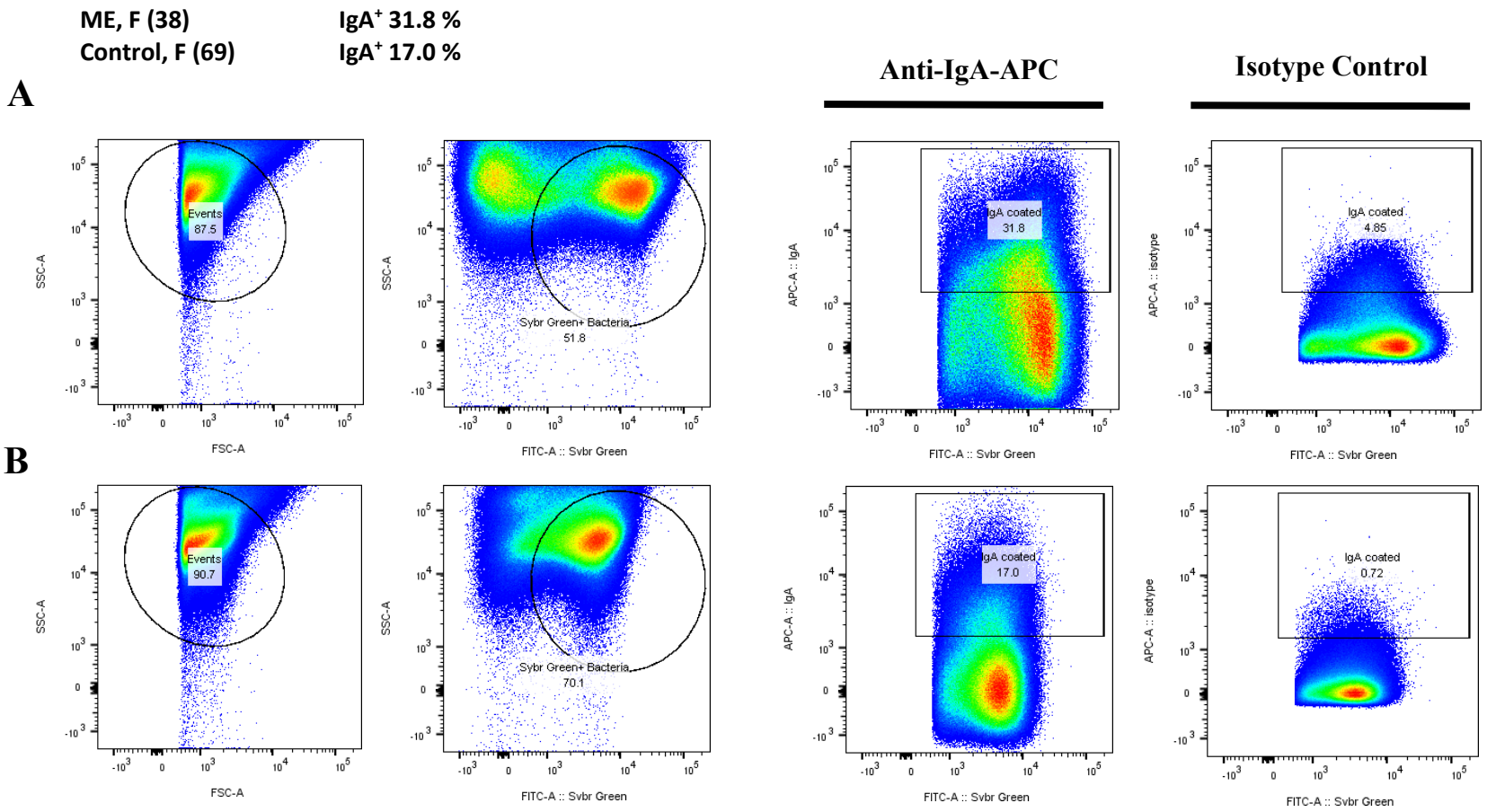

Figure 5.3.13 Flow cytometry data using faecal bacteria isolated from severe ME patient (top row) and their house-hold control (bottom row). Bacterial are gated using Sybr green fluorescence and measured for anti-IgA-APC binding to these cells recorded in the top right quadrant of IgA plots. Isotype control provides indicator for non-specific binding events. Pseudo-colour shows areas of increasing cell numbers. Numbers within each gate, represent the percentage out of total events recorded.

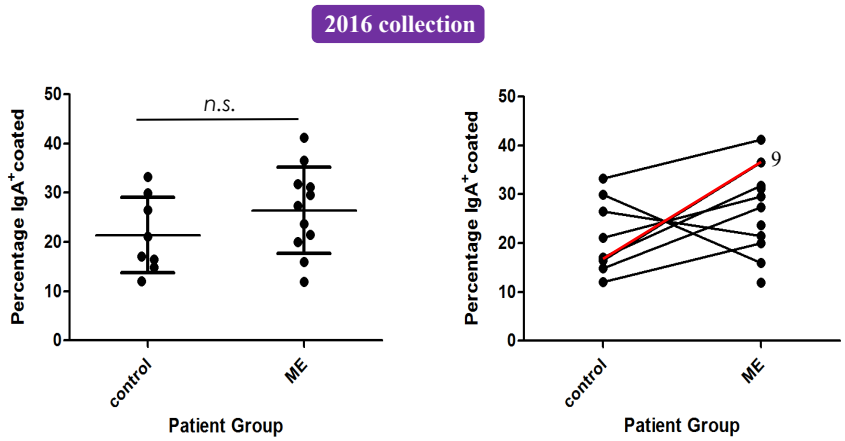

Figure 5.3.14 Summary of the relative abundance of IgA-coated faecal bacteria in 8 pairs of severe, house-bound ME/CFS patients versus house-hold (control) and 3 unmatched patients. Right, paired and unpaired samples; left, lines indicate pairing between patient and house-hold control, red line represents patient 9, see table 5.3.1. Paired t-test did not show any significance difference between the two groups.

In summary, the percentage of IgA-coated faecal bacteria all 19 samples analysed was determined by subtracting non-specific antibody staining as measured using isotype antibodies (figure 5.3.15). The average percentage of IgA^+ bacteria found in severe ME patients was 25.87 ± 7.42% SD versus 20.32 ± 7.35% SD in HHC. Although the differences with mean IgA^+ coated bacterial was not significant when using a paired t test ($p = 0.09$). Non-specific binding events were similar across both groups at 3.56 ± 2.40% SD for ME versus 2.67 ± 2.35% in HHC. When matching patient with their HHC in figure 5.3.14 (right-side plot), there appears to be an emerging trend for severe patients to have more IgA-coated faecal microbes than that of their designed house-hold control. The red line in figure 5.3.14 highlights a severe patient (21, F), and HHC (55, F) (flow data plots shown in figure 5.3.12), which had greatest difference between measured IgA^+ bacteria compared the other pairs.

- *Proportion of observed IgA^+coated faecal bacteria changes with time*

In 2017 an additional 20 faecal samples were studied including some samples from a second stool sample collected from patients and their house-hold control almost a year since the previous collection and analysis. Table 5.1.1 summaries 12 of the original 19 samples visited in 2016 (highlighted in yellow) that were revisited almost a year later

(2017). In addition, 6 new severe ME patients were recruited in 2017 as well as 2 new house-hold controls contributing 2 matched pairs.

In the following chosen examples of this flow data the acquisition of samples has been adapted to show proportions of Sybr green negative ($Sybr^-$) events to establish the proportion of IgA antibody reactivity in each sample that may have occurred in instances where Sybr green staining has been less effective. The percentage of IgA^+ bacteria in figure 5.3.15 shows 27.3% IgA^+ in ME (27, F) compared to 11.3% IgA^+ in the HHC (60, F). Review of the first samples from this pair in 2016 (supplementary S5.2) revealed a profile of 21.5% versus 26.5% IgA^+ in patient and control, respectively. The percentage of $Sybr^-$ IgA^+ events were 6.56% in ME and 10.6% in HHC. Isotype antibody reactivity was higher in HHC at 5.71% compared to 1.54% in ME.

The youngest ME patient within this group was 19 years old in 2017. The patient had also previously donated to this study alongside the same HHC. The samples they provided in 2017, showed similar profile of IgA^+ coated bacteria within both persons, figure 5.3.16. The percentage of IgA^+ bacteria was closely similar, as before, at 11.8% in ME (18, F) and 13.0% in HHC (55, F). In 2016, both these samples had a higher proportion of IgA-coated faecal bacteria with the patient's sample profile was recorded at 29.5% compared to 21.1% in the control (supplementary figure S5.6). Once again, the $Sybr^+$ green staining in figure 5.3.16 appears greater in HHC at 66.7% versus 53.1% in ME. Interestingly, 11.2% of IgA^+ events for HHC were recorded in the $Sybr^-$ region, compared to 4.48% in ME (fig. 5.3.16). Non-specific binding is also higher in HHC sample at 3.95% versus 1.24% in ME.

Figure 5.3.17 is another example of a follow up a year later showing the profile of IgA^+ can change from sample to sample. In this most recent sample, the percentage of IgA^+ bacteria was recorded at 5.09% in ME (38, F) compared with 6.56% in HHC (69, F). The HHC has a greater proportion of $Sybr^-$ IgA^+ events at 11.5% compared with 8.45% in the patient. This is contrasted to the 2016 data obtained for this pair shown previously in figure 5.3.13 which showed 31.8% in the patient compared to 17.0% IgA^+ in the control. Both samples showed low non-specific antibody reactive: 0.27% ME versus 0.55% HHC. Less non-specific antibody binding was seen in the HHC compared to 4.85% in the previous year (figure.5.3.13)

Two non-paired severe ME patients revealed interesting IgA^+ antibody staining patterns. The percentage of Syb^+ IgA^+ in the first patient (40) was 17.9% compared to 2.40% $Sybr^-$ IgA^+ events (figure 5.3.18A). The $Sybr^+$ IgA^+ pattern was the clearest from all samples demonstrating an obvious subpopulation of IgA^+ faecal bacteria. The percentage of non-specific antibody reactivity was all low at 1.03%. This other patient (54) who entirely bed bound (figure 5.3.18B) showed a similar percentage of $Sybr^+$ IgA^+ bacteria at 17.3% and more $Sybr^-$ IgA^+ events recorded 11.4%. Although the staining in this patient was not as discrete as in the previous patient. Isotype antibody reactivity was slightly higher at 4.83%. No data had been collected for these patients the previous year since these patients had not yet been recruited part of the study.

A	ME, F (27)	27.3 %
B	Control F (60)	16.5 %

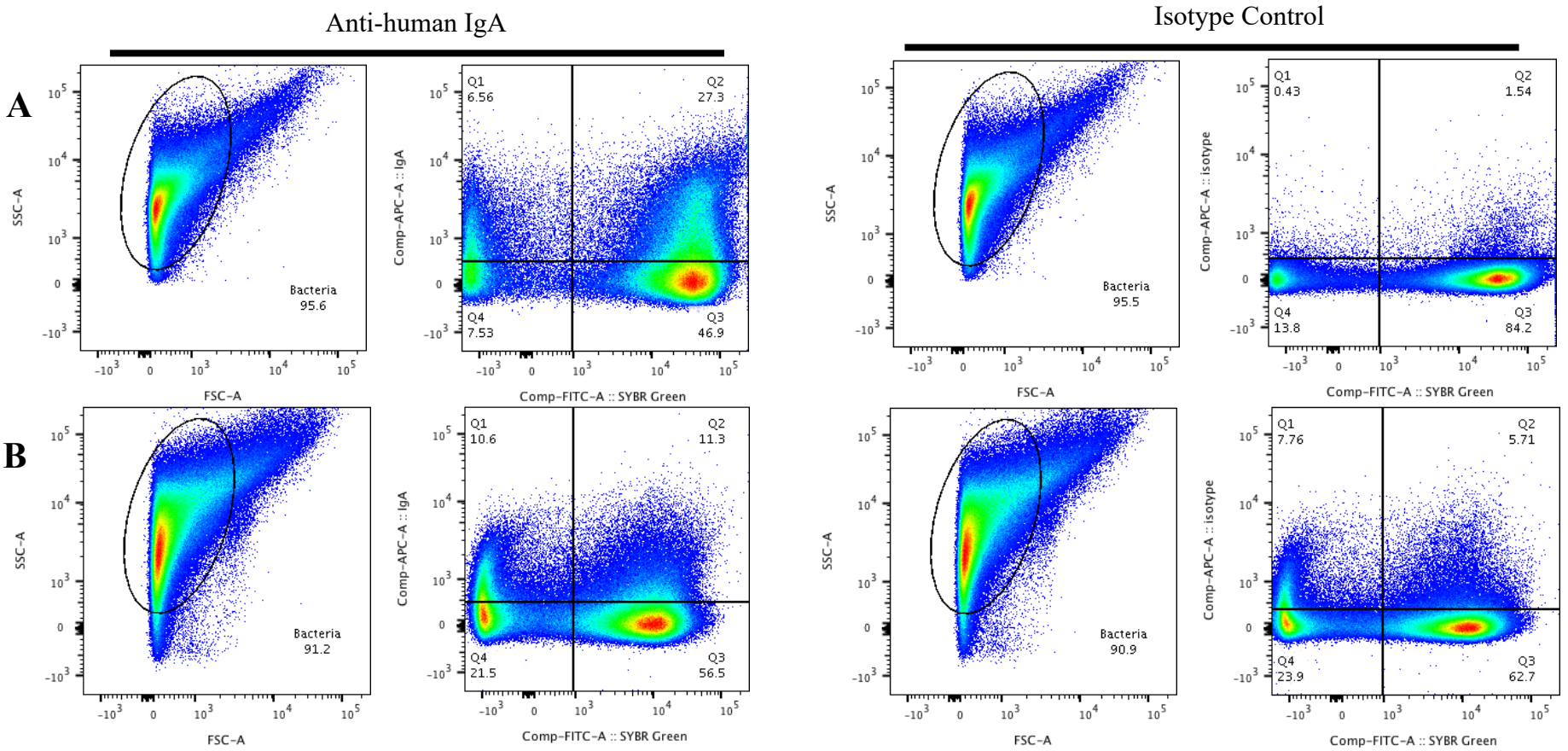

Figure 5.3.15 Flow cytometry data using faecal bacteria isolated from severe ME patient (top row) and their house-hold control (bottom row). Bacteria are gated using Sybr green fluorescence and measured for anti-IgA-APC binding to these cells recorded in the top right quadrant of IgA plots. Isotype control provides indicator for non-specific binding events. Pseudo-colour shows areas of increasing cell numbers. Numbers within each gate, represent the percentage out of total events recorded.

A	ME, F (18)	11.8%
B	Control (55)	13.0%

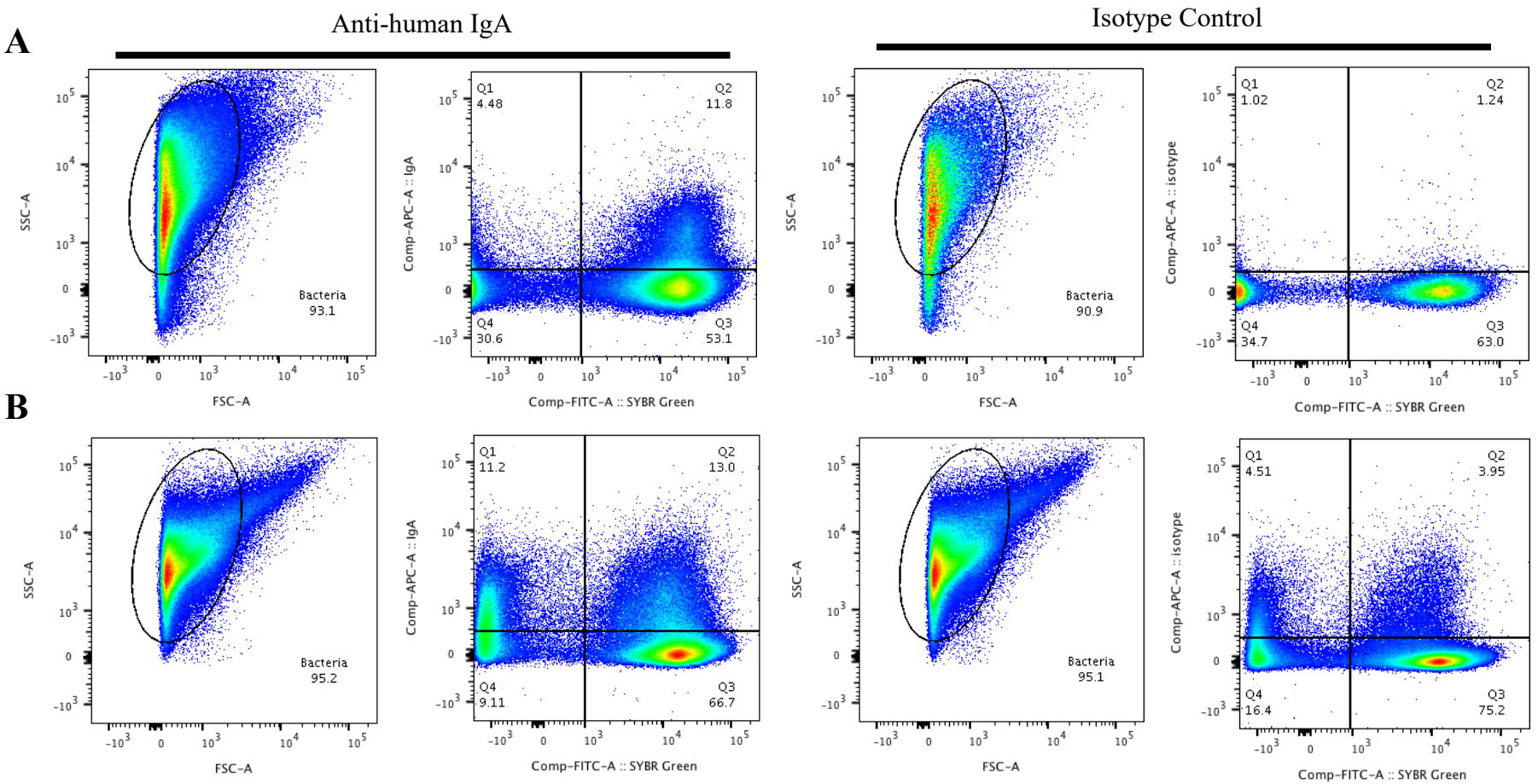

Figure 5.3.16 Flow cytometry data using faecal bacteria isolated from severe ME patient (top row) and their house-hold control (bottom row). Bacteria are gated using Sybr green fluorescence and measured for anti-IgA-APC binding to these cells recorded in the top right quadrant of IgA plots. Isotype control provides indicator for non-specific binding events. Pseudo-colour shows areas of increasing cell numbers. Numbers within each gate, represent the percentage out of total events recorded.

A	ME, F (38)	5.09%
B	Control, F (69)	6.56%

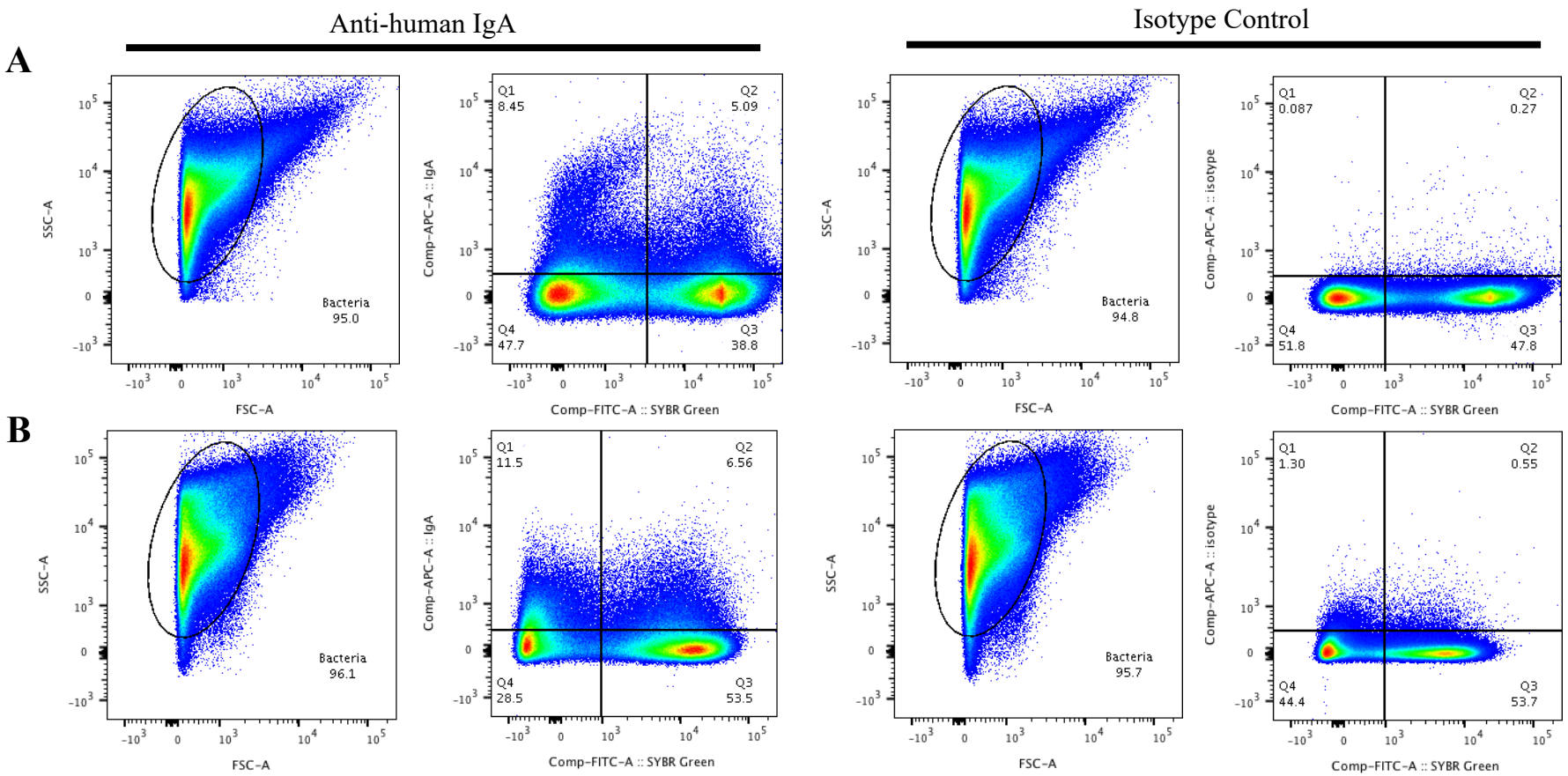

Figure 5.3.17 Flow cytometry data using faecal bacteria isolated from severe ME patient (top row) and their house-hold control (bottom row). Bacteria are gated using Sybr green fluorescence and measured for anti-IgA-APC binding to these cells recorded in the top right quadrant of IgA plots. Isotype control provides indicator for non-specific binding events. Pseudo-colour shows areas of increasing cell numbers. Numbers within each gate, represent the percentage out of total events recorded.

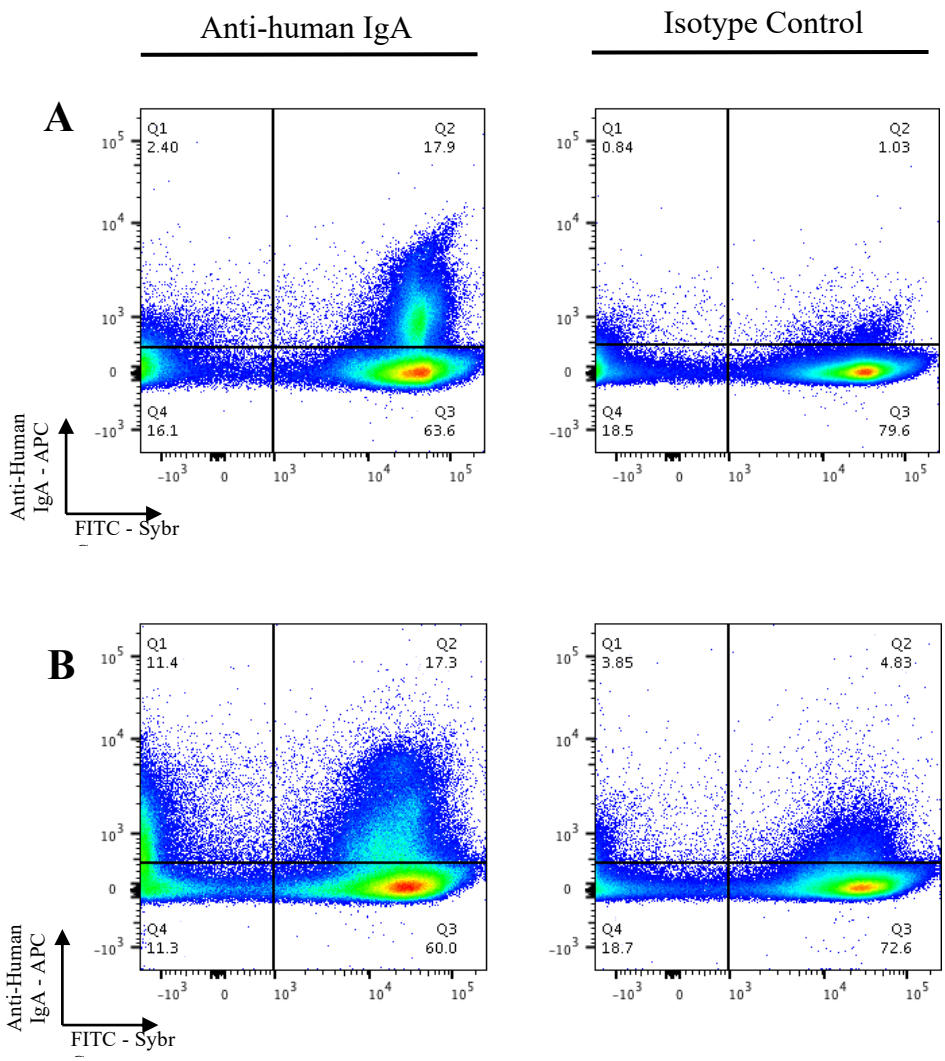

Figure 5.3.18 Discrete IgA-coated bacterial subpopulations measured from faecal suspensions in two unpaired, severe ME patients recruited in 2017. Top (A), F (40) bottom (B), F (54).

The flow cytometry data from the 2017 collections is summarised in figure 5.3.19. The range of IgA-coating of faecal bacteria in severe ME is greater than for house-hold control samples. This is due to one particular ME patient (highlighted as the red line in figure 5.2.19B. The data for this HHC (60) and patient (27) pair is presented in figure 5.3.15. This pair previously studied in 2016 (see supplementary figure 5.2) revealed 26.5% (ME) versus 21.5% (HHC) IgA^+. Comparison of the two time points for the ME patient show the profile is similar at 26.5% in 2016 compared to 27.3% in 2017. Conversely, the HHC decreased from 21.5% in 2016 to 11.3% in 2017. Unfortunately, as can be seen from figure 5.3.19, a reverse trend is found in 2017 showing most ME patients have less of a percentage of IgA^+ faecal bacteria compared to their HHC: mean % IgA^+ in ME was 10.72 ± 4.95 SD versus 9.73 ± 4.14

SD in HHC. There was very little difference on average between non-specific antibody reactivity in ME (1.87 ± 1.15% SD ME compared to 1.46 ± 2.90% SD in HHC).

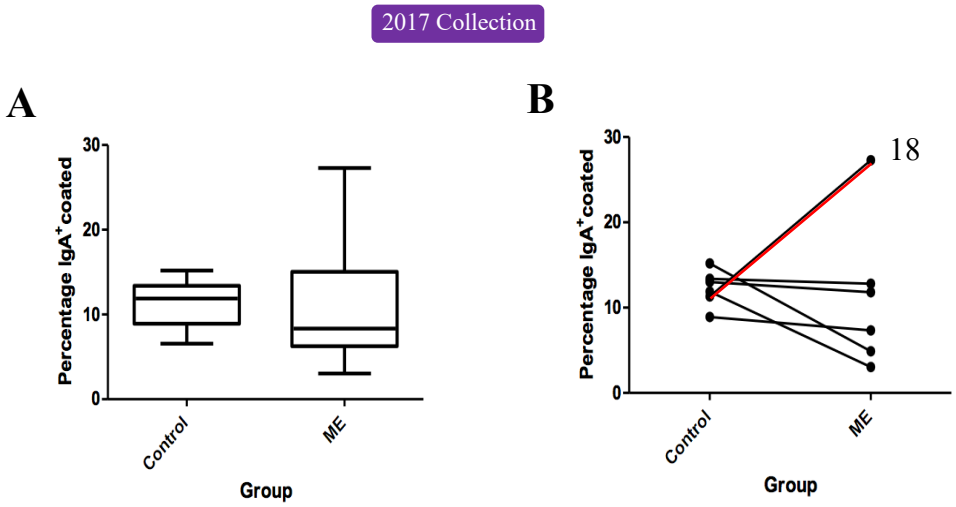

Figure 5.3.19 Summary of the relative proportion of IgA$^+$ faecal bacteria detected in 14 severe, house bound ME patients versus 6 House-Hold Controls (HHC) recruited during 2017. (A) Percentage abundance of IgA-coated faecal bacteria in samples collected in 2017. (B) lines indicated pairing between severe ME patient and house-hold control.

5.3.4 Serological markers of a leaky gut

Thirty-eight complement inactivated serum samples were used to measure endotoxin (LPS) concentration and LPS-binding protein (LBP) as surrogate markers for intestinal permeability. Both screening assays were performed consecutively on same aliquot of serum per patient and house-hold control sample. The endotoxin screen was performed firstly, followed by the LBP assay within 24hrs on serum kept at 4^0C. The serum samples had undergone one freeze-thaw cycle in total. Samples from mild/moderate ME/CFS were more freely available since these patients were able to attend the hospital during a pre-arranged visit during 2015. The data obtained for LPS and LPB in these samples showed no clear differences between these groups (figure 5.3.20).

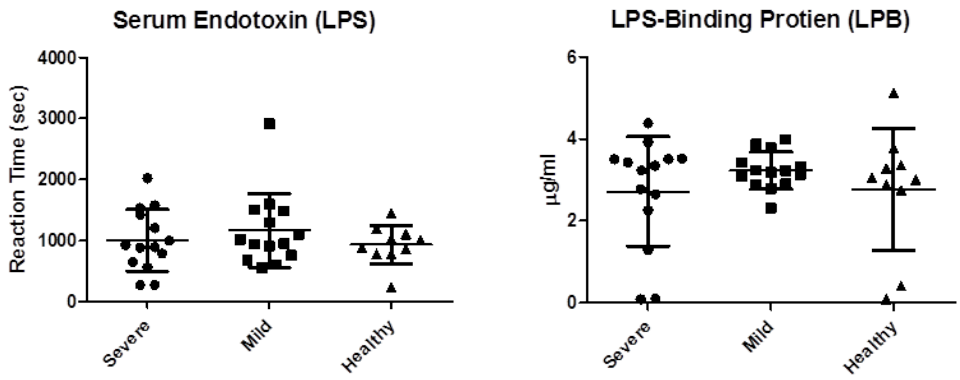

Figure 5.3.20 Serum endotoxin activity and LBP concentrations measured in 14 Severe (S), 14 Mild/moderate ME (M) and 10 House-Hold Controls (HHC) as markers for bacterial translocation. The horizontal bars in both plots for LPS and LPB in figure 5.3.20 represent the median values for reaction time (RT) and concentration (µg/ml) respectively. Error bars represent the standard deviation

5.4 Discussion

The results from this chapter provides a new insight into the pattern of IgA-coated faecal microbes in severe, house-bound ME patients. To date, there are no clinical biomarkers reflecting the status of the intestinal immune system and its interactions with luminal microbes. Previous studies have assessed the composition of the ME/CFS microbiome with data limited to the general ME/CFS population and no information about how changes in the microbiome may relate to severity of ME. Giloteaux et al. and others have reported a general reduction in microbial diversity in the general ME/CFS population as well as increases in Gram negative *Proteobacteria* which are more abundant in inflammatory environments such as IBD and provide source of bacterial LPS (Giloteaux et al., 2016; Sartor, 2011). Based on the current available data, there is a lack of consensus on the precise pattern of dysbiosis and how this is related to causality in ME/CFS. Indeed, any disturbances within the ME microbiome will alter dynamic feedback mechanisms with the gut immune system and reactivity to certain microbes that may give indications of underlying mechanisms driving changes in the immune system. This needs to be addressed in further studies of additional immune parameters for possible additional biomarkers, such as leaky gut.

We hypothesised that severe ME patients have increased intestinal permeability which can impact immunity by allowing intestinal microbes to be exposed directly to the local and subsequently systemic immune systems. The mucosal immune response was examined for production of secretory IgA (sIgA) reactive with faecal bacteria isolated from the patient's own stool. Indeed, faecal bacterial flow cytometry has been established for some time with different variations in faecal sample preparation and staining (van der Waaij et al., 1994). To refine the method used by Palm et al., 2014, faecal microbes were stained with Sybr Green nucleic acid stain to exclude faecal debris, electronic noise and small bubbles registering as events within the flow cytometer. This appeared to work well in most samples, however IgA^+ reactivity was also apparent in Sybr green negative fractions suggesting some microbes may not stain as effectively. The effectiveness of Sybr green staining it likely to depend on the stool consistency and the composition of an individual's microbiota as many bacteria have differences in the structure and design of their cell wall. This is a similar problem to the one discussed earlier regarding DNA extraction from bacteria within complex samples such as human faeces where the diversity and complexity of the community structure of the microbiota is the greatest compared to any other site in or on the human body.

The protocol for detection of IgA-bound faecal bacteria was trialled and optimised with Sybr green staining using one of the first patient/house-hold control samples collected in 2016. The IgA profile in this patient and house-hold control (fig 5.3.11) showed a higher proportion of IgA^+ coated bacteria in ME: 21.3% versus 6.37% in the HHC. This result was encouraging and demanded further investigation using more samples, since potentially, IgA-coating might be a useful immune marker to describe interactions between microbes and the immune system and may have relevance in the context of the status of the integrity of the intestinal barrier. On the latter point, inflammation in active IBD causes tissue damage and destruction of the intestinal barrier and as discussed in the introduction to this chapter, anti-microbial antibodies may have some diagnostic relevance in this process (Mitsuyama et al., 2016; Strober & Fuss, 2011). The integrity of the intestinal barrier is essential for innate immunity via PPRs displayed on the epithelial cells to which commensal bacteria can bind and signal anti-inflammatory immune responses as well as producing anti-inflammatory molecules such as butyrate which further enhance T(reg) responses and HDAC activity to promote changes in gene expression that support epithelial barrier integrity and tolerance to intestinal bacteria (Bordin et al., 2004; Vanhoutvin et al., 2009; Zhou et al., 2018). Without the proper regulation and exclusion from the luminal environment, commensal bacteria can infiltrate the intestinal epithelial barrier providing non-self antigen simulating inflammation and tissue damage by increasing activation immune cells such as DCs and macrophages to produce pro-inflammatory cytokines which favour Th1/Th17 proliferation.

Under normal conditions in the intestine, T-cell independent IgA production is supported through interaction of B cells with DCs which produce retinoic acid inducing α4β7 integrins and chemokine receptor 9 expression on circulating B cells to home to the intestinal mucosa and differentiate within the lamina propria into plasma cells secreting sIgA (Fagarasan et al., 2010; Mora et al., 2006). DC-derived factors such as BAFF and APRIL further bind to B cells and enhance class switch recombination (CSR) from IgM to the IgA isotype (Berkowska et al., 2015). However, an altered pro-inflammatory T cell environment driven by increases in intestinal permeability could led to more T cell dependent production of mucosal IgA secreted by plasma cells in the lamina propria governing somatic hypermutations and enhancing antibody affinity towards specific microbial antigens in the intestine. For example, T-follicular helper (Tfh) cells interact with B cells in the GCs of the lamina propria through CD40L presented on activated CD4+ T cells increasing CD40

intracellular signalling which causes activation-induced cytidine deaminase (AID) within B cells to undergo affinity maturation and CSR to IgA antibody production (Berkowska et al., 2015; Muramatsu et al., 2000; Rescigno, 2014; Shulman et al., 2013). Moreover, Th17 cells and their associated cytokines IL-17, IL21, and IL22 have been shown to induce strong proliferative responses in B cells triggering CSR and increased antibody production with blockading of IL-17 signalling leading to reduction in the size and number of germinal centres where naïve B cells encounter antigen and undergo affinity maturation (Mitsdoerffer et al., 2010). IL-17 has been shown to promote intestinal IgA responses to intestinal infection although it did not affect the development of IgA+ memory B cell responses (Huang et al., 2017). Under homeostatic conditions, DC and Treg cell derived cytokines, TGFβ and IL-10, represent a major T cell independent pathway which leads to the differentiation of B cells into antibody secreting plasma cells with affinities for lipid and carbohydrate structures on bacterial cell surfaces that are consider to be 'natural' of innate antibodies which help stop microbial translocation across the epithelial barrier (Berkowska et al., 2015; Litinskiy et al., 2002; Macpherson et al., 2000). Finally, it has been documented that serum level of IgM and IgA reactive antibodies against bacterial LPS have been found to be higher in patients with CFS as well as in major depression disorder (Maes et al., 2012; Maes, Mihaylova, et al., 2007).

Leaky gut is commonly associated in IBD as a consequence rather than a direct cause with the majority of current IBD therapies target inflammatory pathways with limiting degrees of efficacy (Shimshoni et al., 2015). Potential therapies directed at modulating the microbiome and restoration of the gut barrier are highly likely important targets in future treatments. This is further substantiated by the fact that a high percentage of IgA-coated microbes have been reported in IBD patients and subsequently isolated and sequenced to identify specific bacterial taxa associated with driving inflammation in germ-free mice (Palm et al., 2014). Whilst IBD is an extreme example of loss of intestinal barrier integrity; the increases in the proportion of IgA-coated bacteria may be a new marker for intestinal permeability that can be applied to other diseases associated with permeability and intestinal immune system defects.

A total of 11 severe ME patients and 8 house-hold controls were recruited in 2016. The original recruitment target of 35 patients had previously been determined using a statistical power calculation based on the differences in endotoxin measurements found serum from IBD patients versus healthy controls (Rojo et al., 2007). Home visits required a significant amount of

organisation and coordination to ensure samples were collected and processed as quickly as possible. Unfortunately, it was not possible to perform experiments on fresh samples, so faecal aliquots were processed and stored at -80^{0}C on the day of collection and examined at the end of the recruitment phase. Simultaneous processing of all these samples occurred in a single day and were analysed in a blinded fashion. An emerging trend for increased IgA-coating was found in the majority of severe ME patients compared with their respective house-hold control (HHC), fig. 5.3.14. Most interestingly is patient 9 in this figure which had the second highest proportion of Sybr$^+$ IgA$^+$ bacteria (36.6%) and the biggest increase compared with the HHC. This patient was visited in a completely darkened room and was highly sensitive to any light and sound and speech was difficult. Even though all the patients considered in this work are referred to as severe, there is still considerable variation between them. Whereas, some have no sensitivity to light or sound and are able to manoeuvre around the house, others are almost entirely bed-bound. It is important to note that the conception of this study occurred prior to the 2015 when the Institute of Medicine gave a recommendation to change ME to systemic exertional intolerance disorder (SEID) (IOM et al., 2015). New diagnostic criteria are continuously being reviewed with no consensus on the best criteria to use in ME research.

With the exception of one matched pair, all samples used in this work were gender matched, *see table 5.2.1*. Age is a confounding factor in this study and is known to be important for the immune system (Magrone et al., 2013), but emphasis should be given to the fact that environmentally matched samples obtained from the same house-hold were made a priority for microbiome analysis. Unlike mice, diet and housing factors are almost entirely difficult to control in humans. Therefore, the inclusion of healthy same house-hold controls was an attempt to control for important co-variants of microbiome variation, lifestyle, diet and behaviours. Many of the paired samples are relatives of one another therefore share genetic similarities as well as exposure to the same house-hold environment. Joosens et al. were the first to show unaffected relatives of patients living with Crohn's disease exhibit distinct pattern of intestinal dysbiosis with evidence for decreased species *Collinsella aerofaciens* and *Escherichia coli-Shigella* group and increase RA of *Ruminococcus torques* compared with healthy controls (Joossens et al., 2011). Intestinal permeability has been reported at a two-fold increase in Crohn's and relatives compared to conventional healthy controls suggesting this to be a contributing factor and potential disease mechanism (Hollander et al., 1986). Indeed, first degree relatives of IBD patients have a 1 in 10 risk of developing the condition and taking together with current

microbiome data indicate a significant role for gut dysbiosis and leaky gut in causing disease (Russell & Satsangi, 2004).

The availability of a second stool sample from some of the patients studied in 2016 gave opportunity to re-examine IgA reactivity to faecal microbes in these patients and their HHCs. The level of IgA^+ microbes was similar or decreased in ME. Out of the 12 ME patients revisited, only 6 were included with a HHC. Patient 18, a daughter aged 27 matched with her mother aged 60 in figure 5.3.16 was convincingly higher on this occasion but had previously showed no difference the previous year (supplementary figure 3). The result highlights the dynamic nature of IgA production against intestinal microbes and raises significant questions. For example, are there qualitative differences in the bacterial taxa coated with IgA in severe ME compared with HHC; do systemic IgG antibodies exist against these IgA-coated bacteria? This list is not extensive; however, further work is needed to see how faecal IgA-coated bacteria proportional differ over time and if this can be attributed to disease worsening.

Many of the severe ME patients produced visibly smaller amounts of stool which were compact and hard to manipulate indicating dehydration. This will have an impact of the total number of bacteria within the sample, however IgA measurements are provided as a percentage of total faecal bacteria is not affected by the variation of the numbers of events recorded in each sample. Other research has examined the role of serum IgA against a limited number of enterobacteria using an indirect ELISA containing the LPS of 7 different species (Maes et al., 2007). This work has been further extended to suggest that treatment of a leaky gut can improve ME symptoms based a 'leaky gut diet' and supplementation with L-carnitine, CoQ10, lipoic acid and taurine (Maes et al., 2007). In this case study, this diet focused on exclusion certain dietary allergens, such as dairy, as well as adherence to low-carbohydrate and gluten-free food in a single 13 year old girl who was already lactulose intolerant (Maes et al., 2007).

During the process for obtaining research ethical approval, a new method was explored to help determine if alterations in intestinal barrier permeability exist in ME/CFS patients. Using a novel whole cell bacterial microarray-based approach to screen patients' serum for antibodies against intestinal bacteria immobilised onto a nitrocellulose-coated glass slide. *Bacteroides thetaiotaomicron, Enterococcus gallinarum, Escherichia coli* and *Akkermansia muciniphila* were assessed for their ability to be printed on a microarray, figures 5.3.8 & 5.3.9. Microarray printing offers huge scope to include hundreds of representatives of the

human gut microbiota compared with relative few microbes have been targets for seroreactivity using flow cytometry (Haas et al., 2011). The growth kinetics for each strain enabled calculation of the growth rate, μ, and estimation of the time-point at which cells had reached mid-exponential growth phase for subsequent immobilisation on to the microarray (data not shown). Mid-exponential growth phase was chosen for the purposes of obtaining a high cell viability count so that upon fixing cells in 4% formaldehyde the majority of cells would remain intact ("whole-cell") when screened against patient serum. Thus, any serum antibody reactivity detected will be against bacterial surface antigens such a LPS, fimbriae, or pili etc.

The rationale for using whole cell bacteria immobilised onto a microarray slide, follows that the bacterial cell surface is decorated with an array of molecules such as outer membrane proteins, lipopolysaccharide, flagella (H-antigens), capsules and fimbriae or pili and that the surface molecules are involved in bacterial adherence and are important in establishing an infection (Thirumalapura et al., 2006). Finally, antibodies directed against the bacterial surface antigens can neutralise the bacteria and afford protection particularly against invading extracellular bacteria leaking from the gut.

Systemic priming to intestinal microbes has been documented in IBD and suggested to drive chronic immune activation and consequently disease progression via translocation of intestinal bacteria, including their products such as LPS (Haas et al., 2011; Elkadri et al., 2013). Experiments performed in specific-pathogen free mice demonstrate compartmentalisation between the intestinal mucosal immune system and systemic immunity where IgG responses to commensal bacteria are undetectable unless these mice have been engineered with deficiencies in bacterial sensing through toll-like receptor signalling (Slack et al., 2009). On the contrary, antimicrobial antibodies have been measured healthy humans against a limited number of representatives of commensal bacteria using flow cytometry (Haas et al., 2011). More evidence suggests gram-negative commensals can stimulate systemic immune responses to produce IgG antibodies reactive against commensal antigens, and murein lipoprotein (MLP) on Gram negative bacterial cell walls (Zeng et al., 2016). MLP was found as a major source for stimulating IgG responses in mice and humans. Passive transfer of anti-MLP IgG antibodies in mice to demonstrated protection against *Salmonella* infection (Zeng et al., 2016). This study underpins commensal driven immune response have widespread systemic consequence for the protection against pathogens.

Failed attempts to successfully validate the bacterial array using wild-type OmpA positive and negative stains was further compounded by the time home visits became underway with challenges confronted in obtaining blood necessary to perform this type of screening assay. To that end, the solid phase bacterial microarray assay was abandoned in favour for the ease of availability of stools samples to explore anti-IgA responses to faecal bacteria. LPS-Binding Protein (LPB) is another indicator of LPS leakage into systemic blood serum which could be an effect of microbial translocation. LBP increases binding of circulating LPS to soluble CD14, but its quantification can be more advantageous than detection of LPS alone, since it does not suffer of interference from blood that have been well documented using LAL assays. We found no evidence of these markers being any different in ME patients compared to house-hold controls. This result is in contrast to an earlier report which suggests ME patients have increased bacterial translocation based on elevated plasma LPS, CD14 and LBP concentration in 48 ME/CFS patients and 39 controls, compared to just 12 severe patients and 10 HHCs (Giloteaux et al., 2016). Interestingly we observed much less LBP in both patients and HHC ranging from 8 ng/ml to 4.38 μg/ml compared to a median of 12.38 μg/ml for healthy controls in this previous study. However, our observations for LBP concentration are within the range of healthy humans reported to be between 1.85 – 17.4 μg/ml in serum in a study of serum LBP concentration analysed in 63 severe sepsis and septic shock patients whose level of LBP was found to increase 10 fold in range from 11.8 μg/ml to 275 μg/ml which also reduced LPS activity as expected (Zweigner et al., 2001).

To conclude, the representation of anti-microbial antibodies in patients compared with healthy controls is proposed as an additional marker for interpretation and understanding of how the intestinal microbiota interacts with the immune system in pathological circumstances. Flow cytometry is a well-established technique, shown in this chapter to be suitable for measuring anti-IgA-coating in faecal samples. Skill of the flow cytometer operator is needed to confidently lower the threshold voltages to determine the relatively small size of bacterial cell within the area of the data plot. Bacteria are approximately 1 μm with pure cultures successfully demonstrating light scatter characteristics that were used to examine faecal suspension of bacteria. This can be achieved using forward and side scatter light properties alone, although it is worth noting particles of a similar size that or not microbial, e.g. food particles may also be detected. Thus, the data here has shown that Sybr green appears to be a useful refinement to examine faecal microbes and should be used regularly, but it must also be acknowledged that composition of the microbiota will also impact the success of this labelling. Where possible we

have tried to include data for $Sybr^{-}$ IgA^{+} fractions of the microbiota. From our analyses the differences between the percentage of IgA^{+} coated to total faecal bacteria between severe ME patients and HHCs is inconclusive but quantitative differences are distinct from qualitative differences. Therefore, an outstanding question remains, what are these IgA antibodies specific towards? Future work is needed to isolate these bacteria and identify their taxonomic profile as well as the status of IgA-coated microbes in relation to worsening of symptoms severity for ME/CFS. In the first dataset, from collections made during 2016, we identified a non-significant trend of increased IgA-coated faecal microbes in severe ME compared to house-hold controls. Repeat sample collection, in 2017, reversed this trend. Whilst sample collections for both years were conducted during the season of spring/summer, it is worth noting age, gender and seasonal variations influence SIgA and are indeed reported lower in females, increasing in both genders with age (Weber-Mzell et al., 2004). Certainly, faecal IgA concentration and microbial specificity appear relevant in the context of IBD pathology and gut permeability defects in these cases (Adams et al., 2008; Hollander et al., 1986; Palm et al., 2014; Targan et al., 2005; Viladomiu et al., 2017). The data presented here in severe ME warrant further investigation in larger, better defined patient cohort, preferably taking multiple samples to assess the dynamics of intestinal secreted IgA reactivity over time.

Chapter Six

6 General Discussion

6.0 General Discussion

The original hypothesis for this study suggested increased intestinal permeability exposes the local intestinal immune system to a quantity of non-self-bacterial antigens that facilitates low-grade chronic inflammation and possible autoimmunity (Kelly et al., 2015). The mechanism behind this theory is that chronic immune activation in ME/CFS causes oxidative and nitrosative stress (O&NS) and prolonged levels of pro-inflammatory cytokines via activation of NF-kB (Morris & Maes, 2014). Serum IgM levels against damaged lipid cell membrane components such as palmitic and myristic acid present as neo-epitopes, previously hidden from the immune system (Maes et al., 2006). ROS such as peroxides and superoxides (H_2O_2 and $2O_2^-$) are generated by the immune system to kill pathogens injected by phagocytes (Fang, 2011). Recently a linked has been proposed between chronic immune activation of ROS in serum causes mitochondrial dysfunction (Blomberg et al., 2018). Critically, oxidation of cysteine residues in pyruvate kinase M, an enzyme associated with the pyruvate dehydrogenase complex (PDC) can block production of pyruvate which supplies energy in to the citric acid cycle (Anastasiou et al., 2011).

We anticipated to replicate recently reported disturbances in severe patients, in particular aerobic energy metabolism affected in ME/CFS with increased lactate production (arising from pyruvate) and breakdown of amino acids as an alternative energy source for the citric acid cycle to produce ATP (Fluge et al., 2016; Germain et al., 2017; Naviaux et al., 2016; Yamano et al., 2016). Many individual serum metabolites others have reported were found to be no different in our severe ME patients. In some cases, one or two samples were distinctly separate from the rest of the group and these have been marked with their sample number. Our study is most comparable with Armstrong and colleagues who also used ^{1}H-NMR to analyses serum and faecal water metabolomes (Armstrong et al., 2015, 2017). They, and others, have suggested disturbed energy metabolism through inhibition of glycolysis that may be linked to mitochondrial dysfunction through chronic immune activation of oxidative stress pathways (Armstrong et al., 2017; Fluge et al., 2016). We did not find elevated glucose, or reduced lactate (fig. 4.3.11), glutamate and pyruvate in patients as suggested by Armstrong et al, and therefore cannot conclude glycolysis is being affected. Another metabolite we were expecting to find reduced was hypoxantine, a breakdown product of ATP. Several amino acids were expected to be reduced in the event of them being used as an alternative to carbohydrate energy sources (gluconeogenesis) for the citric acid cycle, but this was not replicated either. To this end, serum citrate

concentration was the same for all groups, (table 4.3.3). Interestingly, faecal y-butyrobetaine was notably higher in 3 severe ME patients, and is a metabolite of L-carnitine which is essential for transfer of acetyl-CoA into the mitochondrial matrix for energy production from the beta oxidation of fatty acids. Increased lactic acid producing bacteria have been reported in CFS patients, but we did not measure any differences in both faecal and serum concentrations for lactate (Sheedy et al., 2009). Based on the serum profile we cannot provide evidence for increased intestinal permeability since microbial-derived metabolite butyrate was not detected. The suggestion of increase amino acids in serum was also not replicated in our cohort, nor were they reduced due to increased bacterial fermentation to reproduce SCFAs (Armstrong et al., 2015).

Both our faecal water and serum metabolome profiling used a small number of samples. Fourteen was the maximum group size, used in serum, for severe ME compared to 34 ME/CFS patients included in Armstrong and colleagues work. The number of patients we analysed the faecal metabolome in was just 11 severe patients and 6 HHC as these samples were collected in 2017. Again, we found no significant changes in the faecal metabolome of ME/CFS patients with respect to increased SCFA production entering energy metabolism, as previously reported (Armstrong et al., 2017). The sequence data (dataset C) for these samples also provided no significant findings, based on 16S V4 amplicon sequences (fig 3.3.32). Earlier collections in 2016 analysed using shotgun metagenomics did provide some significant changes for reduced *F. prausnitzii* and increased *Eggerthella spp*. and *Oscillibacter spp.* in severe ME. Table 3.3.2 compares the overlap of the same patients and HHCs providing samples in 2016 and 2017 to produce both datasets. We had expected to find the opposite of increased SCFAs, particularly the anti-inflammatory mediator butyrate, given its production is associated with *F. prausnitzii* and protection against colitis in rodents (Zhou et al., 2018). Despite re-analysing a different aliquot from some of the same samples collected in 2016 from the same patient, and repeated collections from these patients in 2017 as well as recruiting brand new patients, we did not see a reduction of *F. prausnitzii* in patients based on 16S amplicon sequencing. Many of the patients and HHCs did appear to associate according to their respective pairing based on 16S composition (fig. 4.3.28), which does reflect house-hold exposure and a degree of shared diet can influence the microbiota, although we could not request dietary information.

To perform correlations between the composition of the ME/CFS intestinal microbiome and the faecal and serum metabolomes, we would have needed to compare dataset C with our NMR data, as samples in these datasets were collected at the same time. To that end, we found insufficient difference between severe patients and controls for concentration of metabolites and differences in microbial composition to use a machine learning approach to produce a predictive model for diagnosing severe ME patients from house-hold controls. The relevance here to explain how the structure and metabolic role of the microbiota in various pathophysiological mechanisms, likely to exist in ME/CFS, may more severely disrupt host metabolism in some patients more than others. Such an approach would require many more data points, and a different study design integrating shotgun metagenomics with mass spectrometry to cover ten times more the number of metabolites based on comparison of the number of observations made by Germain and Naviaux. Under half the number of species of bacteria were observed in our shotgun metagenomic dataset compared to Nagy-Szakal and colleagues. The reasons for this were explained earlier, however, it is worth noting we observed 38.64±6.28 SD and 34.62±8.97 SD species in ME/CFS and HHCs, respectively, compared to 74.24±1.67 SE and 77.5±2.07 SE in their ME/CFS cohort and controls, respectively. We were unable re-perform shotgun metagenomics and instead produced dataset C using 16S-targeted amplicon sequencing. The two methods cannot be compared but it is apparent that 16S sequencing does not provide detailed functions of the microbiome and should be replaced with more informative shotgun metagenomic studies which provide functional pathway information that others have reported disturbed in ME/CFS which can then be better integrated with interpretation of faecal and blood metabolomes in patients.

Nagy-Szakal and colleagues reported IBS status significantly altered the composition of the intestinal microbiome in ME/CFS. We did not objectively assess the IBS symptoms in our patients, but it is worth mentioning that all patients did have IBS-like symptoms, particularly abdominal pain and dietary intolerances in most cases to diary. Stress and anxiety are cofounding factors which influence the microbiota and are highly prevalent in ME/CFS patients and may predispose them to IBS (Lakhan & Kirchgessner, 2010). At the genus level, *Faecalibacterium, Roseburia, Dorea, Coprococcus, Clostridium, Ruminococcus* and *Coprocobacillus* were associated with ME/CFS with an emphasis on *Faecalibacterium* and *Alistipes* (Nagy-Szakal et al., 2017). Although, dataset A contains no controls, figure 3.3.5 showed the biggest differences in RA for individual mild/moderate ME/CFS patients

was in the genera, *Faecalibacterium*, as well as *Roseburia*, *Alistipes*, and *Oscillospira.* Interestingly, we found the *Eggerthella* genus was more abundant in our severe ME patients (figure. 3.3.13A) which Nagy-Szakal and colleagues report one of its members *Eggerthella lenta* may be a marker for patients with IBS (Nagy-Szakal et al., 2017). We did not find a significant difference in the relative abundance of the genus *Blautia* between severe patients and HHCs (figure. 3.3.32) despite this being reported to drive separation of ME/CFS without IBS from controls (Nagy-Szakal et al., 2017). *Blautia* can account for anywhere between 2.5% to 16% of the total intestinal microbiota but is usually more abundant in IBS due to higher levels of gases produced as by-products of bacterial fermentation (Eren et al., 2015; Rajilić-Stojanović & de Vos, 2014; Vernocchi et al., 2016). Higher abundance of *Blautia* may also be reflective of *Dorea sp*p. as a major contributor of hydrogen and carbon dioxide gas production, which *Blautia* can convert into acetate (Rajilić-Stojanović & de Vos, 2014). To that end, it is important to separate IBS co-morbidity as a cofounding factor influencing the ME/CFS microbiota and makes it more likely an ME/CFS associated profile will be influenced by low in abundance individual species. In addition to the lack of being able to reproduce increased SCFA production in ME/CFS we did not find any evidence for increased microbial fermentation based on relative abundances of *Clostridium spp*. or *Bacteroides spp.* either. Finally, we cannot conclude there is any difference in the diversity or number of bacteria found in ME/CFS and HHCs.

Germain and colleagues performed pathway analysis on 74 altered metabolites they found using mass spectrometry. This showed taurine metabolism had the highest impact factor in ME/CFS given its decrease in patients, 3 end products in primary bile acid biosynthesis in this metabolic pathway that were also found reduced in ME/CFS patients (Germain et al., 2017). In our severe patient cohort, faecal taurine was only found in 3 patients in high concentration (supplementary 4.1), and importantly none of the HHCs. In these patients it may suggest increased bile salt hydrolysis. Bile salts enable emulsification and digestion of dietary fat, uptake of vitamins, and maintenance of intestinal barrier function, but can become metabolised into secondary and tertiary bile acids by members from diverse genera including *Bacteroides, Clostridium, Lactobacillus, Bifidobacterium, Enterobacter, Eubacterium* and *Escherichia* (Vernocchi et al., 2016). Microbial deconjugation of taurine is the first step which prevents active uptake to the liver for recirculation. High concentration of free bile acids can then become metabolised into secondary bile acids that are able to diffuse lipid bilayers causing disruption to the cell membrane and regeneration of ROS

which can cause DNA damage and mutation and mitochondrial dysfunction that have been associated with a risk of colon cancer (Ajouz et al., 2014; De Boever et al., 2000). Observations of changes in bile acids metabolism in ME/CFS are relevant given they participate in energy regulation, glucose and lipid metabolism (Wahlström et al., 2016). CDCA was lowest in severe ME serum (fig. 4.3.32A) but compared with HHCs does not support evidence of liver toxicity damage as suggested by Germain and colleagues. Conversely active IBD serum provide in the same experiment was statistically higher for CDCA and CA compared to the other groups and may reflect increased bile acid re-uptake due to intestinal barrier breakdown. CDCA concentration may well be expected to be lowest in the severe group given these patients undergo significant periods of fasting or eating very little. This was also reflected by on average less faecal material provided at sample collection compared with HHCs.

In summary, we have been the first to achieve shot metagenomic sequencing in severe, house-bound ME/CFS patients. The rapid evolution of next generation sequencing, guidance in designing the perfect microbiome study from methods of sample collection to analysis have arrived largely after they could be applied to this work. In the previous discussion chapters, it has emerged designing a study on ME/CFS is not straightforward and must be carefully thought out as there are many possible cofounders in these types of studies and is further complicated by the range of symptom complexes within ME/CFS which patients could be selected for and against, e.g. patients with or without IBS or PEM. The choice of these is dependent of the nature of the study and the available resources and methods to clinical assess these patients. The work presented in this thesis attempts to explore the impact of severity of ME/CFS symptoms. How these symptoms are objectively measured along with interpretation of symptoms questionnaires is not agreed internationally. Arranging home visits to patients and coordinating sample collections was enormously time consuming and expensive but did reveal severity of ME/CFS is still largely dependent on a matter of opinion and can have different interpretations and meaning from patient to patient. For example, out of the 17 patients visited, 4 demonstrated extreme hypersensitivity to light and sound. One patient in particular was bed-bound living in the basement to avoid sources of natural or artificial light and was extremely sensitivity to the quietest of sounds. Other severe patients were more mobile around the house, with symptoms vary from day to day.

Our efforts to minimise cofounding factors influencing the microbiome are demonstrated by the inclusion of house-hold controls. We have also taken the approach to adopt a more functional understanding of the microbiome in ME/CFS with the acquisition of ^{1}H-NMR metabolomic profiling from faecal water and serum in an attempt to re-produce findings that have only recently populated the ME/CFS literature in the last two years. Again, these recent findings have come at a time when they could not influence our study design, particularly targeting known compounds in energy and lipid metabolism, as well as controlling for sampling methods and standard operating procedures used in these studies. For example, we originally set out to use serum for anti-microbial detection instead of plasma, which is the biofluid of choice in mass spectrometry studies. To address our hypothesis patients with ME/CFS have increased intestinal permeability we measured the proportion of IgA-coated faecal bacteria, based on the assumption increased IgA production to neutralise intestinal bacterial in a mechanism known as immune exclusion. Although we measured surrogate markers, LPS and LBP, and found no evidence of increased permeability, we gained an insight into the immune system interactions with the intestinal microbiota through sIgA interaction with the patient's own faecal material versus microbes cultured and LPS alone. These results initially showed a trend for increased IgA-coated bacteria in ME/CFS versus HHCs. Almost a year later this trend appeared to reverse. Further work is needed to measure the abundance of bacterial taxa with IgA^{+} and IgA^{-} and to see if these correlate with increased antibodies in serum. This analysis recently been performed in adults versus the elderly and found differences in abundances of *Clostridiaceae* and *Enterobacteriaceae* were lower in the IgA^{+} for the elderly group (Sugahara et al., 2017).

- *Summary*

We draw this thesis work here to a conclusion with the suggestion that more focus is needed for longitudinal shotgun metagenomic studies in ME/CFS to see how functional pathways change in the ME/CFS microbiome and impact the disease with an emphasis of symptom severity and recommendation for the inclusion of house-hold controls. We set out to replicate existing findings of mild to moderately affected ME/CFS patients and to identify significant evidence for intestinal dysbiosis This is the first metabolome-based study of severely affected ME/CFS patients that incorporates the unique feature of same household healthy control subjects to mitigate against major environmental factors that contribute to population-level microbiome variation. On contrary to previous reports in

ME/CFS, our findings fall short of a reduction in the diversity of the severe, house-bound ME microbiome when we compared them with this form of control. Indeed, several applied indices for measuring similarity between groups showed both severe ME and house-hold controls were more compositionally heterogenous than unmatched controls. Based on the current sample size, no clear pattern emerged from this data to suggest a role for specific members on the intestinal microbiome, except for the low abundance of *F. prausnitzii.* However, this species is not specific to ME/CFS and is well associated with IBS symptoms, also highly prevalent amongst the ME/CFS patient population. For that reason, more functional based studies examining the relationship between microbes and the host are encouraged, particularly with respect to microbial-immune and gut-brain signalling. As such, transcriptomic and proteomic analyses may further probe the metabolic activity, beyond the predictive capability of whole-genome sequencing analysis.

Based on comparing more than 50 metabolites in serum and faecal samples our findings do not replicate those of other ME/CFS metabolomics studies. Indeed, the lack of any particular finding consistent with altered metabolism in either faecal and serum metabolome of severe ME/CFS patients was surprising and appears to reject our earlier hypothesis. The only significantly altered serum metabolite we detected was the N-Acetyl groups from α_1-acid glycoprotein which was significantly (p=0.009) increased in severely affected ME/CFS patients. This has previously been identified as a circulating biomarker predictive of the short-term risk of death and of possible relevance to ME/CFS, has been implicated in various pathophysiological mechanisms including inflammation, lipoprotein metabolism, and metabolic homeostasis (Fischer et al., 2014).

Other methodological divergencies include the use of serum, in which small metabolites may be less stable than in plasma, and mass spectrometry in combination with different workflows with the capability of detecting much higher numbers (up to 600 or more) of metabolites (Germain et al., 2017; Naviaux et al., 2016). Targeted acquisition of metabolites in the future should be undertaken using more sophisticated workflows and MS, as previously described (Germain et al., 2017). Our targeted bile acid mass spectrometry analysis and quantitation in ME/CFS patients is a unique aspect of our study and has not been the focus of metabolome studies carried out to this date. However, consideration should be given to food intake and timing of the sample. Therefore, it is recommended integration of targeted metabolomics to characterise the status of energy,

lipid, and amino and bile acid metabolism in severe ME/CFS should also be a priority for future investigation.

Finally, the pathogenesis of ME/CFS is likely to involve disruption of neural, neuro-endocrine and immune signalling pathways communicating along the gut-brain axis. Indeed, GI symptoms and intestinal dysbiosis co-associate in several neurological and (auto)immuno-inflammatory disorders, including ME/CFS. It is apparent the difficulty excluding environmental influences known to cause microbiota population-level changes which make it challenging to identify specific 'diagnostic' microbial signatures. More information is needed to establish models for interaction between microbes and host physiology. Of interest for future studies, are microbial-immune interactions as a key regulator of microbiota-gut-brain communication. To that end, the final chapter of this thesis has shown it is possible to isolate faecal microbes from stool, to evaluate the proportion of faecal microbes bound by intestinal IgA which, we suggest, may be cell sorted and extracted for DNA sequence-based identification. A future objective may be to elucidate specific members of the ME/CFS microbiota eliciting strong mucosal derived and systemic antibody production found in serum, compared with house-hold relatives. A reasonable aim would be to determine the subset phenotype and specificity of T cells for reactivity towards intestinal microbes. Various assays can be used to measure cytokines associated with T-cell induction and proliferation in response towards the patient's endogenous microbiota extracted from faecal samples. Indeed, we hypothesise a leaky gut causes induction and priming of immune cells within the intestinal submucosa which stimulates trafficking of encephalitogenic T cells to cross the blood-brain barrier in to the CNS. Here, flow cytometry would be a powerful method to explore the expression of gut/brain homing markers expressed on the cell surface of these immune cells. This would be a significant attempt to go beyond the descriptive nature of high-throughput 'omics technologies to better understand the potential for microbial-immune interactions to influence ME/CFS pathology, in addition to the metabolism as a feature of the intestinal microbiota.

Additional Materials

Research publication, Study Approvals and Patient Assessment

MICROBIAL ECOLOGY in Health and Disease

COACTION PUBLISHING

ENGIHR SUPPLEMENT

Dysbiosis of the gut microbiota in disease

Simon Carding[1,2], Kristin Verbeke[3], Daniel T. Vipond[1,2], Bernard M. Corfe[4,5]* and Lauren J. Owen[6]

[1]Institute of Food Research, Norwich, UK; [2]Norwich Medical School, University of East Anglia, Norwich, UK; [3]Translational Research in GastroIntestinal Disorders, KU Leuven, Leuven, Belgium; [4]Molecular Gastroenterology Research Group, Department of Oncology, University of Sheffield, Sheffield, UK; [5]Insigneo Institute for in silico Medicine, University of Sheffield, Sheffield, UK; [6]Human Nutrition Unit, Department of Oncology, University of Sheffield, Sheffield, UK

There is growing evidence that dysbiosis of the gut microbiota is associated with the pathogenesis of both intestinal and extra-intestinal disorders. Intestinal disorders include inflammatory bowel disease, irritable bowel syndrome (IBS), and coeliac disease, while extra-intestinal disorders include allergy, asthma, metabolic syndrome, cardiovascular disease, and obesity.

In many of these conditions, the mechanisms leading to disease development involves the pivotal mutualistic relationship between the colonic microbiota, their metabolic products, and the host immune system. The establishment of a 'healthy' relationship early in life appears to be critical to maintaining intestinal homeostasis. Whilst we do not yet have a clear understanding of what constitutes a 'healthy' colonic microbiota, a picture is emerging from many recent studies identifying particular bacterial species associated with a healthy microbiota. In particular, the bacterial species residing within the mucus layer of the colon, either through direct contact with host cells, or through indirect communication via bacterial metabolites, may influence whether host cellular homeostasis is maintained or whether inflammatory mechanisms are triggered. In addition to inflammation, there is some evidence that perturbations in the gut microbiota is involved with the development of colorectal cancer. In this case, dysbiosis may not be the most important factor, rather the products of interaction between diet and the microbiome. High-protein diets are thought to result in the production of carcinogenic metabolites from the colonic microbiota that may result in the induction of neoplasia in the colonic epithelium.

Ever more sensitive metabolomics methodologies reveal a suite of small molecules produced in the microbiome which mimic or act as neurosignallers or neurotransmitters. Coupled with evidence that probiotic interventions may alter psychological endpoints in both humans and in rodent models, these data suggest that CNS-related co-morbidities frequently associated with GI disease may originate in the intestine as a result of microbial dysbiosis. This review outlines the current evidence showing the extent to which the gut microbiota contributes to the development of disease. Based on evidence to date, we can assess the potential to positively modulate the composition of the colonic microbiota and ameliorate disease activity through bacterial intervention.

Keywords: *Microbiome*; *short-chain fatty acids*; *gut health*; *colonic metabolome*; *gut–brain–axis*; *inflammation*

*Correspondence to: Bernard M. Corfe, Molecular Gastroenterology Research Group, Department of Oncology, University of Sheffield, Beech Hill Road, Sheffield, S10 2RX, UK, Email: b.m.corfe@shef.ac.uk

This paper is part of the *Proceedings from the 2013 ENGIHR Conference in Valencia, Spain*. More papers from this supplement can be found at http://www.microbecolhealthdis.net

The human intestinal microbiota is made up of trillions of microorganisms most of which are of bacterial and viral origin that are considered to be non-pathogenic (1, 2). The microbiota functions in tandem with the host's defences and the immune system to protect against pathogen colonisation and invasion. It also performs an essential metabolic function, acting as a source of essential nutrients and vitamins and aiding in the extraction of energy and nutrients, such as short-chain fatty acids (SCFA) and amino acids, from food. Ultimately, the host depends on its intestinal microbiota for a number of vital functions and thus the intestinal microbiota may contribute to health. It is, however, difficult to describe the precise impact of the intestinal microbiota on human health and the involvement in human disease.

Alterations in the microbiota can result from exposure to various environmental factors, including diet, toxins, drugs, and pathogens. Of these, enteric pathogens have the greatest potential to cause microbial dysbiosis as seen in experimental animal models, where foodborne viral

Citation: Microbial Ecology in Health & Disease 2015, **26**: 26191 - http://dx.doi.org/10.3402/mehd.v26.26191

(page number not for citation purpose)

pathogens can trigger both local and systemic inflammation altering the composition of the microbiota and barrier function, as a mechanism for developing autoimmunity, as shown in type 1 diabetes and T-cell mediated destruction of insulin-producing pancreatic β-cells (3–5). Documenting dysbiosis has traditionally relied on classical microbiological techniques and the ability to culture pure isolates for identification and classification, which is necessarily limited to 'culturable' microorganisms. The advent of high-throughput DNA based pyrosequencing technology to classify bacteria and archaea according to individual 16S rRNA sequences directly from human samples (usually faecal in origin) with no need for culturing now provides a rapid and detailed means of profiling complex communities of microorganisms. Since the first application of this technology, it has been shown that the composition of the intestinal microbiota varies substantially amongst individuals (6). This can in part be explained by genetic differences amongst hosts with positive relationships between similarity in dominant faecal microbial communities and genetic relatedness of the host being observed (7). At the phylum level, *Bacteroidetes* and *Firmicutes* dominate with *Proteobacteria*, *Actinobacteria*, *Fusobacteria*, *Spriochaetes*, *Verrucomicrobia*, and *Lentisphaerae* also present (8, 9). Using metagenomic analysis to investigate the functional capability of the intestinal microbiota genome (microbiome), it has been shown that almost 40% of the microbial genes present in each individual are shared with at least half the general population providing evidence for the existence of a functional core, or core microbiome (10). The main approach to studying changes in composition of the intestinal microbiota in relation to disease has relied primarily on the phylogenetic characterisation of the microbiota of diseased individuals in comparison with apparently healthy individuals. However, since there are substantial inter-individual and intra-individual variations in addition to age-related changes in the composition of the intestinal microbiota, it is difficult to establish precise relations between human health and the presence and relative abundance of specific microbial communities. It may be possible in the future to use specific changes in compositional diversity, or even functional diversity, as biomarkers for health or specific diseases. It is important to note, however, that it is questionable whether changes in phylogenetic composition are a cause or consequence of a given disease.

Arguably the strongest evidence of the direct involvement in or requirement for the intestinal microbiota in disease pathogenesis comes from studies using germ-free mouse models of human autoimmune disease in which the requirement for exposure to and colonisation by environmental microorganisms on disease initiation and progression can be determined (Table 1). In most but not all of the disease models, the severity and/or incidence of disease is reduced under germ-free conditions consistent with the microbiota being a 'trigger' for disease progression. However, attempts to identify the members of the 'pathogenic' microbiota (pathobionts) that can reproduce the effect of the microbiota as a whole have to date failed.

It is perhaps not surprising that intestinal dysbiosis is most often associated with GI-related diseases in which alterations in the interaction of the host (immune system) with lumen-derived stimuli and antigens initiate and/or perpetuate uncontrolled inflammation in the intestinal mucosa, and in some cases beyond.

Metabolomic impact of the interaction between diet and the microbiome on human health

Food components that escape digestion in the small intestine, as well as endogenous compounds such as digestive enzymes and shed epithelial cells and associated mucus, enter the colon and become available for fermentation by the colonic microbiota. Bacterial conversion of these compounds results in a wide variety of metabolites that are in close contact with host's cells. In this way, these metabolites can affect the metabolic phenotype of the host and influence the risk of disease (11).

Undigested carbohydrates and proteins constitute the major substrates at the disposal of the microbiota. Fermentation of these substrates results in the production of a range of metabolites including SCFA, branched chain fatty acids, ammonia, amines, phenolic compounds, and gases, including hydrogen, methane, and hydrogen sulphide. In addition, the intestinal microbiota is involved in the production of vitamins, the activation or inactivation of bioactive food components such as isoflavanoids

Table 1. The intestinal microbiota and autoimmunity

Disease	Microbiota status	Disease impact
Inflammatory bowel disease	Germ free, antibiotics or probiotics	No disease or reduced severity
Spontaneous arthritis	Germ free	No disease
Autoimmune arthritis	Germ free	No disease
Autoimmune encephalomyelitis	Germ-free	Weak severity
Systemic lupus erythematosus	Germ free	No change
Type 1 diabetes	Germ free	No disease
Spontaneous ankylosing enteropathy	Germ free or probiotics	No disease

Citation: Microbial Ecology in Health & Disease 2015, **26**: 26191 - http://dx.doi.org/10.3402/mehd.v26.26191

and plant lignans, the conversion of prodrugs to their bioactive forms, and the transformation of bile acids and xenobiotics (12, 13).

Mechanistic effect of metabolites on host health

The SCFA acetate, propionate, and butyrate are the major anions in the colon and are mainly produced by bacterial fermentation of undigested carbohydrates. Up to 95% of produced SCFA are readily absorbed by the colonocytes for use as energy substrates. As colonocytes derive up to 60–70% of their energy needs from SCFA oxidation (14), SCFA provide about 10% of the daily caloric requirements in humans (15). The fraction that is not consumed by the colonocytes is transported across the basolateral membrane to the liver via the portal blood stream. Besides their local role as energy substrates within the colon, SCFA act as signalling molecules involved in systemic lipid metabolism and glucose/insulin regulation (16). These effects are, at least partly, mediated through interaction with two specific G-protein-coupled receptors – GPR41 and GPR43 (later renamed to FFAR3 and FFAR2, respectively) (17) that are widely distributed throughout the human body, including the small intestine and colon (18). Within the cells, SCFA can act as inhibitors of histone deacetylases to induce hyperacetylation of histones which affects gene expression and results in anti-inflammatory properties, induction of growth arrest, and apoptosis (19). However, an integrated understanding of the impact of SCFA on host metabolism requires more quantitative data on fluxes of SCFA in different body compartments. Due to its inaccessibility, little information is available on *in vivo* production rates of SCFA and kinetics of absorption in the large intestine.

Plant polyphenols have been associated with health benefits including anti-inflammatory, antiestrogenic, cardioprotective, chemoprotective, and neuroprotective effects (10). However, the mechanistic evidence *in vivo* is not yet fully understood. The majority of plant polyphenols require metabolic transformation (including deglycation and hydrolysis) to render them biologically active. Within the colon, they are broken down by the microbiota to a variety of small phenolic compounds of which the physiological relevance is not well known (20). In addition, recent studies indicate a selective modulation of the microbiota composition after polyphenol consumption (21). For instance, consumption of red wine polyphenols significantly increases *Enterococcus*, *Prevotella*, *Bacteroides*, *Bifidobacterium*, *Bacteroides uniformis*, *Eggerthella lenta*, and *Blautia coccoides-Eubacterium rectale* numbers in healthy humans (22). Therefore, the health benefits associated with polyphenols should not only be attributed to their bioactive metabolites but also to the modulation of the intestinal microbiota.

Other products of bacterial metabolism have been associated with diseases affecting the liver, cardiovascular system and the kidneys.

In recent years, the gut–liver axis and the impact of the intestinal microbiota on liver function has gained increasing attention. The liver is extensively exposed to metabolites produced at intracolonic fermentation as it receives 70% of its blood supply from the intestine through the portal vein (23). In the early 1980s, a possible causative role of the microbiota in the development of non-alcoholic fatty liver disease (NAFLD) was suggested. In patients that underwent intestinal bypass surgery, hepatic steatosis developed in parallel with bacterial overgrowth. Interestingly, the steatosis regressed after treatment with the antibiotic, metronidazole (24). One of the mechanisms relating the microbiota to NAFLD is bacterial metabolism of choline. In mice susceptible to NAFLD and fed a high-fat diet, choline was increasingly metabolised to methylamines resulting in high urinary excretion of dimethylamine (DMA) and trimethylamine (TMA) and correspondingly low levels of serum phosphatidylcholine (25).

Due to conversion of choline into methylamines by the microbiota, the bioavailability of choline is reduced, resulting in the inability to synthesise phosphatidylcholine with subsequent accumulation of triglycerides in the liver. This mimics choline-deficient diets which have been consistently associated with hepatic steatosis (26).

The bacterial metabolite TMA is consequently absorbed by the intestinal mucosa and transported to the liver via the portal vein where it is oxidised to trimethylamine *N*-oxide (TMAO) by the flavin mono-oxygenase (FMO) enzyme complex. In a metabolomics study profiling the plasma of patients undergoing elective cardiac evaluation, TMAO was identified and confirmed as a predictor of cardiovascular disease (CVD). Subsequent mice experiments confirmed the obligate role of the intestinal microbiota in the formation of TMAO and indicated the pro-atherogenic nature of TMAO by augmentation of cholesterol loaded macrophages and foam cell formation (27). Similarly, metabolism by the intestinal microbiota of dietary L-carnitine, a TMA abundant in red meat, also produced TMAO and accelerated atherosclerosis in mice (28).

Dysbiosis in disease

Dysbiosis and GI-tract-related disorders

Inflammatory bowel disease

Crohn's disease (CD) and ulcerative colitis (UC) are the most prevalent forms of inflammatory bowel disease (IBD), characterised by chronic relapsing inflammation affecting the intestinal mucosa. Although the aetiology of both diseases is unknown, there is increasing evidence that intestinal microbial dysbiosis has a role in the pathogenesis of IBD (29). Overall, patients exhibit a decrease in microbial population and functional diversity and stability of

their intestinal microbiota with decreases in specific *Firmicutes* and a concomitant increase in *Bacteroidetes* and facultative anaerobes such as *Enterobacteriaceae* (30). Significant differences in the microbiota of CD versus UC patients have also been noted (31, 32). In CD, the predominant dysbiosis has been described to be associated with five bacterial species amongst which alterations in the abundance of *Faecalibacterium prausnitzii* is associated with the prolongation of disease remission (32, 33), with this bacterium having a therapeutic effect in experimental models of colitis (34). Conversely, adherent-invasive *E. coli* and *Mycobacterium paratuberculosis* have been implicated in CD pathogenesis although a causal relationship is yet to be demonstrated (35, 36). Indeed, up to now, it is still unclear whether intestinal microbial dysbiosis is a direct cause for the inflammation in IBD, or merely the result of a disturbed environment in the GI-tract. One study that has sought to determine the status of the microbiota in early-diagnosis CD cases is that of Gevers et al. (Cell Host Microbe 2014) (37). This study analysed the microbiota of a large cohort of newly diagnosed paediatric CD patients and found clear differences in bacterial populations between CD and healthy control patients. CD patients had increased abundance of *Enterobacteriaceae*, *Pasteurellaceae*, *Veillonellaceae*, and *Fusobacteriaceae*, and decreased abundance in *Erysipelotrichales*, *Bacteroidales*, and *Clostridiales* compared to healthy control patients. Interestingly, these differences were only revealed when analysing mucosal samples (rather than faecal samples), indicating that the bacteria resident in the mucosal layer may be more significant for disease aetiology.

Dysbiosis and other GI-tract disorders

In addition to IBD, metabolic disorders, obesity, and type 2 diabetes (T2D), the intestinal microbiota has also been implicated in several other (chronic) GI-related diseases and disorders, such as irritable bowel syndrome (IBS), coeliac disease, and colorectal cancer (CRC). In IBS, changes in microbiota composition have been described in the different subtypes of disease compared to healthy individuals (38, 39) although the changes are not uniform (40). Coeliac disease and CRC have also been associated with alterations in microbiota composition with increased diversity and richness observed compared to control subjects (41, 42). In all of these diseases, however, no consistent pattern of microbiota changes has yet been observed. In the case of coeliac disease, however, a recent study has shed light on the interaction between host genetics and microbiota composition in relation to disease development. Expression of the leukocyte antigen DQ2 is a strong risk factor for the development of coeliac disease. Children with this haplotype have an altered microbiota composition (compared to non-HLA DQ2 individuals) prior to clinically apparent disease (43). Coeliac disease results from CD4 T-cell reactivity to dietary gliadin, with some bacterial species being able to digest gliadin and perhaps therefore reduce the immunopathogenicity of ingested gliadin.

Dysbiosis in systemic disease

Metabolic disorders

An increase in the relative abundance of *Firmicutes* and a reduction in the level of *Bacteroidetes* have been observed in both obese mice (44) and humans (45) although these findings have not been replicated in all studies (46–52). Of note, intestinal dysbiosis is not currently used as a factor in diagnosing or predicting onset of a metabolic disease such as obesity or T2D. More subtle changes in the composition of the intestinal microbiota have been described in obese individuals with a reduced compositional microbial diversity compared with lean individuals (7). Additional evidence implicating the intestinal microbiota in obesity originates from obese (*ob*/*ob*) mice that lack expression of the gene encoding leptin, the product of which promotes satiety. In support of the involvement of the microbiota in the development of obesity in these mice, antibiotic treatment conferred changes in the gut microbiota, reducing the incidence of metabolic endotoxemia, inflammation, and several obesity-linked parameters (53). In human populations, it is evident that a high-fat diet and overconsumption of food are responsible for the greater prevalence of obesity and T2D in the West, thus conspiring to alter host metabolism and immune homeostasis via diet-induced changes in the intestinal microbiota. Indeed, the role of the microbiota in metabolism, and notably its ability to harvest energy from food, highlight a significant environmental factor impacting the risk of metabolic disease. A direct link between intestinal microbiota composition and body weight comes from studies using germ-free mice to show that the absence of intestinal microbes protects against diet-induced obesity, and that the intestinal microbiota is involved in the regulation of fat storage (54–56). These and similar studies have led to the proposal that obese individuals are more efficient in converting food into useable energy and in storing this energy in fat than lean individuals, which is related to, and may be a consequence of, the functionality of the intestinal microbiota. Major insights into differences between various physiological states of the host, such as in obese versus lean individuals, should therefore be obtained by studying the functional microbial diversity in addition to phylogenetic diversity. Indeed, an altered representation of bacterial genes and metabolic pathways, including those involved in nutrient harvest, has been found to be related to obesity (7). Also, the amount of SCFA produced by the intestinal microbiota, rather than the changes in the composition of the microbiota, is important in the development of obesity (51). Perhaps unsurprisingly, shifts

Citation: Microbial Ecology in Health & Disease 2015, **26**: 26191 - http://dx.doi.org/10.3402/mehd.v26.26191

in microbiota phyla have also been described in T2D (57), with metagenomics-based studies identifying discriminant metagenomic markers that may differ between different ethnicities of patients (58, 59). The question remains whether dysbiosis of the intestinal microbiota is a direct cause for any metabolism-related disorder, or whether changes in the intestinal microbial communities in affected and obese individuals are an adaptation to a change in the host's diet. Two observations relevant to answering this question are one, that the transfer of microbiota from lean donors into individuals with metabolic syndrome can increase insulin sensitivity and overall amelioration of symptoms of metabolic disease (60) and two, dietary changes in humans leads to rapid and reversible changes in the relative abundance of dominant members of the intestinal microbiota (61).

The potential interaction between host physiology, behaviour, the microbiome, and diet is evidenced in both animal and human studies showing rapid changes in microbiota composition after Roux-en-Y gastric bypass surgery (RYGB) (52, 62) although the impact on metabolite levels has been less explored. Nevertheless, in a non-obese rat model, RYGB surgery resulted in profound metabolic perturbations (63). Besides lower concentrations of oligosaccharides and higher concentrations of SCFA, increased levels of colonic protein fermentation metabolites were found in faecal samples obtained after surgery. These results might point at an incomplete digestion of proteins in the small intestine as a result of the bypass leading to an increased supply of protein to the colon with increased protein fermentation. Interestingly, faecal water samples obtained 2 and 8 weeks after the operation, displayed significantly more cytotoxicity compared to the samples obtained from sham-operated animals (64). It needs to be investigated whether the observed association between increased levels of amino acid fermentation metabolites and increased cytotoxicity also involves a causal relationship. In healthy, normal weight subjects, increased protein fermentation after a high-protein diet was not associated with increased faecal water cytotoxicity (65).

Also, between the large intestine and the kidney, a bi-directional functional relationship exists. Uremia influences the colonic microbial metabolism whereas microbial-related metabolites are involved in the progression of the kidney disease (66). p-Cresyl sulphate and indoxyl sulphate have been most extensively studied and are considered as prototypes of the so-called uremic toxins. They are derived from bacterial fermentation of the aromatic amino acids tyrosine and tryptophan, respectively, followed by sulphation in the colonic mucosa or the liver. Within the plasma, they are highly protein-bound and accumulate when kidney function fails. The free, unbound levels of these solutes increase more than their total plasma levels due to competition for binding sites on plasma proteins (67). In patients with chronic kidney disease, both p-cresyl sulphate and indoxyl sulphate levels have been linked to overall mortality, CVD and progression of the kidney disease (68).

Dysbiosis and CNS-related disorders

Intestinal microbial dysbiosis has also been observed in extra-intestinal diseases and in particular those that may impact on the 'gut–brain–axis' to affect the CNS and behaviour and cognitive function.

Several studies have focused on the possibility that the intestinal microbiota may influence cognitive function and behaviour by direct reprogramming of the hypothalamus–pituitary–adrenal (HPA) axis, a common pathway activated in response to infection and perturbed by psychological stressors. It is known that enteric infections can cause anxiety, depression, and cognitive dysfunction; germ-free mice that have no intestinal microbiota display alterations in stress-responsivity, central neurochemistry, and behaviour indicative of a reduction in anxiety in comparison to conventionalised mice (43). For example, in germ-free mice, increased anxiety-like behaviour has been associated with changes in the production of neurotrophic factors and hormones and expression of their receptors (69). In pathogen-infected mice (70–73), *Campylobacter jejuni* (a common cause of gastroenteritis) can induce anxiety-like behaviour in mice and brainstem activation (the nucleus tractus solitarius and lateral parabrachial nucleus). Commensal bacteria may affect brain changes through GABA, which can directly influence receptors both immune and neural within the ENS and CNS (74, 75). GABA is the main CNS inhibitory neurotransmitter and is involved in regulating physiological and psychological processes. Alterations in central GABA receptor expression are implicated in the pathogenesis of anxiety and depression (76).

Early colonisation of the intestinal tract by microbes is known to be important for the post-natal development of the enteric nervous system (77). Accordingly, intestinal microbiota may have implications on the development and function of the CNS (78, 79).

Evidence of a possible causal role of the intestinal microbiota in the development of autism spectrum disorder (ASD) comes from a maternal immune activation (MIA) mouse model in which pregnant animals after being administered the viral mimetic, ploy(I:C), display increased intestinal permeability and develop stereotypical abnormalities in behaviour, social ability, and communication that resemble ASD (80). MIA offspring display intestinal dysbiosis and an altered serum metabolomic profile, characterised by excessive levels of microbiota-derived 4-ethylphenylsulphate (4EPS), compared to control offspring, with intestinal barrier function being restored and ASD-like symptoms being alleviated after

administering probiotic bacteria. Of particular note, exogenously administered 4EPS, which is structurally related to the toxic sulphated form of *p*-cresol, resulted in an anxiety-like behaviour in naïve mice, suggesting that autism, and maybe other behavioural conditions, involve the GI-tract eventually impacting on the immune, metabolic, and nervous systems.

With the emerging preclinical data and indications in developmental disorders, it is perhaps no coincidence that GI-tract disorders including IBD and IBS are common co-morbidities in debilitating stress-related disorders, including depression and anxiety (81, 82). Recent research suggested that intestinal permeability and bacterial translocation may drive immuno-inflammatory and oxidative and nitrosative stress (IO&NS) pathways in depression and thus play a role in its pathophysiology. Chronic depression in humans was shown to be accompanied by increased immune response (serum IgM and IgA responses) directed against lipopolysaccharide (LPS) products of gram negative gut enterobacteria, that is, *Hafnia alvei*, *Pseudomonas aeruginosa*, Morganella morganii, *Pseudomonas putida*, *Citrobacter koseri*, and *Klebsiella pneumonia* (83). Attempts have been made to examine the potential CNS and behavioural impact of bacteriotherapy in germ-free and pathogen-infected rodents. Germ-free mice exhibit hyper-responsive HPA axis activity following stress as compared to specific-pathogen free mice (78) and this hyper-response of the HPA axis was reversed by *Bifidobacterium infantis* (84). *B. infantis* increased plasma tryptophan levels, decreased serotonin metabolite concentrations in the frontal cortex and dopamine metabolite concentrations in the amygdaloid cortex (85), both of which are implicated in depression (86, 87). In humans, the efficacy of probiotics for mood regulation was suggested in a trial of *Lactobacillus casei* that showed subjects with the lowest scores in the depressed/elated dimension at baseline had significant improvement in mood scores after taking the probiotic compared to the placebo group (88). The combination of *L. helveticus* and *B. longum* reduced anxiety and had beneficial psychological effects with decreased serum cortisol in healthy human volunteers (89).

Functional brain activity measured by functional magnetic resonance (fMRI) showed that a probiotic formulation reduced brain intrinsic connectivity and response to emotive stimuli and changes in midbrain connectivity (90).

However, it should be noted that several studies have failed to observe an effect of probiotic supplementation on anxiety measures in clinical populations, including IBS (91, 92), schizophrenia (93), and rheumatoid arthritis (94). This may be explained in part by the spectrum of doses, species (and combinations thereof), and timings used in probiotic interventions and the lack of a standard trial design.

Future approaches: restoration of the intestinal microbiota through bacteriotherapy

There is huge potential for manipulating the microbiota to sustain, improve, or restore the microbiota in at risk or diseased individuals.

An important pre-requisite for bacteria-based therapy (bacteriotherapy) is defining what constitutes a 'healthy' microbiota during and throughout life, which may be defined differently at the population and individual level. More research is needed to examine species and strain diversity in the GI-tract, the diversity of microbial genes (microbiome), and what their functionality is in the GI-tract throughout human development – from the cradle to the grave! Therapeutically, probiotic-based approaches have been used with some success for centuries (95, 96), as have the more drastic and cruder approach of wholesale microbiota replacement strategies based upon faecal transplantation (97). The application of these procedures is discussed in more detail in a separate review in this supplement – Manipulating the gut microbiota to maintain health and treat disease. The development and use of these and other more refined approaches using chemically defined bacterial products in the clinic will rely on understanding their molecular mechanisms of action and the particular host features requiring personalisation of approach in order to enable bacterial/probiotic therapies to yield their full potential in the treatment and management of human health.

Acknowledgements

The authors thank Dr Nick Chadwick for his support and critical review during the production of this manuscript. The authors acknowledge the support of the European Science Foundation (ESF), in the framework of the Research Networking Programme, The European Network for Gastrointestinal Health Research.

Conflict of interest and funding

The authors have not received any funding or benefits from industry or elsewhere to conduct this study.

References

1. Savage DC. Microbial ecology of the gastrointestinal tract. Ann Rev Microbiol 1977; 31: 107–33.
2. Reyes A, Haynes M, Hanson N, Angly FE, Heath AC, Rohwer F, et al. Viruses in the faecal microbiota of monozygotic twins and their mothers. Nature 2010; 466: 334–8.
3. Kamada N, Seo SU, Chen GY, Nunez G. Role of the gut microbiota in immunity and inflammatory disease. Nat Rev Immunol 2013; 13: 321–35.
4. Tanoue T, Umesaki Y, Honda K. Immune responses to gut microbiota-commensals and pathogens. Gut Microbes 2010; 1: 224–33.
5. Wen L, Ley RE, Volchkov PY, Stranges PB, Avanesyan L, Stonebraker AC, et al. Innate immunity and intestinal microbiota in the development of Type 1 diabetes. Nature 2008; 455: 1109–13.

Citation: Microbial Ecology in Health & Disease 2015, **26**: 26191 - http://dx.doi.org/10.3402/mehd.v26.26191

6. Zoetendal EG, Akkermans AD, De Vos WM. Temperature gradient gel electrophoresis analysis of 16S rRNA from human fecal samples reveals stable and host-specific communities of active bacteria. Appl Environ Microbiol 1998; 64: 3854–9.
7. Turnbaugh PJ, Hamady M, Yatsunenko T, Cantarel BL, Duncan A, Ley RE, et al. A core gut microbiome in obese and lean twins. Nature 2009; 457: 480–4.
8. Rajilic-Stojanovic M, Smidt H, de Vos WM. Diversity of the human gastrointestinal tract microbiota revisited. Environ Microbiol 2007; 9: 2125–36.
9. Zoetendal EG, Rajilic-Stojanovic M, de Vos WM. High-throughput diversity and functionality analysis of the gastrointestinal tract microbiota. Gut 2008; 57: 1605–15.
10. Qin J, Li R, Raes J, Arumugam M, Burgdorf KS, Manichanh C, et al. A human gut microbial gene catalogue established by metagenomic sequencing. Nature 2010; 464: 59–65.
11. Nicholson JK, Holmes E, Kinross J, Burcelin R, Gibson G, Jia W, et al. Host-gut microbiota metabolic interactions. Science 2012; 336: 1262–7.
12. Blaut M, Clavel T. Metabolic diversity of the intestinal microbiota: implications for health and disease. J Nutr 2007; 137: 751S–5S.
13. Marchesi J, Shanahan F. The normal intestinal microbiota. Curr Opin Infect Dis 2007; 20: 508–13.
14. Roediger WEW. Utilization of nutrients by isolated epithelial-cells of the rat colon. Gastroenterology 1982; 83: 424–9.
15. Bergman EN. Energy contributions of volatile fatty-acids from the gastrointestinal-tract in various species. Physiol Rev 1990; 70: 567–90.
16. den Besten G, van Eunen K, Groen AK, Venema K, Reijngoud DJ, Bakker BM. The role of short-chain fatty acids in the interplay between diet, gut microbiota, and host energy metabolism. J Lipid Res 2013; 54: 2325–40.
17. Brown AJ, Goldsworthy SM, Barnes AA, Eilert MM, Tcheang L, Daniels D, et al. The orphan G protein-coupled receptors GPR41 and GPR43 are activated by propionate and other short chain carboxylic acids. J Biol Chem 2003; 278: 11312–9.
18. Layden BT, Angueira AR, Brodsky M, Durai V, Lowe WL. Short chain fatty acids and their receptors: new metabolic targets. Transl Res 2013; 161: 131–40.
19. Schilderink R, Verseijden C, de Jonge WJ. Dietary inhibitors of histone deacetylases in intestinal immunity and homeostasis. Front Immunol 2013; 4: 226. doi: 10.3389/fimmu.2013.00226.
20. Selma MV, Espin JC, Tomas-Barberan FA. Interaction between phenolics and gut microbiota: role in human health. J Agric Food Chem 2009; 57: 6485–501.
21. Cardona F, Andrés-Lacueva C, Tulipani S, Tinahones FJ, Queipo-Ortuño MI. Benefits of polyphenols on gut microbiota and implications in human health. J Nutr Biochem 2013; 24: 1415–22.
22. Queipo-Ortuno MI, Boto-Ordonez M, Murri M, Gomez-Zumaquero JM, Clemente-Postigo M, Estruch R, et al. Influence of red wine polyphenols and ethanol on the gut microbiota ecology and biochemical biomarkers. Am J Clin Nutr 2012; 95: 1323–34.
23. Aron-Wisnewsky J, Gaborit B, Dutour A, Clement K. Gut microbiota and non-alcoholic fatty liver disease: new insights. Clin Microbiol Infect 2013; 19: 338–48.
24. Drenick EJ, Fisler J, Johnson D. Hepatic steatosis after intestinal bypass – prevention and reversal by metronidazole, irrespective of protein-calorie malnutrition. Gastroenterology 1982; 82: 535–48.
25. Dumas ME, Barton RH, Toye A, Cloarec O, Blancher C, Rothwell A, et al. Metabolic profiling reveals a contribution of gut microbiota to fatty liver phenotype in insulin-resistant mice. Proc Natl Acad Sci USA 2006; 103: 12511–6.
26. Corbin KD, Zeisel SH. Choline metabolism provides novel insights into nonalcoholic fatty liver disease and its progression. Curr Opin Gastroenterol 2012; 28: 159–65.
27. Wang Z, Klipfell E, Bennett BJ, Koeth R, Levison BS, Dugar B, et al. Gut flora metabolism of phosphatidylcholine promotes cardiovascular disease. Nature 2011; 472: 57–63.
28. Koeth RA, Wang Z, Levison BS, Buffa JA, Org E, Sheehy BT, et al. Intestinal microbiota metabolism of L-carnitine, a nutrient in red meat, promotes atherosclerosis. Nat Med 2013; 19: 576–85.
29. Baumgart DC, Carding SR. Inflammatory bowel disease: cause and immunobiology. Lancet 2007; 369: 1627–40.
30. Hansen J, Gulati A, Sartor RB. The role of mucosal immunity and host genetics in defining intestinal commensal bacteria. Curr Opin Gastroenterol 2010; 26: 564–71.
31. Frank DN, St Amand AL, Feldman RA, Boedeker EC, Harpaz N, Pace NR. Molecular-phylogenetic characterization of microbial community imbalances in human inflammatory bowel diseases. Proc Natl Acad Sci USA 2007; 104: 13780–5.
32. Sokol H, Pigneur B, Watterlot L, Lakhdari O, Bermudez-Humaran LG, Gratadoux JJ, et al. Faecalibacterium prausnitzii is an anti-inflammatory commensal bacterium identified by gut microbiota analysis of Crohn disease patients. Proc Natl Acad Sci USA 2008; 105: 16731–6.
33. Joossens M, Huys G, Cnockaert M, De Preter V, Verbeke K, Rutgeerts P, et al. Dysbiosis of the faecal microbiota in patients with Crohn's disease and their unaffected relatives. Gut 2011; 60: 631–7.
34. Miquel S, Martin R, Rossi O, Bermudez-Humaran LG, Chatel JM, Sokol H, et al. Faecalibacterium prausnitzii and human intestinal health. Curr Opin Microbiol 2013; 16: 255–61.
35. Darfeuille-Michaud A, Boudeau J, Bulois P, Neut C, Glasser AL, Barnich N, et al. High prevalence of adherent-invasive Escherichia coli associated with ileal mucosa in Crohn's disease. Gastroenterology 2004; 127: 412–21.
36. Rosenfeld G, Bressler B. Mycobacterium avium paratuberculosis and the etiology of Crohn's disease: a review of the controversy from the clinician's perspective. Can J Gastroenterol 2010; 24: 619–24.
37. Gevers D, Kugathasan S, Denson LA, Vazquez-Baeza Y, Van Treuren W, Ren B, et al. The treatment-naive microbiome in new-onset Crohn's disease. Cell Host Microbe 2014; 15: 382–92.
38. Carroll IM, Chang YH, Park J, Sartor RB, Ringel Y. Luminal and mucosal-associated intestinal microbiota in patients with diarrhea-predominant irritable bowel syndrome. Gut Pathog 2010; 2: 19.
39. Krogius-Kurikka L, Lyra A, Malinen E, Aarnikunnas J, Tuimala J, Paulin L, et al. Microbial community analysis reveals high level phylogenetic alterations in the overall gastrointestinal microbiota of diarrhoea-predominant irritable bowel syndrome sufferers. BMC Gastroenterol 2009; 9: 95.
40. Salonen A, de Vos WM, Palva A. Gastrointestinal microbiota in irritable bowel syndrome: present state and perspectives. Microbiology 2010; 156: 3205–15.
41. De Palma G, Nadal I, Medina M, Donat E, Ribes-Koninckx C, Calabuig M, et al. Intestinal dysbiosis and reduced immunoglobulin-coated bacteria associated with coeliac disease in children. BMC Microbiol 2010; 10: 63.
42. Shen XJ, Rawls JF, Randall T, Burcal L, Mpande CN, Jenkins N, et al. Molecular characterization of mucosal adherent bacteria and associations with colorectal adenomas. Gut Microbes 2010; 1: 138–47.
43. Olivares M, Neef A, Castillejo G, Palma GD, Varea V, Capilla A, et al. The HLA-DQ2 genotype selects for early intestinal

microbiota composition in infants at high risk of developing coeliac disease. Gut 2014. doi: 10.1136/gutjnl-2014-306931.
44. Ley RE, Backhed F, Turnbaugh P, Lozupone CA, Knight RD, Gordon JI. Obesity alters gut microbial ecology. Proc Natl Acad Sci USA 2005; 102: 11070–5.
45. Ley RE, Turnbaugh PJ, Klein S, Gordon JI. Microbial ecology: human gut microbes associated with obesity. Nature 2006; 444: 1022–3.
46. Collado MC, Isolauri E, Laitinen K, Salminen S. Distinct composition of gut microbiota during pregnancy in overweight and normal-weight women. Am J Clin Nutr 2008; 88: 894–9.
47. Duncan SH, Lobley GE, Holtrop G, Ince J, Johnstone AM, Louis P, et al. Human colonic microbiota associated with diet, obesity and weight loss. Int J Obes 2008; 32: 1720–4.
48. Kalliomaki M, Collado MC, Salminen S, Isolauri E. Early differences in fecal microbiota composition in children may predict overweight. Am J Clin Nutr 2008; 87: 534–8.
49. Nadal I, Santacruz A, Marcos A, Warnberg J, Garagorri JM, Moreno LA, et al. Shifts in clostridia, bacteroides and immunoglobulin-coating fecal bacteria associated with weight loss in obese adolescents. Int J Obes 2009; 33: 758–67.
50. Santacruz A, Marcos A, Warnberg J, Marti A, Martin-Matillas M, Campoy C, et al. Interplay between weight loss and gut microbiota composition in overweight adolescents. Obesity 2009; 17: 1906–15.
51. Schwiertz A, Taras D, Schafer K, Beijer S, Bos NA, Donus C, et al. Microbiota and SCFA in lean and overweight healthy subjects. Obesity 2010; 18: 190–5.
52. Zhang H, DiBaise JK, Zuccolo A, Kudrna D, Braidotti M, Yu Y, et al. Human gut microbiota in obesity and after gastric bypass. Proc Natl Acad Sci USA 2009; 106: 2365–70.
53. Cani PD, Bibiloni R, Knauf C, Waget A, Neyrinck AM, Delzenne NM, et al. Changes in gut microbiota control metabolic endotoxemia-induced inflammation in high-fat diet-induced obesity and diabetes in mice. Diabetes 2008; 57: 1470–81.
54. Turnbaugh PJ, Ley RE, Mahowald MA, Magrini V, Mardis ER, Gordon JI. An obesity-associated gut microbiome with increased capacity for energy harvest. Nature 2006; 444: 1027–31.
55. Backhed F, Manchester JK, Semenkovich CF, Gordon JI. Mechanisms underlying the resistance to diet-induced obesity in germ-free mice. Proc Natl Acad Sci USA 2007; 104: 979–84.
56. Ridaura VK, Faith JJ, Rey FE, Cheng J, Duncan AE, Kau AL, et al. Gut microbiota from twins discordant for obesity modulate metabolism in mice. Science 2013; 341: 1241214.
57. Larsen N, Vogensen FK, van den Berg FW, Nielsen DS, Andreasen AS, Pedersen BK, et al. Gut microbiota in human adults with type 2 diabetes differs from non-diabetic adults. PLoS One 2010; 5: e9085.
58. Qin J, Li Y, Cai Z, Li S, Zhu J, Zhang F, et al. A metagenome-wide association study of gut microbiota in type 2 diabetes. Nature 2012; 490: 55–60.
59. Karlsson FH, Tremaroli V, Nookaew I, Bergstrom G, Behre CJ, Fagerberg B, et al. Gut metagenome in European women with normal, impaired and diabetic glucose control. Nature 2013; 498: 99–103.
60. Vrieze A, Van Nood E, Holleman F, Salojarvi J, Kootte RS, Bartelsman JF, et al. Transfer of intestinal microbiota from lean donors increases insulin sensitivity in individuals with metabolic syndrome. Gastroenterology 2012; 143: 913–16, e7.
61. Walker AW, Ince J, Duncan SH, Webster LM, Holtrop G, Ze X, et al. Dominant and diet-responsive groups of bacteria within the human colonic microbiota. ISME J 2011; 5: 220–30.
62. Kong LC, Tap J, Aron-Wisnewsky J, Pelloux V, Basdevant A, Bouillot JL, et al. Gut microbiota after gastric bypass in human obesity: increased richness and associations of bacterial genera with adipose tissue genes. Am J Clin Nutr 2013; 98: 16–24.
63. Li JV, Ashrafian H, Bueter M, Kinross J, Sands C, le Roux CW, et al. Metabolic surgery profoundly influences gut microbial-host metabolic cross-talk. Gut 2011; 60: 1214–23.
64. Li JV, Reshat R, Wu Q, Ashrafian H, Bueter M, le Roux CW, et al. Experimental bariatric surgery in rats generates a cytotoxic chemical environment in the gut contents. Front Microbiol 2011; 2: 183.
65. Windey K, De Preter V, Louat T, Schuit F, Herman J, Vansant G, et al. Modulation of protein fermentation does not affect fecal water toxicity: a randomized cross-over study in healthy subjects. PLoS One 2012; 7: e52387. doi: 10.1371/journal.pone.0052387.
66. Evenepoel P, Meijers BKI, Bammens BRM, Verbeke K. Uremic toxins originating from colonic microbial metabolism. Kidney Int Suppl 2009; 76: S12–S9.
67. Sirich TL, Meyer TW, Gondouin B, Brunet P, Niwa T. Protein-bound molecules: a large family with a bad character. Semin Nephrol 2014; 34: 106–17.
68. Poesen R, Meijers B, Evenepoel P. The colon: an overlooked site for therapeutics in dialysis patients. Semin Dial 2013; 26: 323–32.
69. Neufeld K, Kang N, Bienenstock J, Foster J. Reduced anxiety-like behavior and central neurochemical change in germ-free mice. Neurogastroenterol Motil 2011; 23: 255–64, e119.
70. Gaykema R, Goehler LE, Lyte M. Brain response to cecal infection with Campylobacter jejuni: analysis with Fos immunohistochemistry. Brain Behav Immun 2004; 18: 238–45.
71. Goehler LE, Gaykema R, Opitz N, Reddaway R, Badr N, Lyte M. Activation in vagal afferents and central autonomic pathways: early responses to intestinal infection with Campylobacter jejuni. Brain Behav Immun 2005; 19: 334–44.
72. Goehler LE, Park SM, Opitz N, Lyte M, Gaykema R. Campylobacter jejuni infection increases anxiety-like behavior in the holeboard: possible anatomical substrates for viscerosensory modulation of exploratory behavior. Brain Behav Immun 2008; 22: 354–66.
73. Lyte M, Li W, Opitz N, Gaykema R, Goehler LE. Induction of anxiety-like behavior in mice during the initial stages of infection with the agent of murine colonic hyperplasia Citrobacter rodentium. Physiol Behav 2006; 89: 350–7.
74. Li H, Cao Y. Lactic acid bacterial cell factories for gamma-aminobutyric acid. Amino Acids 2010; 39: 1107–16.
75. Lyte M. Probiotics function mechanistically as delivery vehicles for neuroactive compounds: microbial endocrinology in the design and use of probiotics. Bioessays 2011; 33: 574–81.
76. Bravo JA, Forsythe P, Chew MV, Escaravage E, Savignac HM, Dinan TG, et al. Ingestion of Lactobacillus strain regulates emotional behavior and central GABA receptor expression in a mouse via the vagus nerve. Proc Natl Acad Sci USA 2011; 108: 16050–5.
77. Collins J, Borojevic R, Verdu EF, Huizinga JD, Ratcliffe EM. Intestinal microbiota influence the early postnatal development of the enteric nervous system. Neurogastroenterol Motil 2014; 26: 98–107.
78. Sudo N, Chida Y, Aiba Y, Sonoda J, Oyama N, Yu XN, et al. Postnatal microbial colonization programs the hypothalamic-pituitary-adrenal system for stress response in mice. J Physiol 2004; 558: 263–75.
79. Diaz Heijtz R, Wang S, Anuar F, Qian Y, Bjorkholm B, Samuelsson A, et al. Normal gut microbiota modulates brain development and behavior. Proc Natl Acad Sci USA 2011; 108: 3047–52.

80. Hsiao EY, McBride SW, Hsien S, Sharon G, Hyde ER, McCue T, et al. Microbiota modulate behavioral and physiological abnormalities associated with neurodevelopmental disorders. Cell 2013; 155: 1451–63.
81. Cámara RJ, Ziegler R, Begré S, Schoepfer AM, von Känel R. The role of psychological stress in inflammatory bowel disease: quality assessment of methods of 18 prospective studies and suggestions for future research. Digestion 2009; 80: 129–39.
82. Mawdsley J, Rampton D. Psychological stress in IBD: new insights into pathogenic and therapeutic implications. Gut 2005; 54: 1481–91.
83. Maes M, Kubera M, Leunis J-C, Berk M. Increased IgA and IgM responses against gut commensals in chronic depression: further evidence for increased bacterial translocation or leaky gut. J Affect Disord 2012; 141: 55–62.
84. O'Mahony L, McCarthy J, Kelly P, Hurley G, Luo F, Chen K, et al. Lactobacillus and bifidobacterium in irritable bowel syndrome: symptom responses and relationship to cytokine profiles. Gastroenterology 2005; 128: 541–51.
85. Desbonnet L, Garrett L, Clarke G, Kiely B, Cryan J, Dinan T. Effects of the probiotic Bifidobacterium infantis in the maternal separation model of depression. Neuroscience 2010; 170: 1179–88.
86. Myint A-M, Kim YK, Verkerk R, Scharpé S, Steinbusch H, Leonard B. Kynurenine pathway in major depression: evidence of impaired neuroprotection. J Affect Disord 2007; 98: 143–51.
87. Song C, Wang H. Cytokines mediated inflammation and decreased neurogenesis in animal models of depression. Prog Neuropsychopharmacol Biol Psychiatry 2011; 35: 760–8.
88. Benton D, Williams C, Brown A. Impact of consuming a milk drink containing a probiotic on mood and cognition. Eur J Clin Nutr 2006; 61: 355–61.
89. Messaoudi M, Lalonde R, Violle N, Javelot H, Desor D, Nejdi A, et al. Assessment of psychotropic-like properties of a probiotic formulation (Lactobacillus helveticus R0052 and Bifidobacterium longum R0175) in rats and human subjects. Br J Nutr 2011; 105: 755–64.
90. Tillisch K, Labus J, Kilpatrick L, Jiang Z, Stains J, Ebrat B, et al. Consumption of fermented milk product with probiotic modulates brain activity. Gastroenterology 2013; 144: 1394–401.
91. Dapoigny M, Piche T, Ducrotte P, Lunaud B, Cardot J-M, Bernalier-Donadille A. Efficacy and safety profile of LCR35 complete freeze-dried culture in irritable bowel syndrome: a randomized, double-blind study. World J Gastroenterol 2012; 18: 2067.
92. Whorwell PJ, Altringer L, Morel J, Bond Y, Charbonneau D, O'Mahony L, et al. Efficacy of an encapsulated probiotic Bifidobacterium infantis 35624 in women with irritable bowel syndrome. Am J Gastroenterol 2006; 101: 1581–90.
93. Dickerson FB, Stallings C, Origoni A, Katsafanas E, Savage CL, Schweinfurth LA, et al. Effect of probiotic supplementation on schizophrenia symptoms and association with gastrointestinal functioning: a randomized, placebo-controlled trial. Prim Care Companion CNS Disord 2014; 16: pii: PCC. 13m01579.
94. Vaghef-Mehrabany E, Alipour B, Homayouni-Rad A, Sharif S-K, Asghari-Jafarabadi M, Zavvari S. Probiotic supplementation improves inflammatory status in patients with rheumatoid arthritis. Nutrition 2014; 30: 430–5.
95. Gismondo MR, Drago L, Lombardi A. Review of probiotics available to modify gastrointestinal flora. Int J Antimicrob Agents 1999; 12: 287–92.
96. Wilhelm SM, Brubaker CM, Varcak EA, Kale-Pradhan PB. Effectiveness of probiotics in the treatment of irritable bowel syndrome. Pharmacotherapy 2008; 28: 496–505.
97. Brandt LJ, Aroniadis OC. An overview of fecal microbiota transplantation: techniques, indications, and outcomes. Gastrointest Endosc 2013; 78: 240–9.

Faculty of Medicine and Health Sciences Research Ethics Committee

University of East Anglia

Daniel Vipond
MED

Research & Enterprise Services
West Office (Science Building)
University of East Anglia
Norwich Research Park
Norwich, NR4 7TJ

Telephone: +44 (0) 1603 591720

Email: fmh.ethics@uea.ac.uk

Web: www.uea.ac.uk/researchandenterprise

16th July 2015

Dear Daniel

Title: A role for a leaky gut and the intestinal microbiota in the pathophysiology of chronic fatigue syndrome/myalgic encephalomyelitis (CFS/ME)
Reference: 20142015 - 28

Thank you for your e-mail dated 13th July 2015 notifying us of the amendments you would like to make to your above proposal. These have been considered and we can now confirm that your amendments have been approved.

We would like to remind you that following clarification of the NRES approval for the Biorepository/tissue bank to collect tissue, it is now a requirement that researchers such as yourself collecting tissue using the NNUH biorepository process are obliged to bank some of their sample with the tissue bank. This banking will allow other researchers to potentially access and use these samples. Therefore, you will be required to bank some of the tissue that you are collecting as a result of your amendment. Mark Wilkinson will be able to offer you guidance as to how much and in what form you should bank this tissue.

Please can you ensure that any further amendments to either the protocol or documents submitted are notified to us in advance, and also that any adverse events which occur during your project are reported to the Committee.

Please can you also arrange to send us a report once your project is completed.

Yours sincerely,

p.p.

Linda Harvey
Chair Human Tissue - FMH Research Ethics Committee

Cc Simon Carding

Epsom and St Helier NHS
University Hospitals
NHS Trust

Mr Daniel Vipond
[redacted]

Please reply to:
Research and Development General Manager
Research and Development Department
2nd Floor Ferguson House
St Helier Hospital
Wrythe Lane
Carshalton
Surrey SM5 1AA

Tel: 020 8296 4698
Web: www.epsom-sthelier.nhs.uk
Email: yvonne.reilly@esth.nhs.uk

5 March 2015

R&D No: 020S/2014/SMED/D6
(Please quote the R&D Number in all correspondence)

Dear Mr Vipond

Re: NHS Permission

Chief Investigator:	Mr Daniel Vipond
ESTH Collaborator:	Dr Amolak Bansal
Study Title/Acronym:	A role for a leaky gut and the intestinal microbiota in the pathophysiology of Myalgic Encephalomyelitis/Chronic Fatigue Syndrome.
REC No.	20142015-28
Sponsor:	University of East Anglia
NHS Permission Date:	5 March 2015

Thank you for submitting documentation in respect of the above-mentioned study for NHS Permission from Epsom and St Helier University Hospitals NHS Trust (ESTH).

ESTH has granted NHS Permission for the study to proceed on the basis described in the application form, protocol and supporting documentation submitted, subject to the following terms and conditions being satisfied:

1. The study is conducted in accordance with:
   - Research Governance Framework for Health and Social Care, Second Edition, April 2005.
   - Trust Policies and Procedures
   - The Data Protection Act 1998
   - NHS Confidentiality Code of Practice
   - NHS Caldicott Report and Caldicott Guardians
   - The Human Tissue Act 2004
   - Good Clinical Practice
   - Other relevant legislation released during the course of the study.

2. Members of the Research Team who wish to conduct research at ESTH and are not Trust employees must contact the R&D Office to establish appropriate contractual arrangements are in place (e.g. honorary contracts, letters of access), prior to commencement of the research study.

3. Please ensure that you submit a copy of any amendments made to this study to the R&D Office.

4. A requirement of the Research Governance Framework is that Trusts have a duty to monitor research studies. If this study is selected for monitoring, it is your responsibility, as Principal

IFR Institute of Food Research

A role for a leaky gut and the intestinal microbiota in the pathophysiology of ME/CFS

Stool Sample Collection

Unique sample ID:

If you are happy to provide your consent to take part in the study, you will asked to provide a stool sample using a 'sampling kit'. **A blood sample will also be required** which will be arranged to be taking either at the Immunology Dept. D Block, St Helier Hospital or during a scheduled home visit.

Instructions on what to do with the kit are given below:

IMPORTANT INFORMATION

Sample collection will take place between 27th February and 3rd March 2017

Please contact by telephone or email to make arrangements for your sample collection. For severe ME/CFS patients a scheduled Home visit during above dates can be arranged.

Kit contents:

- FECOTAINER® (collection bowl)
- AnaeroGen Compact Sachet
- Zip bag
- Bristol Stool Scale
- Barcode sticker to place on FECOTAINER®

Please ensure your stool sample is collected within no more than 24 hrs prior to scheduled collection day/time

Sample Storage

Place FECOTAINER® with stool sample inside plastic zipped bag, and put into fridge at 4°C

Healthy Volunteers acting as a House-matched control:

Do you live with anybody who would help provide us with a stool sample and by donating blood?

It is helpful, where possible, that we can match each patient sample with a healthy house-matched stool and blood sample, to act as a control.

This will help identify potential disease-specific changes within gut bacteria and metabolism between patient and a healthy volunteer. The importance of house-match is on the basis of a similar environmental exposure and diet if two people are living together, or are related. **Your participation is this study is not affected if no house-matched healthy volunteer is able to participate.**

Kit directions

1. Please record weight of the FECOTAINER®, written on the cellophane of the blue device and record in this space _____ grams.
2. Unwrap FECOTAINER® and fold open the arms, unscrew the top, and depress the centre to form a bowl.
3. Place the device on the toilet basin, and lower the toilet seat downwards to secure in place. Adjust the position how you prefer to ease your sample collect.
4. Perform up to 4 bowl movements into the bowl without urinating in it
5. Next, take the AnaeroGen Compact, tear open, DO NOT USE SCISSORS, take out the sachet and place into the collection bowl. Secure on blue lid.
6. Place entire FECOTAINER® with stool sample inside, into the zippy bag supplied and label your sample with the sticker with your unique Sample ID (matching the number at the top of this page)
7. Place the sample into the fridge & await collection & kept this paper to hand over to the researcher.

To make arrangement for stool sample collection please contact
01603 251433
or preferably email: daniel.vipond@ifr.ac.uk

Norwich Research Park, Colney, Norwich, NR4 7UA, UK
Tel: +44(0) 1603 255000

Version 1.0 14th February 2017

Epsom and St. Helier University Hospitals NHS Trust

Chronic Fatigue Syndrome – Symptom list

Date……

Name…… DoB…… Occupation……

Onset of Fatigue: Acute or Gradual onset Viral symptoms

Brief history of Fatigue:

Main worries now: Getting better Finances Work Serious illness Wasting life

Employment/School F/T P/T – hours/wk……. Nil……since…….

SYMPTOMS	Y/N	COMMENTS
Post Exertional Malaise (PEM)		Time to onset Duration Severity
Non-Restorative sleep		Difficulty getting off to sleep Frequent wakening Early morning wakening Daytime sleeping Obstructive Sleep Apnoea Restless Legs
New Headaches		Frequency Severity Location
Sore throat +/- LN		Frequency
Fever and Sweats		Frequency Mild Mod Severe
Impaired Concentration		Brain fog
Reduced STM		
Arthralgia		Joint swelling Joint stiffness
Myalgia		Never Sometimes All the time Any muscle tenderness?
Intol of sound & light		Overload
Postural instability		
Depression		Mood Anhedonia Libido Appetite Worthlessness Tearful
Anxiety		Persistent Anxiety Episodic anxiety Panic attacks
Fibromyalgia		Severity How many areas

Activities How far can you walk at maximum?

Can you prepare a meal? Y N

Can you wash yourself Y N
Any leisure activity?Walking / Cinema / Eating out / Visiting friends / Other
For how long can you read a book? Watch a film?

Personality before CFS:

Treatments used to date:

GET	Yes	No	When:	Helpful: Yes	No
CBT	Yes	No	When:	Helpful: Yes	No
SSRI	Yes	No	Which drugs	When	How long

Alternative Therapies

Reflexology Homeopathy Acupuncture Pilates Meditation Head Massage

Yoga

Dietary manipulation: No Yes What was this?

Echinacea Ginseng INADA CoQ10 Others

Past Medical History

Past Psychiatric History

Systems Inquiry CVS Resp GI UG NS

Smoke Alcohol Illicit drugs

Present Medication Allergies

Social Support Pets

Family History

Examination

Pulse bp Temperature

Throat Lymphadenopathy

Joint swelling Fibromylagia

Heart Lungs Abdomen Neurology

Investigations

FBC	Hb	WBC	Platelets		
ESR					
AANT	ANA	GPC	AMA	SMA	
Ig's	IgG	IgM	IgA	IMEP	
CRP	TSH	U/E	LFT		
Anti-EM abs	Positive Negative				
ANA	Positive Negative	Pattern	Level		

Assessment

Severity of Fatigue: Mild Moderate Severe Very Severe

Mild – mobile, self caring, light domestic duties, may be working but to detriment of social, family and leisure activities.

Moderate – Reduced mobility, not working, reduced ADL, sleeping in daytime, peaks and troughs of activity.

Severe – few ADL, severe cognitive difficulties, wheelchair dependent for mobility, rarely leave house, often significant worsening of symptoms with any mental or physical exertion

Very severe – no ADL, bedbound most of time, unable to tolerate any noise & are light sensitive, require someone else to wash, toilet and feed them.

Recommendations

Treatment	Comments	Treatment	Comments
GET			
CBT			
SSRI			
Low T4			

REVIEW: *As needed* *3 months* *6 months* *1 year* *Discharge*

Supplementary Data

	10_ME	11_ME	12_ME	13_ME	19_ME	1_ME	3_ME	5_ME	6_ME	7_ME	8_ME	Average
Methanobrevibacter	0	0	0	0	0	15.4285915	0.87880009	0.25515	0	0	4.70525906	1.9334364
Methanosphaera	0	0	0	0	0	0.46347005	0	0	0	0	0	0.0421336
Alloscardovia	0	0	0	0	0	0	0	0	0	1.85511	0	0.1686464
Bifidobacterium	4.31036957	8.4890383	58.59915	4.980439	1.43609014	4.39222044	12.0874812	9.9356	0	7.81759	0	10.18618
Scardovia	0	0	0	0	0	0	0	0	0	0	0.37929992	0.0344818
Adlercreutzia	0.04925	0	0	0.33258993	0	0	0	0.46023	0.17779002	0	0	0.0927145
Atopobium	0	0	0	0	0	0	0	0	0	0.21191	0	0.0192645
Collinsella	4.70980953	3.0210894	0	6.84645863	0	2.08704021	0	0	0.12097001	0	13.3788573	2.7422023
Coriobacteriaceae_noname	0	0	0	0	0	0	0	0	1.09583011	0	0.02732999	0.1021055
Eggerthella	0.71539993	0.93882981	0.89077	0.83193983	0	0	2.16114022	2.36951	0.52515005	1.77808	0.67852986	0.9899409
Gordonibacter	0	0.12233998	0	0.16694997	0	0	0.53353005	0.66265	0	0	0	0.1350427
Slackia	0	0	0	0	0	0	0	0	0	0	1.29438974	0.1176718
Bacteroides	20.5421679	18.8349862	10.26171	17.1565466	36.7682537	1.28433013	31.0265931	0.60495	2.66784027	2.25327	2.81739944	13.110732
Bacteroidales_noname	0.15049998	0	0	2.41760952	0	0	0.52138005	0	0	0	0	0.2808627
Barnesiella	1.23915988	0.16140997	0.47312	5.77211885	0	0	0.31835003	0.01606	0.73777007	0	0	0.7925444
Odoribacter	0.08160999	0	0.04256	0	0	0	0	0	0	0	0	0.0112882
Parabacteroides	0.36640996	4.73978905	0.06679	0.84618983	0	0	3.73056037	0	1.0136901	0	0	0.9784936
Paraprevotella	1.31551987	0	0	0	0	0	0	0	0.20160002	0	0	0.13792
Alistipes	1.79780982	1.78941964	0	4.96723901	0	0.03717	18.8699019	0.29507	0.68282007	0	0	2.5854028
Enterococcus	0	0	0	0	0	0	0	0	0	0.31457	0	0.0285973
Lactobacillus	0	0	0	0	0	0	5.49308055	0	0	2.03104	0	0.684011
Streptococcus	0	0	0	0	0	0	0	0.40238	8.93914089	16.42211	0.18854996	2.3592892
Butyricicoccus	0	0	0	0	0	0	0	0	0	0.0159	0	0.0014455
Clostridium	0.11822999	0.29932994	0.01796	0	0	0.85466009	7.18640072	0	0	1.55062	0	0.9115637
Flavonifractor	0.03171	0	0	0	0	0	0	0	0	0	0	0.0028827
Eubacterium	8.24904918	25.020225	6.14425	4.11896918	4.79896048	1.54914015	1.05976011	11.92396	15.8155016	3.31584	51.6804797	12.152376
Anaerostipes	0	0	0	0	0.37234004	0.02565	0.09652001	0.05127	0	1.73648	0	0.2074782
Blautia	3.40187966	8.90083822	1.6159	2.4917295	2.0363402	2.66457027	0.92656009	14.12867	10.5913111	9.74797	8.63764827	5.9221288
Butyrivibrio	0	0	0	0	0	0	0	0	0	0	0	0
Coprococcus	0.37145996	0.54021989	0.59377	0.60813988	1.13162011	5.56766056	0.24246002	16.74627	0	5.52084	0	2.8474946
Dorea	0.47520995	0.17786996	0.53239	2.95230941	0.9544601	3.61757036	0.39501004	3.88348	2.81214028	4.91421	0.46626991	1.9255382
Lachnospiraceae_noname	0.78092992	0.14460997	0.01607	0.28695994	0.10382001	0	0.93970009	2.38442	0.67286007	1.03447	1.28460974	0.6953136
Roseburia	0.23241998	0.28311994	1.73462	0.37553992	14.0890814	0.23275002	0	3.28879	1.74380017	0	1.63525967	2.1468528
Oscillibacter	0.9807599	0.18850996	0.96966	0.18943996	0.50839005	0.00706	0.13509001	0.75651	1.42944014	0	0	0.4695327
Peptostreptococcaceae_noname	0	0	0	0	0	2.57553026	0	0	0	0.23667	0	0.2556546
Faecalibacterium	8.73221913	0.12602997	4.32493	2.31833954	9.85723099	0.04457	0	0	6.09925061	0.7219	0	2.9294973
Ruminococcaceae_noname	0	0.62632987	0	0	0	0	0	0	0	0	0	0.0569391
Ruminococcus	0	0	8.22607	16.7105867	3.31188033	41.6128442	0	23.04953	5.18818052	33.15199	0	11.931917
Subdoligranulum	5.05242949	10.4021179	0.63076	13.9692772	13.2298913	13.0871413	10.189041	3.29209	34.5304735	1.58648	12.8261174	10.79962
Coprobacillus	0	0	0	0	0	0	0	0.01721	0.61160006	0.27545	0	0.0822055
Erysipelotrichaceae_noname	0.32379997	0	0	0	0	1.44461014	0.46653005	2.82943	0	0.06389	0	0.4662055
Holdemania	0.10910999	0	0	0	0.29729003	0	0	0.00528	0	0	0	0.0374255
Turicibacter	0	0	0	0	0	0.22974002	0	0	0	0	0	0.0208855
Acidaminococcaceae_unclassified	0	0	0	0	0.06949001	0	0	0	0	0	0	0.0063173
Acidaminococcus	0	0	0	0	1.75202018	0	0	0	0	0	0	0.1592746
Dialister	1.33152987	0.41989992	1.45041	0	3.0394003	0.59959006	0	2.49132	0	0	0	0.8483773
Veillonella	0	0	0.01602	0	0	0	0	0	0	2.3649	0	0.2164473
Burkholderiales_noname	0	0	0	0	0	0	0	0	0	0	0	0
Parasutterella	0	0	0	0	0	0	0	0	0	0	0	0
Sutterella	0	0.33334993	1.37245	0	0	0	0	0	0	0	0	0.1550727
Bilophila	1.0182999	0.58485988	0.17091	0.16826997	0	0	0.50772005	0	0	0.06822	0	0.2289345
Citrobacter	0	0	0	0	0	0.20219002	0	0	0	0	0	0.0183809
Enterobacter	3.39422966	0	0	0	0	0	0	0	0	0	0	0.3085663
Enterobacteriaceae_noname	0.19551998	0	0	0	0	0	0	0	0	0	0	0.0177745
Escherichia	0.87524991	0.17987996	0.03973	0	0	0.28197003	2.14150021	0.15017	0.63444006	1.01049	0	0.4830391
Klebsiella	28.9846871	0	0	0	0	0	0	0	0	0	0	2.6349716
Akkermansia	0.06326999	13.6759073	1.81	11.4923577	6.24344062	1.70993017	0.09289001	0	2.93837029	0	0	3.4569242
Epsilon15likevirus	0	0	0	0	0	0	0	0	0.77003008	0	0	0.0700027

Supplementary figure S3.1: Raw abundances of bacterial genera belonging to severe ME patients (dataset B, chapter 3).

	14_ME	15_ME	16_ME	17_ME	18_ME	2_ME	4_ME	9_ME	Average
Methanobrevibacter	0	0	2.17803022	0	0	0	2.0425898	0	0.5275775
Methanosphaera	0	0	0	0	0	0	0	0	0
Alloscardovia	0	0	0	0	0	0	0	0	0
Bifidobacterium	24.3258173	0	2.87945029	21.0126621	0.43925991	4.13946083	0	0	6.5995813
Scardovia	0	0	0	0	0	0	0	0	0
Adlercreutzia	0	0	0	0.15628002	0.07789998	0.21593004	0.75439992	0	0.15056375
Atopobium	0	0	0	0	0	0	0	0	0
Collinsella	5.55620167	4.32737087	6.14365061	0.67007007	0	1.30918026	4.64619954	13.6875986	4.54253396
Coriobacteriaceae_noname	0	0	0	0	0	0	0	0	0
Eggerthella	0	0	0	0.10753001	0	0.10737002	3.22909968	0	0.43049996
Gordonibacter	0	0	0	0	0	0.11910002	0	0	0.0148875
Slackia	0	0	0	0	0	0	0	0	0
Bacteroides	12.3288037	19.5200739	13.1226913	12.8874313	49.2639801	9.0189018	12.9788187	0	16.1400876
Bacteroidales_noname	0	0.95490019	3.53361035	0	0.24317995	1.62688033	0	0	0.79482135
Barnesiella	0	4.45405089	0.88452009	0	2.54694949	0.93055019	0.12093999	0	1.11712633
Odoribacter	0	0	0	0.06154001	0	0	0	0	0.0076925
Parabacteroides	0.55554017	2.94966059	0.72715007	0.50401005	2.54175949	1.0207702	0	0	1.03736132
Paraprevotella	0	0	1.14049011	0	0	0	0	0	0.14256126
Alistipes	13.8410942	12.0271324	23.4168623	4.56782046	3.53325929	0.32753007	1.65026983	0	7.42049607
Enterococcus	0	0	0	0	0	0	0	0	0
Lactobacillus	0	0	0	0	0	0	0	0	0
Streptococcus	1.39616042	1.25511025	0	1.0346401	0.29687994	1.15600023	0.31135997	4.61677954	1.25836631
Butyricicoccus	0	0	0	0	0	0	0	0	0
Clostridium	0	0	0	0.06369001	0	0	0	0	0.00796125
Flavonifractor	0	0	0	0	0	0	0	0	0
Eubacterium	6.681482	0.14091003	2.20187022	1.64443016	2.42071952	36.4113373	16.7484983	28.7026371	11.8689856
Anaerostipes	0	0	0	0	0	0.19954004	0	0.65471993	0.1067825
Blautia	1.53400046	1.84642037	1.50638015	1.77565018	16.3595267	2.79298056	5.79700942	14.3456986	5.7447083
Butyrivibrio	0	0	0	0	5.32584893	0	0	0	0.66573112
Coprococcus	1.39877042	0.89037018	0.88637009	1.78744018	0.91696982	9.72279194	2.20281978	1.89351981	2.46238153
Dorea	0.50822015	3.32715067	1.14861011	0.44989004	0.93528981	3.14496063	5.65632943	11.1521889	3.29032997
Lachnospiraceae_noname	0	0.42354008	0.20145002	0.32161003	0.4837999	0.64487013	0	2.9685597	0.63047873
Roseburia	0.6634202	0.58884012	2.9860003	2.0108702	0.76903985	1.12506023	0.87105991	1.40017986	1.30180883
Oscillibacter	0	0	0.04102	0.59713006	0	0	0	0	0.07976876
Peptostreptococcaceae_noname	0	0	0	0	0	0	0	0	0
Faecalibacterium	6.73152202	0.57292011	23.4556223	8.22818082	1.23591975	11.3703623	15.2508185	15.0264285	10.2339718
Ruminococcaceae_noname	0	0	0	0.93555009	0	0	0	0	0.11694376
Ruminococcus	18.7282656	25.3749651	1.05706011	23.1449623	0	0.40920008	0	0	8.58930665
Subdoligranulum	4.22419127	12.0508824	10.8826211	17.4626417	3.09898938	13.6501327	6.59440934	4.30830957	9.03402219
Coprobacillus	0	0	0	0	0	0	0	0	0
Erysipelotrichaceae_noname	0	0	0	0	0	0	0	1.24337988	0.15542248
Holdemania	0	0	0	0	0	0	0	0	0
Turicibacter	0	0	0	0	0	0	0	0	0
Acidaminococcaceae_unclassified	0	0	0	0	0	0	0	0	0
Acidaminococcus	0	0	0	0	0	0	0	0	0
Dialister	1.22100037	2.89697058	0	0	0	0	0	0	0.51474637
Veillonella	0.30551009	0	0	0	0	0.05569001	0	0	0.04515001
Burkholderiales_noname	0	0.71060014	0	0	0	0	0	0	0.08882502
Parasutterella	0	0	0	0.06392001	0	0	0	0	0.00799
Sutterella	0	0	0	0	0.75578985	0.15200003	0	0	0.11347373
Bilophila	0	0.26325005	0.31304003	0	0.01543	0.14536003	0	0	0.09213501
Citrobacter	0	0	0	0	0	0	0	0	0
Enterobacter	0	0	0	0	0	0	0	0	0
Enterobacteriaceae_noname	0	0	0	0	0	0	0	0	0
Escherichia	0	0	0	0	4.09957918	0.20404004	21.1453779	0	3.18112464
Klebsiella	0	0	0	0	0.56481989	0	0	0	0.07060249
Akkermansia	0	5.42488108	1.29350013	0.51205005	4.07510918	0	0	0	1.41319256
Epsilon15likevirus	0	0	0	0	0	0	0	0	0

Supplementary figure S3.2: Raw abundance table for bacterial genera belonging to HHCs (dataset B, chapter 3)

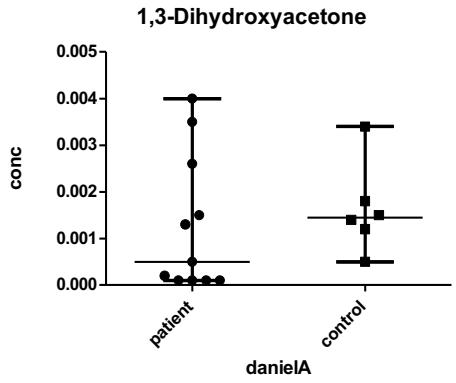
1,3-Dihydroxyacetone
conc
0.005
0.004
0.003
0.002
0.001
0.000
patient
control
danielA

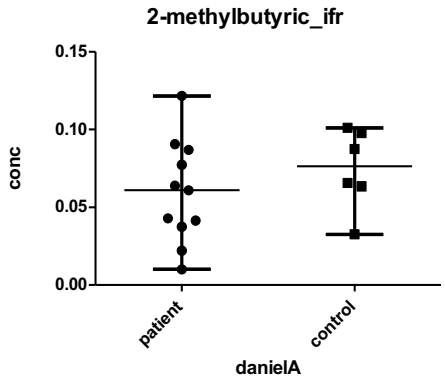
2-methylbutyric_ifr
conc
0.15
0.10
0.05
0.00
patient
control
danielA

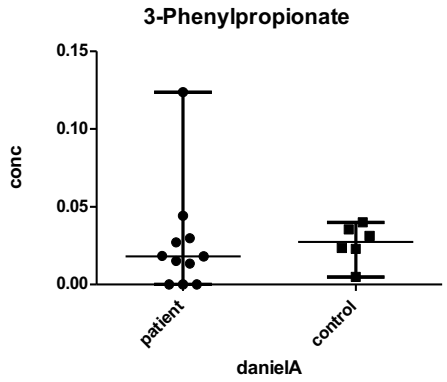
3-Phenylpropionate
conc
0.15
0.10
0.05
0.00
patient
control
danielA

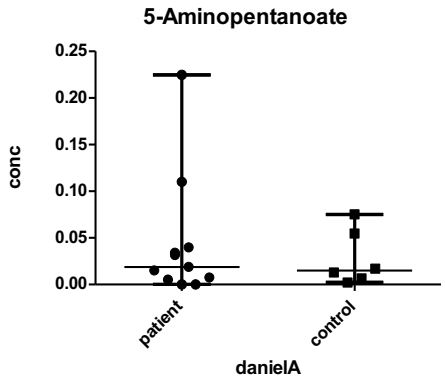
5-Aminopentanoate
conc
0.25
0.20
0.15
0.10
0.05
0.00
patient
control
danielA

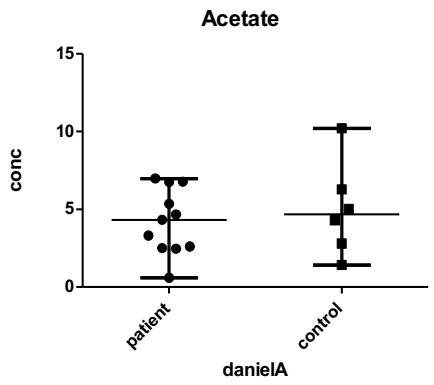
Acetate
conc
15
10
5
0
patient
control
danielA

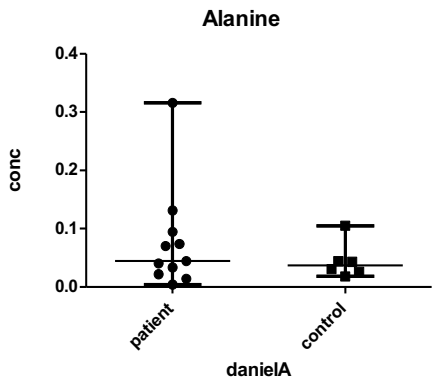
Alanine
conc
0.4
0.3
0.2
0.1
0.0
patient
control
danielA

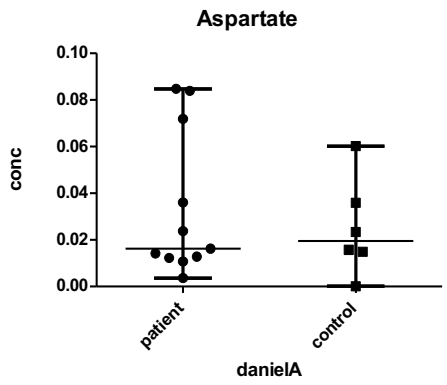
Aspartate
conc
0.10
0.08
0.06
0.04
0.02
0.00
patient
control
danielA

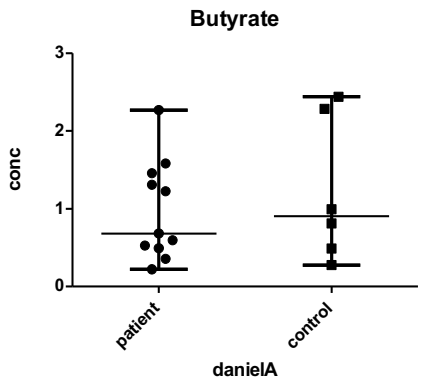
Butyrate
conc
3
2
1
0
patient
control
danielA

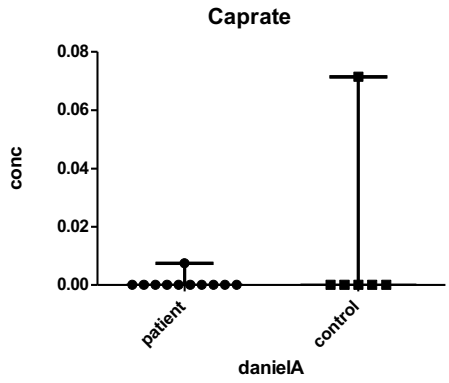
Caprate
0.08
0.06
0.04
0.02
0.00
conc
patient
control
danielA

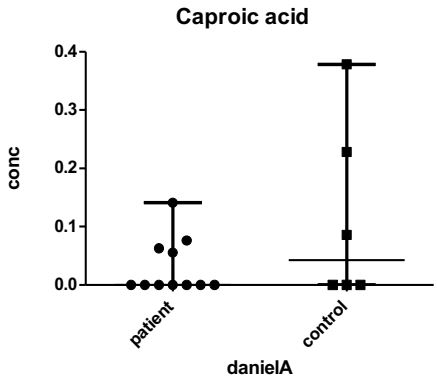
Caproic acid
0.4
0.3
0.2
0.1
0.0
conc
patient
control
danielA

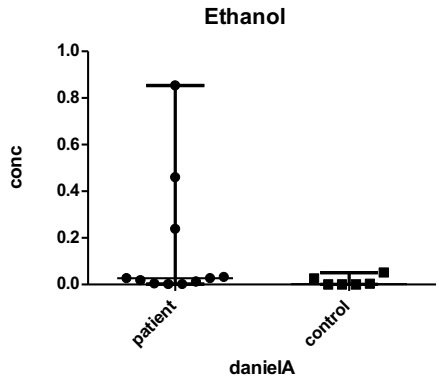
Ethanol
1.0
0.8
0.6
0.4
0.2
0.0
conc
patient
control
danielA

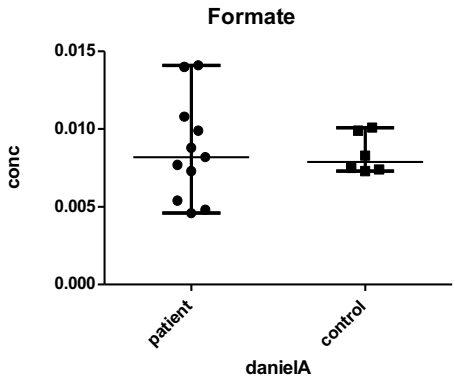
Formate
0.015
0.010
0.005
0.000
conc
patient
control
danielA

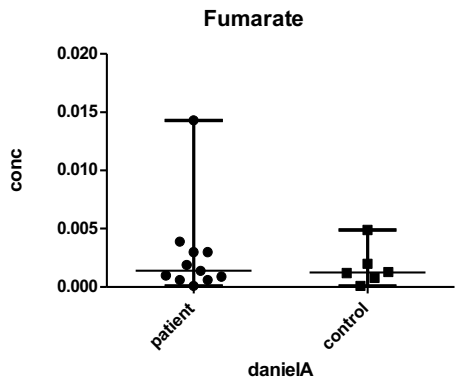
Fumarate
0.020
0.015
0.010
0.005
0.000
conc
patient
control
danielA

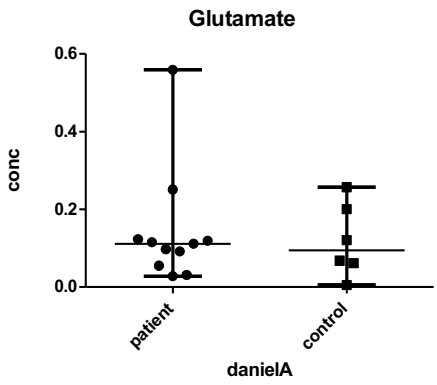
Glutamate
0.6
0.4
0.2
0.0
conc
patient
control
danielA

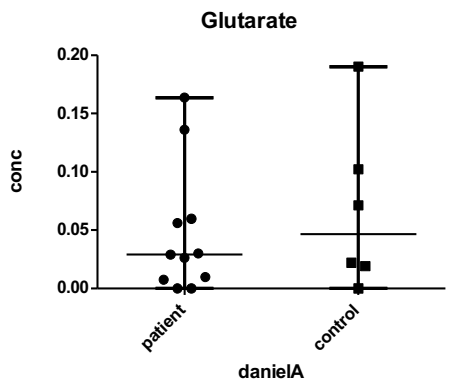
Glutarate
0.20
0.15
0.10
0.05
0.00
conc
patient
control
danielA

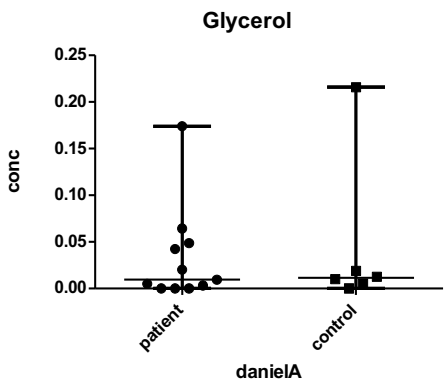
Glycerol
0.25
0.20
0.15
0.10
0.05
0.00
conc
patient
control
danielA

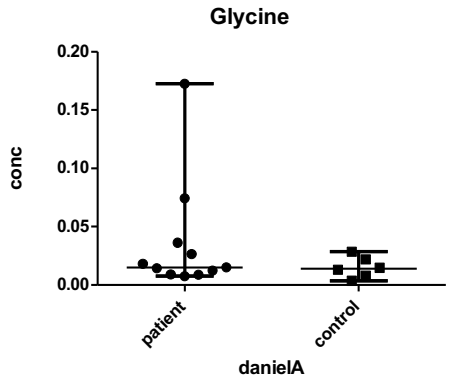
Glycine
conc
0.20
0.15
0.10
0.05
0.00
patient
control
danielA

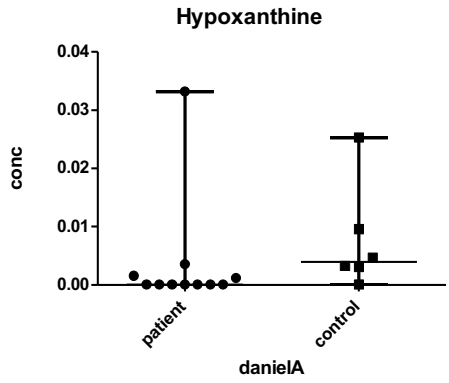
Hypoxanthine
conc
0.04
0.03
0.02
0.01
0.00
patient
control
danielA

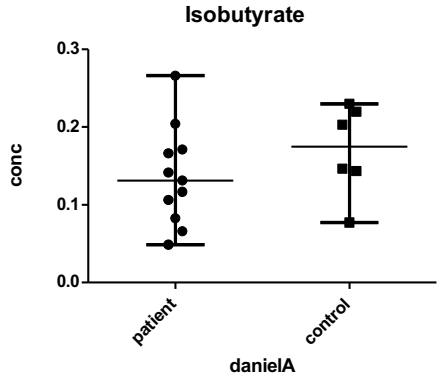
Isobutyrate
conc
0.3
0.2
0.1
0.0
patient
control
danielA

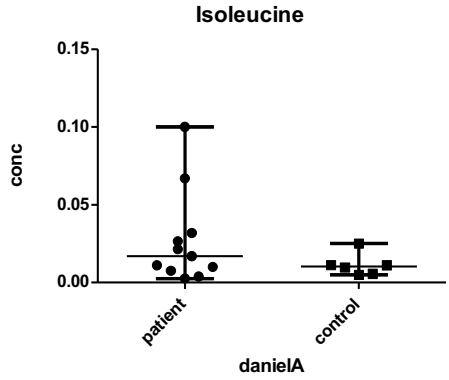
Isoleucine
conc
0.15
0.10
0.05
0.00
patient
control
danielA

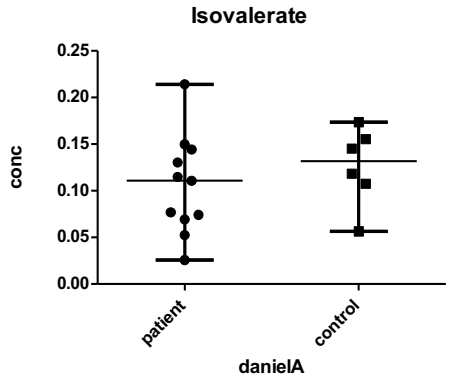
Isovalerate
conc
0.25
0.20
0.15
0.10
0.05
0.00
patient
control
danielA

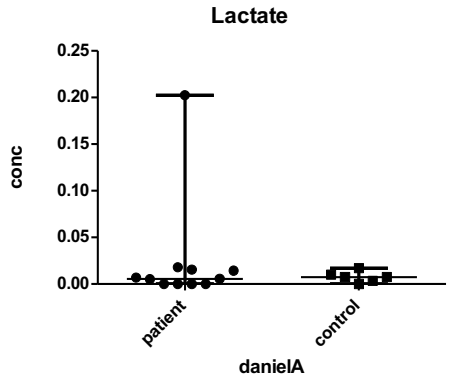
Lactate
conc
0.25
0.20
0.15
0.10
0.05
0.00
patient
control
danielA

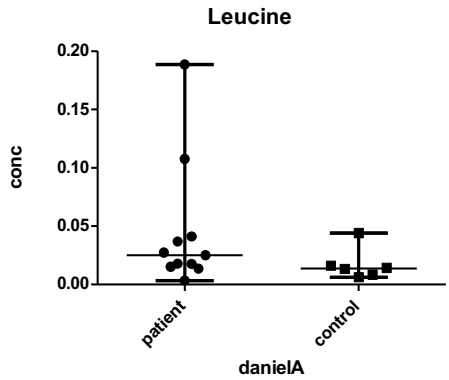
Leucine
conc
0.20
0.15
0.10
0.05
0.00
patient
control
danielA

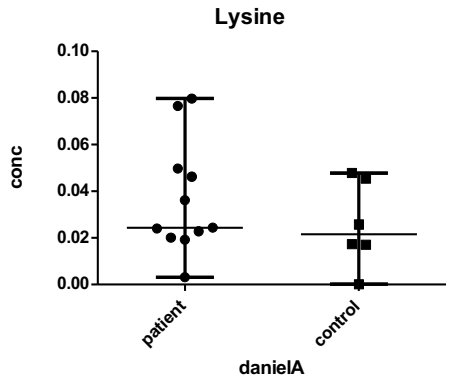
Lysine
conc
0.10
0.08
0.06
0.04
0.02
0.00
patient
control
danielA

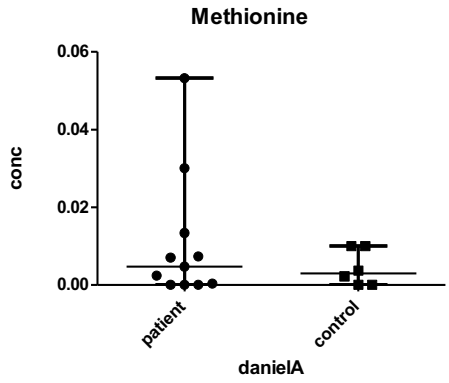
Methionine
0.06
0.04
0.02
0.00
conc
patient
control
danielA

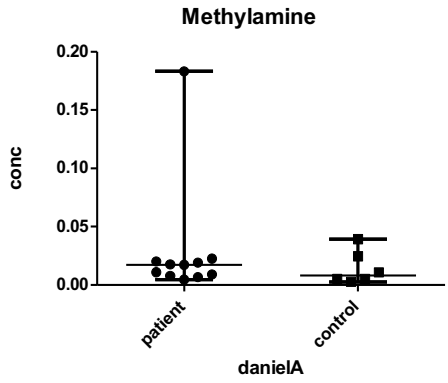
Methylamine
0.20
0.15
0.10
0.05
0.00
conc
patient
control
danielA

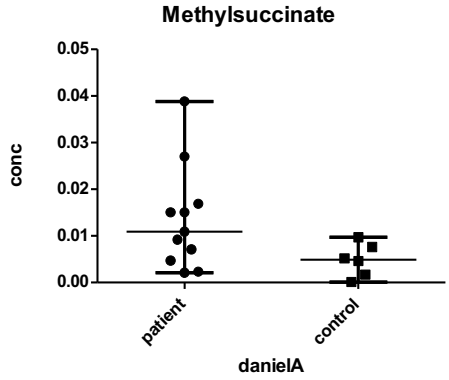
Methylsuccinate
0.05
0.04
0.03
0.02
0.01
0.00
conc
patient
control
danielA

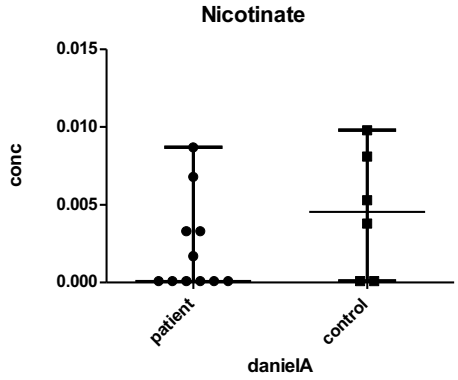
Nicotinate
0.015
0.010
0.005
0.000
conc
patient
control
danielA

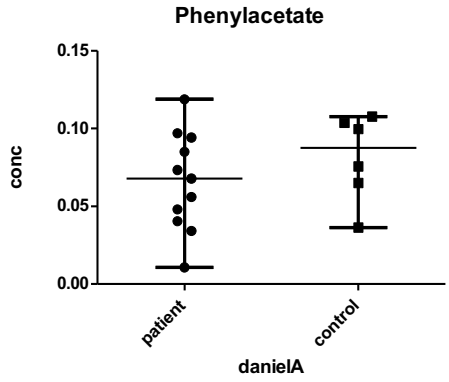
Phenylacetate
0.15
0.10
0.05
0.00
conc
patient
control
danielA

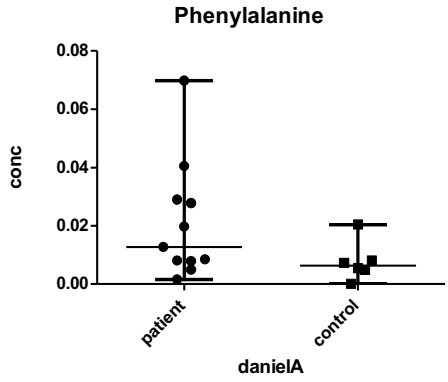
Phenylalanine
0.08
0.06
0.04
0.02
0.00
conc
patient
control
danielA

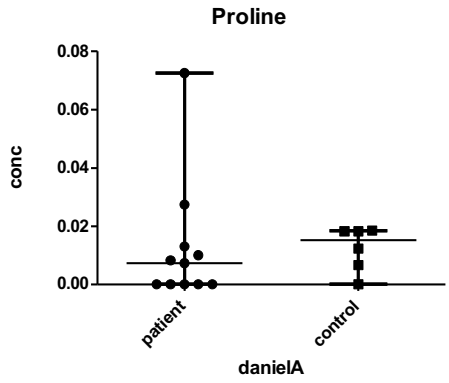
Proline
0.08
0.06
0.04
0.02
0.00
conc
patient
control
danielA

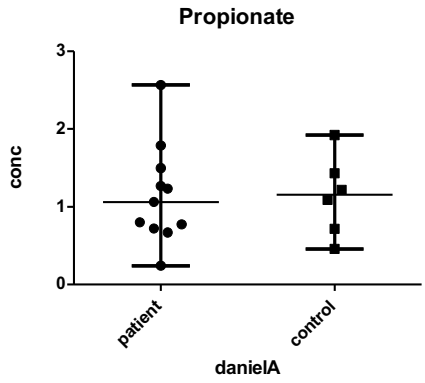
Propionate
3
2
1
0
conc
patient
control
danielA

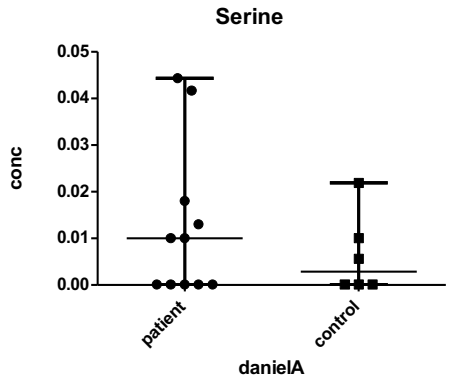
Serine
0.05
0.04
0.03
0.02
0.01
0.00
conc
patient
control
danielA

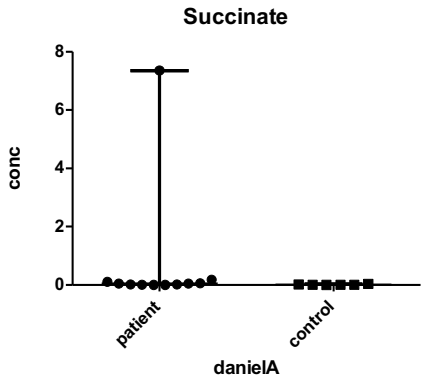
Succinate
8
6
4
2
0
conc
patient
control
danielA

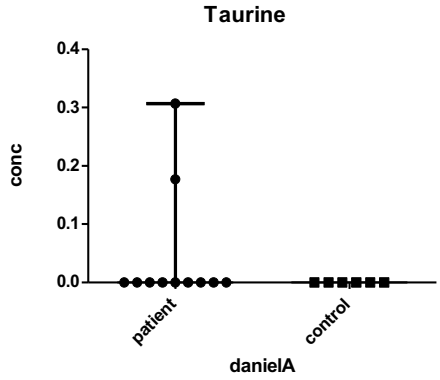
Taurine
0.4
0.3
0.2
0.1
0.0
conc
patient
control
danielA

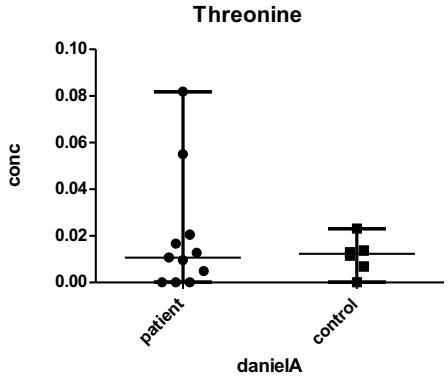
Threonine
0.10
0.08
0.06
0.04
0.02
0.00
conc
patient
control
danielA

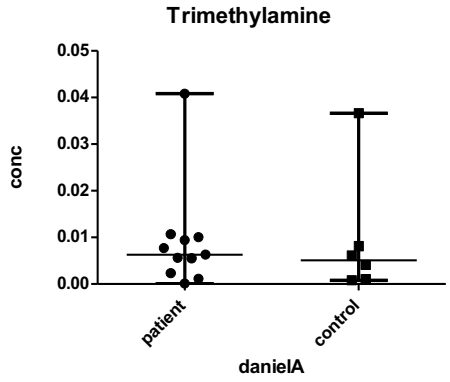
Trimethylamine
0.05
0.04
0.03
0.02
0.01
0.00
conc
patient
control
danielA

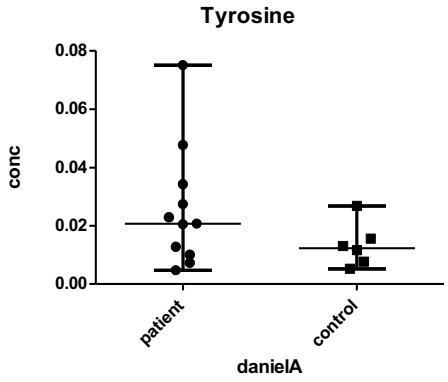
Tyrosine
0.08
0.06
0.04
0.02
0.00
conc
patient
control
danielA

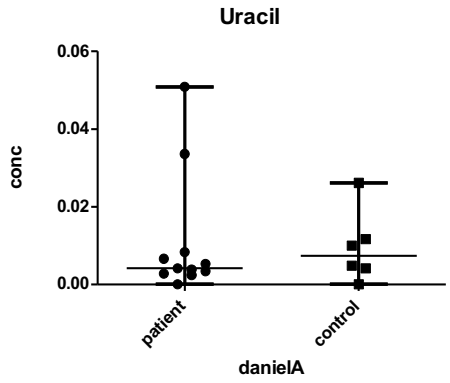
Uracil
0.06
0.04
0.02
0.00
conc
patient
control
danielA

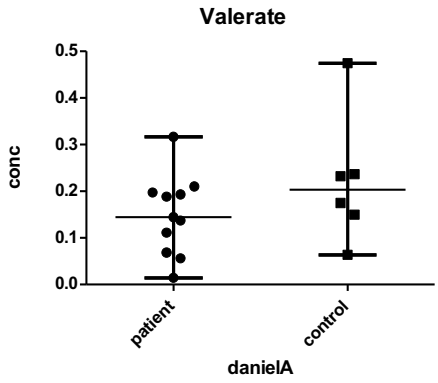
Valerate
0.5
0.4
0.3
0.2
0.1
0.0
conc
patient
control
danielA

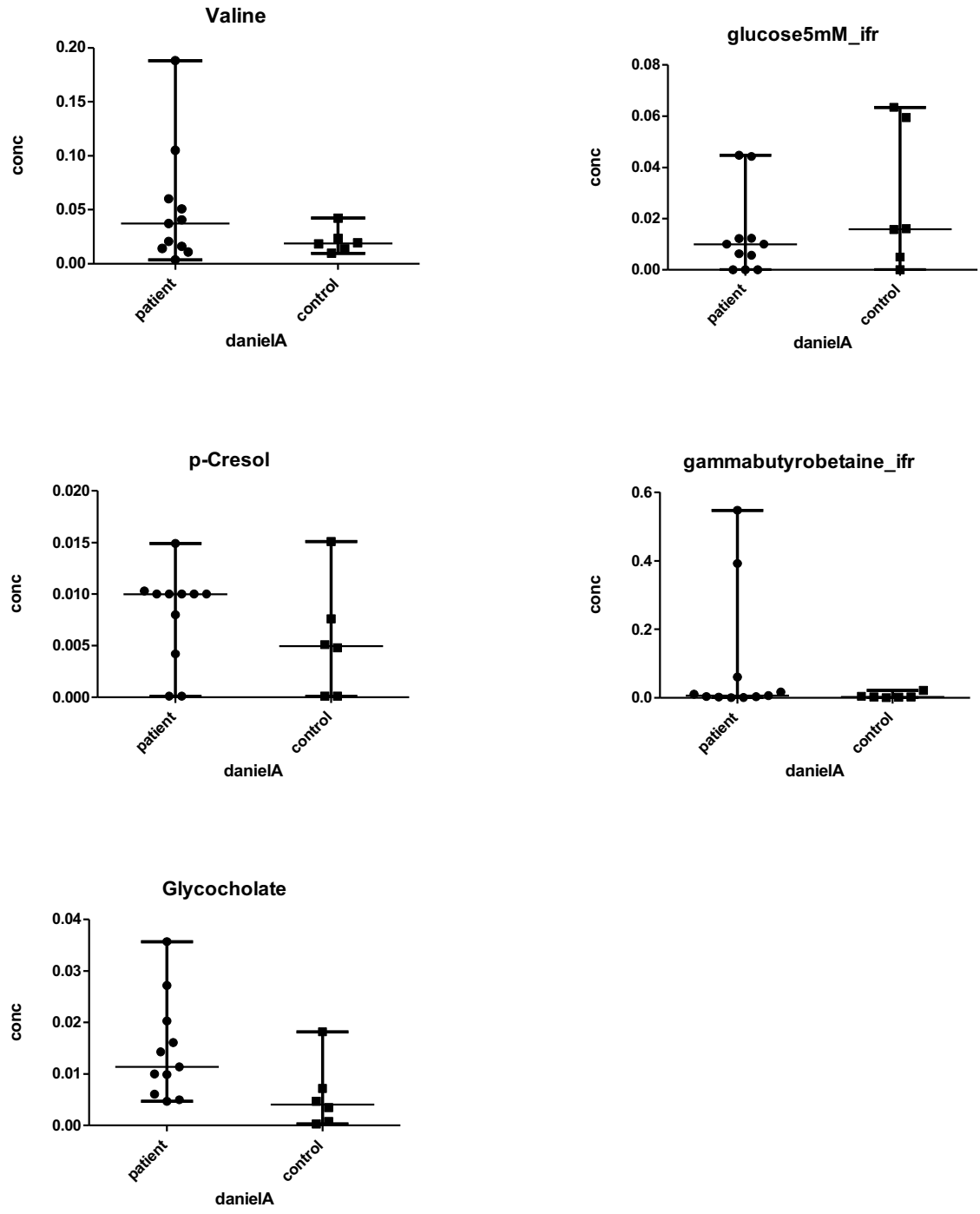

Supplementary figure 4.1: Metabolomic profile of faecal water using ^{1}H-NMR revealed 45 metabolites in 11 house-bound ME patients and 6 HHCs

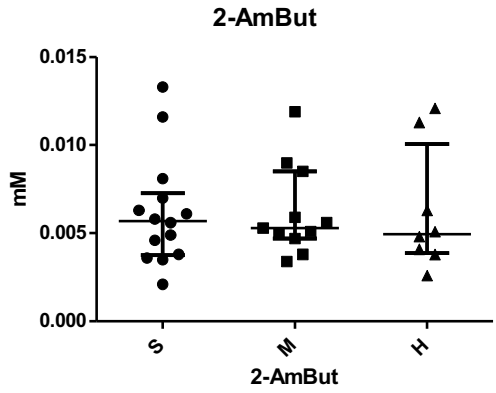
2-AmBut
mM
0.015
0.010
0.005
0.000
S
M
H
2-AmBut

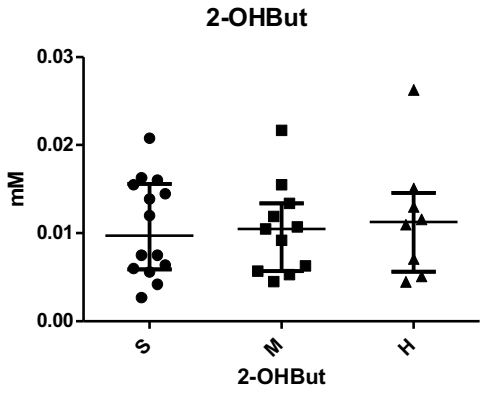
2-OHBut
mM
0.03
0.02
0.01
0.00
S
M
H
2-OHBut

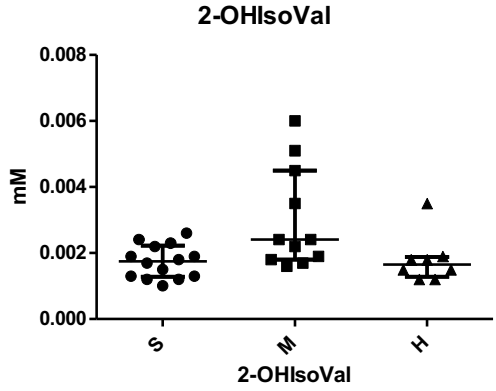
2-OHIsoVal
mM
0.008
0.006
0.004
0.002
0.000
S
M
H
2-OHIsoVal

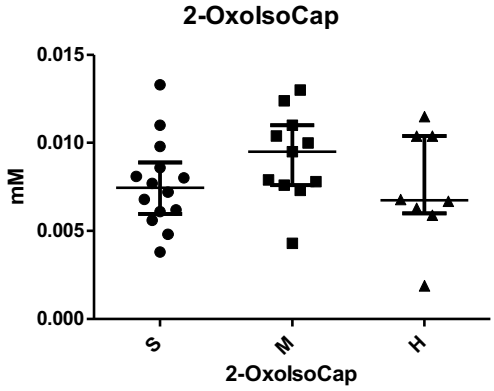
2-OxoIsoCap
mM
0.015
0.010
0.005
0.000
S
M
H
2-OxoIsoCap

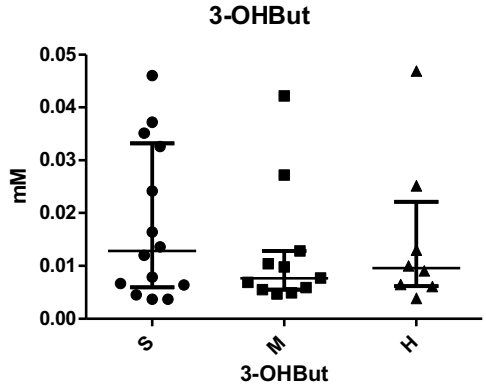
3-OHBut
mM
0.05
0.04
0.03
0.02
0.01
0.00
S
M
H
3-OHBut

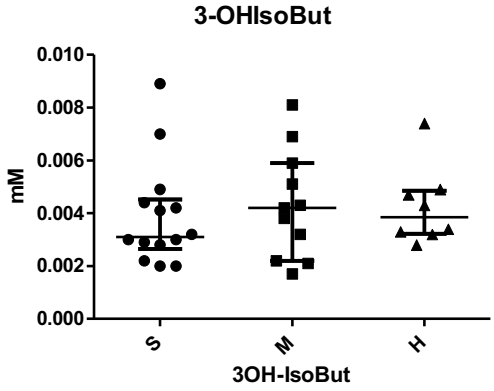
3-OHIsoBut
mM
0.010
0.008
0.006
0.004
0.002
0.000
S
M
H
3OH-IsoBut

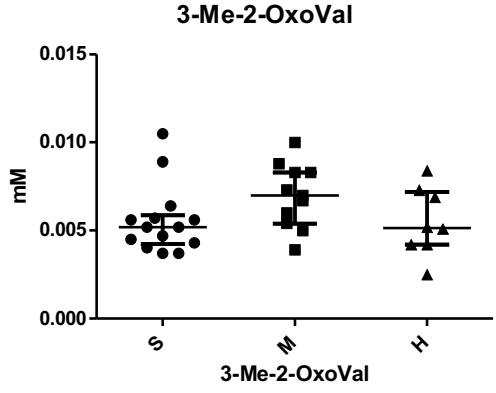
3-Me-2-OxoVal
mM
0.015
0.010
0.005
0.000
S
M
H
3-Me-2-OxoVal

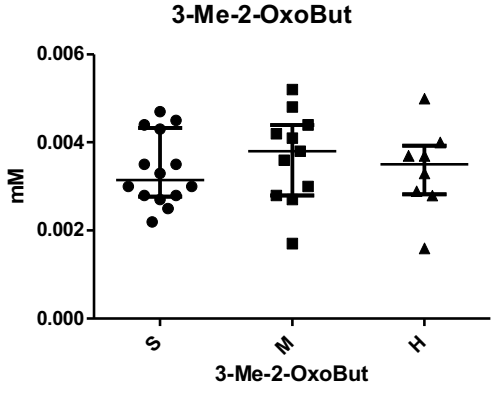
3-Me-2-OxoBut
mM
0.006
0.004
0.002
0.000
S
M
H
3-Me-2-OxoBut

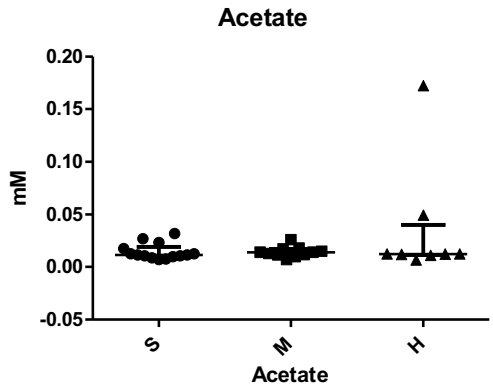
Acetate
0.20
0.15
0.10
0.05
0.00
-0.05
mM
S
M
H
Acetate

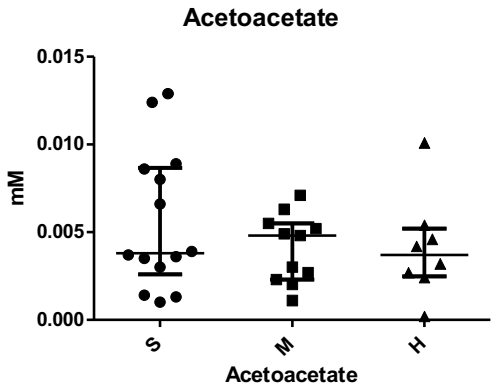
Acetoacetate
0.015
0.010
0.005
0.000
mM
S
M
H
Acetoacetate

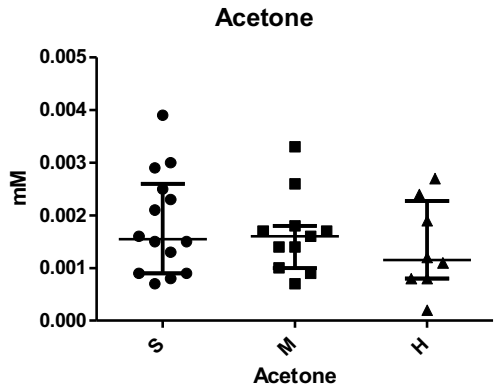
Acetone
0.005
0.004
0.003
0.002
0.001
0.000
mM
S
M
H
Acetone

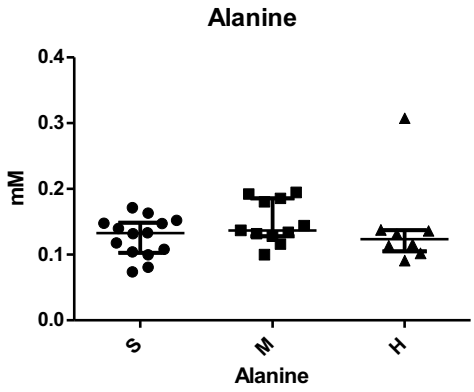
Alanine
0.4
0.3
0.2
0.1
0.0
mM
S
M
H
Alanine

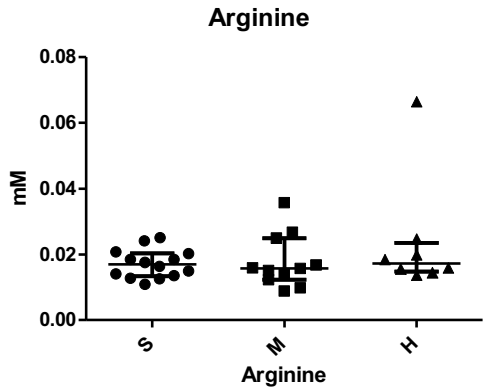
Arginine
0.08
0.06
0.04
0.02
0.00
mM
S
M
H
Arginine

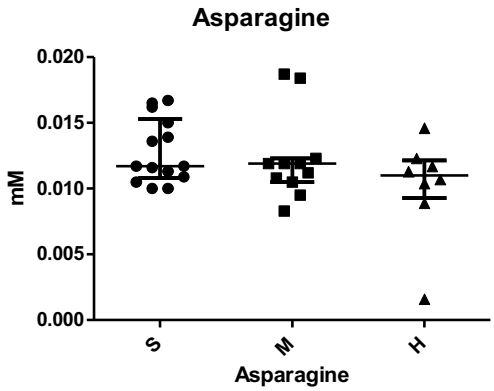
Asparagine
0.020
0.015
0.010
0.005
0.000
mM
S
M
H
Asparagine

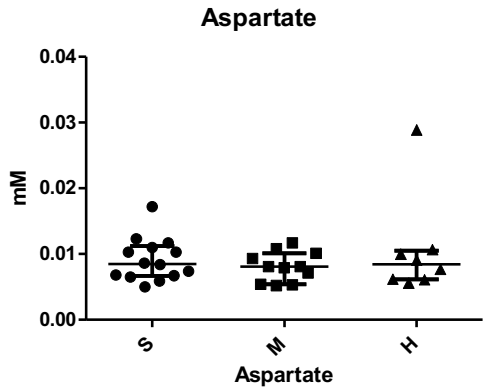
Aspartate
0.04
0.03
0.02
0.01
0.00
mM
S
M
H
Aspartate

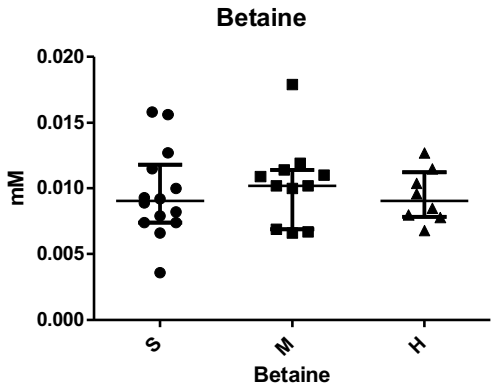
Betaine
0.020
0.015
0.010
0.005
0.000
mM
S
M
H
Betaine

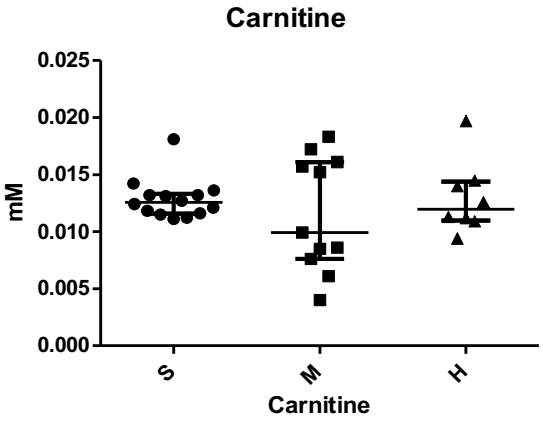
Carnitine
0.025
0.020
0.015
0.010
0.005
0.000
mM
S
M
H
Carnitine

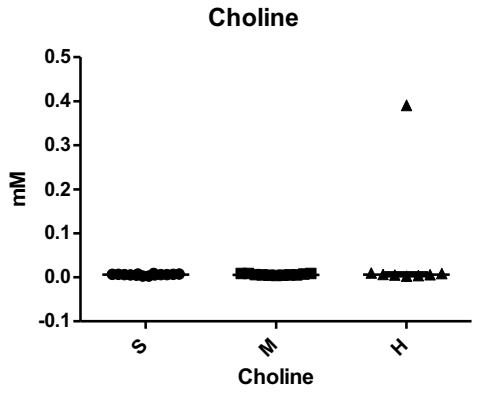
Choline
mM
0.5
0.4
0.3
0.2
0.1
0.0
-0.1
S
M
H
Choline

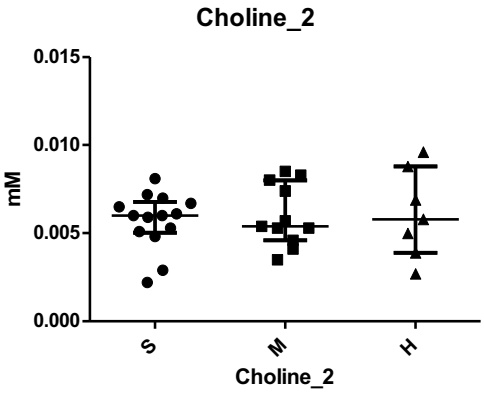
Choline_2
mM
0.015
0.010
0.005
0.000
S
M
H
Choline_2

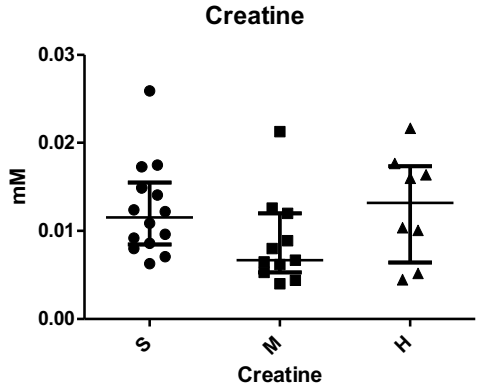
Creatine
mM
0.03
0.02
0.01
0.00
S
M
H
Creatine

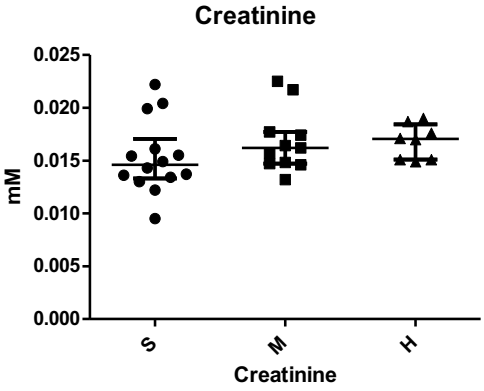
Creatinine
mM
0.025
0.020
0.015
0.010
0.005
0.000
S
M
H
Creatinine

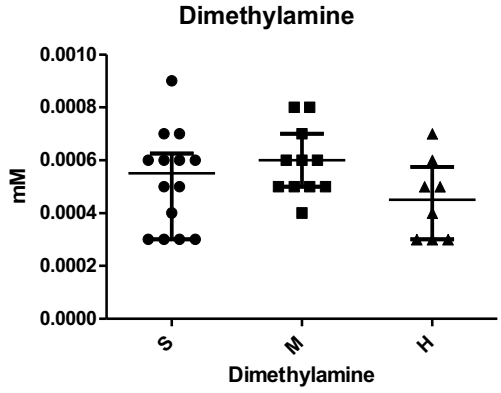
Dimethylamine
mM
0.0010
0.0008
0.0006
0.0004
0.0002
0.0000
S
M
H
Dimethylamine

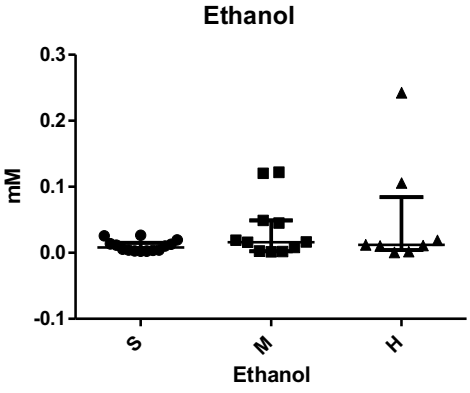
Ethanol
mM
0.3
0.2
0.1
0.0
-0.1
S
M
H
Ethanol

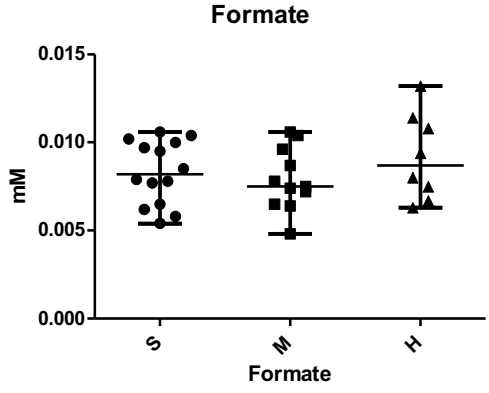
Formate
mM
0.015
0.010
0.005
0.000
S
M
H
Formate

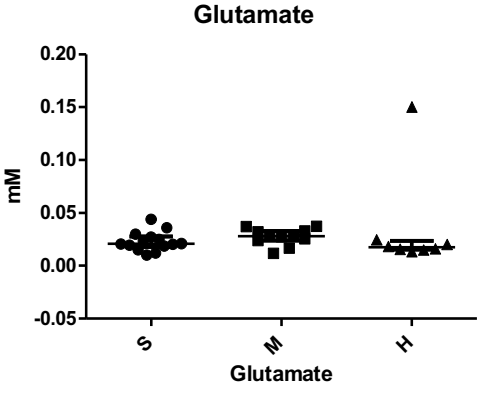
Glutamate
mM
0.20
0.15
0.10
0.05
0.00
-0.05
S
M
H
Glutamate

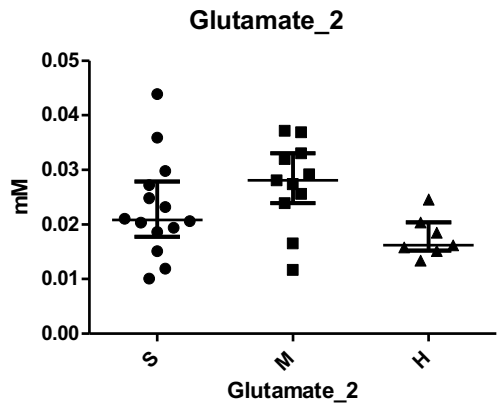
Glutamate_2
mM
0.05
0.04
0.03
0.02
0.01
0.00
S
M
H
Glutamate_2

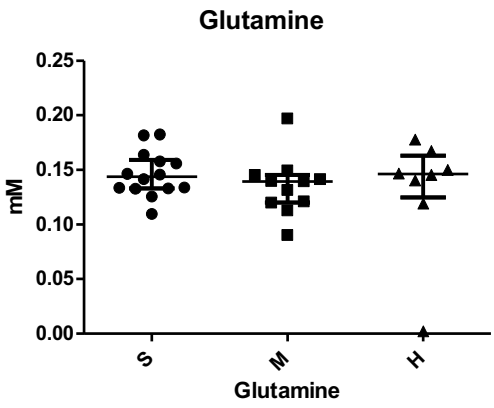
Glutamine
mM
0.25
0.20
0.15
0.10
0.05
0.00
S
M
H
Glutamine

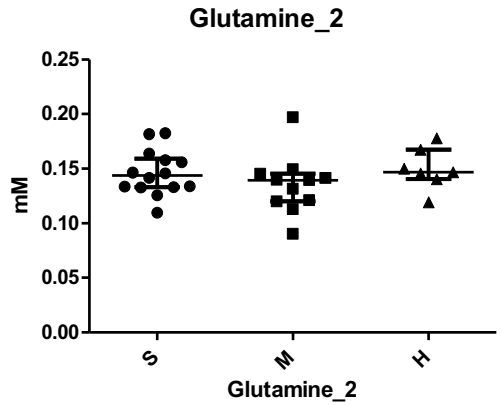
Glutamine_2
mM
0.25
0.20
0.15
0.10
0.05
0.00
S
M
H
Glutamine_2

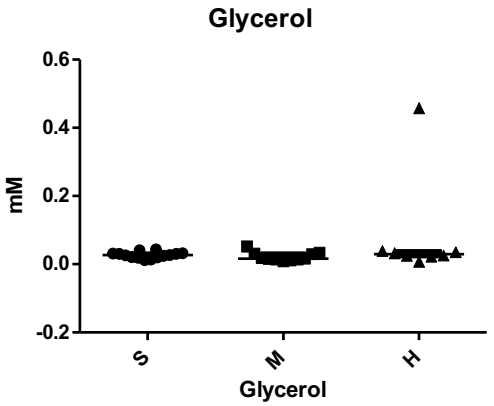
Glycerol
mM
0.6
0.4
0.2
0.0
-0.2
S
M
H
Glycerol

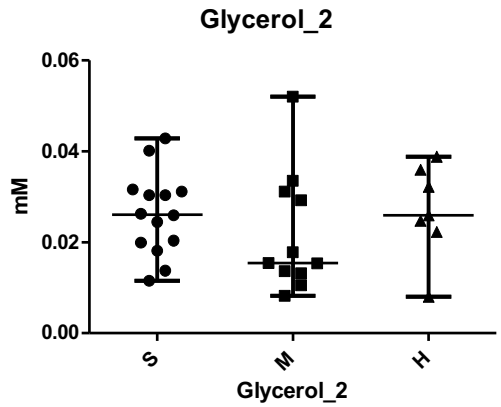
Glycerol_2
mM
0.06
0.04
0.02
0.00
S
M
H
Glycerol_2

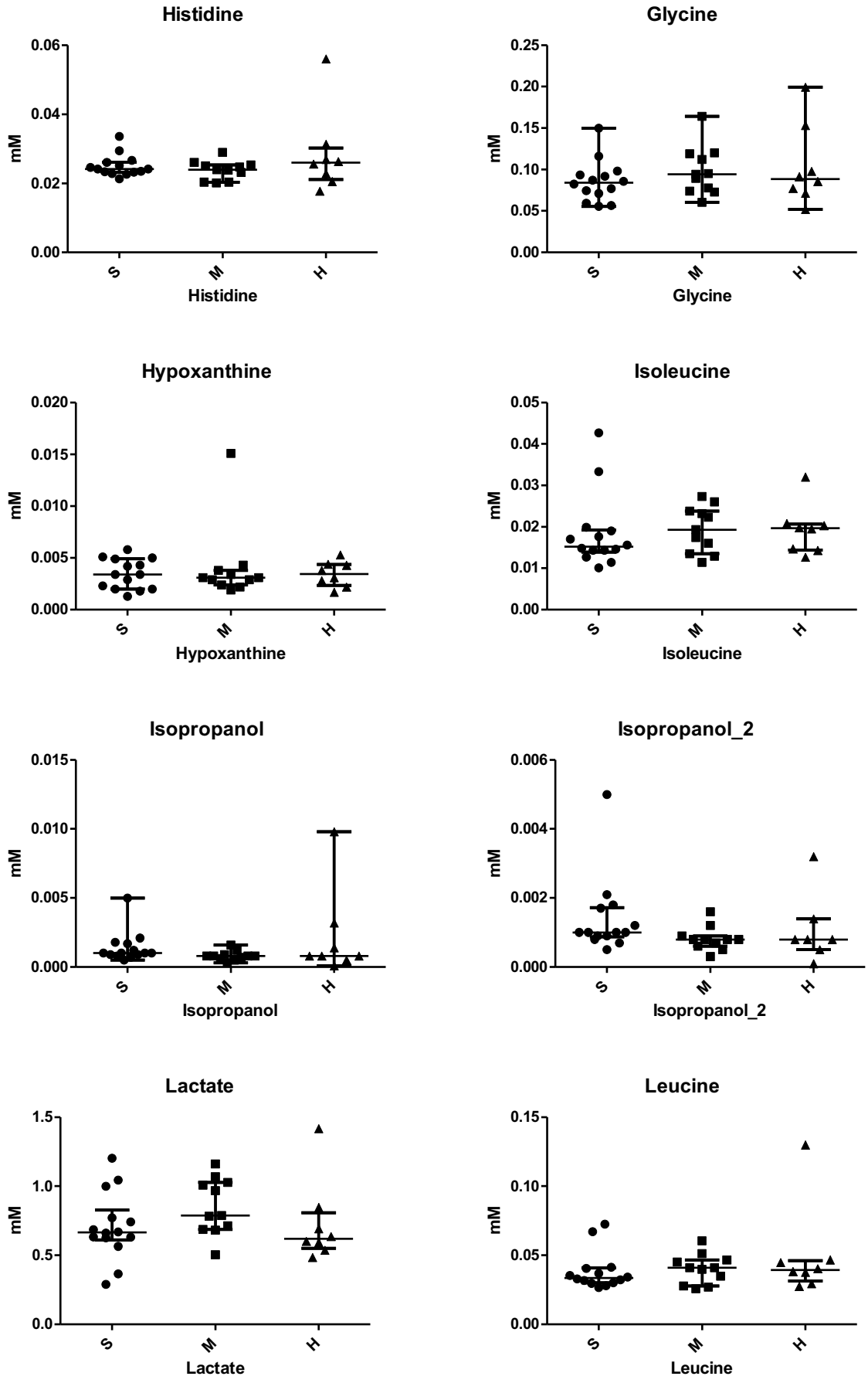
Histidine
0.06
0.04
0.02
0.00
mM
S
M
H
Histidine
Glycine
0.25
0.20
0.15
0.10
0.05
0.00
mM
S
M
H
Glycine
Hypoxanthine
0.020
0.015
0.010
0.005
0.000
mM
S
M
H
Hypoxanthine
Isoleucine
0.05
0.04
0.03
0.02
0.01
0.00
mM
S
M
H
Isoleucine
Isopropanol
0.015
0.010
0.005
0.000
mM
S
M
H
Isopropanol
Isopropanol_2
0.006
0.004
0.002
0.000
mM
S
M
H
Isopropanol_2
Lactate
1.5
1.0
0.5
0.0
mM
S
M
H
Lactate
Leucine
0.15
0.10
0.05
0.00
mM
S
M
H
Leucine

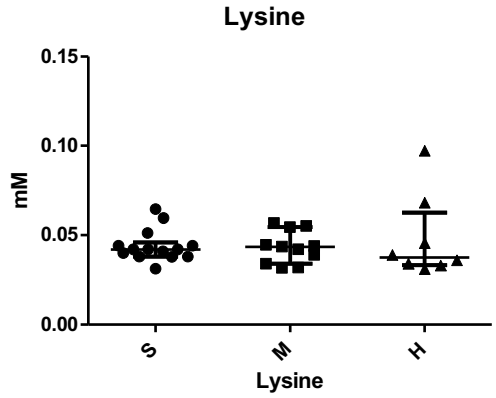
Lysine
0.15
0.10
0.05
0.00
mM
S
M
H
Lysine

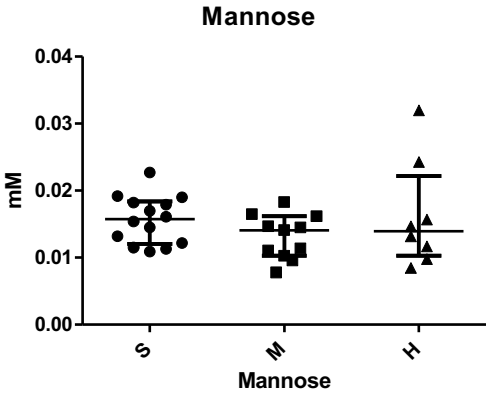
Mannose
0.04
0.03
0.02
0.01
0.00
mM
S
M
H
Mannose

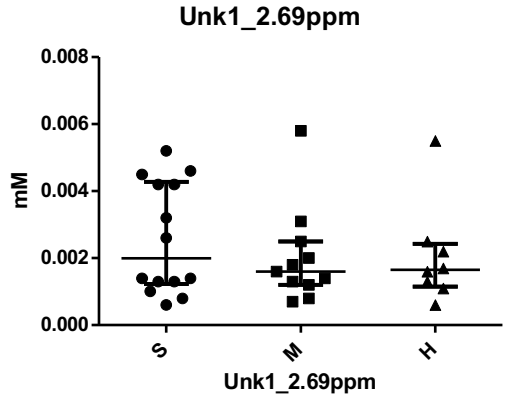
Unk1_2.69ppm
0.008
0.006
0.004
0.002
0.000
mM
S
M
H
Unk1_2.69ppm

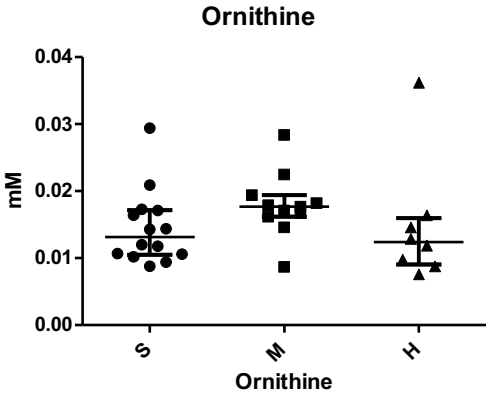
Ornithine
0.04
0.03
0.02
0.01
0.00
mM
S
M
H
Ornithine

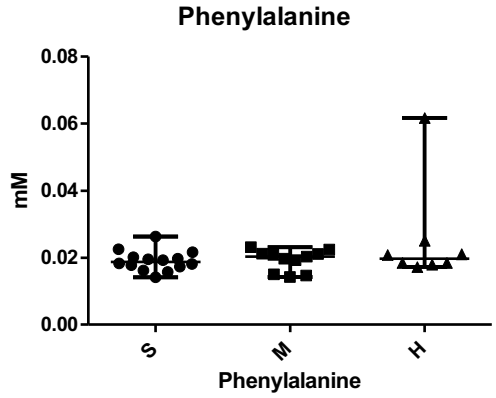
Phenylalanine
0.08
0.06
0.04
0.02
0.00
mM
S
M
H
Phenylalanine

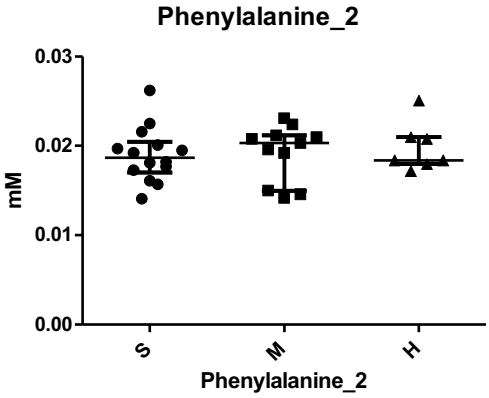
Phenylalanine_2
0.03
0.02
0.01
0.00
mM
S
M
H
Phenylalanine_2

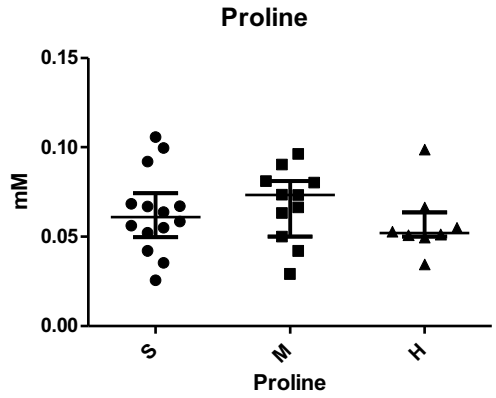
Proline
0.15
0.10
0.05
0.00
mM
S
M
H
Proline

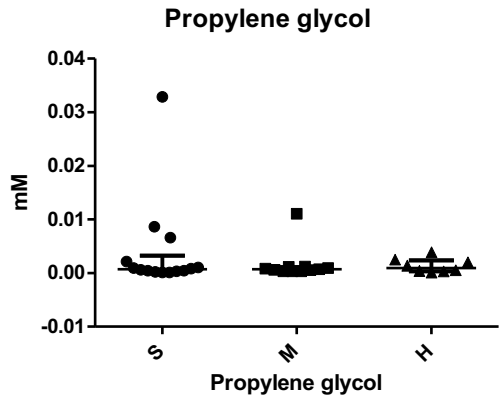
Propylene glycol
0.04
0.03
0.02
0.01
0.00
-0.01
mM
S
M
H
Propylene glycol

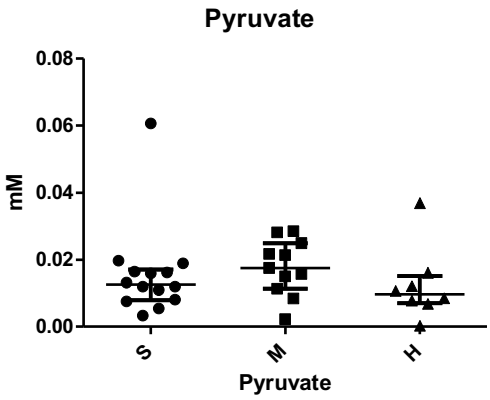
Pyruvate
0.08
0.06
0.04
0.02
0.00
mM
S
M
H
Pyruvate


Sarcosine
0.0008
0.0006
0.0004
0.0002
0.0000
mM
S
M
H
Sarcosine

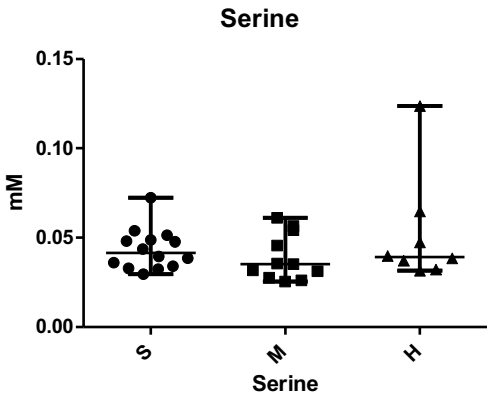
Serine
0.15
0.10
0.05
0.00
mM
S
M
H
Serine

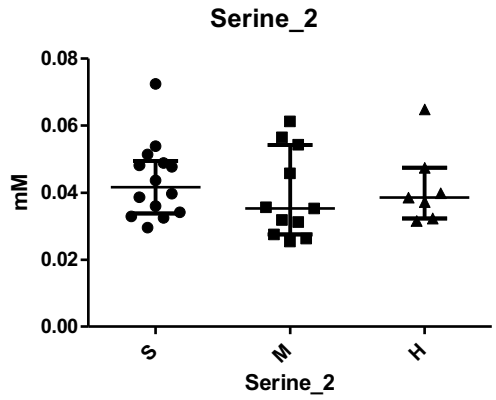
Serine_2
0.08
0.06
0.04
0.02
0.00
mM
S
M
H
Serine_2

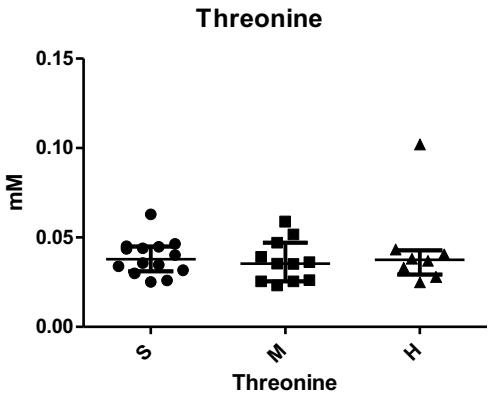
Threonine
0.15
0.10
0.05
0.00
mM
S
M
H
Threonine

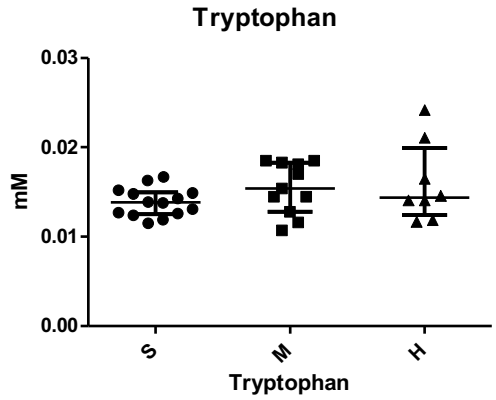
Tryptophan
0.03
0.02
0.01
0.00
mM
S
M
H
Tryptophan

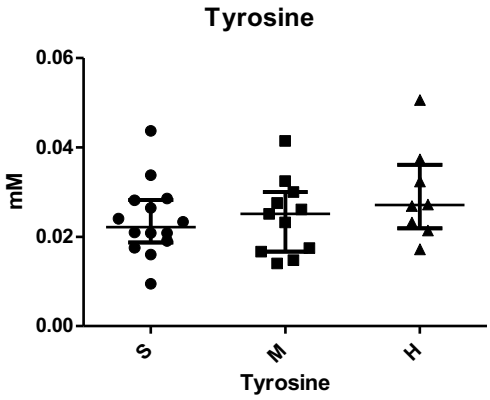
Tyrosine
0.06
0.04
0.02
0.00
mM
S
M
H
Tyrosine

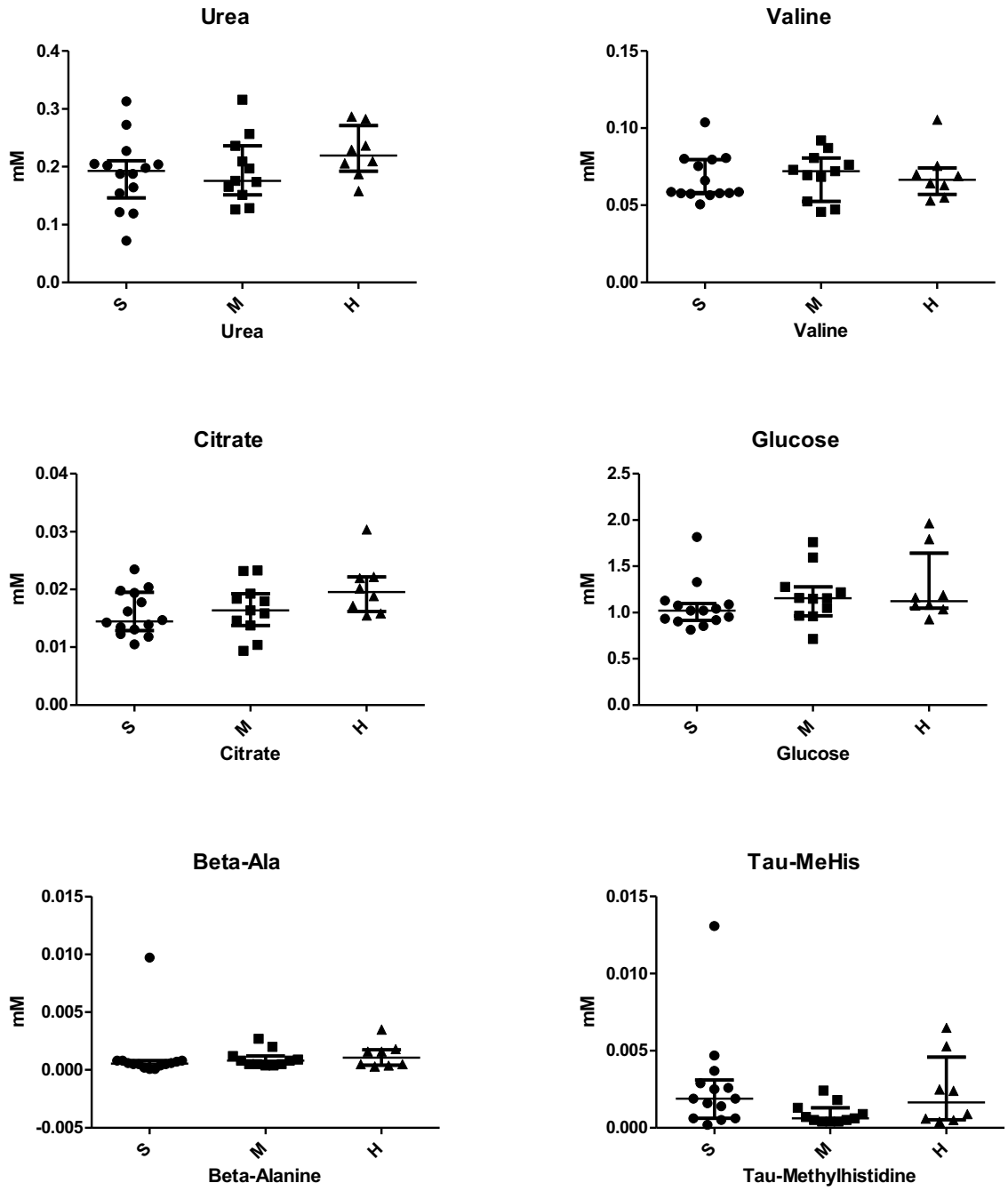

Supplementary figure 4.2: Metabolomic profile of serum using ^{1}H-NMR revealed 53 metabolites in 25 ME/CFS patients (14 severe (S); 11 mild/moderate (M)) and 9 HHCs.

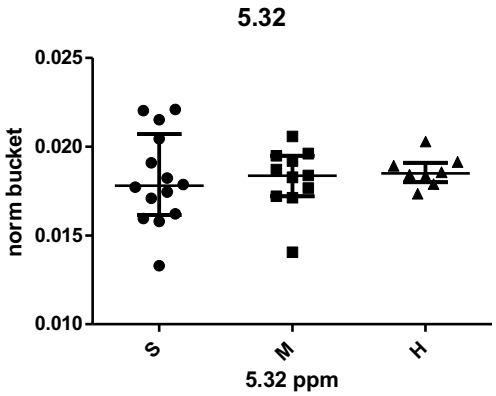
5.32
norm bucket
0.025
0.020
0.015
0.010
S
M
H
5.32 ppm

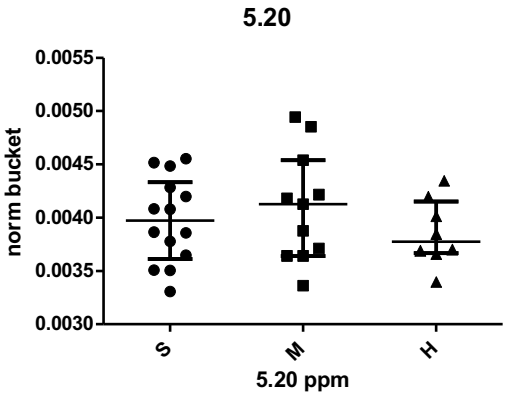
5.20
norm bucket
0.0055
0.0050
0.0045
0.0040
0.0035
0.0030
S
M
H
5.20 ppm

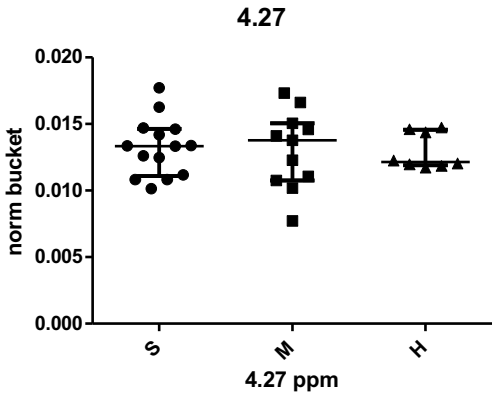
4.27
norm bucket
0.020
0.015
0.010
0.005
0.000
S
M
H
4.27 ppm

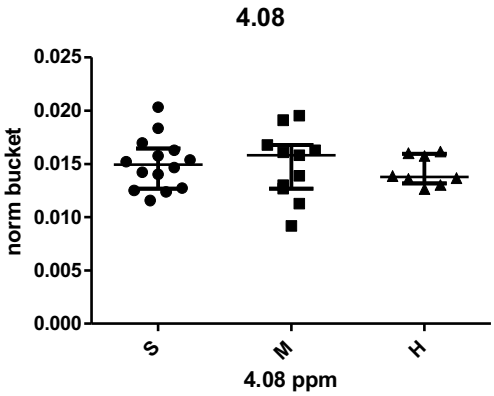
4.08
norm bucket
0.025
0.020
0.015
0.010
0.005
0.000
S
M
H
4.08 ppm

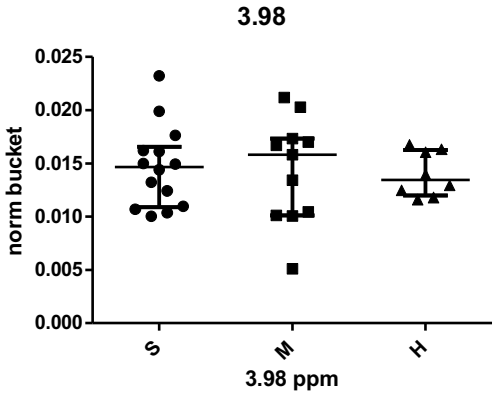
3.98
norm bucket
0.025
0.020
0.015
0.010
0.005
0.000
S
M
H
3.98 ppm

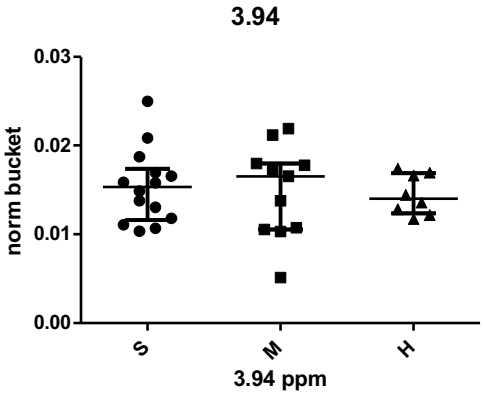
3.94
norm bucket
0.03
0.02
0.01
0.00
S
M
H
3.94 ppm

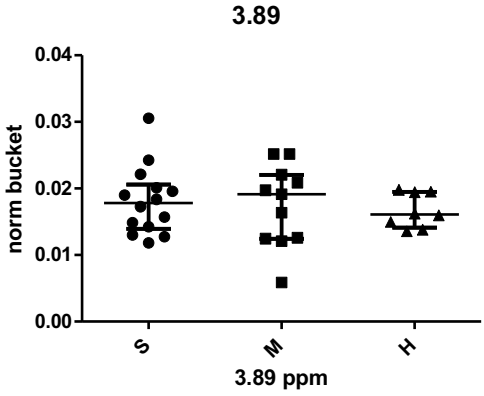
3.89
norm bucket
0.04
0.03
0.02
0.01
0.00
S
M
H
3.89 ppm

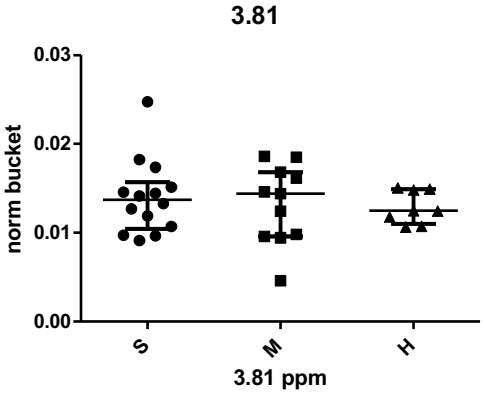
3.81
norm bucket
0.03
0.02
0.01
0.00
S
M
H
3.81 ppm

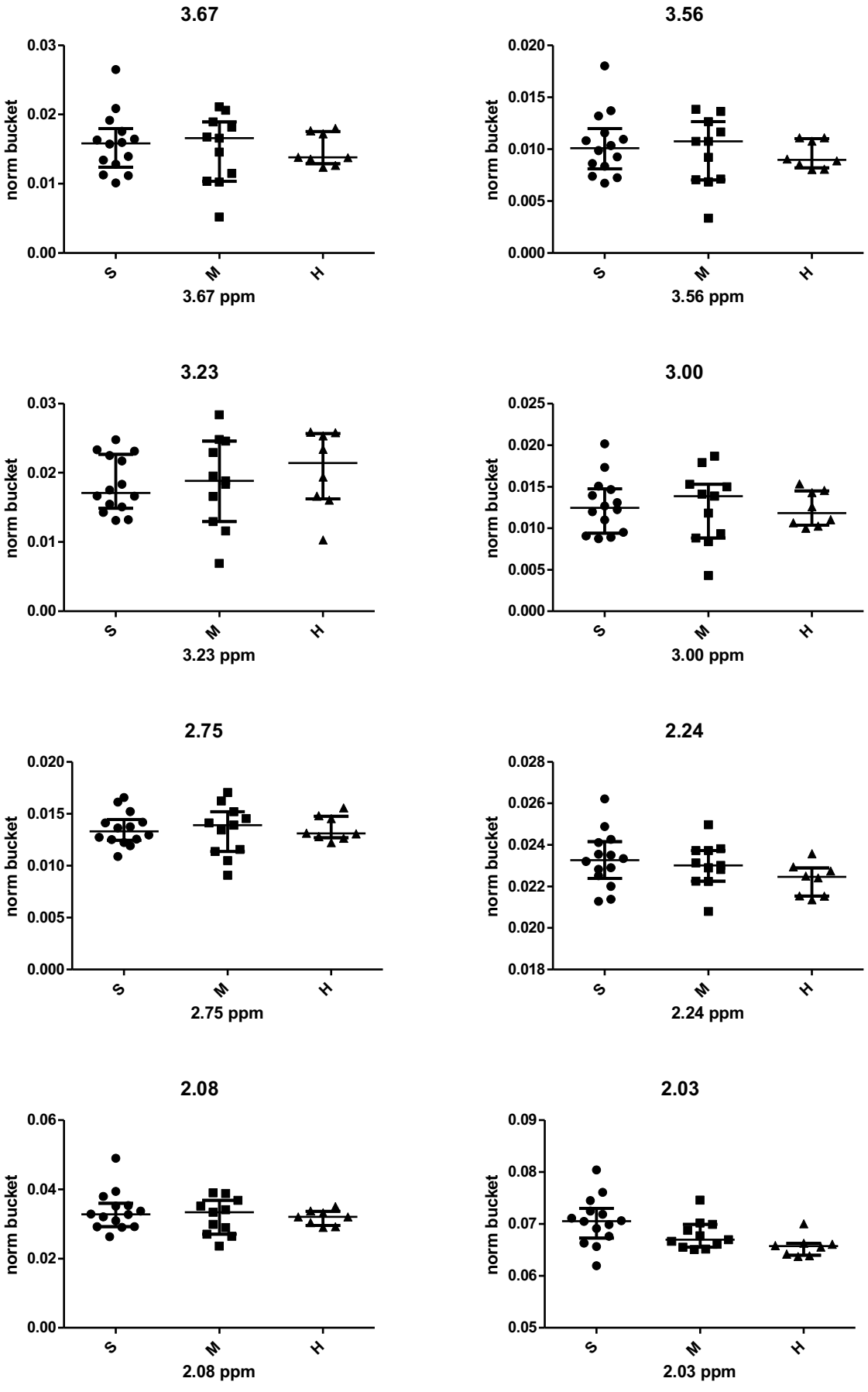
3.67
norm bucket
0.03
0.02
0.01
0.00
S
M
H
3.67 ppm
3.56
norm bucket
0.020
0.015
0.010
0.005
0.000
S
M
H
3.56 ppm
3.23
norm bucket
0.03
0.02
0.01
0.00
S
M
H
3.23 ppm
3.00
norm bucket
0.025
0.020
0.015
0.010
0.005
0.000
S
M
H
3.00 ppm
2.75
norm bucket
0.020
0.015
0.010
0.005
0.000
S
M
H
2.75 ppm
2.24
norm bucket
0.028
0.026
0.024
0.022
0.020
0.018
S
M
H
2.24 ppm
2.08
norm bucket
0.06
0.04
0.02
0.00
S
M
H
2.08 ppm
2.03
norm bucket
0.09
0.08
0.07
0.06
0.05
S
M
H
2.03 ppm

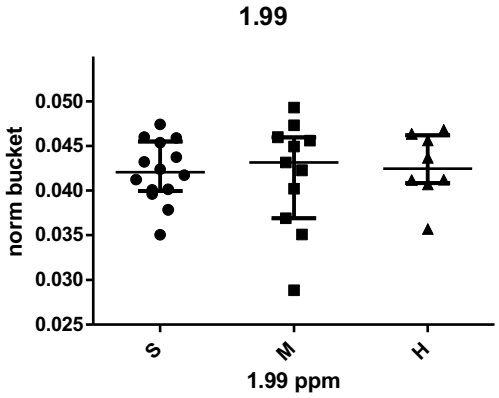
1.99
norm bucket
0.050
0.045
0.040
0.035
0.030
0.025
S
M
H
1.99 ppm

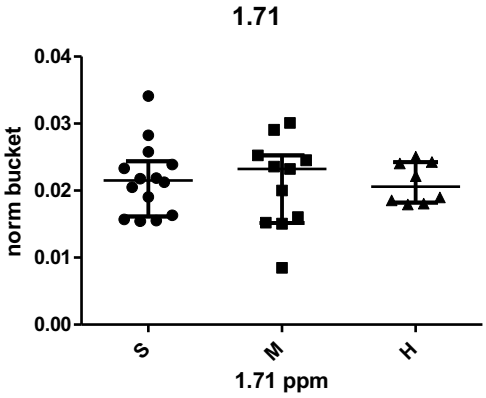
1.71
norm bucket
0.04
0.03
0.02
0.01
0.00
S
M
H
1.71 ppm

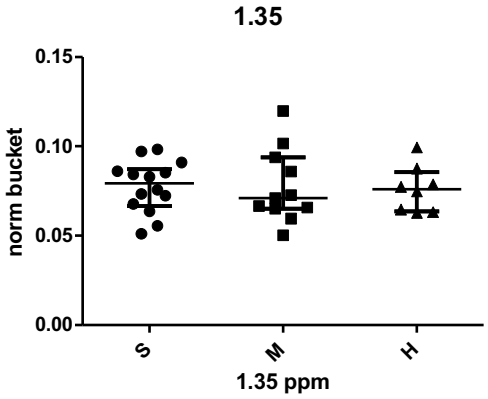
1.35
norm bucket
0.15
0.10
0.05
0.00
S
M
H
1.35 ppm

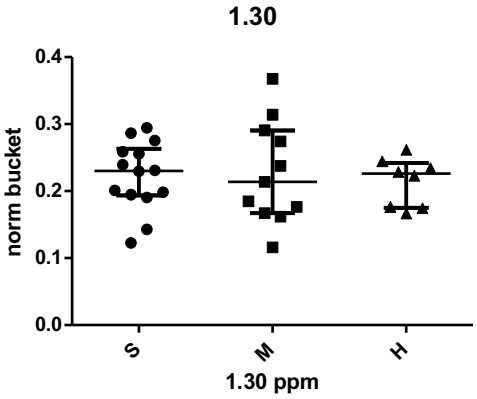
1.30
norm bucket
0.4
0.3
0.2
0.1
0.0
S
M
H
1.30 ppm

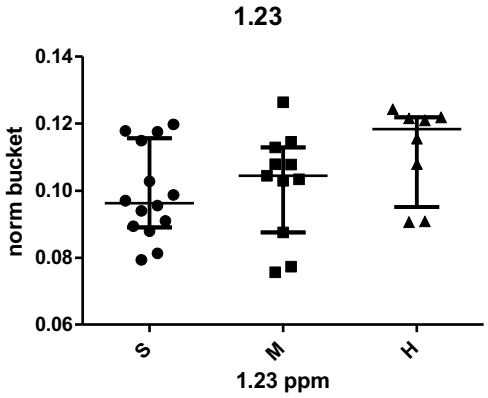
1.23
norm bucket
0.14
0.12
0.10
0.08
0.06
S
M
H
1.23 ppm

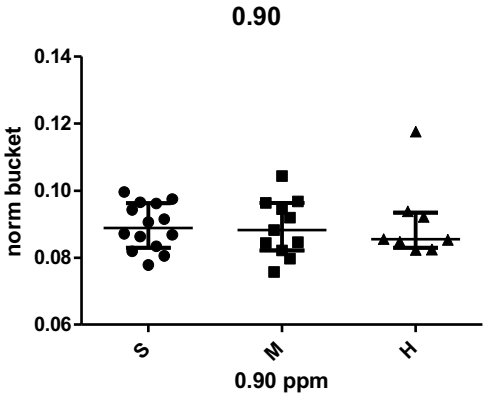
0.90
norm bucket
0.14
0.12
0.10
0.08
0.06
S
M
H
0.90 ppm

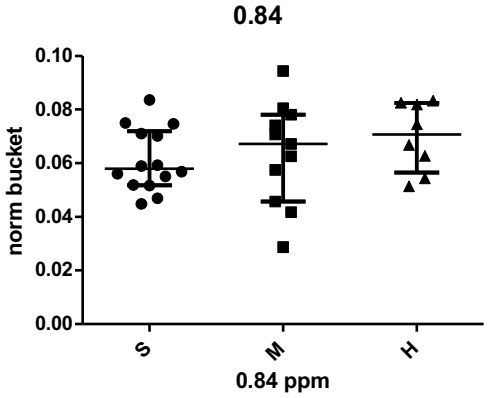
0.84
norm bucket
0.10
0.08
0.06
0.04
0.02
0.00
S
M
H
0.84 ppm

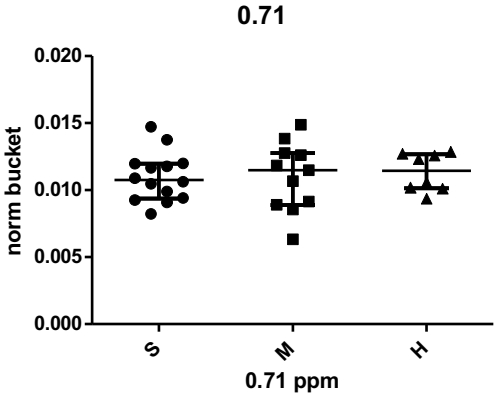
0.71
norm bucket
0.020
0.015
0.010
0.005
0.000
S
M
H
0.71 ppm

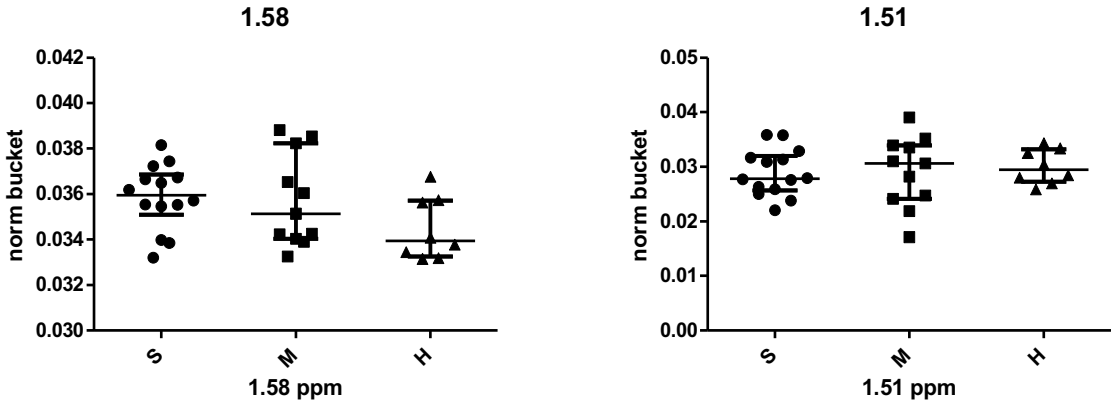

Supplementary figure 4.3: Metabolomic profile of saline diluted serum using diffusion edited spectrum obtained from ^{1}H-NMR revealed 45 metabolites in 14 severe ME, and 11 mild/moderate ME patients and 9 HHCs.

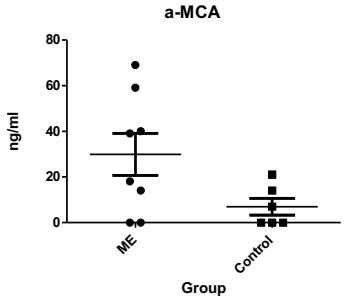
a-MCA
ng/ml
80
60
40
20
0
ME
Control
Group

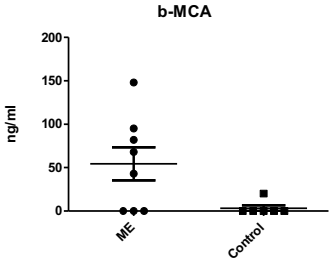
b-MCA
ng/ml
200
150
100
50
0
ME
Control

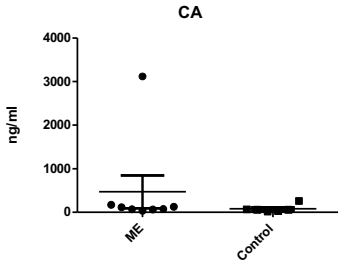
CA
ng/ml
4000
3000
2000
1000
0
ME
Control

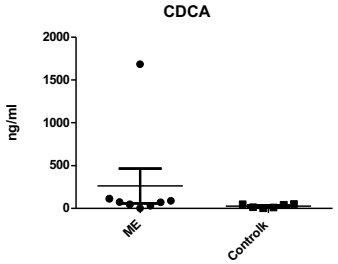
CDCA
ng/ml
2000
1500
1000
500
0
ME
Controlk

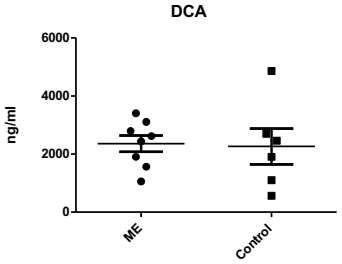
DCA
ng/ml
6000
4000
2000
0
ME
Control

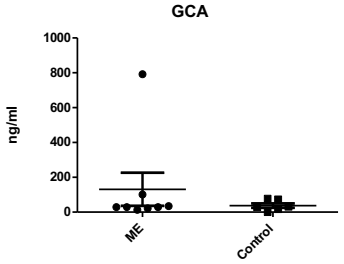
GCA
ng/ml
1000
800
600
400
200
0
ME
Control

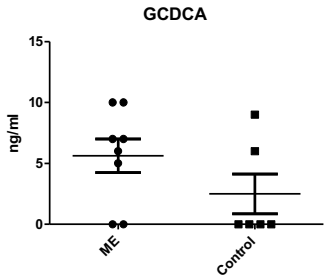
GCDCA
ng/ml
15
10
5
0
ME
Control

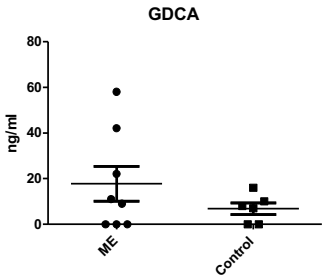
GDCA
ng/ml
80
60
40
20
0
ME
Control

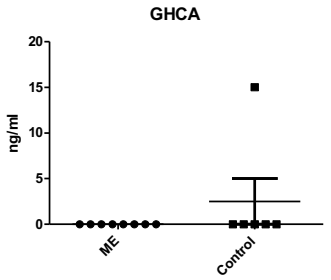
GHCA
ng/ml
20
15
10
5
0
ME
Control

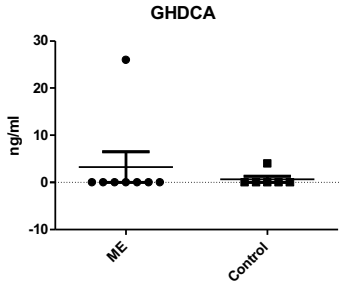
GHDCA
ng/ml
30
20
10
0
-10
ME
Control

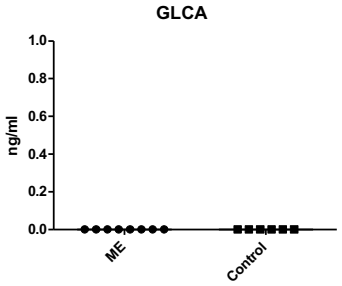
GLCA
ng/ml
1.0
0.8
0.6
0.4
0.2
0.0
ME
Control

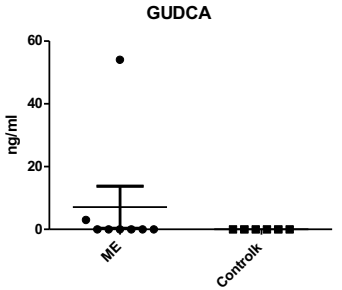
GUDCA
ng/ml
60
40
20
0
ME
Controlk

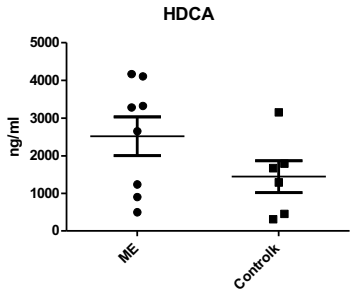
HDCA
ng/ml
5000
4000
3000
2000
1000
0
ME
Controlk

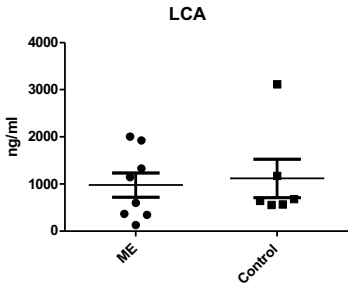
LCA
ng/ml
4000
3000
2000
1000
0
ME
Control

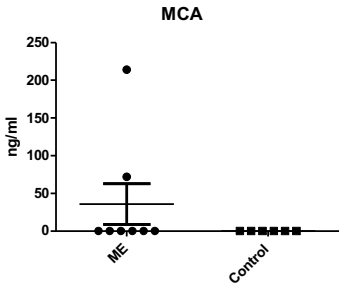
MCA
ng/ml
250
200
150
100
50
0
ME
Control

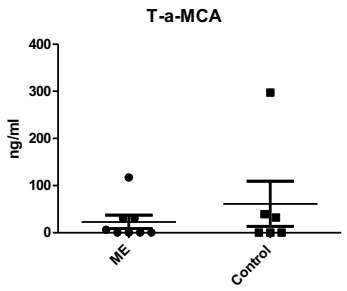
T-a-MCA
ng/ml
400
300
200
100
0
ME
Control

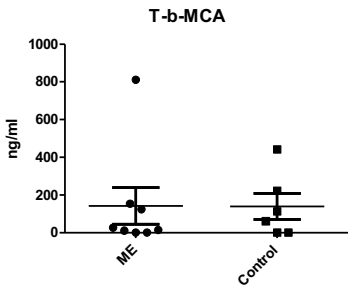
T-b-MCA
ng/ml
1000
800
600
400
200
0
ME
Control

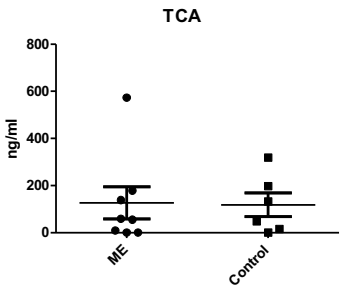
TCA
ng/ml
800
600
400
200
0
ME
Control

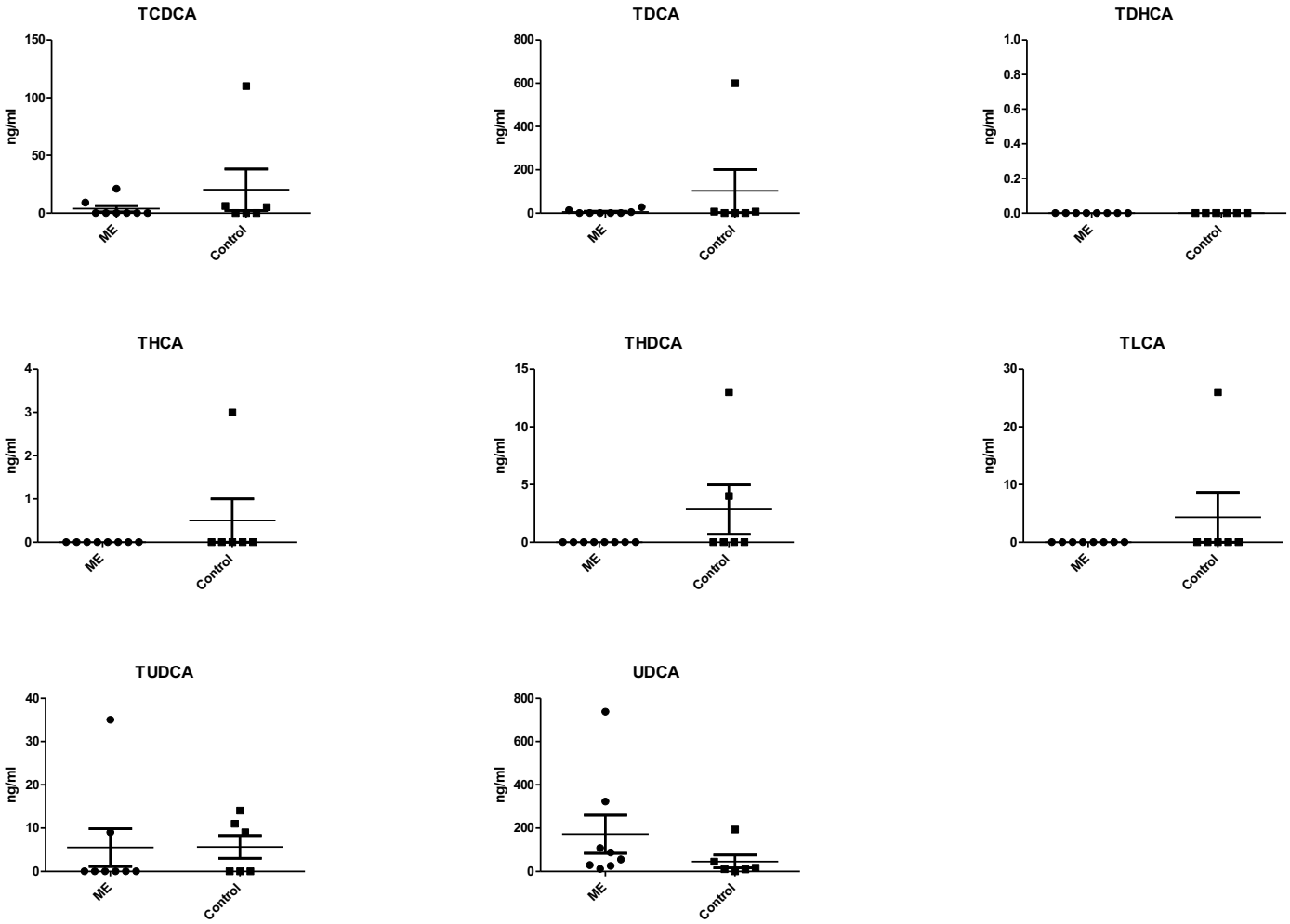

Supplementary figure 4.4: Individual bile acid concentrations in faecal water from 8 ME/CFS patients versus 6 HHCs

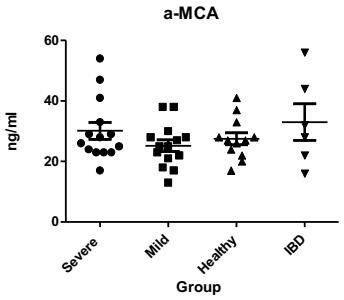
a-MCA
ng/ml
60
40
20
0
Severe
Mild
Healthy
IBD
Group

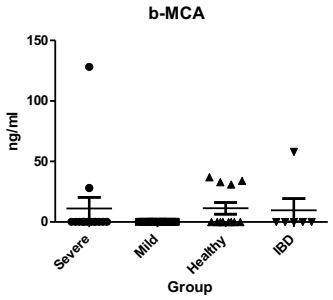
b-MCA
ng/ml
150
100
50
0
Severe
Mild
Healthy
IBD
Group

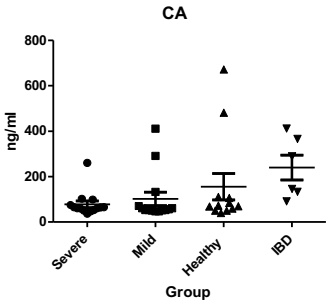
CA
ng/ml
800
600
400
200
0
Severe
Mild
Healthy
IBD
Group

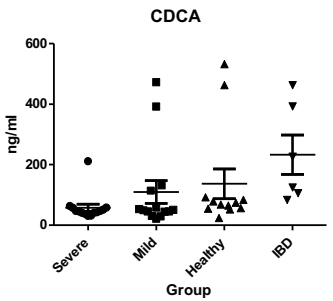
CDCA
ng/ml
600
400
200
0
Severe
Mild
Healthy
IBD
Group

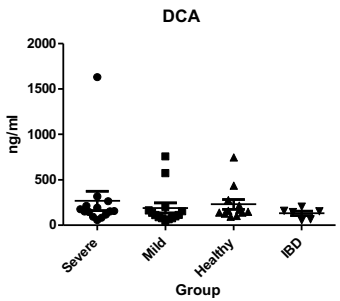
DCA
ng/ml
2000
1500
1000
500
0
Severe
Mild
Healthy
IBD
Group

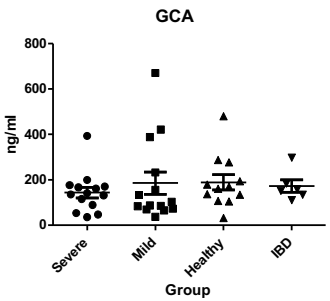
GCA
ng/ml
800
600
400
200
0
Severe
Mild
Healthy
IBD
Group

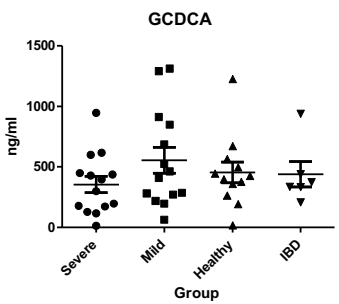
GCDCA
ng/ml
1500
1000
500
0
Severe
Mild
Healthy
IBD
Group

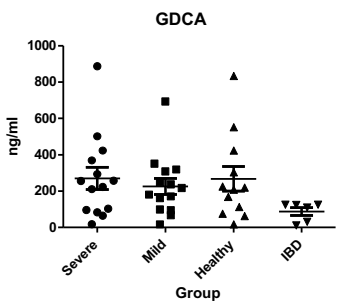
GDCA
ng/ml
1000
800
600
400
200
0
Severe
Mild
Healthy
IBD
Group

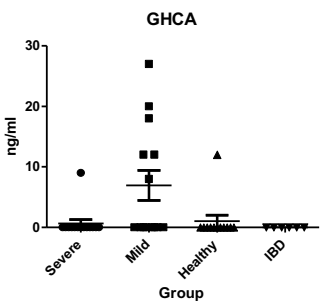
GHCA
ng/ml
30
20
10
0
Severe
Mild
Healthy
IBD
Group

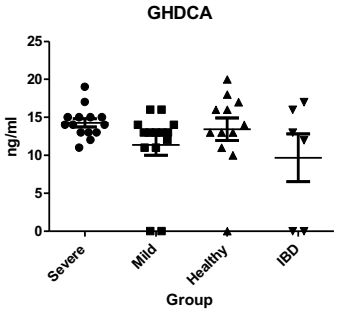
GHDCA
ng/ml
25
20
15
10
5
0
Severe
Mild
Healthy
IBD
Group

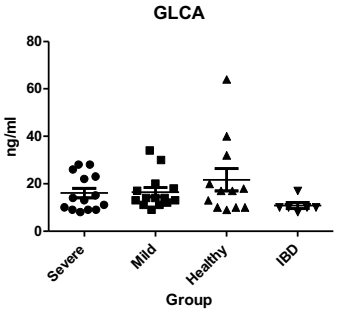
GLCA
ng/ml
80
60
40
20
0
Severe
Mild
Healthy
IBD
Group

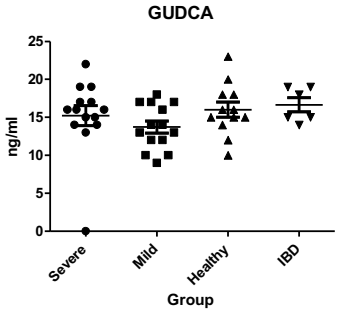
GUDCA
ng/ml
25
20
15
10
5
0
Severe
Mild
Healthy
IBD
Group

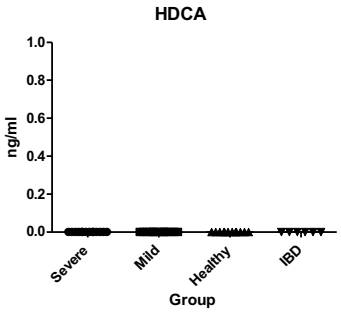
HDCA
ng/ml
1.0
0.8
0.6
0.4
0.2
0.0
Severe
Mild
Healthy
IBD
Group

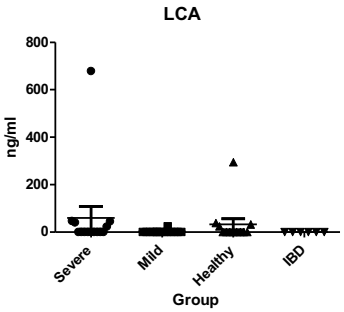
LCA
ng/ml
800
600
400
200
0
Severe
Mild
Healthy
IBD
Group

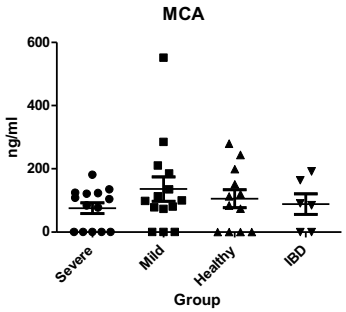
MCA
ng/ml
600
400
200
0
Severe
Mild
Healthy
IBD
Group

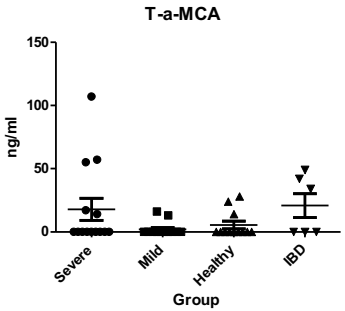
T-a-MCA
ng/ml
150
100
50
0
Severe
Mild
Healthy
IBD
Group

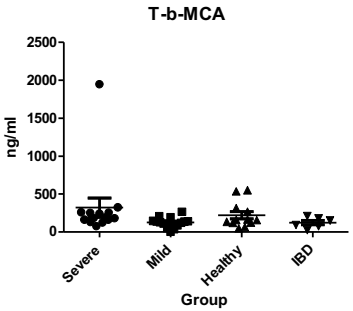
T-b-MCA
ng/ml
2500
2000
1500
1000
500
0
Severe
Mild
Healthy
IBD
Group

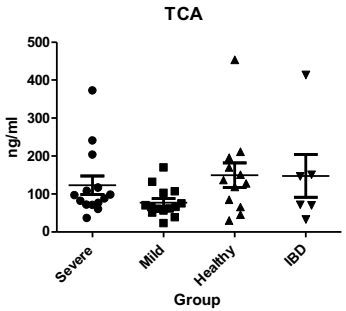
TCA
ng/ml
500
400
300
200
100
0
Severe
Mild
Healthy
IBD
Group

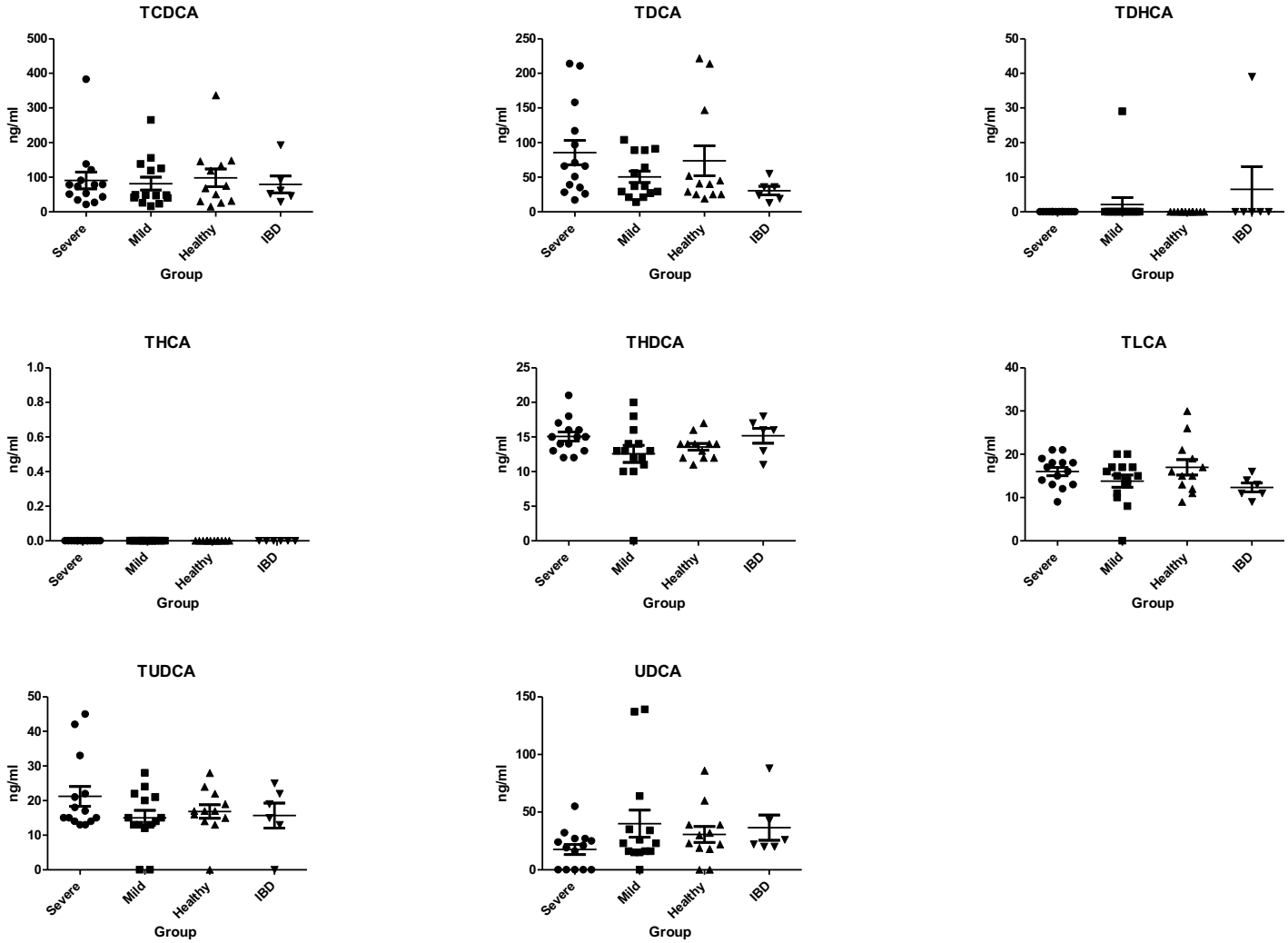

Supplementary figure 4.4: Individual bile acid concentrations in serum of 14 severe ME, 14 mild/moderate ME/CFS, 10 house-hold control & 6 IBD samples

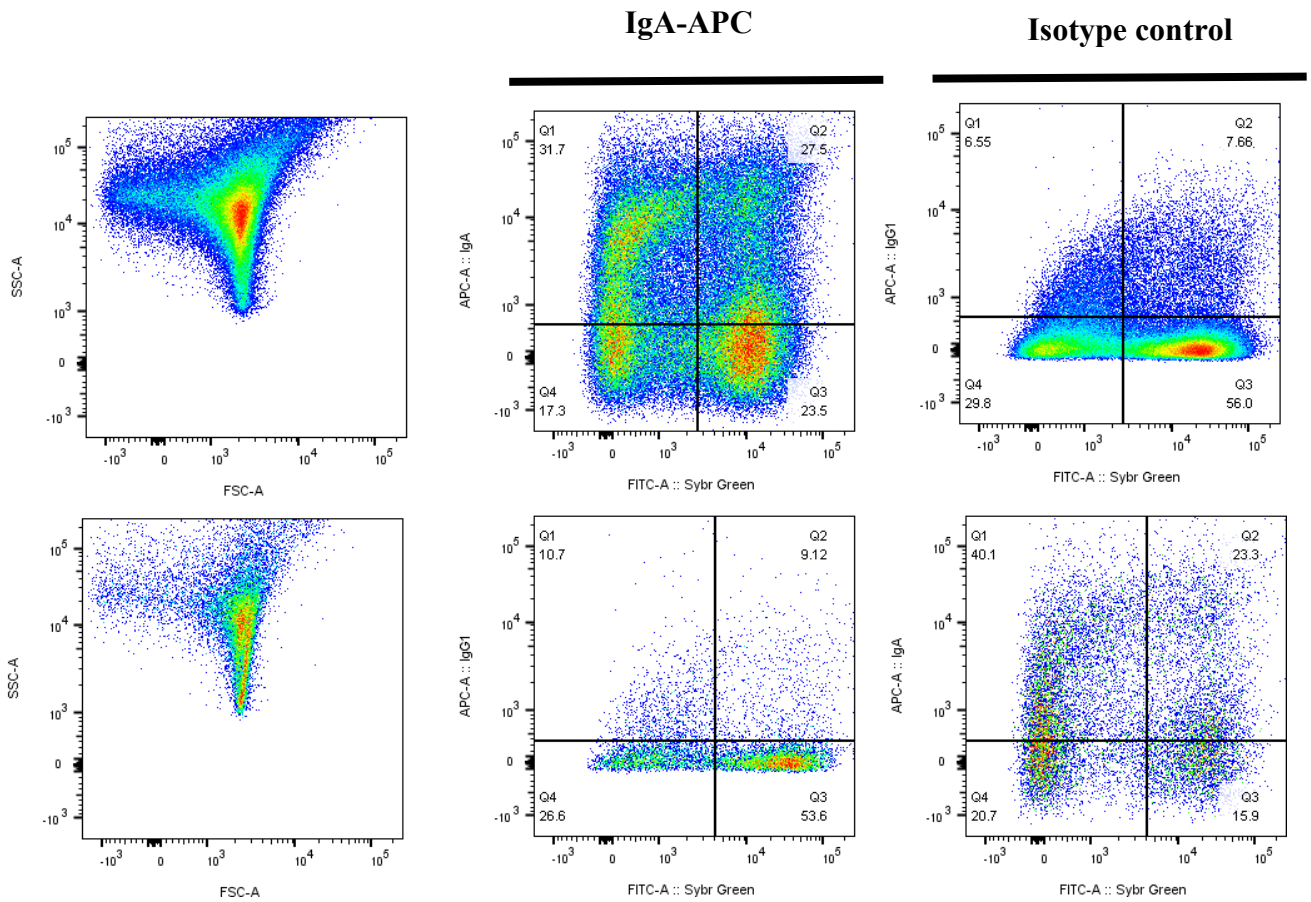

Supplementary figure 5.1 Optimisation of faecal bacterial cell suspension for staining with Sybr green using ME patient faeces. Sybr green concentration (1:10,000) stained 1:100 (top row) versus 1:1000 (bottom row) dilution of faecal bacteria in PBS.

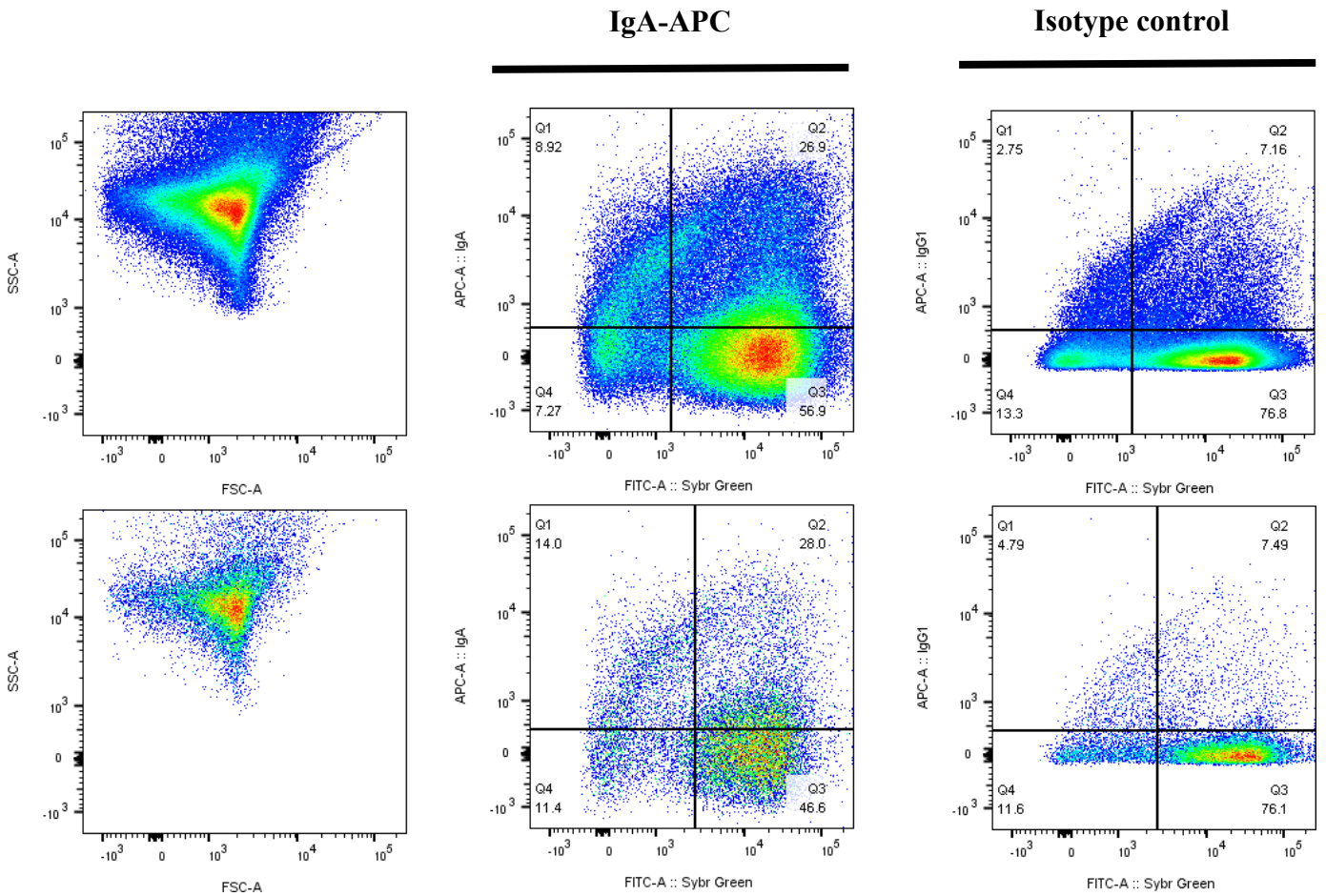

Supplementary figure 5.2 Optimisation of faecal bacterial cell suspension for staining with Sybr green using faeces from ME patient's household control. Sybr green concentration (1:10,000) stained 1:100 (top row) versus 1:1000 (bottom row) dilution of faecal bacteria in PBS.

Paired samples #1

Control, F (30) **12%**

ME, F (57) **20%**

IgA-APC **Isotype control**

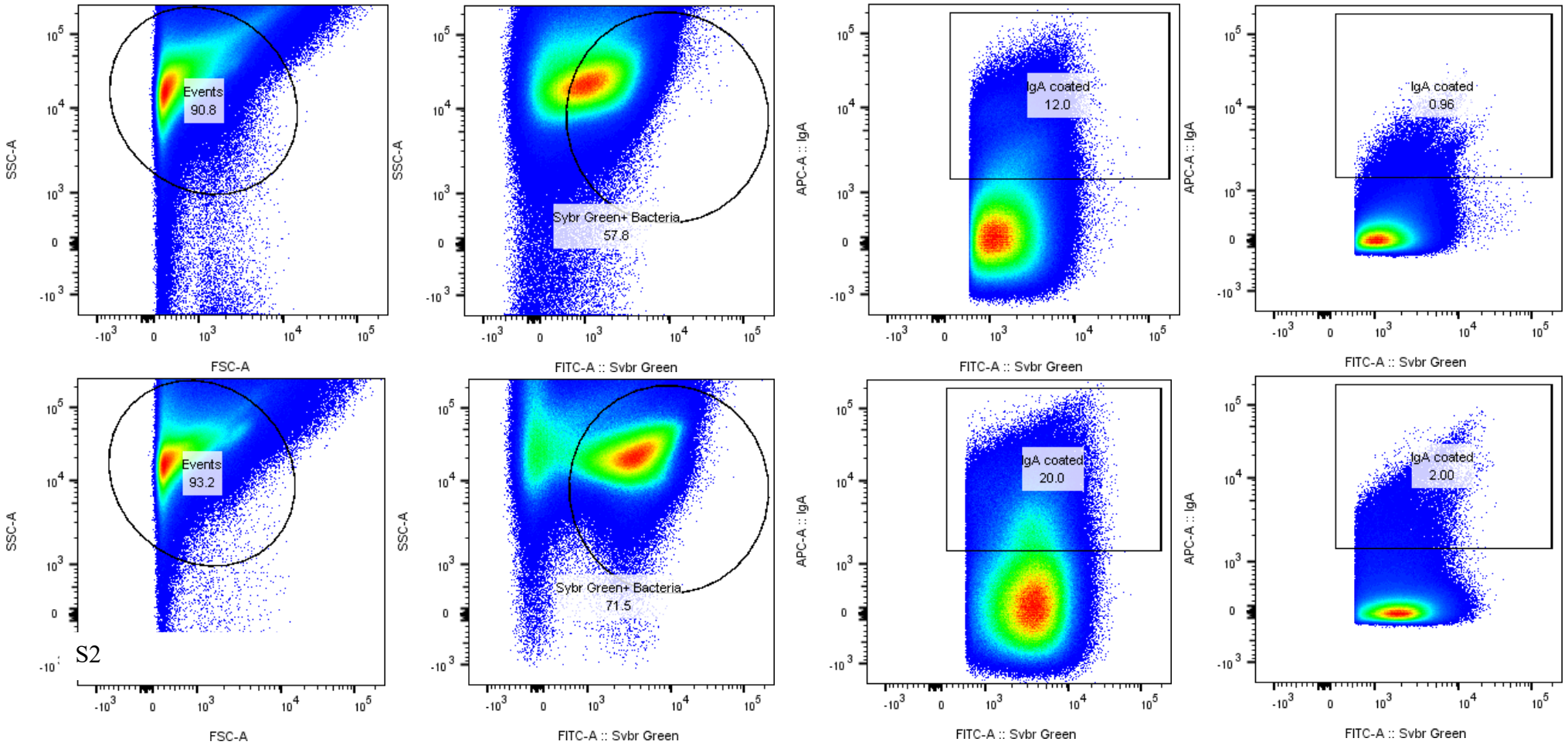

Paired Sample #3

Control, F (60)	**26.5%**
ME, F (27)	**21.5%**

IgA-APC **Isotype control**

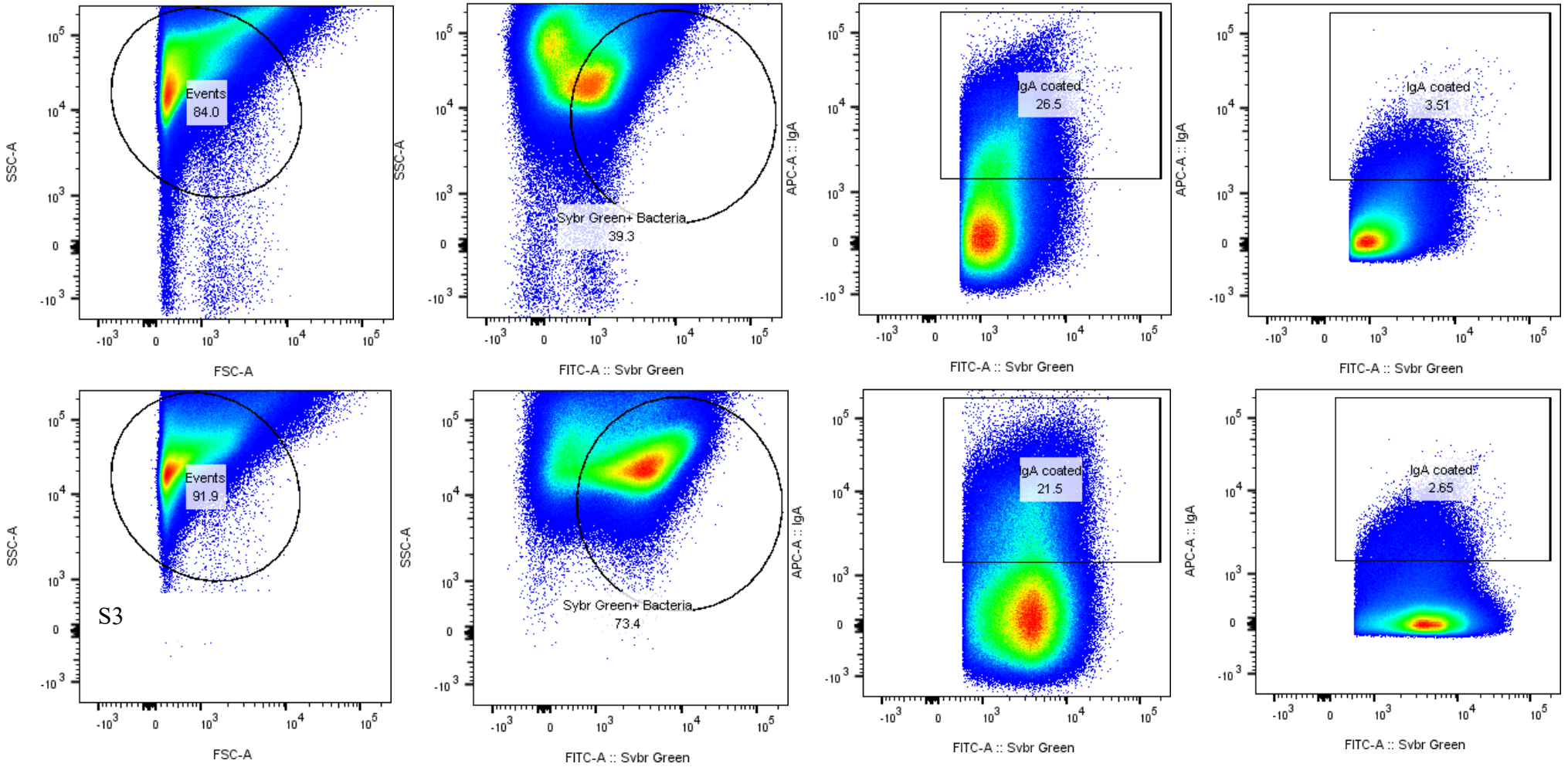

Paired samples #4

ME, F (31)	**41.2%**
Control, F (55)	**33.2%**

IgA-APC **Isotype control**

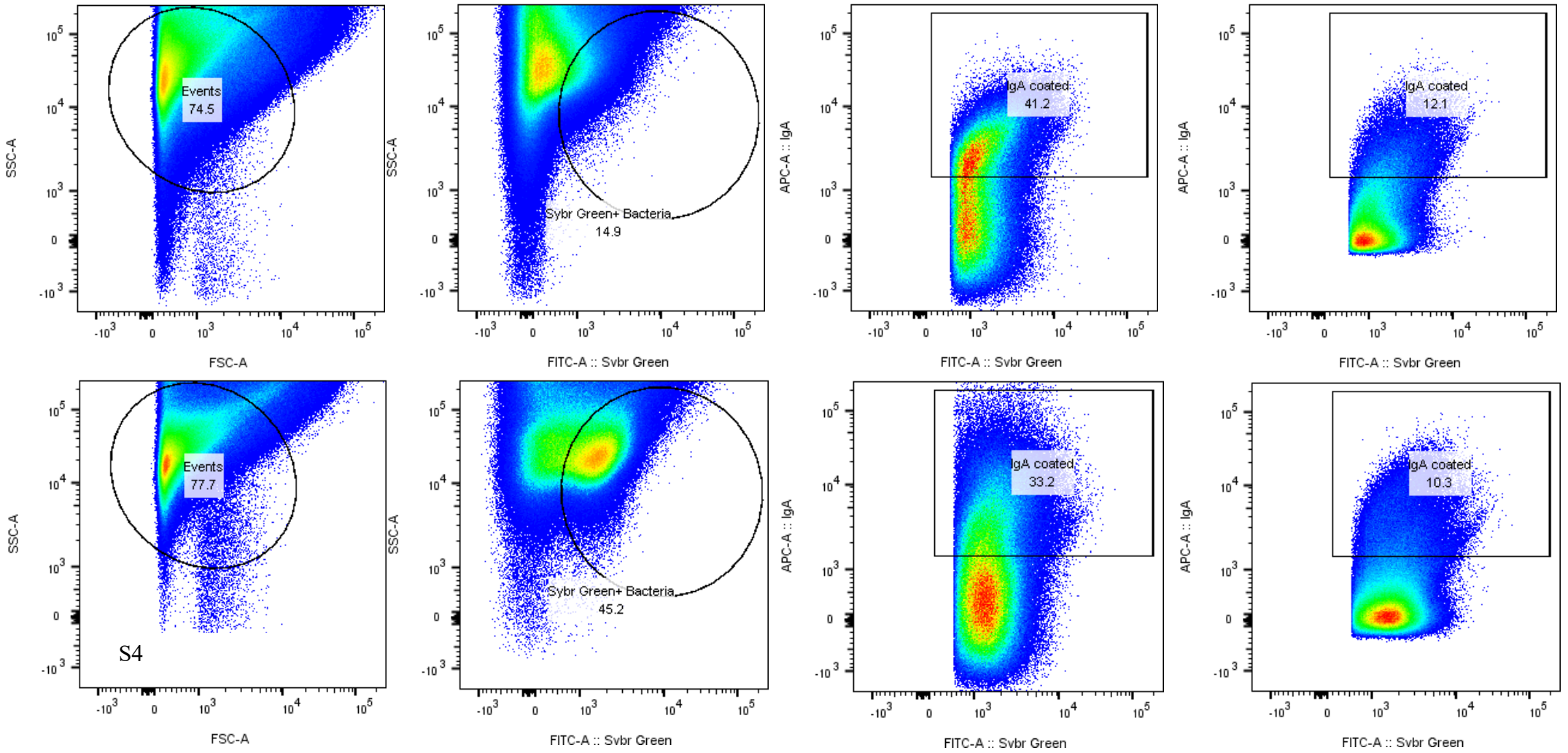

S5

Paired samples #6

Control, F (35)	**29.9%**
ME, F (33)	**16.0**

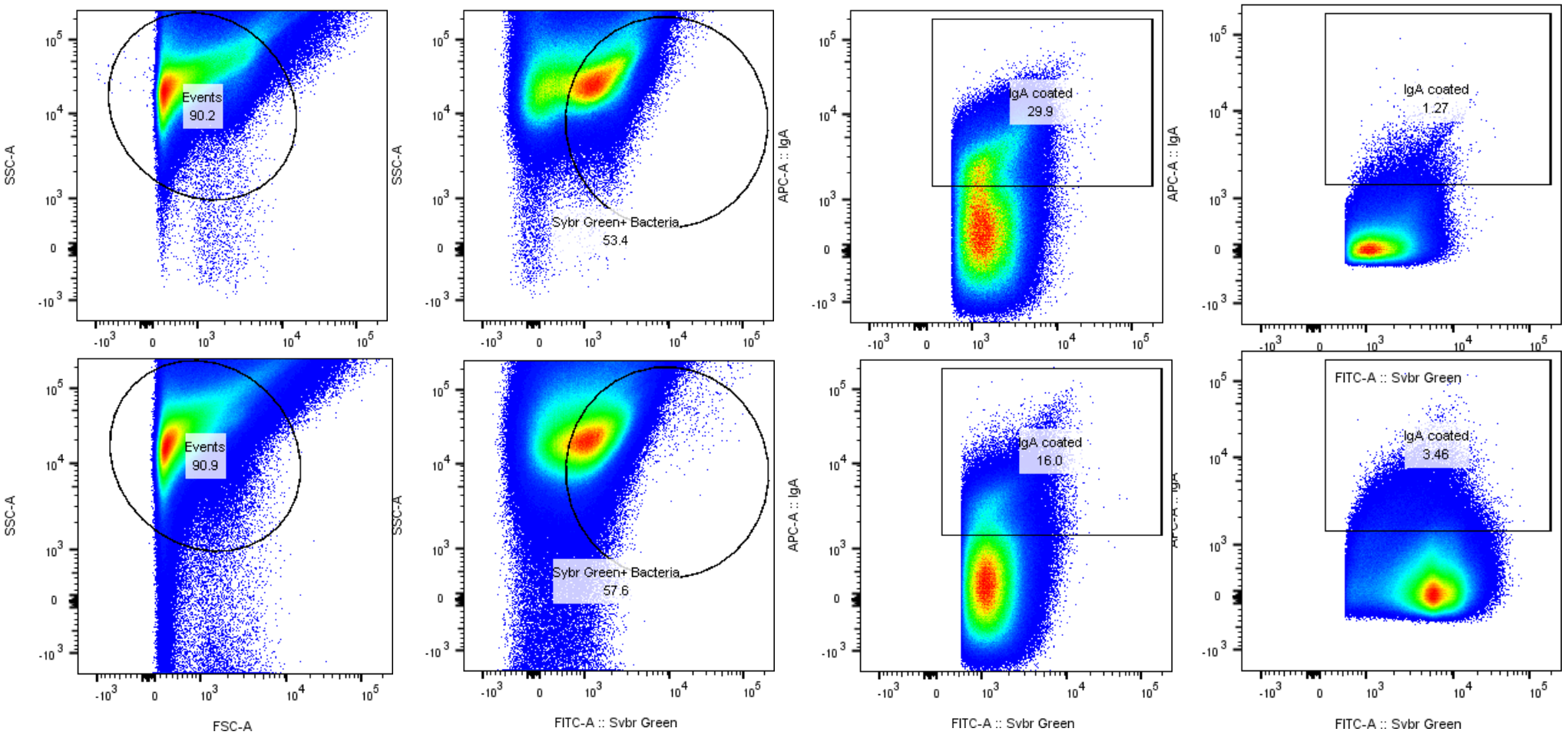

S7

Paired samples #8

Control, F (55)	**21.1%**
ME, F (18)	**29.5%**

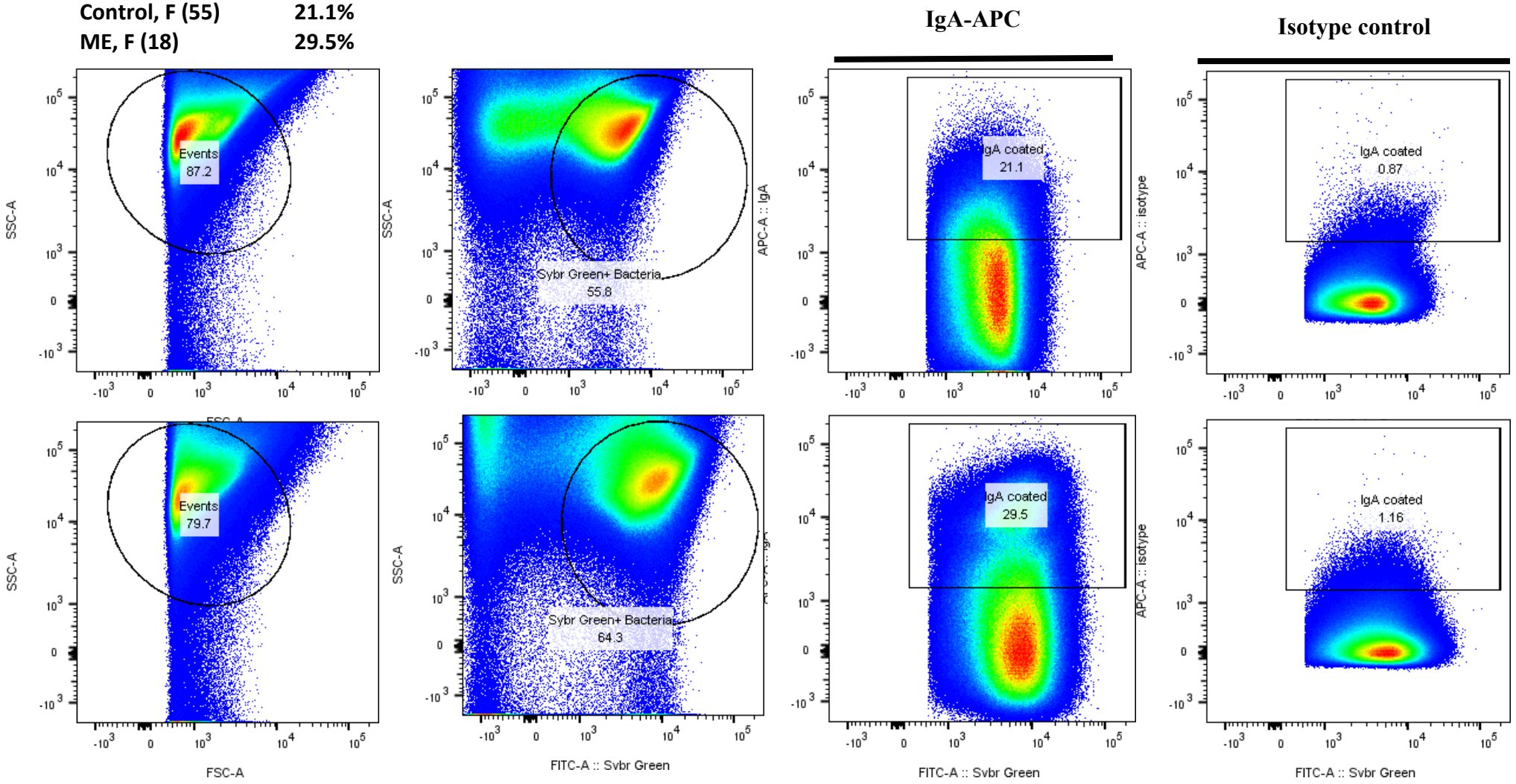

S8

Non-paired sample

15TB100 ME, F (63) **31.1%**

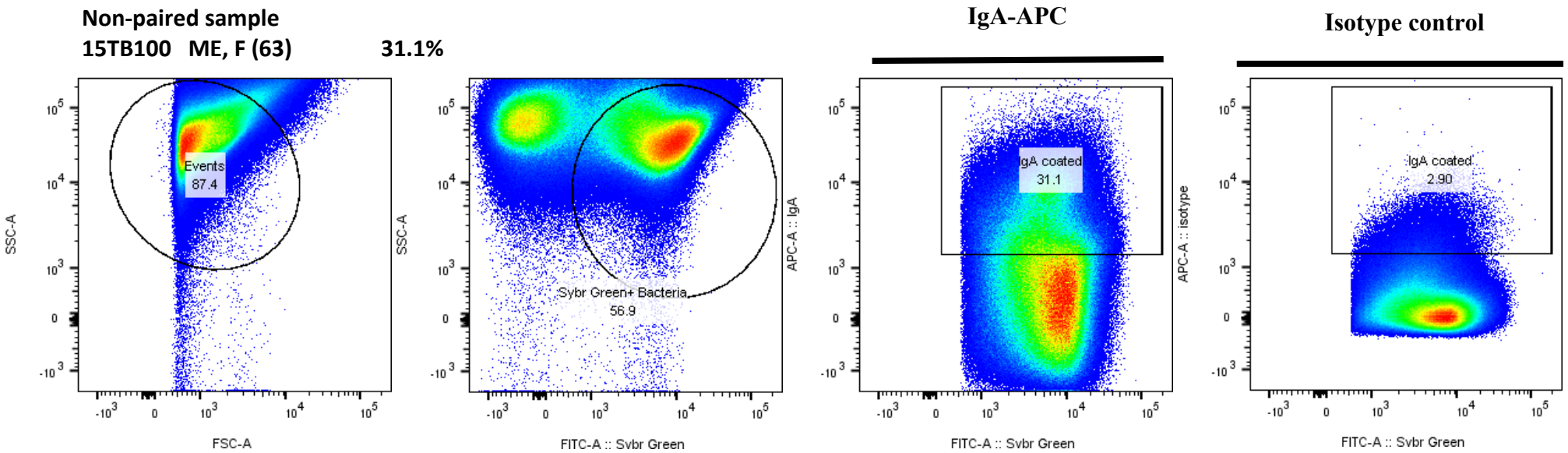

S10

15TB0096 ME, F (56) **23.7% Jones**

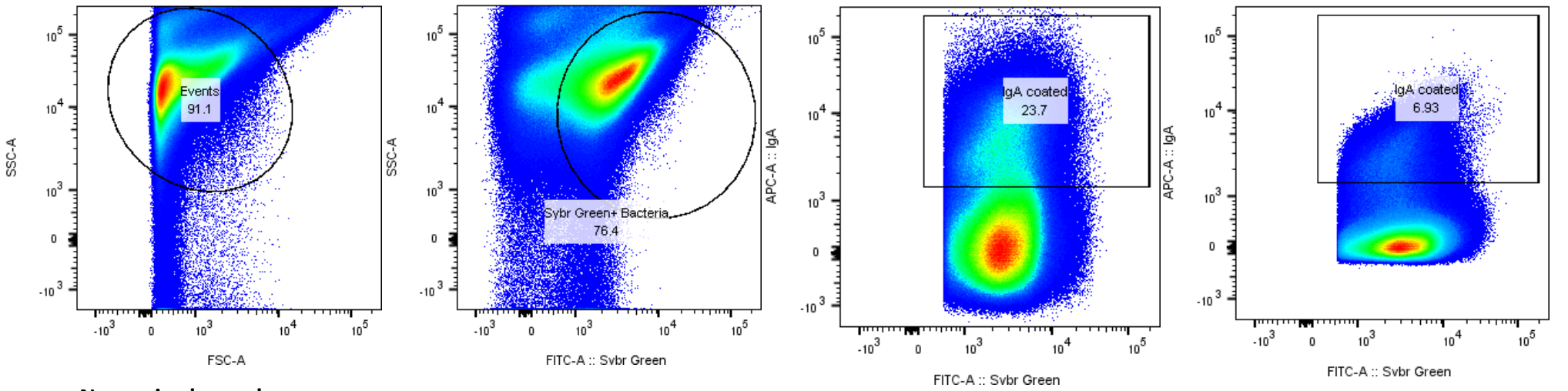

Non-paired samples

15TB0076 ME, F (31) **11.9%**

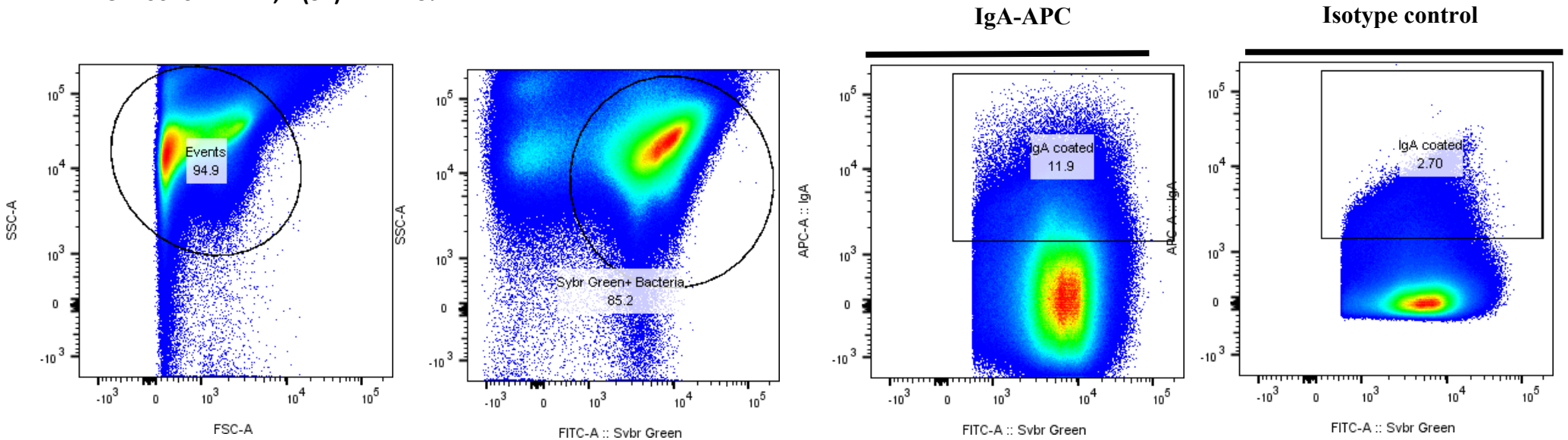

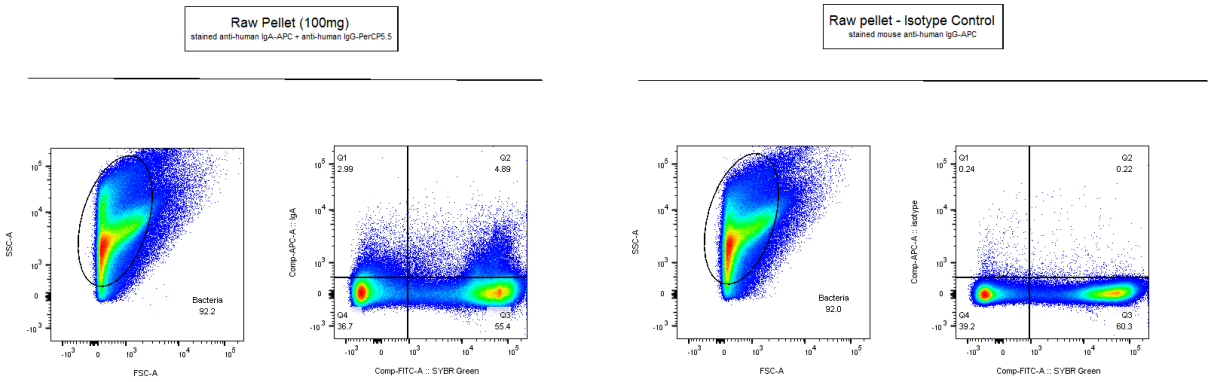

2017 Severe ME, F (37) – Paired 1

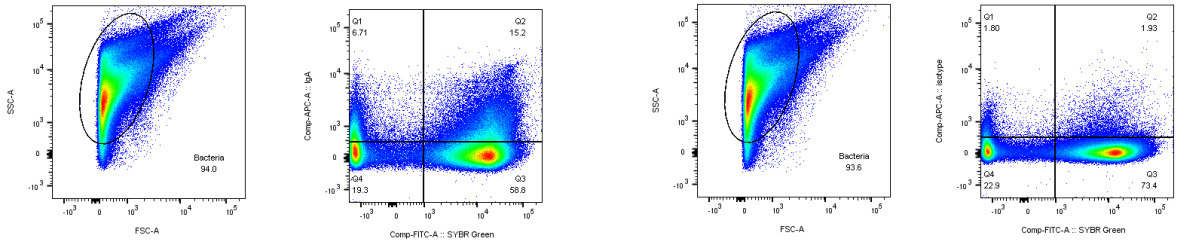

2017 House-Hold Control, F (64) – Paired 1

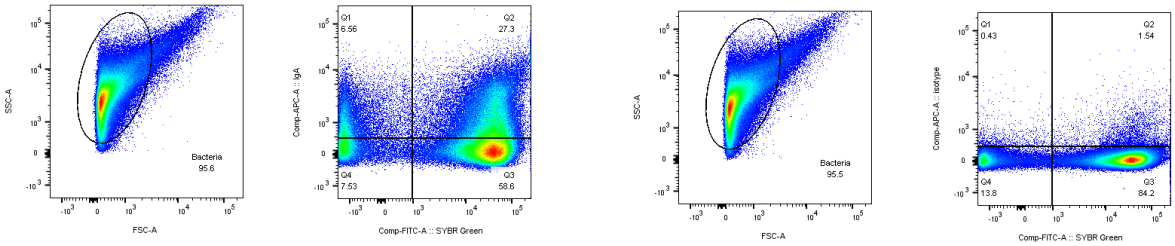

2017 Severe ME, F (27) – Paired 2

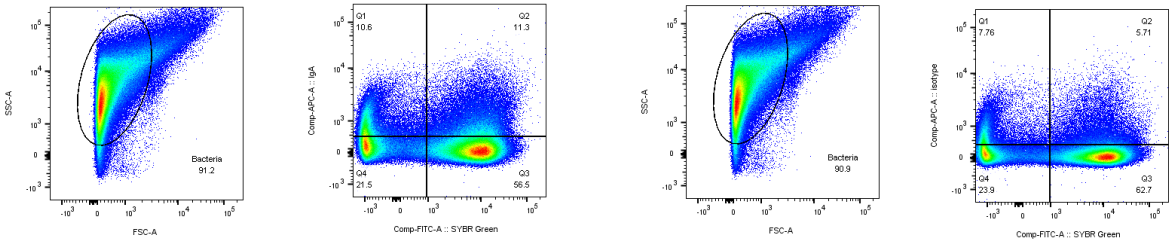

2017 House-Hold Control, F (60) – Paired 2

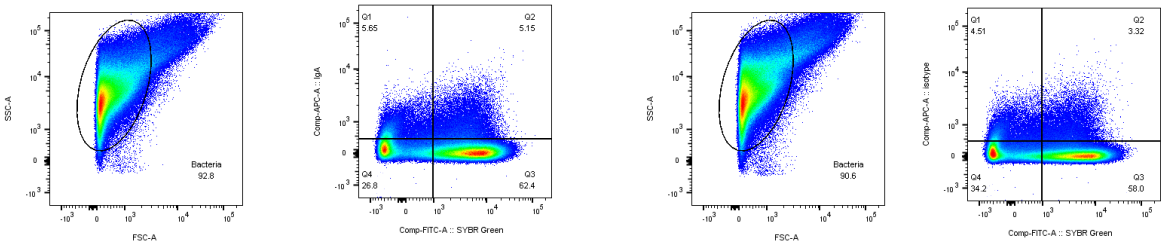

2017 Severe ME, F (63) – New, unpaired

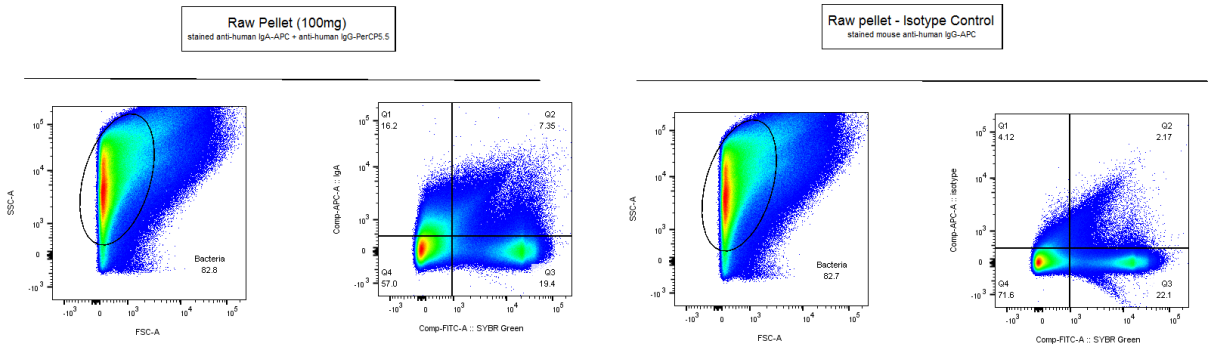

2017 Severe ME, F (21) – Paired 3

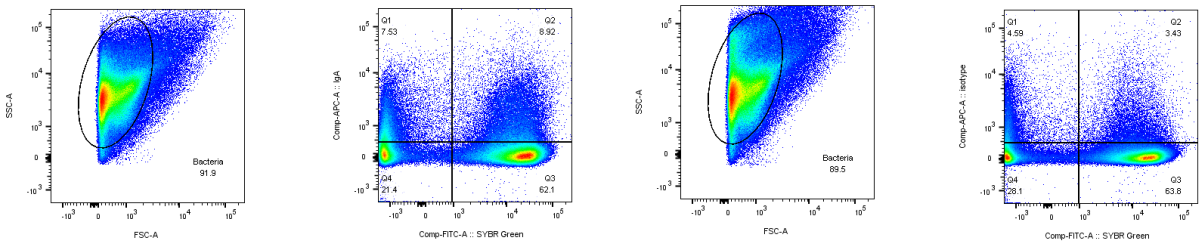

2017 House-Hold Control, F (55) – Paired 3

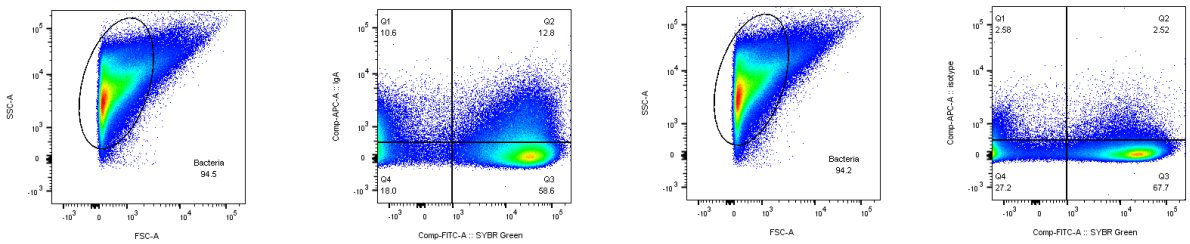

2017 Severe ME, F (58) – Paired 4

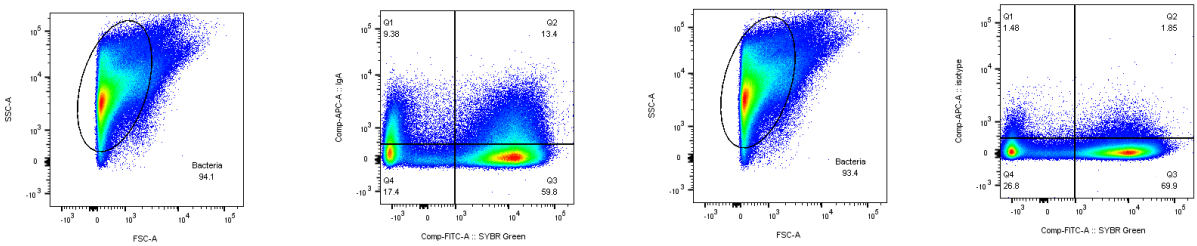

2017 House-Hold Control, M (60) – Paired 4

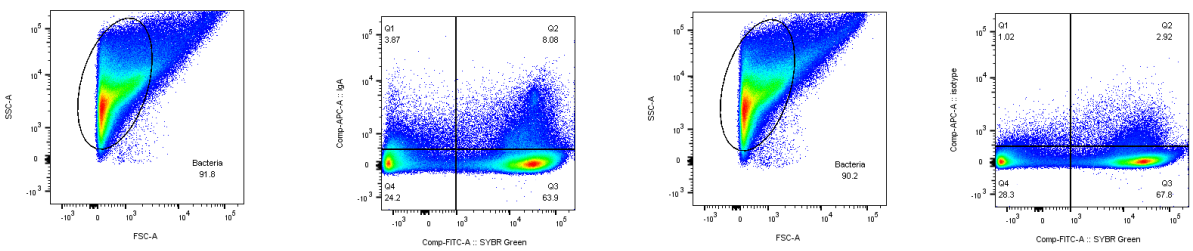

2017 Severe ME, F (56) – Unpaired

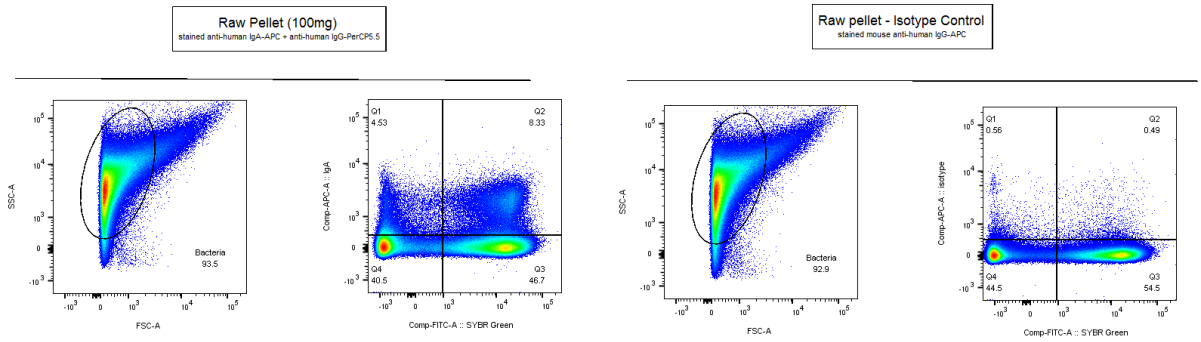

2017 Severe ME, F (63) – Unpaired

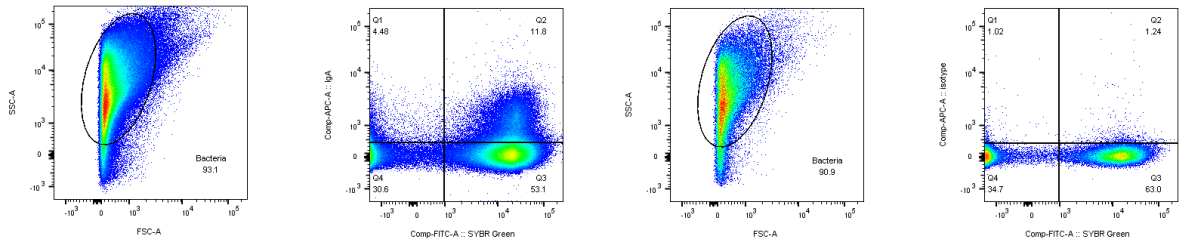

2017 Severe ME, F (18) – Paired 5

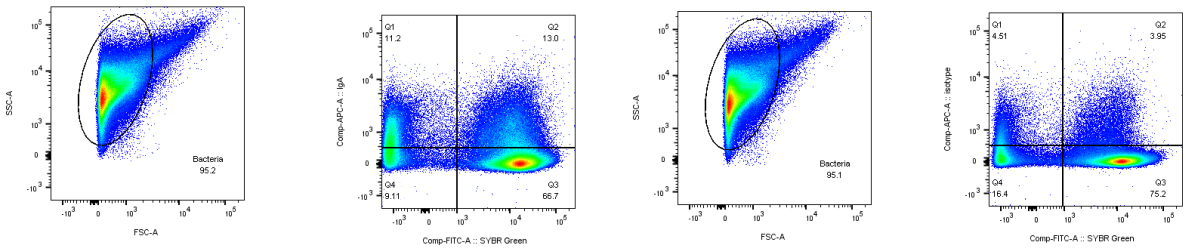

2017 House-Hold Control, F (55) – Paired 5

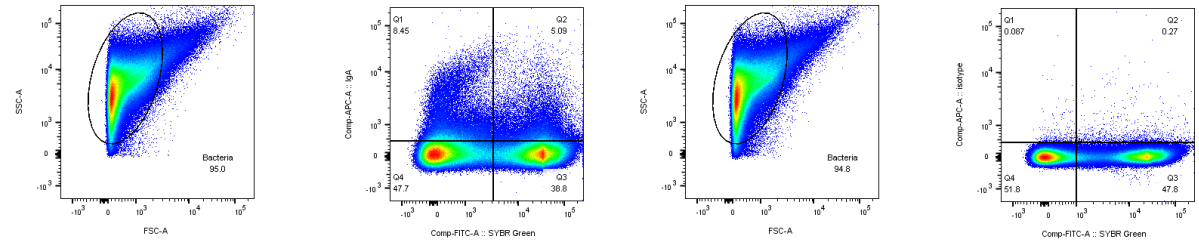

2017 Severe ME, F (38) – Paired 6

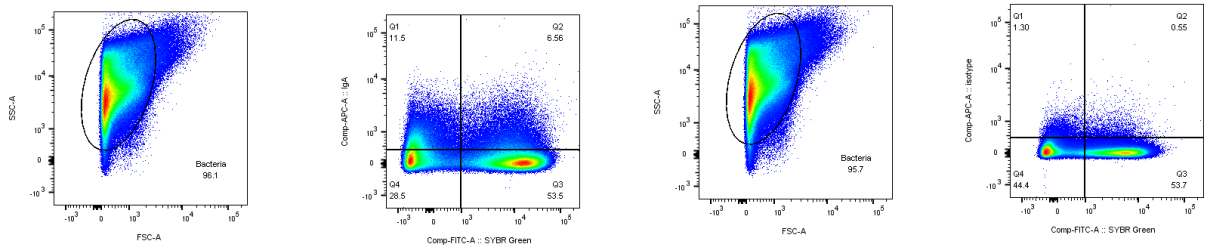

2017 House-Hold Control, F (69) – Paired 6

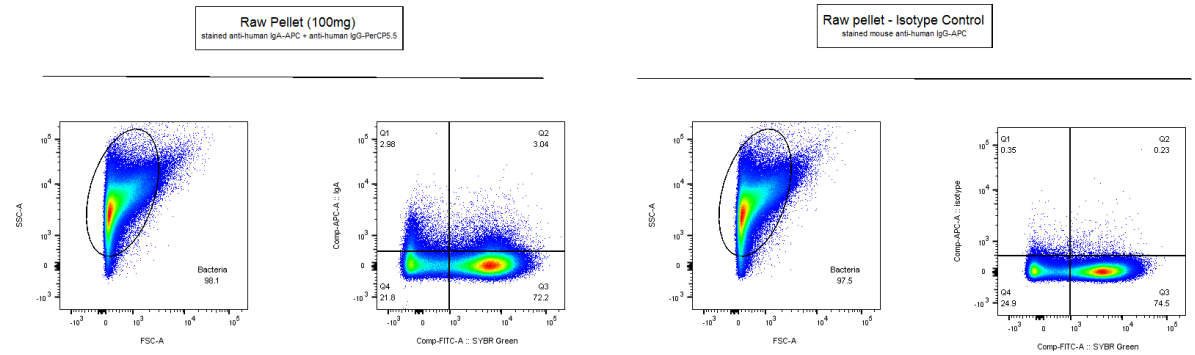

2017 Severe ME, F (44) – Paired 7

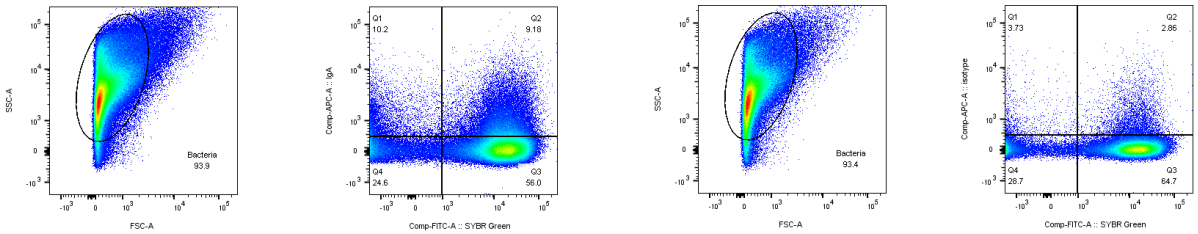

2017 Severe ME, F (61) – Unpaired

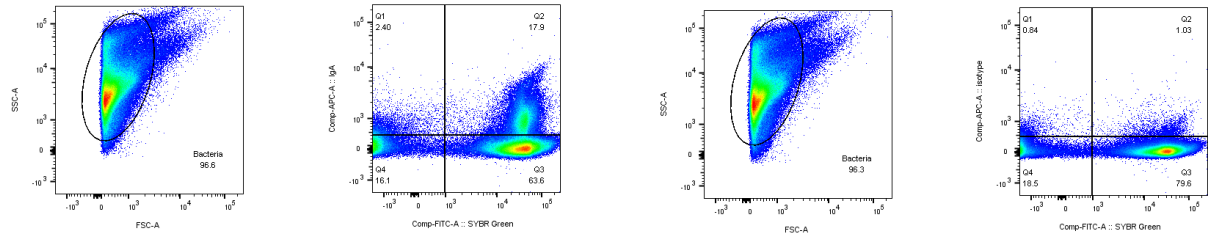

2017 Severe ME, F (40) – Unpaired

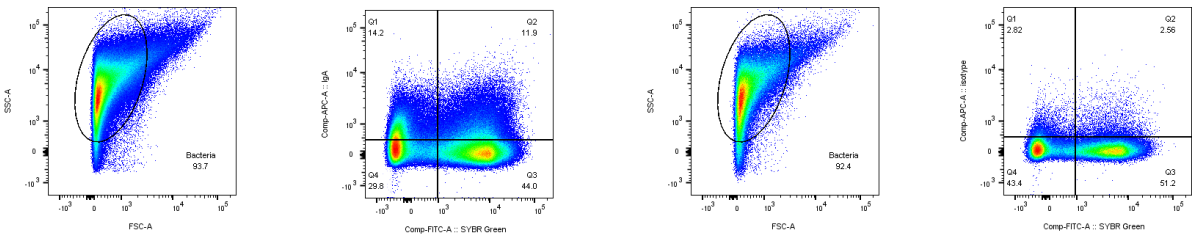

2017 Severe ME, F (70) – Paired 7

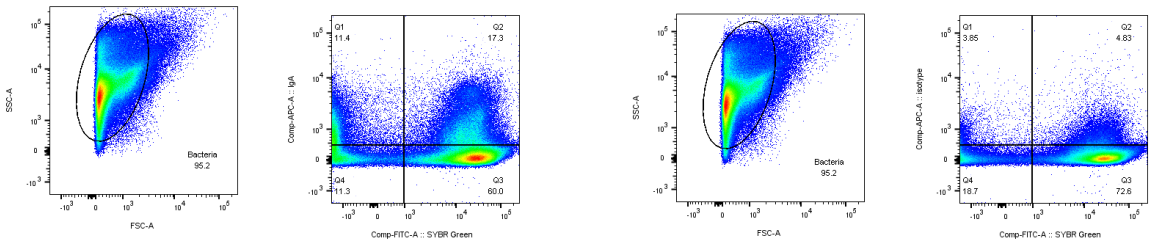

2017 Severe ME, F (54) – Unpaired

References

Abdu, F., & Albaik, M. (2016). Effect of conjugated bile salt taurodeoxycholic acid (TDCA) on mice colonic motor activity. *Periodicum Biologorum*. https://doi.org/10.18054/pb.2016.118.2.3673

Adams, R. J., Heazlewood, S. P., Gilshenan, K. S., O'Brien, M., McGuckin, M. A., & Florin, T. H. J. (2008). IgG antibodies against common gut bacteria are more diagnostic for Crohn's disease than IgG against mannan or flagellin. *American Journal of Gastroenterology*. https://doi.org/10.1111/j.1572-0241.2007.01577.x

Ait-Belgnaoui, A., Durand, H., Cartier, C., Chaumaz, G., Eutamene, H., Ferrier, L., … Theodorou, V. (2012). Prevention of gut leakiness by a probiotic treatment leads to attenuated HPA response to an acute psychological stress in rats. *Psychoneuroendocrinology*. https://doi.org/10.1016/j.psyneuen.2012.03.024

Ajouz, H., Mukherji, D., & Shamseddine, A. (2014). Secondary bile acids: An underrecognized cause of colon cancer. *World Journal of Surgical Oncology*. https://doi.org/10.1186/1477-7819-12-164

Akira, S., & Hemmi, H. (2003). Recognition of pathogen-associated molecular patterns by TLR family. *Immunology Letters*. https://doi.org/10.1016/S0165-2478(02)00228-6

Al-Asmakh, M., & Hedin, L. (2015). Microbiota and the control of blood-tissue barriers. *Tissue Barriers*. https://doi.org/10.1080/21688370.2015.1039691

Almé, B., Bremmelgaard, A., Sjövall, J., & Thomassen, P. (1977). Analysis of metabolic profiles of bile acids in urine using a lipophilic anion exchanger and computerized gas-liquid chromatorgaphy-mass spectrometry. *Journal of Lipid Research*, *18*(3), 339–362. Retrieved from http://www.ncbi.nlm.nih.gov/pubmed/864325

Anastasiou, D., Poulogiannis, G., Asara, J. M., Boxer, M. B., Jiang, J. K., Shen, M., … Cantley, L. C. (2011). Inhibition of pyruvate kinase M2 by reactive oxygen species contributes to cellular antioxidant responses. *Science*. https://doi.org/10.1126/science.1211485

Antvorskov, J. C., Josefsen, K., Engkilde, K., Funda, D. P., & Buschard, K. (2014). Dietary gluten and the development of type 1 diabetes. *Diabetologia*. https://doi.org/10.1007/s00125-014-3265-1

Arentsen, T., Qian, Y., Gkotzis, S., Femenia, T., Wang, T., Udekwu, K., … Diaz Heijtz, R. (2017). The bacterial peptidoglycan-sensing molecule Pglyrp2 modulates brain development and behavior. *Molecular Psychiatry*. https://doi.org/10.1038/mp.2016.182

Armstrong, C. W., McGregor, N. R., Lewis, D. P., Butt, H. L., & Gooley, P. R. (2015). Metabolic profiling reveals anomalous energy metabolism and oxidative stress pathways in chronic fatigue syndrome patients. *Metabolomics*, *11*(6), 1626–1639. https://doi.org/10.1007/s11306-015-0816-5

Armstrong, C. W., McGregor, N. R., Lewis, D. P., Butt, H. L., & Gooley, P. R. (2017). The association of fecal microbiota and fecal, blood serum and urine metabolites in myalgic encephalomyelitis/chronic fatigue syndrome. *Metabolomics*, *13*(1). https://doi.org/10.1007/s11306-016-1145-z

Arumugam, M., Raes, J., Pelletier, E., Le Paslier, D., Yamada, T., Mende, D. R., … Bork, P. (2011). Enterotypes of the human gut microbiome. *Nature*. https://doi.org/10.1038/nature09944

Atarashi, K., Tanoue, T., Oshima, K., Suda, W., Nagano, Y., Nishikawa, H., … Honda, K. (2013). Treginduction by a rationally selected mixture of Clostridia strains from the human microbiota. *Nature*. https://doi.org/10.1038/nature12331

Atarashi, K., Tanoue, T., Shima, T., Imaoka, A., Kuwahara, T., Momose, Y., … Honda, K. (2011). Induction of colonic regulatory T cells by indigenous Clostridium species. *Science*. https://doi.org/10.1126/science.1198469

Aviello, G., & Knaus, U. G. (2017). ROS in gastrointestinal inflammation: Rescue Or Sabotage? *British Journal of Pharmacology*, *174*(12), 1704–1718. https://doi.org/10.1111/bph.13428

Bachstetter, A. D., Van Eldik, L. J., Schmitt, F. A., Neltner, J. H., Ighodaro, E. T., Webster, S. J., … Nelson, P. T. (2015). Disease-related microglia heterogeneity in the hippocampus of Alzheimer's disease, dementia with Lewy bodies, and hippocampal sclerosis of aging. *Acta Neuropathologica Communications*. https://doi.org/10.1186/s40478-015-0209-z

Bäckhed, F., Manchester, J. K., Semenkovich, C. F., & Gordon, J. I. (2007). Mechanisms underlying the resistance to diet-induced obesity in germ-free mice. *Proceedings of the National Academy of Sciences*. https://doi.org/10.1073/pnas.0605374104

Bag, S., Saha, B., Mehta, O., Anbumani, D., Kumar, N., Dayal, M., … Das, B. (2016). An improved method for high quality metagenomics DNA extraction from human and environmental samples. *Scientific Reports*. https://doi.org/10.1038/srep26775

Bailey, M. T., & Coe, C. L. (1999). Maternal separation disrupts the integrity of the intestinal microflora in infant rhesus monkeys. *Developmental Psychobiology*. https://doi.org/10.1002/(SICI)1098-2302(199909)35:2<146::AID-DEV7>3.0.CO;2-G [pii]

Bailey, M. T., Dowd, S. E., Galley, J. D., Hufnagle, A. R., Allen, R. G., & Lyte, M. (2011). Exposure to a social stressor alters the structure of the intestinal microbiota: Implications for stressor-induced immunomodulation. *Brain, Behavior, and Immunity*. https://doi.org/10.1016/j.bbi.2010.10.023

Bajaj, J. S., Heuman, D. M., Hylemon, P. B., Sanyal, A. J., White, M. B., Monteith, P., … Gillevet, P. M. (2014). Altered profile of human gut microbiome is associated with cirrhosis and its complications. *Journal of Hepatology*. https://doi.org/10.1016/j.jhep.2013.12.019

Bajaj, J. S., Ridlon, J. M., Hylemon, P. B., Thacker, L. R., Heuman, D. M., Smith, S., … Gillevet, P. M. (2012). Linkage of gut microbiome with cognition in hepatic encephalopathy. *AJP: Gastrointestinal and Liver Physiology*. https://doi.org/10.1152/ajpgi.00190.2011

Balbo, M., Leproult, R., & Van Cauter, E. (2010). Impact of Sleep and Its Disturbances on Hypothalamo-Pituitary-Adrenal Axis Activity. *International Journal of Endocrinology*. https://doi.org/10.1155/2010/759234

Bansal, A. S. (2016). Investigating unexplained fatigue in general practice with a particular focus on CFS/ME. *BMC Family Practice*, *17*(1), 81. https://doi.org/10.1186/s12875-016-0493-0

Baran, K., Dunstone, M., Chia, J., Ciccone, A., Browne, K. A., Clarke, C. J. P., … Trapani, J. A. (2009). The Molecular Basis for Perforin Oligomerization and Transmembrane Pore Assembly. *Immunity*. https://doi.org/10.1016/j.immuni.2009.03.016

Barr, T. A., Shen, P., Brown, S., Lampropoulou, V., Roch, T., Lawrie, S., … Gray, D. (2012). B cell depletion therapy ameliorates autoimmune disease through ablation of IL-6–producing B cells. *The Journal of Experimental Medicine*. https://doi.org/10.1084/jem.20111675

Barrett, E., Ross, R. P., O'Toole, P. W., Fitzgerald, G. F., & Stanton, C. (2012). γ-Aminobutyric acid production by culturable bacteria from the human intestine. *Journal of Applied Microbiology*. https://doi.org/10.1111/j.1365-2672.2012.05344.x

Baümler, A. J., & Sperandio, V. (2016). Interactions between the microbiota and pathogenic bacteria in the gut. *Nature*. https://doi.org/10.1038/nature18849

Beard, G. (1869). Neurasthenia, or nervous exhaustion. *The Boston Medical and Surgical Journal*, 217–221.

Belenguer, A., Duncan, S. H., Holtrop, G., Anderson, S. E., Lobley, G. E., & Flint, H. J. (2007). Impact of pH on lactate formation and utilization by human fecal microbial

communities. *Applied and Environmental Microbiology*, *73*(20), 6526–6533. https://doi.org/10.1128/AEM.00508-07

Bellavance, M. A., & Rivest, S. (2014). The HPA - immune axis and the immunomodulatory actions of glucocorticoids in the brain. *Frontiers in Immunology*. https://doi.org/10.3389/fimmu.2014.00136

Benckert, J., Schmolka, N., Kreschel, C., Zoller, M. J., Sturm, A., Wiedenmann, B., & Wardemann, H. (2011). The majority of intestinal IgA+ and IgG+ plasmablasts in the human gut are antigen-specific. *Journal of Clinical Investigation*. https://doi.org/10.1172/JCI44447

Benor, S., Russell, G. H., Silver, M., Israel, E. J., Yuan, Q., & Winter, H. S. (2010). Shortcomings of the inflammatory bowel disease Serology 7 panel. *Pediatrics*. https://doi.org/10.1542/peds.2009-1936

Bercik, P., Denou, E., Collins, J., Jackson, W., Lu, J., Jury, J., … Collins, S. M. (2011). The intestinal microbiota affect central levels of brain-derived neurotropic factor and behavior in mice. *Gastroenterology*. https://doi.org/10.1053/j.gastro.2011.04.052

Bercik, P., Park, A. J., Sinclair, D., Khoshdel, A., Lu, J., Huang, X., … Verdu, E. F. (2011). The anxiolytic effect of Bifidobacterium longum NCC3001 involves vagal pathways for gut-brain communication. *Neurogastroenterology and Motility*. https://doi.org/10.1111/j.1365-2982.2011.01796.x

Berkowska, M. A., Schickel, J. N., Grosserichter-Wagener, C., de Ridder, D., Ng, Y. S., van Dongen, J. J., … van Zelm, M. C. (2015). Circulating Human CD27-IgA+ Memory B Cells Recognize Bacteria with Polyreactive Igs. *J Immunol*. https://doi.org/10.4049/jimmunol.1402708

Biagi, E., Nylund, L., Candela, M., Ostan, R., Bucci, L., Pini, E., … de Vos, W. (2010). Through ageing, and beyond: Gut microbiota and inflammatory status in seniors and centenarians. *PLoS ONE*. https://doi.org/10.1371/journal.pone.0010667

Biesmans, S., Meert, T. F., Bouwknecht, J. A., Acton, P. D., Davoodi, N., De Haes, P., … Nuydens, R. (2013). Systemic immune activation leads to neuroinflammation and sickness behavior in mice. *Mediators of Inflammation*. https://doi.org/10.1155/2013/271359

Bilbo, S. D. (2005). Neonatal Infection-Induced Memory Impairment after Lipopolysaccharide in Adulthood Is Prevented via Caspase-1 Inhibition. *Journal of Neuroscience*. https://doi.org/10.1523/JNEUROSCI.1748-05.2005

Bishu, S., Madhavan, D., Perez, P., Civitello, L., Liu, S., Fessler, M., … Pao, M. (2009). CD40 Ligand Deficiency: Neurologic Sequelae With Radiographic Correlation. *Pediatric Neurology*. https://doi.org/10.1016/j.pediatrneurol.2009.07.003

Blease, C., & Geraghty, K. J. (2018). Are ME/CFS Patient Organizations ``Militant''? *Journal of Bioethical Inquiry*. https://doi.org/10.1007/s11673-018-9866-5

Blomberg, J., Gottfries, C. G., Elfaitouri, A., Rizwan, M., & Rosén, A. (2018). Infection elicited autoimmunity and Myalgic encephalomyelitis/chronic fatigue syndrome: An explanatory model. *Frontiers in Immunology*, *9*(FEB). https://doi.org/10.3389/fimmu.2018.00229

Blundell, S., Ray, K. K., Buckland, M., & White, P. D. (2015). Chronic fatigue syndrome and circulating cytokines: A systematic review. *Brain, Behavior, and Immunity*. https://doi.org/10.1016/j.bbi.2015.07.004

Bordin, M., D'Atri, F., Guillemot, L., & Citi, S. (2004). Histone deacetylase inhibitors up-regulate the expression of tight junction proteins. *Molecular Cancer Research : MCR*.

Borody, T. J., & Khoruts, A. (2012). Fecal microbiota transplantation and emerging applications. *Nature Reviews Gastroenterology and Hepatology*. https://doi.org/10.1038/nrgastro.2011.244

Borody, T. J., Nowak, A., & Finlayson, S. (2012). The GI microbiome and its role in Chronic

Fatigue Syndrome: A summary of bacteriotherapy. *Journal of the Australasian College of Nutritional and Environmental Medicine*.

Borre, Y. E., O'Keeffe, G. W., Clarke, G., Stanton, C., Dinan, T. G., & Cryan, J. F. (2014). Microbiota and neurodevelopmental windows: implications for brain disorders. *Trends in Molecular Medicine*. https://doi.org/10.1016/j.molmed.2014.05.002

Bosi, E., Molteni, L., Radaelli, M. G., Folini, L., Fermo, I., Bazzigaluppi, E., … Paroni, R. (2006). Increased intestinal permeability precedes clinical onset of type 1 diabetes. *Diabetologia*. https://doi.org/10.1007/s00125-006-0465-3

Bouskra, D., Brézillon, C., Bérard, M., Werts, C., Varona, R., Boneca, I. G., & Eberl, G. (2008). Lymphoid tissue genesis induced by commensals through NOD1 regulates intestinal homeostasis. *Nature*. https://doi.org/10.1038/nature07450

Bowen, J., Pheby, D., Charlett, A., & McNulty, C. (2005). Chronic Fatigue Syndrome: A survey of GPs' attitudes and knowledge. *Family Practice*. https://doi.org/10.1093/fampra/cmi019

Braniste, V., Al-Asmakh, M., Kowal, C., Anuar, F., Abbaspour, A., Tóth, M., … Pettersson, S. (2014). The gut microbiota influences blood-brain barrier permeability in mice. *Science Translational Medicine*. https://doi.org/10.1126/scitranslmed.3009759

Bravo, J. A., Forsythe, P., Chew, M. V., Escaravage, E., Savignac, H. M., Dinan, T. G., … Cryan, J. F. (2011). Ingestion of Lactobacillus strain regulates emotional behavior and central GABA receptor expression in a mouse via the vagus nerve. *Proceedings of the National Academy of Sciences*. https://doi.org/10.1073/pnas.1102999108

Bray, J. R., & Curtis, J. T. (1957). An ordination of the upland forest communities of southern Wisconsin. *Ecological Monographs*. https://doi.org/10.2307/1942268

Brenu, E. W., Huth, T. K., Hardcastle, S. L., Fuller, K., Kaur, M., Johnston, S., … Marshall-Gradisnik, S. M. (2014). Role of adaptive and innate immune cells in chronic fatigue syndrome/myalgic encephalomyelitis. *International Immunology*. https://doi.org/10.1093/intimm/dxt068

Brenu, E. W., van Driel, M. L., Staines, D. R., Ashton, K. J., Ramos, S. B., Keane, J., … Marshall-Gradisnik, S. M. (2011). Immunological abnormalities as potential biomarkers in Chronic Fatigue Syndrome/Myalgic Encephalomyelitis. *Journal of Translational Medicine*. https://doi.org/10.1186/1479-5876-9-81

Brimmer, D. J., Fridinger, F., Lin, J.-M. S., & Reeves, W. C. (2010). U.S. healthcare providers' knowledge, attitudes, beliefs, and perceptions concerning Chronic Fatigue Syndrome. *BMC Family Practice*. https://doi.org/10.1186/1471-2296-11-28

Broderick, G., Fuite, J., Kreitz, A., Vernon, S. D., Klimas, N., & Fletcher, M. A. (2010). A formal analysis of cytokine networks in Chronic Fatigue Syndrome. *Brain, Behavior, and Immunity*. https://doi.org/10.1016/j.bbi.2010.04.012

Brooks, J. P., Edwards, D. J., Harwich, M. D., Rivera, M. C., Fettweis, J. M., Serrano, M. G., … Buck, G. A. (2015). The truth about metagenomics: Quantifying and counteracting bias in 16S rRNA studies Ecological and evolutionary microbiology. *BMC Microbiology*. https://doi.org/10.1186/s12866-015-0351-6

Brown, K., DeCoffe, D., Molcan, E., & Gibson, D. L. (2012). Diet-induced dysbiosis of the intestinal microbiota and the effects on immunity and disease. *Nutrients*. https://doi.org/10.3390/nu4081095

Brun, P., Giron, M. C., Qesari, M., Porzionato, A., Caputi, V., Zoppellaro, C., … Castagliuolo, I. (2013). Toll-like receptor 2 regulates intestinal inflammation by controlling integrity of the enteric nervous system. *Gastroenterology*. https://doi.org/10.1053/j.gastro.2013.08.047

Brurberg, K. G., Fønhus, M. S., Larun, L., Flottorp, S., & Malterud, K. (2014). Case definitions for chronic fatigue syndrome/myalgic encephalomyelitis (CFS/ME): A systematic review. *BMJ Open*. https://doi.org/10.1136/bmjopen-2013-003973

Bullitt, E. (1990). Expression ofC-fos-like protein as a marker for neuronal activity following noxious stimulation in the rat. *The Journal of Comparative Neurology*. https://doi.org/10.1002/cne.902960402

Bunker, J. J., Erickson, S. A., Flynn, T. M., Henry, C., Koval, J. C., Meisel, M., … Bendelac, A. (2017). Natural polyreactive IgA antibodies coat the intestinal microbiota. *Science*. Retrieved from http://science.sciencemag.org/content/early/2017/09/27/science.aan6619.abstract

Bunker, J. J., Flynn, T. M., Koval, J. C., Shaw, D. G., Meisel, M., McDonald, B. D., … Bendelac, A. (2015). Innate and Adaptive Humoral Responses Coat Distinct Commensal Bacteria with Immunoglobulin A. *Immunity*. https://doi.org/10.1016/j.immuni.2015.08.007

Bunnett, N. W. (2014). Neuro-humoral signalling by bile acids and the TGR5 receptor in the gastrointestinal tract. *Journal of Physiology*. https://doi.org/10.1113/jphysiol.2014.271155

Buscarinu, M. C., Cerasoli, B., Annibali, V., Policano, C., Lionetto, L., Capi, M., … Ristori, G. (2017). Altered intestinal permeability in patients with relapsing–remitting multiple sclerosis: A pilot study. *Multiple Sclerosis Journal*. https://doi.org/10.1177/1352458516652498

Cani, P. D., Bibiloni, R., Knauf, C., Neyrinck, A. M., & Delzenne, N. M. (2008). Changes in gut microbiota control metabolic diet–induced obesity and diabetes in mice. *Diabetes*. https://doi.org/10.2337/db07-1403.Additional

Cao, Y., Shen, J., & Ran, Z. H. (2014). Association between faecalibacterium prausnitzii reduction and inflammatory bowel disease: A meta-analysis and systematic review of the literature. *Gastroenterology Research and Practice*. https://doi.org/10.1155/2014/872725

Caporaso, J. G., Lauber, C. L., Walters, W. A., Berg-Lyons, D., Lozupone, C. A., Turnbaugh, P. J., … Knight, R. (2011). Global patterns of 16S rRNA diversity at a depth of millions of sequences per sample. *Proceedings of the National Academy of Sciences*. https://doi.org/10.1073/pnas.1000080107

Carasi, P., Racedo, S. M., Jacquot, C., Romanin, D. E., Serradell, M. A., & Urdaci, M. C. (2015). Impact of kefir derived lactobacillus kefiri on the mucosal immune response and gut microbiota. *Journal of Immunology Research*. https://doi.org/10.1155/2015/361604

Carding, S., Verbeke, K., Vipond, D. T., Corfe, B. M., & Owen, L. J. (2015). Dysbiosis of the gut microbiota in disease. *Microbial Ecology in Health and Disease*, *26*, 10.3402/mehd.v26.26191. https://doi.org/10.3402/mehd.v26.26191

Carruthers, B. M., Van de Sande, M. I., De Meirleir, K. L., Klimas, N. G., Broderick, G., Mitchell, T., … Stevens, S. (2011). Myalgic encephalomyelitis: International Consensus Criteria. *Journal of Internal Medicine*. https://doi.org/10.1111/j.1365-2796.2011.02428.x

Caruccio, N., Grunenwald, H., Syed, F., & Biotechnologies, E. (2009). Nextera TM technology for NGS DNA library preparation: simultaneous fragmentation and tagging by in vitro transposition. *Nature Methods*. https://doi.org/10.1186/gb-2010-11-12-r119

Cenit, M. C., Sanz, Y., & Codoñer-Franch, P. (2017). Influence of gut microbiota on neuropsychiatric disorders. *World Journal of Gastroenterology*. https://doi.org/10.3748/wjg.v23.i30.5486

Chalder, T., Berelowitz, G., Pawlikowska, T., Watts, L., Wessely, S., Wright, D., & Wallace, E. P. (1993). Development of a fatigue scale. *Journal of Psychosomatic Research*. https://doi.org/10.1016/0022-3999(93)90081-P

Chandrasekharan, B., Bala, V., Kolachala, V. L., Vijay-Kumar, M., Jones, D., Gewirtz, A. T., … Srinivasan, S. (2008). Targeted deletion of neuropeptide Y (NPY) modulates

experimental colitis. *PLoS ONE*. https://doi.org/10.1371/journal.pone.0003304
Chang, S., Kim, Y.-H., Kim, Y.-J., Kim, Y.-W., Moon, S., Lee, Y. Y., … Seong, S.-Y. (2018). Taurodeoxycholate Increases the Number of Myeloid-Derived Suppressor Cells That Ameliorate Sepsis in Mice. *Frontiers in Immunology*, *9*, 1984. https://doi.org/10.3389/fimmu.2018.01984
Chen, J., Chia, N., Kalari, K. R., Yao, J. Z., Novotna, M., Soldan, M. M. P., … Mangalam, A. K. (2016). Multiple sclerosis patients have a distinct gut microbiota compared to healthy controls. *Scientific Reports*. https://doi.org/10.1038/srep28484
Cherrington, C. A., Hinton, M., Pearson, G. R., & Chopra, I. (1991). Short-chain organic acids at pH 5.0 kill Escherichia coli and Salmonella spp. without causing membrane perturbation. *Journal of Applied Bacteriology*. https://doi.org/10.1111/j.1365-2672.1991.tb04442.x
Chiu, I. M., Heesters, B. A., Ghasemlou, N., Von Hehn, C. A., Zhao, F., Tran, J., … Woolf, C. J. (2013). Bacteria activate sensory neurons that modulate pain and inflammation. *Nature*. https://doi.org/10.1038/nature12479
Choo, J. M., Leong, L. E. X., & Rogers, G. B. (2015). Sample storage conditions significantly influence faecal microbiome profiles. *Scientific Reports*. https://doi.org/10.1038/srep16350
Claesson, M. J., Cusack, S., O'Sullivan, O., Greene-Diniz, R., de Weerd, H., Flannery, E., … O'Toole, P. W. (2011). Composition, variability, and temporal stability of the intestinal microbiota of the elderly. *Proceedings of the National Academy of Sciences*. https://doi.org/10.1073/pnas.1000097107
Clarke, G., Grenham, S., Scully, P., Fitzgerald, P., Moloney, R. D., Shanahan, F., … Cryan, J. F. (2013). The microbiome-gut-brain axis during early life regulates the hippocampal serotonergic system in a sex-dependent manner. *Molecular Psychiatry*. https://doi.org/10.1038/mp.2012.77
Claus, S. P., Tsang, T. M., Wang, Y., Cloarec, O., Skordi, E., Martin, F. P., … Nicholson, J. K. (2008). Systemic multicompartmental effects of the gut microbiome on mouse metabolic phenotypes. *Molecular Systems Biology*. https://doi.org/10.1038/msb.2008.56
Clemente, J. C., Manasson, J., & Scher, J. U. (2018). The role of the gut microbiome in systemic inflammatory disease. *Bmj*, j5145. https://doi.org/10.1136/bmj.j5145
Collino, S., Martin, F. P. J., & Rezzi, S. (2013). Clinical metabolomics paves the way towards future healthcare strategies. *British Journal of Clinical Pharmacology*. https://doi.org/10.1111/j.1365-2125.2012.04216.x
Coplan, J. D., Andrews, M. W., Rosenblum, L. A., Owens, M. J., Friedman, S., Gorman, J. M., & Nemeroff, C. B. (1996). Persistent elevations of cerebrospinal fluid concentrations of corticotropin-releasing factor in adult nonhuman primates exposed to early-life stressors: implications for the pathophysiology of mood and anxiety disorders. *Proceedings of the National Academy of Sciences*. https://doi.org/10.1073/pnas.93.4.1619
Correale, J., Fiol, M., & Gilmore, W. (2006). The risk of relapses in multiple sclerosis during systemic infections. *Neurology*. https://doi.org/10.1212/01.wnl.0000233834.09743.3b
Cree, B. A. C., Spencer, C. M., Varrin-Doyer, M., Baranzini, S. E., & Zamvil, S. S. (2016). Gut microbiome analysis in neuromyelitis optica reveals overabundance of Clostridium perfringens. *Annals of Neurology*. https://doi.org/10.1002/ana.24718
Cryan, J. F., & Dinan, T. G. (2015). More than a Gut Feeling: The Microbiota Regulates Neurodevelopment and Behavior. *Neuropsychopharmacology*. https://doi.org/10.1038/npp.2014.224
Curis, E., Crenn, P., & Cynober, L. (2007). Citrulline and the gut. *Current Opinion in Clinical*

Nutrition and Metabolic Care. https://doi.org/10.1097/MCO.0b013e32829fb38d

D., B., R.L., A., T., P., & P., K. (1996). Viral serologies in patients with chronic fatigue and chronic fatigue syndrome. *Journal of Medical Virology*, *50*(1), 25–30. https://doi.org/http://dx.doi.org/10.1002/%28SICI%291096-9071%28199609%2950:1%3C25::AID-JMV6%3E3.0.CO;2-V

D'Amore, R., Ijaz, U. Z., Schirmer, M., Kenny, J. G., Gregory, R., Darby, A. C., … Hall, N. (2016). A comprehensive benchmarking study of protocols and sequencing platforms for 16S rRNA community profiling. *BMC Genomics*. https://doi.org/10.1186/s12864-015-2194-9

Dallman, M. F., Strack, A. M., Akana, S. F., Bradbury, M. J., Hanson, E. S., Scribner, K. A., & Smith, M. (1993). Feast and famine: critical role of glucocorticoids with insulin in daily energy flow. *Frontiers in Neuroendocrinology*. https://doi.org/10.1006/frne.1993.1010

Dantzer, R., O'Connor, J. C., Freund, G. G., Johnson, R. W., & Kelley, K. W. (2008). From inflammation to sickness and depression: When the immune system subjugates the brain. *Nature Reviews Neuroscience*. https://doi.org/10.1038/nrn2297

David, L. A., Maurice, C. F., Carmody, R. N., Gootenberg, D. B., Button, J. E., Wolfe, B. E., … Turnbaugh, P. J. (2014). Diet rapidly and reproducibly alters the human gut microbiome. *Nature*. https://doi.org/10.1038/nature12820

De Boever, P., Wouters, R., Verschaeve, L., Berckmans, P., Schoeters, G., & Verstraete, W. (2000). Protective effect of the bile salt hydrolase-active Lactobacillus reuteri against bile salt cytotoxicity. *Applied Microbiology and Biotechnology*. https://doi.org/10.1007/s002530000330

De Kort, S., Keszthelyi, D., & Masclee, A. A. M. (2011). Leaky gut and diabetes mellitus: What is the link? *Obesity Reviews*, *12*(6), 449–458. https://doi.org/10.1111/j.1467-789X.2010.00845.x

De Magistris, L., Familiari, V., Pascotto, A., Sapone, A., Frolli, A., Iardino, P., … Bravaccio, C. (2010). Alterations of the intestinal barrier in patients with autism spectrum disorders and in their first-degree relatives. *Journal of Pediatric Gastroenterology and Nutrition*. https://doi.org/10.1097/MPG.0b013e3181dcc4a5

De Punder, K., & Pruimboom, L. (2015). Stress induces endotoxemia and low-grade inflammation by increasing barrier permeability. *Frontiers in Immunology*. https://doi.org/10.3389/fimmu.2015.00223

De Smet, I., Van Hoorde, L., Vande Woestyne, M., Christiaens, H., & Verstraete, W. (1995). Significance of bile salt hydrolytic activities of lactobacilli. *Journal of Applied Bacteriology*. https://doi.org/10.1111/j.1365-2672.1995.tb03140.x

Demitrack, M. a, Dale, J. K., Straus, S. E., Laue, L., Listwak, S. J., Kruesi, M. J., … Gold, P. W. (1991). Evidence for impaired activation of the hypothalamic-pituitary-adrenal axis in patients with chronic fatigue syndrome. *The Journal of Clinical Endocrinology and Metabolism*. https://doi.org/10.1210/jcem-73-6-1224

Dermadi, D., Valo, S., Ollila, S., Soliymani, R., Sipari, N., Pussila, M., … Nyström, M. (2017). Western diet deregulates bile acid homeostasis, cell proliferation, and tumorigenesis in colon. *Cancer Research*. https://doi.org/10.1158/0008-5472.CAN-16-2860

Desbonnet, L., Clarke, G., Traplin, A., O'Sullivan, O., Crispie, F., Moloney, R. D., … Cryan, J. F. (2015). Gut microbiota depletion from early adolescence in mice: Implications for brain and behaviour. *Brain, Behavior, and Immunity*. https://doi.org/10.1016/j.bbi.2015.04.004

Di Sabatino, A., Lenti, M. V., Cammalleri, L., Corazza, G. R., & Pilotto, A. (2018). Frailty and the gut. *Digestive and Liver Disease*, *50*(6), 533–541. https://doi.org/10.1016/j.dld.2018.03.010

Dias, D. A., & Koal, T. (2016). Progress in Metabolomics Standardisation and its Significance

in Future Clinical Laboratory Medicine. *EJIFCC*.
Dickson, A., Knussen, C., & Flowers, P. (2007). Stigma and the delegitimation experience: An interpretative phenomenological analysis of people living with chronic fatigue syndrome. *Psychology & Health*. https://doi.org/10.1080/14768320600976224
Dilger, R. N., & Johnson, R. W. (2008). Aging, microglial cell priming, and the discordant central inflammatory response to signals from the peripheral immune system. *Journal of Leukocyte Biology*. https://doi.org/10.1189/jlb.0208108
Dinan, T. G., & Cryan, J. F. (2012). Regulation of the stress response by the gut microbiota: Implications for psychoneuroendocrinology. *Psychoneuroendocrinology*. https://doi.org/10.1016/j.psyneuen.2012.03.007
Dinan, T. G., Stanton, C., & Cryan, J. F. (2013). Psychobiotics: A novel class of psychotropic. *Biological Psychiatry*, *74*(10), 720–726. https://doi.org/10.1016/j.biopsych.2013.05.001
DNAGenotek. (2017). Storage recommendations for OMNIgene ® • GUT samples. Retrieved September 19, 2018, from https://www.dnagenotek.com/us/pdf/PD-PR-00695.pdf
Donaldson, G. P., Ladinsky, M. S., Yu, K. B., Sanders, J. G., Yoo, B. B., Chou, W. C., … Mazmanian, S. K. (2018). Gut microbiota utilize immunoglobulin a for mucosal colonization. *Science*. https://doi.org/10.1126/science.aaq0926
Doolin, K., Farrell, C., Tozzi, L., Harkin, A., Frodl, T., & O'Keane, V. (2017). Diurnal hypothalamic-pituitary-adrenal axis measures and inflammatory marker correlates in major depressive disorder. *International Journal of Molecular Sciences*. https://doi.org/10.3390/ijms18102226
Dowsett, E. G., Ramsay, A. M., McCartney, R. A., & Bell, E. J. (1990). Myalgic encephalomyelitis a persistent enteroviral infection? *Postgraduate Medical Journal*. https://doi.org/10.1136/pgmj.66.777.526
Dunn, A. J. (2000). Cytokine Activation of the HPA Axis. *Annals of the New York Academy of Sciences*. https://doi.org/10.1111/j.1749-6632.2000.tb05426.x
Eckburg, P. B., Bik, E. M., Bernstein, C. N., Purdom, E., Dethlefsen, L., Sargent, M., … Relman, D. A. (2005). Diversity of the human intestinal microbial flora. *Science (New York, N.Y.)*. https://doi.org/10.1126/science.1110591
Edgar, R. C. (2017). UNBIAS: An attempt to correct abundance bias in 16S sequencing, with limited success. *BioRxiv*. https://doi.org/10.1101/124149
Ehrlich, S. D. (2011). MetaHIT: The European Union project on metagenomics of the human intestinal tract. In *Metagenomics of the Human Body*. https://doi.org/10.1007/978-1-4419-7089-3_15
Elsenbruch, S. (2011). Abdominal pain in Irritable Bowel Syndrome: A review of putative psychological, neural and neuro-immune mechanisms. *Brain, Behavior, and Immunity*. https://doi.org/10.1016/j.bbi.2010.11.010
Eren, A. M., Sogin, M. L., Morrison, H. G., Vineis, J. H., Fisher, J. C., Newton, R. J., & McLellan, S. L. (2015). A single genus in the gut microbiome reflects host preference and specificity. *ISME Journal*. https://doi.org/10.1038/ismej.2014.97
Erny, D., De Angelis, A. L. H., Jaitin, D., Wieghofer, P., Staszewski, O., David, E., … Prinz, M. (2015). Host microbiota constantly control maturation and function of microglia in the CNS. *Nature Neuroscience*. https://doi.org/10.1038/nn.4030
Eskilsson, A., Matsuwaki, T., Shionoya, K., Mirrasekhian, E., Zajdel, J., Schwaninger, M., … Blomqvist, A. (2017). Immune-Induced Fever Is Dependent on Local But Not Generalized Prostaglandin E_2 Synthesis in the Brain. *The Journal of Neuroscience*. https://doi.org/10.1523/JNEUROSCI.3846-16.2017
Etemadifar, M., Salari, M., Mirmosayyeb, O., Serati, M., Nikkhah, R., Askari, M., & Fayyazi, E. (2017). Efficacy and safety of rituximab in neuromyelitis optica: Review of evidence. *Journal of Research in Medical Sciences*. https://doi.org/10.4103/1735-1995.200275

Evans, S. S., Repasky, E. A., & Fisher, D. T. (2015). Fever and the thermal regulation of immunity: The immune system feels the heat. *Nature Reviews Immunology*. https://doi.org/10.1038/nri3843

Eyssen, H. J., De Pauw, G., & Van Eldere, J. (1999). Formation of hyodeoxycholic acid from muricholic acid and hyocholic acid by an unidentified gram-positive rod termed HDCA-1 isolated from rat intestinal microflora. *Applied and Environmental Microbiology*, *65*(7), 3158–3163.

EYSSEN, H. J., PARMENTIER, G. G., & MERTENS, J. A. (1976). Sulfated Bile Acids in Germ-Free and Conventional Mice. *European Journal of Biochemistry*, *66*(3), 507–514. https://doi.org/10.1111/j.1432-1033.1976.tb10576.x

Fagarasan, S., Kawamoto, S., Kanagawa, O., & Suzuki, K. (2010). Adaptive Immune Regulation in the Gut: T Cell–Dependent and T Cell–Independent IgA Synthesis. *Annual Review of Immunology*. https://doi.org/10.1146/annurev-immunol-030409-101314

Falk, P. G., Hooper, L. V, Midtvedt, T., & Gordon, J. I. (1998). Creating and maintaining the gastrointestinal ecosystem: what we know and need to know from gnotobiology. *Microbiology and Molecular Biology Reviews : MMBR*. https://doi.org/PMID: PMC98942

Fang, F. C. (2011). Antimicrobial actions of reactive oxygen species. *MBio*. https://doi.org/10.1128/mBio.00141-11

Farzaei, M. H., Bahramsoltani, R., Abdollahi, M., & Rahimi, R. (2016). The role of visceral hypersensitivity in irritable bowel syndrome: Pharmacological targets and novel treatments. *Journal of Neurogastroenterology and Motility*. https://doi.org/10.5056/jnm16001

Farzi, A., Fröhlich, E. E., & Holzer, P. (2018). Gut Microbiota and the Neuroendocrine System. *Neurotherapeutics*, *15*(1), 5–22. https://doi.org/10.1007/s13311-017-0600-5

Fasano, A. (2011). Zonulin and Its Regulation of Intestinal Barrier Function: The Biological Door to Inflammation, Autoimmunity, and Cancer. *Physiological Reviews*. https://doi.org/10.1152/physrev.00003.2008

Fasano, A. (2012). Leaky gut and autoimmune diseases. *Clinical Reviews in Allergy and Immunology*. https://doi.org/10.1007/s12016-011-8291-x

Figueiredo, H. F., Bruestle, A., Bodie, B., Dolgas, C. M., & Herman, J. P. (2003). The medial prefrontal cortex differentially regulates stress-induced c-fos expression in the forebrain depending on type of stressor. *European Journal of Neuroscience*. https://doi.org/10.1046/j.1460-9568.2003.02932.x

Fillatreau, S. (2018). B cells and their cytokine activities implications in human diseases. *Clinical Immunology*. https://doi.org/10.1016/j.clim.2017.07.020

Fine, E. J. (2013). The Alice in Wonderland Syndrome. *Progress in Brain Research*. https://doi.org/10.1016/B978-0-444-63364-4.00025-9

Fletcher, M., Zeng, X., Barnes, Z., Levis, S., & Klimas, N. G. (2009). Plasma cytokines in women with chronic fatigue syndrome. *Journal of Translational Medicine*, *7*(1), 96. https://doi.org/10.1186/1479-5876-7-96

Fluge, Ø., Mella, O., Bruland, O., Risa, K., Dyrstad, S. E., Alme, K., … Tronstad, K. J. (2016). Metabolic profiling indicates impaired pyruvate dehydrogenase function in myalgic encephalopathy/chronic fatigue syndrome. *JCI Insight*, *1*(21). https://doi.org/10.1172/jci.insight.89376

FNM, T. (2017). An Accurate Diagnosis of Myalgic Encephalomyelitis and Chronic Fatigue Syndrome requires strict Clinical Case definitions and Objective Test Methods. *Journal of Medical Diagnostic Methods*, *06*(03). https://doi.org/10.4172/2168-9784.1000249

Font-Nieves, M., Sans-Fons, M. G., Gorina, R., Bonfill-Teixidor, E., Salas-Peŕdomo, A., Maŕquez-Kisinousky, L., … Planas, A. M. (2012). Induction of COX-2 enzyme and down-

regulation of COX-1 expression by lipopolysaccharide (LPS) control prostaglandin E 2 production in astrocytes. *Journal of Biological Chemistry*. https://doi.org/10.1074/jbc.M111.327874

Forbes, J. D., Van Domselaar, G., & Bernstein, C. N. (2016). The gut microbiota in immune-mediated inflammatory diseases. *Frontiers in Microbiology*. https://doi.org/10.3389/fmicb.2016.01081

Forsyth, C. B., Shannon, K. M., Kordower, J. H., Voigt, R. M., Shaikh, M., Jaglin, J. A., … Keshavarzian, A. (2011). Increased intestinal permeability correlates with sigmoid mucosa alpha-synuclein staining and endotoxin exposure markers in early Parkinson's disease. *PLoS ONE*. https://doi.org/10.1371/journal.pone.0028032

Foster, J. A., & McVey Neufeld, K. A. (2013). Gut-brain axis: How the microbiome influences anxiety and depression. *Trends in Neurosciences*. https://doi.org/10.1016/j.tins.2013.01.005

Fouhy, F., Clooney, A. G., Stanton, C., Claesson, M. J., & Cotter, P. D. (2016). 16S rRNA gene sequencing of mock microbial populations- impact of DNA extraction method, primer choice and sequencing platform. *BMC Microbiology*. https://doi.org/10.1186/s12866-016-0738-z

Foxall, P. J., Spraul, M., Farrant, R. D., Lindon, L. C., Neild, G. H., & Nicholson, J. K. (1995). 750 MHz 1H-NMR spectroscopy of human blood plasma. *Journal of Pharmaceutical and Biomedical Analysis*, *11*(4–5), 267–76. https://doi.org/10.1016/0079-6565(95)01013-0

Fragkos, K. C., & Forbes, A. (2018). Citrulline as a marker of intestinal function and absorption in clinical settings: A systematic review and meta-analysis. *United European Gastroenterology Journal*, *6*(2). https://doi.org/10.1177/2050640617737632

Frasca, D., & Blomberg, B. B. (2016). Inflammaging decreases adaptive and innate immune responses in mice and humans. *Biogerontology*. https://doi.org/10.1007/s10522-015-9578-8

Fremont, M., Coomans, D., Massart, S., & De Meirleir, K. (2013). High-throughput 16S rRNA gene sequencing reveals alterations of intestinal microbiota in myalgic encephalomyelitis/chronic fatigue syndrome patients. *Anaerobe*. https://doi.org/10.1016/j.anaerobe.2013.06.002

Friedberg, F., & Jason, L. A. (1998). Understanding chronic fatigue syndrome: An empirical guide to assessment and treatment. *Understanding Chronic Fatigue Syndrome: An Empirical Guide to Assessment and Treatment.*

Fröhlich, E. E., Farzi, A., Mayerhofer, R., Reichmann, F., Jačan, A., Wagner, B., … Holzer, P. (2016). Cognitive impairment by antibiotic-induced gut dysbiosis: Analysis of gut microbiota-brain communication. *Brain, Behavior, and Immunity*. https://doi.org/10.1016/j.bbi.2016.02.020

Fujinami, R. S., Oldstone, M. B., Wroblewska, Z., Frankel, M. E., & Koprowski, H. (1983). Molecular mimicry in virus infection: crossreaction of measles virus phosphoprotein or of herpes simplex virus protein with human intermediate filaments. *Proceedings of the National Academy of Sciences of the United States of America*.

Fukuda, K., Straus, S. E., Hickie, I., Sharpe, M. C., Dobbins, J. G., & Komaroff, A. (1994). The chronic fatigue syndrome: a comprehensive approach to its definition and study. International Chronic Fatigue Syndrome Study Group. *Ann. Intern. Med.* https://doi.org/10.7326/0003-4819-121-12-199412150-00009

Galley, J. D., Nelson, M. C., Yu, Z., Dowd, S. E., Walter, J., Kumar, P. S., … Bailey, M. T. (2014). Exposure to a social stressor disrupts the community structure of the colonic mucosa-associated microbiota. *BMC Microbiology*. https://doi.org/10.1186/1471-2180-14-189

García-cañaveras, J. C., Donato, M. T., & Castell, J. V. (2012). Targeted profiling of circulating and hepatic bile acids in human , mouse and rat using an UPLC-MRM-MS-validated method, 1–28.
Gardiner, B. J., Korman, T. M., & Junckerstorff, R. K. (2014). Eggerthella lenta bacteremia complicated by spondylodiscitis, psoas abscess, and meningitis. *Journal of Clinical Microbiology*. https://doi.org/10.1128/JCM.03158-13
Gareau, M. G., Jury, J., & Perdue, M. H. (2007). Neonatal maternal separation of rat pups results in abnormal cholinergic regulation of epithelial permeability. *AJP: Gastrointestinal and Liver Physiology*. https://doi.org/10.1152/ajpgi.00392.2006
Germain, A., Ruppert, D., Levine, S. M., & Hanson, M. R. (2017). Metabolic profiling of a myalgic encephalomyelitis/chronic fatigue syndrome discovery cohort reveals disturbances in fatty acid and lipid metabolism. *Mol. BioSyst.*, *13*(2), 371–379. https://doi.org/10.1039/C6MB00600K
Ghyselinck, J., Pfeiffer, S., Heylen, K., Sessitsch, A., & De Vos, P. (2013). The effect of primer choice and short read sequences on the outcome of 16S rRNA gene based diversity studies. *PloS One*. https://doi.org/10.1371/journal.pone.0071360
Gilliam, A. G. (1938). Epidemiological study on an epidemic, diagnosed as poliomyelitis, occurring among the personnel of Los Angeles County General Hospital during the summer of 1934. *Public Health Bulletin*.
Giloteaux, L., Goodrich, J. K., Walters, W. A., Levine, S. M., Ley, R. E., & Hanson, M. R. (2016). Reduced diversity and altered composition of the gut microbiome in individuals with myalgic encephalomyelitis/chronic fatigue syndrome. *Microbiome*, *4*(1), 30. https://doi.org/10.1186/s40168-016-0171-4
Glaser, R., & Kiecolt-Glaser, J. K. (2005). Stress-induced immune dysfunction: Implications for health. *Nature Reviews Immunology*. https://doi.org/10.1038/nri1571
Gong, D., Gong, X., Wang, L., Yu, X., & Dong, Q. (2016). Involvement of Reduced Microbial Diversity in Inflammatory Bowel Disease. *Gastroenterology Research and Practice*. https://doi.org/10.1155/2016/6951091
Goodwin, S., McPherson, J. D., & McCombie, W. R. (2016). Coming of age: ten years of next-generation sequencing technologies. *Nat Rev Genet*. https://doi.org/10.1038/nrg.2016.49
Gorelik, L., & Flavell, R. a. (2000). Abrogation of TGFbeta signaling in T cells leads to spontaneous T cell differentiation and autoimmune disease. *Immunity*. https://doi.org/S1074-7613(00)80170-3 [pii]
Gosselin, D., & Rivest, S. (2008). MyD88 signaling in brain endothelial cells is essential for the neuronal activity and glucocorticoid release during systemic inflammation. *Molecular Psychiatry*. https://doi.org/10.1038/sj.mp.4002122
Goto, J., Hasegawa, K., Nambara, T., & Iida, T. (1992). Studies on steroids. CCLIV. Gas chromatographic-mass spectrometric determination of 4- and 6-hydroxylated bile acids in human urine with negative ion chemical ionization detection. *Journal of Chromatography*, *574*(1), 1–7. Retrieved from http://www.ncbi.nlm.nih.gov/pubmed/1629271
Graspeuntner, S., Loeper, N., Künzel, S., Baines, J. F., & Rupp, J. (2018). Selection of validated hypervariable regions is crucial in 16S-based microbiota studies of the female genital tract. *Scientific Reports*. https://doi.org/10.1038/s41598-018-27757-8
Gratton, J., Phetcharaburanin, J., Mullish, B. H., Williams, H. R. T., Thursz, M., Nicholson, J. K., … Li, J. V. (2016a). Optimized Sample Handling Strategy for Metabolic Profiling of Human Feces. *Analytical Chemistry*. https://doi.org/10.1021/acs.analchem.5b04159
Gratton, J., Phetcharaburanin, J., Mullish, B. H., Williams, H. R. T., Thursz, M., Nicholson, J. K., … Li, J. V. (2016b). Optimized Sample Handling Strategy for Metabolic Profiling of Human Feces. *Analytical Chemistry*, *88*(9), 4661–8.

https://doi.org/10.1021/acs.analchem.5b04159
Guo, Y., Li, S.-H., Kuang, Y.-S., He, J.-R., Lu, J.-H., Luo, B.-J., … Qiu, X. (2016). Effect of short-term room temperature storage on the microbial community in infant fecal samples. *Scientific Reports*, *6*(1), 26648. https://doi.org/10.1038/srep26648
Gutzeit, C., Magri, G., & Cerutti, A. (2014). Intestinal IgA production and its role in host-microbe interaction. *Immunological Reviews*. https://doi.org/10.1111/imr.12189
Haas, A., Zimmermann, K., Graw, F., Slack, E., Rusert, P., Ledergerber, B., … Yerly, S. (2011). Systemic antibody responses to gut commensal bacteria during chronic HIV-1 infection. *Gut*. https://doi.org/10.1136/gut.2010.224774
Haney, E., Beth Smith, M. E., McDonagh, M., Pappas, M., Daeges, M., Wasson, N., & Nelson, H. D. (2015). Diagnostic methods for myalgic encephalomyelitis/chronic fatigue syndrome: A systematic review for a national institutes of health pathways to prevention workshop. *Annals of Internal Medicine*. https://doi.org/10.7326/M15-0443
Hanson, M. R., & Giloteaux, L. (2017). The gut microbiome in Myalgic Encephalomyelitis. *Biochemist*, *39*(2), 10–13.
Hapfelmeier, S., Lawson, M. A. E., Slack, E., Kirundi, J. K., Stoel, M., Heikenwalder, M., … Macpherson, A. J. (2010). Reversible microbial colonization of germ-free mice reveals the dynamics of IgA immune responses. *Science*. https://doi.org/10.1126/science.1188454
Hauser, S. L., Waubant, E., Arnold, D. L., Vollmer, T., Antel, J., Fox, R. J., … Smith, C. H. (2008). B-Cell Depletion with Rituximab in Relapsing–Remitting Multiple Sclerosis. *New England Journal of Medicine*. https://doi.org/10.1056/NEJMoa0706383
Häuser, W., Layer, P., Henningsen, P., & Kruis, W. (2012). Functional bowel disorders in adults. *Deutsches Ärzteblatt International*. https://doi.org/10.3238/arztebl.2012.0083
Hawk, C., Jason, L. A., & Peña, J. (2007). Variables That Differentiate Chronic Fatigue Syndrome from Depression. *Journal of Human Behavior in the Social Environment*. https://doi.org/10.1080/10911350802107652
Heijtz, R. D., Wang, S., Anuar, F., Qian, Y., Bjorkholm, B., Samuelsson, A., … Pettersson, S. (2011). Normal gut microbiota modulates brain development and behavior. *Proceedings of the National Academy of Sciences*, *108*(7), 3047–3052. https://doi.org/10.1073/pnas.1010529108
Heikema, A. P., Bergman, M. P., Richards, H., Crocker, P. R., Gilbert, M., Samsom, J. N., … Van Belkum, A. (2010). Characterization of the specific interaction between sialoadhesin and sialylated Campylobacter jejuni lipooligosaccharides. *Infection and Immunity*. https://doi.org/10.1128/IAI.01273-09
Heintz-Buschart, A., & Wilmes, P. (2018). Human Gut Microbiome: Function Matters. *Trends in Microbiology*. https://doi.org/10.1016/j.tim.2017.11.002
Henriksson, A. E., Tagesson, C., Uribe, A., Uvnas-Moberg, K., Nord, C. E., Gullberg, R., & Johansson, C. (1988). Effects of prostaglandin E2 on disease activity, gastric secretion and intestinal permeability, and morphology in patients with rheumatoid arthritis. *Annals of the Rheumatic Diseases*. https://doi.org/10.1136/ard.47.8.620
Herman, J. P., McKlveen, J. M., Ghosal, S., Kopp, B., Wulsin, A., Makinson, R., … Myers, B. (2016). Regulation of the Hypothalamic-Pituitary-Adrenocortical Stress Response. In *Comprehensive Physiology*. https://doi.org/10.1002/cphy.c150015
Herman, J. P., Mcklveen, J. M., Solomon, M. B., Carvalho-Netto, E., & Myers, B. (2012). Neural regulation of the stress response: Glucocorticoid feedback mechanisms. *Brazilian Journal of Medical and Biological Research*. https://doi.org/10.1590/S0100-879X2012007500041
Hoban, A. E., Stilling, R. M., Ryan, F. J., Shanahan, F., Dinan, T. G., Claesson, M. J., … Cryan, J. F. (2016). Regulation of prefrontal cortex myelination by the microbiota.

Translational Psychiatry. https://doi.org/10.1038/tp.2016.42
Hollander, D. (1999). Intestinal permeability, leaky gut, and intestinal disorders. *Current Gastroenterology Reports*. https://doi.org/10.1007/s11894-999-0023-5
Hollander, D., Vadheim, C. M., Brettholz, E., Petersen, G. M., Delahunty, T., & Rotter, J. I. (1986). Increased intestinal permeability in patients with Crohn's disease and their relatives: A possible etiologic factor. *Annals of Internal Medicine*. https://doi.org/10.7326/0003-4819-105-6-883
Holmes, G. P., Kaplan, J. E., Gantz, N. M., Komaroff, A. L., Schonberger, L. B., Straus, S. E., … Brus, I. (1988). Chronic fatigue syndrome: A working case definition. *Annals of Internal Medicine*. https://doi.org/10.7326/0003-4819-108-3-387
Holmes, G. P., Kaplan, J. E., Stewart, J. A., Hunt, B., Pinsky, P. F., & Schonberger, L. B. (1987). A Cluster of Patients With a Chronic Mononucleosis-like Syndrome: Is Epstein-Barr Virus the Cause? *JAMA: The Journal of the American Medical Association*. https://doi.org/10.1001/jama.1987.03390170053027
Hoogland, I. C. M., Houbolt, C., van Westerloo, D. J., van Gool, W. A., & van de Beek, D. (2015). Systemic inflammation and microglial activation: systematic review of animal experiments. *Journal of Neuroinflammation*. https://doi.org/10.1186/s12974-015-0332-6
Hornig, M., Montoya, J. G., Klimas, N. G., Levine, S., Felsenstein, D., Bateman, L., … Lipkin, W. I. (2015). Distinct plasma immune signatures in ME/CFS are present early in the course of illness. *Science Advances*, *1*(1). https://doi.org/10.1126/sciadv.1400121
Hsiao, E. Y., McBride, S. W., Hsien, S., Sharon, G., Hyde, E. R., McCue, T., … Mazmanian, S. K. (2013). Microbiota modulate behavioral and physiological abnormalities associated with neurodevelopmental disorders. *Cell*. https://doi.org/10.1016/j.cell.2013.11.024
Hu, X., Bonde, Y., Eggertsen, G., & Rudling, M. (2014). Muricholic bile acids are potent regulators of bile acid synthesis via a positive feedback mechanism. *Journal of Internal Medicine*, *275*(1), 27–38. https://doi.org/10.1111/joim.12140
Huang, X., Sun, M., Chen, F., Xiao, Y., Chen, L., Yao, S., & Cong, Y. (2017). IL-17 promotes intestinal IgA response to intestinal infection but does not affect memory B cell development. *The Journal of Immunology*, *198*(1 Supplement), 200.16 LP-200.16. Retrieved from http://www.jimmunol.org/content/198/1_Supplement/200.16.abstract
Human Microbiome Project, C. (2012). Structure, function and diversity of the healthy human microbiome. *Nature*. https://doi.org/10.1038/nature11234
Huttenhower, C., Gevers, D., Knight, R., Abubucker, S., Badger, J. H., Chinwalla, A. T., … White, O. (2012). Structure, function and diversity of the healthy human microbiome. *Nature*, *486*(7402), 207–214. https://doi.org/10.1038/nature11234
Illumina. (2014). Nextera ® XT DNA Library Preparation Kit. *Reporter*.
Illumina. (2015). MiSeq System Guide. *Illumina*. https://doi.org/https://support.illumina.com/content/dam/illumina-support/documents/documentation/system_documentation/miseq/miseq-system-guide-15027617-01.pdf
Inoue, D., Tsujimoto, G., & Kimura, I. (2014). Regulation of energy homeostasis by GPR41. *Frontiers in Endocrinology*. https://doi.org/10.3389/fendo.2014.00081
Irvine, E. J., & Marshall, J. K. (2000). Increased intestinal permeability precedes the onset of Crohn's disease in a subject with familial risk. *Gastroenterology*. https://doi.org/10.1053/gast.2000.20231
Ivanov, I. I., Atarashi, K., Manel, N., Brodie, E. L., Shima, T., Karaoz, U., … Littman, D. R. (2009). Induction of Intestinal Th17 Cells by Segmented Filamentous Bacteria. *Cell*. https://doi.org/10.1016/j.cell.2009.09.033
Iwasaki, A., & Kelsall, B. L. (1999). Freshly isolated Peyer's patch, but not spleen, dendritic

cells produce interleukin 10 and induce the differentiation of T helper type 2 cells. *The Journal of Experimental Medicine*. https://doi.org/10.1084/jem.190.2.229

Jackson, M. L., & Bruck, D. (2012). Sleep abnormalities in chronic fatigue syndrome/myalgic encephalomyelitis: A review. *Journal of Clinical Sleep Medicine*, *8*(6), 719–728. https://doi.org/10.5664/jcsm.2276

Jacobson, L. (2014). Hypothalamic-pituitary-adrenocortical axis: Neuropsychiatric aspects. *Comprehensive Physiology*. https://doi.org/10.1002/cphy.c130036

Jammes, Y., Steinberg, J. G., Mambrini, O., Brégeon, F., & Delliaux, S. (2005). Chronic fatigue syndrome: Assessment of increased oxidative stress and altered muscle excitability in response to incremental exercise. *Journal of Internal Medicine*. https://doi.org/10.1111/j.1365-2796.2005.01452.x

Jangi, S., Gandhi, R., Cox, L. M., Li, N., Von Glehn, F., Yan, R., … Weiner, H. L. (2016). Alterations of the human gut microbiome in multiple sclerosis. *Nature Communications*. https://doi.org/10.1038/ncomms12015

Jason, L. A., Brown, M., Evans, M., & Brown, A. (2012). Predictors of Fatigue among Patients with Chronic Fatigue Syndrome. *Journal of Human Behavior in the Social Environment*, *22*(7), 822–832. https://doi.org/10.1080/10911359.2012.707896

Jason, L. A., Evans, M., Porter, N., Brown, M., Brown, A., Hunnell, J., … Friedberg, F. (2010). The development of a revised Canadian myalgic encephalomyelitis chronic fatigue syndrome case definition. *American Journal of Biochemistry and Biotechnology*.

Jason, L. A., Evans, M., So, S., Scott, J., & Brown, A. (2015). Problems in defining post-exertional malaise. *Journal of Prevention and Intervention in the Community*. https://doi.org/10.1080/10852352.2014.973239

Jason, L. A., King, C. P., Richman, J. A., Taylor, R. R., Torres, S. R., & Song, S. (1999). U.S. Case definition of chronic fatigue syndrome: Diagnostic and theoretical issues. *Journal of Chronic Fatigue Syndrome*. https://doi.org/10.1300/J092v05n03_02

Jason, L. A., Porter, N., Brown, M., Anderson, V., Brown, A., Hunnell, J., & Lerch, A. (2009). CFS: A Review of Epidemiology and Natural History Studies. *Bulletin of the IACFS/ME*, *17*(3), 88–106. Retrieved from http://www.pubmedcentral.nih.gov/articlerender.fcgi?artid=3021257&tool=pmcentrez&rendertype=abstract

Jason, L. A., Sunnquist, M., Brown, A., Evans, M., Vernon, S. D., Furst, J. D., & Simonis, V. (2014). Examining case definition criteria for chronic fatigue syndrome and myalgic encephalomyelitis. *Fatigue: Biomedicine, Health & Behavior*. https://doi.org/10.1080/21641846.2013.862993

Jiang, H., Ling, Z., Zhang, Y., Mao, H., Ma, Z., Yin, Y., … Ruan, B. (2015). Altered fecal microbiota composition in patients with major depressive disorder. *Brain, Behavior, and Immunity*. https://doi.org/10.1016/j.bbi.2015.03.016

Jobard, E., Trédan, O., Postoly, D., André, F., Martin, A. L., Elena-Herrmann, B., & Boyault, S. (2016). A systematic evaluation of blood serum and plasma pre-analytics for metabolomics cohort studies. *International Journal of Molecular Sciences*. https://doi.org/10.3390/ijms17122035

Johansson, V., Jakobsson, J., Fortgang, R. G., Zetterberg, H., Blennow, K., Cannon, T. D., … Landén, M. (2017). Cerebrospinal fluid microglia and neurodegenerative markers in twins concordant and discordant for psychotic disorders. *European Archives of Psychiatry and Clinical Neuroscience*. https://doi.org/10.1007/s00406-016-0759-5

Jones, M. B., Highlander, S. K., Anderson, E. L., Li, W., Dayrit, M., Klitgord, N., … Venter, J. C. (2015). Library preparation methodology can influence genomic and functional predictions in human microbiome research. *Proceedings of the National Academy of Sciences*. https://doi.org/10.1073/pnas.1519288112

Joossens, M., Huys, G., Cnockaert, M., De Preter, V., Verbeke, K., Rutgeerts, P., … Vermeire,

S. (2011). Dysbiosis of the faecal microbiota in patients with Crohn's disease and their unaffected relatives. *Gut*. https://doi.org/10.1136/gut.2010.223263

Jovel, J., Patterson, J., Wang, W., Hotte, N., O'Keefe, S., Mitchel, T., … Wong, G. K. S. (2016). Characterization of the gut microbiome using 16S or shotgun metagenomics. *Frontiers in Microbiology*. https://doi.org/10.3389/fmicb.2016.00459

Jurgens, H. A., & Johnson, R. W. (2012). Dysregulated neuronal-microglial cross-talk during aging, stress and inflammation. *Experimental Neurology*. https://doi.org/10.1016/j.expneurol.2010.11.014

Kalsbeek, A., Buijs, R. M., van Heerikhuize, J. J., Arts, M., & van der Woude, T. P. (1992). Vasopressin-containing neurons of the suprachiasmatic nuclei inhibit corticosterone release. *Brain Research*. https://doi.org/10.1016/0006-8993(92)90927-2

Kalsbeek, A., van der Spek, R., Lei, J., Endert, E., Buijs, R. M., & Fliers, E. (2012). Circadian rhythms in the hypothalamo-pituitary-adrenal (HPA) axis. *Molecular and Cellular Endocrinology*. https://doi.org/10.1016/j.mce.2011.06.042

Karst, S. M., Dueholm, M. S., McIlroy, S. J., Kirkegaard, R. H., Nielsen, P. H., & Albertsen, M. (2018). Retrieval of a million high-quality, full-length microbial 16S and 18S rRNA gene sequences without primer bias. *Nature Biotechnology*. https://doi.org/10.1038/nbt.4045

Katon, W., & Russo, J. (1992). Chronic Fatigue Syndrome Criteria: A Critique of the Requirement for Multiple Physical Complaints. *Archives of Internal Medicine*. https://doi.org/10.1001/archinte.1992.00400200042008

Kawamoto, S., Maruya, M., Kato, L. M., Suda, W., Atarashi, K., Doi, Y., … Fagarasan, S. (2014). Foxp3+T Cells Regulate Immunoglobulin A Selection and Facilitate Diversification of Bacterial Species Responsible for Immune Homeostasis. *Immunity*. https://doi.org/10.1016/j.immuni.2014.05.016

Kawamoto, S., Tran, T. H., Maruya, M., Suzuki, K., Doi, Y., Tsutsui, Y., … Fagarasan, S. (2012). The inhibitory receptor PD-1 regulates IgA selection and bacterial composition in the gut. *Science*. https://doi.org/10.1126/science.1217718

Kelly, J. R., Borre, Y., O' Brien, C., Patterson, E., El Aidy, S., Deane, J., … Dinan, T. G. (2016). Transferring the blues: Depression-associated gut microbiota induces neurobehavioural changes in the rat. *Journal of Psychiatric Research*. https://doi.org/10.1016/j.jpsychires.2016.07.019

Kelly, J. R., Kennedy, P. J., Cryan, J. F., Dinan, T. G., Clarke, G., & Hyland, N. P. (2015). Breaking down the barriers: the gut microbiome, intestinal permeability and stress-related psychiatric disorders. *Frontiers in Cellular Neuroscience*. https://doi.org/10.3389/fncel.2015.00392

Kettenmann, H., Hanisch, U.-K., Noda, M., & Verkhratsky, A. (2011). Physiology of Microglia. *Physiological Reviews*. https://doi.org/10.1152/physrev.00011.2010

Khounlotham, M., Kim, W., Peatman, E., Nava, P., Medina-Contreras, O., Addis, C., … Parkos, C. A. (2012). Compromised Intestinal Epithelial Barrier Induces Adaptive Immune Compensation that Protects from Colitis. *Immunity*, *37*(3), 563–573. https://doi.org/10.1016/j.immuni.2012.06.017

Kia, E., MacKenzie, B. W., Middleton, D., Lau, A., Waite, D. W., Lewis, G., … Taylor, M. W. (2016). Integrity of the human faecal microbiota following long-term sample storage. *PLoS ONE*. https://doi.org/10.1371/journal.pone.0163666

Kim, D., Zeng, M. Y., & Núñez, G. (2017). The interplay between host immune cells and gut microbiota in chronic inflammatory diseases. *Experimental & Molecular Medicine*. https://doi.org/10.1038/emm.2017.24

Kimura, I., Inoue, D., Hirano, K., & Tsujimoto, G. (2014). The SCFA receptor GPR43 and energy metabolism. *Frontiers in Endocrinology*. https://doi.org/10.3389/fendo.2014.00085

King, C., Tangye, S. G., & Mackay, C. R. (2008). T follicular helper (TFH) cells in normal and dysregulated immune responses. *Annual Review of Immunology*. https://doi.org/10.1146/annurev.immunol.26.021607.090344

Knight, R., Vrbanac, A., Taylor, B. C., Aksenov, A., Callewaert, C., Debelius, J., … Dorrestein, P. C. (2018). Best practices for analysing microbiomes. *Nature Reviews Microbiology*. https://doi.org/10.1038/s41579-018-0029-9

Koeth, R. A., Levison, B. S., Culley, M. K., Buffa, J. A., Wang, Z., Gregory, J. C., … Hazen, S. L. (2014). γ-butyrobetaine is a proatherogenic intermediate in gut microbial metabolism of L-carnitine to TMAO. *Cell Metabolism*, *20*(5), 799–812. https://doi.org/10.1016/j.cmet.2014.10.006

Kubinak, J. L., & Round, J. L. (2016). Do antibodies select a healthy microbiota? *Nature Reviews Immunology*. https://doi.org/10.1038/nri.2016.114

Kurokawa, K., Itoh, T., Kuwahara, T., Oshima, K., Toh, H., Toyoda, A., … Hattori, M. (2007). Comparative metagenomics revealed commonly enriched gene sets in human gut microbiomes. *DNA Research*. https://doi.org/10.1093/dnares/dsm018

Lakhan, S. E., & Kirchgessner, A. (2010). Gut inflammation in chronic fatigue syndrome. *Nutrition & Metabolism*, *7*(1), 79. https://doi.org/10.1186/1743-7075-7-79

Lambert, G. P. (2009). Stress-induced gastrointestinal barrier dysfunction and its inflammatory effects. *Journal of Animal Science*. https://doi.org/10.2527/jas.2008-1339

Lawley, T. D., & Walker, A. W. (2013). Intestinal colonization resistance. *Immunology*. https://doi.org/10.1111/j.1365-2567.2012.03616.x

Lee, Y.-T., Hu, L.-Y., Shen, C.-C., Huang, M.-W., Tsai, S.-J., Yang, A. C., … Hung, J.-H. (2015). Risk of Psychiatric Disorders following Irritable Bowel Syndrome: A Nationwide Population-Based Cohort Study. *PLOS ONE*. https://doi.org/10.1371/journal.pone.0133283

Lee, Y. K., Menezes, J. S., Umesaki, Y., & Mazmanian, S. K. (2011). Proinflammatory T-cell responses to gut microbiota promote experimental autoimmune encephalomyelitis. *Proceedings of the National Academy of Sciences*. https://doi.org/10.1073/pnas.1000082107

Lewis Price, J. (1961). MYALGIC ENCEPHALOMYELITIS. *The Lancet*, *277*(7180), 737–738. https://doi.org/https://doi.org/10.1016/S0140-6736(61)92893-8

Li, J., Jia, H., Cai, X., Zhong, H., Feng, Q., Sunagawa, S., … Wang, J. (2014). An integrated catalog of reference genes in the human gut microbiome. *Nature Biotechnology*. https://doi.org/10.1038/nbt.2942

Liebich, H. M., & Först, C. (1984). Hydroxycarboxylic and oxocarboxylic acids in urine: products from branched-chain amino acid degradation and from ketogenesis. *Journal of Chromatography*, *309*(2), 225–42. https://doi.org/10.1007/s13398-014-0173-7.2

Litinskiy, M. B., Nardelli, B., Hilbert, D. M., He, B., Schaffer, A., Casali, P., & Cerutti, A. (2002). DCs induce CD40-independent immunoglobulin class switching through BLyS and APRIL. *Nature Immunology*. https://doi.org/10.1038/ni829

Liu, J., Wang, F., Liu, S., Du, J., Hu, X., Xiong, J., … Sun, J. (2017). Sodium butyrate exerts protective effect against Parkinson's disease in mice via stimulation of glucagon like peptide-1. *Journal of the Neurological Sciences*. https://doi.org/10.1016/j.jns.2017.08.3235

Liu, L., Li, Y., Li, S., Hu, N., He, Y., Pong, R., … Law, M. (2012). Comparison of next-generation sequencing systems. *Journal of Biomedicine and Biotechnology*. https://doi.org/10.1155/2012/251364

Liu, X., Hoene, M., Wang, X., Yin, P., Häring, H. U., Xu, G., & Lehmann, R. (2018). Serum or plasma, what is the difference? Investigations to facilitate the sample material selection decision making process for metabolomics studies and beyond. *Analytica*

Chimica Acta. https://doi.org/10.1016/j.aca.2018.03.009
Loebel, M., Grabowski, P., Heidecke, H., Bauer, S., Hanitsch, L. G., Wittke, K., … Scheibenbogen, C. (2016). Antibodies to β adrenergic and muscarinic cholinergic receptors in patients with Chronic Fatigue Syndrome. *Brain, Behavior, and Immunity*. https://doi.org/10.1016/j.bbi.2015.09.013
Loebel, M., Strohschein, K., Giannini, C., Koelsch, U., Bauer, S., Doebis, C., … Scheibenbogen, C. (2014). Deficient EBV-Specific B- and T-Cell Response in Patients with Chronic Fatigue Syndrome, *9*(1). https://doi.org/10.1371/journal.pone.0085387
Looper, K. J., & Kirmayer, L. J. (2004). Perceived stigma in functional somatic syndromes and comparable medical conditions. *Journal of Psychosomatic Research*. https://doi.org/10.1016/j.jpsychores.2004.03.005
Lorusso, L., Mikhaylova, S. V., Capelli, E., Ferrari, D., Ngonga, G. K., & Ricevuti, G. (2009). Immunological aspects of chronic fatigue syndrome. *Autoimmunity Reviews*. https://doi.org/10.1016/j.autrev.2008.08.003
Lowry, S. F., Horowitz, G. D., Jeevanandam, M., Legaspi, A., & Brennan, M. F. (1985). Whole-body protein breakdown and 3-methylhistidine excretion during brief fasting, starvation, and intravenous repletion in man. *Annals of Surgery*, *202*(1), 21–27. https://doi.org/10.1097/00000658-198507000-00003
Luczynski, P., Whelan, S. O., O'Sullivan, C., Clarke, G., Shanahan, F., Dinan, T. G., & Cryan, J. F. (2016). Adult microbiota-deficient mice have distinct dendritic morphological changes: differential effects in the amygdala and hippocampus. *European Journal of Neuroscience*. https://doi.org/10.1111/ejn.13291
Luna, R. A., Oezguen, N., Balderas, M., Venkatachalam, A., Runge, J. K., Versalovic, J., … Williams, K. C. (2017). Distinct Microbiome-Neuroimmune Signatures Correlate With Functional Abdominal Pain in Children With Autism Spectrum Disorder. *Cellular and Molecular Gastroenterology and Hepatology*. https://doi.org/10.1016/j.jcmgh.2016.11.008
Luo, L., Aubrecht, J., Li, D., Warner, R. L., Johnson, K. J., Kenny, J., & Colangelo, J. L. (2018). Assessment of serum bile acid profiles as biomarkers of liver injury and liver disease in humans. *PLoS ONE*, *13*(3), 1–17. https://doi.org/10.1371/journal.pone.0193824
Lyte, M., & Ernst, S. (1992). Catecholamine induced growth of gram negative bacteria. *Life Sciences*. https://doi.org/10.1016/0024-3205(92)90273-R
Lyte, M., Li, W., Opitz, N., Gaykema, R. P. A., & Goehler, L. E. (2006). Induction of anxiety-like behavior in mice during the initial stages of infection with the agent of murine colonic hyperplasia Citrobacter rodentium. *Physiology and Behavior*. https://doi.org/10.1016/j.physbeh.2006.06.019
Machiels, K., Joossens, M., Sabino, J., De Preter, V., Arijs, I., Eeckhaut, V., … Vermeire, S. (2014). A decrease of the butyrate-producing species roseburia hominis and faecalibacterium prausnitzii defines dysbiosis in patients with ulcerative colitis. *Gut*. https://doi.org/10.1136/gutjnl-2013-304833
MacLullich, A. M. J., Beaglehole, A., Hall, R. J., & Meagher, D. J. (2009). Delirium and long-term cognitive impairment. *International Review of Psychiatry (Abingdon, England)*. https://doi.org/10.1080/09540260802675031
Macpherson, A. J., Gatto, D., Sainsbury, E., Harriman, G. R., Hengartner, H., & Zinkernagel, R. M. (2000). A primitive T cell-independent mechanism of intestinal mucosal IgA responses to commensal bacteria. *Science*. https://doi.org/10.1126/science.288.5474.2222
Macpherson, A. J., Geuking, M. B., Slack, E., Hapfelmeier, S., & McCoy, K. D. (2012). The habitat, double life, citizenship, and forgetfulness of IgA. *Immunological Reviews*. https://doi.org/10.1111/j.1600-065X.2011.01072.x
MacPherson, A. J., McCoy, K. D., Johansen, F. E., & Brandtzaeg, P. (2008). The immune

geography of IgA induction and function. *Mucosal Immunology*. https://doi.org/10.1038/mi.2007.6

Macpherson, A. J., & Uhr, T. (2004). Induction of Protective IgA by Intestinal Dendritic Cells Carrying Commensal Bacteria. *Science*. https://doi.org/10.1126/science.1091334

MacPherson, A. J., & Uhr, T. (2004). Compartmentalization of the mucosal immune responses to commensal intestinal bacteria. In *Annals of the New York Academy of Sciences*. https://doi.org/10.1196/annals.1309.005

Macpherson, A., Khoo, U. Y., Forgacs, I., Philpott-Howard, J., & Bjarnason, I. (1996). Mucosal antibodies in inflammatory bowel disease are directed against intestinal bacteria. *Gut*. https://doi.org/10.1136/gut.38.3.365

Maes, M., Coucke, F., & Leunis, J. C. (2007). Normalization of the increased translocation of endotoxin from gram negative enterobacteria (leaky gut) is accompanied bya remission of chronic fatigue syndrome. *Neuroendocrinology Letters*. https://doi.org/NEL280607A13 [pii]

Maes, M., Kubera, M., Leunis, J. C., & Berk, M. (2012). Increased IgA and IgM responses against gut commensals in chronic depression: Further evidence for increased bacterial translocation or leaky gut. *Journal of Affective Disorders*. https://doi.org/10.1016/j.jad.2012.02.023

Maes, M., Kubera, M., Uytterhoeven, M., Vrydags, N., & Bosmans, E. (2011). Increased plasma peroxides as a marker of oxidative stress in myalgic encephalomyelitis/chronic fatigue syndrome (ME/CFS). *Medical Science Monitor : International Medical Journal of Experimental and Clinical Research*, *17*(4), SC11. https://doi.org/10.12659/msm.881699

Maes, M., & Maes, M. (2009). Leaky gut in chronic fatigue syndrome: A review. *Act Nerv Super Rediviva Activitas Nervosa Superior Rediviva Act Nerv Super Rediviva*.

Maes, M., Mihaylova, I., & Leunis, J. C. (2006). Chronic fatigue syndrome is accompanied by an IgM-related immune response directed against neopitopes formed by oxidative or nitrosative damage to lipids and proteins. *Neuroendocrinology Letters*.

Maes, M., Mihaylova, I., & Leunis, J. C. (2007). Increased serum IgA and IgM against LPS of enterobacteria in chronic fatigue syndrome (CFS): Indication for the involvement of gram-negative enterobacteria in the etiology of CFS and for the presence of an increased gut-intestinal permeability. *Journal of Affective Disorders*. https://doi.org/10.1016/j.jad.2006.08.021

Maes, M., Ringel, K., Kubera, M., Anderson, G., Morris, G., Galecki, P., & Geffard, M. (2013). In myalgic encephalomyelitis/chronic fatigue syndrome, increased autoimmune activity against 5-HT is associated with immuno-inflammatory pathways and bacterial translocation. *Journal of Affective Disorders*, *150*(2), 223–230. https://doi.org/10.1016/j.jad.2013.03.029

Maes, M., Twisk, F. N. M., & Johnson, C. (2012). Myalgic Encephalomyelitis (ME), Chronic Fatigue Syndrome (CFS), and Chronic Fatigue (CF) are distinguished accurately: Results of supervised learning techniques applied on clinical and inflammatory data. *Psychiatry Research*. https://doi.org/10.1016/j.psychres.2012.03.031

Maes, M., Twisk, F. N. M., Kubera, M., & Ringel, K. (2012). Evidence for inflammation and activation of cell-mediated immunity in Myalgic Encephalomyelitis/Chronic Fatigue Syndrome (ME/CFS): Increased interleukin-1, tumor necrosis factor-α, PMN-elastase, lysozyme and neopterin. *Journal of Affective Disorders*. https://doi.org/10.1016/j.jad.2011.09.004

Magrone, T., Jirillo, E., Moore, W., Holdeman, L., Ley, R., Peterson, D., … Rehman, T. (2013). The interaction between gut microbiota and age-related changes in immune function and inflammation. *Immunity & Ageing*, *10*(1), 31. https://doi.org/10.1186/1742-4933-10-31

Manfredo Vieira, S., Hiltensperger, M., Kumar, V., Zegarra-Ruiz, D., Dehner, C., Khan, N., … Kriegel, M. A. (2018). Translocation of a gut pathobiont drives autoimmunity in mice and humans. *Science*. https://doi.org/10.1126/science.aar7201

Mariat, D., Firmesse, O., Levenez, F., Guimarăes, V. D., Sokol, H., Doré, J., … Furet, J. P. (2009). The firmicutes/bacteroidetes ratio of the human microbiota changes with age. *BMC Microbiology*, *9*, 1–6. https://doi.org/10.1186/1471-2180-9-123

Maslowski, K. M., Vieira, A. T., Ng, A., Kranich, J., Sierro, F., Di Yu, … MacKay, C. R. (2009). Regulation of inflammatory responses by gut microbiota and chemoattractant receptor GPR43. *Nature*. https://doi.org/10.1038/nature08530

Mayer, E. A. (2011). Gut feelings: The emerging biology of gut-"brain communication. *Nature Reviews Neuroscience*. https://doi.org/10.1038/nrn3071

McEvedy, C. P., & Beard, A. W. (1970). Concept of Benign Myalgic Encephalomyelitis. *British Medical Journal*. https://doi.org/10.1136/bmj.1.5687.11

McManimen, S. L., Sunnquist, M. L., & Jason, L. A. (2016). Deconstructing post-exertional malaise: An exploratory factor analysis. *Journal of Health Psychology*. https://doi.org/10.1177/1359105316664139

Meseguer, V., Alpizar, Y. A., Luis, E., Tajada, S., Denlinger, B., Fajardo, O., … Viana, F. (2014). TRPA1 channels mediate acute neurogenic inflammation and pain produced by bacterial endotoxins. *Nature Communications*. https://doi.org/10.1038/ncomms4125

Mihaylova, I., DeRuyter, M., Rummens, J.-L., Bosmans, E., & Maes, M. (2007). *Decreased expression of CD69 in chronic fatigue syndrome in relation to inflammatory markers: Evidence for a severe disorder in the early activation of T lymphocytes and natural killer cells*. *Neuro endocrinology letters* (Vol. 28).

Miquel, S., Martín, R., Rossi, O., Bermúdez-Humarán, L. G., Chatel, J. M., Sokol, H., … Langella, P. (2013). Faecalibacterium prausnitzii and human intestinal health. *Current Opinion in Microbiology*. https://doi.org/10.1016/j.mib.2013.06.003

Mitra, S., Gilbert, J. a, Field, D., & Huson, D. H. (2010). Comparison of multiple metagenomes using phylogenetic networks based on ecological indices. *The ISME Journal*. https://doi.org/10.1038/ismej.2010.51

Mitsdoerffer, M., Lee, Y., Jager, A., Kim, H.-J., Korn, T., Kolls, J. K., … Kuchroo, V. K. (2010). Proinflammatory T helper type 17 cells are effective B-cell helpers. *Proceedings of the National Academy of Sciences*. https://doi.org/10.1073/pnas.1009234107

Mitsuyama, K., Niwa, M., Takedatsu, H., Yamasaki, H., Kuwaki, K., Yoshioka, S., … Torimura, T. (2016). Antibody markers in the diagnosis of inflammatory bowel disease. *World Journal of Gastroenterology*. https://doi.org/10.3748/wjg.v22.i3.1304

Miyake, S., Kim, S., Suda, W., Oshima, K., Nakamura, M., Matsuoka, T., … Yamamura, T. (2015). Dysbiosis in the gut microbiota of patients with multiple sclerosis, with a striking depletion of species belonging to clostridia XIVa and IV clusters. *PLoS ONE*. https://doi.org/10.1371/journal.pone.0137429

Mm, Z., & Ssung, E. (2017). Das chronische Müdigkeitssyndrom – ein kritischer Diskurs Chronic Fatigue Syndrome : A Critical Review Einleitung Epidemiologie Fallbeispiel Ätiologie und Pathogenese.

Mogensen, T. H. (2009). Pathogen recognition and inflammatory signaling in innate immune defenses. *Clinical Microbiology Reviews*. https://doi.org/10.1128/CMR.00046-08

Montoya, J. G., Holmes, T. H., Anderson, J. N., Maecker, H. T., Rosenberg-Hasson, Y., Valencia, I. J., … Davis, M. M. (2017). Cytokine signature associated with disease severity in chronic fatigue syndrome patients. *Proceedings of the National Academy of Sciences*. https://doi.org/10.1073/pnas.1710519114

Moor, K., Fadlallah, J., Toska, A., Sterlin, D., Balmer, M. L., Macpherson, A. J., … Slack, E. (2016). Analysis of bacterial-surface-specific antibodies in body fluids using bacterial

flow cytometry. *Nature Protocols*. https://doi.org/10.1038/nprot.2016.091
Moos, W. H., Faller, D. V., Harpp, D. N., Kanara, I., Pernokas, J., Powers, W. R., & Steliou, K. (2016). Microbiota and Neurological Disorders: A Gut Feeling. *BioResearch Open Access*. https://doi.org/10.1089/biores.2016.0010
Mora, J. R., Iwata, M., Eksteen, B., Song, S. Y., Junt, T., Senman, B., … Von Andrian, U. H. (2006). Generation of gut-homing IgA-secreting B cells by intestinal dendritic cells. *Science*. https://doi.org/10.1126/science.1132742
Morikawa, M., Derynck, R., & Miyazono, K. (2016). TGF- β and the TGF-β family: Context-dependent roles in cell and tissue physiology. *Cold Spring Harbor Perspectives in Biology*. https://doi.org/10.1101/cshperspect.a021873
Morris, G., Anderson, G., Galecki, P., Berk, M., & Maes, M. (2013). A narrative review on the similarities and dissimilarities between myalgic encephalomyelitis/chronic fatigue syndrome (ME/CFS) and sickness behavior. *BMC Medicine*. https://doi.org/10.1186/1741-7015-11-64
Morris, G., Berk, M., Galecki, P., & Maes, M. (2014). The emerging role of autoimmunity in myalgic encephalomyelitis/chronic fatigue syndrome (ME/cfs). *Molecular Neurobiology*. https://doi.org/10.1007/s12035-013-8553-0
Morris, G., & Maes, M. (2013a). A neuro-immune model of Myalgic Encephalomyelitis/Chronic fatigue syndrome. *Metabolic Brain Disease*. https://doi.org/10.1007/s11011-012-9324-8
Morris, G., & Maes, M. (2013b). Case definitions and diagnostic criteria for myalgic encephalomyelitis and chronic fatigue syndrome: From clinicalconsensus to evidence-based case definitions. *Activitas Nervosa Superior Rediviva*.
Morris, G., & Maes, M. (2014). Oxidative and Nitrosative Stress and Immune-inflammatory Pathways in Patients with Myalgic Encephalomyelitis (ME)/Chronic Fatigue Syndrome (CFS). *Current Neuropharmacology*, *12*(2), 168–185. https://doi.org/10.2174/1570159X11666131120224653
Moya, A., & Ferrer, M. (2016). Functional Redundancy-Induced Stability of Gut Microbiota Subjected to Disturbance. *Trends in Microbiology*. https://doi.org/10.1016/j.tim.2016.02.002
Mulak, A. (2018). A controversy on the role of short-chain fatty acids in the pathogenesis of Parkinson's disease. *Movement Disorders*. https://doi.org/10.1002/mds.27304
Munhoz, C. D. (2006). Chronic Unpredictable Stress Exacerbates Lipopolysaccharide-Induced Activation of Nuclear Factor- B in the Frontal Cortex and Hippocampus via Glucocorticoid Secretion. *Journal of Neuroscience*. https://doi.org/10.1523/JNEUROSCI.4398-05.2006
Muramatsu, M., Kinoshita, K., Fagarasan, S., Yamada, S., Shinkai, Y., & Honjo, T. (2000). Class switch recombination and hypermutation require activation-induced cytidine deaminase (AID), a potential RNA editing enzyme. *Cell*. https://doi.org/10.1016/S0092-8674(00)00078-7
Murr, C., Widner, B., Wirleitner, B., & Fuchs, D. (2002). Neopterin as a Marker for Immune System Activation. *Current Drug Metabolism*. https://doi.org/10.2174/1389200024605082
Nagy-Szakal, D., Williams, B. L., Mishra, N., Che, X., Lee, B., Bateman, L., … Lipkin, W. I. (2017). Fecal metagenomic profiles in subgroups of patients with myalgic encephalomyelitis/chronic fatigue syndrome. *Microbiome*, *5*(1), 44. https://doi.org/10.1186/s40168-017-0261-y
Nakagawa, Y., & Chiba, K. (2014). Role of microglial M1/M2 polarization in relapse and remission of psychiatric disorders and diseases. *Pharmaceuticals*, *7*(12), 1028–1048. https://doi.org/10.3390/ph7121028
Naviaux, R. K., Naviaux, J. C., Li, K., Bright, A. T., Alaynick, W. A., Wang, L., … Gordon, E.

(2016). Metabolic features of chronic fatigue syndrome. *Proceedings of the National Academy of Sciences of the United States of America*, *113*(37), E5472-80. https://doi.org/10.1073/pnas.1607571113

Neufeld, K. M., Kang, N., Bienenstock, J., & Foster, J. A. (2011). Reduced anxiety-like behavior and central neurochemical change in germ-free mice. *Neurogastroenterology and Motility*. https://doi.org/10.1111/j.1365-2982.2010.01620.x

Niblett, S. H., King, K. E., Dunstan, R. H., Clifton-Bligh, P., Hoskin, L. a, Roberts, T. K., … Rothkirch, T. B. (2007). Hematologic and urinary excretion anomalies in patients with chronic fatigue syndrome. *Experimental Biology and Medicine (Maywood, N.J.)*, *232*(8), 1041–9. https://doi.org/10.3181/0702-RM-44

Nimmerjahn, A., Kirchhoff, F., & Helmchen, F. (2005). Neuroscience: Resting microglial cells are highly dynamic surveillants of brain parenchyma in vivo. *Science*. https://doi.org/10.1126/science.1110647

Norman, J. M., Handley, S. A., Baldridge, M. T., Droit, L., Liu, C. Y., Keller, B. C., … Virgin, H. W. (2015). Disease-specific alterations in the enteric virome in inflammatory bowel disease. *Cell*, *160*(3), 447–460. https://doi.org/10.1016/j.cell.2015.01.002

Nouri, M., Bredberg, A., Weström, B., & Lavasani, S. (2014). Intestinal barrier dysfunction develops at the onset of experimental autoimmune encephalomyelitis, and can be induced by adoptive transfer of auto-reactive T cells. *PLoS ONE*. https://doi.org/10.1371/journal.pone.0106335

O'Mahony, S. M., Clarke, G., Dinan, T. G., & Cryan, J. F. (2017). Early-life adversity and brain development: Is the microbiome a missing piece of the puzzle? *Neuroscience*. https://doi.org/10.1016/j.neuroscience.2015.09.068

O'Mahony, S. M., Felice, V. D., Nally, K., Savignac, H. M., Claesson, M. J., Scully, P., … Cryan, J. F. (2014). Disturbance of the gut microbiota in early-life selectively affects visceral pain in adulthood without impacting cognitive or anxiety-related behaviors in male rats. *Neuroscience*. https://doi.org/10.1016/j.neuroscience.2014.07.054

O'Mahony, S. M., Hyland, N. P., Dinan, T. G., & Cryan, J. F. (2011). Maternal separation as a model of brain-gut axis dysfunction. *Psychopharmacology*. https://doi.org/10.1007/s00213-010-2010-9

Ochoa-Repáraz, J., & Kasper, L. H. (2018). The Microbiome and Neurologic Disease: Past and Future of a 2-Way Interaction. *Neurotherapeutics*. https://doi.org/10.1007/s13311-018-0604-9

Ochoa-Reparaz, J., Mielcarz, D. W., Ditrio, L. E., Burroughs, A. R., Begum-Haque, S., Dasgupta, S., … Kasper, L. H. (2010). Central Nervous System Demyelinating Disease Protection by the Human Commensal Bacteroides fragilis Depends on Polysaccharide A Expression. *The Journal of Immunology*. https://doi.org/10.4049/jimmunol.1001443

Oldstone, M. B. (1998). Molecular mimicry and immune-mediated diseases. *The FASEB Journal : Official Publication of the Federation of American Societies for Experimental Biology*.

Solve ME/CFS Initiative (SMCI). (2018). About the disease. Retrieved September 29, 2018, from https://solvecfs.org/about-the-disease/

Opolski, M., & Wilson, I. (2005). Asthma and depression: a pragmatic review of the literature and recommendations for future research. *Clinical Practice and Epidemiology in Mental Health : CP & EMH*. https://doi.org/10.1186/1745-0179-1-18

Org, E., Blum, Y., Kasela, S., Mehrabian, M., Kuusisto, J., Kangas, A. J., … Lusis, A. J. (2017). Relationships between gut microbiota, plasma metabolites, and metabolic syndrome traits in the METSIM cohort. *Genome Biology*. https://doi.org/10.1186/s13059-017-1194-2

Overman, E. L., Rivier, J. E., & Moeser, A. J. (2012). CRF induces intestinal epithelial barrier

injury via the release of mast cell proteases and TNF-α. *PLoS ONE*. https://doi.org/10.1371/journal.pone.0039935
Pabst, O. (2012). New concepts in the generation and functions of IgA. *Nature Reviews Immunology*. https://doi.org/10.1038/nri3322
Palm, N. W., De Zoete, M. R., Cullen, T. W., Barry, N. A., Stefanowski, J., Hao, L., … Flavell, R. A. (2014). Immunoglobulin A coating identifies colitogenic bacteria in inflammatory bowel disease. *Cell*. https://doi.org/10.1016/j.cell.2014.08.006
Pan, X., Elliott, C. T., McGuinness, B., Passmore, P., Kehoe, P. G., Hölscher, C., … Green, B. D. (2017). Metabolomic profiling of bile acids in clinical and experimental samples of Alzheimer's disease. *Metabolites*, *7*(2). https://doi.org/10.3390/metabo7020028
Pandharipande, P. P., Girard, T. D., Jackson, J. C., Morandi, A., Thompson, J. L., Pun, B. T., … Ely, E. W. (2013). Long-Term Cognitive Impairment after Critical Illness. *New England Journal of Medicine*. https://doi.org/10.1056/NEJMoa1301372
Panek, M., Čipčić Paljetak, H., Barešić, A., Perić, M., Matijašić, M., Lojkić, I., … Verbanac, D. (2018). Methodology challenges in studying human gut microbiota – effects of collection, storage, DNA extraction and next generation sequencing technologies. *Scientific Reports*. https://doi.org/10.1038/s41598-018-23296-4
Papadopoulos, A. S., & Cleare, A. J. (2012). Hypothalamic-pituitary-adrenal axis dysfunction in chronic fatigue syndrome. *Nature Reviews Endocrinology*. https://doi.org/10.1038/nrendo.2011.153
Parish, J. G. (1978). Early outbreaks of "epidemic neuromyasthenia." *Postgraduate Medical Journal*, *54*(637), 711–717. https://doi.org/10.1136/pgmj.54.637.711
Parnet, P., Kelley, K. W., Bluthé, R. M., & Dantzer, R. (2002). Expression and regulation of interleukin-1 receptors in the brain. Role in cytokines-induced sickness behavior. *Journal of Neuroimmunology*. https://doi.org/10.1016/S0165-5728(02)00022-X
Patarca-Montero, R. (2004). Medical Etiology, Assessment, and Treatment of Chronic Fatigue and Malaise. *Haworth Prss*, 6–7.
Pender, M. P., Csurhes, P. A., Burrows, J. M., & Burrows, S. R. (2017). Defective T-cell control of Epstein–Barr virus infection in multiple sclerosis. *Clinical & Translational Immunology*, *6*(6), e147. https://doi.org/10.1038/cti.2017.25
Pendergrast, T., Brown, A., Sunnquist, M., Jantke, R., Newton, J. L., Strand, E. B., & Jason, L. A. (2016). Housebound versus nonhousebound patients with myalgic encephalomyelitis and chronic fatigue syndrome. *Chronic Illness*. https://doi.org/10.1177/1742395316644770
Perry, V. H., & Holmes, C. (2014). Microglial priming in neurodegenerative disease. *Nature Reviews Neurology*. https://doi.org/10.1038/nrneurol.2014.38
Perry, V. H., & Teeling, J. (2013). Microglia and macrophages of the central nervous system: The contribution of microglia priming and systemic inflammation to chronic neurodegeneration. *Seminars in Immunopathology*. https://doi.org/10.1007/s00281-013-0382-8
Pijls, K. E., Jonkers, D. M. A. E., Elamin, E. E., Masclee, A. A. M., & Koek, G. H. (2013). Intestinal epithelial barrier function in liver cirrhosis: An extensive review of the literature. *Liver International*, *33*(10), 1457–1469. https://doi.org/10.1111/liv.12271
Pöllinger, B., Krishnamoorthy, G., Berer, K., Lassmann, H., Bösl, M. R., Dunn, R., … Wekerle, H. (2009). Spontaneous relapsing-remitting EAE in the SJL/J mouse: MOG-reactive transgenic T cells recruit endogenous MOG-specific B cells. *The Journal of Experimental Medicine*. https://doi.org/10.1084/jem.20090299
Prawitt, J., Abdelkarim, M., Stroeve, J. H. M., Popescu, I., Duez, H., Velagapudi, V. R., … Staels, B. (2011). Farnesoid X receptor deficiency improves glucose homeostasis in mouse models of obesity. *Diabetes*. https://doi.org/10.2337/db11-0030
Probst, A. J., Weinmaier, T., DeSantis, T. Z., Santo Domingo, J. W., & Ashbolt, N. (2015).

New perspectives on microbial community distortion after whole-genome amplification. *PLoS ONE*. https://doi.org/10.1371/journal.pone.0124158

Psychogios, N., Hau, D. D., Peng, J., Guo, A. C., Mandal, R., Bouatra, S., … Wishart, D. S. (2011). The human serum metabolome. *PLoS ONE*, *6*(2). https://doi.org/10.1371/journal.pone.0016957

Püntener, U., Booth, S. G., Perry, V. H., & Teeling, J. L. (2012). Long-term impact of systemic bacterial infection on the cerebral vasculature and microglia. *Journal of Neuroinflammation*. https://doi.org/10.1186/1742-2094-9-146

Qin, J., Li, R., Raes, J., Arumugam, M., Burgdorf, K. S., Manichanh, C., … Zoetendal, E. (2010). A human gut microbial gene catalogue established by metagenomic sequencing. *Nature*. https://doi.org/10.1038/nature08821

Qiu, X., Zhang, M., Yang, X., Hong, N., & Yu, C. (2013). Faecalibacterium prausnitzii upregulates regulatory T cells and anti-inflammatory cytokines in treating TNBS-induced colitis. *Journal of Crohn's and Colitis*. https://doi.org/10.1016/j.crohns.2013.04.002

Quigley, E. (2018). The Gut-Brain Axis and the Microbiome: Clues to Pathophysiology and Opportunities for Novel Management Strategies in Irritable Bowel Syndrome (IBS). *Journal of Clinical Medicine*, *7*(1), 6. https://doi.org/10.3390/jcm7010006

Quince, C., Walker, A. W., Simpson, J. T., Loman, N. J., & Segata, N. (2017). Shotgun metagenomics, from sampling to analysis. *Nature Biotechnology*. https://doi.org/10.1038/nbt.3935

Rajilić-Stojanović, M., & de Vos, W. M. (2014). The first 1000 cultured species of the human gastrointestinal microbiota. *FEMS Microbiology Reviews*. https://doi.org/10.1111/1574-6976.12075

Ranjan, R., Rani, A., Metwally, A., McGee, H. S., & Perkins, D. L. (2016). Analysis of the microbiome: Advantages of whole genome shotgun versus 16S amplicon sequencing. *Biochemical and Biophysical Research Communications*. https://doi.org/10.1016/j.bbrc.2015.12.083

Rao, A. V., Bested, A. C., Beaulne, T. M., Katzman, M. A., Iorio, C., Berardi, J. M., & Logan, A. C. (2009). A randomized, double-blind, placebo-controlled pilot study of a probiotic in emotional symptoms of chronic fatigue syndrome. *Gut Pathogens*. https://doi.org/10.1186/1757-4749-1-6

Ravi, R. K., Walton, K., & Khosroheidari, M. (2018). MiSeq: A Next Generation Sequencing Platform for Genomic Analysis. In J. K. DiStefano (Ed.), *Disease Gene Identification: Methods and Protocols* (pp. 223–232). New York, NY: Springer New York. https://doi.org/10.1007/978-1-4939-7471-9_12

Rea, K., Dinan, T. G., & Cryan, J. F. (2016). The microbiome: A key regulator of stress and neuroinflammation. *Neurobiology of Stress*. https://doi.org/10.1016/j.ynstr.2016.03.001

Reeves, W. C., Lloyd, A., Vernon, S. D., Klimas, N., Jason, L. A., Bleijenberg, G., … Unger, E. R. (2003). Identification of ambiguities in the 1994 chronic fatigue syndrome research case definition and recommendations for resolution. In *BMC health services research*. https://doi.org/10.1186/1472-6963-3-25

Rescigno, M. (2014). Tfr Cells and IgA Join Forces to Diversify the Microbiota. *Immunity*. https://doi.org/10.1016/j.immuni.2014.06.012

Reynolds, K. J., Vernon, S. D., Bouchery, E., & Reeves, W. C. (2004). The economic impact of chronic fatigue syndrome. *Cost Effectiveness and Resource Allocation : C/E*. https://doi.org/10.1186/1478-7547-2-4

Rhee, S. H., Pothoulakis, C., & Mayer, E. A. (2009). Principles and clinical implications of the brain-gut-enteric microbiota axis. *Nature Reviews Gastroenterology and Hepatology*. https://doi.org/10.1038/nrgastro.2009.35

Ridlon, J. M., Kang, D. J., Hylemon, P. B., & Bajaj, J. S. (2014). Bile acids and the gut microbiome. *Current Opinion in Gastroenterology*. https://doi.org/10.1097/MOG.0000000000000057

Rintala, A., Pietilä, S., Munukka, E., Eerola, E., Pursiheimo, J. P., Laiho, A., … Huovinen, P. (2017). Gut microbiota analysis results are highly dependent on the 16s rRNA gene target region, whereas the impact of DNA extraction is minor. *Journal of Biomolecular Techniques*. https://doi.org/10.7171/jbt.17-2801-003

Rios, D., Wood, M. B., Li, J., Chassaing, B., Gewirtz, A. T., & Williams, I. R. (2016). Antigen sampling by intestinal M cells is the principal pathway initiating mucosal IgA production to commensal enteric bacteria. *Mucosal Immunology*. https://doi.org/10.1038/mi.2015.121

Rivas, J. L., Palencia, T., Fernández, G., & García, M. (2018). Association of T and NK cell phenotype with the diagnosis of myalgic encephalomyelitis/chronic fatigue syndrome (ME/CFS). *Frontiers in Immunology*, *9*(MAY), 1–13. https://doi.org/10.3389/fimmu.2018.01028

Rivest, S. (2001). How circulating cytokines trigger the neural circuits that control the hypothalamic-pituitary-adrenal axis. *Psychoneuroendocrinology*. https://doi.org/10.1016/S0306-4530(01)00064-6

Rizzatti, G., Lopetuso, L. R., Gibiino, G., Binda, C., & Gasbarrini, A. (2017). Proteobacteria: A common factor in human diseases. *BioMed Research International*. https://doi.org/10.1155/2017/9351507

Robinson, C. K., Brotman, R. M., & Ravel, J. (2016). Intricacies of assessing the human microbiome in epidemiologic studies. *Annals of Epidemiology*. https://doi.org/10.1016/j.annepidem.2016.04.005

Rodríguez, J. M., Murphy, K., Stanton, C., Ross, R. P., Kober, O. I., Juge, N., … Collado, M. C. (2015). The composition of the gut microbiota throughout life, with an emphasis on early life. *Microbial Ecology in Health & Disease*, *26*(0). https://doi.org/10.3402/mehd.v26.26050

Roessner, U. (2001). Metabolic Profiling Allows Comprehensive Phenotyping of Genetically or Environmentally Modified Plant Systems. *THE PLANT CELL ONLINE*. https://doi.org/10.1105/tpc.13.1.11

Rojo, Ó. P., San Román, A. L., Arbizu, E. A., Martínez, A. D. L. H., Sevillano, E. R., & Martínez, A. A. (2007). Serum lipopolysaccharide-binding protein in endotoxemic patients with inflammatory bowel disease. *Inflammatory Bowel Diseases*. https://doi.org/10.1002/ibd.20019

Round, J. L., & Mazmanian, S. K. (2009). The gut microbiota shapes intestinal immune responses during health and disease. *Nature Reviews Immunology*. https://doi.org/10.1038/nri2515

Röuthig, H. -Jürgen, Bernhardt, W., & Afting, E. -G. (1984). Excretion of total and muscular Nτ-methylhistidine and creatinine in muscle diseases. *Muscle & Nerve*, *7*(5), 374–379. https://doi.org/10.1002/mus.880070506

Rowland, I., Gibson, G., Heinken, A., Scott, K., Swann, J., Thiele, I., & Tuohy, K. (2018). Gut microbiota functions: metabolism of nutrients and other food components. *European Journal of Nutrition*. https://doi.org/10.1007/s00394-017-1445-8

Russell, R. K., & Satsangi, J. (2004). IBD: A family affair. *Best Practice and Research: Clinical Gastroenterology*, *18*(3), 525–539. https://doi.org/10.1016/j.bpg.2003.12.006

Sacquet, E., Parquet, M., Riottot, M., Raizman, a, Jarrige, P., Huguet, C., & Infante, R. (1983). Intestinal absorption, excretion, and biotransformation of hyodeoxycholic acid in man. *Journal of Lipid Research*, *24*(5), 604–613.

Sait, L. C., Galic, M., Price, J. D., Simpfendorfer, K. R., Diavatopoulos, D. A., Uren, T. K., … Strugnell, R. A. (2007). Secretory antibodies reduce systemic antibody responses

against the gastrointestinal commensal flora. *International Immunology*. https://doi.org/10.1093/intimm/dxl142

Sampson, T. R., Debelius, J. W., Thron, T., Janssen, S., Shastri, G. G., Ilhan, Z. E., … Mazmanian, S. K. (2016). Gut Microbiota Regulate Motor Deficits and Neuroinflammation in a Model of Parkinson's Disease. *Cell*, *167*(6), 1469–1480.e12. https://doi.org/10.1016/j.cell.2016.11.018

Sapone, A., De Magistris, L., Pietzak, M., Clemente, M. G., Tripathi, A., Cucca, F., … Fasano, A. (2006). Zonulin upregulation is associated with increased gut permeability in subjects with type 1 diabetes and their relatives. *Diabetes*, *55*(5), 1443–1449. https://doi.org/10.2337/db05-1593

Sartor, R. B. (2011). Key questions to guide a better understanding of host-commensal microbiota interactions in intestinal inflammation. *Mucosal Immunology*. https://doi.org/10.1038/mi.2010.87

Sayin, S. I., Wahlström, A., Felin, J., Jäntti, S., Marschall, H. U., Bamberg, K., … Bäckhed, F. (2013). Gut microbiota regulates bile acid metabolism by reducing the levels of tauro-beta-muricholic acid, a naturally occurring FXR antagonist. *Cell Metabolism*. https://doi.org/10.1016/j.cmet.2013.01.003

Schwiertz, A., Spiegel, J., Dillmann, U., Grundmann, D., Bürmann, J., Faßbender, K., … Unger, M. M. (2018). Fecal markers of intestinal inflammation and intestinal permeability are elevated in Parkinson's disease. *Parkinsonism and Related Disorders*. https://doi.org/10.1016/j.parkreldis.2018.02.022

Scully, P., McKernan, D. P., Keohane, J., Groeger, D., Shanahan, F., Dinan, T. G., & Quigley, E. M. M. (2010). Plasma cytokine profiles in females with irritable bowel syndrome and extra-intestinal co-morbidity. *American Journal of Gastroenterology*. https://doi.org/10.1038/ajg.2010.159

Sender, R., Fuchs, S., & Milo, R. (2016). Revised Estimates for the Number of Human and Bacteria Cells in the Body. *PLoS Biology*. https://doi.org/10.1371/journal.pbio.1002533

Services, H., Insti-, N., & Control, D. (2015). Beyond Myalgic Encephalomyelitis / Chronic Fatigue Syndrome Redefining an Illness. *Institute of Medicine of the National Academies*. https://doi.org/10.1001/jama.2015.1346.Conflict

Shanks, N., Larocque, S., & Meaney, M. J. (1995). Neonatal endotoxin exposure alters the development of the hypothalamic-pituitary-adrenal axis: early illness and later responsivity to stress. *The Journal of Neuroscience : The Official Journal of the Society for Neuroscience*. https://doi.org/10.1523/JNEUROSCI.15-01-00376.1995

Shapiro, H., Kolodziejczyk, A. A., Halstuch, D., & Elinav, E. (2018). Bile acids in glucose metabolism in health and disease. *The Journal of Experimental Medicine*. https://doi.org/10.1084/jem.20171965

Sharkey, K. A., & Savidge, T. C. (2014). Reprint of: Role of enteric neurotransmission in host defense and protection of the gastrointestinal tract. *Autonomic Neuroscience: Basic and Clinical*. https://doi.org/10.1016/j.autneu.2014.03.004

Shaw, A. G., Sim, K., Powell, E., Cornwell, E., Cramer, T., McClure, Z. E., … Kroll, J. S. (2016). Latitude in sample handling and storage for infant faecal microbiota studies: The elephant in the room? *Microbiome*. https://doi.org/10.1186/s40168-016-0186-x

Sheedy, J. R., Wettenhall, R. E. H., Scanlon, D., Gooley, P. R., Lewis, D. P., Mcgregor, N., … De Meirleir, K. L. (2009). Increased D-lactic acid intestinal bacteria in patients with chronic fatigue syndrome. *In Vivo*, *23*(4), 621–628. https://doi.org/10.1097/00006123-200108000-00033

Shen, Y., Zhang, C., & Chen, Y. (2015). TGF-β in Inflammatory Bowel Diseases: A Tale of the Janus-Like Cytokine. *Critical Reviews in Eukaryotic Gene Expression*. https://doi.org/10.1615/CritRevEukaryotGeneExpr.2015013974

Shih, D. M., Shaposhnik, Z., Meng, Y., Rosales, M., Wang, X., Wu, J., … Lusis, A. J. (2013). Hyodeoxycholic acid improves HDL function and inhibits atherosclerotic lesion formation in LDLR-knockout mice. *FASEB Journal*, *27*(9), 3805–3817. https://doi.org/10.1096/fj.12-223008

Shimshoni, E., Yablecovitch, D., Baram, L., Dotan, I., & Sagi, I. (2015). ECM remodelling in IBD: Innocent bystander or partner in crime? The emerging role of extracellular molecular events in sustaining intestinal inflammation. *Gut*. https://doi.org/10.1136/gutjnl-2014-308048

Shulman, Z., Gitlin, A. D., Targ, S., Jankovic, M., Pasqual, G., Nussenzweig, M. C., & Victora, G. D. (2013). T follicular helper cell dynamics in germinal centers. *Science (New York, N.Y.)*. https://doi.org/10.1126/science.1241680

Sierra, A., Gottfried-Blackmore, A., Milner, T. A., McEwen, B. S., & Bulloch, K. (2008). Steroid hormone receptor expression and function in microglia. *GLIA*. https://doi.org/10.1002/glia.20644

Silverman, M. N., Pearce, B. D., Biron, C. A., & Miller, A. H. (2005). Immune Modulation of the Hypothalamic-Pituitary-Adrenal (HPA) Axis during Viral Infection. *Viral Immunology*. https://doi.org/10.1089/vim.2005.18.41

Singh, P., Agnihotri, A., Pathak, M. K., Shirazi, A., Tiwari, R. P., Sreenivas, V., … Makharia, G. K. (2012). Psychiatric, somatic and other functional gastrointestinal disorders in patients with irritable bowel syndrome at a tertiary care center. *Journal of Neurogastroenterology and Motility*. https://doi.org/10.5056/jnm.2012.18.3.324

Slack, E., Hapfelmeier, S., Stecher, B., Velykoredko, Y., Stoel, M., Lawson, M. A. E., … Macpherson, A. J. (2009). Innate and adaptive immunity cooperate flexibly to maintain host-microbiota mutualism. *Science*. https://doi.org/10.1126/science.1172747

Smith, E. A., & MacFarlane, G. T. (1998). Enumeration of amino acid fermenting bacteria in the human large intestine: Effects of pH and starch on peptide metabolism and dissimilation of amino acids. *FEMS Microbiology Ecology*, *25*(4), 355–368. https://doi.org/10.1016/S0168-6496(98)00004-X

Smythies, L. E., Shen, R., Bimczok, D., Novak, L., Clements, R. H., Eckhoff, D. E., … Smith, P. D. (2010). Inflammation anergy in human intestinal macrophages is due to Smad-induced IkappaBalpha expression and NF-kappaB inactivation. *Journal of Biological Chemistry*. https://doi.org/10.1074/jbc.M109.069955

Speight, N. (2013). Myalgic encephalomyelitis/chronic fatigue syndrome: Review of history, clinical features, and controversies. *Saudi Journal of Medicine and Medical Sciences*, *1*(1), 11. https://doi.org/10.4103/1658-631X.112905

Staff, M. (1957). An outbreak of encephalomyelitis in the royal free hospital group, London, in 1955. *British Medical Journal*, *2*(5050), 895–904. https://doi.org/10.1136/bmj.2.5050.895

Staley, C., Weingarden, A. R., Khoruts, A., & Sadowsky, M. J. (2017). Interaction of gut microbiota with bile acid metabolism and its influence on disease states. *Applied Microbiology and Biotechnology*. https://doi.org/10.1007/s00253-016-8006-6

Stellwag, E. J., & Hylemon, P. B. (1976). Purification and characterization of bile salt hydrolase from Bacteroides fragilis subsp. fragilis. *BBA - Enzymology*. https://doi.org/10.1016/0005-2744(76)90068-1

Stilling, R. M., Ryan, F. J., Hoban, A. E., Shanahan, F., Clarke, G., Claesson, M. J., … Cryan, J. F. (2015). Microbes & neurodevelopment - Absence of microbiota during early life increases activity-related transcriptional pathways in the amygdala. *Brain, Behavior, and Immunity*. https://doi.org/10.1016/j.bbi.2015.07.009

Strober, W., & Fuss, I. J. (2011). Proinflammatory cytokines in the pathogenesis of inflammatory bowel diseases. *Gastroenterology*.

https://doi.org/10.1053/j.gastro.2011.02.016
Stromnes, I. M., & Goverman, J. M. (2006). Active induction of experimental allergic encephalomyelitis. *Nature Protocols*. https://doi.org/10.1038/nprot.2006.285
Studer, N., Desharnais, L., Beutler, M., Brugiroux, S., Terrazos, M. A., Menin, L., … Hapfelmeier, S. (2016). Functional Intestinal Bile Acid 7α-Dehydroxylation by Clostridium scindens Associated with Protection from Clostridium difficile Infection in a Gnotobiotic Mouse Model. *Frontiers in Cellular and Infection Microbiology*. https://doi.org/10.3389/fcimb.2016.00191
Sudo, N., Chida, Y., Aiba, Y., Sonoda, J., Oyama, N., Yu, X. N., … Koga, Y. (2004). Postnatal microbial colonization programs the hypothalamic-pituitary-adrenal system for stress response in mice. *Journal of Physiology*, *558*(1), 263–275. https://doi.org/10.1113/jphysiol.2004.063388
Sugahara, H., Okai, S., Odamaki, T., Wong, C. B., Kato, K., Mitsuyama, E., … Shinkura, R. (2017). Decreased taxon-specific IgA response in relation to the changes of gut microbiota composition in the Elderly. *Frontiers in Microbiology*. https://doi.org/10.3389/fmicb.2017.01757
Sullivan, A., Nord, C. E., & Evengård, B. (2009). Effect of supplement with lactic-acid producing bacteria on fatigue and physical activity in patients with chronic fatigue syndrome. *Nutrition Journal*. https://doi.org/10.1186/1475-2891-8-4
Sullivan, E. L., Nousen, E. K., & Chamlou, K. A. (2014). Maternal high fat diet consumption during the perinatal period programs offspring behavior. *Physiology and Behavior*. https://doi.org/10.1016/j.physbeh.2012.07.014
Summerfield, J. A., Billing, B. H., & Shackleton, C. H. (1976). Identification of bile acids in the serum and urine in cholestasis. Evidence for 6alpha-hydroxylation of bile acids in man. *The Biochemical Journal*, *154*(2), 507–16. https://doi.org/10.1042/bj1540507
Suzuki, K., Meek, B., Doi, Y., Muramatsu, M., Chiba, T., Honjo, T., & Fagarasan, S. (2004). Aberrant expansion of segmented filamentous bacteria in IgA-deficient gut. *Proceedings of the National Academy of Sciences*. https://doi.org/10.1073/pnas.0307317101
Syed, F., Grunenwald, H., & Caruccio, N. (2009). Next-generation sequencing library preparation: Simultaneous fragmentation and tagging using in vitro transposition. *Nature Methods*. https://doi.org/10.1038/nmeth1109-802
Takahashi, S., Fukami, T., Masuo, Y., Brocker, C. N., Xie, C., Krausz, K. W., … Gonzalez, F. J. (2016). Cyp2c70 is responsible for the species difference in bile acid metabolism between mice and humans. *Journal of Lipid Research*, *57*(12), 2130–2137. https://doi.org/10.1194/jlr.M071183
Tannock, G. W., & Savage, D. C. (1974). Influences of dietary and environmental stress on microbial populations in the murine gastrointestinal tract. *Infection and Immunity*, *9*(3), 591–598.
Targan, S. R., Landers, C. J., Yang, H., Lodes, M. J., Cong, Y., Papadakis, K. A., … Hershberg, R. M. (2005). Antibodies to CBir1 flagellin define a unique response that is associated independently with complicated Crohn's disease. *Gastroenterology*. https://doi.org/10.1053/j.gastro.2005.03.046
Taub, D. D. (2008). Neuroendocrine interactions in the immune system. *Cellular Immunology*. https://doi.org/10.1016/j.cellimm.2008.05.006
Telesford, K. M., Yan, W., Ochoa-Reparaz, J., Pant, A., Kircher, C., Christy, M. A., … Kasper, L. H. (2015). A commensal symbiotic factor derived from Bacteroides fragilis promotes human CD39+Foxp3+ T cells and Treg function. *Gut Microbes*. https://doi.org/10.1080/19490976.2015.1056973
Theorell, J., Bileviciute-Ljungar, I., Tesi, B., Schlums, H., Johnsgaard, M. S., Asadi-Azarbaijani, B., … Bryceson, Y. T. (2017). Unperturbed Cytotoxic Lymphocyte Phenotype and

Function in Myalgic Encephalomyelitis/Chronic Fatigue Syndrome Patients. *Frontiers in Immunology*. https://doi.org/10.3389/fimmu.2017.00723

Thevaranjan, N., Puchta, A., Schulz, C., Naidoo, A., Szamosi, J., Verschoo, C., … Bowdish, D. (2017). Age-Associated Microbial Dysbiosis Promotes Intestinal Permeability, Systemic Inflammation, and Macrophage Dysfunction. *Cell Host Microbe*. https://doi.org/10.1016/j.chom.2017.03.002

Thieben, M. J., Sandroni, P., Sletten, D. M., Benrud-Larson, L. M., Fealey, R. D., Vernino, S., … Low, P. a. (2007). Postural orthostatic tachycardia syndrome: the Mayo clinic experience. *Mayo Clinic Proceedings. Mayo Clinic*. https://doi.org/10.4065/82.3.308

Thirumalapura, N. R., Ramachandran, A., Morton, R. J., & Malayer, J. R. (2006). Bacterial cell microarrays for the detection and characterization of antibodies against surface antigens. *Journal of Immunological Methods*. https://doi.org/10.1016/j.jim.2005.11.016

Thursby, E., & Juge, N. (2017). Introduction to the human gut microbiota. *The Biochemical Journal*. https://doi.org/10.1042/BCJ20160510

Tibble, J. A., Sigthorsson, G., Bridger, S., Fagerhol, M. K., & Bjarnason, I. (2000). Surrogate markers of intestinal inflammation are predictive of relapse in patients with inflammatory bowel disease. *Gastroenterology*. https://doi.org/10.1053/gast.2000.8523

Tsigos C, Kyrou I, Kassi E, et al. (2016). Stress, Endocrine Physiology and Pathophysiology.

Turlej-Rogacka, A., Schellemans, H., Chapelle, S., Bryssinck, L., Xavier, B. B., Lammens, C., … Malhotra-Kumar, S. (2017). Comparison of six commercial kits for DNA extraction from human faecal samples, (April), 11–12.

TURNBULL, A. V., & RIVIER, C. L. (1999). Regulation of the Hypothalamic-Pituitary-Adrenal Axis by Cytokines: Actions and Mechanisms of Action. *Physiological Reviews*. https://doi.org/10.1152/physrev.1999.79.1.1

Twisk, F. (2018). Dutch Health Council Advisory Report on Myalgic Encephalomyelitis and Chronic Fatigue Syndrome: Taking the Wrong Turn. *Diagnostics (Basel, Switzerland)*. https://doi.org/10.3390/diagnostics8020034

Twisk, F. N. M. (2014). The status of and future research into Myalgic Encephalomyelitis and Chronic Fatigue Syndrome: The need of accurate diagnosis, objective assessment, and acknowledging biological and clinical subgroups. *Frontiers in Physiology*. https://doi.org/10.3389/fphys.2014.00109

Unger, M. M., Spiegel, J., Dillmann, K.-U., Grundmann, D., Philippeit, H., Bürmann, J., … Schäfer, K.-H. (2016). Short chain fatty acids and gut microbiota differ between patients with Parkinson's disease and age-matched controls. *Parkinsonism & Related Disorders*. https://doi.org/10.1016/j.parkreldis.2016.08.019

Vaiserman, A. M., Koliada, A. K., & Marotta, F. (2017). Gut microbiota: A player in aging and a target for anti-aging intervention. *Ageing Research Reviews*. https://doi.org/10.1016/j.arr.2017.01.001

Van'T Leven, M., Zielhuis, G. A., Van Der Meer, J. W., Verbeek, A. L., & Bleijenberg, G. (2010). Fatigue and chronic fatigue syndrome-like complaints in the general population*. *European Journal of Public Health*. https://doi.org/10.1093/eurpub/ckp113

van der Waaij, L. A., Mesander, G., Limburg, P. C., & van der Waaij, D. (1994). Direct flow cytometry of anaerobic bacteria in human feces. *Cytometry*, *16*(3), 270–279. https://doi.org/10.1002/cyto.990160312

Van Deusen, E. H. (1869). Observations on a form of nervous prostration, (neurasthenia) culminating in insanity. *Amer. J. Insanity*, *25*((4)), 445–461.

Vandeputte, D., Tito, R. Y., Vanleeuwen, R., Falony, G., & Raes, J. (2017). Practical considerations for large-scale gut microbiome studies. *FEMS Microbiology Reviews*.

https://doi.org/10.1093/femsre/fux027
Vanhoutvin, S. A. L. W., Troost, F. J., Hamer, H. M., Lindsey, P. J., Koek, G. H., Jonkers, D. M. A. E., … Brummer, R. J. M. (2009). Butyrate-Induced Transcriptional Changes in Human Colonic Mucosa. *PLoS ONE*. https://doi.org/10.1371/journal.pone.0006759
Vanuytsel, T., Van Wanrooy, S., Vanheel, H., Vanormelingen, C., Verschueren, S., Houben, E., … Tack, J. (2014). Psychological stress and corticotropin-releasing hormone increase intestinal permeability in humans by a mast cell-dependent mechanism. *Gut*. https://doi.org/10.1136/gutjnl-2013-305690
Varrin-Doyer, M., Spencer, C. M., Schulze-Topphoff, U., Nelson, P. A., Stroud, R. M., Bruce, B. A., & Zamvil, S. S. (2012). Aquaporin 4-specific T cells in neuromyelitis optica exhibit a Th17 bias and recognize Clostridium ABC transporter. *Annals of Neurology*. https://doi.org/10.1002/ana.23651
Verma, S., Nakaoke, R., Dohgu, S., & Banks, W. A. (2006). Release of cytokines by brain endothelial cells: A polarized response to lipopolysaccharide. *Brain, Behavior, and Immunity*. https://doi.org/10.1016/j.bbi.2005.10.005
Vernocchi, P., Del Chierico, F., & Putignani, L. (2016). Gut microbiota profiling: Metabolomics based approach to unravel compounds affecting human health. *Frontiers in Microbiology*. https://doi.org/10.3389/fmicb.2016.01144
Vighi, G., Marcucci, F., Sensi, L., Di Cara, G., & Frati, F. (2008). Allergy and the gastrointestinal system. *Clinical and Experimental Immunology*. https://doi.org/10.1111/j.1365-2249.2008.03713.x
Viladomiu, M., Kivolowitz, C., Abdulhamid, A., Dogan, B., Victorio, D., Castellanos, J. G., … Longman, R. S. (2017). IgA-coated E. Coli enriched in Crohn's disease spondyloarthritis promote TH17-dependent inflammation. *Science Translational Medicine*. https://doi.org/10.1126/scitranslmed.aaf9655
Visser, J., Rozing, J., Sapone, A., Lammers, K., & Fasano, A. (2009). Tight junctions, intestinal permeability, and autoimmunity: Celiac disease and type 1 diabetes paradigms. *Annals of the New York Academy of Sciences*. https://doi.org/10.1111/j.1749-6632.2009.04037.x
Wahlström, A., Sayin, S. I., Marschall, H. U., & Bäckhed, F. (2016). Intestinal Crosstalk between Bile Acids and Microbiota and Its Impact on Host Metabolism. *Cell Metabolism*. https://doi.org/10.1016/j.cmet.2016.05.005
Waldecker, M., Kautenburger, T., Daumann, H., Busch, C., & Schrenk, D. (2008). Inhibition of histone-deacetylase activity by short-chain fatty acids and some polyphenol metabolites formed in the colon. *Journal of Nutritional Biochemistry*. https://doi.org/10.1016/j.jnutbio.2007.08.002
Walker, A. W., Martin, J. C., Scott, P., Parkhill, J., Flint, H. J., & Scott, K. P. (2015). 16S rRNA gene-based profiling of the human infant gut microbiota is strongly influenced by sample processing and PCR primer choice. *Microbiome*. https://doi.org/10.1186/s40168-015-0087-4
Wang, G. Y., Zhu, Z. M., Cui, S., & Wang, J. H. (2016). Glucocorticoid induces incoordination between glutamatergic and gabaergic neurons in the amygdala. *PLoS ONE*. https://doi.org/10.1371/journal.pone.0166535
Wang, H., Gong, J., Wang, W., Long, Y., Fu, X., Fu, Y., … Hou, X. (2014). Are there any different effects of Bifidobacterium, Lactobacillus and Streptococcus on intestinal sensation, barrier function and intestinal immunity in PI-IBS mouse model? *PLoS ONE*. https://doi.org/10.1371/journal.pone.0090153
Wang, L., Christophersen, C. T., Sorich, M. J., Gerber, J. P., Angley, M. T., & Conlon, M. A. (2012). Elevated fecal short chain fatty acid and ammonia concentrations in children with autism spectrum disorder. *Digestive Diseases and Sciences*. https://doi.org/10.1007/s10620-012-2167-7

Wang, Y., & Qian, P. Y. (2009). Conservative fragments in bacterial 16S rRNA genes and primer design for 16S ribosomal DNA amplicons in metagenomic studies. *PLoS ONE*. https://doi.org/10.1371/journal.pone.0007401

Wang, Z., Roberts, A. B., Buffa, J. A., Levison, B. S., Zhu, W., Org, E., … Hazen, S. L. (2015). Non-lethal Inhibition of Gut Microbial Trimethylamine Production for the Treatment of Atherosclerosis. *Cell*. https://doi.org/10.1016/j.cell.2015.11.055

Watts, A. G. (2005). Glucocorticoid regulation of peptide genes in neuroendocrine CRH neurons: A complexity beyond negative feedback. *Frontiers in Neuroendocrinology*. https://doi.org/10.1016/j.yfrne.2005.09.001

Wei, M., Shinkura, R., Doi, Y., Maruya, M., Fagarasan, S., & Honjo, T. (2011). Mice carrying a knock-in mutation of Aicda resulting in a defect in somatic hypermutation have impaired gut homeostasis and compromised mucosal defense. *Nature Immunology*. https://doi.org/10.1038/ni.1991

Wherry, E. J. (2011). T cell exhaustion. *Nature Immunology*. https://doi.org/10.1038/ni.2035

Whitehead, L. (2009). The Measurement of Fatigue in Chronic Illness: A Systematic Review of Unidimensional and Multidimensional Fatigue Measures. *Journal of Pain and Symptom Management*, *37*(1), 107–128. https://doi.org/10.1016/j.jpainsymman.2007.08.019

Wichmann, A., Allahyar, A., Greiner, T. U., Plovier, H., Lundén, G. Ö., Larsson, T., … Bäckhed, F. (2013). Microbial modulation of energy availability in the colon regulates intestinal transit. *Cell Host and Microbe*. https://doi.org/10.1016/j.chom.2013.09.012

Williams, Y. (2014). Chronic Fatigue Syndrome: Case Definitions and Diagnostic Assessment. *N Y State Psychol*, *26*(4), 41–45. https://doi.org/10.1016/j.clinbiochem.2015.06.023.Gut-Liver

Willing, B. P., Vacharaksa, A., Croxen, M., Thanachayanont, T., & Finlay, B. B. (2011). Altering host resistance to infections through microbial transplantation. *PLoS ONE*. https://doi.org/10.1371/journal.pone.0026988

Wintzingerode, F. V., Göbel, U. B., & Stackebrandt, E. (1997). Determination of microbial diversity in environmental samples: Pitfalls of PCR-based rRNA analysis. *FEMS Microbiology Reviews*. https://doi.org/10.1016/S0168-6445(97)00057-0

Wohleb, E. S., McKim, D. B., Sheridan, J. F., & Godbout, J. P. (2015). Monocyte trafficking to the brain with stress and inflammation: A novel axis of immune-to-brain communication that influences mood and behavior. *Frontiers in Neuroscience*. https://doi.org/10.3389/fnins.2014.00447

Wong, S. H., Kwong, T. N. Y., Chow, T. C., Luk, A. K. C., Dai, R. Z. W., Nakatsu, G., … Sung, J. J. Y. (2017). Quantitation of faecal Fusobacterium improves faecal immunochemical test in detecting advanced colorectal neoplasia. *Gut*. https://doi.org/10.1136/gutjnl-2016-312766

Wu, H. J., & Wu, E. (2012). The role of gut microbiota in immune homeostasis and autoimmunity. *Gut Microbes*. https://doi.org/10.4161/gmic.19320

Wu, J. Y., Jiang, X. T., Jiang, Y. X., Lu, S. Y., Zou, F., & Zhou, H. W. (2010). Effects of polymerase, template dilution and cycle number on PCR based 16 S rRNA diversity analysis using the deep sequencing method. *BMC Microbiology*. https://doi.org/10.1186/1471-2180-10-255

Yamano, E., Sugimoto, M., Hirayama, A., Kume, S., Yamato, M., Jin, G., … Kataoka, Y. (2016). Index markers of chronic fatigue syndrome with dysfunction of TCA and urea cycles. *Scientific Reports*. https://doi.org/10.1038/srep34990

Yang, B., Wang, Y., & Qian, P. Y. (2016). Sensitivity and correlation of hypervariable regions in 16S rRNA genes in phylogenetic analysis. *BMC Bioinformatics*. https://doi.org/10.1186/s12859-016-0992-y

Yang, Z. Z., Grote, D. M., Xiu, B., Ziesmer, S. C., Price-Troska, T. L., Hodge, L. S., … Ansell, S. M. (2014). TGF-β upregulates CD70 expression and induces exhaustion of effector memory T cells in B-cell non-Hodgkin's lymphoma. *Leukemia*. https://doi.org/10.1038/leu.2014.84

Yarza, P., Yilmaz, P., Pruesse, E., Glöckner, F. O., Ludwig, W., Schleifer, K. H., … Rosselló-Móra, R. (2014). Uniting the classification of cultured and uncultured bacteria and archaea using 16S rRNA gene sequences. *Nature Reviews Microbiology*. https://doi.org/10.1038/nrmicro3330

Yu, Q. J., Yu, S. Y., Zuo, L. J., Lian, T. H., Hu, Y., Wang, R. D., … Zhang, W. (2018). Parkinson disease with constipation: Clinical features and relevant factors. *Scientific Reports*. https://doi.org/10.1038/s41598-017-16790-8

Yu, X., Stavrakis, S., Hill, M. A., Huang, S., Reim, S., Li, H., … Kem, D. C. (2012). Autoantibody activation of beta-adrenergic and muscarinic receptors contributes to an "autoimmune" orthostatic hypotension. *Journal of the American Society of Hypertension*. https://doi.org/10.1016/j.jash.2011.10.003

Yu, Z., Kastenmüller, G., He, Y., Belcredi, P., Möller, G., Prehn, C., … Wang-Sattler, R. (2011). Differences between human plasma and serum metabolite profiles. *PLoS ONE*. https://doi.org/10.1371/journal.pone.0021230

Zamvil, S. S., Spencer, C. M., Baranzini, S. E., & Cree, B. A. C. (2018). The Gut Microbiome in Neuromyelitis Optica. *Neurotherapeutics*, *15*(1), 92–101. https://doi.org/10.1007/s13311-017-0594-z

Zarrinpar, A., Chaix, A., Xu, Z. Z., Chang, M. W., Marotz, C. A., Saghatelian, A., … Panda, S. (2018). Antibiotic-induced microbiome depletion alters metabolic homeostasis by affecting gut signaling and colonic metabolism. *Nature Communications*, *9*(1), 2872. https://doi.org/10.1038/s41467-018-05336-9

Zenewicz, L. A., Yancopoulos, G. D., Valenzuela, D. M., Murphy, A. J., Stevens, S., & Flavell, R. A. (2008). Innate and Adaptive Interleukin-22 Protects Mice from Inflammatory Bowel Disease. *Immunity*. https://doi.org/10.1016/j.immuni.2008.11.003

Zeng, M. Y., Cisalpino, D., Varadarajan, S., Hellman, J., Warren, H. S., Cascalho, M., … Núñez, G. (2016). Gut Microbiota-Induced Immunoglobulin G Controls Systemic Infection by Symbiotic Bacteria and Pathogens. *Immunity*. https://doi.org/10.1016/j.immuni.2016.02.006

Zhan, Y., Paolicelli, R. C., Sforazzini, F., Weinhard, L., Bolasco, G., Pagani, F., … Gross, C. T. (2014). Deficient neuron-microglia signaling results in impaired functional brain connectivity and social behavior. *Nature Neuroscience*. https://doi.org/10.1038/nn.3641

Zhang, J., Li, H., Zhou, H., Fang, L., Xu, J., Yan, H., … Jia, W. (2017). Lowered fasting chenodeoxycholic acid correlated with the decrease of fibroblast growth factor 19 in Chinese subjects with impaired fasting glucose. *Scientific Reports*. https://doi.org/10.1038/s41598-017-06252-6

Zhang, L., Gough, J., Christmas, D., Mattey, D. L., Richards, S. C. M., Main, J., … Kerr, J. R. (2010). Microbial infections in eight genomic subtypes of chronic fatigue syndrome/myalgic encephalomyelitis. *Journal of Clinical Pathology*, *63*(2), 156–164. https://doi.org/10.1136/jcp.2009.072561

Zhang, M., Zhou, Q., Dorfman, R. G., Huang, X., Fan, T., Zhang, H., … Yu, C. (2016). Butyrate inhibits interleukin-17 and generates Tregs to ameliorate colorectal colitis in rats. *BMC Gastroenterology*. https://doi.org/10.1186/s12876-016-0500-x

Zhang, Y., & Klaassen, C. D. (2010). Effects of feeding bile acids and a bile acid sequestrant on hepatic bile acid composition in mice. *Journal of Lipid Research*, *51*(11), 3230–3242. https://doi.org/10.1194/jlr.M007641

Zhernakova, A., Kurilshikov, A., Bonder, M. J., Tigchelaar, E. F., Schirmer, M., Vatanen, T., …

Fu, J. (2016). Population-based metagenomics analysis reveals markers for gut microbiome composition and diversity. *Science*. https://doi.org/10.1126/science.aad3369

Zhou, L., Zhang, M., Wang, Y., Dorfman, R. G., Liu, H., Yu, T., … Yu, C. (2018). Faecalibacterium prausnitzii Produces Butyrate to Maintain Th17/Treg Balance and to Ameliorate Colorectal Colitis by Inhibiting Histone Deacetylase 1. *Inflammatory Bowel Diseases*, *24*(9), 1926–1940. https://doi.org/10.1093/ibd/izy182

Zhou, Q., Zhang, B., & Nicholas Verne, G. (2009). Intestinal membrane permeability and hypersensitivity in the irritable bowel syndrome. *Pain*. https://doi.org/10.1016/j.pain.2009.06.017

Zijlmans, M. A. C., Korpela, K., Riksen-Walraven, J. M., de Vos, W. M., & de Weerth, C. (2015). Maternal prenatal stress is associated with the infant intestinal microbiota. *Psychoneuroendocrinology*. https://doi.org/10.1016/j.psyneuen.2015.01.006

Zimomra, Z. R., Porterfield, V. M., Camp, R. M., Johnson, J. D., Akaogi, J., Yamada, H., … Peebles, R. (2011). Time-dependent mediators of HPA axis activation following live Escherichia coli. *American Journal of Physiology. Regulatory, Integrative and Comparative Physiology*. https://doi.org/10.1152/ajpregu.00301.2011

Zweigner, J., Gramm, H. J., Singer, O. C., Wegscheider, K., & Schumann, R. R. (2001). High concentrations of lipopolysaccharide-binding protein in serum of patients with severe sepsis or septic shock inhibit the lipopolysaccharide response in human monocytes. *Blood*. https://doi.org/10.1182/blood.V98.13.3800

Zwielehner, J., Liszt, K., Handschur, M., Lassl, C., Lapin, A., & Haslberger, A. G. (2009). Combined PCR-DGGE fingerprinting and quantitative-PCR indicates shifts in fecal population sizes and diversity of Bacteroides, bifidobacteria and Clostridium cluster IV in institutionalized elderly. *Experimental Gerontology*. https://doi.org/10.1016/j.exger.2009.04.002